Journal of Chemistry

Natural Bioactive Compounds: Chemistry, Extraction, and Applications

Lead Guest Editor: Muhammad Zia-Ul-Haq
Guest Editors: Romina Alina Vlaic Marc and Marwa Abdelaziz Ali Fayed

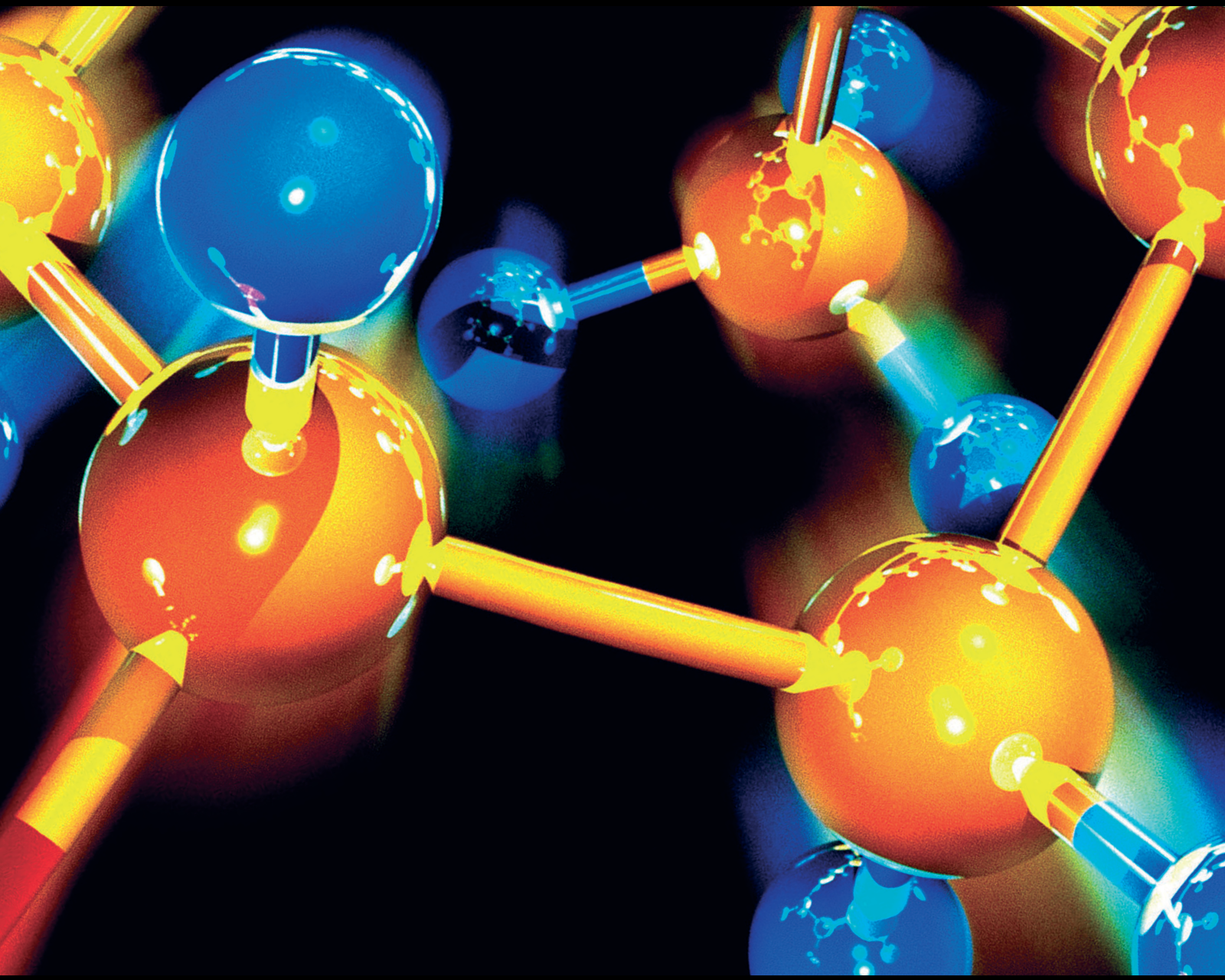

Natural Bioactive Compounds: Chemistry, Extraction, and Applications

Journal of Chemistry

Natural Bioactive Compounds: Chemistry, Extraction, and Applications

Lead Guest Editor: Muhammad Zia-Ul-Haq
Guest Editors: Romina Alina Vlaic Marc and
Marwa Abdelaziz Ali Fayed

Chief Editor

Kaustubha Mohanty, India

Associate Editors

Mohammad Al-Ghouti, Qatar
Tingyue Gu, USA
Teodorico C. Ramalho, Brazil
Artur M. S. Silva, Portugal

Academic Editors

Jinwei Duan , China
Luqman C. Abdullah, Malaysia
Dr Abhilash, India
Amitava Adhikary, USA
Amitava Adhikary, USA
Mozhgan Afshari, Iran
Daryoush Afzali, Iran
Mahmood Ahmed, Pakistan
Islam Al-Akraa, Egypt
Juan D. Alché, Spain
Gomaa A. M. Ali, Egypt
Mohd Sajid Ali, Saudi Arabia
Shafaqat Ali, Pakistan
Patricia E. Allegretti, Argentina
Marco Anni, Italy
Alessandro Arcovito, Italy
Hassan Arida, Saudi Arabia
Umair Ashraf, Pakistan
Narcis Avarvari, France
Davut Avci, Turkey
Chandra Azad, USA
Mohamed Azaroual, France
Rasha Azzam, Egypt
Hassan Azzazy, Egypt
Renal Backov, France
Suresh Kannan Balasingam, Republic of Korea
Sukanta Bar, USA
Florent Barbault, France
Maurizio Barbieri, Italy
James Barker, United Kingdom
Salvatore Barreca, Italy
Jorge Barros-Velázquez, Spain
THANGAGIRI Baskaran, India
Haci Baykara, Ecuador
Michele Benedetti, Italy
Laurent Billon, France
Marek Biziuk, Poland
Jean-Luc Blin, France
Tomislav Bolanca, Croatia
Ankur Bordoloi, India
Cato Brede, Norway
Leonid Breydo, USA
Wybren J. Buma, The Netherlands
J. O. Caceres, Spain
Patrizia Calaminici, Mexico
Claudio Cameselle, Spain
Joaquin Campos, Spain
Dapeng Cao, China
Domenica Capasso, Italy
Stefano Caporali, Italy
Zenilda Cardeal, Brazil
Angela Cardinali, Italy
Stefano Carli, Italy
Maria F. Carvalho, Portugal
Susana Casal, Portugal
David E. Chavez, USA
Riccardo Chelli, Italy
Zhongfang Chen, Puerto Rico
Vladislav Chrastny, Czech Republic
Roberto Comparelli, Italy
Filomena Conforti, Italy
Luca Conti, Italy
Christophe Coquelet, France
Filomena Corbo, Italy
Jose Corchado, Spain
Maria N. D.S. Cordeiro, Portugal
Claudia Crestini, Italy
Gerald Culioli, France
Nguyen Duc Cuong, Vietnam
Stefano D'Errico, Italy
Matthias D'hooghe, Belgium
Samuel B. Dampare, Ghana
Umashankar Das, Canada
Victor David, Romania
Annalisa De Girolamo, Italy
Antonio De Lucas-Consuegra, Spain
Marcone A. L. De Oliveira, Brazil
Paula G. De Pinho, Portugal
Damião De Sousa, Brazil
Francisco Javier Deive, Spain
Tianlong Deng, China

Contents

Contents

Hindawi
Journal of Chemistry
Volume 2023, Article ID 6504505, 15 pages
https://doi.org/10.1155/2023/6504505

Research Article

Biological Activities and GC-MS Analysis of *Aloe vera* and *Opuntia ficus-indica* Extracts

Afaf Alghamdi,[1] Wafa Alshehri ,[1] Bayan Sajer,[2] Mada Ashkan,[3] Ruba Ashy,[1] Rukaia Gashgari,[1] and Haifa Hakmi[1]

[1]*Department of Biological Sciences, College of Science, University of Jeddah, Jeddah, Saudi Arabia*
[2]*Department of Biological Sciences, College of Science, King Abdulaziz University, Jeddah 80200, Saudi Arabia*
[3]*Biological Sciences Department, College of Science & Art, King Abdulaziz University, Rabigh 21911, Saudi Arabia*

Correspondence should be addressed to Wafa Alshehri; waalshehri@uj.edu.sa

Received 28 October 2022; Revised 26 February 2023; Accepted 5 April 2023; Published 9 May 2023

Academic Editor: Muhammad Zia-Ul-Haq

To evaluate the potential antimicrobial activity, *Aloe vera* and *Opuntia ficus-indica* plants were collected from the Jeddah, Al Baha, and Taif areas of the Kingdom of Saudi Arabia (SA), and their ethanolic extracts were screened by gas chromatography mass spectrometry (GC–MS/MS). The di(2-propylpentyl) ester and hexadecenoic acid ethyl ester of phthalic acid were the most abundant compounds in the *A. vera* extract, and 1-(benzyloxy)-3,5-dinitrobenzene and phenol, 5-ethenyl-2-methoxy were the most abundant compounds in the *O. ficus-indica* extract. The antimicrobial activity of aqueous and ethanolic extracts of these plants against seven fungi and five pathogenic bacteria was also tested. Among all the tested fungi, *A. chevalieri* showed the largest inhibition zone when treated with the *A. vera* gel ethanolic extract, followed by *P. funiculosum* and *P. minioluteum*, which were more sensitive to and showed larger inhibition zones upon treatment with aqueous extract. For the *O. ficus-indica* ethanolic extract, T. funiculosus showed the largest inhibition zone. The aqueous extract of the *O. ficus-indica* showed low antimicrobial activity against all tested fungi. By contrast, both the *A. vera* and *O. ficus-indica* extracts showed antibacterial activity against *S. aureus*, *Shigella* sp., *E. coli*, and *MRSA* except *S. typhimurium*, which was the most resistant bacterium to both the aqueous and ethanol extracts of *A. vera* and *O. ficus-indica.*

1. Introduction

Cacti and cacti-like plants are important food sources for wild animals besides their use in medicine, chemical, spinning, and cosmetic industry. These plants are a low-cost source of readily available raw materials [1, 2] for various uses. As medicinal plants, they are rich sources of novel antimicrobial agents [3]. Throughout human history, various infectious diseases have been treated with traditional herbal medicines. A wide range of medicinal plant parts are extracted as raw drugs that possess various medicinal properties [3]. The antimicrobial agents of *A. vera* gel effectively kill or greatly reduce the growth of a wide range of pathogens [4–7]. Both *Opuntia* and *Aloe* species have wide applications, as bactericidal, antibiotic, fungicidal, and anti-inflammatory agents; in tissues as moisturizing creams; and as pain relievers for joint and muscle pain [6, 8–11]. Several studies have reported that *A. vera* gel is effective against both Gram-positive and -negative bacteria [12]. Irshad and Butt [13] found that *A. vera* gel has a good antibacterial effect toward some bacteria, such as *Escherichia coli*, *Salmonilla typhimurium*, *Bacillus subtilis*, *Staphylococcus epidermidis*, and *Pseudomonas.* Jain et al. [12] reported that bioactive components in *A. vera* crude extracts have powerful antibacterial activity. Hence, higher concentrations of *A. vera* extracts can be utilized as secondary antibacterial agents for the treatment of some diseases. Another study reported the antibacterial properties of *A. vera* gel ethanolic extracts towards selected pathogens [6]. Arbab et al. [14] stated that *A. vera* is effective against infections caused by *Staphylococcus aureus*, *Staphylococcus epidermidis*, *Pseudomonas aeruginosa*, and *Streptococcus pyogenes*.

Pourmajed et al. [15] showed that the ethanolic extracts of the *O. ficus-indica* possess antimicrobial activity against *E. coli* isolated from patients with urinary tract infection (UTI). The ethyl acetate extract of the cactus showed antibacterial activity against five food-borne bacteria, namely, *B. subtilis*, *Staphylococcus aureus* subsp. *aureus*, *E. coli*, *S. typhimurium*, and *Pseudomonas fluorescens*. No study exists exploring the chemical composition and antimicrobial activities of *O. ficus-indica* and *A. vera* plants. Hence, current study was designed to evaluate these parameters of both plants collected from Jeddah, Taif, and Al Baha, in SA, by screening their ethanolic extracts using GC–MS/MS.

2. Materials and Methods

2.1. Collection of Plant Samples. The fresh naturally grown stems, leaves, and roots of *A. vera* and *O. ficus-indica* were harvested from the Jeddah, Taif, and Al Baha areas, in SA, in September 2019 and January 2020. The selected plants are listed in Table 1.

2.2. Preparation of Plant Extracts

2.2.1. Aqueous Extract. The *Opuntia ficus-indica* (leaves and stems) were soaked in a solution of sodium hypochlorite (0.1%; w/v) for disinfection and removal of any adherent soil material [16]. The samples were washed with distilled water to remove the sodium hypochlorite. The leaves and stems samples were taken by cutting 1/2 inch from the plant base to remove the yellow sap material and 1/2 inch from the apex. These were then cut into two or more parts for easy handling. The spiny leaf margins were removed using a clean knife. The inner gel was carefully scraped out using a clean spoon to avoid the green areas. The gel was mixed using a grinder to obtain a juice gel. The juice gel was heated in a hot water bath at 70°C for 20 min. The juice was then filtrate to obtain a clear juice gel.

2.2.2. Ethanol Extract. The fresh stems of cacti and fresh leaves of cacti-like plants were rinsed several times with both tap water and distilled water [17]. 95 g of the samples were then grounded in an electrical blender to obtain a fine paste by adding a few drops of 99% ethanol. The gel was equally distributed in conical flasks, after which 150 mL of 99% alcohol was added to all conical flasks. Subsequently, the flasks were kept in a rotary shaker for 3 days. The gel was filtered using Whatman filter paper no.1 (Filter Papers Grade 1, Turkey), evaporated in a heating mantle yielding 14.8 g powder, which was stored in a screw cap test tube at 4°C. 10 mg/ml of the powder, and was used later on in the antimicrobial activity testing.

2.3. Pathogenic Microorganisms. Seven pathogenic fungi (Aspergillus chevalieri (MT487830.1), *Aspergillus terreus* (MT558939.1), *Penicillium funiculosum* (JX500735.1), *Talaromyces funiculosus* (KX262973.1), *Penicillium minioluteum* (JN620402.1), *Aspergillus niger* (MT628904.1), *Curvularia khuzestanica* (MH688044.1)), and five human pathogenic bacteria (*Escherichia coli* (11775), *Staphylococcus aureus* (12600), *Shigella* sp., methicillin-resistant *Staphylococcus aureus* (33591), and *Salmonella typhimurium* (14028)) were obtained from the King Fahad Researcher Centre in Jeddah and used during the experiment.

2.3.1. Determination of Antimicrobial Activity. PDA medium was used for subcultivation of the fungal and bacterial strains. Each microbe was evenly inoculated on the PDA media in plates using the streak method. Filter papers (5 mm diameter) were completely immersed in the aqueous and ethanol extracts of *A. vera* and *O. ficus-indica* extract and then placed on the agar surface. The plates were incubated for 2–5 days at 37°C and 28°C for fungal and bacterial growth, respectively. All experiments were performed thrice [18]. The antimicrobial activity was determined by observing the inhibition zone.

2.3.2. Antimicrobial Sensitivity Test on Microbes (Positive Control). For the positive control samples for microbe inhibition, the antibiotic itraconazole was used for fungi and ciprofloxacin for bacteria.

2.3.3. Antimicrobial Effect of Solvents (Negative Control). Ethanol and distilled water were used as negative control.

2.4. Gas Chromatography-Mass Spectrometry Conditions. About 500 μL ethanol and 500 μL samples were added. The mixture was vortexed for 30 seconds and then injected for GC–MS analysis.

2.4.1. Gas Chromatography–Mass Spectrometry (GC–MS/MS) for Aloe vera. The *A. vera* extracts were analyzed by gas chromatography (Agilent 7890A GC System). A Hp-5 ms fused silica capillary column was used (5% phenyl/95% dimethylsiloxane 30 M × 0.25 mm film thickness 0.32 Lm). The oven temperature was 110°C (isothermal for 2 minutes), with an increase to 200°C (10°C/min) and then 280°C (5°C/min), with final temperature (isothermal for 9 minutes).

The carrier gas used was helium (flow rate of 1 mL/min). GC–MS analyses were performed using an Agilent Technologies 7000 GC/MS Triple Quad coupled to an Agilent Technologies 7693 Autosampler. The capillary column and GC conditions were calculated as described above. MS spectra were recorded at 70 eV, and the scanning rate was 1 scan/s with a run time of 90 minutes [19].

2.4.2. Gas Chromatography–-Mass Spectrometry (GC–MS/MS) for Opuntia ficus-Indica. Gas chromatographic analysis was performed using an Agilent Technologies 7890A GC System. The separation was achieved using an HP-5 ms fused silica capillary column (30 m × 0.25 mm i.d., 0.25 mm film thickness). The GC oven temperature was programmed for an increase from 40°C (5 min) to 250°C @ 2°C/min, held for 15 minutes and eventually increased to 270°C@ 10°C/min. Helium was used as a carrier gas, with a 1.0 mL/min flow

Table 1: List of Cacti and cacti-like plants utilized in this study.

No	Scientific name	Family	Common name	Part of plant used	Collection site
1	*Aloe vera*	*Asphodalaceae*	*Aloe vera*	Roots and leaves	Jeddah
2	*Opuntia ficus-indica*	Cactaceae	*Opuntia* Teen Shouki Barshoumi	Roots and stems	Albaha and Taif

rate, and injector and detector temperature of 250°C, and 280°C, respectively. A fused silica HP-Innowax polyethylene glycol capillary column (50 m × 0.20 mm i.d., 0.20 mm film thickness) was used. A mixture of aliphatic hydrocarbons (C8–C30) in hexane was directly injected into the GC injector under the abovementioned temperature program to calculate the retention index (as the Kovats index) of each compound. GC–MS analysis was performed on an Agilent Technologies 7000 GC/MS Triple Quad coupled to an Agilent Technologies7693 Autosampler. The separation was performed using a fused silica HP-5 capillary column (30 m × 0.25 mm i.d., 0.33 mm film thickness). The GC oven temperature was programmed similarly to in the gas chromatographic analyses. The MS scan conditions were source temperature, 25°C; interface temperature, 290°C; electron energy, 70 eV; and mass scan range, 40–450 AMU [20].

2.5. Statistical Analysis. Using the Windows Microsoft Excel 2013 software, version 15.0, analyzing the results was carried out using a one-way analysis of variance (ANOVA) test to determine any significant differences between the antimicrobial effect in both cacti and cacti-like plants. All columns versus control and the P value <0.05 are considered as significant.

3. Results

3.1. Determination of Antimicrobial Activity of Aloe vera Extract. The antimicrobial activity of *A. vera* extracted using two solvents, aqueous and ethanol, showed different response against the selected fungi and bacteria. Among all tested fungi, the largest inhibition zone for ethanol extracts was observed with *A. chevalieri* (1.00 ± 0.50 mm), while *P. funiculosum* and *P. minioluteum* were the most sensitive for aqueous extracts, with inhibition zones of 0.57 ± 0.40 and 0.43 ± 0.23 mm), respectively. *A. terreus* and *A. niger* were the most resistant fungi, with no activity revealed for both the aqueous and ethanol extracts. The aqueous extract of *A. vera* showed antibacterial activity against *S. aureus, Shigella* sp., and *E. coli*, with inhibition zones of 1.10 ± 0.10, 0.47 ± 0.25, and 0.40 ± 0.10 mm, respectively. MRSA showed the largest inhibition zone with ethanol extract (0.70 ± 0.26 mm). *S. typhimurium* was the most resistant bacteria, with no activity being shown for either the aqueous or ethanol extracts of *A. vera* (Tables 2 and 3).

ANOVA showed that the *A. vera* aqueous extract has the highest antibacterial activity with an average value of 0.4592 while the ethanolic extract has the highest antifungal activity with an average value of 0.2331. There is a statistically significant difference between aqueous and ethanolic extracts ($P < 0.05$) (Table 4).

3.2. Determination of Antimicrobial Activity of Opuntia ficus-Indica Extract. The antimicrobial activity of *O. ficus-indica* aqueous and ethanolic extracts, showed different response against the selected pathogens. Among tested fungi, T. funiculosus showed the largest inhibition zone against ethanolic extract (0.40 ± 0.10 mm), while P. funiculosum showed a smaller zone of inhibition against ethanolic extract (0.07 ± 0.06 mm). The aqueous extract showed low antimicrobial activity with all tested fungi, ranging from 0.13 to 0.17. The *O. ficus-indica* aqueous extract showed significant antibacterial activity against MRSA, *Shigella* sp., and *S. aureus.* MRSA showed the largest inhibition zone of 1.43 ± 0.40 mm, followed by *Shigella* sp. and *S. aureus*, with inhibition zones of 0.73 ± 0.06 and 0.66 ± 0.20 mm, respectively, against aqueous extracts. *S. typhimurium* was the most resistant bacteria, with no activity for either the aqueous or ethanolic extracts (0.00) (Tables 5 and 6).

The ANOVA showed that the *Opuntia ficus-indica* aqueous and ethanolic extracts have the highest antibacterial activity with an average of (0.59, 0.198), respectively. There is a statistically significant difference between aqueous and ethanolic extracts ($p < 0.05$) (Table 7).

3.3. GC–MS Analysis of Aloe vera Ethanolic Extract. The GC–MS/MS analysis for A. vera was performed for 18 identified compounds. The well-known phthalic acid, di(2-propylpentyl) ester (92.4%) was identified as the major compound, followed by hexadecenoic acid, ethyl ester (91.8%), lidocaine (89%), trib utyl acetyl citrate (88.1%), ethyl oleate (86.0%), 1,4-benzenedi carboxylic acid, bis(2-ethylhexyl)ester (80.8%), pyrolo[3,2-d]py rimidin-2,4(1H,3H)-dione (77.3%), phenol,4-[(5,6,7,8-tetrahy dro-1,3-dioxolo[4,5-g]isoquinolin-5yl)methyl],(R)- (76.4%), 3-methyl-1,2,3,4 tetrahydro-gamma-carboline (73.4%), 2,2 dim ethyl-5-phenyl-3(2H)furanone (71.7%), 1,2 benzenedi-carbox ylic acid,bis(2-methylpropyl)ester (71.2%), 2-fluoro-6-trifluoro methylbenzoic acid, 4-nitrophenyl ester (71.2%), 4-(benzyl-eth yl-amino)-butyric acid, methyl ester (70.7%), (2-aziridinyl ethyl)amine (69.8%), 3-methyl-4-nitrophenyl pentafluoro benzyl ether (67.7%), methane, difluoroiodo- (66.5%), pyrro le,2-methyl-5-phenyl- (66.0%), and benzamide,2-methoxy-N-b enzyl-N-phenethyl- (65.6%) (Figures 1 and 2).

3.4. GC–MS of O. ficus-Indica Ethanolic Extracts. The GC–MS analysis of *O. ficus-indica* led to 34 compounds, namely, 1-(benzyloxy)-3,5-dinitrobenzene (81.5%), phenol, 5-ethenyl-2-methoxy- (80.7%), hexadecanoic acid, ethyl ester (80.6%), 1,3-pentadiyne,1,5,5,5-nitropyrimidine (77.0%), benzene,1fluoro-4-methyl(75.6%), trifluoromethylthiocyanate (74.4%),1-(benzyloxy)-3,5dinitro-benzene (74.2%), furan,2-methoxy-(74.1%), phthalic acid, di(oct-3-yl)ester (72.1%), acetic acid,(4-chloro-2-methylphenoxy)-heptadecyl ester (71.6%), pyridine,3-propyl-(71.1%), benzphetamine (71.0%), l-alanine,

Table 2: Antifungal activities of aqueous and ethanolic extract of *A. vera*.

No	Fungi	Inhibition zone (mm)			
		A. vera aqueous extract (30 μ/disc)	*A.vera* ethanolic extract (30 μ/disc)	Itraconazole (positive control) (30 μ/disc)	Distilled water (negative control) (30 μ/disc)
1	*A. chevalieri*	0.33 ± 0.12	1.00 ± 0.50	0.27 ± 0.12	0.00
2	*T. funiculosus*	0.27 ± 0.06	0.13 ± 0.12	0.13 ± 0.06	0.00
3	*A. terreus*	0.00	0.00	1.7 ± 0.06	0.00
4	*P. funiculosum*	0.57 ± 0.40	0.20 ± 0.10	0.23 ± 0.15	0.00
5	*P.minioluteum*	0.43 ± 0.23	0.23 ± 0.23	1.33 ± 0.47	0.00
6	*A. niger*	0.00	0.00	1.20 ± 0.36	0.00
7	*C. khuzestanica*	0.07 ± 0.06	0.07 ± 0.06	0.20 ± 0.10	0.00

All values are expressed as mean ± SD.

Table 3: Antibacterial activities of aqueous and ethanolic extract of *A. vera*.

No	Bacteria	Inhibition zone (mm)			
		A. vera aqueous extract (30 μ/disc)	*A. vera* ethanolic extract (30 μ/disc)	Ciprofoxacin (positive control) (30 μ/disc)	Distilled water (negative control) (30 μ/disc)
1	*Staph. aureus*	1.10 ± 0.10	0.00	2.00 ± 0.00	0.00
2	*Shigella sp.*	0.47 ± 0.25	0.17 ± 0.06	0.23 ± 0.06	0.00
3	*S.thypimurium*	0.00	0.00	1.33 ± 0.3	0.00
4	MRSA	0.33 ± 0.06	0.70 ± 0.26	1.83 ± 0.3	0.00
5	*E.coli*	0.40 ± 0.10	0.07 ± 0.06	1.97 ± 0.06	0.00

All values are expressed as mean ± SD.

Table 4: One-way ANOVA for antifungal and antibacterial activity of *A.vera* extracts.

No	Bacteria	Inhibition zone (mm)			
		A. vera aqueous extract (30 μ/disc)	*A. vera* ethanolic extract (30 μ/disc)	Ciprofoxacin (positive control) (30 μ/disc)	Distilled water (negative control) (30 μ/disc)
1	*Staph. aureus*	1.10 ± 0.10	0.00	2.00 ± 0.00	0.00
2	*Shigella sp.*	0.47 ± 0.25	0.17 ± 0.06	0.23 ± 0.06	0.00
3	*S.thypimurium*	0.00	0.00	1.33 ± 0.3	0.00
4	MRSA	0.33 ± 0.06	0.70 ± 0.26	1.83 ± 0.3	0.00
5	*E.coli*	0.40 ± 0.10	0.07 ± 0.06	1.97 ± 0.06	0.00

Table 5: Antifungal activities of aqueous and ethanolic extract of *O. ficus-indica*.

No	Fungi	Inhibition zone (mm)			
		O. ficus-indica aqueous extract (30 μ/disc)	*O. ficus-indica* ethanol extract (30 μ/disc)	Antibiotic itraconazole (positive control) (30 μ/disc)	Distilled water (negative control) (30 μ/disc)
1	*A. chevalieri*	0.10 ± 0.10	0.13 ± 0.06	0.27 ± 0.12	0.00
2	*T. funiculosus*	0.10 ± 0.10	0.40 ± 0.10	0.13 ± 0.06	0.00
3	*A. terreus*	0.00	0.20 ± 0.10	1.66 ± 0.06	0.00
4	*P. funiculosum*	0.07 ± 0.06	0.07 ± 0.06	0.23 ± 0.15	0.00
5	*P. minioluteum*	0.00	0.13 ± 0.06	1.33 ± 0.47	0.00
6	*A. niger*	0.17 ± 0.06	0.13 ± 0.06	1.20 ± 0.36	0.00
7	*C. khuzestanica*	0.13 ± 0.06	0.17 ± 0.57	0.20 ± 0.10	0.00

All values are expressed as mean ± SD.

n-propargyloxycarbonyl-, ethyl ester (70.4%), 2-aminohydra tropic acid (69.8%), thiophene,3-methyl- (69.6%), cyanogen-chloride (69.2%), alanine, N-methyl-n-propoxycarbonyl-, nonyl ester (69.1%), 3-amino2,4dimethylpentane (68.1%), 2,2′-bioxirane (68.2%), hydrazine-carbo-thioamide, N-methyl-(67.7%), 4-methyl-2,4-bis(p-hydroxy-phenyl)pent-1-ene,2TM Sderivative (67.6%), phthalic acid,bis(2-pentyl) ester (67.5%), phthalic acid, butyl hexyl ester (67.4%), 2-butynedinitrile (67.2%), bis(2-ethylhexyl)phthalate (67.1%), silane, dimethyl(4methoxyphenoxy)heptadecyloxy- (67.0%), 4-hexen-2-one(66.4%), furfural (66.4%), 1-penten-3-one (65.7%) and 2propanol,1,3-dibromo (65.1%) (Figures 3 and 4).

Table 6: Antibacterial activities of aqueous and ethanolic extract of *O. ficus-indica*.

No	Bacteria	Inhibition zone (mm)			
		O. ficus-indica aqueous extract (30 μ/disc)	*O. ficus-indica* ethanolic extract (30 μ/disc)	Ciprofoxacin (positive control) (30 μ/disc)	Distilled water (negative control) (30 μ/disc)
1	*Staph .aureus*	0.66 ± 0.20	0.00	2.00 ± 0.00	0.00
2	*Shigella sp.*	0.73 ± 0.06	0.10 ± 0.10	0.23 ± 0.06	0.00
3	*S. thypimurium*	0.00	0.00	1.33 ± 0.28	0.00
4	MRSA	1.43 ± 0.40	0.76 ± 0.25	1.83 ± 0.28	0.00
5	*E.coli*	0.13 ± 0.06	0.13 ± 0.06	1.97 ± 0.06	0.00

All values are expressed as mean ± SD.

Table 7: One-way ANOVA for antifungal and antibacterial activity of *O. ficus-indica* extracts.

	Average	Variance	*P* value
Antifungal activity of *O. ficus-indica* aqueous extract	0.0814	0.0040	0.0019
Antifungal activity of *O. ficus-indica* ethanolic extract	0.1757	0.0113	
Antibacterial activity of *O. ficus-indica* aqueous extract	0.59	0.3224	0.0011
Antibacterial activity of *O. ficus-indica* ethanolic extract	0.198	0.1021	

Coppounds in Aloe vera			
Classes of compounds	Bioactive Compounds	MW	Molecular
long-chain fatty acid ethyl ester	Phthalic acid, di (2-propylpentyl) ester	402.5	$C_{26}H_{26}O_4$
long-chain fatty acid ethyl ester	Hexadecanoic acid, ethyl ester	284.4	C18H36O2
Monocarboxylic acid amide	Lidocaine	234.34	$C_{14}H_{22}N_2O$
plasticizers	Tributyl acetylcitrate	402.5	C20H34O8
polyphenols	Pyrolo[3,2-d] pyrimidin-2,4 (1H,3H)-dione	151.12	$C_6H_5N_3O_2$
Ester	2-Fluoro-6-trifluoromethylbenzoic acid, 4-nitrophenyl ester	329.2	$C_{14}H_7F_4NO_4$
plasticizers	1,2-Benzenedicarboxylic acid, bis (2-methylpropyl) ester	278.3	$C_{16}H_{22}O_4$
Pyrroles	Pyrrole, 2-methyl-5-phenyl-	157.21	$C_{11}H_{11}N$
polyphenols	Benzamide, 2-methoxy-N-benzyl-N-phenethyl	257.29	$C_{15}H_{15}NO_3$

Figure 1: The various compounds found in *A. vera*.

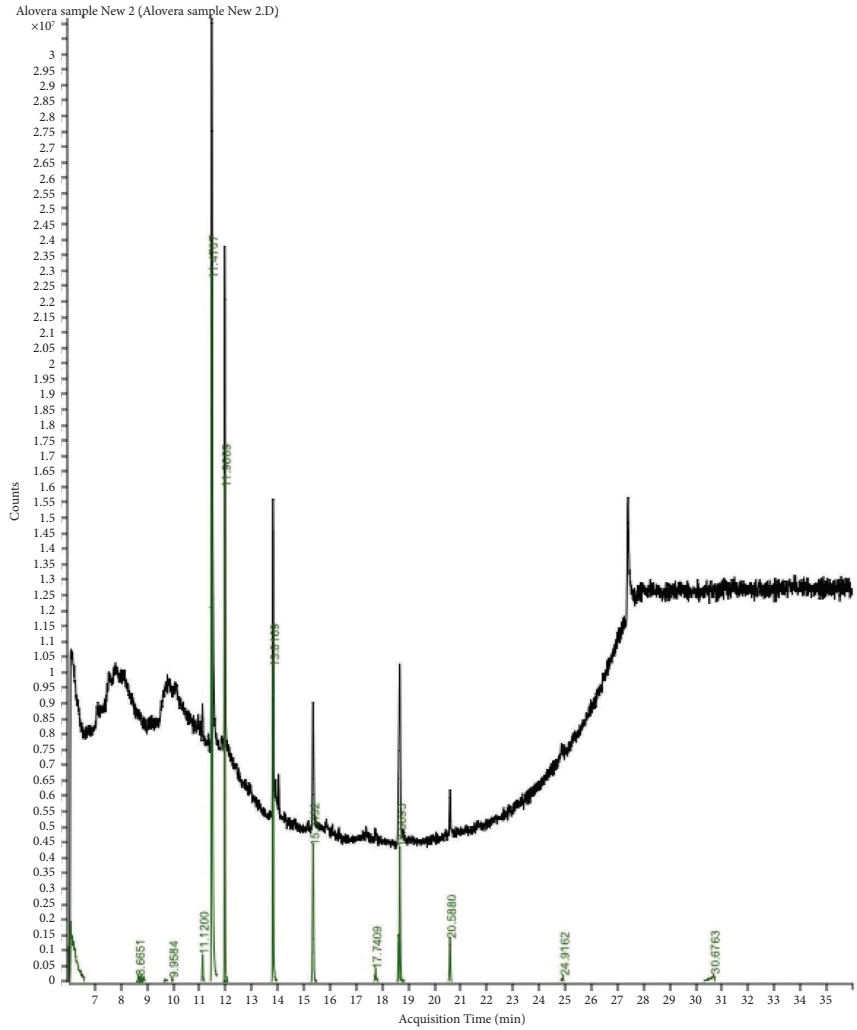

Figure 2: Continued.

Compound name	GCMS Analyses	Structure
Phthalic acid, di (2-propylpentyl) ester	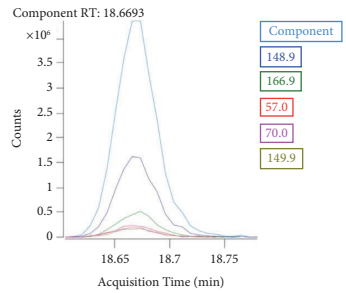	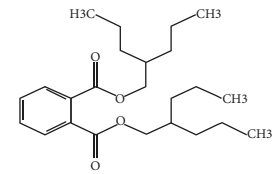
Hexadecanoic acid, ethyl ester	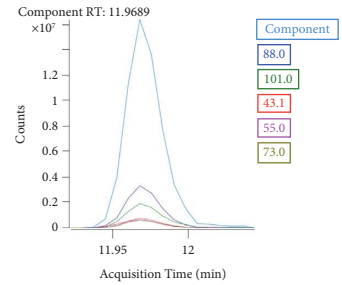	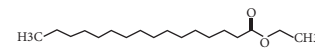
Lidocaine	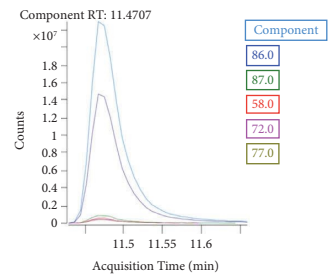	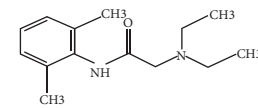
Tributyl acetylcirate	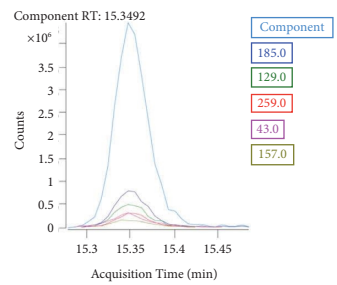	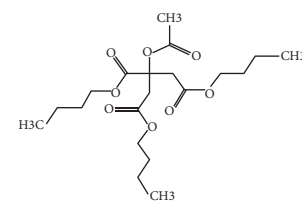
Ethyl Oleate	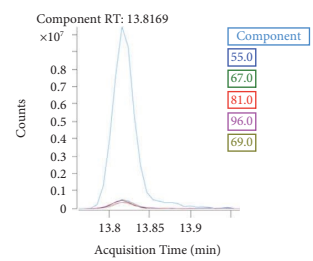	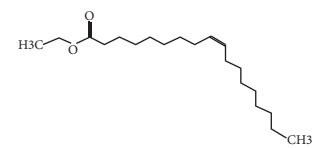

Figure 2: Continued.

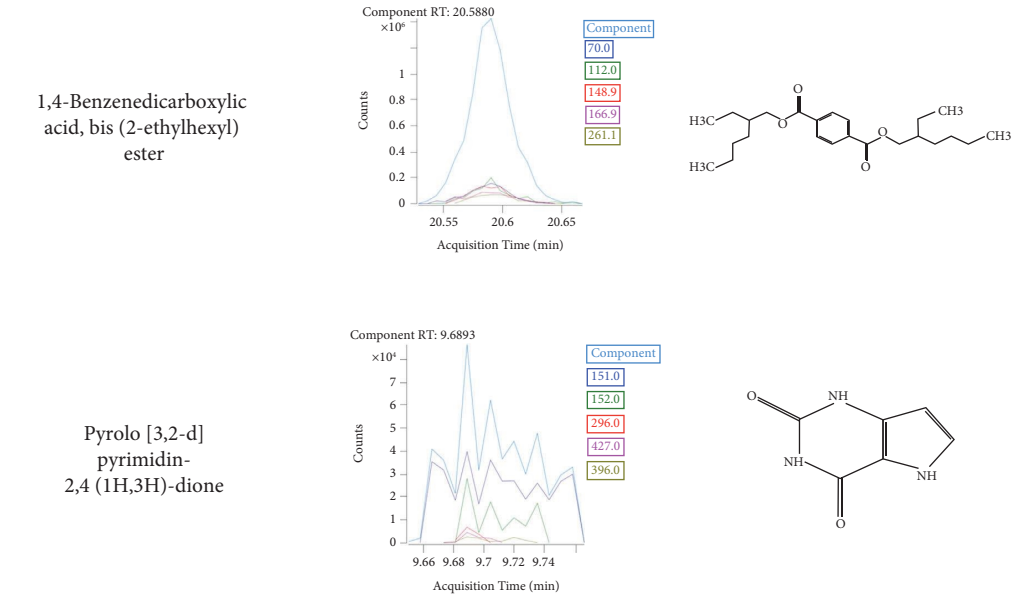

Figure 2: Active metabolites of *Aloe vera* ethanolic extract using GC–MS/MS. Base peak chromatogram of *Aloe vera* ethanolic extract (A) and identified secondary metabolites. A: The chromatogram obtained from the GCMS of O. *ficus-indica* ethanolic extract.

3.5. The Biological Activities of A. vera and O. ficus-Indica Compounds. GC–MS was conducted using the National Institute Standard and Technology (NIST) database. In total, 18 and 34 compounds were studied from *A. vera* and *O. ficus-indica*, respectively. Hexadecenoic acid, ethyl ester, found in extracts of both plants, has antioxidant, nematicide, hypocholesterolemic, pesticide, lubricant, antiandrogenic, flavor, and hemolytic activity [21–23]. Javahershenas and Khalafy [24] showed that pyrolo[3,2-d] pyrimidin-2,4(1H,3H)-dione has antimicrobial, antibacterial, antifungal, anti-inflammatory, antitumor, antioxidant, antiviral, anti-HIV, anti-asthmatic, and anticoagulant activity. Benzamide,2-methoxy-*N*-benzyl-*N*-phenethyl has antibacterial and antifungal activity [25, 26]. Phthalic acid, di(2-propylpentyl) ester, tributyl acetyl citrate, phthalic acid, di(oct-3-yl)ester, 1,2-benzenedicarboxylic acid, bis(2-methylpropyl)ester, and pyrrole,2-methyl-5-phenyl-, all have antimicrobial activity [27–31]. However, 2-fluoro-6-trifluoromethylbenzoic acid, 4-nitrophenyl ester is an acidifier and an arachidonic acid inhibitor, which increases aromatic amino acid decarboxylase activity, according to [32] (Tables 8 and 9).

4. Discussion

The present study aimed to evaluate the potential antimicrobial activity of *O. ficus-indica* and *Aloe vera* plants collected from Saudi Arabia. To our best knowledge, this is the first report of being tested on the selected microbial species from Saudi Arabia.

The results showed that *A. vera* extract has higher antifungal activity than the *O. ficus-indica* extract, as evidenced by the larger inhibition zone. The ethanolic extract of both plants had a significant effect on the microbes. The best results in terms of inhibition were observed against A. chevalieri and P. funiculosum were with *A. vera* ethanolic and aqueous extract, respectively. For *S. aureus* and *Shigella* sp., the best inhibition was observed with the aqueous extract, and for MRSA, this was with the ethanolic extract of *A. vera*.

The *O. ficus-indica* extract showed the best inhibition result with *T. funiculosus* using the ethanolic extract, while the aqueous extract showed insignificant effects against all fungi. The best inhibitory activity with both aqueous and ethanolic extract was observed for MRSA, followed by *Shigella* sp., and then *S. aureus* but only with the aqueous extract. *O. ficus-indica* has a stronger effect on bacteria than fungi, while *A. vera* has good effects on both fungi and bacteria. Both *S. aureus* and *B. subtilis* are significantly inhibited by *A. vera* gel extract [33]. Previous studies showed that the *A. vera* has a significant effect on *S. aureus* and *B. subtilis* and an insignificant effect on *A. ficuum* [34]. Ethanolic extract of *A. vera* had a greater inhibition zone than methanolic extract with *S. aureus*, *B. subtilis, E. coli*, and *S. typhimurium*. *A. vera* and *O. ficus-indica* ethanolic extracts had inhibitory effects on *E. coli*, *S. aureus*, *Acinetobacter*, and *S. epidermidis* with different concentrations [6]. Both plant extracts had a significant impact on the aforementioned bacteria [35]. Antimicrobial activity of the *O. ficus-indica* seeds oil against *C. albicans*, *E. coli*, *S. aureus*, *L. monocytogenes*, *P. aeruginosa*, *S. cerevisiae*, *and S. typhimurium* [36] showed that the oil extracts have high antimicrobial activity against Gram-positive and -negative bacteria.

The discovery of novel antimicrobial metabolites from medicinal plants such as *A. vera* and *O. ficus-indica* is an important alternative to overcome the increasing drug

Coppounds in *O. ficus-indica*			
Classes of compounds	Bioactive Compounds	MW	Molecular
Ketones	4-Hexen-2-one	98.14	$C_6H_{10}O$
Organosulfur	Thiophene, 3-methyl-	98.16	$CH_3C_4H_3S$
long-chain fatty acid ethyl ester	Phthalic acid, di (oct-3-yl) ester	418.6	$C_{24}H_{38}O_4$
Polyphenols	4-Methyl-2,4-bis (p-hydroxyphenyl)pent-1-ene, 2TMS derivative	268.3	$C_{18}H_{20}O_2$
long-chain fatty acid ethyl ester	Phthalic acid, bis (2-pentyl) ester	306.4	$C_{20}H_{30}O_4$
long-chain fatty acid ethyl ester	Hexadecanoic acid, ethyl ester	284.4	$C_{18}H_{36}O_2$
Anorectic	Benzphetamine	239.3	$C_{17}H_{21}N$
Plasticizers	Bis (2-ethylhexyl) phthalate	390.5	$C_{24}H_{38}O_4$
Fatty acid	2-Aminohydratropic acid	165.19	$C_9H_{11}NO_2$
Local anaesthetic	Tolycaine	278.35	$C_{15}H_{22}N_2O_3$
Hydrocarbons	1,3-Pentadiyne, 1,5,5,5-tetrafluoro-	136.05	C_5F_4
Amino acids derivative	l-Alanine, n-propargyloxycarbonyl-, ethylester	199.20	$C_9H_{13}NO_4$
long-chain fatty acid ethyl ester	Phthalic acid, butyl hexyl ester	306.3	$C_{18}H_{26}O_4$
polyhenols	1- (Benzyloxy)-3,5-dinitrobenzene	274.2	$C_{13}H_{10}N_2O_5$
Hydrocarbons	2-Butynedinitrile	76	C_4N_2
Aldehyde	2-Propanol, 1,3-dibromo	217.89	$C_3H_6Br_2O$
Aliphatic amine	3-Amino-2,4-dimethylpentane	115.22	$C_7H_{17}N$
Polyphenols	Phenol, 5-ethenyl-2-methoxy-	150.17	$C_9H_{10}O_2$
Ketone	1-Penten-3-one	84	C_5H_8O
Terpenes	Silane, dimethyl (4-methoxyphenoxy)heptadecyloxy-	436.7	$C_{26}H_{48}O_3Si$
Pyrimidines	5-Pyrimidinol, 2-methyl-	94	$C_5H_6N_2$
Amino acids derivative	Alanine, N-methyl-n-propoxycarbonyl-, nonyl ester	259.34	$C_{13}H_{25}NO_4$
polyphenols	Acetic acid, (4-chloro-2-methylphenoxy)-, heptadecylester	439	$C_{26}H_{43}ClO_3$
Pyridines	Pyridine, 3-propyl-	121	$C_8H_{11}N$
polyphenols	Phenol, 5-ethenyl-2-methoxy-	150	$C_9H_{10}O_2$

Figure 3: The various compounds found in *O. ficus-indica*.

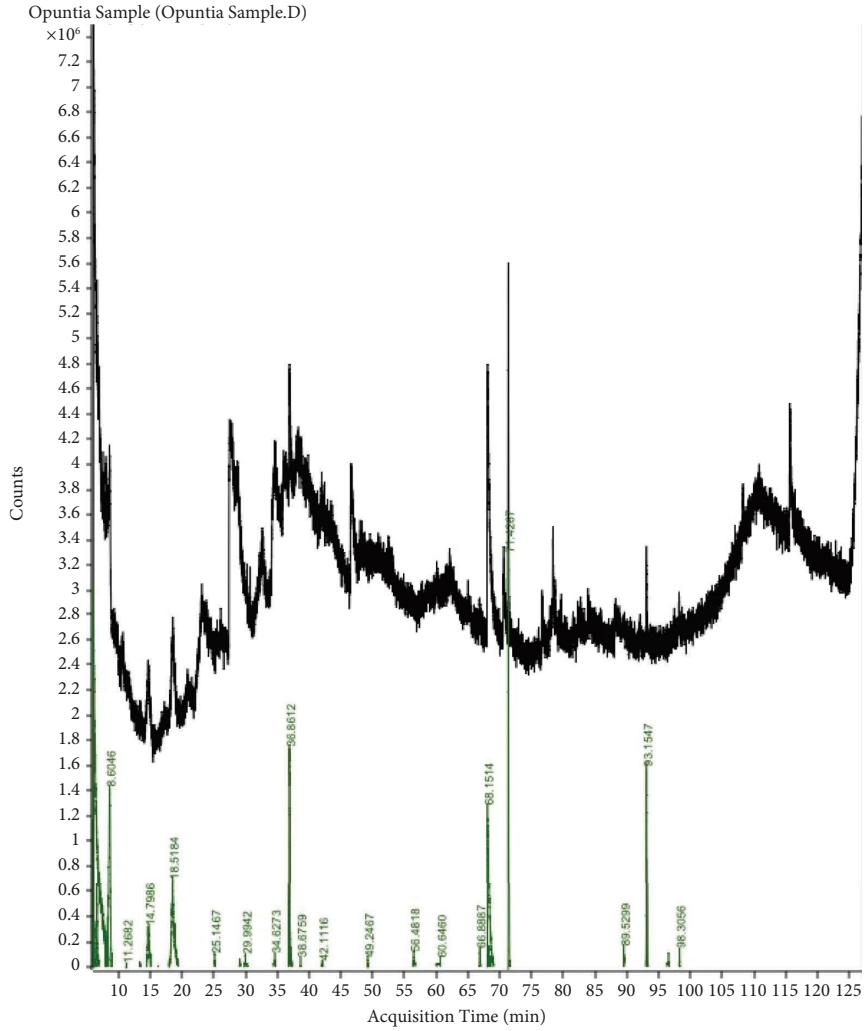

Figure 4: Continued.

Compound name	GC MS Analyses	Structure
1-(Benzyloxy)-3,5-dinitrobenzene	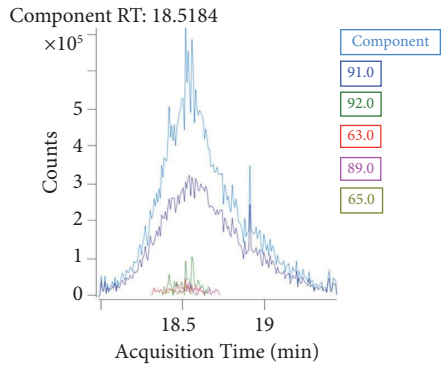	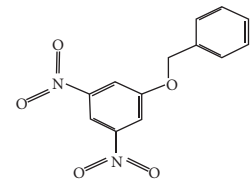
Hexadecanoic acid, ethyl ester	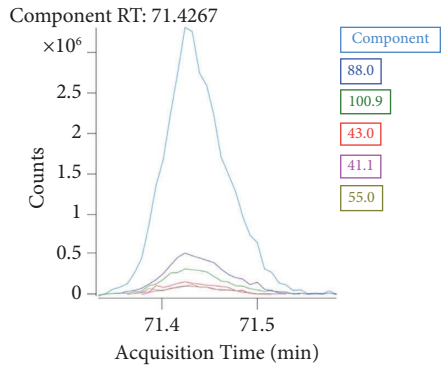	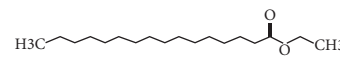
Phenol, 5-ethenyl-2-methoxy-	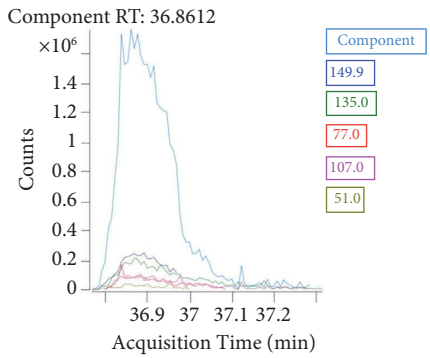	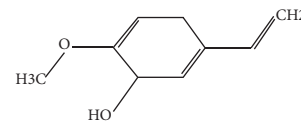
1,3-Pentadiyne, 1,5,5,5-tetrafluoro-	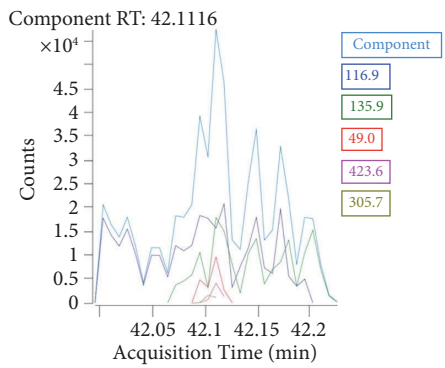	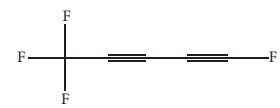

Figure 4: Continued.

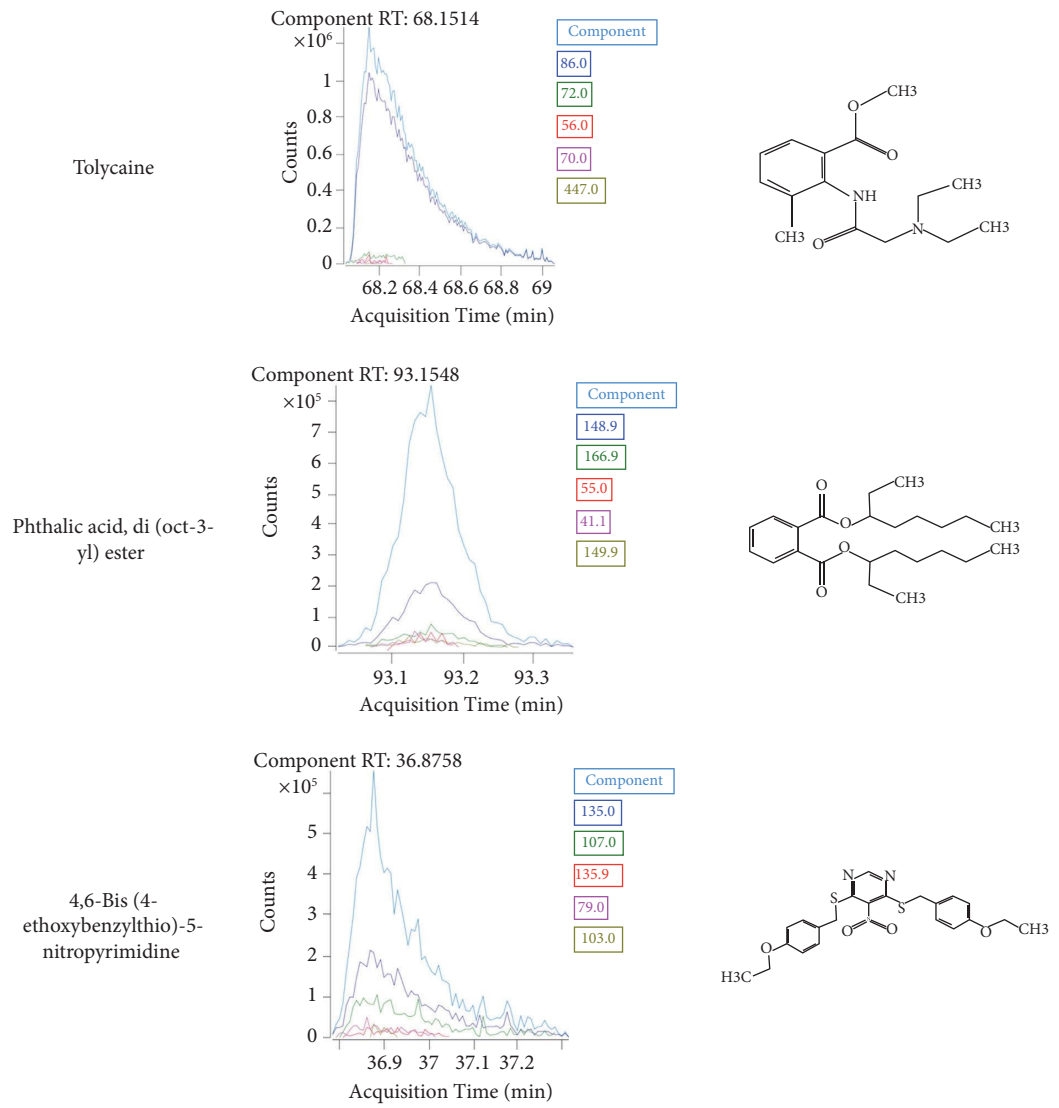

Figure 4: Active metabolites in *O. ficus-indica* extract identified by GC–MS. Base peak chromatogram of *O. ficus-indica* methanolic extract (A) and identified secondary metabolites. A: The GCMS chromatogram of the A. vera ethanolic extract.

Table 8: Biological activities of *A. vera* compounds.

No	RT	Compound	Match factor	Biological activity
1	18.6693	Phthalic acid, di(2-propylpentyl) ester	92.4	Antimicrobial [30]
2	11.9689	Hexadecanoic acid, ethyl ester	91.8	Antioxidant, nematicide, hypocholesterolemic, pesticide, luubricant, antiandrogenic, flavor, hemolytic [22, 23]
3	11.4707	Lidocaine	89.4	Anaesthetic, antiarrhythmic (DrugBank accession number DB00281)
4	15.3492	Tributyl acetylcitrate	88.1	Anticancer, antimicrobial activity [28]
5	9.6893	Pyrolo[3,2-d]pyrimidin-2,4(1H,3H)-dione	77.3	Antimicrobial, antibacterial, antifungal, anti-inflammatory, antitumor, antioxidant, antiviral, anti-HIV agents, antiasthmatic, anticoagulant. [24]
6	30.6763	2-Fluoro-6-trifluoromethylbenzoic acid, 4-nitrophenyl ester	71.2	Acidifier, arachidonic acid inhibitor, increase aromatic amino acid decarboxylase activity [32]
7	11.1200	1,2-Benzenedicarboxylic acid, bis(2-methylpropyl) ester	71.2	Antimicrobial, α-Glucosidase inhibition, and the in vivo hypoglycemic effect. [29]
9	8.8667	Pyrrole, 2-methyl-5-phenyl-	66.0	Antimicrobial, inti-inflammatory, antitumor [27]
10	24.9162	Benzamide, 2-methoxy-*N*-benzyl-*N*-phenethyl	65.6	Antifungal and antibacterial. [26]

Table 9: Biological activities of *O. ficus-indica* compounds.

No	RT	Compound	Match factor	Biological activity
1	71.4267	Hexadecanoic acid, ethyl ester	80.6	Antioxidant, nematicide, hypocholesterolemc, pesticide, lubricant, antiandrogenic, flavor, and hemolytic [22, 23]
2	68.1514	Tolycaine	78.8	Reduce the pain of injection, use in dental injection. (DrugBank)
3	93.1548	Phthalic acid, di(oct-3-yl) ester	72.1	Antimicrobial and antifouling. [31]
4	93.1547	Bis(2-ethylhexyl) phthalate	67.1	Antibacterial and antifungal agent. [25, 28]

resistance in humans. The plant extracts with known antimicrobial properties can be of great importance for therapeutic treatments. *O. ficus-indica* has been used traditionally for controlling many different pathogenic bacterial infections [37].

Endophytic fungi isolated from *A. vera* (*Penicillium* sp., *Aspergillus* sp., and *F. oxysporum*) showed a moderate inhibition zone when treated with methanol extract [38]. The *A. vera* extracts showed antibacterial activity against both Gram-positive and -negative isolates, while the leaf extracts did not show any such activity [4]. Ethanolic extract of *A. vera* inhibited the growth of *E. coli*, *S. aureus*, and *C. albicans* with zones of inhibition of 6, 5, and 4 mm, respectively, while aqueous extract had zones of inhibition of 6, 4, and 3 mm, respectively [7]. The methanolic extract of *A. vera* inhibited the growth of *E. coli* (3 mm) only.

A. vera extracts showed greater antibacterial activity against Gram-positive bacteria as compared to Gram-negative bacteria [6]. With respect to individual pathogens, the ethanolic extract showed greater inhibition than the methanolic extract, while significantly lower inhibition was observed with acetone extract. *A. vera* distilled extract was effective against *P. aeruginosa* [5]. *A. vera* sterol extract had great antifungal activity against *A. niger*, *A. terreus*, and *Penicillium* sp. and antibacterial activity against *S. aureus*, *E. coli*, and *S. typhimurium* [39]. *A. vera* extract has antimicrobial activity against *S. aureus*, *E. coli*, and *Shigella* [40]. Both *A. barbadensis* juice and gel inhibited the growth of *C. albicans*, *E. coli* and *P. fluorescens* better than that of *A. arborescens* [41].

A. vera extracts showed low antifungal activity against the *Aspergillus* and *Penicillium* strains and strong activity against the *Alternaria spp2* strain [42]. The cactus pear fruit (*O. ficus-indica)* extracts clearly showed positive action against the bacterial and fungal species [43]. However, the extract did not show any activity against *A. niger* for more than 2 days, unlike *C. albicans*, which can resist the inhibitory activity of the extract for periods longer than 2 days. Good antibacterial activity of the *O. ficus-indica* skin fruit extracts has been revealed against both Gram-positive and Gram-negative bacterial isolates [44]. However, the extraction of *A. vera* showed low antifungal activity on the *Aspergillus* strains and *Penicillium* strains and strong activity against the *Alternaria spp2* strain [42]. *A. niger* showed a large inhibition zone with the alcohol and aqueous extracts of *A. vera*, and no zone was observed with *C. albicans* [45].

GC–MS was conducted using the National Institute Standard and Technology (NIST) database. The spectrum of the unknown components was compared with the spectrum of the known components stored in the NIST library. The essential oil composition of the skin, pulp, and seeds from the *O. ficus-indica* fruits was analyzed by hydrodistillation (HD) followed by gas chromatography–mass spectrometry (GC–MS) to investigate the compounds in processed fruit [20]. Prickly pear has a high bioactive potential, being an important source of bioactive compounds and an excellent source of dietary antioxidants [46]. The antioxidant and antimicrobial compounds highlight the importance of *O. ficus-indica* as a crop [20]. Twelve compounds were identified from *A. vera*, including hexadecenoic acid, octadecanoic acid, tricosane, 1-octadecanol, and trace amounts of sterols [39]. The ethanolic and aqueous extracts of the bagasse (byproducts of *A. vera* processing leaves) have shown antioxidant and antifungal activity [47].

The antioxidant properties of *A. vera* flowers could have an important application in the food industry, providing an income for farmers if the flowers are considered as a byproduct rather than a residue. Natural products with antioxidant properties have been extensively utilized as health-promoting products and natural additives in the food industry [48]. *A. vera* compounds have anticancer and antimicrobial activity [19].

We investigated the activity of 18 and 34 compounds from *A. vera* and *O. ficus-indica*, respectively. The studied compounds showed biological activity similar to the results reported earlier, with similar antioxidant, antifungal, antibacterial, antiviral, and anti-inflammatory properties. These plants may offer a new source of antibacterial and antifungal agents with significant activity against infective microorganisms [3]. However, our results should be verified through further investigations on the antimicrobial activity of these cacti-like plants and other aspects. Based on the results obtained in this research, those types of polyphenols compounds obtained in *A. vera* and *O. ficus-indica* may be a potential target in the future to explore antifungal and microbial benefits for humanity.

5. Conclusions

Extracts from cacti and cacti-like plants possess antifungal and antibacterial activity against various pathogens. These extracts can be used as natural alternatives to synthetic antifungal treatments in fungi management. GC–MS clearly shows more polyphenols in *A. vera* extract as phthalic acid di(2-propylpentyl) ester and hexadecenoic acid ethyl ester, and 1-(benzyloxy)-3,5-dinitrobenzene and phenol, 5-ethenyl-2-methoxy in the *O. ficus-indica* extract. These compounds have a biological activity such as antimicrobial and antioxidant, which means that these plant extracts can be used in

medical and cosmetic products against fungi and bacteria. In the future study, we would like to use the HPLC for both plant extracts and study the phenol, flavonoids, and alkaloids compounds.

Abbreviations

NC-endophytes:	Nonclavicipitaceous endophytes
C-endophytes:	Clavicipitaceous endophytes
DSE:	Dark septate endophytes'
WHO:	World Health Organization
MRSA:	Methicillin-resistant *Staphylococcus aureus*
GC-MS:	Gas chromatography-mass spectrometry
PDA:	Potato dextrose agar
PDB:	Potato dextrose broth
EDTA:	Ethylenediamine tetracetic acid
Tris:	(Hydroxymethyl) aminomethane
TAE:	(Tris-acetate-EDTA) buffer
NaCl:	Sodium chloride
BLAST:	Basic local alignment search tool
PCR:	Polymerase chain reaction
ITS:	Internal transcribed spacer
UV:	Ultraviolet
NCBI:	National Center for Biotechnology Information
CF:	Colonization frequency
NIST:	National Institute Standard and Technology
HD:	Hydro distillation.

Data Availability

All datasets generated or analyzed during this study are included in this article.

Conflicts of Interest

The authors declare that there are no conflicts of interest.

Authors' Contributions

All authors have made substantial, direct, and intellectual contribution to the work and approved it for publication.

References

[1] J. D. Mauseth, *Botany: An Introduction To Plant Biology*, Jones & Bartlett Learning, Burlington, MA, USA, 2019.

[2] T. S. Suryanarayanan, S. K. Wittlinger, and S. H. Faeth, "Endophytic fungi associated with cacti in Arizona," *Mycological Research*, vol. 109, no. 5, pp. 635–639, 2005.

[3] S. Pooja and G. Vidyasagar, "Antimicrobial activity of opuntia cochenillifera (L.) mill fruit and cladode extracts," *International Journal of Pharmacology, Phytochemistry and Ethnomedicine*, vol. 84, 2016.

[4] A. Bashir, B. Saeed, T. Y. Mujahid, and N. Jehan, "Comparative study of antimicrobial activities of Aloe vera extracts and antibiotics against isolates from skin infections," *African Journal of Biotechnology*, vol. 10, no. 19, pp. 3835–3840, 2011.

[5] D. Gharibi, M. Khosravi, Z. Hosseini, F. Boroun, S. K. Barzgar, and A. Forughi Far, "Antibacterial effects of aloe vera extracts on some human and animal bacterial pathogens," *Journal of Medical Microbiology and Infectious Diseases*, vol. 3, no. 1, pp. 6–10, 2015.

[6] R. Lawrence, P. Tripathi, and E. Jeyakumar, "Isolation, purification and evaluation of antibacterial agents from Aloe vera," *Brazilian Journal of Microbiology*, vol. 40, no. 4, pp. 906–915, 2009.

[7] M. C. Stanley, O. E. Ifeanyi, and O. G. Eziokwu, "Antimicrobial effects of Aloe vera on some human pathogens," *International Journal of Current Microbiology and Applied Sciences*, vol. 3, no. 3, pp. 1022–1028, 2014.

[8] J.-L. Rios and M. C. Recio, "Medicinal plants and antimicrobial activity," *Journal of Ethnopharmacology*, vol. 100, no. 1-2, pp. 80–84, 2005.

[9] O. Rosca-Casian, M. Parvu, L. Vlase, and M. Tamas, "Antifungal activity of Aloe vera leaves," *Fitoterapia*, vol. 78, no. 3, pp. 219–222, 2007.

[10] A. F. Silva-Hughes, D. E. Wedge, C. L. Cantrell et al., "Diversity and antifungal activity of the endophytic fungi associated with the native medicinal cactus Opuntia humifusa (Cactaceae) from the United States," *Microbiological Research*, vol. 175, pp. 67–77, 2015.

[11] A. Surjushe, R. Vasani, and D. Saple, "Aloe vera: a short review," *Indian Journal of Dermatology*, vol. 53, no. 4, pp. 163–166, 2008.

[12] S. Jain, N. Rathod, R. Nagi et al., "Antibacterial effect of Aloe vera gel against oral pathogens: an in-vitro study," *Journal of Clinical and Diagnostic Research: Journal of Clinical and Diagnostic Research*, vol. 10, no. 11, pp. ZC41–ZC44, 2016.

[13] S. Irshad and M. Butt, "In-vitro Antibacterial Activity of Aloe Barbadensis Miller (Aloe Vera)," *International research journal of pharmaceuticals*, vol. 1, no. 2, pp. 59–64, 2011.

[14] S. Arbab, H. Ullah, W. Weiwei et al., "Comparative study of antimicrobial action of aloe vera and antibiotics against different bacterial isolates from skin infection," *Veterinary Medicine and Science*, vol. 7, no. 5, pp. 2061–2067, 2021.

[15] R. Pourmajed, M. Jabbari Amiri, P. Karami, and A. Khaledi, "Antimicrobial effect of opuntia ficus-indica extract on Escherichia coli isolated from patients with urinary tract infection," *Iranian Journal of Public Health*, vol. 50, no. 3, pp. 634–636, 2021.

[16] M. Mulik and M. Phale, "Extraction, purification and identification of aloe gel from Aloe vera (Aloe barbadensis Miller)," *Journal of Natural Products*, vol. 5, no. 3, pp. 111–115, 2009.

[17] V. B. M Shilpa, A. V. Shetty, M. S. R. Reddy, and P. Pund, "Antifungal activity of aloe vera leaf and gel extracts against Candida albicans: an in vitro study," *World Journal of Dentistry*, vol. 11, no. 1, pp. 36–40, 2020.

[18] S. Mushtaq, A. Ali, I. Khokhar, and I. Mukhtar, "Antagonisitic potential of soil bacteria against food borne fungi," *World Applied Sciences Journal*, vol. 11, no. 8, pp. 966–969, 2010.

[19] M. Saljooghianpour and T. A. Javaran, "Identification of phytochemical components of aloe plantlets by gas chromatography-mass spectrometry," *African Journal of Biotechnology*, vol. 12, no. 49, pp. 6876–6880, 2013.

[20] P. Zito, M. Sajeva, M. Bruno, S. Rosselli, A. Maggio, and F. Senatore, "Essential oils composition of two Sicilian cultivars of Opuntia ficus-indica (L.) Mill.(Cactaceae) fruits (prickly pear)," *Natural Product Research*, vol. 27, no. 14, pp. 1305–1314, 2013.

[21] P. Lakshmi and P. Rajalakshmi, "Identification of phyto components and its biological activities of aloe vera through

the gas chromatography-mass spectrometry," *International Research Journal of Pharmacy*, vol. 2, no. 5, pp. 247–249, 2011.

[22] B. Parthipan, M. Suky, and V. Mohan, "GC-MS analysis of phytocomponents in pleiospermium alatum (wall. Ex wight & arn.) swingle,(rutaceae)," *Journal of Pharmacognosy and Phytochemistry*, vol. 4, no. 1, 2015.

[23] T. Tyagi and M. Agarwal, "Phytochemical screening and GC-MS analysis of bioactive constituents in the ethanolic extract of Pistia stratiotes L. and Eichhornia crassipes (Mart.) solms," *Journal of Pharmacognosy and Phytochemistry*, vol. 6, no. 1, pp. 195–206, 2017.

[24] R. Javahershenas and J. Khalafy, "A new synthesis of pyrrolo [3, 2-d] pyrimidine derivatives by a one-pot, three-component reaction in the presence of L-proline as an organocatalyst," *Heterocyclic Communications*, vol. 24, no. 1, pp. 37–41, 2018.

[25] M. A. A. Al-Bari, M. S. A. Bhuiyan, M. E. Flores, P. Petrosyan, M. García-Varela, and M. A. U. Islam, "Streptomyces bangladeshensis sp. nov., isolated from soil, which produces bis-(2-ethylhexyl) phthalate," *International Journal of Systematic and Evolutionary Microbiology*, vol. 55, no. 5, pp. 1973–1977, 2005.

[26] T. Belz, S. Ihmaid, J. Al-Rawi, and S. Petrovski, "Synthesis characterization and antibacterial, antifungal activity of N-(benzyl carbamoyl or carbamothioyl)-2-hydroxy substituted benzamide and 2-benzyl amino-substituted benzoxazines," *International journal of medicinal chemistry*, vol. 2013, Article ID 436397, 20 pages, 2013.

[27] V. Bhardwaj, D. Gumber, V. Abbot, S. Dhiman, and P. Sharma, "Pyrrole: a resourceful small molecule in key medicinal hetero-aromatics," *RSC Advances*, vol. 5, no. 20, pp. 15233–15266, 2015.

[28] N. Binh, P. Lam, and C. Diep, "Bioactive compounds from marine fungus Penicillium citrinum strain nd7c by gas chromatographymass spectrometry," *Pharmaceutical Chemistry Journal*, vol. 5, no. 1, pp. 211–224, 2018.

[29] M. P. S. Govindappa, V. Vinay, and R. Channabasava, "Chemial composition of methanol etract of endophytic fungi, Alternaria sp. of tebebuia argentea and their antimicrobial and antioxidant activity," *International Journal of Biological & Pharmaceutical Research*, vol. 5, no. 11, pp. 861–869, 2014.

[30] O. Osuntokun and G. Cristina, "Bio isolation, chemical purification, identification, antimicrobial and synergistic efficacy of extracted essential oils from stem bark extract of Spondias mombin(Linn)," *International Journal of Molecular Biology*, vol. 4, no. 4, pp. 135–143, 2019.

[31] J. Rani and M. Kapoor, "Gas chromatography-mass spectrometric analysis and identification of bioactive constituents of Catharanthus roseus and its antioxidant activity," *Asian Journal of Pharmaceutical and Clinical Research*, vol. 12, no. 3, pp. 461–465, 2019.

[32] M. H. Kumar, K. Prabhu, M. R. K. Rao et al., "The GC MS study of one ayurvedic medicine, vasakadyaristam," *Research Journal of Pharmacy and Technology*, vol. 12, no. 2, p. 569, 2019.

[33] G. Yebpella, H. M. M. Adeyemi, C. Hammuel, A. Magomya, A. Agbaji, and E. Okonkwo, "Phtyochemical screening and comparative study of antimicrobial activity of Aloe vera various extracts," *African Journal of Microbiology Research*, vol. 5, no. 10, pp. 1182–1187, 2011.

[34] K. Shahzad, R. Ahmad, S. Nawaz, S. Saeed, and Z. Iqbal, "Comparative antimicrobial activity of Aloe vera gel on microorganisms of public health significance," *Pharmacologyonline*, vol. 1, pp. 416–423, 2009.

[35] L. Q. yaseen, S. H. Nayyef, N. I. Salih, and M. A. Mustafa, "Antimicrobial activity of aloe vera and opuntia Ficus extract against certain pathogenic bacteria," *European Journal of Molecular & Clinical Medicine*, vol. 7, no. 9, pp. 422–428, 2020.

[36] E. Ramírez-Moreno, R. Cariño-Cortés, N. D. S. Cruz-Cansino et al., "Antioxidant and antimicrobial properties of cactus pear (Opuntia) seed oils," *Journal of Food Quality*, vol. 2017, Article ID 3075907, 8 pages, 2017.

[37] J. M. Feugang, P. Konarski, D. Zou, F. C. Stintzing, and C. Zou, "Nutritional and medicinal use of Cactus pear (Opuntia spp.) cladodes and fruits," *Frontiers in Bioscience*, vol. 11, no. 1, pp. 2574–2589, 2006.

[38] A. B. Gangurde, P. R. Jagtap, M. A. Vyawahare, G. P. Kukreja, and R. S. Mane, "Production, purification and evaluation of different functional groups from endophytic Penicillium species derived bioactive compounds isolated from Aloe vera," *International journal of chemical studies*, vol. 3, no. 2, pp. 35–38, 2019.

[39] R. Bawankar, V. Deepti, P. Singh, R. Subashkumar, G. Vivekanandhan, and S. Babu, "Evaluation of bioactive potential of an Aloe vera sterol extract," *Phytotherapy Research*, vol. 27, no. 6, pp. 864–868, 2013.

[40] F. Nejatzadeh-Barandozi, "Antibacterial activities and antioxidant capacity of Aloe vera," *Organic and medicinal chemistry letters*, vol. 3, no. 1, pp. 5–8, 2013.

[41] K. Kupnik, M. Primožič, Ž. Knez, and M. Leitgeb, "Antimicrobial efficiency of aloe arborescens and aloe barbadensis natural and commercial products," *Plants*, vol. 10, no. 1, p. 92, 2021.

[42] I. Laib, F. Boubrik, and M. Barkat, "Optimization of the extraction parameters of Aloe Vera polyphenols and study of antioxidant and antifungal activities: application to molds isolated from durum wheat," *Acta Scientifica Naturalis*, vol. 6, no. 1, pp. 79–90, 2019.

[43] A. Bargougui, H. Maatoug Tag, M. Bouaziz, and S. Triki, "Antimicrobial, antioxidant, total phenols and flavonoids content of four cactus (Opuntia ficus-indica) cultivars," *Biomedical & Pharmacology Journal*, vol. 12, no. 3, pp. 1353–1368, 2019.

[44] G. Welegerima and A. Zemene, "Antibacterial activity of Opuntia ficus-indica skin fruit extracts," *Biotechnology International*, vol. 10, pp. 74–83, 2017.

[45] J. Saniasiay, R. Salim, I. Mohamad, and A. Harun, "Antifungal effect of Malaysian Aloe vera leaf extract on selected fungal species of pathogenic otomycosis species in in vitro culture medium," *Oman Medical Journal*, vol. 32, no. 1, pp. 41–46, 2017.

[46] M. A. Silva, T. G. Albuquerque, P. Pereira et al., "Opuntia ficus-indica (L.) mill.: a multi-benefit potential to Be exploited," *Molecules*, vol. 26, no. 4, p. 951, 2021.

[47] M. L. Flores-López, A. Romaní, M. A. Cerqueira, R. Rodríguez-García, D. Jasso de Rodríguez, and A. A. Vicente, "Compositional features and bioactive properties of whole fraction from Aloe vera processing," *Industrial Crops and Products*, vol. 91, pp. 179–185, 2016.

[48] A. Martínez-Sánchez, M. E. López-Cañavate, J. Guirao-Martínez, M. J. Roca, and E. Aguayo, "Aloe vera flowers, a byproduct with great potential and wide application, depending on maturity stage," *Foods*, vol. 9, no. 11, p. 1542, 2020.

Hindawi
Journal of Chemistry
Volume 2023, Article ID 6111058, 11 pages
https://doi.org/10.1155/2023/6111058

Research Article

Phytoconstituent Isolation and Cytotoxicity Evaluation of the Egyptian *Cassia occidentalis* L. Possessing Selective Activity against Lung Carcinoma

Hanaa M. Sayed,[1] Mahmoud A. Ramadan,[1] Heba H. Salem,[2] and Marwa A. A. Fayed[3]

[1]*Department of Pharmacognosy, Faculty of Pharmacy, Assiut University, Assiut 71526, Egypt*
[2]*Department of Pharmacognosy, Faculty of Pharmacy, Northern Border University, Rafha Region, Arar, Saudi Arabia*
[3]*Department of Pharmacognosy, Faculty of Pharmacy, University of Sadat City, Sadat City 32897, Egypt*

Correspondence should be addressed to Marwa A. A. Fayed; marwa.fayed@fop.usc.edu.eg

Received 24 August 2022; Revised 22 November 2022; Accepted 20 March 2023; Published 8 April 2023

Academic Editor: Ashanul Haque

Ethyl acetate fraction column chromatographic analysis was used to isolate eleven compounds (numerically tagged 1–10) from *Cassia occidentalis* L. in this study. Two unique metabolites, including a neolignan compound designated as occidentalignan I (9) and a flavonoidal glycoside, chrysin-7-O-α-L-rhamnopyranosyl (10), were identified, while silybin A (8) was the first flavonolignan to be isolated from the Fabaceae family. Four compounds, including β-sitosterol-3-*O*-β-D-glucopyranoside (1), stigmasterol-3-*O*-β-D-glucopyranoside (2), betulinic acid (3), and vanillic acid (4) were isolated from *C. occidentalis* for the first time. In addition, four known compounds, cinnamic acid (5), p-hydroxybenzoic acid (6), β- resorcylic acid (7), and citric acid (11), were also detected. The *in-vitro* cytotoxicity assessment of the methanolic extract of *C. occidentalis* on seven cancer cell lines, including A-549, Colo-205, Huh-7, HCT-116, PANC-1, SKOV-3, and BNL, demonstrated its selective potent cytotoxicity on lung cancer cells without affecting normal BNL cells. In contrast, the methanolic extract showed moderate activity on Colo-205 and Huh-7 and nearly no activity on HCT-116, PANC-1, and SKOV-3 cell lines. These results suggest that the methanolic extract of *C. occidentalis* is an excellent candidate with potential antiproliferative activity against lung cancer; however, further studies are necessary to clarify its mechanism of action.

1. Introduction

Cancer treatment remains a significant healthcare challenge that constantly necessitates the discovery of new therapeutic candidates. Numerous synthetic cancer medications are currently available; however, the majority exhibit fatal drawbacks to normal healthy cells, such as cell toxicity, genotoxicity, carcinogenicity, and teratogenic effects [1]. Thus, despite their high efficiency in targeted cancer cell treatments, the adverse effects of these available agents limit their use as synthetic chemotherapeutics. Consequently, there is an urgency to discover new sources for safe anticancer agents with selective activity on cancer cells and without harmful effects on normal cells. Nature is a rich source of highly effective therapeutic agents with the capacity to treat several deadly ailments at very low toxicity margins.

C. occidentalis L. is a pharmacologically significant herb and a candidate with crucial anticarcinogenic properties. The herb belongs to the family Fabaceae (Leguminosae), and its different tissues have been used in folk medicine. *C. occidentalis* is native to the western hemisphere, principally South and Central America, and was introduced to India and China and then to African countries, such as Egypt and Libya [2, 3]. The extract of the whole plant has been used ethnomedicinally to cure eye inflammation, while it is extensively used in Jamaica to treat various diseases, such as eczema, constipation, diarrhea, venereal diseases, fever, dysentery, and cancer [4]. Infusions of *C. occidentalis* roots have been used for stomach pain, whereas uses in veterinary

medicine as antidotes for animal treatments have been reported. In addition, boiled *C. occidentalis* roots are used to treat constipation, whooping cough, and lactogogue [5], while its decoction mixed with black pepper is used in the treatment of filarial disease [6]. In Brazil, the roots are also used as a tonic, antidiuretic, and febrifuge and in the treatment of liver diseases, anemia, fever, and tuberculosis [7].

C. occidentalis L. leaves have been used topically as a paste for the treatment of wounds, cutaneous diseases, sores, bone fractures, ringworms, fever, and throat infections, while their extracts have also been shown to pharmacologically possess antibacterial, antimalarial, antimutagenic [8–10], immunosuppressive [11], anticarcinogenic, and hepatoprotective activities [10, 12, 13]. Other uses, such as anti-inflammatory, antidermatophyte, antibacterial, antiplasmodial, antifertility, antimalarial, and antidiabetic activities, as well as its capacity to repair, protect, and normalize liver functions have been reported [10, 14].

Previous studies on *Cassia* species reported the isolation and identification of a wide range of secondary metabolites with numerous biological potentials. Consequently, this study explored *C. occidentalis* with an aim to elucidate its phytochemical and biological properties and to extensively demonstrate evidence of its usage in various pharmaceutical products.

2. Methods and Materials

2.1. Ethical Statement. All experiments and procedures were performed by following the relevant guidelines and regulations of the Faculty of Pharmacy, Assiut University, Assiut, Egypt.

2.2. General Experimental Procedures. Infrared (IR) spectra were recorded on a Shimadzu Infrared-400 spectrometer (Kyoto, Japan) and ultraviolet (UV) spectra were obtained on a Shimadzu 1601 UV/VIS spectrophotometer. Nuclear magnetic resonance spectroscopy (NMR) spectra were obtained on a Bruker Avance III 400 spectrometer using precoated silica gel 60 F_{254} TLC (0.25 mm, Merck, Germany) and RP-18 F_{254} plates (0.25 mm, Merck, Germany). In electron-ionization mass spectrometry (EIMS), measurements were obtained on a Bruker, Mass DIP meth-mass spectrometer.

2.3. Plant Material. The whole aerial flowering parts of *C. occidentalis* were collected between April and July 2014, from plants cultivated at the Experimental Station, Faculty of Pharmacy, Assiut University, Assiut, Egypt. The plant was identified by Dr. A. A. Fayed, Prof. of Plant Taxonomy, Faculty of Science, Assiut University, Assiut, Egypt. A voucher sample was kept in the Herbarium of the Pharmacognosy Department, Faculty of Pharmacy, Assiut University, Assiut, Egypt.

2.4. Extraction and Fractionation. The air-dried powdered samples from whole aerial flowering parts (3 kg) of *C. occidentalis* L. were extracted by maceration in 70% methanol (10 L × 4). The alcoholic extract was concentrated, and 350 g of the solvent-free residue (11.7%) was mixed with 500 mL of distilled water and then was subjected to successive solvent fractionation with *n*-hexane, chloroform, ethyl acetate, and *n*-butanol till complete exhaustion, followed by extract storage in a vacuum desiccator until use. After monitoring all fractions with TLC using different solvent systems and spraying with different reagents, the ethyl acetate fraction was selected for column chromatographic isolation of compounds as it contained several different compounds of important chemical classes with vital biological functions, such as flavonoids and phenolics.

2.5. Phytochemical Studies

2.5.1. Column Chromatographic Separations. The ethyl acetate fraction (40 g) was subjected to vacuum liquid chromatography with chloroform-methanol gradient elution. Five subfractions labeled as COEt-I-COEt-V.Subfraction COEt-II (7.5 g) were rechromatographed on silica gel column chromatography (280 g) and eluted with a chloroform-methanol gradient. Fractions of 50 mL each were collected and monitored by thin-layer chromatography (TLC). Similar fractions were collected and grouped. Fractions eluted with chloroform/methanol in the ratios of 9 : 1, 8 : 2, and 7 : 3 generated 50, 20, and 25 mg of compounds **(1)**, **(2)**, and **(5)**, respectively. Subfraction COEt-III (8.5 g) was rechromatographed on silica gel column chromatography (320 g) and eluted with a chloroform/methanol gradient. Fractions of 50 mL each were collected and grouped. Fractions eluted with chloroform/methanol in the ratios of 9 : 1, 8 : 2, and 6 : 4 yielded 18 g, 22 mg, and 18 mg of compounds **(6)**, **(7)**, and **(4)**, respectively. Subfraction COEt-IV (9.5 g) was rechromatographed on silica gel column chromatography (350 g) and then eluted with a chloroform/methanol gradient in the ratios of 8 : 2, 7 : 3, 6 : 4, and 1 : 1 to generate compounds **(3)**, **(9)**, and **(8)** with 15, 25, and 30 mg, respectively. Subfraction COEt-V (9 g) was rechromatographed on silica gel column chromatography (300 g) and eluted with a chloroform/methanol gradient in the ratios of 7 : 3, 6 : 4, and 1 : 1 to yield compounds **(10)** and **(11)** with mass of 18 and 25 mg, respectively.

2.5.2. Acid Hydrolysis. A solution of the isolated glycoside (5 mg in 10 mL MeOH) was treated with 1.5 mL of 3% H_2SO_4 and heated at 100°C for 1 h. The aglycone was extracted with ethyl acetate, concentrated under reduced pressure, and identified by co-TLC with an authentic sample by using a suitable system. The sugars in the aqueous layer were identified by paper chromatography with authentic standards using system n-butanol-acetic acid-water (4 : 1 : 2 drops) v/v and sprayed with aniline hydrogen phthalate [15].

2.6. Pharmacological Studies

2.6.1. In Vitro Assay

(1) Cell Culture. The lung cancer (A-549), colorectal cancer (Colo-205), liver cancer (Huh-7), colon cancer (HCT-116), pancreatic cancer (PANC-1), and ovarian cancer (SKOV-3) cell lines, as well as normal hepatocyte cell line (BNL) were obtained from Nawah Scientific Inc. (Mokatam, Cairo, Egypt). Cell lines were maintained in a Roswell Park Memorial Institute (RPMI) medium supplemented with 100 mg/mL of streptomycin, 100 units/mL of penicillin, and 10% of heat-inactivated fetal bovine serum and then incubated at 37°C in a humidified 5% (v/v) CO_2 atmosphere [16].

(2) Cytotoxicity Assay. Cell viability was assessed using a sulforhodamine B (SRB) assay. About 100 L of cell suspension (5×10^3 cells) was transferred to a 96-well plate and incubated in a complete medium for 24 h. The cells were then treated with 100 L of medium containing samples at 10 and 100 g/mL concentrations. After 72 h of exposure, the cells were fixed by replacing the medium with 150 L of 10% trichloroacetic acid and incubating at 4°C for 1 h. Subsequently, the trichloroacetic acid solution was removed and the cells were washed five times with distilled water. Approximately, 70 L of SRB solution (0.4% w/v) was added and the mixture was incubated in the dark at an ambient temperature for 10 min. The plates were then washed three times with 1% acetic acid and allowed to air-dry overnight. After drying, 150 L of 10 mM tris (hydroxymethyl) aminomethane (TRIS) was added to dissolve the protein-bound SRB stain, and then the absorbance was measured at 540 nm using a BMG LABTECH-FLUOstar Omega microplate reader (Ortenberg, Germany) [16].

2.7. Statistical Analysis. Data are expressed as mean ± SD for all parameters. Graph Pad Prism software package was used for multiple comparisons of data, and a one-way analysis of variance (ANOVA) test was used to infer statistical significance at $P < xx$.

3. Results and Discussion

3.1. Phytochemical Studies

3.1.1. Screening and Isolation of Compounds. Silica gel column chromatographic analysis of the ethyl acetate fraction obtained from the whole aerial flowering parts of *C. occidentalis* identified eleven compounds labeled **1**–**11** (Figure 1). The structures of these compounds were identified and confirmed by one-dimensional (1D) and 2D NMR analysis and mass measurements and by comparing results with the reported data that were previously published.

Four known compounds (**1**–**4**) identified as *β*-sitosterol-3-*O*-*β*-D-glucopyranoside (**1**), stigmasterol-3-*O*-*β*-D-glucopyranoside (**2**), betulinic acid (**3**), and vanillic acid (**4**) were for the first time in *Cassia occidentalis* L, while in addition, three known compounds, cinnamic acid (**5**), *p*-hydroxybenzoic acid (**6**), and *β*- resorcylic acid **(7),** were also identified. Silybin A (**8**) is the first flavonolignan to be identified in the family Fabaceae and could serve as a taxonomic marker of *C. occidentalis*. All physical and spectral data of these compounds were consistent with those reported in the previous data (8).

Compound (1) was isolated as a granular powder (50 mg, MeOH), and electron-ionization mass spectrometry (EI-MS), *m*/*z* (rel.int%), of 413 $[M\text{-sugar}]^+$ (10%), 394 (20%), 399 (10%), 264 (20%), 83 (60%), and 57 (100%) was detected (Figure S1). On the basis of the EI-MS, ^{1}H-, and ^{13}C-NMR (Figures S2 and S3) and by comparison with the literature [17, 18], compound (1) was identified as *β*-sitosterol-3-*O*-*β*-D-glucopyranoside (**1**). To our knowledge, this study represents the first report of its isolation from *C. occidentalis* L.

Compound (2) was isolated as a white granular powder (20 mg, MeOH), and electron-ionization mass spectrometry (EI-MS), *m*/*z* (rel.int%), of 411 $[M\text{-sugar}]^+$(5%), 394 (5%), 300 (30%), 255 (20%), 83 (30%), and 70 (100%) was observed (Figure S4). On the basis of EI-MS, ^{1}H-, and ^{13}C-NMR (Figures S5 and S6) and by comparison with the literature [18, 19], compound (2) was identified as stigmasterol-3-*O*-*β*-D-glucopyranoside (**2**). To our knowledge, this represents its first isolation from *C. occidentalis*.

Compound (3) was isolated as a white needle-shaped substance (15 mg, MeOH) with a melting point (m.p) of 295–298°C. EI-MS, *m*/*z* (rel.int%), of 456 $[M]^+$ (60%), 411 $[M\text{-}COOH]^+$ (5%), 438 $[M\text{-}H_2O]^+$ (5%), 248 (10%), 207 (22%), and 189 (20%) was detected (Figure S7). The ^{1}H-NMR spectrum analysis of compound (3) (Table S1 and Figure S8) showed that it exhibited a triterpenoid skeleton that revealed the presence of six methyl group signals, and five of them at δ_H 0.65, 0.76, 0.89, 0.91, and 0.93 parts per million (ppm) were assigned to Me-25, Me-23, Me-24, Me-27, and Me-26, respectively. In addition, a vinylic methyl at δ_H 1.64 ppm assigned to Me-30, a methine proton at δ_H 2.97 ppm (1H, m) attributed to H-19, and one oxymethine proton at δ_H 3.33 ppm (overlapped with solvent signal) assigned to H-3 were detected, which were confirmed by IR band at ν 3400 cm^{-1} [20]. Two olefinic protons at δ_H 4.56 and 4.69 ppm were attributed to H-29a and H29b, respectively. The mass spectrum (Figure S7) showed a molecular ion peak at *m*/*z* 456, which corresponded to a molecular formula $C_{30}H_{48}O_3$, with characteristic mass fragments at *m*/*z* 411, 219, 248, 218, and 207, typical of betulinic acid [21]. The ^{13}C-NMR spectrum of compound (3) (Table S1; Figures S9 and S10) confirmed its triterpenoid nature and revealed signals for thirty carbons. The compound exhibited a carbonyl carboxylic acid moiety at δ_C 177.77 ppm assigned to C-28, in addition to two olefinic carbons at δ_C 110.11 and 150.78 ppm assigned to C-29 and C-20, respectively, and one oxymethine at δ_C 78.70, suggesting a lupane skeleton. Previous studies suggested that the compound was betulinic acid [21]; thus, it was designated as betulinic acid (**3**). To our knowledge, this represents its first isolation from *C. occidentalis*.

Compound (4) was isolated as a white amorphous powder (18 mg, MeOH). EI-MS, *m*/*z* (rel.int%), of 168 $[M]^+$ (10%), 153 $[M\text{-}CH_3]^+$ (15%), 137 $[M\text{-}OCH_3]^+$ (60%), 129

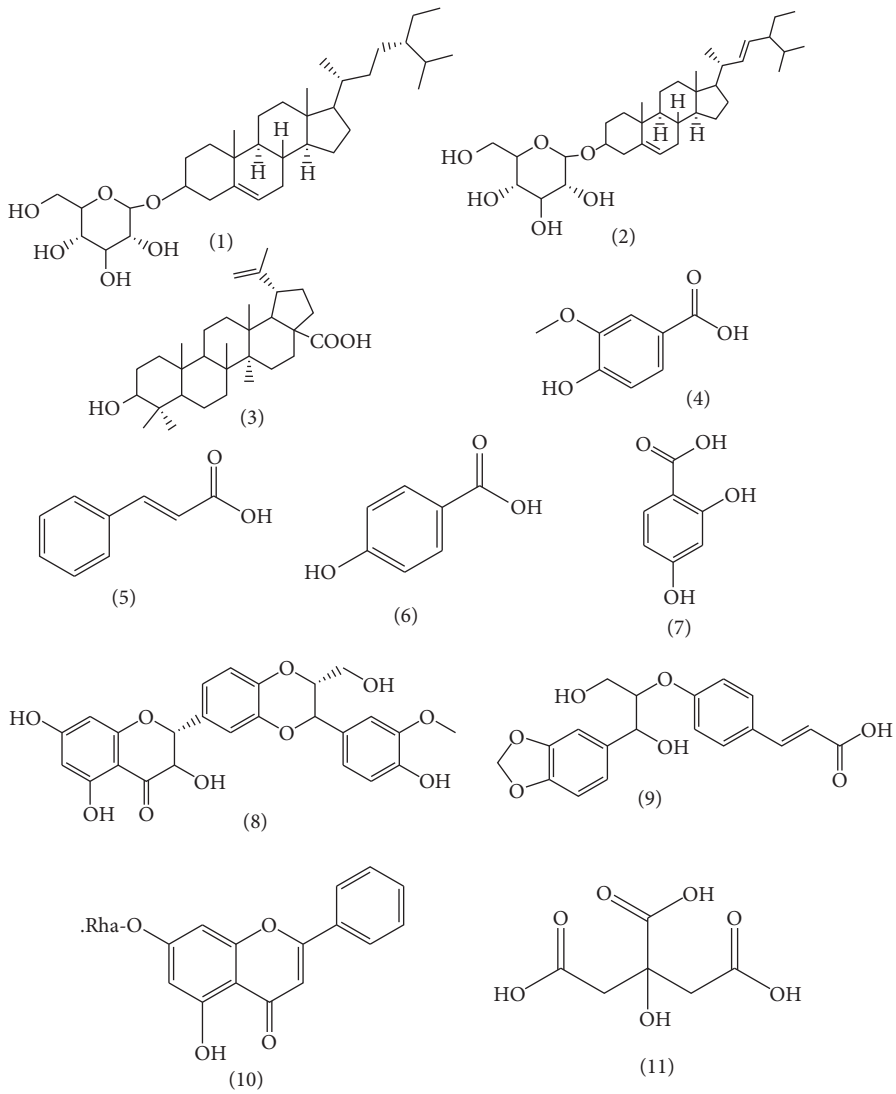

Figure 1: Structures of compounds isolated from the whole aerial flowering parts of *C. occidentalis* L.

(90%), 111 (50%), and 87 (100%) was observed (Figure S11). Analysis of ^{1}H- and ^{13}C-NMR spectra data of compound (4) (Table S2; Figures S12 and S13) showed that it exhibited three signals in the aromatic region at δ_H 7.45 ppm (1H, s), 6.84 ppm (1H, d, J = 8.8 Hz), and 7.44 ppm (1H, d, J = 8.8 Hz), indicating the presence of a trisubstituted benzene ring. A singlet corresponding to three protons at δ_H 3.80 ppm suggested the presence of a methoxy group, which was confirmed by δ_C 55.97 ppm and another singlet at δ_H 9.01 ppm for the aromatic hydroxyl group. The ^{13}C-NMR spectrum revealed seven aromatic carbon signals, with downfield one at δ_C 167.80 ppm being attributed to a carboxy carbonyl group, while the other six signals were similar to the previously reported compounds [22, 23]. The mass with the molecular ion peak at m/z 168 and ^{13}C-NMR spectral data of compound (4) suggested a molecular formula of $C_8H_8O_4$, thus the compound was considered to be 3-methoxy, 4-hydroxy benzoic acid (vanillic acid) (**4**), which to our knowledge represents its first isolation from *C. occidentalis*.

Compound (5) was isolated as white crystals (25 mg, MeOH) with an m.p of 133135°C. EI-MS, m/z (rel.int%), of 148 $[M]^+$ (77%), 147 $[M\text{-}1]^+$ (100%), 131 $[M\text{-}OH]^+$ (27%), 103 $[M\text{-}45]^+$ (69%), 91 (40%), and 77 (65%) was detected (Figure S14). Compound (5) exhibited a ^{1}H-NMR spectrum (Table S3 and Figure S15) for a monosubstituted phenyl ring at δ_H 7.68 ppm (2H, d, J = 8.0 Hz) corresponding to H-2 and H-6, in addition to AB system with resonance at δ_H 7.60 and 6.54 ppm that had a large coupling constant, indicating a transgeometry. The ^{13}C- and ^{13}C-DEPT (distortionless enhancement by polarization transfer) NMR spectra of compound (5) (Table S3; Figures S16, and S17) displayed seven carbon signals, with one of them being attributed to acid carbonyl at δ_C 168.05 ppm, which predicted a cinnamic acid structure. The mass spectrum (Figure S7) exhibited a molecular ion peak at m/z 148 that corresponded to $C_9H_8O_2$, thus validating the predicted structure. The resulting spectral data were consistent with that of cinnamic acid in a previous study [24], and it was therefore isolated as

cinnamic acid (**5**), which to our knowledge represents its first isolation from the genus *Cassia*.

Compound (6) was isolated as a white needle-shaped compound (18 mg, MeOH) with m.p of 215–217°C. EI-MS, *m*/*z* (rel.int%), of 138 $[M]^+$ (70%), 121 $[M\text{-}OH]^+$ (100%), 93 $[M\text{-}COOH]^+$ (32%), and 65 (40%) was obtained (Figure S18). The ^{1}H-NMR spectrum analysis of the compound (Table S4 and S19) showed that it exhibited two doublet signals at δ_H 7.80 ppm (2H, d, J = 8.4 Hz) and 6.83 ppm (2H, d, J = 8.4 Hz), which were equivalent to protons attributed to a paradisubstituted benzene ring, in addition to the two downfield singlet signals at δ_H 12.28 and 10.32 ppm that corresponded to carboxylic OH and 4-OH groups. The ^{13}C- and DEPT ^{13}C-NMR (Figures S20 and S21) spectra revealed five signals, which could be attributed to seven carbons including a signal at δ_C 167.64 ppm that corresponded to carboxy carbonyl. The DEPT experiment revealed three quaternary carbons, which were attributed to C-1 and C-4 at the δ_C 121.84 and 162.06 ppm and a carboxylic one at δ_C 167.64. The mass spectrum (Figure S18) generated a molecular ion peak at *m*/*z* 138, which predicted a molecular formula of $C_7H_6O_3$. The obtained data were consistent with those of *p*-hydroxybenzoic acid [25], thus the compound was identified as *p*-hydroxybenzoic acid (**6**), which to our knowledge represents its first isolation from the genus *Cassia*.

Compound (7) was isolated as a white needle-shaped compound (22 mg, MeOH) with m.p of 208–211°C. EI-MS, *m*/*z* (rel.int%), of 154 $[M]^+$ (30%), 136 $[M\text{-}H_2O]^+$ (100%), 108 $[M\text{-}COOH]^+$ (46%), and 80 (60%) was obtained (Figure S22). Its ^{1}H-NMR spectrum (Table S5 and Figure S23) exhibited three aromatic proton signals, which were characteristic to the trisubstituted benzene ring at δ_H 7.18 ppm (1H, br.s), 6.78 ppm (1H, d, J = 8.8 Hz), and 6.96 ppm (1H, d, J = 8.8 Hz), which were assigned to H-3, H-5, and H-6, respectively. An additional downfield singlet at δ_H 9.30 ppm for phenolic hydroxyl was also detected. The ^{13}C-NMR spectrum of compound (7) (Table S5 and Figure S24) showed seven carbon signals and included a signal at δ_C 172.14 ppm, which was assigned to the carboxy carbonyl group. DEPT experiment (Figure S25) revealed four quaternary carbons attributed to C-1, C-2, and C-4 at δ_C 113.08, 149.83, and 154.57 ppm, respectively, in addition to a carboxylic group at δ_C 172.14. The mass spectrum (Figure S22) revealed a molecular ion peak at *m*/*z* 154 that predicted a molecular formula of $C_7H_6O_4$. The obtained data suggested that the compound was 2,4-dihydroxy benzoic acid, and previous spectral data report [23] confirmed its identity as 2,4-dihydroxy benzoic acid (β-resorcylic acid) (**7**), which to our knowledge represents its first isolation from the genus *Cassia*.

Compound (8) was isolated as a yellowish-white granular powder (30 mg, MeOH). The UV spectral analysis of the compound λ_{max} (MeOH) showed absorption at 217, 290, and 330 nm. The IR (KBr) spectrum showed the following absorption bands at ν cm^{-1} 3431 (phenolic OH), 1704 (C=O), 1552, 1440, 1250, 1237, 1080, 992, and 680 (aromatic system). EI-MS, m/*z* (rel.int%), of 482 $[M]^+$ (21%), 465 $[M\text{-}OH]^+$ (8%), 195 (3%), 109 (16%), 180 [M-cinnamoyl]$^+$ (30%), 153 (60%), 137 (90%), 133 (10%), and 124 (100%) (Figure S26) was obtained. The ^{1}H-NMR spectrum evaluation of the compound (Table S6 and Figure S27) displayed typical features of 5,7-dihydroxy-substituted flavonol skeleton [15] with signals at δ_H 5.88 ppm (1H, br.s, H-6), 5.92 ppm (1H, br.s, H-8), 5.08 ppm (1H, d, J = 7.2 Hz), and 4.62 ppm (1H, m), which were characteristic to the H-2 and H-3 of the dihydro-flavonol skeleton [26]. In addition, the six protons in the aromatic region could be attributed to the two sets of 1, 3, and 4-trisubstituted aromatic rings, with one belonging to the B-ring of the dihydro-flavonol group at δ_H 7.09 ppm (1H, br.s.), 6.97 ppm (1H, d, J = 8.0 Hz), 6.99 ppm, and (1H, d, J = 8.0 Hz) for H-2′, 5′, and 6′, respectively, while the other belonging to the cinnamic alcohol groups at δ_H 7.01 (1H,br.s.), 6.81 (1H,d, J = 8.0 Hz), and 6.87 (1H,d, J = 8.0 Hz) for H-2″, H-5″, and H-6″, respectively. Four protons at δ_H 4.90 ppm (1H, d, J = 8.0 Hz, H-7″), 4.17 ppm (1H, m, H-8″), 3.55 ppm (1H, m, H-9a″), and 3.40 ppm (1H, m, H-9b″) could be assigned to a propanol moiety connected to a dioxane ring [26]. The ^{1}H-NMR spectra also exhibited a three-proton singlet at δ_H 3.78 ppm that was assigned to the aromatic methoxy group and three hydroxyls attached to the aromatic skeleton at δ_H 11.89, 10.24, and 9.15 ppm (each as one proton singlet), which suggested the 5-OH, 7-OH, and 4″-OH groups, respectively, and were confirmed by the IR absorption band at 3431 cm^{-1}. In addition, two proton signals were attributed to olefinic hydroxyls at δ_H 5.81 ppm (1H, d, J = 6.0 Hz) and 4.91 ppm (1H, d, J = 7.6 Hz) for 3-OH and 9″-OH, respectively. The mass spectrum (Figure S26) showed a molecular ion peak at *m*/*z* 482 and the ^{13}C-NMR spectrum (Table S6 and Figure S28) revealed 25 carbon signals, suggesting a molecular formula of $C_{25}H_{22}O_{10}$. Carbon signals at δ_C 83.02 and 71.80 ppm corresponded to C-2 and C-3, in addition to the downfield one at δ_C 198.20 ppm, which was assigned to the C-4, thereby confirming a dihydro-flavonol skeleton with hydroxylated C-5 and C-7 [27]. The remaining ^{13}C-NMR signals were consistent with those previously reported for a flavonolignan skeleton [26, 28]. The DEPT experiment (Table S6 and Figure S29) detected 1, 1, 12, and 11 signals for methoxy, CH_2, CH, and quaternary carbons, respectively. The obtained data suggested a dihydro-flavonol skeleton and a lignan moiety, and their connection was verified by comparing the obtained spectral data with those in the literature [28]. Complete assignment of the ^{1}H- and ^{13}C-NMR signals was achieved by analyzing their ^{1}H^{1}H correlation spectroscopy (COSY), heteronuclear single quantum coherence (HSQC), and heteronuclear multiple bond correlation (HMBC) spectra (Figures S30–S32). The stereochemistry of compound (8) was based on the carbon chemical shifts, which shared a close resemblance with those previously reported for silybin A (**8**) (2R,3R)-3,5,7-trihydroxy-2-[(2S,3S)-3-(4-hydroxy-3-methoxyphenyl)-2-hydroxymethyl-2,3-dihydro-benzol [1, 4] dioxin-6-yl]-chroman-4-one [28]. On the basis of previously reported spectral data and by comparison with the available literature [26, 28], compound (8) was verified to be silybin A (**8**). To our knowledge, this represents its first isolation from

Table 1: ^{1}H-NMR, ^{13}C-NMR, DEPT, and HMBC (400 and 100 MHz, DMSO-d_6) data of compound(**9**).

Carbon no.	^{1}H-NMR (m, in Hz)	^{13}C-NMR	DEPT	HMBC
1	—	131.30	C	—
2	7.17 (1H, br.s)	104.40	CH	3, 4, 6
3	—	148.40	C	—
4	—	148.20	C	—
5	6.91 (1H, *d*, *J* = 7.6 Hz)	109.0	CH	1, 3, 4
6	6.98 (1H, *d*, *J* = 7.6 Hz)	123.0	CH	1, 2, 4
7	3.52 (1H, m)	70.10	CH	-—
8	3.41 (1H, m)	73.20	CH	—
9	9_a 4.20 (1H, m) 9_b 4.46 (1H, m)	62.50	CH_2	—
1′	—	148.40	C	—
2′,6′	6.94 (2H, *d*, *J* = 8.1 Hz)	126.10	CH	1′, 3′, 4′, 5′
4′	—	131.30	C	—
3′,5′	6.87 (2H, *d*, *J* = 8.1 Hz)	138.20	CH	1′, 4′, 7′, 2′, 6′
7′	7.21 (1H, *d*, *J* = 14.8 Hz)	142.40	CH	3′, 5′, 9′
8′	6.67 (1H, *d*, *J* = 14.8 Hz)	121.20	CH	3′, 5′, 9′
9′	—	164.90	C	—
9′-OH	13.13 (1H, br.s.)	—	—	—
O-CH_2-O	6.02 (s)	101.70	CH_2	3, 4

Table 2: UV spectral data of compound **(10)** in methanol and with different ionizing and complexing reagents.

Band	λ_{max} (nm)										
	MeOH	+NaOMe		+$AlCl_3$		+$AlCl_3$/HCl		+NaOAc		+NaOAc/H_3BO_3	
	λ_{max}	λ_{max}	Δ λ_{max}	λ_{max}	Δ λ_{max}	λ_{max}	Δ λ_{max}	λ_{max}	Δ λ_{max}	λ_{max}	Δ λ_{max}
II	283	290	+7	295	+12	293	+8	285	+3	290	+7
I	335	350	+15	386	+56	370	+45	345	+15	344	+9

the genus *Cassia* and family Fabaceae; thus, it might serve as a taxonomic marker of *C. occidentalis* as flavonolignans have not been reported in the family.

Compound 9 was obtained as a yellow granular powder (25 mg, MeOH). EI-MS, *m*/*z* (rel.int%), of 358 $[M]^+$ (27%), 357 $[M\text{-}H]^+$ (89%), 341 $[M\text{-}OH]^+$ (2%), 327 $[M\text{-}CH_2OH]^+$ (3%), 313 $[M\text{-}COOH]^+$ (2%), 300 (36%), 287 [M-propenoic acid]$^+$ (3%), 195 (5%), 163 (13%), and 71 [propenoic acid] (45%) was obtained (Figure S33). The molecular formula was established to be $C_{19}H_{18}O_7$, which implied 11 degrees of unsaturation. The IR (KBr) spectrum showed the following absorption bands at ν cm^{-1} 3400 (OH), 2830, 1705 (C=O), 1601, 1580, 1509, 1280, 750 (C=C aromatic ring), 1038, and 930 (methylenedioxy). The ^{1}H-NMR spectrum (Table 1 and Figure S34) first revealed the protons in the aromatic region at δ_H 6.98–7.17 ppm that displayed seven signals, which were attributed to two metadisubstituted and paradisubstituted phenyl rings, then followed by two transolefinic protons at δ_H 6.67 and 7.21 (d, *J* = 14.8 Hz) [29] and one methylenedioxy group at δ_H 6.02 ppm [29]. In addition, four signals at δ_H 3.52–3.41 ppm could be attributed to the protons attached to carbons with adjacent oxygen, leading to the assignment of an oxyneolignan structure with propenyl moiety. Based on signal characteristics (HSQC, COSY, and HMBC), protons at δ_H 7.17 ppm (1H, s), 6.91 ppm (1H, d, *J* = 7.6 Hz), and 6.98 ppm (1H, d, *J* = 7.6 Hz) could be assigned to H-2, H-5, and H-6 (ring A), while protons at δ_H 6.94 ppm (2H, d, *J* = 8.1 Hz) and 6.87 ppm (2H, d, *J* = 8.1 Hz) were assigned to the *para*disubstituted phenyl ring (ring B). Besides, the ^{13}C-NMR indicated the presence of 19 carbons, while DEPT ^{13}C-NMR data (Table 1; Figures S35 and S36), confirmed the presence of two phenylpropanoid units [30]. The DEPT experiment revealed the presence of an alcoholic methylene signal at δ_C 62.50 ppm and a signal at δ_C 101.70 ppm, confirming the methylenedioxy group [29]. In addition, six quaternary carbons at δ_C 131.30, 148.40, and 148.20 ppm were assigned to C-1, C-3, and C-4 of ring A, while the signals at δ_C 148.40 and 131.30 ppm were assigned to C-1′ and C-4′ of ring B, in addition to carboxylic carbonyl at δ_C 164.90 ppm, which confirmed the *trans*substituted neolignan. The NMR results and the detection of significant mass peaks at *m*/*z* 71 and 287 confirmed the presence of propenoic (acrylic) acid moiety [30]. Complete assignment of the ^{1}H- and ^{13}C-NMR signals was confirmed from their ^{1}H-^{1}H COSY, HSQC, and HMBC (Figures S37–S39) spectra analysis. The spectral data and their comparison with similar compounds in the literature [29–31] could assign compound **9** as (E)-3-[4-(1-(benzol) [d] [1, 3] dioxol-6-yl)-1, 3-dihydroxy propan-2) phenyl] propanoic acid, which can loosely be called occidentalignan I (**9**). This represents a new compound and the first report of its isolation from *C. occidentalis* [32].

Table 3: ^{1}H-NMR, ^{13}C-NMR, and DEPT (400 and 100 MHz, DMSO-d_6) data of compound **(10)**.

Carbon no.	^{1}H-NMR (m, in Hz)	^{13}C-NMR	DEPT
2	—	164.92	C
3	6.93 (1H, s)	105.61	CH
4	—	182.31	C
5	—	161.91	C
6	6.20 (1H, *d*, $J = 1.6$ Hz)	99.50	CH
7	—	163.65	C
8	6.51 (1H, *d*, $J = 1.6$ Hz)	94.60	CH
9	—	157.92	C
10	—	104.41	C
1′	—	131.15	C
2′, 6′	8.04 (2H, *d*, $J = 8.0$ Hz)	126.84	CH
3′, 5′	7.59 (3H, *dd*, $J = 8.0$, 1.8 Hz)	129.60	CH
4′		132.48	CH
1″	4.81 (1H, s)	101.91	CH
2″	3.08–3.63 (remaining sugar protons, m)	72.16	CH
3″		72.85	CH
4″		73.97	CH
5″		68.16	CH
6″	1.10 (3H, *d*, $J = 6.40$ Hz)	18.44	CH
5-OH	12.80 (1H, s)	—	—

Compound 10 was obtained as a yellow amorphous powder (18 mg, MeOH). EI-MS (Figure S40) showed a molecular ion peak at m/z 254 [M-sugar]$^+$ and a calculated molecular formula of $C_{15}H_{10}O_4$ (chrysin). The UV spectral data in MeOH (Table 2) showed two absorption bands at λ_{max} 283 nm (band II) and 335 nm (band I), which were the characteristic of the flavone skeleton [15], with 5-OH (bathochromic replaced in band I with $AlCl_3$) and the absence of dihydroxyl substitution at C-4` or C-7 position (no shift with NaOMe (band I) or with NaOAc (band II)). The ^{1}H-, ^{13}C-, and DEPT ^{13}C-NMR spectra of compound **10** (Table 3; Figures S41–S43) exhibited a characteristic pattern of flavone skeleton [15], similar to those of chrysin [33]. In addition, it displayed anomeric sugar proton at δ_H 4.81 ppm (1H, s) with a δ_C at 101.91 as well as an upfield three-proton signal at δ_H 1.10 ppm (3H, d, $J = 6.40$ Hz) attributed to the methyl group of rhamnose moiety, which was confirmed by CH_3 signal at δ_C 18.44 ppm. The appearance of carbon signal at δ_C 68.16 ppm was attributed to C-5, indicating α-L-rhamnose [27]. Glycosylation of chrysin was determined to occur at the C-7 (no NaOAC bathochromic shift in band II), which was confirmed by the upfield shift of C-7 by 1.33 ppm in the ^{13}C-NMR spectrum in comparison to chrysin. The ^{13}C-NMR data displayed 15 carbon signals of a flavone skeleton [27] at δ_C 72.16–68.16, which could be assigned to the sugar moiety. The DEPT experiment revealed seven quaternary carbon and 13 CH signals. Acid hydrolysis of compound **(10)** as described in the methods resulted in the identification of a hydrolysate. The aglycone was confirmed to be chrysin by direct comparison with an authentic sample, and the sugar fraction was identified as L-rhamnose using paper chromatography. From the spectral data and their comparison with similar compounds in the literature [34], compound (10) was identified as chrysin-7-*O*-α-L-rhamnopyranosyl (**10**), which to our knowledge represents a new compound and the first report of its isolation from a plant-based natural source.

Compound (11) was isolated from ethyl acetate fraction as a colorless needle-shaped substance (25 mg, MeOH) with an m.p of 152-153°C. EI-MS, m/z (rel.int%), of 192 [M]$^+$ (5%), 147 [M-COOH]$^+$ (5%), 102 [M-2COOH]$^+$ (25%), 57 [M-3COOH]$^+$ (32%), and 45 (100%) was observed (Figure S44). The ^{1}H-NMR spectrum of compound (11) (Table S7 and Figure S45) exhibited two sets of enantiotropic pairs of hydrogen with an identical chemical shift at δ_H 2.60 and 2.72 ppm, each for two protons with a coupling constant of 15.6 Hz. The ^{13}C-NMR spectrum (Table S7 and Figure S46) displayed four carbon signals attributed to six carbons, with two downfield signals being assigned to three carboxylic groups at δ_C 175.03 and 171.77 ppm (for two chemically equivalent groups), in addition to an oxygenated carbon at δ_C 72.91 and two chemically equivalent ethylenic carbons at δ_C 43.20. Mass spectrum (Figure S44) showed a molecular ion peak at m/z 192 with a calculated molecular formula of $C_6H_8O_7$ and characteristic mass peaks at m/z 147, 102, and 57 for successive loss of three carboxylic groups, which was confirmed from the ^{13}C-NMR data. The obtained spectral data were inconsistent with those previously reported for citric acid [35]. Based on the comparison between previously identified and published spectral data [35], compound (11) was identified as citric acid (**11**), representing its isolation from the genus *Cassia*.

3.2. Pharmacological Studies

3.2.1. In Vitro Cytotoxicity assay. The total methanolic extract of the whole aerial flowering parts of *C. occidentalis* was screened for its cytotoxic activity (Table 4). As reported, the cytotoxicity of *C. occidentalis* is due to anthraquinones (major active constituents in the plant) which are found in high concentrations. Since this class of compounds (anthraquinones) is present in higher concentrations in the total extract than other fractions, it was chosen in our study to confirm the plant's activity [36] against seven cancer cell lines, including lung cancer (A-549), colorectal carcinoma (Colo-205), hepatocellular carcinoma (Huh-7), colon cancer (HCT-116), pancreatic cancer (PANC-1), ovarian cancer (SKOV-3), and mouse normal liver cells BNL, using SRB screening assay at sample concentrations of 10 and 100 g/mL. The cytotoxic activity revealed that the extract exhibited selective potent cytotoxicity on lung cancer cells without affecting BNL normal cells, while the extract showed moderate activity on Colo-205 and Huh-7 and nearly no activity on HCT-116, PANC-1, and SKOV-3 cell lines.

The optical microscope-stained images (Figure 2) recorded the SRB cytotoxicity assay results for the total methanolic extract of the whole aerial flowering parts of *C. occidentalis* at the two tested concentration points against

Table 4: Rapid SRB cytotoxicity screening results of total methanolic extract from the whole aerial flowering parts of *C. occidentalis* on several cell lines.

Conc. of the tested sample (μg/mL)	Cell viability (%)						
	Cancer cell lines						Normal cell line
	A-549	Colo-205	Huh-7	HCT-116	PANC-1	SKOV-3	BNL
10	98.5338	100.512	96.0551	98.9648	100.038	102.567	99.0442
100	65.9283	83.916	93.2841	98.6645	93.1391	100.09	96.3608

±SD ($n = 3$).

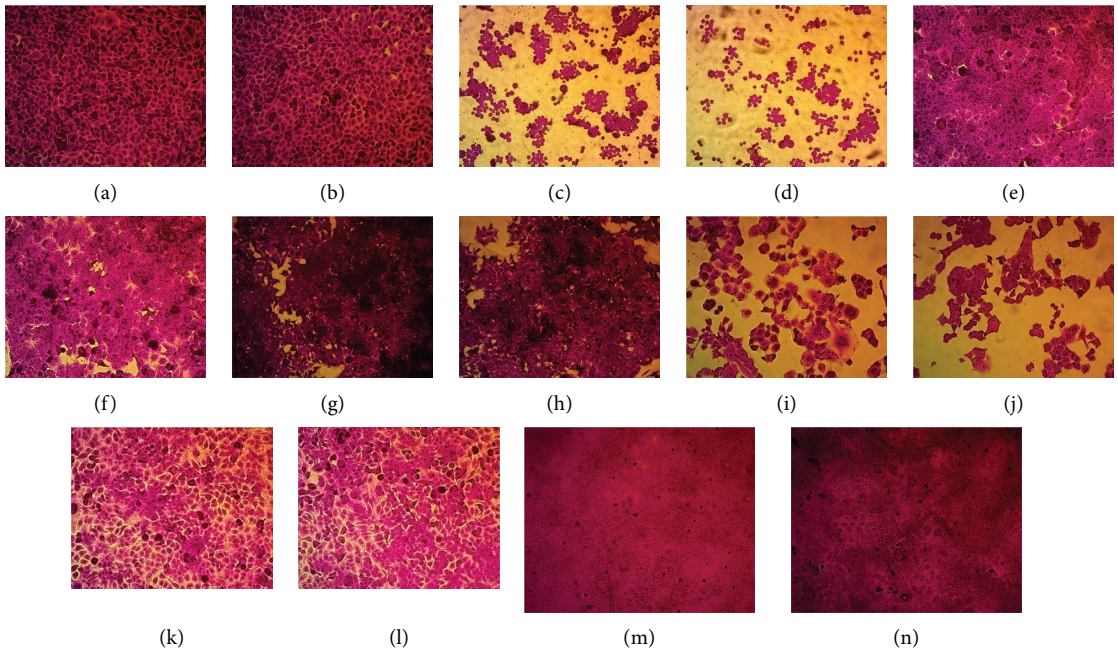

Figure 2: The optical microscope stained images of cytotoxicity assays of the seven cell lines: (a) A-549 (10 μg/mL), (b) A-549 (100 μg/mL), (c) colo-205 (10 μg/mL), (d) colo-205 (100 μg/mL), (e) huh-7 (10 μg/mL), (f) huh-7 (100 μg/mL), (g) HCT-116 (10 μg/mL), (h) HCT-116 (100 μg/mL), (i) PANC-1 (10 μg/mL), (j) PANC-1 (100 μg/mL), (k) SKOV-3 (10 μg/mL), (l) SKOV-3 (100 μg/mL), (m) BNL (10 μg/mL), and (n) BNL (100 μg/mL), magnification power: 200×.

the seven cell lines. As a result, clear significant morphological changes in lung cancer cells were detected at both extract concentrations, while moderate changes were observed at higher (100 g/mL) concentrations on Colo-205 and Huh-7. In contrast, no changes were detected on HCT-116, PANC-1, and SKOV-3. These results confirmed the cytotoxic activity of the total methanolic extract of *C. occidentalis* on the A-549 cell line.

To investigate the safety of *C. occidentalis* methanolic extract on normal cells and its selective cytotoxicity on cancer cells, the cytotoxic activity was tested against mouse normal liver cells BNL. The results showed the percentage cell viability of 96.3608 for the methanolic extract at a concentration of 100 μg/mL against the BNL normal cell line. In contrast, it demonstrated a potent cytotoxic effect with a percentage cell viability of 65.9283 on the A-549 cell line with the same concentration, which suggested its safety on normal cell lines and selective cytotoxicity on lung cancer cell lines.

4. Conclusion

In summary, this study used ethyl acetate fraction column chromatography to isolate eleven compounds of different classes from the whole aerial flowering parts of *C. occidentalis*. Two new metabolites, including a neolignan, designated as occidentalignan I (**9**) and a flavonoidal glycoside, named chrysin-7-*O*-α-L-rhamnopyranosyl (**10**), were identified based on spectroscopic evidence. In addition, a flavonolignan compound, silybin A (**8**), was isolated for the first time from the family Fabaceae, while four compounds, including β-sitosterol-3-*O*-β-D-glucopyranoside (**1**), stigmasterol-3-*O*-β-D-glucopyranoside (**2**), betulinic acid (**3**), and vanillic acid (**4**), as well as four known compounds, cinnamic acid (**5**), *p*-hydroxybenzoic acid (**6**), β-resorcylic acid (**7**), and citric acid (**11**), were isolated for the first time in *C. occidentalis* L. *In vitro* cytotoxicity assessment of the methanolic extract on seven different cancer cell lines, A-549, Colo-205, Huh-7, HCT-116, PANC-1, SKOV-3, and

BNL, showed a selective potent cytotoxicity of *C. occidentalis* extract on lung cancer cells without affecting BNL normal cells. The extract also showed moderate activity on Colo-205 and Huh-7, and nearly no activity on HCT-116, PANC-1, and SKOV-3. These results indicate that the *Cassia occidentalis* methanolic extract is potentially a good candidate for the treatment of lung cancer cell lines; however, further studies are required to clarify its underlying mechanism of action.

Abbreviations

A-549: Lung cancer
br.s: Broad singlet
BNL: Normal hepatocyte cell line
COEt: *Cassia occidentalis* ethyl acetate extract
Colo-205: Colorectal cancer
DEPT: Distortions enhancement by polarization transfer
EI-MS: Electron ionization-mass spectrometry
HMBC: Heteronuclear multiple bond correlation
HSQC: Heteronuclear single-quantum correlation
Huh-7: Liver cancer
HCT-116: Colon cancer
PANC-1: Pancreatic cancer
SKOV-3: Ovarian cancer
TLC: Thin-layer chromatography.

Data Availability

All data generated or analyzed during this study are included in this published article and its supplementary materials.

Conflicts of Interest

The authors declare that they have no conflicts of interest.

Authors' Contributions

All authors conceptualized the study, curated the data, performed the formal analysis, acquired the funding, investigated the data, developed the methodology, administered the project, collected the resources, developed the software, visualized, validated, and supervised the study, wrote of the original draft, and reviewed and edited the data.

Acknowledgments

The authors acknowledge the Pharmacognosy Department, Faculty of Pharmacy, Assiut University, Assiut, Egypt, for supporting to perform this work in their labs.

Supplementary Materials

Supplementary Figure (S1): EI-MS spectrum of compound (1). Supplementary Figure (S2): 1H-NMR spectrum of compound (1) (DMSO-d6-400 MHz). Supplementary Figure (S3): 13C-NMR spectrum of compound (1) (DMSO-d6-100 MHz). Supplementary Figure (S4): EI-MS spectrum of compound (2). Supplementary Figure (S5): 1H-NMR spectrum of compound (2) (DMSO-d6-400 MHz). Supplementary Figure (S6): 13C-NMR spectrum of compound (2) (DMSO-d6-100 MHz). Supplementary Figure (S7): EI-MS spectrum of compound (3). Supplementary Figure (S8): 1H-NMR spectrum of compound (3) (DMSO-d6-400 MHz). Supplementary Figure (S9): 13C-NMR spectrum of compound (3) (DMSO-d6- 100 MHz). Supplementary Figure (S10): Expansion of 13C-NMR spectrum of compound (3) (DMSO-d6- 100 MHz). Supplementary Figure (S11): EI-MS spectrum of compound (4). Supplementary Figure (S12): 1H-NMR spectrum of compound (4) (DMSO-d6-400 MHz). Supplementary Figure (S13): 13C-NMR spectrum of compound (4) (DMSO-d6-100 MHz). Supplementary Figure (S14): EI-MS spectrum of compound (5). Supplementary Figure (S15): H-NMR spectrum of compound (5) (DMSO-d6-400 MHz). Supplementary Figure (S16): 13C-NMR spectrum of compound (5) (DMSO-d6-100 MHz). Supplementary Figure (S17): DEPT 13C-NMR spectrum of compound (5) (DMSO-d6-100 MHz). Supplementary Figure (S18): EI-MS spectrum of compound (6). Supplementary Figure (S19): 1H-NMR spectrum of compound (6) (DMSO-d6-400 MHz). Supplementary Figure (S20): 13C-NMR spectrum of compound (6) (DMSO-d6-100 MHz). Supplementary Figure (S21): DEPT 13C-NMR spectrum of compound (6) (DMSO-d6- 100 MHz). Supplementary Figure (S22): EI-MS spectrum of compound (7). Supplementary Figure (S23): 1H-NMR spectrum of compound (7) (DMSO-d6-400 MHz). Supplementary Figure (S24): 13C-NMR spectrum of compound (7) (DMSO-d6-100 MHz). Supplementary Figure (S25): DEPT 13C-NMR spectrum of compound (7) (DMSO-d6-100 MHz). Supplementary Figure (S26): EI-MS spectrum of compound (8). Supplementary Figure (S27): 1H-NMR spectrum of compound (8) (DMSO-d6-400 MHz). Supplementary Figure (S28): 13C-NMR spectrum of compound (8) (DMSO-d6-100 MHz). Supplementary Figure (S29): DEPT 13C-NMR spectrum of compound (8) (DMSO-d6-100 MHz). Supplementary Figure (S30): 1H-1H COSY spectrum of compound (8) (DMSO-d6). Supplementary Figure (S31): HSQC spectrum of compound (8) (DMSO-d6). Supplementary Figure (S32): HMBC spectrum of compound (8) (DMSO-d6). Supplementary Figure (S33): EI-MS spectrum of compound (9). Supplementary Figure (S34): 1H-NMR spectrum of compound (9) (DMSO-d6-400 MHz). Supplementary Figure (S35): 13C-NMR spectrum of compound (9) (DMSO-d6-100 MHz). Supplementary Figure (S36): DEPT 13C-NMR spectrum of compound (9) (DMSO-d6-100 MHz). Supplementary Figure (S37): 1H-1H COSY spectrum of compound (9) (DMSO-d6). Supplementary Figure (S38): HSQC spectrum of compound (9) (DMSO-d6). Supplementary Figure (S39): Extended HSQC spectrum of compound (9) (DMSO-d6). Supplementary Figure (S40): EI-MS spectrum of compound (10). Supplementary Figure (S41): 1H-NMR spectrum of compound (10) (DMSO-d6-400 MHz). Supplementary Figure (S42): DEPT 13C-NMR spectrum of compound (10) (DMSO-d6- 100 MHz). Supplementary Figure (S43): DEPT 13C-NMR spectrum of

compound (10) (DMSO-d6-100 MHz). Supplementary Figure (S44): EI-MS spectrum of compound (11). Supplementary Figure (S45): 1H-NMR spectrum of compound (11) (DMSO-d6-400 MHz). Supplementary Figure (S46): 13C-NMR spectrum of compound (11) (DMSO-d6-100 MHz). Supplementary Table (S1): 1H-, 13C-, and 13C-NMR (400 and 100 MHz, DMSO-d6) data of compound (3). Supplementary Table (S2): 1H- and 13C-NMR (400 and 100 MHz, DMSO-d6) data of compound (4). Supplementary Table (S3): 1H-, 13C-, and DEPT 13C-NMR (400 and 100 MHz, DMSO-d6) data of compound (5). Supplementary Table (S4): 1H-, 13C-, and DEPT 13C-NMR (400 and 100 MHz, DMSO-d6) data of compound (6). Supplementary Table (S5): 1H-, 13C-, and DEPT 13C-NMR (400 and 100 MHz, DMSO-d6) data of compound (7). Supplementary Table (S6): 1H-, 13C-, and DEPT 13C-NMR (400 and 100 MHz, DMSO-d6) data of compound (8). Supplementary Table (S7): 1H- and 13C-NMR (400 and 100 MHz, DMSO-d6) data of compound (11). (*Supplementary Materials*)

References

[1] E. D. Tetzlaff, J. D. Cheng, and J. A. Ajani, "Review of docetaxel in the treatment of gastric cancer," *Therapeutics and clinical risk management*, vol. 4, no. 5, pp. 999–1007, 2008.

[2] R. A. Rutter, *Catalogo de Plants Utiles de la Amazonia Peruana Instituto Lingusitico de Verano*, Ministerio de Educacion/Instituto Linguistico de Verano, Yarinacocha, Peru, 1990.

[3] Í. F. da Silva and E. A. Vieira, "Phytotoxic potential of Senna occidentalis (L.) Link extracts on seed germination and oxidative stress of Ipê seedlings," vol. 21, no. 4, pp. 770–779, 2019.

[4] A. Payne-Jackson, M. C. Alleyne, and M. C. Alleyne, *Jamaican folk medicine: A source of healing*, University of West Indies Press, Mona, Jamaica, 2004.

[5] A. C. Jain and R. Saksena, "A study of ethoxymethylation in the 3-position of chroman-4-ones," *Proceedings of the Indian Academy of Sciences - Chemical SciencesProceedings/Indian Academy of Sciences*, vol. 103, no. 1, pp. 25–31, 1991.

[6] J. Holder and M. Lee, *Environmental protection, law and policy: Text and materials*, Cambridge University Press, Cambridge, UK, 2007.

[7] R. Coimbra, "Manual de fitoterapia," in *Manual de fitoterapia*,p. 335, Elsevier, Amsterdam, Netherlands, 1994.

[8] N. P. M. S. Sharma, "In vitro inhibition of carcinogen-induced mutagenicity by Cassia occidentalis and Emblica officinalis," *Drug Chem Toxicol*, vol. 23, no. 3, pp. 477–84, 2000.

[9] M. B. P. L. M. Delmut, J. R. L. M. L. Paula, E. C. J. R. Conceição, A. S. E. C. Santos, I. A. H. A. S. Pfrimer, and G. Cai, "Cassia occidentalis: effect on healing skin wounds induced by Bothrops moojeni in mice," *journal of Pharmaceutical Technology and Drug Research*, vol. 2, no. 10, 2013.

[10] A. Lum Nde, "Ethnobotanical, phytochemical, toxicology and anti-diabetic potential of Senna occidentalis (L.) link; A review," *Journal of Ethnopharmacology*, vol. 283, Article ID 114663, 2022.

[11] B. Bin-Hafeez, "Protective effect of Cassia occidentalis L. on cyclophosphamide-induced suppression of humoral immunity in mice," *J Ethnopharmacol*, vol. 75, no. 1, pp. 13–8, 2001.

[12] V. Arya, Y. Sanjay, K. Sandeep, and J. P. Yadav, "Antimicrobial Activity of Cassia occidentalis L (Leaf) against various Human Pathogenic Microbes," 2010, https://www.researchgate.net/profile/Ved-Arya-2/publication/288262077_Antimicrobial_Activity_of_Cassia_occidentalis_L_Leaf_against_various_Human_Pathogenic_Microbes/links/555c645108aec5ac2232d02a/Antimicrobial-Activity-of-Cassia-occidentalis-L-Leaf-against-var.

[13] I. S. Sadiq, A. B. Bello, S. G. Tureta et al., "Phytochemistry and Antimicrobial Activities of Cassia Occidentalis Used for Herbal Remedies," *JOURNAL OF CHEMICAL ENGINEERING*, vol. 1, no. 1, 2012.

[14] M. Bhagat and A. Saxena, "Evaluation of Cassia occidentalis for in vitro cytotoxicity against human cancer cell lines and antibacterial activity," *Indian J Pharmacol*, vol. 42, no. 4, pp. 234–237, 2010.

[15] T. J. Mabry, K. R. Markham, and M. B. Thomas, *The Systematic Identification of Flavonoids*, Springer-Verlage, Heidelberg Germany, 1970.

[16] S. Basiouni, "Characterization of Sunflower Oil Extracts from the Lichen Usnea barbata," vol. 10, no. 9, p. 353, 2020.

[17] E. Abdou, "Assessment of the hepatoprotective effect of developed lipid-polymer hybrid nanoparticles (LPHNPs) encapsulating naturally extracted β-Sitosterol against CCl4 induced hepatotoxicity in rats," *Scientific Reports*, vol. 9, no. 1, Article ID 19779, 2019.

[18] L. L. A. M. Pierri, "Isolation and Characterization of Stigmasterol and β-sitosterol from Odontonema strictum (Acanthaceae)," *JIBS*, vol. 2, no. 1, pp. 88–95, 2015.

[19] M. A. El-Shanawany, H. Sayed, S. R. M. Ibrahim, and M. A. A. Fayed, "Stigmasterol Tetracosanoate, a New Stigmasterol Ester from the Egyptian Blepharis ciliaris," *Drug Res*, vol. 65, no. 7, pp. 347–353, 2015.

[20] R. M. A. W. Silverstein, *Spectroscopic Identification of Organic Compounds*, John Wiley and Sons, Hoboken, NJ, USA, 6 edition, 1998.

[21] A. Haque, "Isolation of Betulinic Acid and 2,3-Dihydroxyolean-12-en-28-oic Acid from the Leaves of Callistemon linearis," *Dhaka University Journal of Science*, vol. 61, no. 2, pp. 211-212, 2013.

[22] M. El-Shanawany, "Chemical constituents, anti-inflammatory, and antioxidant activities of Anisotes trisulcus," *Bulletin of Faculty of Pharmacy, Cairo University*, vol. 52, no. 1, pp. 9–14, 2014.

[23] B. Juurlink, "Hydroxybenzoic acid isomers and the cardiovascular system," *Nutrition Journal*, vol. 13, no. 1, p. 63, 2014.

[24] R. Liu, A. Li, and A. Sun, "Preparative isolation and purification of hydroxyanthraquinones and cinnamic acid from the chinese medicinal herb Rheum officinale Baill. by high-speed counter-current chromatography," *J Chromatogr A*, vol. 1052, no. 1-2, pp. 217–21, 2004.

[25] R. Dhakal, "Phytochemical Constituents of the Bark of Vitex negundo L," *Journal of Nepal Chemical Society*, vol. 23, pp. 89–92, 2009.

[26] D. Y. Lee and Y. Liu, "Molecular structure and stereochemistry of silybin A, silybin B, isosilybin A, and isosilybin B, Isolated from Silybum marianum (milk thistle)," *J Nat Prod*, vol. 66, no. 9, pp. 1171–4, 2003.

[27] P. K. Agrawal, *Carbon 13 NMR of Flavonoids*, Elseiver, New york, NY, USA, 1989.

[28] N. Kim, "COMPLETE isolation and characterization of silybins and isosilybins from milk thistle (Silybum marianum)," *Org Biomol Chem*, vol. 1, no. 10, pp. 1684–9, 2003, http://www.rsc.org/suppdata/ob/b3/b300099k/.

[29] G. Y. Cao, "New neolignans from the seeds of Myristica fragrans that inhibit nitric oxide production," *Food chemistry*, vol. 173, pp. 231–237, 2015.

[30] L. Zhu, F. Yan, J. Chen, N. Zhang, X. Zhang, and X. S. Yao, "8-O-4'Neolignan Glycosides from the Aerial Parts of Matteuccia struthiopteris," *Chinese Chemical Letters*, vol. 27, pp. 63–65, 2016.

[31] J. M. J. K. Sinkkonen, "Lignans from the bark extract of Pinus sylvestris L," *Magn Reson Chem*, vol. 44, no. 6, pp. 633–6, 2006.

[32] https://Scifinder.cas.org/scifinder/view/scifinder/scifinderExplorerjsf.

[33] H. Liu, Y. Mou, J. Zhao et al., "Flavonoids from Halostachys caspica and their antimicrobial and antioxidant activities," *Molecules*, vol. 15, no. 11, pp. 7933–7945, 2010.

[34] S. S. A. V. V. I. Azimova, *Natural Compounds, Flavonoids, Plant Sources, Structure and Properties*, Springers, New York, Heidellerg Dordrecht, London, New York, 2013.

[35] G. Del Campo, I. Berregi, R. Caracena, and J. I. Santos, "Quantitative analysis of malic and citric acids in fruit juices using proton nuclear magnetic resonance spectroscopy," *Analytica Chimica Acta*, vol. 556, no. 2, pp. 462–468, 2006.

[36] G. K. Panigrahi, M. K. Suthar, N. Verma et al., "Investigation of the interaction of anthraquinones of Cassia occidentalis seeds with bovine serum albumin by molecular docking and spectroscopic analysis: correlation to their in vitro cytotoxic potential," *Food Research International*, vol. 77, no. 3, pp. 368–377, 2015.

Hindawi
Journal of Chemistry
Volume 2023, Article ID 3469727, 9 pages
https://doi.org/10.1155/2023/3469727

Research Article

Comparative Study of Antioxidant, Antidiabetic, Cytotoxic Potentials, and Phytochemicals of Fenugreek (*Trigonella foenum-graecum*) and Ginger (*Zingiber officinale*)

Javaria Hafeez,[1] Muhammad Naeem,[2] Tayyab Ali,[1] Bushra Sultan,[1] Fatma Hussain,[1] Haroon Ur Rashid,[3] Muhammad Nadeem,[4] and Ibrahim Shirzad[5]

[1]*Clinico-Molecular Biochemistry Laboratory, Department of Biochemistry, University of Agriculture, Faisalabad 38000, Pakistan*
[2]*College of Life Science, Hebei Normal University, Shijiazhuang 050024, China*
[3]*Department of Computer Science and Information Technology, University of Lahore, Sargodha, Pakistan*
[4]*Department of Management Sciences, National University of Modern Languages, Multan, Pakistan*
[5]*Quality Control Laboratories, Food and Drug Authority, Kabul, Afghanistan*

Correspondence should be addressed to Ibrahim Shirzad; ibrahim410660@gmail.com

Received 31 August 2022; Revised 13 October 2022; Accepted 23 March 2023; Published 31 March 2023

Academic Editor: Marwa Fayed

Trigonella foenum-graecum and *Zingiber officinale* are used as traditional medicinal plants for the treatment of infectious and inflammatory diseases. However, a comparative analysis and bioactivities of *T. foenum-graecum* and *Z. officinale* lack some necessary information for therapeutic purposes. This study was designed to evaluate the biochemical characterizations and biological efficacy of *T. foenum-graecum* and *Z. officinale* as antioxidant, antidiabetic, antiamnesic, and cytotoxic agents. Antioxidant activity was determined by DPPH free radical scavenging assay. Antidiabetic potentials were evaluated by glycation, alpha-amylase, and acetylcholinesterase inhibition assays. We performed biochemical characterization through analyses of high-performance liquid chromatography (HPLC) and FTIR (Fourier transform infrared spectroscopy). Results revealed that total phenolic contents (TPCs) (g GAE/100 g) of *T. foenum-graecum* and *Z. officinale* were 5.74 ± 0.81 g and 6.15 ± 0.06 g, respectively, and total flavonoid contents (TFCs) varied from 1.51 ± 0.58 g CE/100 g to 17.54 ± 0.58. DPPH scavenging potentials of *T. foenum-graecum* and *Z. officinale* extract were 50.27% and 88.82%, respectively. Antiglycation potentials of *T. foenum-graecum* and *Z. officinale* showed a maximum activity at 16–29% and 96%. Alpha-amylase and alpha-glucosidase inhibition ranged from 9.43–24.95 and 10.52–27.89 and 54.97%, respectively. All the test samples of *T. foenum-graecum* and *Z. officinale* showed acetylcholinesterase inhibition potential at 0.37–46.88%. HPLC analysis of *T. foenum-graecum* revealed the presence of quercetin, gallic acid, caffeic acid, vanillic acid, syringic acid, and cumeric acid, while *Z. officinale* revealed the quercetin, gallic acid, vanillic acid, benzoic acid, chlorogenic acid, p.Coumaric acid, ferulic acid, and cinnamic acid. FTIR analysis revealed the presence of aldehydes, ketones, aromatic compounds, amines, and carbonyl groups in *T. foenum-graecum*, while alcohol, alkane, alkene, ketone, amine, and ether are bioactives present in the methanolic extract of *Z. officinale*. It was concluded that a comparative analysis of *T. foenum-graecum* and *Z. officinale* showed that *Z. officinale* showed higher therapeutic effects.

1. Introduction

Different synthetic drugs and chemical compounds have been used for the treatment of infectious diseases. However, the application of phytomedicines has increased attention recently due to their therapeutic advantages over allopathic medicines like bioavailability, high solubility, and fewer side effects [1]. The extensive use of plant-derived medicines and medicinal plants in traditional cultures globally has enhanced the incorporation of phytochemicals into contemporary products for disease treatment and health promotion [2]. Medicinal plants contain secondary metabolites, also

known as phytochemicals, which encompass a large variety of natural products, including phenolics, flavonoids, alkaloids, glycosides, saponins, steroids, and tannins [2].

T. foenum-graecum is used as a traditional medicinal plant around the world due to its diverse nature of phytoconstituents, such as steroids, saponins, diosgenin, gitogenin, glycosides, hydrocarbons, amino acids, and gingerol [3]. Along with it, *Z. officinale* is also used as a phytomedicine for the treatment of infectious and metabolic diseases [4]. *Z. officinale* is a rich source of bioactive compounds, electrolytes, vitamins, volatile oily components, gingerols, heptanoids, alkaloids, sulphates, steroidal derivatives, and glycosides isolated [5]. Due to the presence of these bioactive compounds and secondary metabolites, *T. foenum-graecum* and *Z. officinale* are potentially employed for the treatment of inflammatory and infectious diseases.

Ginger (*Z. officinale*) is well known for its potential against several diseases like cancers, hepatocellular carcinoma [6], diabetes mellitus [7], osteoarthritis, and myocardial infarction [8]. *Z. officinale* is also used for bacterial infections, boosts immunity, and enhances gastrointestinal functions [9]. Several studies revealed *Z. officinale* exhibited high potential in reducing oxidative stress and thus minimized the production of free radical species in living tissues [10]. It also activates the different genes responsible for suppressing tumor function, thus exhibiting anticancerous potential [11, 12].

T. foenum-graecum is used as a medicinal plant for the treatment of diabetes mellitus [13], rheumatic arthritis, injuries, muscular weakness, throat infections, hypertension [14], neurological disorders, and cardiac diseases [15]. Several studies showed the androgenic and anabolic effects of *T. foenum-graecum* in human reproductive physiology. The hydrolysates proteins obtained from the rhizome extract *T. foenum-graecum* showed anticancer potential as they minimized the levels of reactive oxygen species. Hydrolysates are a rich source of protein and are also used for the treatment of colorectal cancers [16].

Keeping in view of the literature update, we hypothesized that a comparative analysis of extracts of *T. foenum-graecum* leaf and *Z. officinale* rhizome might add sufficient knowledge to the scientific data. The biological potential of *T. foenum-graecum* leaf and *Z. officinale* rhizome lack the necessary information for therapeutic applications. However, this type of comparative study approach was not reported in the literature before. This study aimed to evaluate *in vitro* antioxidant, antidiabetic, and antiamnesic activities of *T. foenum-graecum* leaf and *Z. officinale* rhizome. In addition, we performed biochemical characterization through high-performance liquid chromatography (HPLC) and FTIR (Fourier transform infrared spectroscopy) for the identification of bioactive compounds and functional groups.

2. Materials and Methods

2.1. Plant Materials. *T. foenum-graecum* (fenugreek) leaves and *Z. officinale* rhizome samples were bought from the vendor market of Faisalabad and were identified by the Department of Botany, University of Agriculture Faisalabad [17].

2.2. Preparations of Extracts. Extracts of ground rhizomes and leaves were prepared by using *n*-hexane, ethanol, and methanol, along with water extract. The first extraction was carried out by maceration method in methanol for three consecutive days with repeated filtrations. The semisolid final extract was dissolved in water and then fractionated into ethanol and *n*-hexane solvents [18].

2.3. Total Phenolic Content (TPC). Total phenolic contents were measured by following the Folin–Ciocalteu method [18]. In this method, the reaction mixture was prepared by dissolving the 1.58 mL distilled water into 20 μL test samples. Then, 3 mL Na_2CO_3 (1% w/v) was mixed into the reaction mixture, and incubation was carried out at 25°C for 10 minutes. At wavelength 750 nm, the blue color compound was produced, which showed the highest absorption, and it indicated the number of phenolics present in test samples.

2.4. Total Flavonoid Content (TFC). Total flavonoid contents were measured by following the aluminium trichloride ($AlCl_3$) colorimetric method [19]. In this method, plant extract (50 μL) was mixed with 160 μL of $NaNO_2$, along with 1.26 mL of distilled water, and incubation was carried out at 25°C for 10 minutes. Then, 1 mL of NaOH and 10% 300 μL of $AlCl_3$ were added to the reaction mixture. The absorbance was measured at 510 nm, which indicated the number of flavonoids present in test samples.

2.5. DPPH Radical Scavenging Assay. The antioxidant potential of extracts was determined using the 2,2-diphenyl-1-picrylhydrazyl (DPPH) free radical scavenging method. Extracts and 5 mL DPPH were mixed together and were kept at 25°C temperature for 30 minutes. Butylated hydroxytoluene was used as a standard [20]. The antioxidant activity was calculated by using the following formula:

$$\%\text{DPPH inhibition} = 100\text{X}[\text{A Blank} - \text{A Sample/A Blank}]. \quad (1)$$

2.6. Antidiabetic Activity

2.6.1. Glycation Inhibition Assay. Test samples, D-glucopyranose (100.0 mg) and serum protein (10.0 mg), were mixed together into a 67 mM solution of sodium phosphate and maintained at pH 7.2. The reaction mixture was then incubated at 37°C for 48 hours. Absorbance was measured at 540 nm by using the spectrophotometer. Samples without D-glucose and metformin were used as controls [21]. The % inhibition was calculated as follows:

$$\%\text{ Inhibitory Activity} = 100\text{ x}[\text{Abs c/Abs ex} - \text{Abs c}]. \quad (2)$$

2.6.2. Alpha-Amylase Inhibitory Activity. Alpha-amylase inhibition activity of extracts was measured by using the colorimetric method. In this method, 500 μL of alpha-amylase enzyme (porcine pancreatic) was prepared into

0.02 M buffer maintained at pH 6.9 and the test samples (500 μL) were incubated at 25°C for 10 minutes. Then, 1 mL of dinitrosalicylic acid (DNS) reagent was added to the reaction mixture and heated in a boiling water bath for 30 minutes. Buffer was used as negative control, and the acarbose drug positive was used as a positive control. Absorbance was measured at 540 nm by using the spectrophotometer [20]. The % inhibition was calculated as follows:

$$\%\ \text{Alpha} - \text{Amylase inhibition: } (\text{Ac} - \text{As/Ac}) \times 100, \quad (3)$$

where Ac is absorbance of the control and As is absorbance of test samples.

2.6.3. Acetylcholinesterase Inhibitory Activity. Acetylcholinesterase inhibitory activity of plant extracts was measured by mixing Ellman's reagent, phosphate buffer, and acetylcholinesterase. The reaction mixture was incubated at 25°C for 10 minutes. Then, a substrate (acetylcholine iodide) was added to the reaction mixture and absorbance was measured at 412 nm [22]. Extraction solvent was used as a negative control, whereas physostigmine was used as a positive control. Percentage acetylcholinesterase (AChE) inhibition was calculated by following the formula:

$$\text{Acetylcholinesterase (AChE) inhibition: Absorbance (Control} - \text{Sample)/Absorbance control]} \times 100. \quad (4)$$

2.7. Chemical Characterization

2.7.1. HPLC Analysis. HPLC was performed for the identification of different compounds in plant extracts. HPLC analysis was performed at Hi-Tech Laboratory, University of Agriculture, Faisalabad, Pakistan, under chromatographic conditions solvent A (acetic acid, water 6 : 94) and solvent B (acetonitrile). Shim-pack CLC ODS (C-18) column was used as a stationary phase with a 1 mL·min^{-1} flow rate. Phenols and flavonoids were identified at 280 nm on the basis of comparison (retention times of peaks) of plant samples [23].

2.7.2. FTIR Analysis. Fourier transform infrared spectroscopy was performed for the structural identification of functional groups of different compounds in extracts. A thin film was prepared by mixing the powdered samples and potassium bromide and infrared spectrum were measured at 4 cm^{-1} resolution and 25°C temperature. OPUS software was used to measure the IR spectra. The results were compared with standards for the detection of active groups [24].

2.7.3. Statistical Analysis. Data were subjected to analysis of variance (ANOVA), and a comparison between the means of two activities was carried out by using SPSS with the level of p significant at <0.05. Data were finally expressed as mean ± SD or percentage.

3. Results and Discussion

3.1. Chemical Characterization

3.1.1. HPLC Analysis. Table1 and Figure 1 show the different compounds in the extract of *Z. officinale* identified by the HPLC chromatogram. The HPLC analysis revealed the existence of phenolic acids and flavonoids, i.e., quercetin (18.17 ppm), gallic acid (2.71 ppm), vanillic acid (5.68 ppm), benzoic acid (15.93 ppm), chlorogenic acid (17.22 ppm), p-coumaric acid (1.16 ppm), ferulic acid (3.13 ppm), and cinnamic acid (0.37 ppm). Table 2 and Figure 2 show the different compounds in the extract of *T. foenum-graecum* identified by the HPLC chromatogram. Quercitin was determined at the peak of 3.073, having a concentration of 4.12 ppm. While gallic acid, caffeic acid, vanillic acid, syringic acid, and M. cumeric acid were determined at peaks 4.487, 12.340, 12.973, 15.507, and 19.733, respectively, having concentrations of 0.43 ppm, 0.57 ppm, 0.61 ppm, 0.15 ppm, and 0.14 ppm.

Our results are agreed with the previous studies. A recent study reported that luteolin (15.80%), apigenin (14.41%), and glycosides (12.02%) were identified in the rhizome of *Z. officinale* [25]. Another study revealed that nonacylated compounds, apigenin (8.82%) and kaempferol (9.61%) derivatives and acylated apigenin (6.59%), glycosides (6.59%), and luteolin (5.60%), were screened in *Z. officinale*, respectively. These flavonoids were found to be the major compounds with 87.80% of the total identified compounds. The other compounds were present at lower relative percentages [26]. Another study revealed that quercetin and kaempferol isolated *T. foenum-graecum* leaves with concentration values of 12.6 mg/g and 11.2 mg/g, respectively [27].

3.1.2. FTIR Analysis. Table 1 and Figure 3 show the different peaks of functional groups in the extract of *Z. officinale* identified by FTIR analysis. The broad peak of the O-H and N-H bond at 3276.3 cm^{-1} indicates alcohols and secondary amines. Peaks at 928.1 cm^{-1} as well as 991.5 cm^{-1} and 2926.0 cm^{-1} elucidate alkenes and alkanes, which projected out of plane bending due to =C-H and stretching of CH_2, respectively. Table 2 and Figure 4 show the different peaks of functional groups in the extract of *T. foenum-graecum* identified by the FTIR analysis. Three functional groups were identified at medium peak, four at strong peak and one functional group at weak peak type in the range of 1000–3000. In medium peak type C-H, N-H, N-H, and O-H functional groups were identified at peaks 2900, 3400, 1530, and 1440, respectively, whereas in strong peak type functional groups -CH, N-O, S=O, and C=C were determined at

Table 1: Chemical characterization of *Zingiber officinale*.

Sr.no	*Compound name*	*HPLC Peak area*	*Amount (ppm)*
1	Quercetin	341.037	18.17
2	Gallic acid	75.336	2.71
3	Vanillic acid	91.680	5.68
4	Benzoic acid	150.354	15.93
5	Chlorogenic acid	220.818	17.22
6	p-Coumaric acid	81.639	1.16
7	Ferulic acid	42.235	3.13
8	Cinnamic acid	28.439	0.37

Sr.no	*Wave number (cm^{-1})*	*FTIR Functional group*	*Type of bond*
1	3276.3	Secondary amide, alcohol	N-H stretching, O-H stretch
2	2926.0	Alkane	$-CH_2$ stretching
3	1636.3	Alkene, primary amines, water, ketone	C=C stretching, N-H bending, H-O-H, C=C-C=O
4	1148.0	Amine, alcohol	C-N, O-H stretching
5	1075.3	Amines, alcohol	C-N stretching, C-O stretching
6	991.5	Alkene	=C-H
7	928.1	Alkenes	=C-H
8	861.0	Ether	C-O stretching

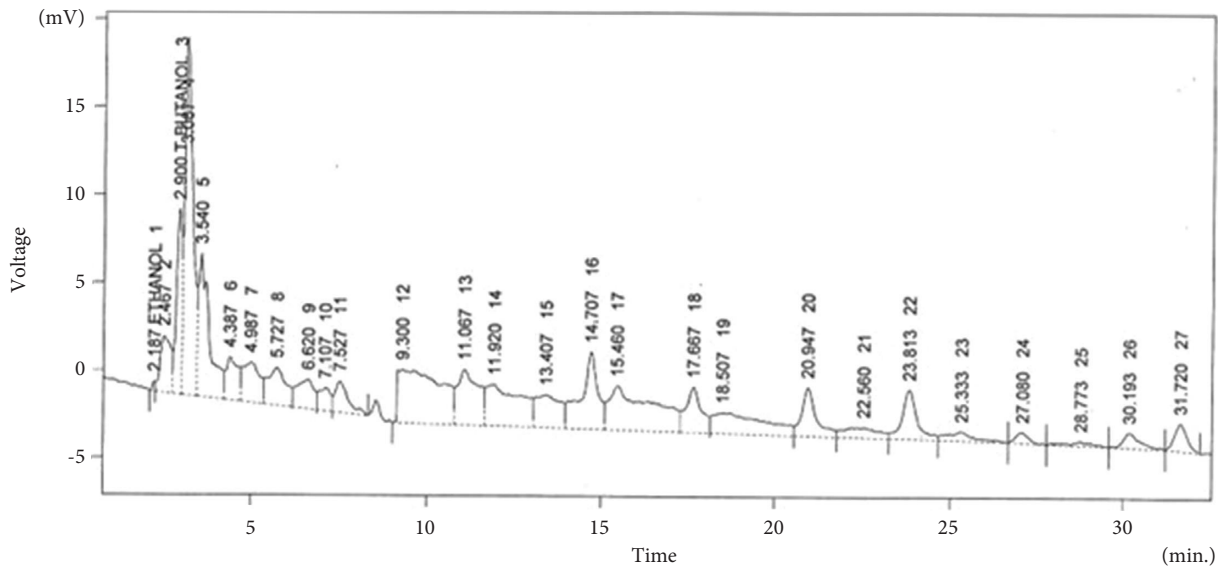

Figure 1: Representative HPLC chromatogram of *Zingiber officinale*.

peaks 2820, 1520, 1190, and 990, respectively. Only one peak type was weak, identified at 1800 with functional group C-H. This data indicated the presence of polyphenols, alcohols, and carboxylic compounds. In a previous study, aldehyde and ketone functional groups were identified at 1705 cm^{-1}.

According to the previous studies, *Z. officinale* exhibited wave numbers at 3443, 2970, 1475, 1439, 1386, and 1238 (cm^{-1}) due to C-H/O-H stretch, C=C (aromatic), C-N (nitrile), C-O (acid and ester stretch), respectively [28]. A recent study revealed that *Z. officinale* exhibited N-H stretch of proteins, a symmetric stretch of C-O of COO groups, CH_2 bending of lipids and symmetric and asymmetric stretch of P=O of nucleic acids at 3290, 1236, 1400, and 1236 wave numbers (cm^{-1}), respectively [29]. Previous studies showed that the carbonyl group was found at 1790 cm^{-1} in *T. foenum-graecum* leaves extract. Aromatic functional groups, including C-H, O-H, and N-H were identified at a spectral range of 3800 cm^{-1}–2600 cm^{-1} [30]. A recent study revealed that recognized peaks within similar spectral ranges that suggested the presence of methylene, carbonyl, and phenolic compounds similar to the current study [31].

3.1.3. Antioxidant Activity. Table 3 shows that TPC in the extracts of *Z. officinal* rhizome lies in the range of 3.16 ± 0.77–6.15 ± 0.06 (GAE/100 g), while Table 4 shows

Table 2: Structural data analysis of *Trigonella foenum-graecum* leaves.

		HPLC		
Retention time	*Area (mV. s)*	*Area (%)*	*Amount (ppm)*	*Compound name*
3.07	77.54	12.2	4.12	Quercetin
4.49	12.09	1.9	0.43	Gallic acid
12.34	3.58	0.5	0.57	Caffeic acid
12.97	9.26	1.5	0.61	Vanillic acid
15.51	5.24	1.0	0.15	Syringic acid
19.73	3.75	0.5	0.14	m.Cumeric acid
		FTIR		
Frequency range	*Wave number*	*Peak type*	*Functional group*	*Type of bonding*
2840–3000	2900	Medium	-CH	Saturated -CH
2800–3000	2820	Strong	-CH	Saturated -CH
3400–3300	3400	Medium	N-H	N-H stretching
1550–1500	1520	Strong	N-O	N-O stretching
1440–1395	1440	Medium	O-H	O-H bending
1200–1185	1190	Strong	S=O	S=O stretching
995–985	990	Strong	C=C	C=C bending
1870–1540	1800	Weak	C-H	C-H bending

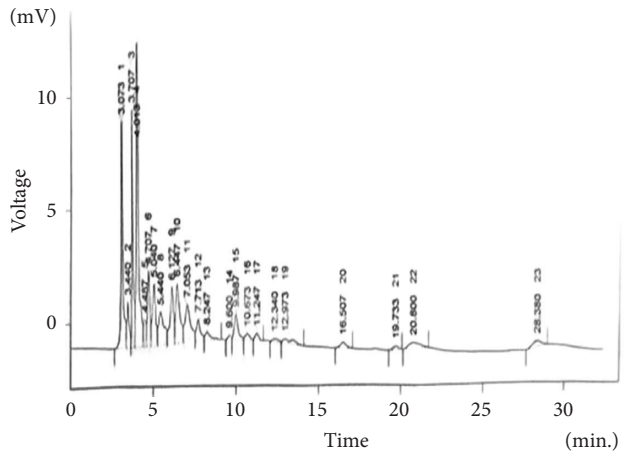

Figure 2: HPLC chromatogram of *Trigonella foenum-graecum* leaves.

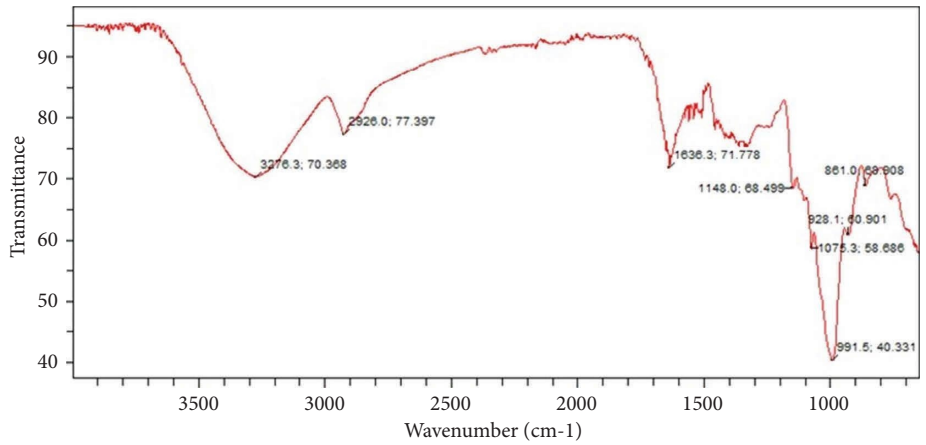

Figure 3: Representative FTIR spectrum of *Zingiber officinale*.

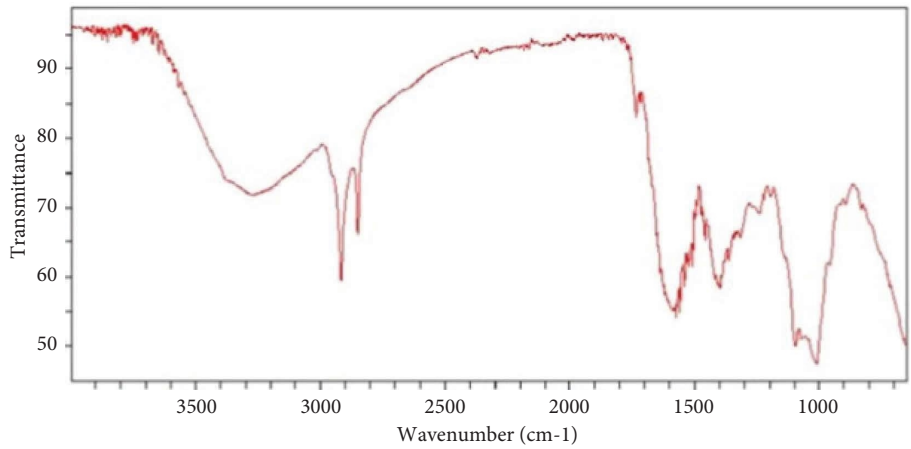

Figure 4: Representative FTIR spectrum of *Trigonella foenum-graecum* leaves.

Table 3: Different extracts and biological efficacies of *Zingiber officinale* rhizome.

Activities	Methanol	Ethanol	*n*-hexane	Aqueous	Control
TFC	10.04 ± 0.18	9.52 ± 0.10	7.09 ± 0.14	9.93 ± 0.09	—
TPC	5.56 ± 0.82	6.15 ± 0.06	3.75 ± 0.92	3.16 ± 0.77	—
DPPH (IC_{50})	21.11	88.82	38.14	50.23	90
Glycation	67	96	20	69	53
Alpha-amylase	28	54.97	6.01	15.27	13.58
AChE	40.8	17.3	46.88	0.37	59.51

Data expressed as mean ± SD or percentage. TPC: total phenolic contents expressed as g gallic acid equivalents/100 g dry weight; TFC: total flavonoid contents expressed as g catechin equivalents/100 g dry weight; DPPH: 2,2-diphenyl l-picrylhydrazyl. Positive controls: BHT; butylated hydroxytoluene (antioxidant activity), metformin (antiglycation assay), glucobay (*α*-amylase inhibitory assay), and physostigmine (AChE inhibitory assay).

Table 4: Different extracts and biological efficacies of *Trigonella foenum-graecum* leaf.

Sample	ME	EE	NHE	AE	Control
Antioxidant contents and activity					
TFC	2.38 ± 0.26	1.88 ± 0.31	1.51 ± 0.58	2.93 ± 0.09	—
TPC	6.23 ± 0.76	6.18 ± 0.06	5.75 ± 0.86	5.74 ± 0.81	—
DPPH	32.56	45.78	38.14	50.27*	90
Antidiabetic activity—percentage inhibition					
Glycation	29*	23	16	20	53
Alpha-amylase	24.95*	17.93	11.30	9.43	48.20
Antiamnesic activity					
AChE inhibition	14.08	8.37	4.62	10.37	59.51

Data expressed as mean ± SD or percentage of triplicate measurements. * Significant at $p < 0.05$. ME: methanol extract; EE: ethanol extract; NHE: *n*-hexane extract; AE: aqueous extract. TPC: total phenolic contents expressed as g gallic acid equivalents/100 g dry weight; TFC: total flavonoid contents expressed as g catechin equivalents/100 g dry weight; DPPH: 2,2-diphenyl l-picrylhydrazyl free radical scavenging potential expressed as percentage. Positive controls: BHT; butylated hydroxytoluene (antioxidant activity), metformin (antiglycation assay), physostigmine (AChE inhibitory assay), glucobay (alpha-amylase inhibitory assay), and acarbose (alpha-glucosidase).

that different extract fractions of *T. foenum-graecum* leaves with TPC in the range 5.74 ± 0.81–6.23 ± 0.76 (GAE/100 g). Total flavonoid contents (TFC) varied from 3.52 ± 0.13–17.54 ± 0.58 (GAE/100 g) in the extract fractions of *Z. Officinale* rhizome. TFC (g CE/100 g) in different extract fractions of *T. foenum-graecum* leaves varied from 1.51 ± 0.58–2.93 ± 0.09 (GAE/100 g). Free radical scavenging activity was maximally (88.82%) shown by ethanol fraction while minimum (21.11%) by methanol fraction in *Z. officinale* rhizome extracts. Regarding antioxidant activity in the *T. foenum-graecum* leaf extracts, DPPH reducing activity was observed in the case of aqueous extract (50.27%).

Oxidative stress is induced during lipid and carbohydrate metabolisms that lead to damage to the biological membranes and biomolecules [32]. The presence of phytochemicals such as polyphenols supports the use of medicinal plants in alternative and traditional medicines and has received continued attention since being responsible for supporting plant, animal, and human health [2, 33]. The phenolic compounds, including flavonoids, contribute to

human health through antioxidant activity, free radical scavenging, and antimicrobial properties [2].

Our findings are agreed with the previous studies. A recent study revealed that *T. foenum-graecum* had 46.08 ± 0.15 mg GAE/g phenolic compounds, 13.02 ± 0.44 mg/g flavonoids content, and $45.41 \pm 2.1\%$ antioxidant activity (DPPH) [34]. Another study reported that methonolic extract of *Z. officinale* possessed 13.5 ± 2.26 g GAE/100 g phenolic contents [35]. As reported earlier, *Z. officinale* extract possessed 2.80 mg CE/g flavonoid contents, which agreed with the current study. A recent study showed that methanolic extract *Z. officinal* exhibited 15% DPPH scavenging activity [36], and the aqueous extract showed 52.50% radical scavenging activity [37], which is in agreement with the findings of the present study.

3.1.4. Antidiabetic Potential. Table 3 shows the results of the antidiabetic potential of the rhizome extract of *Z. officinal*. Ethanol fractions of *Z. officinal* showed a 96% antiglycation effect. The ethanol fraction of *Z. officinale* showed maximum (54.97%) inhibition of α-amylase. Table 4 shows the results of the antidiabetic potential of *T. foenum-graecum* leaf extract, showing inhibitions of alpha-amylase are 9.43 to 24.95%.

Secondary metabolites like polyphenols are helpful for controlling the glycemic index in diabetic patients [38]. Previous studies reported that an aqueous fraction of *Z. officinale* exhibited α-amylase inhibition activity by 50% (3.14 ± 0.05 mg·ml^{-1}) in a dose-dependent manner and also indicated that phytoconstituents of *Z. officinale* can actively inhibit amylase enzyme and glycation processes [39]. Another study revealed aqueous extract of *Z. officinale* showed α-amylase 68% inhibition which also supports our findings [40].

Another study revealed the glycation potential of ethanolic and aqueous extracts of *T. foenum-graecum*. The hindrance of alpha-amylase and alpha-glucosidase activities reduces the production of monosaccharides and absorption through intestinal epithelial cells and controls hyperglycemia [41].

3.1.5. Acetylcholinesterase Inhibitory Activity. Table 3 shows the inhibitory effect of the extract of *Z. officinale* on acetylcholinesterase activity. Results revealed that the extract of *Z. officinale* showed a maximum of 46.88% inhibitory effect on acetylcholinesterase activity. Table 4 shows that all the test samples of *T. foenum-graecum* showed 4.62%–14.08% acetylcholinesterase inhibitions.

Alzheimer's disease, the most prevalent type of neurological disorder, has fewer treatment opportunities. The activity of acetylcholinesterase is linked with Alzheimer's disease, which can be blocked through the action of medicinal plants. Plant-based medications have the neuroprotective potential for controlling neurodegenerative disorders [42]. Previous studies showed that *Z. officinale* extract showed more than 80% acetylcholine esterase inhibition [43]. Similarly, another study reported 2.422 ± 0.133 mg/mL AChE inhibition by *Z. officinale* extract [44]. Another study revealed that *T. foenum-graecum* seed has a potential AchE inhibitory activity and is considered a promising therapeutic option to treat Alzheimer's disease [45]. A recent study showed the positive healing efficacies of *T. foenum-graecum* in neurodegenerative conditions. Several studies have reported antidepressant and antianxiety effects along with modulation of cognitive behaviour by *T. foenum-graecum* [46].

4. Conclusion

T. foenum-graecum and *Z. officinale* are consumed as traditional medicinal plants worldwide and are also used as phytomedicine for the treatment of infectious diseases and bacterial infections, having numerous medicinal properties. The comparative analysis of *T. foenum-graecum* and *Z. officinale* showed that *Z. officinale* showed higher therapeutic effects due to the presence of quercetin, gallic acid, caffeic acid, vanillic acid, syringic acid, cumeric acid, benzoic acid, chlorogenic acid, p.Coumaric acid, ferulic acid, and cinnamic acid. This research laid the foundation for the discovery of optimized, cost-effective*in vitro* bioassays of active constituents of different plants. *T. foenum-graecum* and *Z. officinale* could be used as nutraceutical adjuncts as they have immense prospects to be further explored in animal and human trials. Furthermore, these medicinal plants are potential sources of significant natural antioxidant and marked antimicrobial agents. Furthermore, isolation, purification, and investigations of the bioactive constituents of these plants are required to reveal more health benefits for the public and therapeutics uses in the medical field.

Data Availability

The data used to support the findings of this study are available from the corresponding authors upon request.

Conflicts of Interest

The authors declare that they have no conflicts of interest.

Authors' Contributions

Conception and design of the study were performed by Javaria Hafeez; data acquisition was performed by Muhammad Naeem, Tayyab Ali, and Javaria Hafeez; data analysis and interpretation were performed by Haroon Ur Rashid, Muhammad Nadeem, Fatma Hussain, and Bushra Sultan; drafting manuscript was performed by Ibrahim Shirzad, Muhammad Naeem, Tayyab Ali, and Javaria Hafeez; critical revision of manuscript was performed by Muhammad Naeem, Tayyab Ali, Ibrahim Shirzad, and Fatma Hussain; and final approval was performed by Ibrahim Shirzad, Fatma Hussain, Muhammad Naeem, Tayyab Ali, Bushra Sultan, and Javaria Hafeez.

References

[1] R. Mohammadinejad, A. Shavandi, and D. S. Raie, "Plant molecular farming: production of metallic nanoparticles and therapeutic proteins using green factories," vol. 21, no. 8, 2019.

[2] M. Soleimani, A. Arzani, V. Arzani, and T. H. Roberts, "Phenolic compounds and antimicrobial properties of mint and thyme," *Journal of Herbal Medicine*, vol. 36, Article ID 100604, 2022.

[3] S. D. Robert, A. A. S. Ismail, and W. I. Wan Rosli, "*Trigonella foenum-graecum* seeds lowers postprandial blood glucose in overweight and obese individuals," *Journal of Nutrition and Metabolism*, vol. 2014, Article ID 964873, 5 pages, 2014.

[4] M. Zhang, R. Zhao, D. Wang et al., "Ginger (*Zingiber officinale Rosc.*) and its bioactive components are potential resources for health beneficial agents," *Phytotherapy Research*, vol. 35, no. 2, pp. 711–742, 2021.

[5] K. Tanaka, M. Arita, H. Sakurai, N. Ono, and Y. Tezuka, "Analysis of chemical properties of edible and medicinal ginger by metabolomics approach," *BioMed Research International*, vol. 2015, Article ID 671058, 7 pages, 2015.

[6] M. Aviram and M. Rosenblat, "Pomegranate protection against cardiovascular sdiseaes," *Evidence-based Complementary and Alternative Medicine*, vol. 2012, Article ID 382763, 2012.

[7] M. Talebi, S. İlgün, V. Ebrahimi et al., "*Zingiber officinale* ameliorates Alzheimer's disease and Cognitive Impairments: lessons from preclinical studies," *Biomedicine & Pharmacotherapy*, vol. 133, Article ID 111088, 2021.

[8] Y. Dong, K. W. Yao, and J. Wang, "[Pharmacological effects and clinical applications of *Zingiber officinale* and its processed products]," *Zhongguo Zhongyao Zazhi*, vol. 43, no. 10, pp. 2020–2024, May 2018.

[9] V. Ebrahimzadeh Attari, A. Malek Mahdavi, Z. Javadivala, S. Mahluji, S. Zununi Vahed, and A. Ostadrahimi, "A systematic review of the anti-obesity and weight lowering effect of ginger (*Zingiber officinale Roscoe*) and its mechanisms of action," *Phytotherapy Research*, vol. 32, no. 4, pp. 577–585, 2018.

[10] B. G. Eid, H. Mosli, A. Hasan, and H. M. El-Bassossy, "Ginger ingredients alleviate diabetic prostatic complications: effect on oxidative stress and fibrosis," *Evidence-based Complementary and Alternative Medicine*, vol. 2017, Article ID 6090269, 12 pages, 2017.

[11] Y. Liu, J. Liu, and Y. Zhang, "Research progress on chemical constituents of zingiber officinale roscoe," *BioMed Research International*, vol. 2019, Article ID 5370823, 2019.

[12] S. Prasad and A. K. Tyagi, "Ginger and its constituents: role in prevention and treatment of gastrointestinal cancer," *Gastroenterology Research and Practice*, vol. 2015, pp. 1–11, 2015.

[13] G. A. Geberemeskel, Y. G. Debebe, and N. A. Nguse, "Antidiabetic effect of fenugreek seed powder solution (*Trigonella foenum-graecum L.*) on hyperlipidemia in diabetic patients," *Journal of Diabetes Research*, vol. 2019, Article ID 8507453, 8 pages, 2019.

[14] S. Oufquir, M. Ait Laaradia, Z. El Gabbas et al., "*Trigonella foenum-Graecum L.* Sprouted seed extract: its chemical HPLC analysis, abortive effect, and neurodevelopmental toxicity on mice," *Evidence-based Complementary and Alternative Medicine*, vol. 2020, pp. 1–10, 2020.

[15] S. Goyal, N. Gupta, and S. Chatterjee, "Investigating therapeutic potential of *Trigonella foenum-graecum L.* As our defense mechanism against several human diseases," *Journal of Toxicology*, vol. 2016, Article ID 1250387, 10 pages, 2016.

[16] A. Allaoui, S. Gascón, S. Benomar et al., "Protein hydrolysates from fenugreek (*Trigonella foenum graecum*) as nutraceutical molecules in colon cancer treatment," *Nutrients*, vol. 11, no. 4, pp. 724–750, 2019.

[17] N. Mehmood, M. Zubaır, K. Rızwan, N. Rasool, M. Shahid, and V. Uddin Ahmad, "Antioxidant, antimicrobial and phytochemical analysis of *Cichorium intybus* seeds extract and various organic fractions," *Iranian Journal of Pharmaceutical Research*, vol. 11, no. 4, pp. 1145–1151, 2012.

[18] F. Hussain, A. Akram, J. Hafeez, and M. Shahid, "Biofunctional characterization of red, black and white ginseng (*Panax ginseng meyer*) root extracts," *Revista Mexicana de Ingenieria Quimica*, vol. 20, no. 1, pp. 175–186, 2020.

[19] A. M. Chahardehi, D. Ibrahim, and S. F. Sulaiman, "Antioxidant activity and total phenolic content of some medicinal plants in Urticaceae family," *The Journal of Applied Biological Sciences*, vol. 3, no. 2, pp. 25–29, 2009.

[20] F. Hussain and F. Ikram, "Antioxidant and antidiabetic potential of saponin fraction isolated from moringa oleifera leaves," *Biological Sciences - PJSIR*, vol. 63, no. 2, pp. 86–92, 2020.

[21] H. Matsuda, T. Wang, H. Managi, and M. Yoshikawa, "Structural requirements of flavonoids for inhibition of protein glycation and radical scavenging activities," *Bioorganic & Medicinal Chemistry*, vol. 11, no. 24, pp. 5317–5323, 2003.

[22] A. Rahman, M. I. Choudhary, and W. J. Thomsen, *Bioassay Techniques for Drug Development, Bioassay Tech*, CRC Press, Boca Raton, FL, USA, 2001.

[23] M. S. Pak-Dek, A. Osman, and N. G. Sahib, "Effects of extraction techniques on phenolic components and antioxidant activity of Mengkudu (*Morinda citrifolia L.*) leaf extracts," *Journal of Medicinal Plants Research*, vol. 5, no. 20, pp. 5050–5057, 2011.

[24] S. K. Sachin, K. V Ashwini, and C. V Kawade Ashwini, "Isolation and standardization of gingerol from ginger rhizome by using TLC, HPLC, and identification tests," *The Pharma Innovation Journal*, vol. 6, no. 2, pp. 179–182, 2017.

[25] S. Tanweer, T. Mehmood, S. Zainab, Z. Ahmad, and A. Shehzad, "Comparison and HPLC quantification of antioxidant profiling of ginger rhizome, leaves and flower extracts," *Clinical Phytoscience*, vol. 6, no. 1, p. 12, 2020.

[26] H. Tohma, İ. Gülçin, E. Bursal, A. C. Goren, S. H. Alwasel, and E. Koksal, "Antioxidant activity and phenolic compounds of ginger (*Zingiber officinale Rosc.*) determined by HPLC-MS/MS," *Journal of Food Measurement and Characterization*, vol. 11, no. 2, pp. 556–566, 2017.

[27] T. Visuvanathan, L. T. L. Than, J. Stanslas, S. Y. Chew, and S. Vellasamy, "Revisiting *Trigonella foenum-graecum L.*: pharmacology and therapeutic potentialities," *Plants*, vol. 11, no. 11, p. 1450, 2022.

[28] G. A. Otunola, A. J. Afolayan, E. O. Ajayi, and S. W. Odeyemi, "Characterization, antibacterial and antioxidant properties of silver nanoparticles synthesized from aqueous extracts of Allium sativum, Zingiber officinale, and Capsicum frutescens Allium sativum, Zingiber officinale, and Capsicum frutescens," *Pharmacogn Magazine*, vol. 13, no. 50, p. 201, 2017.

[29] U. A. Awan, S. Ali, A. M. Shahnawaz et al., "Biological activities of *Allium sativum* and *Zingiber officinale* extracts on clinically important bacterial pathogens, their phytochemical and FT-IR spectroscopic analysis," *Pakistan journal of pharmaceutical sciences*, vol. 30, no. 3, pp. 729–745, 2017.

[30] B. Sambandam, D. Thiyagarajan, A. Ayyaswamy, and P. Raman, "Extraction and isolation of flavonoid quercetin from the leaves of *Trigonella foenum-graecum* and their antioxidant activity," *International Journal of Pharmacy and Pharmaceutical Sciences*, vol. 8, no. 6, pp. 120–124, 2016.

[31] S. Akbari, N. H. Abdurahman, R. M. Yunus, O. R. Alara, and O. O. Abayomi, "Extraction, characterization and antioxidant activity of fenugreek (*Trigonella-Foenum Graecum*) seed oil," *Materials Science for Energy Technologies*, vol. 2, no. 2, pp. 349–355, 2019.

[32] F. Hussain and H. U. R. Kayani, "Aging - oxidative stress, antioxidants and computational modeling," *Heliyon*, vol. 6, no. 5, Article ID e04107, 2020.

[33] R. Kiani, A. Arzani, and S. A. M. Mirmohammady Maibody, "Polyphenols, flavonoids, and antioxidant activity involved in salt tolerance in wheat, *Aegilops cylindrica* and *their amphidiploids*," *Frontiers of Plant Science*, vol. 12, pp. 1–13, 2021.

[34] B. B. Aggarwal, S. Prasad, S. Reuter et al., "Identification of novel anti-inflammatory agents from ayurvedic medicine for prevention of chronic diseases ;reverse pharmacology; and ;bedside to bench; approach," *Current Drug Targets*, vol. 12, no. 11, pp. 1595–1653, 2011.

[35] R. R. Singh, C. V. Raju, I. P. Lakshmisha et al., "Analysis of in-vitro antioxidant activities of crude potato peel and ginger extract," *Natl. J. Life Sci.*vol. 13, pp. 7–12, 2016.

[36] A. Ghasemzadeh, H. Z. E. Jaafar, and A. Rahmat, "Antioxidant activities, total phenolics and flavonoids content in two varieties of Malaysia young ginger (*Zingiber officinale Roscoe*)," *Molecules*, vol. 15, no. 6, pp. 4324–4333, 2010.

[37] S. Ghosh and P. Bhateja, "A process for standardization of ayurvedic polyherbal formulation (churna) for antioxidant activity," *RRJoPS*, vol. 5, no. 2, pp. 1–7, 2014.

[38] F. Shidfar, A. Rajab, T. Rahideh, N. Khandouzi, S. Hosseini, and S. Shidfar, "The effect of ginger (*Zingiber officinale*) on glycemic markers in patients with type 2 diabetes," *Journal of Complementary and Integrative Medicine*, vol. 12, no. 2, pp. 165–170, 2015.

[39] G. Oboh, A. J. Akinyemi, A. O. Ademiluyi, and S. A. Adefegha, "Inhibitory effects of aqueous extracts of two varieties of ginger on some key enzymes linked to type-2 diabetes in vitro," *Journal of Food and Nutrition Research*, vol. 49, no. 1, pp. 14–20, 2010.

[40] N. B. Abdulrazaq, M. M. Cho, N. N. Win, R. Zaman, and M. T. Rahman, "Beneficial effects of ginger *(Zingiber officinale)* on carbohydrate metabolism in streptozotocin-induced diabetic rats," *The British Journal of Nutrition*, vol. 108, no. 7, pp. 1194–1201, 2012.

[41] K. Papoutsis, J. Zhang, M. C. Bowyer, N. Brunton, E. R. Gibney, and J. Lyng, "Fruit, vegetables, and mushrooms for the preparation of extracts with α-amylase and α-glucosidase inhibition properties: a review," *Food Chemistry*, vol. 338, Article ID 128119, September 2020.

[42] F. Fernandes, M. F. Barroso, A. De Simone et al., "Multi-target neuroprotective effects of herbal medicines for Alzheimer's disease," *Journal of Ethnopharmacology*, vol. 290, February, Article ID 115107, 2022.

[43] M. Mathew and S. Subramanian, "In vitro evaluation of anti-Alzheimer effects of dry ginger (*Zingiber officinale Roscoe*) extract," *Indian Journal of Experimental Biology*, vol. 52, no. 6, pp. 606–612, 2014.

[44] C. Sutalangka and J. Wattanathorn, "Neuroprotective and cognitive-enhancing effects of the combined extract of *Cyperus rotundus* and *Zingiber officinale*," *BMC Complementary and Alternative Medicine*, vol. 17, no. 1, pp. 1–11, 2017.

[45] A. Prema, A. J. Thenmozhi, T. Manivasagam, M. M. Essa, M. D. Akbar, and M. Akbar, "Fenugreek seed powder nullified aluminium chloride induced memory loss, biochemical changes, Aβ burden and apoptosis via regulating Akt/GSK3β signaling pathway," *PLoS One*, vol. 11, no. 11, Article ID e0165955, 2016.

[46] S. Zameer, A. K. Najmi, D. Vohora, and M. Akhtar, "A review on therapeutic potentials of *Trigonella foenum graecum* (fenugreek) and its chemical constituents in neurological disorders: complementary roles to its hypolipidemic, hypoglycemic, and antioxidant potential," *Nutritional Neuroscience*, vol. 21, no. 8, pp. 539–545, Article ID 1327200, 2017.

Hindawi
Journal of Chemistry
Volume 2023, Article ID 8315711, 11 pages
https://doi.org/10.1155/2023/8315711

Research Article

Antioxidant Activity of Flavonoids and Phenolic Acids from *Dodonaea angustifolia* Flower: HPLC Profile and PASS Prediction

Fekade Beshah Tessema,[1,2] **Yilma Hunde Gonfa**,[1,3] **Tilahun Belayneh Asfaw**,[1,4] **Mesfin Getachew Tadesse**,[1,5] **and Rakesh Kumar Bachheti**[1,5]

[1]*Department of Industrial Chemistry, Addis Ababa Science and Technology University, Addis Ababa, Ethiopia*
[2]*Department of Chemistry, Faculty of Natural and Computational Science, Woldia University, Woldia, Ethiopia*
[3]*Department of Chemistry, Faculty of Natural and Computational Science, Ambo University, Ambo, Ethiopia*
[4]*Department of Chemistry, College of Natural and Computational Science, Gondar University, Gondar, Ethiopia*
[5]*Centre of Excellence in Biotechnology and Bioprocess, Addis Ababa Science and Technology University, Addis Ababa, Ethiopia*

Correspondence should be addressed to Rakesh Kumar Bachheti; rkbachheti@gmail.com

Received 4 November 2022; Revised 23 November 2022; Accepted 19 December 2022; Published 30 March 2023

Academic Editor: Marwa Fayed

Background. *Dodonaea angustifolia* is a known medicinal plant across East Arica. The flower of *D. angustifolia* is not well investigated in terms of phytochemistry and biological activities. This study aims to investigate the presence of flavonoids and phenolic acids in the flower of *D. angustifolia* and its antioxidant activity. *Methods*. Preliminary phytochemical screening was carried out using the standard protocols. Antioxidant activity evaluation using DPPH assay and total phenol content (TPC) and total flavonoid content (TFC) determinations in the flower extract were compared with the values of the leaf extract. UHPLC-DAD analysis was managed to develop the profile of the flower extract. Prediction of biological activity spectra for substances (PASS) was done using an online server for antioxidant and related activities. *Results*. Preliminary phytochemical screening and TPC and TFC values confirmed the presence of flavonoids and phenolic acids. From the HPLC analysis of flavonoids, quercetin, myricetin, rutin, and phenolic acids such as chlorogenic acid, gallic acid, and syringic acid were detected and quantified. The biological activity spectrum was predicted for the detected and quantified polyphenols. *Conclusions*. *D. angustifolia* flower is a rich source of flavonoids and phenolic acids, which are extractable and can be checked for further biological activity. It was possible to identify and quantify phenolic compounds through HPLC analysis in the methanol extract of *D. angustifolia* flower. The PASS biological activity prediction results showed that there were stronger antioxidant activities for the identified flavonoids. Future work will emphasize the isolation and characterization of active principles responsible for bioactivity.

1. Introduction

Dodonaea angustifolia Lf (syn*: Dodonaea viscosa*) is a species belonging to the family Sapindaceae and known for many therapeutic purposes [1]. Locally, in Ethiopia, it is known by the names such as Karkare (Agew), Kitkitta (Amh, Gur), Termien (Geez), Ettecca (Oro), Intanca (Sid), Tahses (Tre, Tya), and Den (Som) [2, 3]. The plant is an erect bushy shrub 5–8 m high, with simple and alternate leaves, yellowish-green small flowers stacked without petals, yellowish-green capsule fruits, and flowering after the rainy season from August to September [3]. It occurs in most parts of Ethiopia and is pantropically known for fast-growing and used for soil stabilizing and reforestation activities [1].

Ethno-medicinal reports showed that parts of this plant are known to cure different human and cattle ailments. The roots are used for toothache and wound healing [4], parasitic worms [5], and tapeworms [6, 7]. Roots with leaves have

been used for trachoma [8]. Leaf decoctions, juice, and extracts of *D. angustifolia* are used for the treatment of taeniasis [9], liver ailment [10], wound healing [8, 11, 12], eye infection, herps and fire burn [13], malaria [12, 14], cancer [15], and skin infection and wound [16–18]. The leaves are also used externally for itchy skin and as a remedy for skin rashes [19]. It is also reported that the leaf extract is known for mild purgative and soared throat [17] and hemorrhoid [20]. As an ointment for head swelling, bursting, and hair fungus, dried, powdered leaves and a paste made of oil have been employed [12].

A large group of phytochemicals have been reported from *Dodonaea* species. Melaku et al. isolated pinocembrin (flavanone), santin (flavanol), and clerodane diterpenes using bioassay-guided extraction and chromatographic separation [21] from *D. angustifolia*. Similarly, Omosa et al. reported flavonoids (3,4′,5,7-tetrahydroxy-6-ethoxyflavone, 5-hydroxy-3,4′,7-trimethoxyflavone, isokaempferide, kumatakenin, rhamnocitrin, and diterpenoids ((ent-3β,8α)-15,16-epoxy-13(16),14-labdadiene-3,8-diol, 2β-hydroxyhardwickiic acid, and dodonic acid) from the leaf extract of same species using chromatographic separation [22]. Methoxymkapwanin and Mkapwanin were also isolated from the leaf surface exudate using serial extraction and column chromatography fractionation [23].

From earlier investigations, both crude methanol extract [24] and quercetin derivatives [22, 25, 26] isolated from *D. angustifolia* showed antibactericidal efficacy against gram-positive and gram-negative bacteria. The aqueous extract demonstrated analgesic and antipyretic potential in mice and rats [27]. Ethanol extract displayed a combination of antioxidant and antiproliferative properties with little to no damage to normal cells [28, 29]. Nonpolar extracts of the leaves of *D. angustifolia* inhibited the viral growth at subtoxic concentrations [30]. Crude extract of both the leave [31, 32] and root [33] showed the strong antiplasmodial activity against *P. berghei* infected mice. This is in agreement with its medicinal use traditionally to treat malaria [34]. The antihelminthic property of *D. angustifolia* was reasoned out for the polyphenols present, including kaempferol, quercetin, and myricetin-based flavanol [35].

D. angustifolia is a medicinal plant frequently used to treat toothache, microbial infections, and fever [36]. It showed antifungal activities and was found to be nontoxic. It is also used with other medicinal plants for musculoskeletal ailments [37] and bone fracture [6] with a higher informant agreement ratio.

The biological activity spectrum predicts many different compounds' biological activity types. Since it is solely dependent on the compound's structure, it is regarded as an intrinsic property of the substance [38]. The multilevel neighborhoods of atoms (MNA), which are original descriptors, are used in PASS (prediction of activity spectra for substances) to characterize chemical structure [39]. A MOL or SDF (structure data file formats) with the structural details of the molecules being studied serves as the input data for PASS. MNA descriptors are generated automatically using the data from the input files. Using data from MNA descriptors for both active and inactive compounds, for each activity, two probabilities are computed: Pa is the probability that a compound is active, while Pi is the probability that a compound is inactive. Pa and Pi have values that range from 0.000 to 1.000 since they represent probabilities (with 3 appropriate decimals determined) and Pa + Pi < 1 since these probabilities are computed independently. Pa and Pi can be thought of as measurements of the substance being studied that fall within the categories of active and inactive substances, respectively [38].

The antioxidant action of flavonoids and phenolic acids includes suppressing the formation of reactive oxygen species by inhibiting the respective enzymes, scavenging free radicals, and triggering antioxidant defence [40]. These phytochemicals also protect the disintegration of the lipid of biomembrane by preventing or hindering lipid peroxidation [41]. Flavonoids are synthesized by plants following a microbial infection and are known to possess antioxidant and antibacterial activities. The mechanism and activity level depends on the polyphenols' specific structural variety [41]. Flavonoids have a more significant number of physiological activities promoting human health and minimizing the risk of being infected by a broad spectrum of pathogens.

Flowers of *D. angustifolia* are ideal for bee forage and are considered a major agricultural value of the plant [3]. The seasonal flower of this plant is not well investigated in terms of phytochemistry and biological activities. Other parts including leaves, seeds, stem bark, and roots were investigated for their phytochemical constituents [22, 23, 26] and biological activities [21, 22, 25, 27, 31, 33, 34].

This study aimed to investigate the profile and antioxidant activity of the flower of *D. angustifolia* and compare it to the plant's leave. For this purpose, HPLC analysis and PASS online prediction of biological activities were used.

2. Materials and Methods

2.1. Chemicals and Reagents. All the extraction chemicals and reagents used for the total content of phenol and flavonoid determination were of AR grade. While for HPLC analysis and the antioxidant activity evaluation, HPLC grade solvents and reagents were used. Water was distilled and purified by MQ (18.2) at 21°C in a water purification system (Purelab flex 4 Elga). Phenolic acid standards: syringic acid, chlorogenic acid, and gallic acid; flavonoid standards: myricetin, quercetin, rutin, and kaempferol references purchased from Sigma (>99.9%, Sigma, China). 2, 2-Diphenyl-1-picrylhydrazyl (DPPH) for antioxidant test and ascorbic acid are obtained from Sigma (>99.9%, Sigma, China).

2.2. Plant Material Collection and Pretreatment. The flower part of *D. angustifolia* was collected from Addis Ababa Science and Technology University campus. Ato Melaku Wondafrash identified the plant and a herbarium sample was deposited at the national herbarium (voucher number: FB-001/11) in the College of Science, Addis Ababa University, Ethiopia. Following collection, the samples were

cleaned with tap water and then distilled water to get rid of dirt and other debris. Then, the samples were chopped into smaller sizes and spread onto clean polyethylene plastic sheets at room temperature (23 ± 3°C). The air-dried samples were ground using a sample grinder (stainless steel 700 g electric grains, spices, herbs, cereals, and dry food grinding mill, China).

2.3. Ultrasonic Assisted Extraction (UAE). The extracts of air-dried and blended leaves and flower samples of *D. angustifolia* (5 g of each) were obtained from an intelligent ultrasonic processor (SJIA-950W, probe Φ 6) sonicator in 25 mL methanol. The method optimization of UAE followed a method reported by Zakaria et al. [42], with minor modifications considering the bioactive components we are dealing with. Briefly, the settings for sonication were temperature 35°C, time 15 min, and power rate 50%. Up on the optimized method suggested by Zakaria et al. (2021), the nature of the solvent (methanol) was expected to compromise the polarity difference between the phenolic acid and flavonoid with varied polarity. The temperature is also reasonable for the extraction of bioactive components. After 2x successive sonication for each aliquot extract, the extracts were centrifuged using proanalytical @ 600 (10x) for 20 min. Whatman no. 1 filter paper was then used to filter the supernatant, adjusted to a volume of 50 ml, and kept in an amber vial for further analysis.

2.4. Preliminary Phytochemical Screening. Using standard procedures [43], the presence of alkaloids, flavonoids, phenolics, tannins, steroids, triterpenoids, saponins, glycosides, carboxylic acids, anthraquinones, and essential oil was assessed. Briefly, to check for the presence of alkaloids, Wagner's reagent was used. Triterpenoids were checked by using Salkowski's reaction. The presence of flavonoids was confirmed by the lead acetate test showing yellow precipitate. Acetic anhydride test was carried out to check the presence of steroids. The presence of tannins was checked by adding 10% of NaOH and shaking well for an emulsion formation. Saponins were checked by foam test, where plant extract was mixed with water and shaken vigorously to see persistent foam for 10 min. Glycosides were checked using an aqueous NaOH test from the methanol extracts. Borntrager's test determined the presence of anthraquinones. An effervescence test using a sodium bicarbonate solution was used to check carboxylic acid's presence. To check for the presence of volatile oils, fluorescence tests were conducted. Details of the screening tests are shown in Table 1. The phytochemicals present in the methanol extracts of the leaves and flowers of *D. angustifolia* were compared.

2.5. Evaluation of Antioxidant Activity. We used the DPPH radical assay because it is easily available, has better radical scavenging potential, and is a commonly used free radical to evaluate the antioxidant potential of plant extracts [44, 45]. Modified protocol for the effect of free-radical scavenging on the DPPH assay from Banothu et al. [46] was followed. More briefly, to 0.25 mL of sample solution, 0.75 mL of DPPH was added and the reaction was left in the dark for 30 minutes. As a control, 0.25 mL of methanol and 0.75 mL of DPPH solution were combined. The standard utilized was ascorbic acid. In a 50 mL brown volumetric flask, 1.9716 mg of DPPH was dissolved in methanol to prepare DPPH solution and then adjusted to nearly 1.000 absorbance. A standard solution of ascorbic acid was prepared at a 1000 ppm concentration by dissolving 0.10 g in 100 ml of methanol for the calibration curve. From this stock solution, 25, 50, 100, 150, 200, 250, 300, 350, 400, 450, and 500 mg/L concentrations were prepared. The flower sample extract (0.1 g/mL) was diluted with methanol using 5, 10, 25, 50, 100, 150, and 200 dilution factors. The absorbance was measured using a JASCO V-770 spectrophotometer (Jasco, USA) at 517 nm with a 1 mm path length in a rectangular cell holder (500 μL cuvette). The percentage of inhibition is used to measure radical scavenging activity. The following formula was used to determine the DPPH radical scavenging capacity:

$$\text{scavenging activity (\%)} = \left(\frac{\text{absorbance}_{\text{control}} - \text{absorbance}_{\text{sample}}}{\text{absorbance}_{\text{control}}}\right) x\ 100 \quad (1)$$

IC_{50} values were computed from the relation log (sample) vs absorbance (normalized) using graph pad prism 8 software as suggested for better IC_{50} estimation [47].

2.6. Total Phenol and Total Flavonoid Content Determination. The total phenol content (TPC) of the flower sample extract was determined by the Folin–Ciocalteu colorimetric method as described by McDonald et al. [48] with some modifications. More briefly, 0.2 mL of 2% Na_2CO_3 was added to the mixture after 0.4 mL of the extract and 0.4 mL of Folin–Ciocalteu reagent (10x diluted) were combined. Various concentrations of sample extracts were checked, and the one with dilution factor 5 was used for the determination as the absorbance was between 0.1 to 1 (within Beer's Law) following consistent color changes. For control, a reagent without the methanol extract was used. The V-770 UV-Vis spectrophotometer (Jasco, USA) was used to measure the absorbance at 765 nm in triplicate after the mixture was incubated at room temperature for 35 minutes. The standard gallic acid was prepared for calibration at 1000 ppm and was serially diluted and 6.25, 12.5, 25, 50, 100, 150, 200, 250, and 500 mg/L standard solutions were prepared. Equation (2) was used to calculate TPC as the milligrams of gallic acid equivalent (GAE) per gram of extract (dry weight).

Table 1: Qualitative tests for phytochemical screening [43].

SN	Phytochemical groups	Test	Procedure	Observations (indicating positive test)
1	Alkaloids	Wagner's test	Few mL filtrates (50 gm solvent-free extract is mixed with a few mL dil. HCl and then filtered) + 1-2 drops of Wagner's reagent (along the sides of the test tube)	A brown/reddish precipitate
2	Glycosides	Aqueous NaOH test	Alcoholic extract + dissolved in 1 mL of water + a few drops of aqueous NaOH solution	A yellow color
3	Flavonoids	Lead acetate test	1 mL of plant extract + few drops of 10% lead acetate solution	A yellow precipitate
4	Phenolic compounds	Ferric chloride test	Extract aqueous solution + few drops 5% ferric chloride sol	Dark green/bluish black color
5	Tannins	10% NaOH test	0.4 mL of plant extract + 4 mL of 10% NaOH + shaken well	Formation of emulsion (hydrolysable tannins)
6	Saponins	Foam test	0.5 gm of plant extract + 2 mL of water (vigorously shaken)	Persistent foam for 10 min
7	Steroids	Acetic anhydride test	0.5 mL of plant extract + 2 mL of acetic anhydride + 2 mL of conc. H_2SO_4	Change in color from violet to blue/green
8	Triterpenoids	Salkowski's test	Filtrate (equal quantity of chloroform is treated with plant extract and filtered) + a few drops of conc. H_2SO_4 (shaken well and allowed to stand)	Golden yellow layer (at the bottom)
9	Anthraquinones	Borntrager's test	10 mL of 10% ammonia sol. + Few ml filtrating (shaken vigorously for 30 sec.)	A pink, violet, or red-colored solution
10	Carboxylic acid	Effervescence test	1 mL of plant extract + 1 mL of sodium bicarbonate solution	Appearance of effervescence
11	Volatile oils	Fluorescence test	10 mL of extract, filtered till saturation, exposed to UV light	Bright pinkish fluorescence

$$\text{Concentration } (mg/100\ g) = \frac{C\ x\ V\ x\ DF}{m}\ x\ 100, \quad (2)$$

where C is the concentration obtained from the calibration curve in mg/L, V is the final volume of the sample in L, m is the mass of the sample powder taken for extraction, and DF is the dilution factor.

Total flavonoid content (TFC) was determined using Chang et al.'s aluminum chloride colorimetric method [49] with slight modifications. More briefly, the mixture of 0.3 mL extract and 0.3 mL of 2% $AlCl_3$, 0.3 mL of 1% $NaNO_2$, and 0.3 mL of 5% NaOH were mixed and incubated at room temperature for a total of 30 min. Sample extracts were prepared in a similar way as for the TPC determination mentioned above. Methanol was used as a control. Absorbance was recorded in triplicate at λ 314 nm using a V-770 UV-Vis spectrophotometer (Jasco, USA). A standard stock solution of quercetin (1000 ppm) (mg/L) was prepared. The calibration standards were also prepared similarly. TFC was calculated as milligrams of quercetin equivalent (QE) per gram of the flower extract (dry weight).

2.7. HPLC Analysis. Stock solutions for standards (1 mg/mL) of both phenolic acids and flavonoids were prepared by dissolving an appropriate amount in methanol. Calibration standard solutions at 6 concentrations ranging from 2.5 to50 mg/mL were prepared and obtained by appropriate dilutions from the stock solutions in the selected mobile phase. The selected mobile phase was a binary isocratic elution consisting of (A) methanol and (B) acidified (1% acetic acid) ultra-pure water (60/40, v/v). The 10 μL injection volume was used at a flow rate of 0.8 mL/min.

Ultrahigh-performance liquid chromatography coupled with a diode array detector (Ultimate 3000 UHPLC-DAD, Thermo Scientific Dionex, USA) was used to separate the analytes via chromatography. The UHPLC system was equipped with a pump (model: LPG-3400SD), autosampler (model: WPS-3000TSL), and temperature-controlled column compartment (model: TCC-3100). Monitoring and quantitation were performed at 254 nm, 272 nm, 360 nm, and 372 nm. Chromeleon (c) Dionex version 7.2.4.8179 was used for instrument control and data acquisition. Chromatographic separation was performed on reverse phase column (Acclaim (TM) 102 with Fortis 5 μm, C18 (column dimension: 4.6 × 250 mm) Thermo Scientific Technologies, USA) operated at 30°C. Using these conditions, flavonoids and phenolic acid with external standards were separated within 25 min per sample. By comparing the retention times of the various compounds to standards, the individual compounds were identified and quantified. The amounts of the flavonoids and phenolic acids in the methanol extract of *D. angustifolia* flower were calculated using equation (2) [50].

2.8. PASS (Prediction of Activity Spectra for Substances) Test. PASS prediction for the flavonoids, phenolic acids, and reference antioxidant (ascorbic acid) was performed using the PASS online web server (http://www.pharmaexpert.ru/passonline). The PASS prediction uses canonical smiles to determine the probability of being active (Pa) and probability of being inactive (Pi) values. Pa and Pi values indicate a compound's biological activity. The biological activities selected were those activities related in one way or another to antioxidant activity [51]. Interpretation of the result as recommended by Langunin et al. [39] and Maharani et al. [52] was as follows:

(i) If Pa > 0.7, the compound is very active and is likely to display the aforementioned activity in trials conducted in a wet lab.

(ii) If 0.5 < Pa < 0.7 is likely to exhibit the activity and there is a lower chance than in the first case, then the compound will demonstrate the activity in a wet lab experiment.

(iii) If Pa < 0.5, the compound is unlikely to show the respective activity in the wet lab.

The 2.0 version of PASS online was used to perform the PASS test [53]. First, SMILES were retrieved for the candidate's compounds from PubChem (http://pubchem.ncbi.nlm.nih.gov), then the MOL or SDF file for the compounds was given as input to the PASS software and activity prediction was performed (get prediction). Before conducting lab testing, it was crucial to confirm the results of the PASS biological activity test. The probability activity score would display the findings and indicate the likelihood of success if lab tests were conducted.

3. Results

3.1. Phytochemical Screening. The preliminary phytochemical screening revealed that the methanol extracts of the flower and the leaves were almost comparable qualitatively for the tested secondary metabolites. The glycoside, saponin, triterpenoid, and anthraquinone tests indicated more concentration in the leaves than in the flowers. Alkaloids and tannins were not detected in the flower extract (Table 2).

3.2. Antioxidant Activity Evaluation. The IC_{50} values and % radical scavenging activity are almost identical for the leaf and flower extracts.

3.3. Total Phenol and Total Flavonoid Determination. Equation of calibration curve for TPC determination was $y = 0.0023x - 0.0693$, where $R^2 = 0.9981$, and for TFC determination was $y = 0.002x + 0.0399$, where $R^2 = 0.9971$.

3.4. HPLC Analysis. The number of components identified by HPLC analysis was 15 using a polar solvent system (Figure 1). Among these 6 were determined by using an external standard method on UHPLC-DAD (Table 3). The concentration (mg/100 g) was computed using $V = 0.050$ L and $m = 5.0046$ g on the equation given above in the method section.

Among the investigated flavonoids, myricetin took the lead with a concentration of 219.35 mg/100 g. Quercetin was

Table 2: Test result for qualitative phytochemical screening for leaves and flowers.

SN	Phytochemical groups	Test	Methanol extract of leaves of *D. angustifolia*	Methanol extract of flowers of *D. angustifolia*
1	Alkaloids	Wagner's test	+	−
2	Glycosides	Aqueous NaOH test	++	+
3	Flavonoids	Lead acetate test	++	++
4	Phenolic compounds	Ferric chloride test	++	++
5	Tannins	10% NaOH test	+	−
6	Saponins	Foam test	++	+
7	Steroids	Acetic anhydride test	+	+
8	Triterpenoids	Salkowski's test	++	+
9	Carboxylic acid	Effervescence test	++	+
10	Anthraquinones	Borntrager's test	++	+
11	Volatile oils	Fluorescence test	+	+

Result indications: ++ = present in appreciable amount; + = present in low amount; − = negative result.

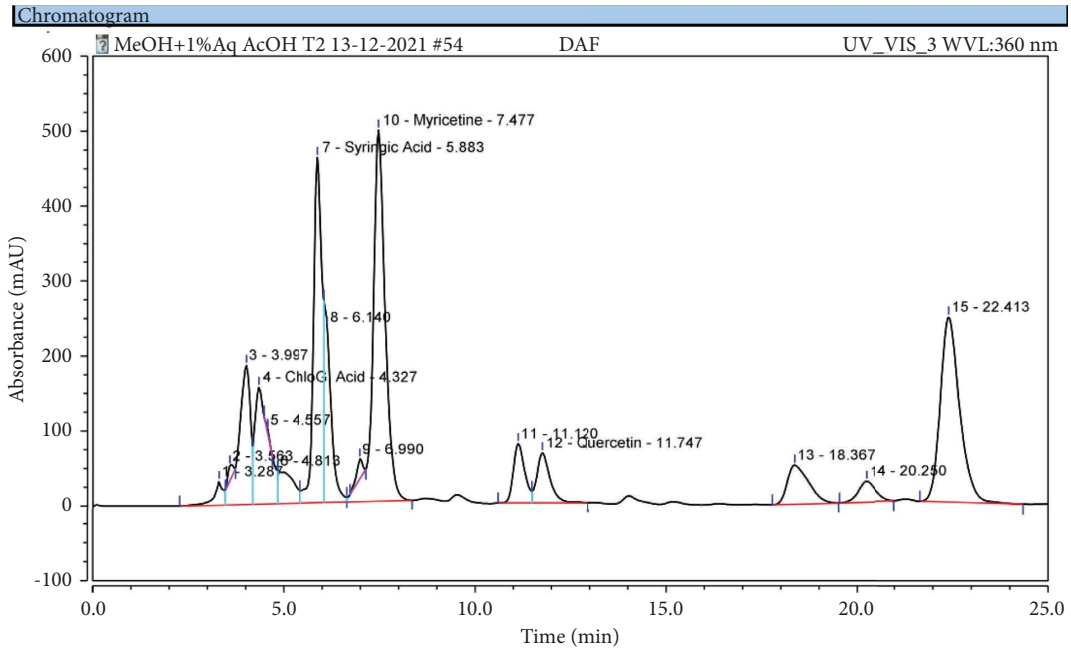

Figure 1: UHPLC-DAD chromatogram for the methanol extract of *D. angustifolia* flower.

Table 3: HPLC data table for the identified components of *D. angustifolia* flower.

Compound	Retention time (min)	Amount (mg/L)	Concentration (mg/100 g)	Remark
Chlorogenic acid	4.327	24.58 ± 1.76	24.56 ± 1.75	Phenolic acid
Syringic acid	5.883	81.42 ± 1.79	81.35 ± 1.79	Phenolic acid
Myricetin	7.477	219.55 ± 9.61	219.35 ± 9.6	Flavonoid
Quercetin	11.747	11.7 ± 1.13	11.69 ± 1.13	Flavonoid
Rutin	20.110	5.8 ± 0.74	5.8 ± 0.74	Flavonoid
Gallic acid	3.971	7.51 ± 0.23	7.51 ± 0.23	Phenolic acid
Kaempferol	12.767	No data	No data	Flavonoid

20x less than myricetin. The concentrations of rutin and gallic acid were found to be less than 10 mg/100 g. The concentration of syringic acid was 4x larger than chlorogenic acid. The data for kaempferol could not appear on the chromatogram and data table for unknown reasons after initially being tracked in the standard mixture. This might be due to precipitation and/or degradation of kaempferol at high temperatures (analysis temperature at 35°C). The rutin and gallic acid are not shown on the chromatogram due to the smaller amounts compared to the others.

3.5. PASS Prediction of Biological Activity. Biological activities used to describe the mechanism of antioxidant activity are considered in the PASS test. Other activities such as antimutagenic, cardioprotection, anticarcinogenic,

chemopreventive, proliferative disease treatment, antibacterial, antiprotozoal, antifungal, anti-inflammatory, and antiviral activities were also considered. The PASS results (Supplement 1) are summarized for the compounds considered in Table 4.

4. Discussion

From the preliminary phytochemical screening test result (shown in Table 2), the leaves and flowers of *D. angustifolia* were similar in the constituency of the major phytochemical groups. Moreover, the results obtained for the leaf extract are in close agreement with the literature report [51]. Generally, the screening study indicated that flavonoids and phenolic compounds are the major constituents of the leaf and flower extracts of *D. angustifolia* [54].

The radical scavenging activity of both the leaves and flowers of *D. angustifolia* was assessed using the DPPH method. The percentage of inhibition used to measure the DPPH radical scavenging activity using the formula is as follows: percentage effect (E %) = $(\text{Abs}_{\text{control}} - \text{Abs}_{\text{sample}}) \times 100/\text{Abs}_{\text{control}}$. As one can see from the structures of the flavonoids and phenolic acids, the presence of a more significant number of hydroxyl groups can result in higher antioxidant activity. As shown in Tables 5–7 and Figure 2, there is no significant difference in the antioxidant activity and TPC and TFC values between the leaves and flower parts of *D. angustifolia*.

Mobile phase selection for HPLC–DAD method for both extract samples was one of the big challenges to get better separation as the polarity of phenolic acids and flavonoids are closer. To come up with a solution for such problems, we have considered the advantage of the gradient method [55] for HPLC analysis. However, we successfully used isocratic elution for our flower sample. As shown on the chromatogram (Figure 1), the peak shape and separation were good for the selected polar solvent system. Methanol extract of *D. angustifolia* leaves was not showing separate peaks for the identified polyphenols in the case of the flower. Additional methods like hyphenation with mass spectroscopy should be considered for further component identifications.

The flavonoids (flavanols) considered in our study are sourced similarly following closely related biosynthesis in most cases. They are even common in dietary sources [56]. Flavonoids occur in most plant parts, specifically photosynthesizing plant cells as major coloring components of flowering plants [41]. For flowers, the matrix's complexity may be lower compared to the leaves where chlorophyll and related components are more concentrated.

Investigations of phenolic acids and flavonoids among the phytochemicals from natural products are usually conducted using HPLC analysis with a DAD detector [57]. Such analysis has been attempted by Mizzi et al. (2020) [55]. Due to the complexity of the matrix analysis, it is not simple to do such an investigation for medicinal plants. Alam et al. [58] and Thomas et al. [59] mention an HPLC method using a gradient of acetonitrile and methanol to estimate some of these phenolics in *Moringa oleifera*. As the retention times of these compounds are closer to each other, making simultaneous measurements of both the groups was not possible in our case. Less than 1 mg/100 g of concentration was reported for rutin, myricetin, and gallic acid for *D. viscosa* flower [60]. Tong et al. reported gallic acid and quercetin 19.68 and 5.95 mg/100 g, respectively, from the flower of the same *Dodonaea* species [61]. In this study, HPLC analysis results are 5 to 220 mg/100 g for both flavonoids and phenolic acids. Myricetin was nearly 220 mg/100 g dry weight basis. Because of the few attempts on the synonym *Dodonaea* species, it is impossible to compare the results from this current investigation.

Biological activities predicted by PASS include main pharmacological effects, mechanisms of action, specific toxicities, interactions with antitargets, metabolic actions, influence in gene expression, and action on transporters [38, 53]. Biological activities related to antioxidant activity were selected for discussion from the activity spectrum of the individual flavonoids and phenolic acids under consideration. The Pi values were not significant for decision-making of inactivity for most of the compounds considered. On average, each of the considered flavonoids was predicted to have 90 pharmacological activities with Pa value greater than 0.700, which was doubled that of the standard reference compound. The gallic acid and syringic acid predicted pharmacological activities were 375 and 220, respectively. As a result, the flower of *D. angustifoli*a can be considered a potential pharmacological agent [62], which is consistent with the therapeutic use of the plant's leaves.

The antioxidant and other related activities of the four flavonoids, quercetin, rutin, myricetin, and kaempferol, have been predicted. Similarly, three phenolic acids, namely, gallic acid, syringic acid, and chlorogenic acid have been predicted using PASS. The PASS results were compared with ascorbic acid as a reference standard (Table 4). The Pa values for the flavonoids and chlorogenic acid were greater than 0.700. This indicates that the antioxidant activities of these compounds are very likely to be positive if attempted via wet lab experiments. These results agreed with the DPPH assay results of the extracts. The Pa value for ascorbic acid, a standard reference for *in vitro* antioxidant activity, was comparable with the flavonoids, more specifically myricetin and rutin.

Activities such as free radical scavengers, peroxidase inhibitors, membrane integrity agonists, dioxygenase inhibiter, and NADPH oxidase inhibitors refer to the mechanisms of action for the antioxidant activity by the respective compounds [51]. The Pa values of these activities were also greater than 0.700, indicating all to be among the possible mechanisms of action for the antioxidant activities of the compounds considered in this investigation. Considering the activation of internal antioxidants with Pa values less than 0.300, the polyphenols' role in the activation of internal antioxidant enzymes was not expected.

The Pa values related to the antioxidant activity such as antimutagenic, cardioprotective, anticarcinogenic, chemopreventive, and proliferative disease treatment were also greater than 0.700. Except for minor inconsistencies in the treatment of proliferative illnesses, the compounds under

Table 4: Probability of activity (Pa) summary for the flavonoids and phenolic acids.

SN	Activity	Standard	Polyphenols					
		AA	F1	F2	F3	F4	PA1	PA2	PA3
1	Antioxidant	0.928	0.872	0.923	0.856	0.924	0.520	0.403	0.785
2	Free radical scavenger	0.564	0.811	0.988	0.771	0.832	0.570	0.619	0.856
3	Peroxidase inhibitor	0.252	0.962	0.987	0.956	0.966	0.891	0.846	0.855
4	Membrane integrity agonist	0.815	0.973	0.984	0.974	0.968	0.890	0.837	0.940
5	Membrane integrity antagonist	0.561	0.454	0.758	0.530	0.410	0.543	0.627	0.304
6	Quercetin 2,3-dioxygenase inhibitor	0.206	0.934	0.371	0.951	0.917	0.422	nd	nd
7	NADPH oxidase inhibitor	nd	0.928	0.850	0.889	0.939	0.509	0.520	
8	Antimutagenic	nd	0.940	0.503	0.948	0.963	0.597	0.821	0.409
9	Cardioprotection	0.229	0.833	0.988	0.814	0.886	0.468	0.463	nd
10	Anticarcinogenic	0.332	0.757	0.983	0.715	0.784	0.395	0.413	0.846
11	Chemopreventive	0.382	0.717	0.968	0.669	0.734	0.406	0.452	0.833
12	Proliferative disease treatment	nd	0.614	0.952	0.602	0.645	0.324	0.317	0.769
13	Antibacterial	0.377	0.387	0.677	0.395	0.421	0.418	0.395	0.537
14	Antiprotozoal (Leishmania)	0.205	0.575	0.907	0.554	0.521	0.329	0.347	0.655
15	Antifungal	0.332	0.490	0.784	0.495	0.508	0.398	0.366	0.638
16	Anti-inflammatory	0.779	0.689	0.728	0.676	0.720	0.548	0.498	0.598
17	Antiviral (herps)	0.418	0.484	0.526	0.483	0.500	0.404	0.377	0.411
18	Antiviral (influenza)	0.459	0.403	0.743	0.400	0.444	0.654	0.607	0.537
19	Antiviral (hepatitis B)	0.180	0.498	0.451	0.496	0.519	nd	nd	0.528

Pa, probability to be active and no data; codes for compounds: AA, ascorbic acid; F1, quercetin; F2, rutin; F3, kaempferol; F4, myricetin; PA1, gallic acid; PA2, syringic acid; PA3, chlorogenic acid.

Table 5: Result summary of IC_{50} and R^2 values.

	Log (inhibitor) vs. normalized response: variable slope			
Sample	LogIC50	HillSlope	IC_{50}	R squared
DAF	−0.162 ± 0.003	−5.547 ± 0.218	0.689 ± 0.005	0.997 ± 001
DAL	−0.156 ± 0.001	−5.121 ± 0.036	0.698 ± 0.002	0.995 ± 002
Ascorbic acid	−0.9075 ± 0.01	−3.439 ± 0.02	0.1237 ± 0.01	0.991 ± 0.02

DAF: *D. angustifolia* flower part; DAL: *D. angustifolia* leaf part.

Table 6: % radical scavenging activity.

Concentrations (mg/mL)	% RSA of DAL	% RSA of DAF
5	22.98	22.60
10	34.46	34.99
25	55.72	54.67
50	82.72	85.11
100	93.74	94.46
150	93.12	94.40
200	92.11	94.78
250	91.32	94.31

Table 7: Total phenol and total flavonoid content for the flower and leaf extracts.

Sample	TPC (mg/100 g)	TFC (mg/100 g)
DAF	502.71 ± 7.56	488.23 ± 23
DAL	765.85 ± 16.95	700.66 ± 39.14

consideration were also most likely projected to be similarly potent. Other activities such as antibacterials, antiprotozoal, antifungal, anti-inflammatory, and antiviral activities were predicted to show activities less likely in the wet lab experiments. Here, the probability will be less than the first case as Pa values are between 0.500 and 0.700, with few irregularities among the compounds and the activities. As flavonoids display varied cellular effects, they affect the overall process of carcinogenesis by varied mechanisms [63].

Phenolic acids: syringic acid, chlorogenic acid, gallic acid, and flavonoids: quercetin, myricetin, rutin, and kaempferol are common in food substances, including alcoholic drinks and fruits [56]. Phenolic compounds are known to impart beneficial properties such as antimicrobial,

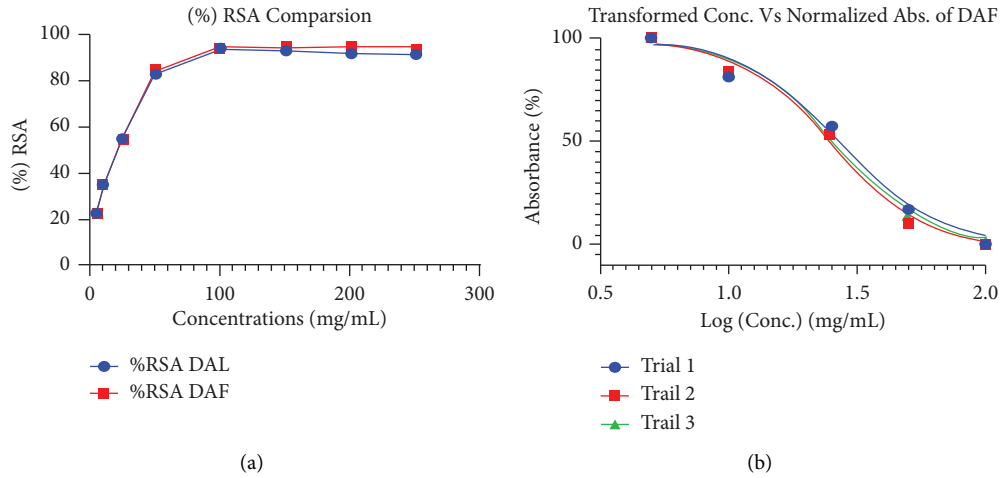

Figure 2: (a) Graph comparisons for % RSA and (b) log (conc.) vs. normalized absorbance.

preservatives, antioxidants [55], and other varied physiological properties [64]. Antioxidant properties dictate so many pharmacological activities such as cardioprotective, anticarcinogenic, gastroprotective, anti-inflammation, and antimicrobial effects in the human body, and hence they are considered nutraceuticals [65]. As an example, rutin and quercetin showed the gastroprotective effects due to their antioxidant properties [66]. This is also shown on the biological activity spectrum for PASS online prediction. The mechanisms of such pharmacological activities include enzyme inhibition, disruption of cell membranes, blocking viral attachments and cell penetration, and activating the host cell's self-defense mechanism [67].

5. Conclusions

D. angustifolia flower is a rich source of phytochemicals, which are extractable and can be checked for further biological activities depending on the phytochemical screening. A preliminary phytochemical study, the DPPH radical scavenging activity, and TPC, and TFC determinations all confirmed that the flowers and leaves of *D. angustifolia* are nearly similar in terms of phytoconstituency. From HPLC analysis, phenolic compounds identified clearly in the methanol extract of *D. angustifolia* flower include flavonoids: quercetin, myricetin, rutin, and phenolic acids: chlorogenic acid, syringic acid, and gallic acid. PASS biological activity prediction results show the stronger antioxidant activity of the identified flavonoids. Future work will emphasize the isolation and characterization of active principles responsible for bioactivity.

Data Availability

The data used to support this study are available in this article and the supplementary materials.

Conflicts of Interest

The authors declare that they have no conflicts of interest.

Acknowledgments

The authors acknowledge Dr. Belete Adefrse for his help in providing standards and Industrial Chemistry Department, Addis Ababa Science and Technology University and Woldia University for the opportunity to do this investigation.

Supplementary Materials

Supplementary file 1. PASS Data. (*Supplementary Materials*)

References

[1] F. Beshah, Y. Hunde, M. Getachew, R. K. Bachheti, A. Husen, and A. Bachheti, "Ethnopharmacological, phytochemistry and other potential applications of *Dodonaea* genus: a comprehensive review," *Current Research in Biotechnology*, vol. 2, pp. 103–119, 2020.

[2] E. Dagne, "Natural Database for Africa (NDA) Verion 2.0," Addis Ababa, Ethiopia, 2011, http://alnapnetwork.com/NDA.aspx.

[3] R. Fichtl and A. Adi, *Honeybee flora of Ethiopia*, Margraf Verlag, Weikersheim, Germany, 1994.

[4] T. T. Jima and M. Megersa, "Ethnobotanical study of medicinal plants used to treat human diseases in berbere district, bale zone of oromia regional state, south East Ethiopia," *Evidence-based Complementary and Alternative Medicine*, vol. 2018, Article ID 8602945, 16 pages, 2018.

[5] A. Belayneh, Z. Asfaw, S. Demissew, and N. F. Bussa, "Medicinal plants potential and use by pastoral and agro-pastoral communities in Erer Valley of Babile Wereda, Eastern Ethiopia," *Journal of Ethnobiology and Ethnomedicine*, vol. 8, no. 1, pp. 42–11, 2012.

[6] G. Chekole, Z. Asfaw, and E. Kelbessa, "Ethnobotanical study of medicinal plants in the environs of Tara-gedam and Amba remnant forests of Libo Kemkem District, northwest Ethiopia," *Journal of Ethnobiology and Ethnomedicine*, vol. 11, no. 1, p. 4, 2015.

[7] S. Zerabruk and G. Yirga, "Traditional knowledge of medicinal plants in Gindeberet district, Western Ethiopia," *South African Journal of Botany*, vol. 78, pp. 165–169, 2012.

[8] G. Chekole, "Ethnobotanical study of medicinal plants used against human ailments in Gubalafto District, Northern

Ethiopia," *Journal of Ethnobiology and Ethnomedicine*, vol. 13, no. 1, p. 55, 2017.

[9] B. Desta, "Ethiopian traditional herbal drugs. Part I: studies on the toxicity and therapeutic activity of local taenicidal medications," *Journal of Ethnopharmacology*, vol. 45, no. 1, pp. 27–33, 1995.

[10] S. Suleman and T. Alemu, "A survey on utilization of ethnomedicinal plants in nekemte town, East wellega (oromia), Ethiopia," *Journal of Herbs, Spices, and Medicinal Plants*, vol. 18, no. 1, pp. 34–57, 2012.

[11] G. Seyoum and G. Zerihun, "An ethnobotanical study of medicinal plants in Debre Libanos Wereda, Central Ethiopia," *African Journal of Plant Science*, vol. 8, no. 7, pp. 366–379, 2014.

[12] A. Belayneh and N. F. Bussa, "Ethnomedicinal plants used to treat human ailments in the prehistoric place of Harla and Dengego valleys, eastern Ethiopia," *Journal of Ethnobiology and Ethnomedicine*, vol. 10, no. 1, pp. 18–17, 2014.

[13] A. Teklay, B. Abera, and M. Giday, "An ethnobotanical study of medicinal plants used in Kilte Awulaelo District, Tigray Region of Ethiopia," *Journal of Ethnobiology and Ethnomedicine*, vol. 9, no. 1, pp. 65–23, 2013.

[14] S. Asnake, T. Teklehaymanot, A. Hymete, B. Erko, and M. Giday, "Survey of medicinal plants used to treat malaria by sidama people of boricha district, sidama zone, south region of Ethiopia," *Evidence-based Complementary and Alternative Medicine*, vol. 2016, Article ID 9690164, 9 pages, 2016.

[15] T. T. Ayele, "A review on traditionally used medicinal plants/herbs for cancer therapy in Ethiopia: current status, challenge, and future perspectives," *Organic Chemistry: Current Research*, vol. 7, no. 2, pp. 1–8, 2018.

[16] A. Enyew, Z. Asfaw, E. Kelbessa, and R. Nagappan, "Ethnobotanical study of traditional medicinal plants in and around Fiche District, Central Ethiopia," *Current Research Journal of Biological Sciences*, vol. 6, no. 4, pp. 154–167, 2014.

[17] A. Hassan-abdallah, A. Merito, S. Hassan et al., "Medicinal plants and their uses by the people in the Region of Randa, Djibouti," *Journal of Ethnopharmacology*, vol. 148, no. 2, pp. 701–713, 2013.

[18] T. Birhanu, D. Abera, and E. Ejeta, "Ethnobotanical study of medicinal plants in selected horro gudurru woredas, western Ethiopia," *Journal of Biology, Agriculture and Healthcare*, vol. 5, no. 1, pp. 83–94, 2015.

[19] G. L. Alemayehu, "Ethnobotanical Study on Medicinal Plants Used by Indigenous Local Communities in Minjar-Shenkora Wereda, North Shewa Zone of Amhara Region, Ethiopia," *Journal of Medicinal Plants Studies*, vol. 3, no. 6, pp. 1–11, 2010.

[20] T. Teklehaymanot, "Ethnobotanical study of knowledge and medicinal plants use by the people in Dek Island in Ethiopia," *Journal of Ethnopharmacology*, vol. 124, no. 1, pp. 69–78, 2009.

[21] Y. Melaku, T. Worku, Y. Tadesse et al., "Antiplasmodial compounds from leaves of *Dodonaea angustifolia*," *Current Bioactive Compounds*, vol. 13, no. 3, pp. 268–273, 2017.

[22] L. K. Omosa, B. Amugune, B. Ndunda et al., "Antimicrobial flavonoids and diterpenoids from *Dodonaea angustifolia*," *South African Journal of Botany*, vol. 91, pp. 58–62, 2014.

[23] L. K. Omosa, J. O. Midiwo, S. Derese, A. Yenesew, M. G. Peter, and M. Heydenreich, "Neo -Clerodane diterpenoids from the leaf exudate of *Dodonaea angustifolia*," *Phytochemistry Letters*, vol. 3, no. 4, pp. 217–220, 2010.

[24] R. Naidoo, M. Patel, Z. Gulube, and I. Fenyvesi, "Inhibitory activity of *Dodonaea viscosa* var. *angustifolia* extract against *Streptococcus mutans* and its biofilm," *Journal of Ethnopharmacology*, vol. 144, no. 1, pp. 171–174, 2012.

[25] B. Mengiste, Y. Hagos, and F. Moges, "Invitro antibacterial screening of extracts from selected Ethiopian medicinal plants," *Momona Ethiop J Sci*, vol. 6, no. 1, pp. 102–110, 2014.

[26] T. Ngabaza, M. M. Johnson, S. Moeno, and M. Patel, "Identification of 5,6,8-Trihydroxy-7-methoxy-2-(4-methoxyphenyl)-4H-chromen-4-one with antimicrobial activity from *Dodonaea viscosa* var. *angustifolia*," *South African Journal of Botany*, vol. 112, pp. 48–53, 2017.

[27] G. J. Amabeoku, P. Eagles, G. Scott, I. Mayeng, and E. Springfield, "Analgesic and antipyretic effects of *Dodonaea angustifolia* and *Salvia africana-lutea*," *Journal of Ethnopharmacology*, vol. 75, no. 2-3, pp. 117–124, 2001.

[28] J. Tauchen, I. Doskocil, C. Caffi et al., "In vitro antioxidant and anti-proliferative activity of Ethiopian medicinal plant extracts," *Industrial Crops and Products*, vol. 74, pp. 671–679, 2015.

[29] K. Teshome, T. Gebre-mariam, K. Asres, and E. Engidawork, "Toxicity studies on dermal application of plant extract of *Dodonaea viscosa* used in Ethiopian traditional medicine," *Phytotherapy Research*, vol. 24, no. 1, pp. 60–69, 2010.

[30] K. Asres, F. Bucar, T. Kartnig, M. Witvrouw, C. Pannecouque, and E. De Clercq, "Antiviral activity against human immunodeficiency virus type 1 (HIV-1) and type 2 (HIV-2) of ethnobotanically selected Ethiopian medicinal plants," *Phytotherapy Research*, vol. 15, pp. 62–69, 2001.

[31] T. Deressa, Y. Mekonnen, and A. Animut, "Vivo antimalarial activities of Clerodendrum myricoides, Dodonea angustifolia and Aloe debrana against Plasmodium berghei," *The Ethiopian Journal of Health Development*, vol. 24, no. 1, pp. 1–5, 2010.

[32] C. N. Muthaura, J. Keriko, C. Mutai et al., "Antiplasmodial potential of traditional phytotherapy of some remedies used in treatment of malaria in Meru – tharaka Nithi County of Kenya," *Journal of Ethnopharmacology*, vol. 175, pp. 315–323, 2015.

[33] W. Amelo, P. Nagpal, and E. Makonnen, "Antiplasmodial activity of solvent fractions of methanolic root extract of *Dodonaea angustifolia* in *Plasmodium berghei* infected mice," *BMC Complementary and Alternative Medicine*, vol. 14, pp. 462–467, 2014.

[34] B. Mengiste, E. Makonnen, and K. Urga, "In vivo antimalarial activity of *Dodonaea angustifolia* seed extracts against *Plasmodium berghei* in mice model," *Momona Ethiopian Journal of Science*, vol. 4, no. 1, pp. 47–63, 2012.

[35] G. Mengistu, H. Hoste, M. Karonen, J. P. Salminen, W. H. Hendriks, and W. Pellikaan, "The in vitro anthelmintic properties of browse plant species against *Haemonchus contortus* is determined by the polyphenol content and composition," *Veterinary Parasitology*, vol. 237, pp. 110–116, 2017.

[36] Z. K. S. Mcotshana, L. J. McGaw, D. Kemboi et al., "Cytotoxicity and antimicrobial activity of isolated compounds from *Monsonia angustifolia* and *Dodonaea angustifolia*," *Journal of Ethnopharmacology*, vol. 301, Article ID 115170, 2023.

[37] S. Esakkimuthu, S. Mutheeswaran, P. Elankani, P. Pandikumar, and S. Ignacimuthu, "Quantitative analysis of medicinal plants used to treat musculoskeletal ailments by non-institutionally trained siddha practitioners of Virudhunagar district, Tamil Nadu, India," *Journal of Ayurveda and Integrative Medicine*, vol. 12, no. 1, pp. 58–64, 2021.

[38] V. V. Poroikov, D. A. Filimonov, W. D. Ihlenfeldt et al., "PASS biological activity spectrum predictions in the enhanced open NCI Database Browser," *Journal of Chemical Information and Computer Sciences*, vol. 43, no. 1, pp. 228–236, 2003.

[39] A. Lagunin, A. Stepanchikova, D. Filimonov, and V. Poroikov, "PASS: prediction of activity spectra for biologically active substances," *Bioinformatics*, vol. 16, no. 8, pp. 747-748, 2000.

[40] A. Mishra, S. Kumar, and A. K. Pandey, "Scientific Validation of the Medicinal Efficacy of Tinospora Cordifolia," *Science World Journal*, vol. 2013, Article ID 292934, 8 pages, 2013.

[41] C. S. Tiwari and N. Husain, "Biological activities and role of flavonoids in human health - a review," *Indian Journal of Scientific Research*, vol. 12, no. 2, pp. 193–196, 2017.

[42] F. Zakaria, J.-K. Tan, S. M. Mohd Faudzi, M. B. Abdul Rahman, and S. E. Ashari, "Ultrasound-assisted extraction conditions optimisation using response surface methodology from Mitragyna speciosa (Korth.) Havil leaves," *Ultrasonics Sonochemistry*, vol. 81, Article ID 105851, 2021.

[43] J. R. Shaikh and M. Patil, "Qualitative tests for preliminary phytochemical screening: an overview," *International Journal of Chemical Studies*, vol. 8, no. 2, pp. 603–608, 2020.

[44] D. M. Kasote, G. K. Jayaprakasha, and B. S. Patil, "Leaf disc assays for rapid measurement of antioxidant activity," *Scientific Reports*, vol. 9, no. 1, pp. 1884–1910, 2019.

[45] R. Salazar, M. E. Pozos, P. Cordero, J. Perez, M. C. Salinas, and N. Waksman, "Determination of the antioxidant activity of plants from northeast Mexico," *Pharmaceutical Biology*, vol. 46, no. 3, pp. 166–170, 2008.

[46] V. Banothu, C. Neelagiri, U. Adepally, J. Lingam, and K. Bommareddy, "Phytochemical screening and evaluation of in vitro antioxidant and antimicrobial activities of the indigenous medicinal plant *Albizia odoratissima*," *Pharmaceutical Biology*, vol. 55, no. 1, pp. 1155–1161, 2017.

[47] Z. Chen, R. Bertin, and G. Froldi, "EC_{50} estimation of antioxidant activity in DPPH assay using several statistical programs," *Food Chemistry*, vol. 138, no. 1, pp. 414–420, 2013.

[48] S. McDonald, P. D. Prenzler, M. Antolovich, and K. Robards, "Phenolic content and antioxidant activity of olive extracts," *Food Chemistry*, vol. 73, no. 1, pp. 73–84, 2001.

[49] C. C. Chang, M. H. Yang, H. M. Wen, and J. C. Chern, "Estimation of total flavonoid content in propolis by two complementary colometric methods," *Journal of Food and Drug Analysis*, vol. 10, no. 3, pp. 178–182, 2020.

[50] E. C. Oliveira, E. I. Muller, F. Abad, J. Dallarosa, and C. Adriano, "Internal standard versus external standard calibration: an uncertainty case study of a liquid chromatography analysis," *Química Nova*, vol. 33, no. 4, pp. 984–987, 2010, http://scholar.google.com/scholar?hl=en&btnG=Search&q=intitle:Quim.+Nova,#0%5Cnhttp://www.scielo.br/pdf/qn/v33n4/41.pdf.

[51] J. M. Lü, P. H. Lin, Q. Yao, and C. Chen, "Chemical and molecular mechanisms of antioxidants: experimental approaches and model systems," *Journal of Cellular and Molecular Medicine*, vol. 14, no. 4, pp. 840–860, 2010.

[52] M. G. Maharani, S. R. Lestari, and B. Lukiati, "Molecular docking studies flavonoid (Quercetin, Isoquercetin, and Kaempferol) of single bulb garlic *(Allium sativum)* to inhibit lanosterol synthase as antihypercholesterol therapeutic strategies," *AIP Conference Proceedings*, vol. 2231, p. 2020, 2020.

[53] D. A. Filimonov, A. A. Lagunin, T. A. Gloriozova et al., "Prediction of the biological activity spectra of organic compounds using the pass online web resource," *Chemistry of Heterocyclic Compounds*, vol. 50, no. 3, pp. 444–457, 2014.

[54] S. O. Anode, T. Abraha, and S. Araya, "Phytochemical analysis of *Dodonaea angustifolia* plant extracts," *International Journal of Herbal Medicine*, vol. 6, no. 5, pp. 37–42, 2018.

[55] L. Mizzi, C. Chatzitzika, R. Gatt, and V. Valdramidis, "HPLC analysis of phenolic compounds and flavonoids with overlapping peaks," *Food Technology and Biotechnology*, vol. 58, no. 1, pp. 1–12, 2020.

[56] A. P. B. Gollucke, D. A. Ribeiro, and O. J. Aguiar, "Polyphenols as supplements in foods and beverages: recent methods, benefits, and risks," *Polyphenols in Human Health and Disease*, vol. 1, pp. 71–77, 2014.

[57] H. Kelebek, M. Jourdes, S. Selli, and P. L. Teissedre, "Comparative evaluation of the phenolic content and antioxidant capacity of sun-dried raisins," *Journal of the Science of Food and Agriculture*, vol. 93, no. 12, pp. 2963–2972, 2013.

[58] P. Alam, S. F. Elkholy, S. A. Mahfouz, P. Alam, and M. A. Sharaf-Eldin, "HPLC based estimation and extraction of rutin, quercetin and gallic acid in *Moringa oleifera* plants grown in Saudi Arabia," *Journal of Chemical and Pharmaceutical Research*, vol. 8, no. 8, pp. 1243–1246, 2016, https://www.jocpr.com/.

[59] A. Thomas, A. Kanakdhar, A. Shirsat, S. Deshkar, and L. Kothapalli, "A high performance thin layer chromatographic method using a design of experiment approach for estimation of phytochemicals in extracts of *Moringa oleifera* leaves," *Turkish Journal of Pharmaceutical Sciences*, vol. 17, no. 2, pp. 148–158, 2020.

[60] M. N. Malik, I. Haq, H. Fatima et al., "Bioprospecting *Dodonaea viscosa* Jacq.: a traditional medicinal plant for antioxidant, cytotoxic, antidiabetic and antimicrobial potential," *Arabian Journal of Chemistry*, vol. 15, no. 3, Article ID 103688, 2022.

[61] Z. W. Tong, H. Gul, M. Awais et al., "Determination of in vivo biological activities of Dodonaea viscosa flowers against CCl_4 toxicity in albino mice with bioactive compound detection," *Scientific Reports*, vol. 11, no. 1, Article ID 13336, 2021.

[62] V. Poroikov, D. Filimonov, A. Lagunin, and A. Stepanchikova, "PASS: prediction of biological activity spectra for substances," *Bioinformatics*, vol. 16, no. 8, pp. 747-748, 2000.

[63] S. Ramos, "Effects of dietary flavonoids on apoptotic pathways related to cancer chemoprevention," *The Journal of Nutritional Biochemistry*, vol. 18, no. 7, pp. 427–442, 2007.

[64] S. Bajkacz, I. Baranowska, B. Buszewski, B. Kowalski, and M. Ligor, "Determination of flavonoids and phenolic acids in plant materials using SLE-SPE-UHPLC-MS/MS method," *Food Analytical Methods*, vol. 11, no. 12, pp. 3563–3575, 2018.

[65] A. Tapas, D. Sakarkar, and R. Kakde, "Flavonoids as nutraceuticals: a review," *Tropical Journal of Pharmaceutical Research*, vol. 7, no. 3, pp. 1089–1099, 2008.

[66] M. Morsy and A. El-Sheikh, "Prevention of gastric ulcers," in *Peptic Ulcer Disease*, J. Chai, Ed., InTech, Rang-Du-Fliers, France, 2011.

[67] M. Friedman, "Overview of antibacterial, antitoxin, antiviral, and antifungal activities of tea flavonoids and teas," *Molecular Nutrition and Food Research*, vol. 51, no. 1, pp. 116–134, 2007.

Hindawi
Journal of Chemistry
Volume 2023, Article ID 4170703, 19 pages
https://doi.org/10.1155/2023/4170703

Research Article

Molecular Dynamics Simulation and Pharmacoinformatic Integrated Analysis of Bioactive Phytochemicals from *Azadirachta indica* (Neem) to Treat Diabetes Mellitus

Asif Abdullah,[1] Partha Biswas,[2] Md. Sahabuddin,[1] Afiya Mubasharah,[1] Dhrubo Ahmed Khan,[2] Akram Hossain,[3] Tanima Roy,[4] Nishat Md. R. Rafi,[3] Dipta Dey,[5] Md. Nazmul Hasan,[2] Shabana Bibi,[6,7] Mahmoud Moustafa,[8,9] Ali Shati,[9] Hesham Hassan,[10,11] and Ruchika Garg[12]

[1]*Department of Biomedical Engineering, Jashore University of Science and Technology, Jashore 7408, Bangladesh*
[2]*Laboratory of Pharmaceutical Biotechnology and Bioinformatics, Department of Genetic Engineering and Biotechnology, Jashore University of Science and Technology, Jashore 7408, Bangladesh*
[3]*Department of Biomedical Engineering, Khulna University of Engineering and Technology, Khulna 9203, Bangladesh*
[4]*Military Institute of Science and Technology, Dhaka, Bangladesh*
[5]*Biochemistry and Molecular Biology Department, Life Science Faculty, Bangabandhu Sheikh Mujibur Rahman Science and Technology University, Gopalgonj 8100, Bangladesh*
[6]*Department of Bioscience, Shifa Tameer-e-Millat University, Islamabad 44000, Pakistan*
[7]*Yunnan Herbal Laboratory, College of Ecology and Environmental Sciences, Yunnan University, Kunming 650091, China*
[8]*Department of Biology, Faculty of Science, King Khalid University, Abha, Saudi Arabia*
[9]*Department of Botany and Microbiology, Faculty of Science, South Valley University, Qena, Egypt*
[10]*Department of Pathology, College of Medicine, King Khalid University, Abha, Saudi Arabia*
[11]*Department of Pathology, Faculty of Medicine, Assiut University, Assiut, Egypt*
[12]*University School of Pharmaceutical Sciences, Rayat Bahra University, Mohali 140413, Punjab, India*

Correspondence should be addressed to Md. Nazmul Hasan; mn.hasan@just.edu.bd, Shabana Bibi; shabana.bibi.stmu@gmail.com, and Ruchika Garg; ruchika.p88@gmail.com

Received 1 September 2022; Revised 29 October 2022; Accepted 28 November 2022; Published 3 March 2023

Academic Editor: Romina Alina Marc (Vlaic)

Diabetes mellitus is a chronic hormonal and metabolic disorder in which our body cannot generate necessary insulin or does not act in response to it, accordingly, ensuing in discordantly high blood sugar (glucose) levels. Diabetes mellitus can lead to systemic dysfunction in the multiorgan system, including cardiac dysfunction, severe kidney disease, lowered quality of life, and increased mortality risk from diabetic complications. To uncover possible therapeutic targets to treat diabetes mellitus, the in silico drug design technique is widely used, which connects the ligand molecules with target proteins to construct a protein-ligand network. To identify new therapeutic targets for type 2 diabetes mellitus, *Azadirachta indica* is subjected to phytochemical screening using in silico molecular docking, pharmacokinetic behavior analysis, and simulation-based molecular dynamic analysis. This study has analyzed around 63 phytochemical compounds, and the initial selection of the compounds was made by analyzing their pharmacokinetic properties by comparing them with Lipinski's rule of 5. The selected compounds were subjected to molecular docking. The top four ligand compounds were reported along with the control drug nateglinide based on their highest negative molecular binding affinity. The protein-ligand interaction of selected compounds has been analyzed to understand better how compounds interact with the targeted protein structure. The results of the in silico analysis revealed that 7-Deacetyl-7-oxogedunin had the highest negative docking score of −8.9 Kcal/mol and also demonstrated standard stability in a 100 ns molecular dynamic simulation performed with insulin receptor ectodomain. It has been found that these substances may rank among the essential supplementary antidiabetic drugs for treating type 2 diabetes mellitus. It is suggested that more in vivo and in vitro research studies be carried out to support the conclusions drawn from this in silico research strategy.

1. Introduction

The ability of the body to exert control over and use sugar (glucose) as fuel is reduced in type 2 diabetes. Due to this chronic (long-term) illness, too much sugar circulates in the blood. The most notable metabolic dysfunctions associated with type 2 diabetes, often known as diabetes mellitus, are insulin resistance and cell dysfunction. Early in the condition, circulating insulin levels are higher to compensate for insulin resistance, but insulin production eventually becomes insufficient, and hyperglycemia develops [1, 2]. One of the human body's most significant regulators of energy balance is insulin. Insulin control issues disrupt energy homeostasis, which leads to type 2 diabetes mellitus [3, 4]. The human insulin receptor is a tyrosine kinase that is homodimeric and disulfide-linked $(\alpha\beta)2$ [5, 6]. Even though the receptor's signaling is essential in various diseases, thorough and atomic-level knowledge is still unclear on how insulin builds up at the receptor and triggers signal transduction. One challenge is that the isolated, soluble receptor ectodomain (sIR), which is suitable for structural biology studies, lacks the remarkable affinity and poor cooperativity of insulin binding that the hormone receptor (hIR) offers. The pancreas secretes insulin hormones [7, 8]. The ability of a cell to absorb blood glucose as an energy source is controlled by insulin through its interaction with the insulin receptor protein found on the cell's surface. In type 2 diabetes, insulin binds to the insulin receptor as it should. Still, the signal is not carried through into cells resulting in the cells not absorbing sufficient glucose, and the elevated blood glucose levels that result over time harm organs [9–11].

Many modern pharmaceuticals are directly or indirectly produced from plants, which have long been a reliable supply of medicines. According to ethnobotanical studies, approximately 800 plants may have antidiabetic qualities [12, 13]. Drug development is an expensive and time-consuming procedure that calls for numerous clinical trials. High throughput virtual screening and de novo structure-based rational drug design are two in silico methods for drug discovery that have shown potential [14–16]. Virtual screening is now widely used to uncover novel compounds like drugs. In silico virtual screening has become a valuable and time- and money-saving addition to in vitro screening for discovering and developing novel effective compounds [17–20]. Ligand-based virtual screening and receptor-based virtual screening are the two main screening procedures for finding potential compounds from a chemical database that are likely to interact favorably with the target binding sites [21, 22].

The 3d structure of a protein and protein-ligand complex is essential in molecular modeling for lead discovery [23–25]. Quantitative structure-activity relationships (QSAR), biological tests, and pharmacophore analysis can all be used to improve and create new leads [26–28]. Structure-based drug design assists in creating more potent and significant molecules during the drug development process [29–31].

The movement of each molecule in a molecular system is predicted by molecular dynamics (MD) simulations, which depend on a general physics model governing interatomic interactions [32–34]. The general concept of MD simulation is simple. Given the coordinates of every atom in a biomolecular system, it is possible to determine the force each atom experiences from all the other atoms in the system [35, 36] (for example, a protein encircled by a lipid bilayer and potentially some water). Thus, it is possible to forecast each atom's spatial position as a function of time using Newton's equations of motion. One, in particular, goes across time, estimating the forces acting on each atom and modifying every atom's position and speed based on all of those forces. A three-dimensional movie that shows how the system was configured at each point during the simulated period can be compared to the resulting trajectory [37, 38].

Finding a ligand that delivers a specific signaling profile and binding to the target is a common goal of drug development. This is true, in particular for signaling receptors [39, 40]. It is possible to use a full agonist, which vigorously stimulates the signaling and activation of the receptor, a partial agonist, which revitalizes signaling only slightly, and a neutral antagonist [41, 42], which inhibits the body's natural agonists from binding but does not signal on its own, or an inverse agonist, which decreases signaling below basal levels [43, 44]. The drug must stabilize receptor conformational states and, consequently, particular binding pocket conformational states to produce a specific signaling profile. An agonist, for instance, keeps active states above inactive states. The binding pocket's conformational changes have unique signaling patterns. This information might be available through MD simulations [37, 43].

Pharmacokinetic studies are an integral aspect of a new medicine development program. They are used to determine the time course of medicine and significant metabolite concentrations in tubes and other natural fluids to learn about immersion, distribution, metabolism, and elimination. Pharmacokinetics (PK) is commonly utilized in preclinical investigations to evaluate toxicological outcomes. In phase I cure forbearance studies, beast chronic toxicity data can be used to influence lozenge selection and escalation approaches. Pharmacokinetically guided cure escalation (PGDE) methods facilitate the use of preclinical pharmacokinetic data for clinical cure finding in phase I research. In clinical trials, PK is critical for cure detection and escalation investigations [44–46].

Every stage in the discovery and development of a drug requires consideration of chemical properties like absorption, distribution, metabolism, excretion, and toxicity (ADMET). It is crucial to develop effective compounds with improved ADMET characteristics [47]. The notion of drug-likeness is a helpful guideline during the early phases of medication development [48]. The first and most well-knownrule-based filters were proposed by Lipinski and colleagues in 1997. They included the molecular weight (MW) 500, the octanol/water partition coefficient (A log P) 5, the number of hydrogen bond donors (HBDs), and the

number of hydrogen bond acceptors (HBAs), all of which must be greater than or equal to 5 [49–51]. Ghose and colleagues calculated that, of the 6304 compounds in the CMC (comprehensive medicinal chemistry) database, more than 80% met the following requirements: −0.4 A log P 5.6, 160 MW 480, 40 MR (molar refractivity), and 20 to 70 atoms in total [52]. 7 drug development can be sped up by using filters that compare compounds to drugs based on their physicochemical properties. But 14 numerous studies have demonstrated the limitations of drug-likeness rules or filters based on physicochemical characteristics [53, 54].

Several studies have shown the efficacy of neem in treating diabetes meatus. However, the phytochemical screening of ligands, specific pharmacokinetic behavior analysis-related study, and molecular dynamics simulation study of ligands derived from neem is still not performed. Therefore, we aim to analyze the following parameters to have a deep view of new oral drug candidates and potential inhibitors against insulin receptor ectodomains derived from the neem tree via in silico studies.

2. Materials and Methods

2.1. Preparation of Protein. The RCSB protein data bank (PDB) (https://www.rcsb.org/) contains the 3D experimental tertiary structures of the protein insulin receptor ectodomain. Three hundred six amino acids (AA) make up the protein sequence known as the insulin receptor ectodomain protein with the PDB id 1i44 [55]. The proteins' PDB structures were assembled using the following criteria: water, metal ions, side chains, and cofactors were excluded, as well as crystallographic protein structure and expressed in humans. Then, the Chimera software mixed polar hydrogen atoms with nonpolar hydrogen atoms. Finally, the Gasteiger charges of the system were determined.

2.2. Selection of Ligands. The large variety of chemical spaces covered by phytochemicals derived from naturally occurring medicinal plants can be employed in drug development and discovery. The IMPPAT (Indian medicinal plants, phytochemistry, and therapeutics) database, which contains >1742 Indian medicinal plants and >9500 phytochemical substances, is used to improve natural product-based medication discovery [56, 57]. The chemicals from Azadirachta indica (neem tree) have been compiled using the IMPPAT journal after extensive literature reviews. The compounds discovered in the database were made by accurately classifying the atoms in AutoDock 4, combining nonpolar hydrogens, finding aromatic carbons, and creating a "torsion tree." It has been found that most of the particles in the compound have the same sort of atom as the AD4 atom.

2.3. Molecular Docking. These days, molecular docking is an integral part of structural biology and is primarily employed for CADD. The techniques aid in predicting which small molecule will attach to a target macromolecule (such as a protein, enzyme, or drug) most advantageously [58, 59]. The PyRx virtual screening software integrated with the AutoDock Vina platform was used to conduct a molecular docking analysis to assess the molecular binding energy of the requisite protein with the chosen phytochemicals [60, 61].

A library of chemicals can be tested against a specific therapeutic target using PyRx, an open-source virtual screening program. It mostly appears in CADD techniques. PyRx becomes a more dependable CADD tool with the addition of AutoDock 4 and AutoDock Vina as docking wizards and a simple user interface. The ideal protein and ligand binding configurations were found using the molecular docking PyRx tools AutoDock Vina wizard [62]. Utilizing the default setup parameters of the PyRx virtual screening tools, the binding energy with the highest negative number (kcal/mol) was selected as a `preferred drug candidate for further experiments. The protein-ligands complex's binding interaction was eventually visualized using the Ligplot + Version 2.2 tools [63].

2.4. MM-GBSA Analysis. MMGBSA is known as the molecular mechanics-generalized born surface area which can be performed to calculate ligand binding free energies and ligand strain energies for a set of ligands and a single receptor [64, 65]. After completing the interaction binding affinity analysis, the MMGBSA was conducted by utilizing the prime model of Schrödinger suite 2020-3 (maestro application, paid version). This study analyzed the relative binding free affinity of the ligand compounds Vilasinin (PubChem-102090424), Nimbidinin (PubChem-101306757), 7-Deacetyl-7-oxogedunin (PubChem-1886), and PubChem-122801 with the 1I44 protein complex.

2.5. Pharmacokinetic Property and QSAR Analysis. In CADD, the term "PK" refers to the computer-based timing of drug absorption, distribution, metabolism, and excretion (ADME). The flow of drugs into and out of the body as a function of intensity and duration is described by PK (ADME) features as a whole [66]. In the early stages of CADD, the integrity and effectiveness of substances are supported and defined by their pharmacokinetic properties. The study used the SwissADME (http://www.swissadme.ch) website to look at the early-stage PK characteristics of the medications we chose [67]. The SwissADME server is a free online web-based server widely used to predict the pharmacokinetic properties and drug-likeness characteristics of simple molecules. Thus, the pharmacokinetic property is analyzed using the SwissADME server. The PKCSM website is used to predict toxicity (https://biosig.unimelb.edu.au/pkcsm/) [68]. Finally, the quantitative structure-activity relationship (QSAR) assessment for the top ligands was carried out on the PASS server (https://www.pharmaexpert.ru/passonline) to validate antidiabetic, anticancer, and antiviral activity.

2.6. Molecular Dynamic Simulation. To determine the stability of the targeted protein, insulin receptor ectodomain's (PDB ID : 1I44) interaction with the four possible ligand

molecules was chosen and subjected to 100 nanoseconds MD simulations. The "Desmond v3.6 Program" from Schrödinger (https://www.schrodinger.com/ac) was used to model the molecular dynamics of the protein-ligand complex structures [69].

To establish the desired this framework, a predetermined TIP3P water strategy was developed to establish a specific volume with periodic orthorhombic coordinates separated by 10 mm. The necessary ions, for example, 0+ and 0.15 M salts, were randomly added to the solvent solution to neutralize the framework electrically. The solvency protein system was constructed utilizing a ligand complex, and the system framework was reduced using the default protocol. This was accomplished totally inside the Desmond module by applying the force field settings OPLS3e [70]. In NPT assemblies, which were held at 101,325 bar (1 atm) pressure and 300 K with 50 PS capture sessions totaling 1.2 kcal/mole energy coming before them, the Nosé–Hoover temperature combination and the isotropic approach were used.

The screenshots of the molecular dynamic simulation were produced using Schrödinger's maestro application, version 9.5. The Simulations interaction diagram derived from the Desmond modules of the Schrödinger suite has been used to analyze the simulation event and assess the dependability of the MD simulation. The stability of the protein-ligand complex structure was evaluated based on the trajectory performance, root mean square fluctuation (RMSF), root mean square deviation (RMSD), solvent-accessible surface area (SASA) value, intramolecular hydrogen bonds, the radius of gyration (Rg) value, protein-ligand contacts (P-L), the polar surface area (PSA), and MolSA. The root means square deviation (RMSD) in molecular dynamics simulations is the arithmetic mean distance generated by a single atom's motion over the period of a certain amount of time relative to a reference time [71, 72]. The RMSD of the structural atoms of a protein, such as heavy particles, backbone, C, and sidechain, were first measured before the root mean square deviation of protein-suited ligand compounds from all timescales, which were realigned and compared against the reference time (in our study 100 ns). The following equation (equation (1)) can be used to determine the RMSD of an MD simulation concerning the period of x.

$$\mathrm{RMSD} = \sqrt{\frac{\sum_{i=0}^{N}\left[m_i * \left(X_i - Y_i\right)^2\right.}{M}}. \tag{1}$$

N stands for the number of selected atoms, r' for the bit's position in the system x after the reference system's point has been superimposed, and j for the reference time. Most commonly, local changes in the conformational shape of proteins have been detected and tracked using the root mean square fluctuation (RMSF) [73]. The RMSF estimation of a molecular dynamic's simulation of a protein with 2 residues can be obtained using the continuity equation (2).

$$\mathrm{RMSF} = \sqrt{\frac{1}{T}\sum_{T_j}^{T}\left(X_i\left(t_j\right) - x_j\right)^2}. \tag{2}$$

3. Result and Findings

3.1. Molecular Docking Result Analysis. The process of drug development has become more reliant on molecular docking. Advances in computer hardware and a rise in the number of and ease of access to small molecule and protein structures, have facilitated the development of new techniques, making docking more popular in both commercial and academic contexts since its inception in the 1980s. The methods for enhancing several drug development tasks with docking have evolved throughout time. Docking was initially created and utilized as a stand-alone technique, but it is now routinely combined with other computational techniques in integrated workflows.

The desired intermolecular framework within a drug compound and a macromolecule can be developed through molecular docking. A molecular docking study was first conducted to determine the optimal intermolecular interaction between the phytochemical ligand compounds with the target protein by a group of Python tools called PyRx. Using the AutoDock Vina wizard, we performed molecular docking between 63 phytochemicals and the target protein. The phytochemical compound's molecular docking revealed binding affinities that range from −4.5 to −8.9 kcal/mol.

The top 6.35% of 63 phytochemicals (a total of 4) had a better binding affinity than nateglinide and were chosen based on binding affinity. This study utilized Nateglinide as a control ligand because of its previously reported inhibitory effect against the human insulin receptor ectodomain, which binds with a docking score of −7.1 kcal/mol. The compounds with the best docking score and binding affinity are listed in Table 1.

3.2. MM-GBSA Result Analysis. The greater the negative free energies of the binding value, the stronger the binding between the ligand compound with the targeted protein complex (Table 2). The findings showed that the Vilasinin (PubChem CID-102090424) with 1I44 protein complex possessed strong binding free energy −53.644. In contrast, PubChem CID-122801, Nimbidinin (Pubchem-101306757), 7-Deacetyl-7-oxogedunin (PubChem CID-1886), and Nateglinide (PubChem CID-5311309 (Control)) with 1I44 protein complex have been shown excellent binding free energy −48.984, −41.589, −41.461, and −40.984 consecutively.

3.3. Analysis of Protein-Ligand Interactions. The interactions between protein and ligand molecules are necessary for most biological processes. All biological processes depend on the ligand-mediated signaling that occurs through molecular complementarity. At the molecular level, biological recognition is produced by this type of protein-ligand chemical interaction. Establishing specialized sites designed to bind small-molecule ligands having standard affinities adjusted to the requirements of the cell is essential for the evolution of protein function. Cooperation between ligands and the target protein is essential for regulating biological processes

Table 1: List of the selected best four ligands and nateglinide (control drug) with their PubChem CID chemical name, two-dimensional (2D) chemical structure, and docking score.

Compound CID	Compound name	Chemical structure	Docking score
CID-1886	7-Deacetyl-7-oxogedunin	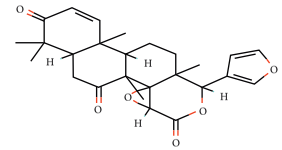	−8.9
CID 122801	[1S, 2R, 4S, 10R, 11R, 16R)-6-(Furan-3-yl)-1, 7, 11, 15-pentamethyl-5, 14-dioxo-3 oxapentacyclo [8.8.0.02, 4.02, 7.011, 16] octadec-12-en-18-yl] acetate	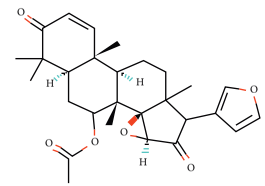	−8.5
CID 102090424	Vilasinin	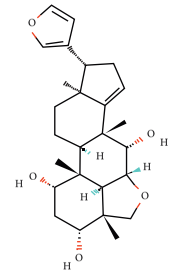	−8.2
CID 101306757	Nimbidinin	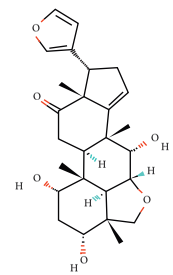	−7.9
CID 5311309 (control)	Nateglinide	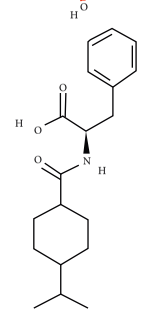	−7.1

Table 2: MMGBSA calculation by maestro application of schrodinger package software.

Protein ID	Ligand PubChem CID	Ligand name	MMGBSA dG bind score (kcal/mol)
1I44	1886	7-Deacetyl-7-oxogedunin	−41.461
1I44	122801	[1S, 2R, 4S, 10R, 11R, 16R)-6-(Furan-3-yl)-1,7,11,15-pentamethyl-5, 14-dioxo-3 oxapentacyclo [8.8.0.02, 4.02, 7.011, 16] octadec-12-en-18-yl] acetate	−48.984
1I44	102090424	Vilasinin	−53.644
1I44	101306757	Nimbidinin	−41.589
1I44	5311309 (control)	Nateglinide	−40.984

that clash with one another. The molecular mechanisms governing protein compatibility changes between low and high-affinity states affect cellular function through collaborative protein-ligand interactions.

The creation of small-molecule drug compounds for the treatment of disease is made possible by the atomic resolution structures of protein-ligand complexes. The Ligplot + Version 2.2 tools were used to show how the selected four ligands interacted with the target protein in Table 3. In terms of the chemical CID 1886 has been formed with two hydrogen bonds, Trp1200 (A) (3.34 Å) and Asp1229 (A) (3.13 Å), and a hydrophobic bond with Ser1204 (A), Glu1207 (A), Pro1231 (A), Gln1211 (A), Leu1213 (A), Phe1221 (A), Leu1228 (A), Try1227 (A), and Tyr1210 (A).

In terms of the chemical CID 122801, it has been revealed that when it comes into contact with the appropriate protein PDB-1I44. From the Ligplot + visualizer, it can be visualized that the hydrogen bond has been formed with Asp1083 (A) (2.91 Å) and supported by 12 hydrophobic bonds (Val1010 (A), Gly1149 (A), Val1060 (A), Met1070 (A), Lys1030 (A), Met1139 (A), Asn1137 (A), Arg1136 (A), Gln1004 (A), Gly1082 (A), Gly1003 (A), and Leu1002 (A)). "The insulin Receptor Ectodomain-Vilasinin" complex was supported by one hydrogen bond Lys1030 (A) (3.08 Å) and fourteen hydrophobic bonds (Ala1028 (A), Met1079 (A), Leu1078 (A), Met1039 (A), Val1010 (A), Leu1002 (A), Gly1082 (A), Gly1003 (A), Arg1136 (A), Asp1083 (A), Gln1004 (A), Asn1137 (A), Ser1006 (A), and Gly1005 (A)) (Figure 1), whereas Nimbidinin interacts with insulin receptor ectodomain protease was supported by two hydrogen bonds (Asp1232 (A) (2.82 Å) and Glu1207 (A) (3.30 Å) and nine hydrophobic bonds (Pro1104 (A), Thr1203 (A), Asn1233 (A), Met1109 (A), Pro1235 (A), Pro1103 (A), Ser1204 (A), Leu1205 (A), and Pro1231 (A)) (Figure 1). In addition, the control drug nateglinide possesses the interaction with the targeted protein by one hydrogen bond with Met1079 (A) (2.94 Å) and eleven hydrophobic bonds, including Ala1029 (A), Lys1030 (A), Val1060 (A), Met1139 (A), Met1076 (A), Val1010 (A), Leu1002 (A), Asp1083 (A), Gly1083 (A), Gly1082 (A), and Leu1078 (A).

3.4. Pharmacokinetic Property and QSAR Analysis. The study of a small molecule candidate's dynamic motions inside the body, and the ADME characteristics of a chemical that resembles a drug, is known as pharmacokinetics. The term "PK" refers to a class of xenobiotic regulatory procedures that is necessary throughout the drug discovery process, especially in preclinical studies. It employs several mathematical equations to create a model and offers data on the xenobiotics in the body over time. In addition, PK traits can aid in understanding and predicting biological functions, such as a compound's harmful or beneficial effects. The PKCSM server and SwissADME server were utilized in the study of the necessary PK parameters of the four selected potential phytocompounds that were chosen. The ADME features of the selected compounds, such as lipophilicity (dissolve in oils, fats, and nonpolar solvents), drug-likeness, and water solubility, have been found using the server. In the investigation, the PK characteristics of all of the identified compounds were found to be efficacious and druggable. The compounds studied in this paper have no violation according to Lipinski's rule of 5 and Ghose and colleague's rule. Pk properties, including several hydrogen bond donors and acceptors, molecular weight, molar refractivity, and Log p value, are noted in Tables 4 and 5.

Table 4 has depicted important pharmacokinetic parameters to show the credentials of the selected phytocompounds to be selected as a preferable alternative for present-age diabetic medicine. The molecular weight of the following drug compounds is within the range of 350–480 which firmly supports the ADMET rules of both Lipinski's Rule of 5 and Ghose and Colleagues' rules. All the compounds possess more hydrogen bond donors than the control drug. In the case of hydrogen bonds acceptors, CID 1886 and CID 122801 don't possess any hydrogen bond acceptors, whereas CID 102090424 and CID 101306757 contain 3 hydrogen bond acceptors each, and the control drug CID 5311309 got 2 hydrogen bond acceptors. The logP values are reported as 4.1981, 4.6291, 3.6435, 2.82225, and 4.1981 for compound CID 1886, CID122801, CID 102090424, CID 101306757, and CID 5311309 (Control), respectively. Other important pharmacokinetic parameters including molar refractivity, Intestinal absorption, total clearance, and CaCO2 permeability also have been reported within a standard range as shown in Table 4.

In Table 5, different toxicity-related parameters for the selected phytocompounds have been demonstrated. From Table 5, we can see that no compounds have shown AMES toxicity or working as hERG I or hERG II inhibitors. The maximum tolerated dose in humans for CID 1886 is 0.48; for CID 122801, the value is −0.658. For CID 102090424 compound, the maximum tolerated dose is −0.69. For CID 101306757 compound, the maximum tolerated dose is −0.625. And lastly, for CID 5311309 (control) compound, the maximum tolerated dose is 0.292. From the column where the rat acute toxicity (LD50) has been depicted, we can see the LD50 values are the compounds are 2.791, 2.694, 2.716, 3.71, and 2.022 for CID 1886, CID 122801, CID 102090424, CID 101306757, and CID 5311309 (control) respectively. The oral rat chronic toxicity (LOAEL) values of those compounds are 0.66, 0.534, 1.715, 2.28, and 1.977 followed by the CID sequence mentioned previously. This work also evaluated the hepatotoxicity and skin sensitiveness of the compounds. It has been found that only CID 102090424 has hepato-toxicity, whereas all the other compounds are reported safe from hepatotoxicity as well as skin sensation parameters in the following in silico study. The T. pyriformis toxicity and minnow toxicity also showed the druggability of the selected phytocompounds.

Moreover, the quantitative structure-activity relationship (QSAR) assessment showed that these ligand compounds possessed potent antidiabetic, anticancer, and antiviral activity (Table 6). Here, the compounds CID-122801, CID-102090424, CID 101306757, and CID 5311309 (control) possessed potent antidiabetic properties, whereas CID-122801, CID-102090424, CID 101306757, and CID 5311309 (control) have reported antiviral activity. All the compounds also showed potential to be selected as an anticancer compound according to the QSAR analysis.

Table 3: Molecular interactions between the chosen phytochemicals and the targeted receptor are tabulated in the docking score.

Compounds	Docking score (kcal/mol)	Interaction of the hydrogen bond	Interaction of the hydrophobic bond
7-Deacetyl-7-oxogedunin (CID-1886)	−8.9	Trp1200 (A) (3.34 Å) and Asp1229 (A) (3.13 Å)	Ser1204 (A), Glu1207 (A), Pro1231 (A), Gln1211 (A), Leu1213 (A), Phe1221 (A), Leu1228 (A), Try1227 (A), and Tyr1210 (A)
[1S, 2R, 4S, 10R, 11R, 16R)-6-(Furan-3-yl)-1,7,11,15-pentamethyl-5, 14-dioxo-3 oxapentacyclo [8.8.0.02, 4.02, 7.011, 16] octadec-12-en-18-yl] acetate (CID 122801)	−8.5	Asp1083 (A) (2.91 Å)	Val1010 (A), Gly1149 (A), Val1060 (A), Met1070 (A), Lys1030 (A), Met1139 (A), Asn1137 (A), Arg1136 (A), Gln1004 (A), Gly1082 (A), Gly1003 (A), and Leu1002 (A)
Vilasinin (CID 102090424)	−8.2	Lys1030 (A) (3.08 Å)	Ala1028 (A), Met1079 (A), Leu1078 (A), Met1039 (A), Val1010 (A), Leu1002 (A), Gly1082 (A), Gly1003 (A), Arg1136 (A), Asp1083 (A), Gln1004 (A), Asn1137 (A), Ser1006 (A), and Gly1005 (A)
Nimbidinin (CID 101306757)	−7.9	Asp1232 (A) (2.82 Å) and Glu1207 (A) (3.30 Å)	Pro1104 (A), Thr1203 (A), Asn1233 (A), Met1109 (A), Pro1235 (A), Pro1103 (A), Ser1204 (A), Leu1205 (A), and Pro1231 (A)
Nateglinide (CID 5311309)	−7.1	Met1079 (A) (2.94 Å)	Ala1029 (A), Lys1030 (A), Val1060 (A), Met1139 (A), Met1076 (A), Val1010 (A), Leu1002 (A), Asp1083 (A), Gly1083 (A), Gly1082 (A), and Leu1078 (A)

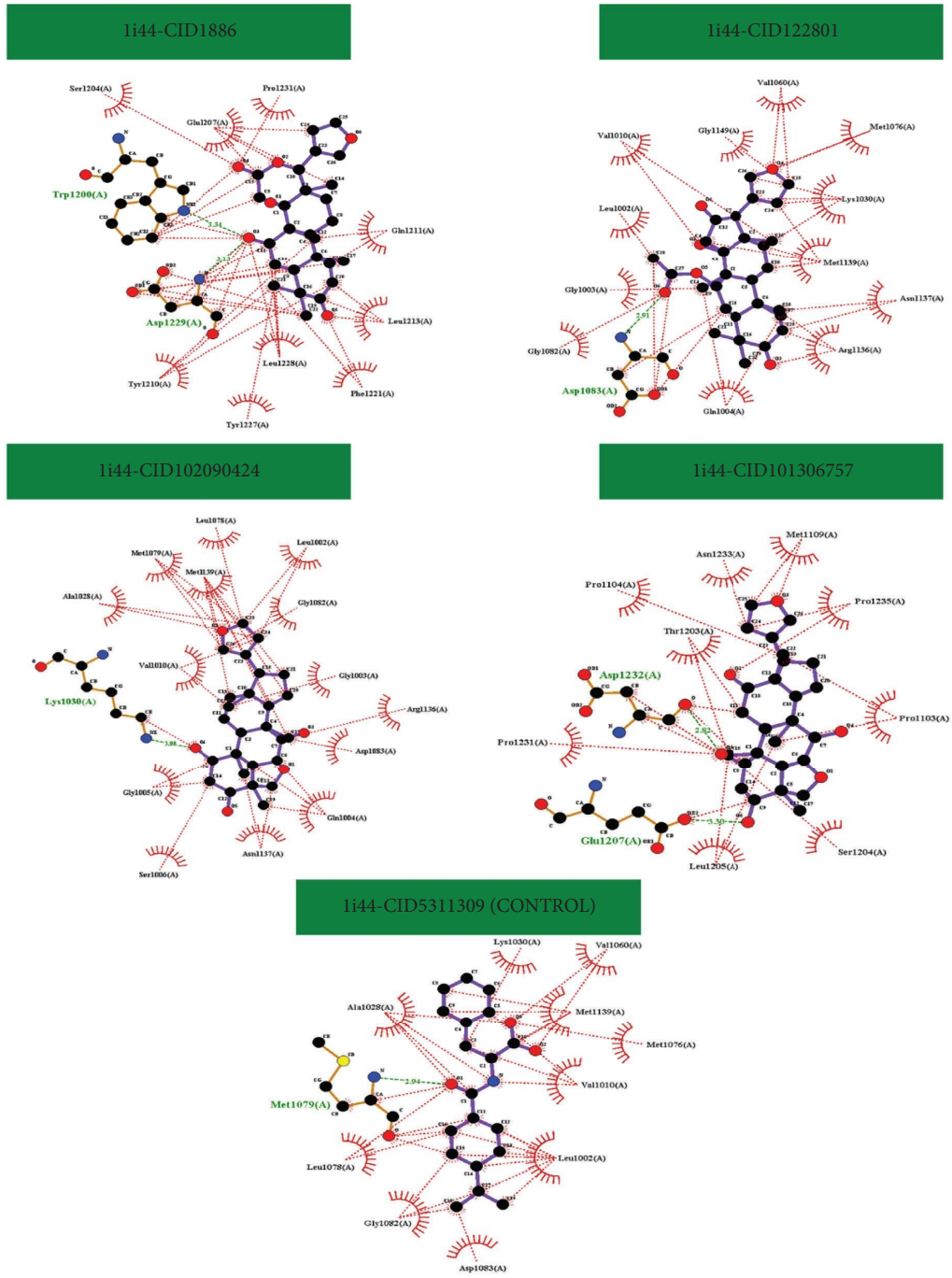

Figure 1: Interaction between the insulin receptor ectodomain (PDB 1I44) with compound CID 1886, CID 122801, CID 102090424, and CID 101306757.

Table 4: The complete pharmacophore and pharmacokinetic profiling of the selected ligands.

Compound ID	MW (g/mol)	HBA	HBD	LogP	MR	IAb	TCl	CaP
CID-1886	438.52	6	0	4.1981	115.34	99.394	0.093	0.883
CID-122801	466.57	6	0	4.6291	124.96	100	0.33	1.154
CID-102090424	428.569	5	3	3.6435	117.11	97.403	0.36	0.702
CID-101306757	442.54	6	3	2.8225	117.31	86.847	1.21	2.094
CID 5311309 (control)	317.42	2	2	4.1981	91.75	99.405	0.108	0.878

Units of physiochemical properties: MW, molecular weight (g/mol); HBA, hydrogen bond acceptor; HBD, hydrogen bond donor; LogP, estimated octanol/coefficient of liquid fraction; MR, molecular refractivity. Units of pharmacokinetics properties: IAb, intestinal absorption (% absorbed); TCl, total clearance (log mL/min/kg); Caco2 permeability (log Papp in 10^{-6} cm/s).

Table 5: Table depicting the toxicity properties of selected compounds showing compound CID, AMES toxicity, max. Tolerated dose (human), hERG I inhibitor, hERG II inhibitor, oral rat acute toxicity, (LD50) oral rat chronic toxicity (LOAEL), hepato-toxicity, skin sensitisation, T. pyriformis toxicity, and minnow toxicity.

Compound CID	AMES toxicity	Max. tolerated dose (human)	hERG I inhibitor	hERG II inhibitor	Oral rat acute toxicity (LD50)	Oral rat chronic toxicity (LOAEL)	Hepato-toxicity	Skin sensitisation	*T. pyriformis* toxicity	Minnow toxicity
CID 1886	No	−0.48	No	No	2.791	0.66	No	No	0.304	−0.07
CID 122801	No	−0.658	No	No	2.694	0.534	No	No	0.306	0.243
CID 102090424	No	−0.69	No	No	2.716	1.715	Yes	No	0.359	1.129
CID 101306757	No	−0.625	No	No	3.71	2.28	No	No	0.287	2.354
CID 5311309 (control)	No	0.292	No	No	2.022	1.977	No	No	0.284	0.796

Table 6: QSAR-based bioactivity prediction for ligand validation.

Compounds CID	Prediction of activity spectra for substances (Pa = 0.3 to 0.7)		
	Antidiabetic	Anticancer	Antiviral
CID-1886	×	√	√
CID-122801	√	√	√
CID-102090424	√	√	√
CID-101306757	√	√	×
CID 5311309 (control)	√	√	√

QSAR: quantitative structure-activity relationship; Pa: prediction of activity score as per PASS server. Pa score of 0.3 to 0.7 signifies moderate activity. ×: Pa score less than 0.3; √: Pa score in the range 0.3 to 0.7.

3.5. Analysis of MD Simulation Parameters. The conformational stability and several intramolecular interaction parameters of a protein-ligand complex are studied in real time using MD simulation in CADD. The conformational alteration that a complex system experiences when it is placed in an artificial environment can also be ascertained using this method. To comprehend the conformational variations and rearrangements of the protein in complex, a 100 ns MD simulation of the protein in combination with the particular ligand was carried out in this study. Initially, the terminal snapshots from the 100 ns MDS trajectories were used to examine intermolecular behavior.

The average change in the RMSD of the protein-ligand interaction is quite acceptable, with a range of 1–4. If the RMSD value is greater than 1–4, a significant conformational shift in the protein structure has occurred. To examine the conformational change of the target protein combination with the two ligand molecules included by the 4-ligand molecule and control drug, a 100 ns MD simulation was performed, and the related RMSD value was determined.

The ligand complex vilasinin, which had fewer fluctuations, had an average RMSD that ranged from 1.2 to 2.4. The RMSD value of the compound, which changed within a very small range and dropped outside the permissible range, indicates that the protein-ligand complex structure depicted in Figure 2 is conformationally stable.

The RMSF can facilitate in identifying and characterizing the adjacent alterations that arise within the configuration of the protein when a particular ligand compound attaches with remnants. The RMSF of the compounds with the targeted protein model was established for analyzing the changes in protein structure resulting from the attachment of specific ligands with a particular residual site, as illustrated in Figure 3.

Alpha helices and beta strands, which are among the most rigid secondary structural elements, were shown to have a minimum observation rate between 7 and 275 amino acid residues. Due to the existence of these domains, the C- and N- termini of the protein exhibit the majority of the variation. Therefore, it is discovered that there is a low fluctuation probability for the displacement of a single atom in the four-ligand complex and control medication under examination in the simulation environment.

The radius of gyration (RG) of the interaction between protein and ligand can be determined by the positioning of an interaction system's atoms across its axis. Since it divulges alteration in complex compactness gradually, the computation of the radius of gyration is one of the most crucial signs to look for when predicting the structural functioning of a macromolecule.

The stability of 7-Deacetyl-7-oxogedunin, [(1S, 2R, 4S, 10R, 11R, 16R)-6-(Furan-3-yl)-1,7,11,15,15-pentamethyl-5,14-dioxo-3 oxapenta-cyclo [8.8.0.02, 4.02, 7.011, 16] octadec-12-en-18-yl] acetate, Vilasinin, Nimbidinin, and Nateglinide together with the target protein was also explored in terms of the radius of gyration over a 100 ns simulation run, as depicted in Figure 4. The mean rg value for 7-Deacetyl-7-oxogedunin is 3.75, and for CID 122801, CID 102090424, CID 5311309, and Nateglinide (control drug), the average rg value is 4. This result shows that the protein's binding site does not undergo significant structural alterations upon binding the selected ligand compounds.

The confirmation of structural identity and the actions of biological macromolecules are governed by SASA concentration. When amino acid residues are attached to a surface of a protein, it functions as active sites and/or get interconnected with other molecules and ligands, a molecule's solventlike behavior (hydrophilic or hydrophobic), and the elements of protein-ligand interactions are better known.

The SASA for the selected compounds was in the range of 50 to 40, showing standard exposure of the selected compound with an amino acid residue in the complex systems (Figure 5).

The MolSA is equivalent to the Van der Waals surface area, which was discovered using a 1.4 probe radius. In our in silico analysis, each ligand had the standard Van der Waals surface area (Figure 6). In addition, only molecule of nitrogen and oxygen atoms contribute to PSA. Here, the targeted protein showed a significant PSA value for each ligand molecule (Figure 7).

Using the simulation interactions diagram, the intricate structure of a protein with the indicated ligands and their intermolecular interactions have been studied during a simulation time of 100 ns (SID).

The interactions between the chosen ligand molecules and proteins are influenced by various factors, including the hydrogen bond, noncovalent bond (hydrophobic bond), ionic bond, and water bridge bond. Figure 8 evaluates and depicts the chosen ligand compounds and the control drug. To help build a stable binding with the intended protein, all compounds generated many connections throughout the course of the 100 ns simulation via hydrogen, hydrophobic, ionic, and water bridge bonding and maintained these contacts up until the simulation was over.

4. Discussion

A drug candidate must have good activity against the therapeutic target to achieve the appropriate ADMET properties at a therapeutic dose [74]. ADME, linked to pharmacokinetic characteristics, significantly impacts a drug's activity. The pharmacokinetic parameters are obligatory to create a medication candidate that will successfully complete the required clinical trials and must be adjusted in time for the drug design process [75–77].

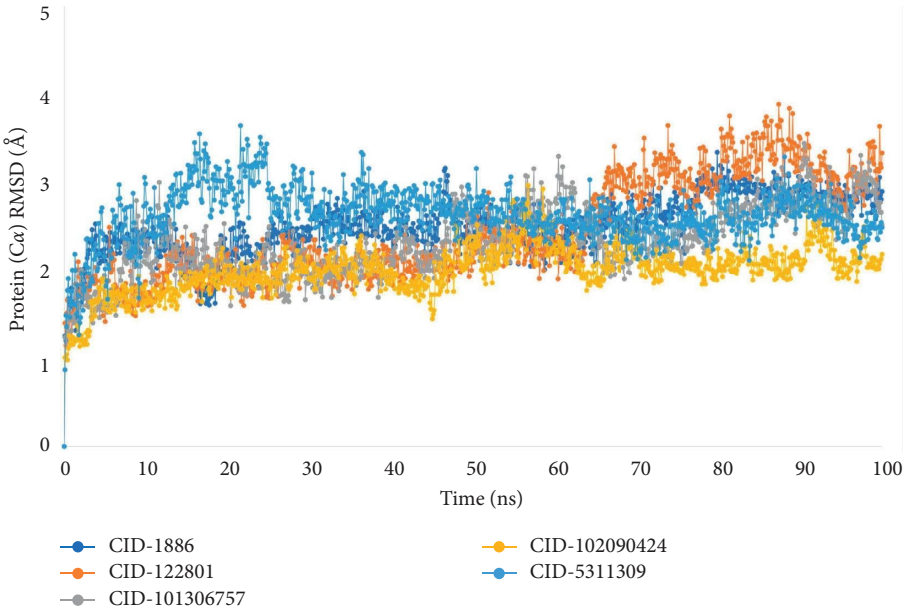

Figure 2: The RMSD values for the 4 ligand molecules and the nateglinide control for the 1i44 protein model. The selected compounds with the CIDs 1886, 122801, 101306757, 102090424, and 5311309 in relationship with the protein were represented by the hues dark blue, orange, gray, yellow, and light blue, respectively, while the control medicine had the CIDs 5311309 in association with the protein.

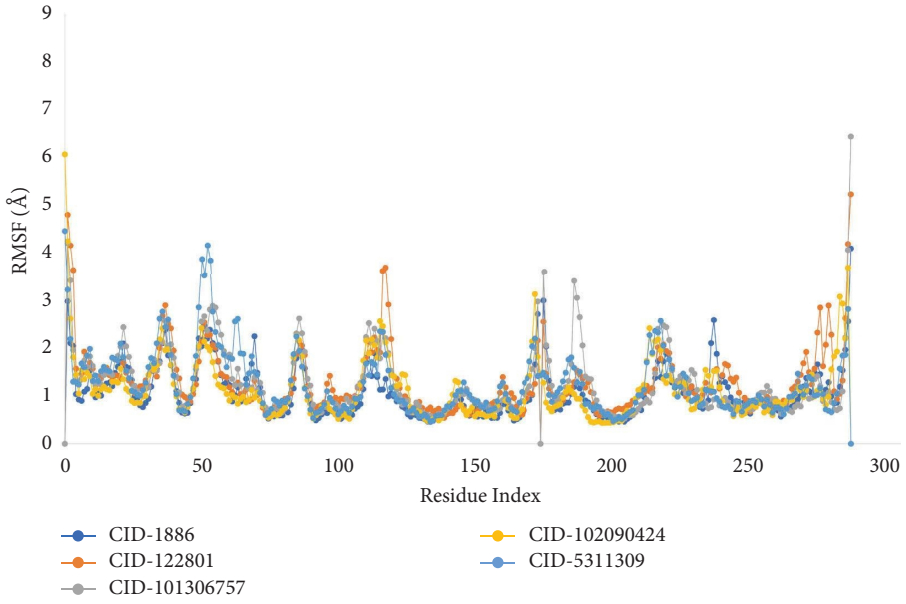

Figure 3: The graph displays the RMSF values for the 1i44 protein model using 4 ligand compounds and 1 control drug that were recovered from the C atoms of the complex system. The markers blue, orange, gray, yellow, and light blue are used to depict the selected compounds and had the CIDs 1886, 122801, 101306757, 102090424, and 5311309, respectively.

According to Lipinski and Ghose's drug likeliness qualities, the compounds investigated in this investigation did not exhibit severe toxicity or any other violations. The pharmacokinetics and drug-likeness properties of the investigated compounds were calculated. The compound selected after docking with the most promising result shows no violation in both Lipinski's rule of 5 and Ghose and colleagues' rule. The selected ligands followed the following parameters: $160 \leq MW \leq 480$, $-0.4 \leq WLOGP \leq 5.6$, $MLOGP \leq 4.15$, N or $O \leq 10$, NH or $OH \leq 5$, $40 \leq$ Molar Refractivity ≤ 130, and $20 \leq$ Atoms ≤ 70. No compound has shown any adverse toxic effect during the in-silico toxicity analysis [78–80]. Furthermore, the QSAR analysis depicted that all the compounds possessed effective antidiabetic, anticancer, and antiviral activity.

Analysis of biomolecular interactions and the interface between protein architecture and activity can benefit the development of new medications and performance data

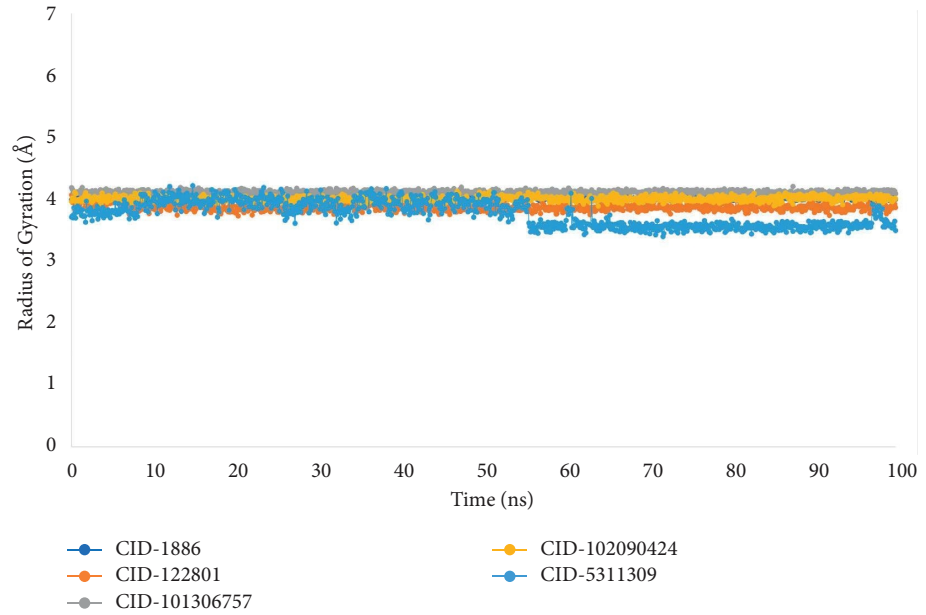

Figure 4: The radius of gyration (Rg) of the protein-ligand interaction was calculated using the 100 ns simulation. The markers blue, orange, gray, yellow, and light blue are used to depict the selected ligand compounds that contain the CID 1886, CID 122801, CID 101306757, CID 102090424, and CID 5311309, respectively, in association with the protein.

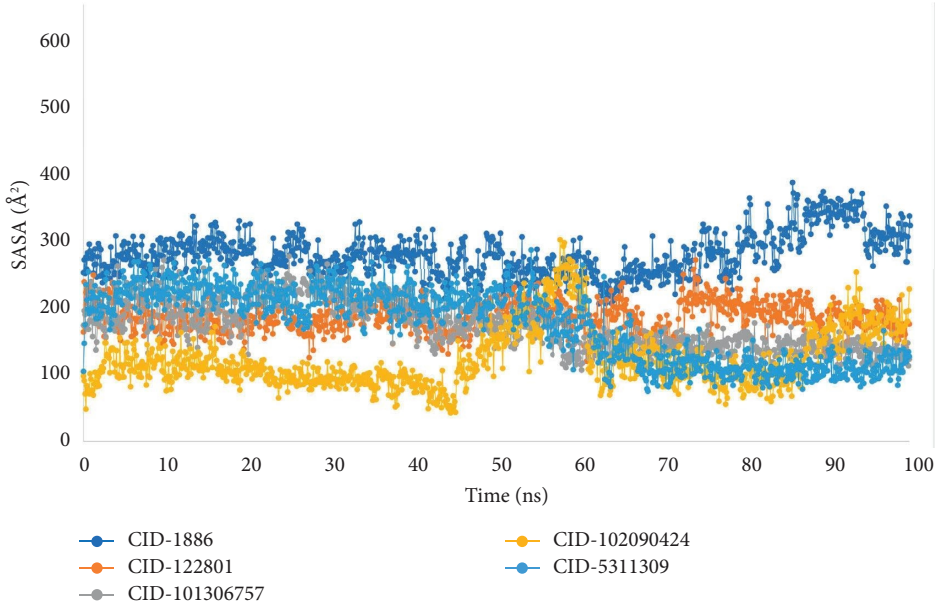

Figure 5: From the 100 ns simulated interaction diagram, the solvent accessible surface area (SASA) of the protein-ligand interaction compounds was estimated. The markers blue, orange, gray, yellow, and light blue are used to depict the protein in association with the chosen ligand molecules CID 1886, CID 122801, CID 101306757, CID 102090424, and CID 5311309, respectively.

from dynamic trajectory analysis, also known as the molecular dynamic simulation (MDS) [18, 81]. The Schrödinger package software from the Desmond application was utilized in our study to execute a 100 ns MDS with the selected physiologic and physicochemical parameters. This simulation trajectory of the simulation tool has allowed accurate analysis of the root mean square deviation (RMSD), root mean square fluctuation (RMSF), the radius of gyration (Rg), hydrogen bond number, and solvent accessible surface area (SASA) [82]. The RMSD of the selected 1i44 model protein was used to evaluate the protein structure's dependability and conformational fluctuations; a lower value indicates the most stable molecules. RMSD values under 1.5 are typically suggestive of more consistency in docking because RMSD values over 1.5 represent the average binding positions. The RMSD values for the protein-ligand interactions in our study were within a typical range, i.e., average mean values of 4 (the lowest value for the selected

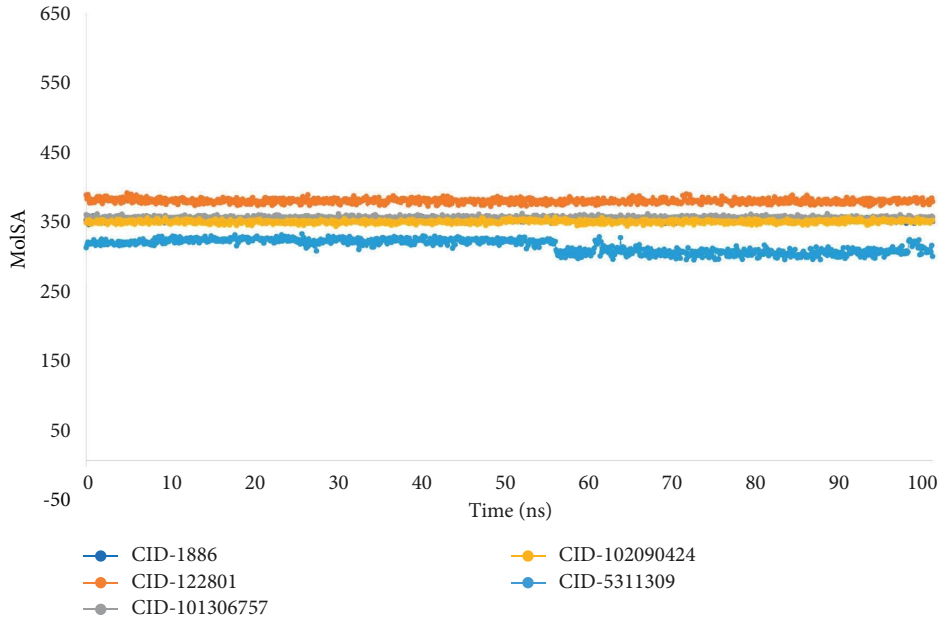

Figure 6: The 100 ns simulated interaction diagram was used to calculate the molecular surface area (MolSA) of the protein-ligand interaction complexes. The markers blue, orange, gray, yellow, and light blue are used to depict the selected ligand compounds CID 1886, CID 122801, CID 101306757, CID 102090424, and CID 5311309, respectively, in association with the protein.

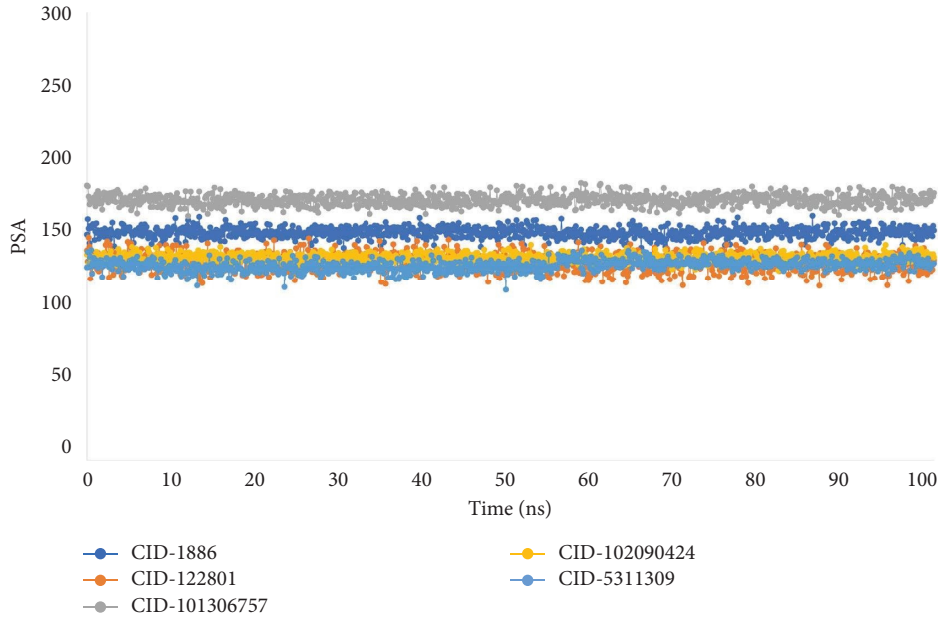

Figure 7: From the 100 ns simulated interaction diagram, the polar surface area (PSA) of the protein-ligand interaction compounds was estimated. The markers blue, orange, gray, yellow, and light blue are used to depict the selected ligand compounds CID 1886, CID 122801, CID 101306757, CID 102090424, and CID 5311309, respectively, in association with the protein.

ligand compounds is approximately 1.0, and maximum values of 4, indicating a more advantageous docking position and no disruption of the protein-ligand structure). In Figure 2, The average protein fluctuations can be measured using the RMSF as a reference point. RMSF graphs demonstrate how the average protein fluctuations relate to changes at the residue level. The RMSF of the target protein is depicted in Figure 3.

The number of intramolecular bonds found in the ligand compound Vilasinin, which is more stable in conformation than the other ligand compound, was higher than the total number of intermolecular bonds created between the macromolecule and its ligand compounds (Figure 8). For ligand 7-Deacetyl-7-oxogedunin, the SID diagram observed that the interaction fraction value had reached the highest value at ASP 1229, created by hydrogen bonds and water

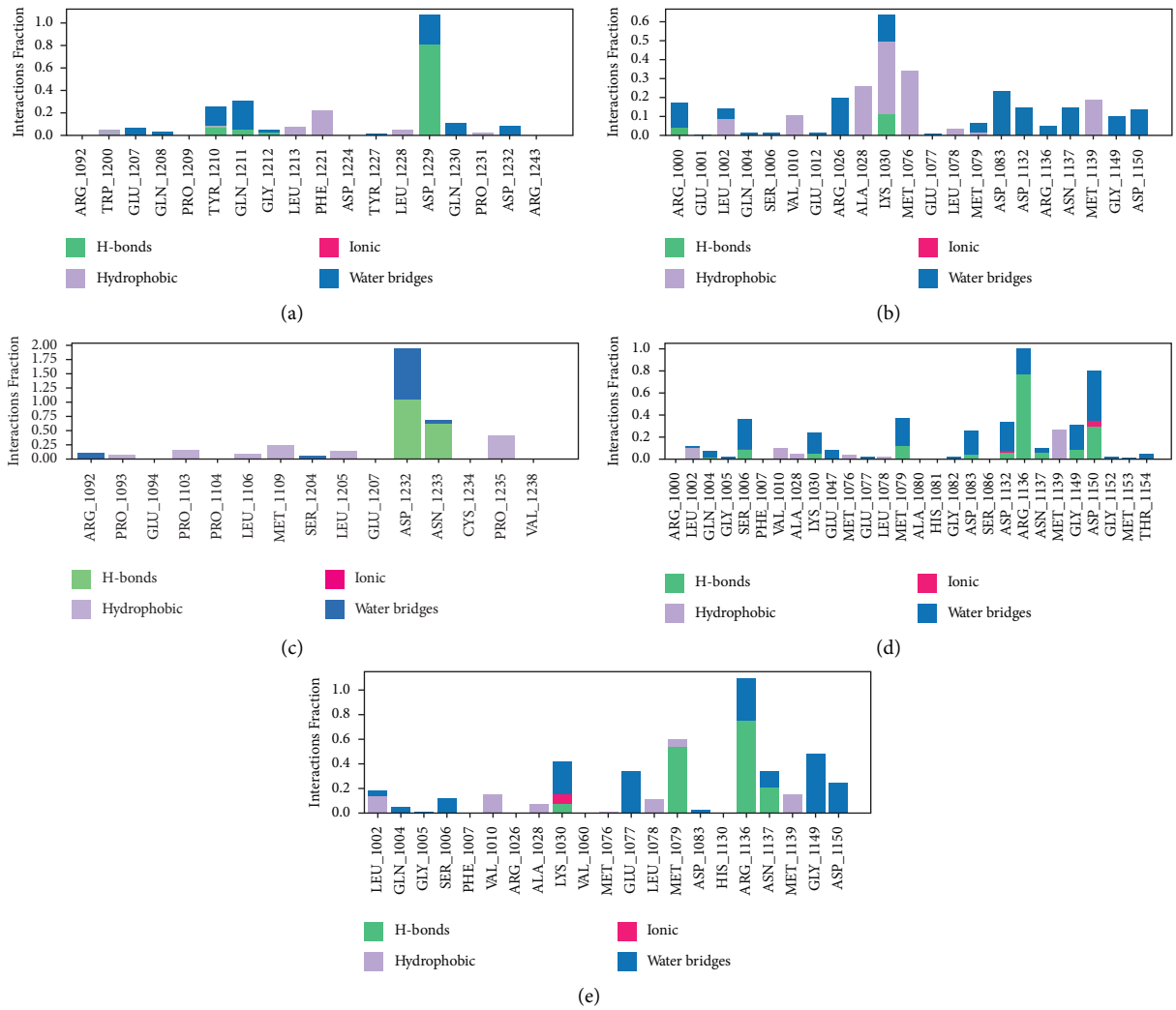

FIGURE 8: The interactions between proteins and ligands identified during the 100 ns simulation are shown in the stacked bar charts. In this section, the interactions of the chosen ligand molecules are demonstrated. Figures (a)–(e) in the image above represented, respectively, the intermolecular fractions for the compounds CID 1886, CID 122801, CID 101306757, CID 102090424, and CID 5311309.

bridges showing that specific interaction has been maintained over the 100 ns simulation time. The IFV for compound having compound CID 122801 has shown everyday interaction by forming hydrogen bonds, hydrophobic bonds, and water bridges with the highest value of 0.6 with Lys 1030. Vilasinin has formed water bridges and hydrogen bond interactions with the highest value of 2 with ASP 1232. The stacked chart bar for Nimbidinin showed the highest IFV with ARG 1136 by forming hydrogen bonds and water bridges having the highest value of 1. The SID diagram also showed that the highest IFV value of the control drug Nateglinide is formed by water bridges and hydrogen bonds with ARG 1136. The Result shows that the molecular stability of the selected phytocompounds is similar to the control drug nateglinide with the insulin receptor ectodomain.

The protein-ligandssolvent-accessible surface area (SASA) was also estimated using simulated trajectories to determine the dimensional changes of the drug-like molecules along the simulation trajectory [15, 83].

One of the most significant SASA values is related to the unstable structure, which has hydrophobic amino acid residues close to the water molecule [84, 85]. All chosen compounds have conventional SASA values, as shown by the MDS trajectory's SASA result (Figure 5). The MolSA and PSA validation graph shows that all ligand compounds have potential advantages over the control medication (Figures 6 and 7).

In addition, Rg measures the separation between the end of the protein and the centre mass of the protein. As a result, this metric provides additional information about the protein's folding properties while measuring how compact the protein molecule is [86]. A significant Rg value indicates slack packing, whereas a lower Rg value indicates compact packing [83]. The summary of the Rg values in Figure 4 reveals that the protein-containing compounds all displayed average compactness.

5. Conclusion

Four phytocompounds were selected from a total of 63. The following compounds are projected to have the best drug-like properties based on the virtual-mediated ADMET

screening employed in this procedure. These ligand molecules, which are similar to the reference medication nateglinide, have the highest affinities for the insulin receptor, according to molecular docking studies. Notably, these drug-like compounds had longer interactions with the target protein's active site residues. Interestingly, the highest positive values were observed for the compounds in the simulation study that evaluated the quality of these molecules' interactions with the target receptor. Due to their ability to block the appropriate insulin receptor, these drugs may delay the development of diabetes mellitus. These top four phytocompounds could be used to treat diabetes, but more (in vivo and in vitro) study is needed to confirm their safety attributes.

As the next generation of pharmaceuticals develops, the management of diabetes mellitus will advance. Even though these are only a few examples of the variety of related development initiatives and cutting-edge tactics being utilized to treat type 2 diabetes, the following research has discussed several distinct therapeutic approaches for treating DM. Future generations of antidiabetic drugs will need to find solutions to a variety of real-world issues, including overlapping safety concerns, side effects, drug-drug interactions, dose and futility restrictions, and other issues that currently limit their use in certain situations. Thus, all significant problems would be solved, and the chosen phytocompounds would function as efficient complementary treatments for type 2 Diabetes Mellitus.

Data Availability

Data sharing does not apply to this article as no datasets were generated or analyzed during the current study.

Conflicts of Interest

The authors declare that there are no conflicts of interest.

Authors' Contributions

Conceptualization was carried out by A. A. and P. B.; investigation, data curation, and manuscript writing were carried out by A. A., P. B., M. S., A. M., D. A. K., A. H., T. R., N. M. R. R., and D. D.; visualization was carried out by A. A., P. B., M. S., A. H., D. D., M. N. H., and S. B.; review and editing were carried out by A. A., P. B., M. S., D. A. K., A. H., D. D., M. N. H., S. B., and R. G.; supervision was carried out by M. S., M. N. H., and S. B.; funding acquisition was carried out by M. M., A. S., and H.H. All authors read and approved the final version of the manuscript. Asif Abdullah and Partha Biswas these authors provide equal contributions to this current scientific research work.

Acknowledgments

The authors thank the Deanship of Scientific Research, King Khalid University, Saudi Arabia, for funding this work under Grant no. R.G.P. 1/290/43.

Supplementary Materials

The steps involved in the research study are represented. (*Supplementary Materials*)

References

[1] American Diabetes Association, "Diagnosis and classification of diabetes mellitus," *Diabetes Care*, vol. 32, no. 1, pp. S62–S67, 2009.

[2] M. A. Rahman, M. H. Rahman, M. S. Hossain et al., "Molecular insights into the multifunctional role of natural compounds: autophagy modulation and cancer prevention," *Biomedicines*, vol. 8, no. 11, p. 517, 2020.

[3] O. O. Oguntibeju, "Type 2 diabetes mellitus, oxidative stress and inflammation: examining the links," *International journal of physiology, pathophysiology and pharmacology*, vol. 11, no. 3, pp. 45–63, 2019.

[4] M. A. Rahman, M. H. Rahman, P. Biswas et al., "Potential therapeutic role of phytochemicals to mitigate mitochondrial dysfunctions in alzheimer's disease," *Antioxidants*, vol. 10, no. 1, p. 23, 2020.

[5] K. M. Ferguson, C. Hu, and M. A. Lemmon, "Insulin and epidermal growth factor receptor family members share parallel activation mechanisms," *Protein Science*, vol. 29, no. 6, pp. 1331–1344, 2020.

[6] M. N. H. Zilani, M. A. Islam, P. Biswas et al., "Metabolite profiling, anti-inflammatory, analgesic potentials of edible herb Colocasia gigantea and molecular docking study against COX-II enzyme," *Journal of Ethnopharmacology*, vol. 281, Article ID 114577, 2021.

[7] F. Weis, J. G. Menting, M. B. Margetts et al., "The signalling conformation of the insulin receptor ectodomain," *Nature Communications*, vol. 9, no. 1, p. 4420, 2018.

[8] R. Vozdek, Y. Long, and D. K. Ma, "The receptor tyrosine kinase HIR-1 coordinates HIF-independent responses to hypoxia and extracellular matrix injury," *Science Signaling*, vol. 11, no. 550, Article ID eaat0138, 2018.

[9] S. Al Azad, S. Ahmed, P. Biswas et al., "Quantitative analysis of the factors influencing IDA and TSH downregulation in correlation to the fluctuation of activated vitamin D3 in women," *JABET*, vol. 12, 2022.

[10] D. Dey, M. M. Hasan, P. Biswas et al., "Investigating the anticancer potential of salvicine as a modulator of topoisomerase II and ROS signaling cascade," *Frontiers in Oncology*, vol. 12, Article ID 899009, 2022.

[11] N. Ferdausi, S. Islam, F. H. Rimti et al., "Point-specific interactions of isovitexin with the neighboring amino acid residues of the hACE2 receptor as a targeted therapeutic agent in suppressing the SARS-CoV-2 influx mechanism," *Journal of advanced veterinary and animal research*, vol. 9, no. 2, pp. 230–240, 2022.

[12] H. Rasouli, R. Yarani, F. Pociot, and J. Popović-Djordjević, "Anti-diabetic potential of plant alkaloids: revisiting current findings and future perspectives," *Pharmacological Research*, vol. 155, Article ID 104723, 2020.

[13] P. Biswas, D. Dey, A. Rahman et al., "Analysis of SYK gene as a prognostic biomarker and suggested potential bioactive phytochemicals as an alternative therapeutic option for colorectal cancer: an in-silico pharmaco-informatics investigation," *Journal of Personalized Medicine*, vol. 11, no. 9, p. 888, 2021.

[14] M. Batool, B. Ahmad, and S. Choi, "A structure-based drug discovery paradigm," *International Journal of Molecular Sciences*, vol. 20, no. 11, p. 2783, 2019.

[15] D. Dey, P. Biswas, P. Paul et al., "Natural flavonoids effectively block the CD81 receptor of hepatocytes and inhibit HCV infection: a computational drug development approach," *Molecular Diversity*, vol. 1, 2022.

[16] M. M. Hasan, M. N. H. Zilani, S. Akter et al., "UHPLC-Q/Orbitrap/MS based chemical fingerprinting and hepatoprotective potential of a medicinal plant, Morinda angustifolia Roxb," *South African Journal of Botany*, vol. 148, pp. 561–572, 2022.

[17] B. J. Neves, R. C. Braga, C. C. Melo-Filho, J. T. Moreira-Filho, E. N. Muratov, and C. H. Andrade, "QSAR-based virtual screening: advances and applications in drug discovery," *Frontiers in Pharmacology*, vol. 9, p. 1275, 2018.

[18] D. Dey, R. Hossain, P. Biswas et al., "Amentoflavone derivatives significantly act towards the main protease (3CL(PRO)/M(PRO)) of SARS-CoV-2: in silico admet profiling, molecular docking, molecular dynamics simulation, network pharmacology," *Molecular Diversity*, vol. 10, pp. 1–15, 2022.

[19] A. Hasan, P. Biswas, T. A. Bondhon et al., "Can artemisia herba-alba Be useful for managing COVID-19 and comorbidities?" *Molecules*, vol. 27, no. 2, p. 492, 2022.

[20] A. K. M. H. Morshed, S. Al Azad, M. A. R. Mia et al., "Oncoinformatic screening of the gene clusters involved in the HER2-positive breast cancer formation along with the in silico pharmacodynamic profiling of selective long-chain omega-3 fatty acids as the metastatic antagonists," *Molecular Diversity*, vol. 26, 2022.

[21] A. J. Banegas-Luna, J. P. Cerón-Carrasco, and H. Pérez-Sánchez, "A review of ligand-based virtual screening web tools and screening algorithms in large molecular databases in the age of big data," *Future Medicinal Chemistry*, vol. 10, no. 22, pp. 2641–2658, 2018.

[22] A. C. Kaushik, S. Kumar, D. Q. Wei, and S. Sahi, "Structure based virtual screening studies to identify novel potential compounds for GPR142 and their relative dynamic analysis for study of type 2 diabetes," *Frontiers of Chemistry*, vol. 6, p. 23, 2018.

[23] F. Stanzione, I. Giangreco, and J. C. Cole, "Use of molecular docking computational tools in drug discovery," *Progress in Medicinal Chemistry*, vol. 60, pp. 273–343, 2021.

[24] S. K. Baral, P. Biswas, M. A. Kaium et al., "A comprehensive discussion in vaginal cancer based on mechanisms, treatments, risk factors and prevention," *Frontiers in Oncology*, vol. 12, Article ID 883805, 2022.

[25] S. Bibi, M. M. Hasan, P. Biswas et al., "Chapter 7 - phytonutrients in the management of lipids metabolism," in *The Role of Phytonutrients in Metabolic Disorders*, H. Khan, E. K. Akkol, and M. Daglia, Eds., pp. 195–236, Academic Press, Cambridge, Massachusetts, 2022.

[26] D. Dey, T. I. Ema, P. Biswas et al., "Antiviral effects of bacteriocin against animal-to-human transmittable mutated sars-cov-2: a systematic review," *Front Agr Sci Eng*, vol. 8, no. 4, pp. 603–622, 2021.

[27] R. A. Khan, R. Hossain, A. Siyadatpanah et al., "Diterpenes/diterpenoids and their derivatives as potential bioactive leads against dengue virus: a computational and network pharmacology study," *Molecules*, vol. 26, no. 22, p. 6821, 2021.

[28] M. Munshi, M. N. H. Zilani, M. A. Islam et al., "Novel compounds from endophytic fungi of Ceriops decandra inhibit breast cancer cell growth through estrogen receptor alpha in in-silico study," *Informatics in Medicine Unlocked*, vol. 32, Article ID 101046, 2022.

[29] R. P. Bhole, C. G. Bonde, S. C. Bonde, R. V. Chikhale, and R. D. Wavhale, "Pharmacophore model and atom-based 3D quantitative structure activity relationship (QSAR) of human immunodeficiency virus-1 (HIV-1) capsid assembly inhibitors," *Journal of Biomolecular Structure and Dynamics*, vol. 39, no. 2, pp. 718–727, 2021.

[30] A. K. Maurya, V. Mulpuru, and N. Mishra, "Discovery of novel coumarin analogs against the α-glucosidase protein target of diabetes mellitus: pharmacophore-based QSAR, docking, and molecular dynamics simulation studies," *ACS Omega*, vol. 5, no. 50, pp. 32234–32249, 2020.

[31] X. Y. Feng, W. Q. Jia, X. Liu et al., "Identification of novel PPARα/γ dual agonists by pharmacophore screening, docking analysis, ADMET prediction and molecular dynamics simulations," *Computational Biology and Chemistry*, vol. 78, pp. 178–189, 2019.

[32] S. A. Hollingsworth and R. O. Dror, "Molecular dynamics simulation for all," *Neuron*, vol. 99, no. 6, pp. 1129–1143, 2018.

[33] M. S. Rahman, M. N. H. Zilani, M. A. Islam et al., "In vivo neuropharmacological potential of gomphandra tetrandra (wall.) sleumer and in-silico study against β-amyloid precursor protein," *Processes*, vol. 9, no. 8, p. 1449, 2021.

[34] M. T. Sarker, S. Saha, P. Biswas et al., "Identification of blood-based inflammatory biomarkers for the early-stage detection of acute myocardial infarction," *Network Modeling Analysis in Health Informatics and Bioinformatics*, vol. 11, no. 1, p. 28, 2022.

[35] M. A. Islam, M. N. H. Zilani, P. Biswas et al., "Evaluation of in vitro and in silico anti-inflammatory potential of some selected medicinal plants of Bangladesh against cyclooxygenase-II enzyme," *Journal of Ethnopharmacology*, vol. 285, Article ID 114900, 2022.

[36] M. Sohel, P. Biswas, M. Al Amin et al., "Genistein, a potential phytochemical against breast cancer treatment-insight into the molecular mechanisms," *Processes*, vol. 10, no. 2, p. 415, 2022.

[37] P. Gkeka, G. Stoltz, A. Barati Farimani et al., "Machine learning force fields and coarse-grained variables in molecular dynamics: application to materials and biological systems," *Journal of Chemical Theory and Computation*, vol. 16, no. 8, pp. 4757–4775, 2020.

[38] R. Hossain, D. Dey, P. Biswas et al., "Chlorophytum borivilianum (musli) and cimicifuga racemosa (black cohosh)," in *Herbs, Shrubs, and Trees of Potential Medicinal Benefits*, pp. 45–82, CRC Press, Boca Raton, Florida, 2022.

[39] M. Al Saber, P. Biswas, D. Dey et al., "A comprehensive review of recent advancements in cancer immunotherapy and generation of CAR T cell by CRISPR-cas9," *Processes*, vol. 10, no. 1, p. 16, 2021.

[40] P. Biswas, D. Dey, P. K. Biswas et al., "A comprehensive analysis and anti-cancer activities of quercetin in ROS-mediated cancer and cancer stem cells," *International Journal of Molecular Sciences*, vol. 23, no. 19, Article ID 11746, 2022.

[41] P. K. Paul, S. Azad, M. H. Rahman et al., "Catabolic profiling of selective enzymes in the saccharification of non-food lignocellulose parts of biomass into functional edible sugars and bioenergy: an in silico bioprospecting," *Journal of advanced veterinary and animal research*, vol. 9, no. 1, pp. 19–32, 2022.

[42] H. Ahmed, A. R. Mahmud, M. F. R. Siddiquee et al., "Role of T cells in cancer immunotherapy: opportunities and challenges," *Cancer Pathogenesis and Therapy*, vol. 23, 2022.

[43] R. O. Dror, D. H. Arlow, P. Maragakis et al., "Activation mechanism of the β2-adrenergic receptor," *Proceedings of the National Academy of Sciences*, vol. 108, no. 46, pp. 18684–18689, 2011.

[44] W. Huang, A. Manglik, A. J. Venkatakrishnan et al., "Structural insights into μ-opioid receptor activation," *Nature*, vol. 524, no. 7565, pp. 315–321, 2015.

[45] A. Arefin, T. Ismail Ema, T. Islam et al., "Target specificity of selective bioactive compounds in blocking α-dystroglycan receptor to suppress Lassa virus infection: an in silico approach," *Journal of biomedical research*, vol. 35, no. 6, pp. 459–473, 2021.

[46] P. Biswas, M. M. Hasan, D. Dey et al., "Candidate antiviral drugs for COVID-19 and their environmental implications: a comprehensive analysis," *Environmental Science and Pollution Research*, vol. 28, no. 42, Article ID 59570, 59593 pages, 2021.

[47] C. Y. Jia, J. Y. Li, G. F. Hao, and G. F. Yang, "A drug-likeness toolbox facilitates ADMET study in drug discovery," *Drug Discovery Today*, vol. 25, no. 1, pp. 248–258, 2020.

[48] L. L. G. Ferreira and A. D. Andricopulo, "ADMET modeling approaches in drug discovery," *Drug Discovery Today*, vol. 24, no. 5, pp. 1157–1165, 2019.

[49] P. Zhou, X. L. Yang, X. G. Wang et al., "A pneumonia outbreak associated with a new coronavirus of probable bat origin," *Nature*, vol. 579, no. 7798, pp. 270–273, 2020.

[50] X. Chen, H. Li, L. Tian, Q. Li, J. Luo, and Y. Zhang, "Analysis of the physicochemical properties of Acaricides based on lipinski's rule of five," *Journal of Computational Biology*, vol. 27, no. 9, pp. 1397–1406, 2020.

[51] C. M. Chagas, S. Moss, and L. Alisaraie, "Drug metabolites and their effects on the development of adverse reactions: revisiting Lipinski's Rule of Five," *International Journal of Pharmaceutics*, vol. 549, no. 1-2, pp. 133–149, 2018.

[52] M. Zurnacı, M. Şenturan, N. Şener et al., "Studies on antimicrobial, antibiofilm, efflux pump inhibiting, and ADMET properties of newly synthesized 1, 3, 4-thiadiazole derivatives," *ChemistrySelect*, vol. 6, no. 45, pp. 12571–12581, 2021.

[53] S. O. Olubode, M. O. Bankole, P. A. Akinnusi et al., "Molecular modeling studies of natural inhibitors of androgen signaling in prostate cancer," *Cancer Informatics*, vol. 21, Article ID 117693512211185, 2022.

[54] P. M. Glassman and V. R. Muzykantov, "Pharmacokinetic and pharmacodynamic properties of drug delivery systems," *Journal of Pharmacology and Experimental Therapeutics*, vol. 370, no. 3, pp. 570–580, 2019.

[55] J. H. Till, A. J. Ablooglu, M. Frankel, S. M. Bishop, R. A. Kohanski, and S. R. Hubbard, "Crystallographic and solution studies of an activation loop mutant of the insulin receptor tyrosine kinase: insights into kinase mechanism," *Journal of Biological Chemistry*, vol. 276, no. 13, Article ID 10049, 10055 pages, 2001.

[56] K. Mohanraj, B. S. Karthikeyan, R. P. Vivek-Ananth et al., "IMPPAT: a curated database of Indian medicinal plants, Phytochemistry and therapeutics," *Scientific Reports*, vol. 8, no. 1, p. 4329, 2018.

[57] R. Vivek-Ananth, K. Mohanraj, A. K. Sahoo, and A. J. b. Samal, "Imppat 2.0: an enhanced and expanded phytochemical atlas of Indian medicinal plants," *bioRxiv*, vol. 2022, Article ID 496609, 2022.

[58] L. Pinzi and G. Rastelli, "Molecular docking: shifting paradigms in drug discovery," *International Journal of Molecular Sciences*, vol. 20, no. 18, p. 4331, 2019.

[59] J. Fan, A. Fu, and L. Zhang, "Progress in molecular docking," *Quantitative Biology*, vol. 7, no. 2, pp. 83–89, 2019.

[60] J. Eberhardt, D. Santos-Martins, A. F. Tillack, and S. Forli, "AutoDock vina 1.2.0: new docking methods, expanded force field, and Python bindings," *Journal of Chemical Information and Modeling*, vol. 61, no. 8, pp. 3891–3898, 2021.

[61] O. Trott and A. J. Olson, "AutoDock Vina: improving the speed and accuracy of docking with a new scoring function, efficient optimization, and multithreading," *Journal of Computational Chemistry*, vol. 31, no. 2, pp. 455–461, 2010.

[62] R. P. Pawar and S. H. Rohane, "Role of autodock vina in PyRx molecular docking," *Asian Journal of Research in Chemistry*, vol. 14, pp. 132–134, 2021.

[63] R. A. Laskowski and M. B. Swindells, "LigPlot+: multiple ligand-protein interaction diagrams for drug discovery," *Journal of Chemical Information and Modeling*, vol. 51, no. 10, pp. 2778–2786, 2011.

[64] S. Genheden and U. Ryde, "How to obtain statistically converged MM/GBSA results," *Journal of Computational Chemistry*, vol. 31, no. 4, pp. 837–846, 2010.

[65] F. Godschalk, S. Genheden, P. Söderhjelm, and U. Ryde, "Comparison of MM/GBSA calculations based on explicit and implicit solvent simulations," *Physical Chemistry Chemical Physics*, vol. 15, no. 20, pp. 7731–7739, 2013.

[66] J. Shen, F. Cheng, Y. Xu, W. Li, and Y. Tang, "Estimation of ADME properties with substructure pattern recognition," *Journal of Chemical Information and Modeling*, vol. 50, no. 6, pp. 1034–1041, 2010.

[67] A. Daina, O. Michielin, and V. Zoete, "SwissADME: a free web tool to evaluate pharmacokinetics, drug-likeness and medicinal chemistry friendliness of small molecules," *Scientific Reports*, vol. 7, no. 1, Article ID 42717, 2017.

[68] D. E. V. Pires, T. L. Blundell, and D. B. P. K. C. S. M. Ascher, "pkCSM: predicting small-molecule pharmacokinetic and toxicity properties using graph-based signatures," *Journal of Medicinal Chemistry*, vol. 58, no. 9, pp. 4066–4072, 2015.

[69] A. M. Omar, A. S. Aljahdali, M. K. Safo, G. A. Mohamed, and S. R. M. Ibrahim, "Docking and molecular dynamic investigations of phenylspirodrimanes as cannabinoid receptor-2 agonists," *Molecules*, vol. 28, no. 1, p. 44, 2022.

[70] F. Ahammad, R. Alam, R. Mahmud et al., "Pharmacoinformatics and molecular dynamics simulation-based phytochemical screening of neem plant (Azadiractha indica) against human cancer by targeting MCM7 protein," *Briefings in Bioinformatics*, vol. 22, no. 5, Article ID bbab098, 2021.

[71] O. Carugo, "How root-mean-square distance (r.m.s.d.) values depend on the resolution of protein structures that are compared," *Journal of Applied Crystallography*, vol. 36, no. 1, pp. 125–128, 2003.

[72] K. Sargsyan, C. Grauffel, and C. Lim, "How molecular size impacts RMSD applications in molecular dynamics simulations," *Journal of Chemical Theory and Computation*, vol. 13, no. 4, pp. 1518–1524, 2017.

[73] L. Martínez, "Automatic identification of mobile and rigid substructures in molecular dynamics simulations and fractional structural fluctuation analysis," *PLoS One*, vol. 10, no. 3, Article ID e0119264, 2015.

[74] S. Saleem, S. Bibi, Q. Yousafi et al., "Identification of effective and nonpromiscuous antidiabetic drug molecules from penicillium species," *Evidence-based Complementary and Alternative Medicine*, vol. 2022, Article ID 7040547, pp. 1–15, 2022.

[75] M. A. Alamri, A. Altharawi, A. B. Alabbas, M. A. Alossaimi, and S. M. Alqahtani, "Structure-based virtual screening and molecular dynamics of phytochemicals derived from Saudi medicinal plants to identify potential COVID-19 therapeutics," *Arabian Journal of Chemistry*, vol. 13, no. 9, pp. 7224–7234, 2020.

[76] M. H. Rahman, P. Biswas, D. Dey et al., "An in-silico identification of potential flavonoids against kidney fibrosis targeting tgfßr-1," *Life*, vol. 12, no. 11, p. 1764, 2022.

[77] P. Paul, P. Biswas, D. Dey et al., "Exhaustive plant profile of "dimocarpus longan lour" with significant phytomedicinal properties: a literature based-review," *Processes*, vol. 9, no. 10, p. 1803, 2021.

[78] M. Abdalla, R. K. Mohapatra, A. K. Sarangi et al., "In silico studies on phytochemicals to combat the emerging COVID-19 infection," *Journal of Saudi Chemical Society*, vol. 25, no. 12, Article ID 101367, 2021.

[79] R. K. Mohapatra, M. Azam, P. K. Mohapatra et al., "Computational studies on potential new anti-Covid-19 agents with a multi-target mode of action," *Journal of King Saud University Science*, vol. 34, no. 5, Article ID 102086, 2022.

[80] R. K. Mohapatra, K. Dhama, A. A. El-Arabey et al., "Repurposing benzimidazole and benzothiazole derivatives as potential inhibitors of SARS-CoV-2: DFT, QSAR, molecular docking, molecular dynamics simulation, and in-silico pharmacokinetic and toxicity studies," *Journal of King Saud University Science*, vol. 33, no. 8, Article ID 101637, 2021.

[81] K. Kousar, A. Majeed, F. Yasmin, W. Hussain, and N. Rasool, "Phytochemicals from selective plants have promising potential against SARS-CoV-2: investigation and corroboration through molecular docking, MD simulations, and quantum computations," *BioMed Research International*, vol. 2020, Article ID 6237160, pp. 1–15, 2020.

[82] S. Bibi, M. S. Khan, S. A. El-Kafrawy et al., "Virtual screening and molecular dynamics simulation analysis of Forsythoside A as a plant-derived inhibitor of SARS-CoV-2 3CLpro," *Saudi Pharmaceutical Journal*, vol. 30, no. 7, pp. 979–1002, 2022.

[83] P. Biswas, O. Hany Rumi, D. Ahmed Khan et al., "Evaluation of melongosides as potential inhibitors of NS2B-NS3 activator-protease of dengue virus (serotype 2) by using molecular docking and dynamics simulation approach," *Journal of Tropical Medicine*, vol. 2022, Article ID 7111786, pp. 1–13, 2022.

[84] A. A. Zaki, A. Ashour, S. S. Elhady, K. M. Darwish, and A. A. Al-Karmalawy, "Calendulaglycoside A showing potential activity against SARS-CoV-2 main protease: molecular docking, molecular dynamics, and SAR studies," *Journal of traditional and complementary medicine*, vol. 12, no. 1, pp. 16–34, 2022.

[85] P. Biswas, S. A. Polash, D. Dey et al., "Advanced implications of nanotechnology in disease control and environmental perspectives," *Biomedicine & Pharmacotherapy*, vol. 158, Article ID 114172, 2023.

[86] P. Robustelli, S. Piana, and D. E. Shaw, "Developing a molecular dynamics force field for both folded and disordered protein states," *Proceedings of the National Academy of Sciences of the United States of America*, vol. 115, no. 21, Article ID E4758, e4766 pages, 2018.

Hindawi
Journal of Chemistry
Volume 2023, Article ID 6316589, 14 pages
https://doi.org/10.1155/2023/6316589

Research Article

Natural Bioactive Compounds Promote Cell Apoptosis in Gastric Cancer Treatment: Evidence from Network Pharmacological Study and Experimental Analysis

Yan Wang, Haiyang Wang, and Shun Xu

College of Chemistry and Green Catalysis Center, Zhengzhou University, Zhengzhou 450001, Henan Province, China

Correspondence should be addressed to Shun Xu; shxuzz@zzu.edu.cn

Received 4 September 2022; Revised 9 November 2022; Accepted 25 November 2022; Published 6 February 2023

Academic Editor: Marwa Fayed

Background. Gastric cancer (GC) is one of the most lethal cancers. Shenlian capsule (SLC) is a Chinese patent medicine made from 11 herbs containing numerous plant-derived compounds, and the clinical trials of SLCs confirmed that they had effective adjuvant therapy for a variety of cancer such as lung cancer and gastric cancer. Moreover, the HPLC fingerprint of SLCs was established from other research to find potential components. In this study, network pharmacology-based research was used to identify combinations with molecules, targets, and pathways to explore their interaction mechanisms. *Methods*. The Traditional Chinese Medicine Systems Pharmacology (TCMSP) database and the Traditional Chinese Medicine Integrated Database (TCMID) were widely implemented in selecting the active chemical components of SLCs with an oral bioavailability (OB) ≥ 30% and drug-likeness (DL) ≥ 18%. In addition, the TCMSP and TCMID databases obtained the targets of SLCs, and PharmMapper (PM) was used to predict targets of SLCs. Gastric cancer-related genes were provided by the GeneCards and TTD databases. Subsequently, the drug/target/pathway network was established and visualized using Cytoscape software. Then, Gene Ontology (GO) and Kyoto Encyclopedia of Genes and Genome (KEGG) enrichment analyses were used to predict the potential genes and pathways of gastric cancer. Molecular docking was performed to study the interaction between ligands and targets; the interaction was visualized using Discovery Studio and PyMOL. Finally, the potential primary mechanism used by SLCs against gastric cancer was verified by cell experiments, including MTT cell apoptosis assay, flow cytometry cell cycle assay, and western blotting with HGC-27 cells (undifferentiated). *Results*. Of 213 active chemical components from SLCs, 35 primary active chemical components were identified, and 10 potential critical targets were selected from the 185 intersections of the targets of SLCs and GC, such as RAC-alpha serine/threonine kinase 1 (AKT1), cellular tumor antigen p53 (TP53), interleukin-6 (IL6), caspase-3 (CASP3), vascular endothelial growth factor A (VEGFA), and epidermal growth factor receptor (EGFR). GO and KEGG enrichment analysis provided the PI3K/AKT, TNF, and p53 signaling pathways, which may be the primary signaling pathways modulating gastric cancer. Molecular docking verified targets such as AKT1, TP53, EGFR, and CASP3, which exhibited satisfactory binding capacity with active ingredients. Experiments with HCG-27 cells confirmed that SLCs may provide favorable treatment for GC by promoting CASP3 and TP53 expression to induce cell apoptosis and provided the predictions for network pharmacology and molecular docking. MTT and flow cytometry assays verified that SLCs promoted cell apoptosis and inhibited cell proliferation by triggering G0/G1 and S cell cycle arrest. In addition, western blot analysis confirmed that SLCs promoted TP53 and CASP3 overexpression, which led to HGC-27 gastric cell apoptosis. *Conclusions*. Our results confirmed that SLCs inhibit proliferation of HGC-27 gastric cell by promoting cell apoptosis and, therefore, have potential in the treatment of advanced gastric cancer. P53 signaling pathway was the key pathway. In addition, quercetin, matrine, and ursolic acid might be the main active ingredients.

1. Introduction

Gastric cancer (GC), a common malignant tumor, has become the fourth most lethal cancer worldwide, as reported in the 2020 GLOBOCAN project by the International Agency for Research on Cancer (IARC) [1]. Gastric cancer is classically divided into intestinal and diffuse histologic types, and most cases of gastric cancer were induced by infection with the bacterium *Helicobacter pylori* [2]. Currently, patients with advanced gastric cancer usually choose

chemotherapy and radiotherapy as the major treatment due to a lack of effective surgical treatments and a late diagnosis. Despite this, the survival rate for patients with advanced gastric cancer remains dismal [3, 4]. Doxorubicin hydrochloride (Dox), irinotecan (CPT-11), and esophagogastroduodenoscopy (EGD) are commonly used to treat gastric cancer. However, drug resistance is frequently observed in the treatment of GC, and therefore, it is necessary to find new and effective drugs for treatment. Natural bioactive compounds have potential as a cancer therapy; therefore, the uses of natural bioactive compounds have become one of the hottest topics worldwide.

Traditional Chinese medicine (TCM) has been widely used in the treatment of cancer because natural bioactive compounds have the capability of exerting synergistic effects upon multiple targets [5–7]. To exemplify, Xiao-Ai-Ping (XAP) injection has been effectively used to treat gastric cancer and lung cancer [8, 9], and Weikang Keli has also been used for gastric cancer therapy in cell experiments [10]. Thus, there is promising potential for TCM to be used to treat advanced gastric cancer.

Shenlian capsule (SLC) is a Chinese patent medicine that is prepared from 11 Chinese herbs: Danshen (Radix Salviae Miltiorrhizae/Chinese salvia (Salvia miltiorrhiza Bunge)), Kushen (Radix Sophorae Flavescentis Radix/shrubby sophora (*Sophora flavescens* Aiton)), Banzhilian (Herba Scutellariae Barbatae/barbed skullcap (Scutellaria barbata D. Don.)), Shandougen (Radix et Rhizome Sophorae Tonkinensis/bushy sophora (Sophora tonkinensis Gagnep.)), Baibiandou (Semen Lablab Album/hyacinth bean (Dolichos lablab L.)), Sanleng (Rhizoma Sparganii/common bur-reed (Sparganium stoloniferum Buch.-Ham.)), Ezhu (Rhizoma Curcumae (Zedoariae)/zedoary root (Cucurma zedoaria (Christm.) Roscoe), Fangji (Radix Stephaniae Tetrandrae/stephania root (Stephania tetrandra S. Moore)), Wumei (Fructus Mume/dried black plum (Prunus mume (Sieb. et Zucc.))), Buguzhi (Fructus Psoraliae/babchi (Psoralea corylifolia L.)), and Kuxingren (Semen Armeniacae Amarum/apricot seeds (Prunus armeniaca L.)). SLCs have already been used for the treatment of lung cancer and gastric cancer. The high performance liquid chromatography (HPLC) fingerprint of Shenlian also established by Han' s team to find the potential ingredients of SLCs. Nine components were identified such as oxymatrine, matrine, tetrandrine, fangchinoline, amygdalin, oleanolic acid, ursolic acid, psoralen, and angelicin [11–13]. Several clinical trials in China have confirmed that adjuvant treatment with SLCs was effective with bevacizumab injection, epirubicin hydrochloride injection, cisplatin injection, or fluorouracil injection for advanced gastric cancer [14, 15]. However, the treatment and action mechanisms of the SLC remain undefined. Thus, a network pharmacology-based study, which was proposed by Hopkins and relies on network database retrieval, system biology, and pharmacology, should be undertaken to elucidate SLCs' potential treatment mechanism in gastric cancer [16–18]. Network pharmacology-based studies have the ability to determine the primary potential ingredients, targets, and pathways involved [19, 20].

To further identify the mechanism of action of the SLCs, molecular docking was used to validate combination ingredients with targets [21]. The binding energy and bond interacitons between ingredients and targets interpreted the biological activity of the SLCs' main ingredients.. By also conducting MTT cell apoptosis assay, flow cytometry, and western blot analysis, the specific mechanisms used by the SLC to regulate gastric cancer cell apoptosis, cell cycle arrest, and their signal transduction pathways were elucidated [22]. Finally, the mechanisms used by the SLC against GC were clarified through the above research, and a schematic flow diagram is shown in Figure 1.

2. Methods

2.1. Main Active Ingredients and Target Identification. The main active chemical ingredients in all the herbs in the SLC were found in the Traditional Chinese Medicine Systems Pharmacology (TCMSP; https://tcmsp-e.com/tcmsp.php) database and Traditional Chinese Medicine Integrated Database (TCMID; https://www.megabionet.org/tcmid/). These components were identified based on oral bioavailability (OB) ≥ 30% and drug-likeness (DL) ≥ 18%. The targets of the main components were obtained from TCMSP and TCMID, and the predictions of the SLC's potential targets were obtained from the PharmMapper database (PM; https://www.lilab-ecust.cn/pharmmapper/) based on a z score ≥4. The UniProt database (https://www.uniprot.org/) and DrugBank database (https://www.drugbank.ca) provided the human genes related to these targets. GC targets were selected from the GeneCards database (https://www.genecards.org/) and TTD database (https://bidd.nus.edu.sg/group/ttd/ttd.asp) by searching using the keywords "gastric cancer," "stomach cancer," and "gastric carcinoma."

2.2. Drugs/Targets/Pathways and Protein-Protein Interaction Network Construction. The targets and potential active ingredients were imported into Cytoscape (v. 3.8.0) for the construction of a drug/target/pathway network. By selecting high-degree targets and active ingredients, key targets and main active ingredients were mined. Protein-protein interaction (PPI) networks were constructed using STRING tools (https://string-db.org) and Cytoscape to find the potential leader targets.

2.3. GO and KEGG Enrichment Analysis. Gene Ontology (GO) and Kyoto Encyclopedia of Genes and Genome (KEGG) enrichment analyses were applied from the DAVID database (https://david.ncifcrf.gov/) based on a P value < 0.05 as the condition to visualize the results and confirm key signaling pathways.

2.4. Molecular Docking Analyses. The 3D structures of proteins were downloaded from the Research Collaboratory for Structural Bioinformatics (RCSB) Protein Data Bank database (https://www.rcsb.org/). The chosen scientific name of the source organism was *Homo sapiens*, and it was refined at resolutions of 1.0–3.0 A°. Ligands were downloaded from TCMSP and TCMID and generated using

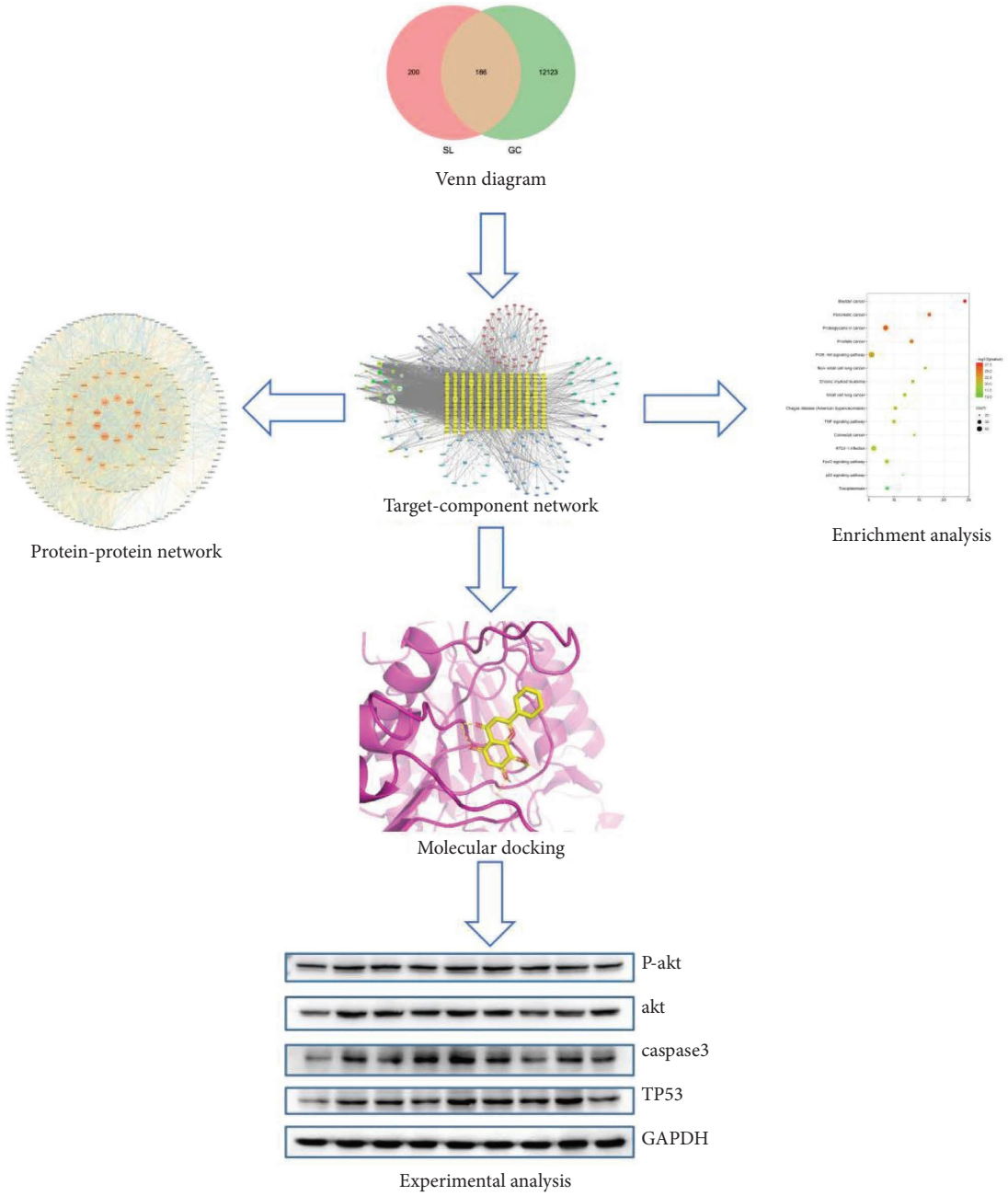

Figure 1: Schematic flow diagram showing the steps used for determining the active ingredients, network pharmacology analysis, molecular docking, and experimental analysis of SLCs.

ChemDraw (v. 14.0). AutoDockTools (v. 1.5.6) was used to prepare the input files, and AutoDock Vina was used to calculate the affinities between these proteins and ligands. Then, the docking results, which are docking binding energies based on the threshold conditions of ≤ -8.0 kcal/mol, were collected and were then integrated and visualized using PyMOL (v. 2.3.0) and Discover Studio (v. 2017).

2.5. Experimental Analysis

2.5.1. Cell Culture. HGC-27 (undifferentiated) gastric cells were provided by Procell Life Science & Technology (Wuhan, China). The cells were grown in Roswell Park Memorial Institute (RPMI)-1640 medium with fetal bovine serum (20%, FBS) (HyClone, China) and a mixture of 1% antibiotics (streptomycin 100 U/mL and penicillin 100 U/mL) in an incubator containing 5% CO_2 at 37°C. The culture medium was replaced every 2-3 days at both the apical and basolateral ends. After 90% confluence, the cells were subcultured on plates.

2.5.2. MTT Analysis. HGC-27 cells were digested with trypsin to produce a single-cell suspension, followed by their seeding in a 96-well plate at 3×10^4 cells/well. After incubation for 24 h, the cells were incubated with different

concentrations of SLC solution (0 g/L, 0.25 g/L, 0.5 g/L, 1 g/L, 2 g/L, and 4 g/L) in a constant temperature incubator at 37°C for 48 h. After the end of the culture, 100 μL MTT was added to each well. After 4 h, the MTT solution was removed, and 150 μL DMSO was added. The plate was then shaken for 10 min at a low speed, and the OD value was determined at 490 nm by an enzyme labeling instrument.

2.5.3. Investigation of Apoptosis and Cell Cycle through Flow Cytometry. The HGC-27 cells were divided into three groups: blank, control (SLC 0 g/L), and experimental (SLC 2 g/L and 4 g/L). Then, the HGC-27 cells were inoculated into a 6-well plate. After 48 h of corresponding treatment in an incubator containing 5% CO_2 at 37°C, cells from each group were collected and washed using phosphate-buffered saline (PBS), 0.5 mL trypsin was added, and the cells were then centrifuged. Flow cytometry was subsequently performed to analyze the cell cycle.

2.5.4. Western Blotting. The samples were lysed on ice for 20 min and centrifuged for 20 min (12,000 rpm, 4°C), and the supernatant was then removed. Then, the concentrations of proteins were measured using a BCA Protein Assay Kit (Solarbio, Beijing, China). After adjusting the protein concentration using 5× loading buffer and PBS, the samples were boiled at 95°C for 5 min and prepared for electrophoresis. After electrophoresis, electroblotting was performed to transfer the proteins to a polyvinylidene fluoride (PVDF) membrane. Five percent nonfat milk was used to block the PVDF membranes for 2 h, and then western blotting was performed with the primary antibodies against CASP3, Akt, phosphorylated Akt, and p53 at 4°C for 12 h. All of the primary antibodies were diluted in a ratio of 1 : 1000. After that, Tris-buffered saline (TBS) containing 0.1% Tween-20 (TBST) was used to wash the PVDF membranes 3 times, for 10 min each time. Horseradish peroxidase (HRP)-conjugated secondary antibodies were diluted in a ratio of 1 : 1500 and incubated with the PVDF membranes for 1 h at room temperature. The PVDF membranes were then washed with TBST 3 times and 10 min each time. The enhancement solution in the ECL reagent was mixed with the stable peroxidase solution in a 1 : 1 ratio, and the immunoreactive protein bands were imaged by a fully automated chemiluminescence image analysis system. Then, TBST was used to wash the PVDF membranes 3 times, for 5 min each time, and the PVDF membranes were then recovered and regenerated. The PVDF membranes were blocked again and incubated with secondary antibodies, with the other parameters remaining unchanged. ImageJ software (National Institutes of Health, Bethesda, MD, USA) was used for the gray value analysis.

3. Results

3.1. Main Active Ingredients and Target Identification. A total of 386 potential targets were identified from the TTD database and GeneCards database. After comparison with the targets of the SLC, 185 potential targets associated with GC and the SLC were obtained from the database screening and prediction, as shown in Figure 2.

There were 855 active components retrieved from the TCMSP database and the TCMID in which OB ≥ 30% and DL ≥ 18%. Some of the basic information about these active components is shown in Table 1.

3.2. Drug/Target/Pathway and Protein-Protein Interaction Network Construction. The active components and targets were input into Cytoscape to construct the network of "drugs/targets/pathways," as shown in Figure 3. Thirty-five main potential active ingredients were mined from the network, as shown in Table 2. It has already been shown that common ingredients such as quercetin, ursolic acid, and kaempferol possess anticancer activity. Thus, they might be the main potential ingredients. In addition, wogonin and moslosooflavone may also play a very important role in the treatment of GC.

The protein-protein interaction network diagrams were obtained from STRING tools and Cytoscape, as shown in Figure 4. The protein-protein interaction network diagrams indicated that AKT1, TP53, VEGFA, and CASP3 might be key targets.

3.3. GO and KEGG Enrichment Analysis. The main potential genes and pathways were determined using GO and KEGG enrichment analysis, as shown in Figures 5 and 6. The primary signaling pathways may be those of PI3K-Akt, TNF, FoxO, and p53. The pathways in cancer were the most significantly enriched. The PI3K-Akt signaling pathway regulates cell survival and cell cycle, the TNF signaling pathway, and the FoxO signaling pathway. The p53 signaling pathway regulates cell apoptosis. These pathways had well correlation with AKT1, TP53, CASP3, and EGFR that were the main potential genes of SLC because these pathways are highly involved in cancer development. The main potential ingredients of SLC like quercetin, matrine, ursolic acid, and stigmasterol can exert antitumor effects by altering cell cycle progression, inhibiting cell proliferation, promoting apoptosis, inhibiting angiogenesis and metastasis progression, and affecting autophagy found from previous studies. Hence, the main potential ingredients of SLC could regulate the expression of BP, CC, and MF to regulate cell apoptosis and cell cycle. The SLC regulated well with the expression of these pathways when administered for treatment for advanced gastric cancer.

3.4. Molecular Docking Analyses. Ten proteins and 35 ingredients were selected for the molecular docking analysis. Several results of molecular docking are shown in Table 3. The key targets such as AKT1, TP53, and CASP3 were able to strongly bind with quercetin, wogonin, and (2R)-5,7-dihydroxy-2-(4-hydroxyphenyl)chroman-4-one, as shown in Figure 7. To exemplify, the binding energy between wogonin and TP53 was approximately −7.9 kcal/mol. Val147 and Pro223 were involved in pi-sigma bonding, and Cys220

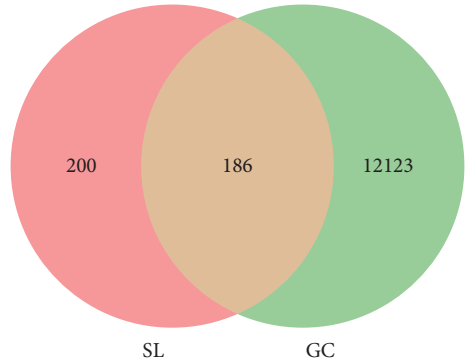

Figure 2: Venn diagram of common targets between the SLC and GC. After searching databases, 186 common targets were found.

Table 1: Potential ingredients in SLC (OB ≥ 30%, DL ≥ 0.18).

MOLID	Ingredients	OB (%)	DL
MOL008601	Methyl arachidonate	46.9	0.23
MOL000098	Quercetin	46.43	0.28
MOL000449	Stigmasterol	43.83	0.76
MOL000422	Kaempferol	41.88	0.24
MOL000511	Ursolic acid	16.77	0.75
MOL000263	Oleanolic acid	29.02	0.76
MOL001484	Inermine	75.18	0.54
MOL003627	Sophocarpine	64.26	0.25
MOL003648	Inermin	65.83	0.54
MOL003673	Wighteone	42.8	0.36
MOL003676	Sophoramine	42.16	0.25
MOL003680	Sophoridine	60.07	0.25
MOL000392	Formononetin	69.67	0.21
MOL004580	cis-Dihydroquercetin	66.44	0.27
MOL005944	Matrine	63.77	0.25
MOL006562	Leontalbinine	62.08	0.25
MOL006564	(+)-Allomatrine	58.87	0.25
MOL006566	(+)-Lehmannine	58.34	0.25
MOL006568	Isosophocarpine	61.57	0.25
MOL006571	Anagyrine	62.01	0.24
MOL006573	13,14-Dehydrosophoridine	65.34	0.25
MOL006582	5α,9α-Dihydroxymatrine	40.93	0.32
MOL006583	7,11-Dehydromatrine	44.43	0.25
MOL006596	Glyceollin	97.27	0.76
MOL003347	Hyperforin	44.03	0.60
MOL000006	Luteolin	36.16	0.25
MOL006613	Kushenin	47.62	0.38
MOL006619	Kushenol J	51.39	0.74
MOL006620	Kushenol J_qt	50.86	0.24
MOL006622	Kushenol O	42.41	0.76
MOL006623	Kushenol T	51.28	0.64
MOL006626	Leachianone G	60.97	0.40
MOL006627	Lehmanine	62.23	0.25
MOL006628	(+)-Lupanine	52.71	0.24
MOL006630	Norartocarpetin	54.93	0.24
MOL000456	Phaseolin	78.2	0.73
MOL006649	Sophranol	55.42	0.28
MOL006650	(−)-Maackiain-3-O-glucosyl-6′-O-malonate	48.69	0.52
MOL006652	Trifolirhizin	48.5	0.74
MOL001484	Inermine	75.18	0.54
MOL000354	Isorhamnetin	49.6	0.31
MOL003627	Sophocarpine	64.26	0.25
MOL003629	Daidzein-4,7-diglucoside	47.27	0.67
MOL003633	Oxynarcotine	56.74	0.60

Table 1: Continued.

MOLID	Ingredients	OB (%)	DL
MOL003647	Sophojaponicin	41.51	0.79
MOL003656	Lupiwighteone	51.64	0.37
MOL003663	Sophoranol	67.32	0.28
MOL003675	3,4,5,6-Tetradehydrospartein-2-one	71.26	0.24
MOL003677	Sophoranol	62.77	0.28
MOL000392	Formononetin	69.67	0.21
MOL007085	Salvilenone	30.38	0.38
MOL000915	(1S,10S),(4S,5S)-Germacrone-1(10),4-diepoxide	30.48	0.18
MOL000173	Wogonin	30.68	0.23
MOL001297	trans-Gondoic acid	30.7	0.20
MOL005030	Gondoic acid	30.7	0.20
MOL001735	Dinatin	30.97	0.27
MOL010922	Diisooctyl succinate	31.62	0.23
MOL007145	Salviolone	31.72	0.24
MOL006563	(+)-9-alpha-Hydroxymatrine	32.04	0.29
MOL007059	3-beta-Hydroxymethyllenetanshiquinone	32.16	0.41
MOL002331	N-Methylflindersine	32.36	0.18
MOL007143	Salvilenone I	32.43	0.23
MOL003644	Withaferine	33.14	0.73
MOL002719	6-Hydroxynaringenin	33.23	0.24
MOL002714	Baicalein	33.52	0.21
MOL007049	4-Methylenemiltirone	34.35	0.23

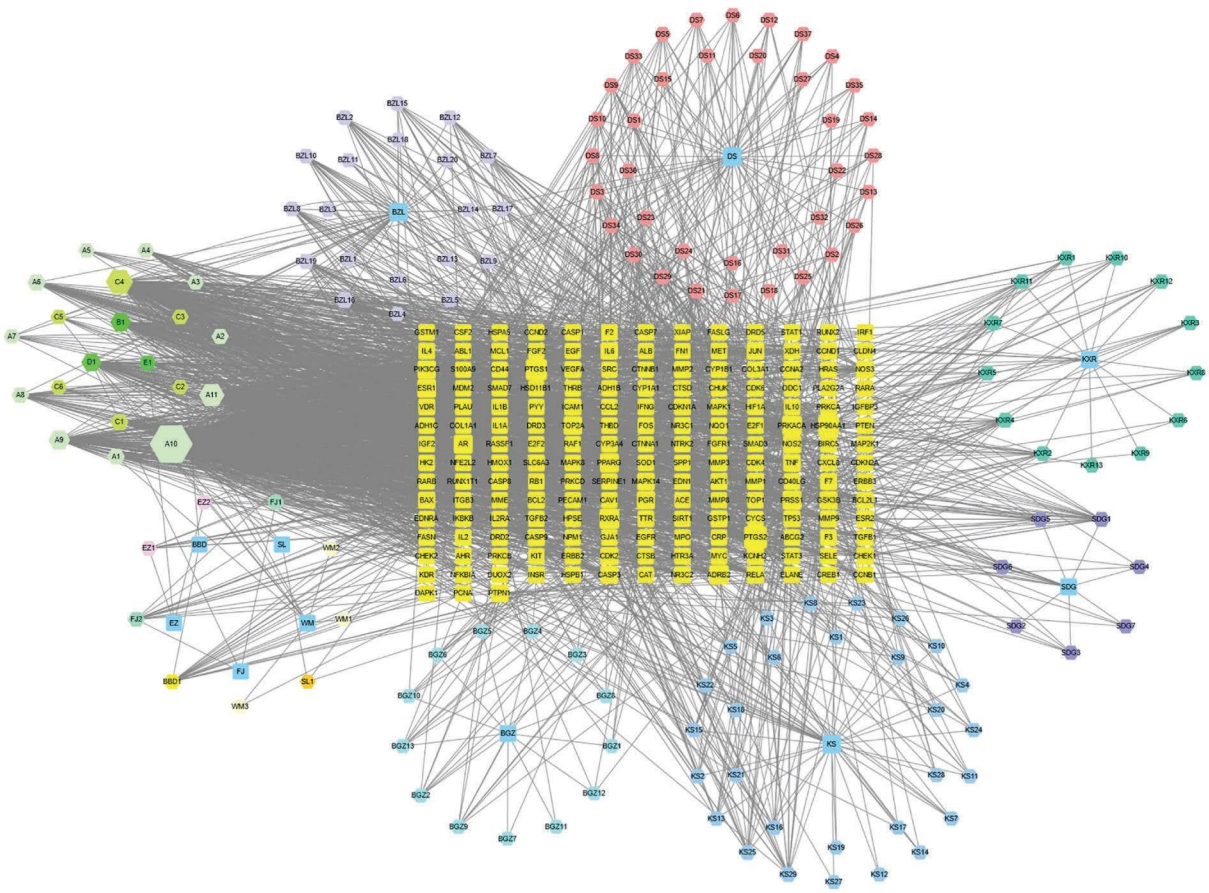

Figure 3: Drug/target/pathway network for SLC and GC. A1–A11, B1, C1–C6, D1, and E1 were common potential active ingredients. Other 21 potential ingredients like wogonin and rhamnazin had high degrees and betweenness that exceed the average value. Thus, 35 main potential active ingredients were mined for further research.

Table 2: Thirty-five main potential active ingredients in SLC.

Name	ID	Degree	Betweenness
Quercetin	A10	432	0.323217
Ursolic acid	C4	181	0.097642
Luteolin	A11	150	0.088354
Formononetin	A9	95	0.020403
Kaempferol	B1	74	0.038225
beta-Sitosterol	D1	68	0.015347
Wighteone	A6	42	0.005507
Wogonin	BZL16	36	0.039156
Stigmasterol	C1	33	0.012039
Matrine	A8	30	0.014486
(2R)-5,7-Dihydroxy-2-(4-hydroxyphenyl)chroman-4-one	A1	27	0.008905
Baicalein	BZL19	23	0.017185
Isorhamnetin	SDG1	22	0.011682
Tanshinone IIA	DS21	22	0.028999
Inermine	A2	20	0.003451
Inermin	A4	20	0.003451
beta-Carotene	BBD1	19	0.01471
8-Isopentenyl-kaempferol	KS29	18	0.006275
Rhamnazin	BZL8	18	0.0044
Moslosooflavone	BZL10	17	0.004829
Salvilenone	DS29	17	0.003735
Danshexinkun D	DS30	17	0.008629
Licochalcone B	KXR2	16	0.003991
Glabridin	KXR4	16	0.004015
Phaseolin	KS25	15	0.003611
5-Hydroxy-7,8-dimethoxy-2-(4-methoxyphenyl) chromone	BZL2	15	0.003367
Tetrandrine	FJ2	15	0.0194
Lupiwighteone	SDG5	15	0.002831
Rivularin	BZL15	14	0.004003
Hederagenin	E1	14	0.01254
Chrysin-5-methylether	BZL12	13	0.002947
Cryptotanshinone	DS3	13	0.008271
Tanshinone VI	DS24	13	0.004279
Miltirone	DS34	13	0.002486
Phaseol	KXR5	13	0.003233

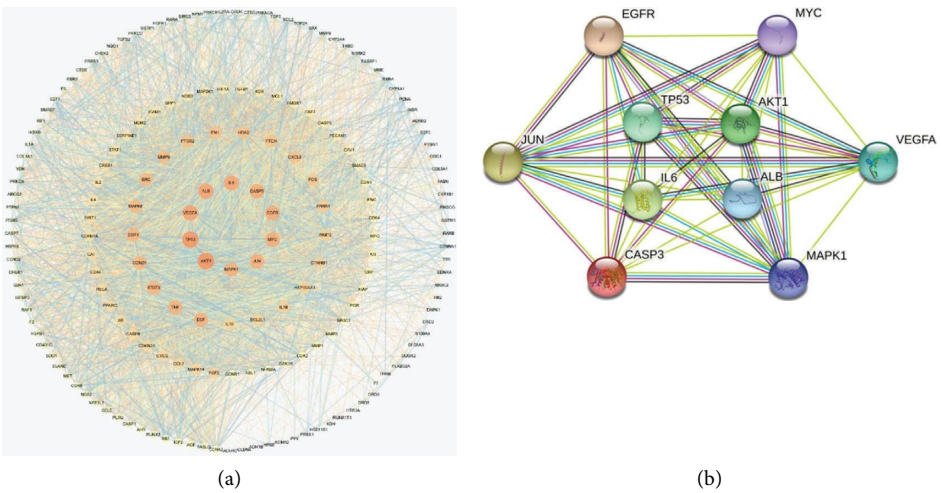

(a) (b)

Figure 4: Protein-protein interaction of expression genes: (a) the combination of all types of expression genes and (b) 10 high-degree gene combinations.

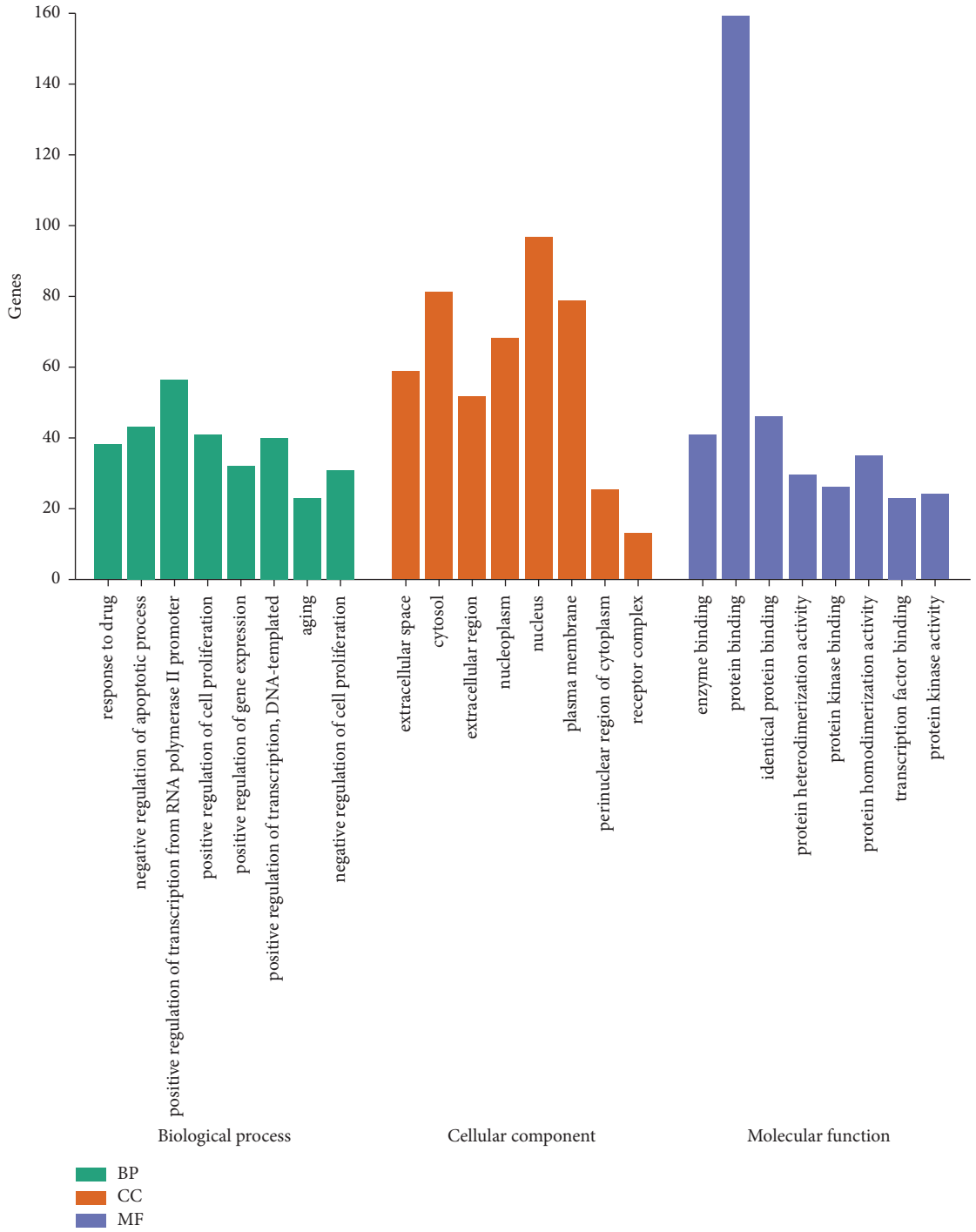

Figure 5: GO enrichment analysis of putative target genes. The top eight functions for biological process, cellular component, and molecular function. BP, CC, and MF had direct correlation between cell cycle, cell apoptosis, and the ingredients of SLC.

formed pi-sulfur interactions with the cyclic ring. Pro153 and Pro222 formed pi-alkyl interactions with the cyclic ring, which shows the potential hydrophobic interactions. Glu221 formed amide-pi stacked interactions with the cyclic ring. The molecular docking results indicated that there was stronger binding activity of the SLC's active ingredients with the primary targets of GC, which may imply that the SLC regulates the expression of the main pathways by combining with key targets. Besides, the results of binging energy between main ingredients such as stigmasterol, matrine, and main targets such as AKT1, TP53, CASP3, and EGFR also suggested that the main ingredients can control cell apoptosis and cell cycle to reduce the content of cancer cells The molecular docking results are shown in Table 3.

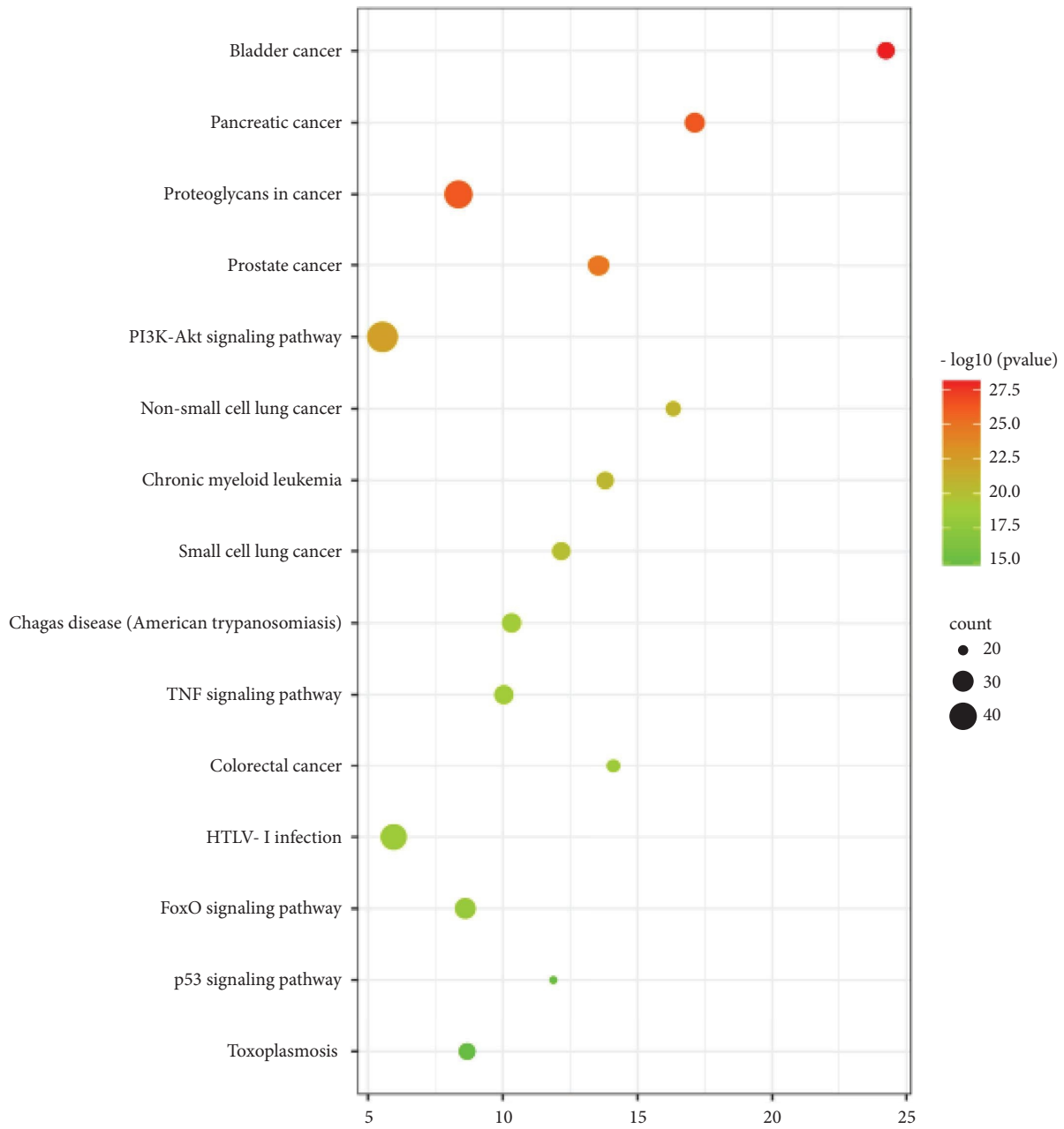

Figure 6: KEGG pathway enrichment analysis of putative target genes. There were twelve KEGG pathways with a significant P value <0.001. The targets of SLC had direct or indirect correlation with the KEGG pathways which correlated well with cancer. Thus, the ingredients of SLC could regulate these pathways such as TNF signaling pathway and PI3K-Akt signaling pathway to treatment.

3.5. Experimental Analysis

3.5.1. MTT Analysis. The SLC's antitumor effect on GC was confirmed by MTT assay, as shown in Figure 8. The results show that there was excellent effectiveness by the mid and high concentrations of the SLC in killing HGC-27 undifferentiated gastric cancer cells. The highest inhibition rate was up to 79.57% with different concentrations of the SLC solution (4 g/L) in a constant temperature incubator at 37°C for 48 h. Low cell viability was aided by the variety of ingredients, and the problem of drug resistance was solved. Therefore, the results of MTT analysis corroborate well with the conclusions of molecular docking. The ingredients of SLC such as quercetin, ursolic acid, stigmasterol, and matrine combined with key targets to prohibit cell apoptosis.

3.5.2. Investigation of Apoptosis and Cell Cycle through Flow Cytometry. To investigate the effect of the SLC combination on the cell cycle distribution, flow cytometry was used, as shown in Figure 9. The results collectively show that the SLC exerts a mild effect on the cell cycle in HGC-27 cells. Cells

Table 3: The molecular docking results of 4 key targets with 10 potential ingredients.

Target (PDB ID)	Ligand	Binding energy (kcal/mol)
AKT1 (6hhf)	Quercetin	−9.2
AKT1 (6hhf)	Ursolic acid	−8.9
AKT1 (6hhf)	Luteolin	−9.6
AKT1 (6hhf)	Formononetin	−9.3
AKT1 (6hhf)	Kaempferol	−9.2
AKT1 (6hhf)	beta-Sitosterol	−10.4
AKT1 (6hhf)	Wighteone	−10.0
AKT1 (6hhf)	Wogonin	−9.4
AKT1 (6hhf)	Stigmasterol	−10.7
AKT1 (6hhf)	Matrine	−8.3
TP53 (5g6o)	Quercetin	−7.9
TP53 (5g6o)	Ursolic acid	−7.3
TP53 (5g6o)	Luteolin	−8.2
TP53 (5g6o)	Formononetin	−8.1
TP53 (5g6o)	Kaempferol	−7.1
TP53 (5g6o)	beta-Sitosterol	−7.0
TP53 (5g6o)	Wighteone	−8.1
TP53 (5g6o)	Wogonin	−7.9
TP53 (5g6o)	Stigmasterol	−7.2
TP53 (5g6o)	Matrine	−8.0
CASP3 (3gjr)	Quercetin	−6.8
CASP3 (3gjr)	Ursolic acid	−8.7
CASP3 (3gjr)	Luteolin	−7.1
CASP3 (3gjr)	Formononetin	−7.3
CASP3 (3gjr)	Kaempferol	−6.7
CASP3 (3gjr)	beta-Sitosterol	−7.8
CASP3 (3gjr)	Wighteone	−7.6
CASP3 (3gjr)	Wogonin	−7.2
CASP3 (3gjr)	Stigmasterol	−7.8
CASP3 (3gjr)	Matrine	−8.1
EGFR (3lzb)	Quercetin	−8.0
EGFR (3lzb)	Ursolic acid	−6.7
EGFR (3lzb)	Luteolin	−8.0
EGFR (3lzb)	Formononetin	−7.6
EGFR (3lzb)	Kaempferol	−8.1
EGFR (3lzb)	beta-Sitosterol	−8.0
EGFR (3lzb)	Wighteone	−8.4
EGFR (3lzb)	Wogonin	−8.0
EGFR (3lzb)	Stigmasterol	−8.7
EGFR (3lzb)	Matrine	−8.5

were blocked in S phase at medium SLC concentrations and blocked in G1 phase at high SLC concentrations. The results of the flow cytometry assay proved that the main mechanism of action was regulation of apoptosis instead of decreasing cell proliferation. The results of flow cytometry evidenced the predictions of network pharmacology and molecular docking. SLC regulated cell cycle to promote apoptosis of HGC-27 cells.

3.5.3. Western Blotting. To confirm the results of network pharmacology, western blotting was used, as shown in Figure 10. We inferred that the SLC enhances proapoptotic gene expression, such as that of caspase-3 and TP53, to promote apoptosis. This result confirmed the potential targets studied from network pharmacology and molecular docking. We also verified the results of network pharmacology research. However, the inhibition of Akt and phosphorylated Akt was insufficient. We speculated that the reason for this may be a lack of effect on the cell cycle by the SLC. Quercetin, ursolic acid, stigmasterol, and matrine played very important role in the treatment. The results of western blotting justified that these main ingredients of SLC promote cell apoptosis to treat GC.

4. Discussion

Natural bioactive compounds are widely used to treat various diseases, especially cancers [23]. Natural products with potential for gastric cancer treatment have received much attention [24]. The possible mechanisms responsible for the effect of the SLCs in the treatment of advanced gastric cancer were proposed in this study. The main natural bioactive compounds of SLCs were identified by HPLC, and network pharmacology was used to identify the main potential active ingredients and targets [25]. SLCs may fortify

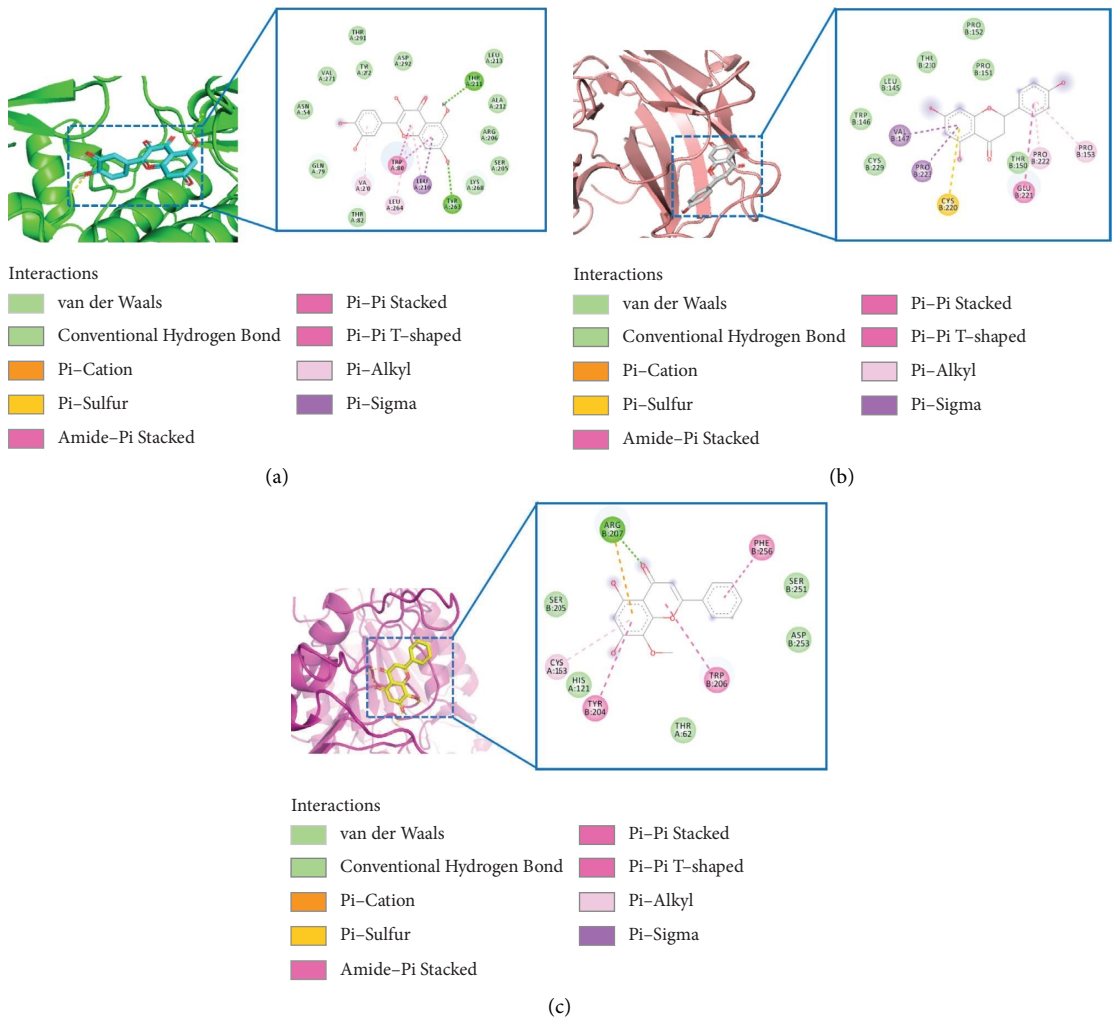

Figure 7: The molecular docking analysis of (a) AKT1 binding with quercetin, (b) TP53 binding with wogonin, and (c) CASP3 binding with (2R)-5,7-dihydroxy-2-(4-hydroxyphenyl) chroman-4-one. Hydrogen bonds, pi-pi stacked, pi-sigma, and van der Waals forces contributed to the interaction between the targets and the ingredients.

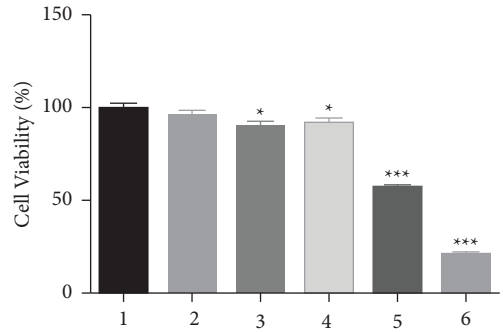

Figure 8: MTT assay. From left to right, the SLC concentrations were 0, 0.2, 0.5, 1, 2, and 4 g/L in turn. Each group was treated with the SLC for 48 h ($^{*}P < 0.1$ and $^{***}P < 0.001$). The cell viability of group 6 reached a plateau at ~20%.

the p53 signaling pathway and inhibit the PI3K/AKT signaling pathway to promote gastric cancer cell apoptosis. The p53 and PI3K/AKT signaling pathways play an important role in the apoptotic signaling circuitry [25, 26]. GO and KEGG enrichment analysis revealed that TP53, caspase-3, and AKT1 might be the key targets [27]. Network pharmacology study pointed out the relationship between ingredients of SLC such as quercetin, matrine, ursolic acid, and stigmasterol and key targets such as AKT1, EGFR, CASP3, and TP53, as shown in Figures 5 and 6. The main ingredients

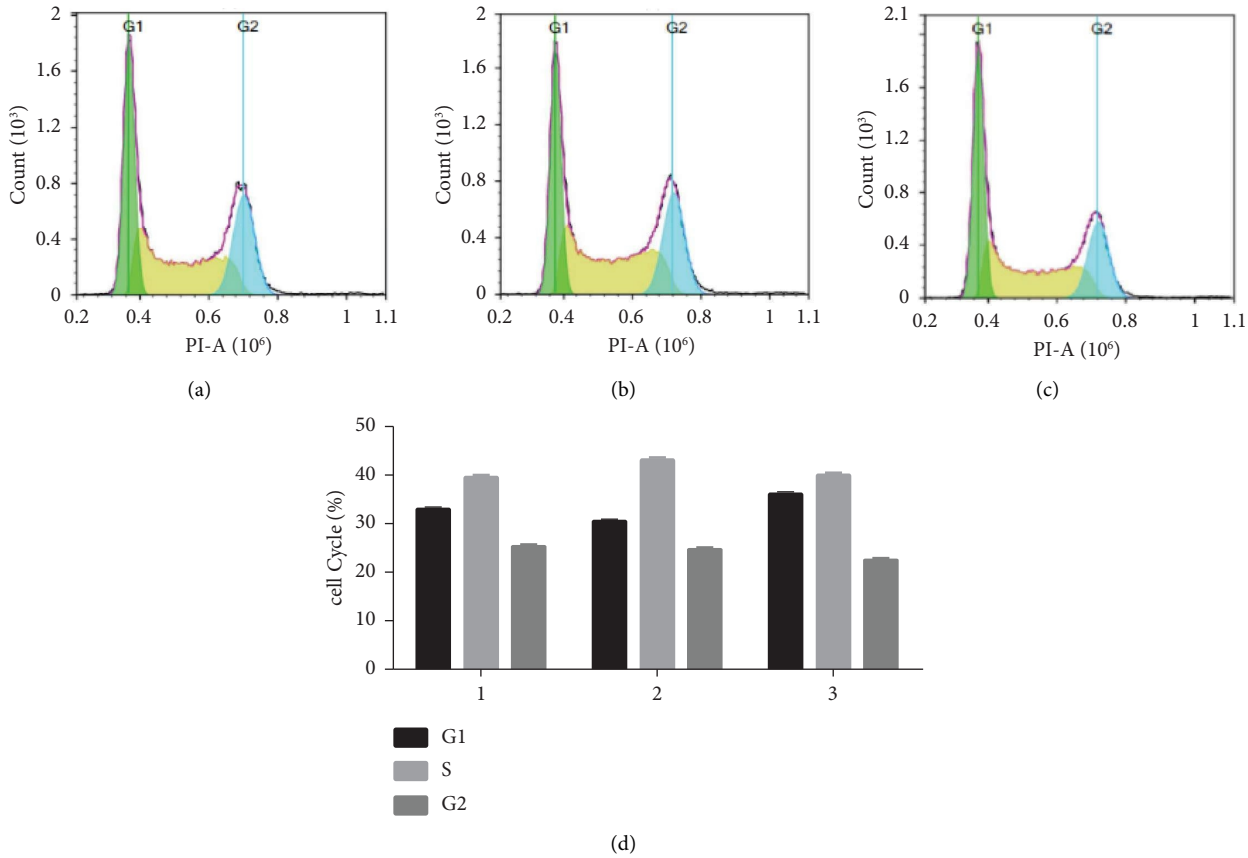

Figure 9: Flow cytometry analysis of HGC-27 cells. From left to right, the SLC concentrations were 0, 2, and 4 g/L. Each group was treated with SLCs for 48 h. HGC-27 cells were arrested in G1/S phase because of ingredients of SLCs.

of SLC might promote cell apoptosis and regulate cell cycle for GC therapy, and quercetin, matrine, and stigmasterol might be the main active natural bioactive compounds. In addition, numerous studies have already identified that these ingredients are potential anticancer agents and natural bioactive compounds can be expected to address clinical drug resistance [28–30], and the accuracy of the prediction was confirmed.

Furthermore, molecular docking revealed the results of ingredients binding to targets. There were excellent docking results for quercetin, beta-sitosterol, ursolic acid, matrine, and stigmasterol. These main ingredients were docked with main targets such as AKT1, CASP3, TP53, and EGFR. The results of molecular docking confirmed that SLC's ingredients could combine with these key targets to control PI3K-Akt signaling pathway, p53 signaling pathway, and TNF signaling pathway. This matched the network pharmacology study's interpretation and offered a cell experimental basis for the use of key targets as therapeutic targets. This adds further evidence that the natural bioactive compounds in SLC have promising effect on GC.

Moreover, the results of cell experimental were in a good agreement with the network pharmacology and molecular docking results. The MTT assay and flow cytometry also confirmed that SLCs can prompt the apoptosis and inhibit proliferation of HGC-27 cells. Although the SLC exerted a mild effect on the cell cycle in HGC-27 cells, cell viability decreased to 11.43% after HGC-27 cells were incubated with high concentrations of the SLC. This matches the results of previous studies and pointed out that the ingredients of SLC could promote cell apoptosis and control cell cycle to reduce the viability of HGC-27 cells in vitro. Western blotting confirmed that the SLC upregulated the protein expression of TP53 and caspase-3 protein, which consequently promoted cell apoptosis [31–34]. This confirmed that the ingredients of SLC regulated the expression of the TNF signaling pathway and p53 signaling pathway and led to cell apoptosis. The accuracy of network pharmacology and molecular docking prediction results must be verified by experimental assay.

Nevertheless, we systematically demonstrated the potential mechanism of the SLCs and confirmed that the SLC's action in the treatment of advanced gastric cancer is the regulation of the p53 signaling pathway overexpression. The main active natural bioactive compounds might be quercetin, matrine, ursolic acid, and stigmasterol. As a TCM that is rich in plant-derived compounds, there is great potential for the SLC to play a more significant role in the treatment of advanced gastric cancer. Moreover, the natural bioactive compounds such as quercetin, matrine, and ursolic acid are

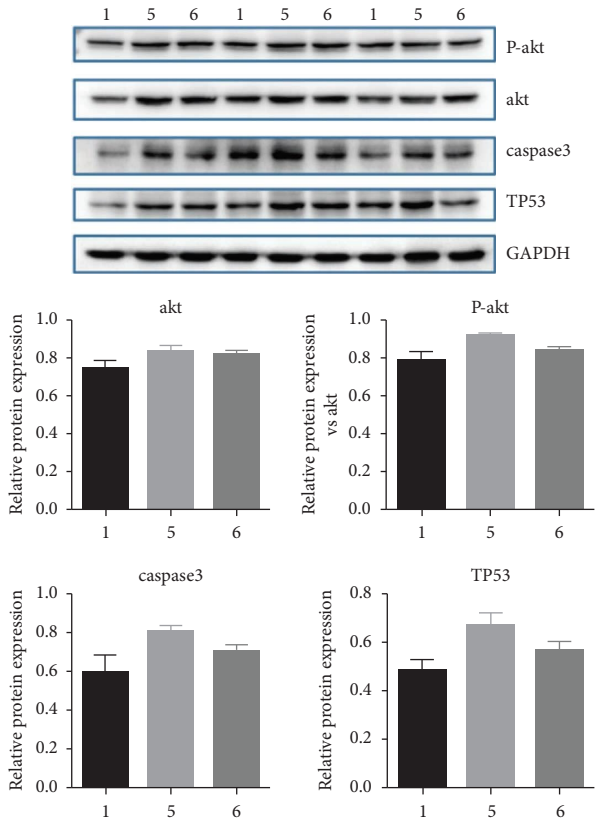

Figure 10: Western blot assay of phosphorylated Akt, Akt, CASP3, and TP53. From left to right, the SLC concentrations were 0, 2, and 4 g/L. Caspase3 and TP53 of HGC-27 cells were overexpressed after treated with SLC concentrations.

useful in the therapy of gastric cancer. Natural products are considered a source for bioactive compounds and have potential for developing some novel therapeutic agents.

Data Availability

All the data and materials used in the current study are available from the corresponding author upon reasonable request.

Disclosure

The funders had no role in the study design, data collection and analysis, decision to publish, or preparation of the manuscript.

Conflicts of Interest

The authors declare that they have no conflicts of interest.

Acknowledgments

This study was supported by the Postgraduate Education Reform and Quality Improvement Project of Henan Province (YJS2021AL014 and YJS2022ZX06). This study was also supported by the National Supercomputing Center in Zhengzhou. The authors thank LetPub (https://www.letpub.com/) for its linguistic assistance during the preparation of this manuscript.

Supplementary Materials

Supplementary Figure 1: the drug/target/pathway network. Supplementary Figure 2: the raw data of MTT assay. Supplementary PDF1: the raw data of flow cytometry W1. Supplementary PDF2: the raw data of flow cytometry W2. Supplementary PDF3: the raw data of flow cytometry W3. Supplementary PDF4: the raw data of western blot. (*Supplementary Materials*)

References

[1] H. Sung, J. Ferlay, R. L. Siegel et al., "Global cancer statistics 2020: GLOBOCAN estimates of incidence and mortality worldwide for 36 cancers in 185 countries," *CA: A Cancer Journal for Clinicians*, vol. 71, no. 3, pp. 209–249, 2021.

[2] A. H. Chang and J. Parsonnet, "Role of bacteria in oncogenesis," *Clinical Microbiology Reviews*, vol. 23, no. 4, pp. 837–857, 2010.

[3] R. E. Sexton, M. N. Al Hallak, M. Diab, and A. S. Azmi, "Gastric cancer: a comprehensive review of current and future treatment strategies," *Cancer & Metastasis Reviews*, vol. 39, no. 4, pp. 1179–1203, 2020.

[4] Z. Song, Y. Wu, J. Yang, D. Yang, and X. Fang, "Progress in the treatment of advanced gastric cancer," *Tumor Biology*, vol. 39, no. 7, Article ID 101042831771462, 2017.

[5] K. Wang, Q. Chen, Y. Shao et al., "Anticancer activities of TCM and their active components against tumor metastasis," *Biomedicine & Pharmacotherapy*, vol. 133, Article ID 111044, 2021.

[6] Y. Liu, S. Yang, K. Wang et al., "Cellular senescence and cancer: focusing on traditional Chinese medicine and natural products," *Cell Proliferation*, vol. 53, no. 10, Article ID e12894, 2020.

[7] Y. Xiang, Z. Guo, P. Zhu, J. Chen, and Y. Huang, "Traditional Chinese medicine as a cancer treatment: modern perspectives of ancient but advanced science," *Cancer Medicine*, vol. 8, no. 5, pp. 1958–1975, 2019.

[8] X. L. Hu and X. S. Liu, "Clinical effect of Xiaoaiping injection combined with gemcitabine and carboplatin in treatment of IIIB and IV non-small cell lung cancer," *Drug Evaluation Research*, vol. 40, pp. 266–269, 2017, in China.

[9] J. R. Liu, Y. H. An, W. B. Yang, and K. Zhao, "Clinical study on Xiaoaiping injection combined with GP regimen in the treatment of advanced lung squamous cell carcinoma," *Medical Innovation of China*, vol. 13, pp. 97–101, 2016, in China.

[10] J. Huo, F. Qin, X. Cai et al., "Chinese medicine formula 'Weikang Keli' induces autophagic cell death on human gastric cancer cell line SGC-7901," *Phytomedicine*, vol. 20, no. 2, pp. 159–165, 2013.

[11] Y. C. Hung, T. L. Pan, and W. L. Hu, "Roles of reactive oxygen species in anticancer therapy with salvia miltiorrhiza Bunge," *Oxidative Medicine and Cellular Longevity*, vol. 2016, Article ID 5293284, 10 pages, 2016.

[12] X. Cao and Q. He, "Anti-tumor activities of bioactive phytochemicals in *Sophora flavescens* for breast cancer," *Cancer Management and Research*, vol. 12, pp. 1457–1467, 2020.

[13] Q. Han, Z. Bin, L ping, and G. Zhi-hu, "Quality evaluation of Shenlian capsules by HPLC fingerprint and pattern

recognition," *Chinese Journal of Pharmaceutical Analysis*, vol. 40, no. 07, pp. 1300–1308, 2020, in China.
[14] Z. Diao, "The clinical effects of Shenlian capsule, trastuzumab combined with SOX regimen in the treatment for HER-2 positive advanced gastric carcinoma," *International Journal of Translation & Community Medicine*, vol. 40, no. 117, pp. 1020–1024, 2018, in China.
[15] T. XiaoHui, "Clinical study on Shenlian capsule combined with DP therapeutic regimen in treatment of advanced gastric cancer," *Drugs and Clinic*, vol. 33, no. 8, pp. 2055–2059, 2018, in China.
[16] A. L. Hopkins, "Network pharmacology: the next paradigm in drug discovery," *Nature Chemical Biology*, vol. 4, no. 11, pp. 682–690, 2008.
[17] B. Boezio, K. Audouze, P. Ducrot, and O. Taboureau, "Network-based approaches in pharmacology," *Molecular Informatics*, vol. 36, no. 10, Article ID 1700048, 2017.
[18] C. Nogales, Z. M. Mamdouh, M. List, C. Kiel, A. I. Casas, and H. H. Schmidt, "Network pharmacology: curing causal mechanisms instead of treating symptoms," *Trends in Pharmacological Sciences*, vol. 43, no. 2, pp. 136–150, 2022.
[19] X. Wang, Z. Y. Wang, J. H. Zheng, and S. Li, "TCM network pharmacology: a new trend towards combining computational, experimental and clinical approaches," *Chinese Journal of Natural Medicines*, vol. 19, no. 1, pp. 1–11, 2021.
[20] R. Zhang, X. Zhu, H. Bai, and K. Ning, "Network pharmacology databases for traditional Chinese medicine: review and assessment," *Frontiers in Pharmacology*, vol. 10, p. 123, 2019.
[21] L. Pinzi and G. Rastelli, "Molecular docking: shifting paradigms in drug discovery," *International Journal of Molecular Sciences*, vol. 20, no. 18, p. 4331, 2019.
[22] T. Hussain, S. Bajpai, M. Saeed et al., "Potentiating effect of ethnomedicinal plants against proliferation on different cancer cell lines," *Current Drug Metabolism*, vol. 19, no. 7, pp. 584–595, 2018.
[23] S. Wang, S. Long, Z. Deng, and W. Wu, "Positive role of Chinese herbal medicine in cancer immune regulation," *The American Journal of Chinese Medicine*, vol. 48, no. 7, pp. 1577–1592, 2020.
[24] J. Xu, F. Kang, W. Wang, S. Liu, J. Xie, and X. Yang, "Comparison between heat-clearing medicine and antirheumatic medicine in treatment of gastric cancer based on network pharmacology, molecular docking, and tumor immune infiltration analysis," *Evidence-based Complementary and Alternative Medicine*, vol. 2022, 21 pages, 2022.
[25] M. J. Duffy, N. C. Synnott, and J. Crown, "Mutant p53 as a target for cancer treatment," *European Journal of Cancer*, vol. 83, pp. 258–265, 2017.
[26] M. Osaki, M. Oshimura, and H. Ito, "PI3K-Akt pathway: its functions and alterations in human cancer," *Apoptosis*, vol. 9, no. 6, pp. 667–676, 2004.
[27] J. Kania, S. J. Konturek, K. Marlicz, E. G. Hahn, and P. Konturek, "Expression of survivin and caspase-3 in gastric cancer," *Digestive Diseases and Sciences*, vol. 48, no. 2, pp. 266–271, 2003.
[28] M. Reyes-Farias and C. Carrasco-Pozo, "The anti-cancer effect of quercetin: molecular implications in cancer metabolism," *International Journal of Molecular Sciences*, vol. 20, no. 13, p. 3177, 2019.
[29] A. J. Vargas, S. Sittadjody, T. Thangasamy, E. E. Mendoza, K. H. Limesand, and R. Burd, "Exploiting tyrosinase expression and activity in melanocytic tumors: quercetin and the central role of p53," *Integrative Cancer Therapies*, vol. 10, no. 4, pp. 328–340, 2011.
[30] M. S. Bin Sayeed and S. S. Ameen, "Beta-sitosterol: a promising but orphan nutraceutical to fight against cancer," *Nutrition and Cancer*, vol. 67, no. 8, pp. 1216–1222, 2015.
[31] J. Chen, "The cell-cycle arrest and apoptotic functions of p53 in tumor initiation and progression," *Cold Spring Harbor Perspectives Medicine*, vol. 6, no. 3, Article ID a026104, 2016.
[32] X. Wang, E. R. Simpson, and K. A. Brown, "p53: protection against tumor growth beyond effects on cell cycle and apoptosis," *Cancer Research*, vol. 75, no. 23, pp. 5001–5007, 2015.
[33] A. G. Porter and R. U. Jänicke, "Emerging roles of caspase-3 in apoptosis," *Cell Death & Differentiation*, vol. 6, no. 2, pp. 99–104, 1999.
[34] S. Nagata, "Apoptosis and clearance of apoptotic cells," *Annual Review of Immunology*, vol. 36, no. 1, pp. 489–517, 2018.

Hindawi
Journal of Chemistry
Volume 2023, Article ID 5224921, 10 pages
https://doi.org/10.1155/2023/5224921

Research Article

Emodin Alleviates Lupus Nephritis in Rats by Regulating M1/M2 Macrophage Polarization

Weijian Xiong, Ying Li, Ling Zhang, Yanying Xiong, Jin Zhong, Xunjia Li, Yan Luo, Hong Liu, Renhong Kang, and Yunjie Chen

Department of Nephrology, Chongqing Traditional Chinese Medicine Hospital, Chongqing 400000, China

Correspondence should be addressed to Ying Li; sabrina_pipi@cdutcm.edu.cn and Ling Zhang; 1648770473@qq.com

Received 26 August 2022; Revised 23 September 2022; Accepted 28 September 2022; Published 4 February 2023

Academic Editor: Muhammad Zia-Ul-Haq

Lupus nephritis (LN) is one of the most common clinical manifestations of systemic lupus erythematosus (SLE), causing death and disability. The current research study explored whether there was any improvement effect on LN after emodin administration. Network pharmacology was used to screen the target genes of emodin for the treatment of LN. LPS and IL-4 were employed for RAW264.7 macrophage M1/M2 polarization induction, and 0.1% $HgCl_2$ was used for the LN rat model's establishment. Flow cytometry was performed to detect the effect of 20, 40, and 80 μM emodin on RAW264.7 macrophage polarization. HE and PAS staining were subsequently conducted to detect 70 mg/kg emodin action on renal injury in LN rats. The effect of emodin on the content of urinary proteins and dsDNA antibodies was also determined. The results indicated that peroxisome proliferators-activated receptors gamma (PPARG) may be a target gene of emodin in LN, and emodin had no significant toxicity to macrophages at different concentrations. Compared with the control, emodin significantly inhibited LPS-induced polarization in M1 macrophages and improved that of IL-4-induced M2 macrophages. Besides, emodin alleviated kidney injury and markedly reduced the levels of urinary protein and dsDNA antibodies in rats. Moreover, after targeting interference with the PPARG expression, the improvement effect of emodin on LN is significantly reduced, indicating that emodin may relieve the symptoms of LN by activating the PPARG expression. Our study revealed that PPARG may be applied as a new therapy for LN.

1. Introduction

Systemic lupus erythematosus (SLE), a serious systemic autoimmune disease, affects most females of childbearing age, especially pregnant women [1]. During the disease progression of SLE patients, there are often severe inflammatory responses, immune dysfunction, abnormal recognition of autoantibodies and nonautoantibodies, and immune tolerance disorders during the progression of the disease. Clinically, more than half of SLE patients present with symptoms of kidney injury, which eventually progress to lupus nephritis (LN) if left untreated. The clinical symptoms of LN include hematuria, proteinuria, elevated markers of renal injury, as well as serum creatinine, antidouble-stranded DNA titers, a progressive decline in renal function, and eventual death due to renal failure [2–4]. Hematuria, proteinuria, renal injury, elevated markers of renal failure, and renal failure are also present.

The pathological mechanism of LN has not been clarified, but some studies have confirmed that abnormal activation and differentiation of immunocytes play key biological roles in LN pathogenesis [5, 6]. The infiltrating cells and macrophages in the kidney of LN patients can be roughly polarized into two phenotypes, namely M1-type macrophages secreting inducible nitric oxide synthase (iNOS) and M2-type macrophages secreting arginase-1 (Arg-1). In LN, M1 macrophages exert a proinflammatory and profibrotic role, while M2 macrophages are responsible for antiinflammation, which promotes the reconstruction and repair of injured body sites [7]. The most ideal goal of the treatment of autoimmune diseases is immune reconstruction to restore the body's immune tolerance to autoantigens, but it has not been achieved so far. Immunosuppressive therapy is still the main treatment for autoimmune diseases in clinical practice. Most of the

mechanisms of existing immunosuppressive agents are cytotoxicity, antimetabolism, and inhibition of signal transduction, which often have inhibitory or even killing effects on immune cells and cells of other systems, causing a wide range of adverse reactions [8].

Emodin, known as 1,3,8-trihydroxy-6-methylanthraquinone, is a free anthraquinone derivative and a major effective monomer of rhubarb. Emodin is one of the most common traditional Chinese medicines and has abundant resources and broad research prospects. The main effect of emodin is to treat dry stools and hot knot constipation. Emodin has recently indicated multiple pharmacological effects, such as antiallergy, antitumor, antiviral, antibacterial, antiosteoporosis, antidiabetes, immunity inhibition, nerve protection, and liver protection [9–11]. Additional studies have also demonstrated the anti-inflammation action of emodin. Emodin can dose-dependently hinder IκB degradation and NF-κB activation after LPS induction, which reduces concentrations of inflammatory cytokines IL-6 and IL-1β and the expressions of chemokines CCL2 and IL-8 [12]. Ha et al. have indicated the roles of emodin dose-dependently in inhibiting the secretion of inflammatory mediators IL-6, IL-8, IL-1β, and TNF-α and downregulating VEGF, MMP-1, MMP-13, and PGE2 levels in a rheumatoid arthritis cell model. It is suggested that emodin inhibits the production of inflammatory cytokines and VEGF due to its anti-inflammation function [13]. The study by Alisi et al. has shown that emodin restricts the increase of TNF-α induced by hyper glucose and high-fat diets in rats, thus hiding steatohepatitis [14]. The results of Song et al. have indicated that emodin can enhance the left ventricular function of rats with experimental autoimmune myocarditis by gavage, thereby reducing the severity of myocarditis [15].

Unluckily, few scientific reports have been found investigating the ameliorative effects of emodin on LN. To the best of our knowledge, only Liu et al. found that emodin inhibits proliferation and promotes apoptosis in LN patients' kidney fibroblasts, which may improve the prognosis of LN [16]. Recently, emodin has been reported to inhibit T-lymphocyte-like receptor 4 expression in renal tubular epithelial cells induced by lipopolysaccharide, and downregulate the synthesis of IL-6 and TNF-α [17]. Meanwhile, the number of regulatory T cells can be increased, and dendritic cells can be mediated by emodin during the processes of differentiation and maturation [18]. The findings demonstrated the role of emodin in the regulation of immune responses. Therefore, the present work attempted to investigate whether emodin can improve LN symptoms by affecting macrophages, and hopefully offer a theoretical basis for the application of emodin again LN.

2. Methods

2.1. Network Pharmacology. The predicted targets of emodin were exported using the websites PubChem (https://pubchem.ncbi.nlm.nih.gov) and SwissTargetPrediction (https://www.swisstargetprediction.ch/), and the disease targets of LN were obtained from GeneCards (https://www.genecards.org). Overlapped targets of emodin and LN were uploaded to STRING and information on protein-protein interaction (PPI) was collected for the construction of a PPI network diagram. To illustrate the role of emodin targets in gene function and signaling pathways, ClueGo, a plug-in of Cytoscape 3.6.1, was employed for GO enrichment analysis and KEGG pathway annotation to identify possible targets of emodin in LN treatment, and the analysis results were visualized.

2.2. Cell Culture. The macrophage RAW264.7 cell line (SCSP-5036) was obtained from the Cell Bank of the Chinese Academy of Sciences. DMEM containing 10% FBS (Gibco, USA), 1% Glutamax (35050061, Invitrogen, USA), and 1% sodium pyruvate 100 mM Solution (11360070, Invitrogen, USA) was used for culture with 5% CO_2 at 37°C.

2.3. Preparation of Emodin. Emodin (HY-14393, CAS No. 518-82-1) was purchased from MedChemExpress, USA. For introduction experiments, emodin was dissolved in dimethyl sulfoxide at 20, 40, and 80 mM and diluted 1000 times to 20, 40, and 80 μM when used. For in vivo experiments, emodin was dissolved in 0.5% carboxymethylcellulose at 4 mg/mL.

2.4. MTT Assay. We employed the MTT cell proliferation and cytotoxicity assay kit (M1020, Solarbio, Beijing, China) to determine cell viability. Following cell collection in the logarithmic phase, the cells were inoculated into 96-well plates at a density of 1×10^6/mL, or 100 μL per well. Culture at 37°C and 5% CO_2 for 12 hours. The 96-well plates were removed and cultured with low, medium, and high concentrations (20, 40, and 80 μM) of emodin for 6 and 12 h, respectively. After the supernatant was carefully sucked away, 90 μL DMEM and 10 μL MTT solutions were added for culture for another 4 h. The supernatant was discarded again. Of 110 μL formazan solution was supplied to each well and mixed well by vibrating 10 min mildly to fully dissolve the crystals. The absorbance of each well was detected at 490 nm by ELISA. Cell viability was computed using the formula as follows:

$$\text{Cell viability} = \frac{\left(A_{\text{test}} - A_{\text{blank}}\right)}{\left(A_{\text{control}} - A_{\text{blank}}\right)} \times 100\%. \quad (1)$$

2.5. Flow Cytometry. RAW264.7 cells at a density of 1×10^6/mL were inoculated into 6-well plates, 2 mL for each well, and placed in the cell incubator for further culture overnight until they adhered to the wall. Then we discarded the medium and washed it twice with PBS. The polarization of RAW264.7 M1 was induced by 1 μg/mL LPS. The control group was cultured with a complete medium. The LPS group was cultured with a complete medium containing 1 μg/mL LPS. Low, medium, and high dose emodin groups were cultured with a complete medium containing 1 μg/mL LPS + 20 μM emodin, 1 μg/mL LPS + 40 μM emodin, and 1 μg/mL LPS + 80 μM emodin, respectively. Raw264.7 M2 polarization was induced by 20 ng/mL IL-4. The grouping

and dosage of emodin in M2 polarization detection were the same as in M1 polarization detection. After the cells were cultured for 48 h, the M1 marker $F4/80^+CD86^+$ and the M2 marker $F4/80^+CD206^+$ were detected by flow cytometry.

2.6. Lentivirus Transfection. The targeted interference of the PPARG lentivirus vector was constructed by Chongqing Biomedicine Biotechnology Co. Ltd. RAW264.7 cells were inoculated onto plates, cultured for 12 h, and divided into 3 groups. The blank group had no virus infection, the vector group was given a negative control virus, and the interference group had a lentivirus containing the PPARG interference sequence. 48 h after infection, the culture solution was replaced with DMEM medium containing 4 mg/L puromycin for 2 days to screen for resistant cells. The cells were then used for flow cytometry detection.

2.7. Animal Modeling and Grouping. Twenty SPF SD rats (male, weighing 180–220 g) were provided by Chongqing Enswell Biotechnology Co., Ltd. After 7 days of adaptive feeding in the animal room, the laboratory animals were grouped into control, model, emodin, and PPARG lentivirus interference groups. The experiment lasted for 14 days. Except for the control group, which was injected with an identical volume of pH = 3.8 water for injection (prepared with 0.1 M hydrochloric acid), the LN model was established by subcutaneous injection of 0.1% $HgCl_2$ (1 mg/kg) into a foot pad, once every 2 days. The emodin treatment group received an intraperitoneal injection of 70 mg/kg of emodin per day. The lentivirus group was first injected in situ with PPARG lentivirus at 5 injection sites (10 μL for each site) and then injected with emodin at 70 mg/kg daily. Animal room temperature was maintained at 23–25°C with 12 h/12 h light and dark alternately. Eating and drinking were provided ad libitum.

2.8. Detection of Urinary Protein and Double-Stranded DNA Antibodies in Rats. Following 24 h of the last administration, urine and blood samples of rats were collected using a sterile centrifugal tube, and urine protein and serum dsDNA antibody levels of rats were detected as per the instructions of ELISA kits. Rat urine protein detection kits (RX302447R) and dsDNA antibody detection kits (RX302544R) were from Quanzhou Ruixin Biotechnology Co., Ltd.

2.9. HE Staining. Twenty-four hours following the last administration, laboratory animals were anesthetized by intraperitoneal injection of 2% pentobarbital sodium (0.2 mL/100 g) and then sacrificed. Kidney tissue was collected for 24 h of fixation using 4% paraformaldehyde. The tissue was paraffin-embedded as usual and sectioned subsequently. Xylene was used for dewaxing twice, 5 min each. anhydrous ethanol was used for immersion twice, 5 min each. 95%, 85%, and 75% ethanol were treated for 2 min at each concentration. Distilled water was used for immersion for 2 min, and then the samples were stained with hematoxylin staining solution for 10 min followed by a 10-second rinse using running water. The differentiation solution was differentiated for 5 seconds, and the water was washed for 30 seconds. The eosin staining solution was dyed for 2 min and then washed with running water for 5 s. The samples were soaked with ethanol at 75%, 85%, 95%, and 100% (I) for 3 s and 100% ethanol (II) for 1 min, followed by xylene transparency twice, each time for 1 min. Finally, the section was sealed with neutral gum and photographed under a microscope (CX43, Olympus, Japan).

2.10. PAS Staining. Paraffin sections of kidney tissue were taken and rinsed with running water for 2 min, then rinsed with distilled water twice. The slices were placed and kept in an oxidizer at room temperature for 5 min, rinsed once with tap water, and then immersed twice in distilled water. Slices were immersed in Schiff staining solution and dyed in dark at room temperature for 10 min following a 10-min cycle of rinsing with running water. The slices were kept in the hematoxylin staining solution for 2 min. An acidic differentiation solution was used for differentiation for 5 s. After rinsing with tap water for 10 min, step-by-step ethanol dehydration and transparent xylene and neutral gum sealing were performed according to the HE staining steps.

2.11. Data Analysis. GraphPad 8.0 was employed for data analysis, which was then expressed as mean ± standard deviation. A one-way ANOVA was used for multiple group comparisons and $P < 0.05$ was regarded as statistically significant.

3. Results

3.1. PPAGR may be the Target Gene for Emodin in Treating LN. Through network pharmacology analysis, 70 genes were predicted to intersect with LN (Figure 1(a)), and the top five connected nodes by degree were HSP90AA1, EGFR, ESR1, BCL2L1, and RRARG. According to the analysis results and literature review, PPARG played an essential role in macrophage polarization, and it was speculated that it also played an important role in the emodin improvement of LN. GO functional enrichment analysis was also carried out to analyze overlapped genes, and the top 10 terms were subsequently visualized. As shown in Figure 1(b), among the first 10 items, one of them belongs to molecular function, heat shock protein binding. The other 9 are biological processes, which are related to inflammatory response regulation and macrophage differentiation and activation. It is suggested that emodin may be associated with macrophages in alleviating LN symptoms. In KEGG enrichment analysis results, the PI3K-Akt signaling pathway enrichment index was the highest (Figure 1(c)), indicating that emodin regulation of the disease may be achieved by regulating PPARG activation of this signaling pathway.

3.2. Emodin Has No Significant Toxicity to Macrophages. To verify whether there is any influence of emodin at different concentrations on RAW264.7 cell viability,

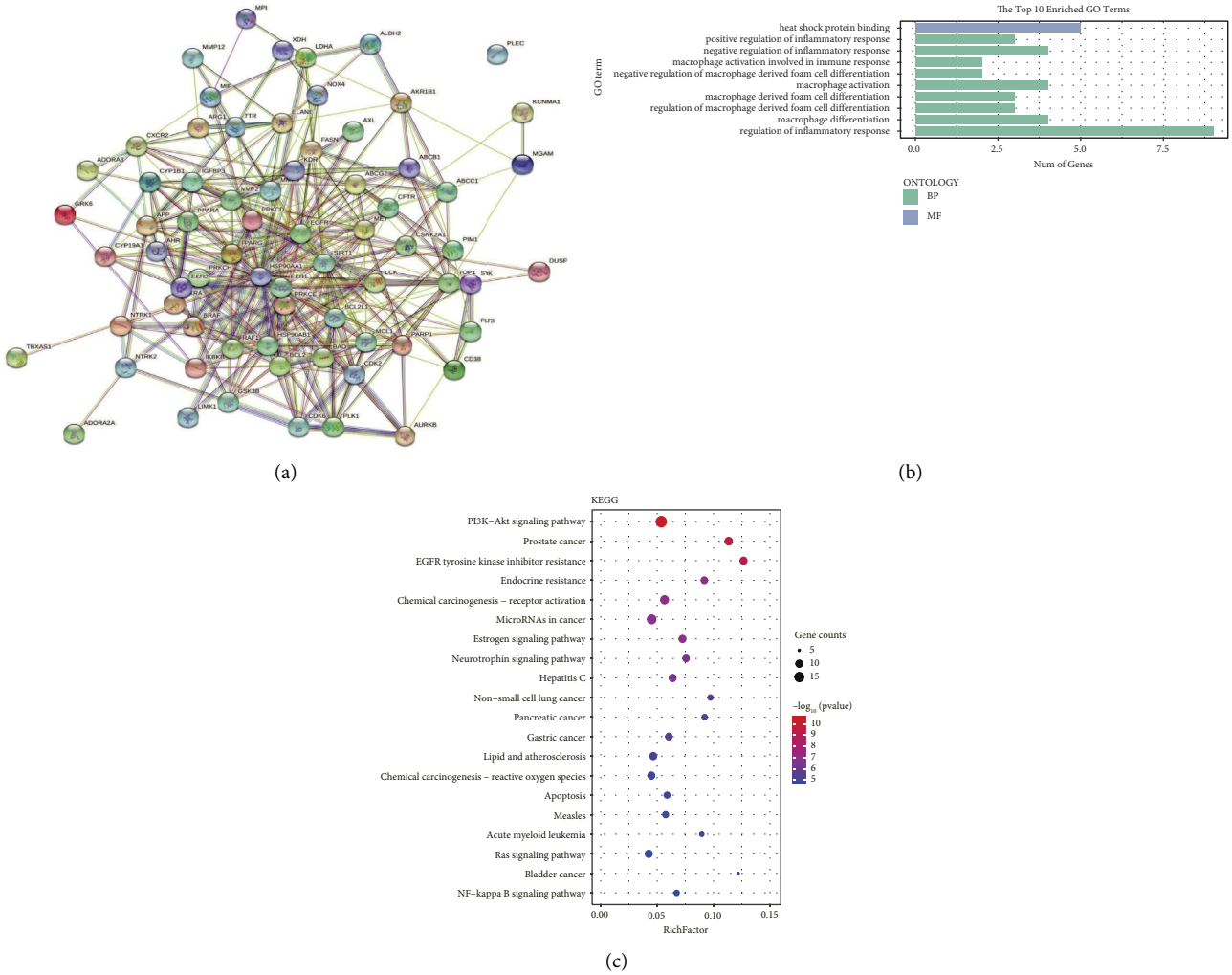

Figure 1: Results of network pharmacology analysis. (a) GO enrichment analysis; (b) PPI network diagram; and (c) KEGG enrichment analysis.

RAW264.7 cells were treated with low, medium, and high concentrations (20, 40, and 80 μM) of emodin for 6 h and 12 h, respectively. MTT results showed that no significant decrease in cell viability was observed regardless of whether emodin was used for 6 h (Figure 2(a)) or 12 h (Figure 2(b)), indicating that emodin had no significant toxicity to cells at 20, 40, and 80 μM.

3.3. Emodin Drives Macrophage Polarization Toward Anti-Inflammatory M2 Phenotypes. The polarization direction of macrophages is positively associated with the inflammatory response during persistent tissue injury, and network pharmacological analysis suggested that macrophages play a role in the improvement of LN. Therefore, M1-type polarization markers F4/80$^+$CD86$^+$ and M2-type polarization markers F4/80$^+$CD206$^+$ were detected by flow cytometry for evaluating emodin's action on cell polarization, implying that the detection rates of F4/80$^+$CD86$^+$ and F4/80$^+$CD206$^+$ were markedly higher than control after LPS and IL-4 induction, respectively (Figures 3(a) and 3(b)) ($P < 0.01$). Compared with the LPS group, emodin at low, medium, and high concentrations significantly reduced the macrophages polarized towards M1 phenotypes ($P < 0.01$). However, only medium- and high-concentration emodin greatly promoted the macrophages polarized towards M2 phenotypes ($P < 0.01$) compared with IL-4 group.

3.4. Interference with PPARG Expression Decreases M2 Phenotypes Polarization. To verify if PPARG can affect the therapeutic effect of LN, this study used lentiviral vectors to target macrophages infected by PPARG for 2 d and induced macrophage polarization with IL-4 and LPS, respectively. The detection rate of M1 macrophage marker F4/80$^+$CD86$^+$ indicated a marked increase after lentivirus interfered with the PPARG gene versus LPS + vector group (Figure 4(a)) ($P < 0.01$). The detection rate of M2 macrophage marker F4/80$^+$CD206$^+$ was also much higher than that of the IL-4 + vector group (Figure 4(b)) ($P < 0.01$), suggesting that PPARG gene exerts a decisive role in macrophage polarization.

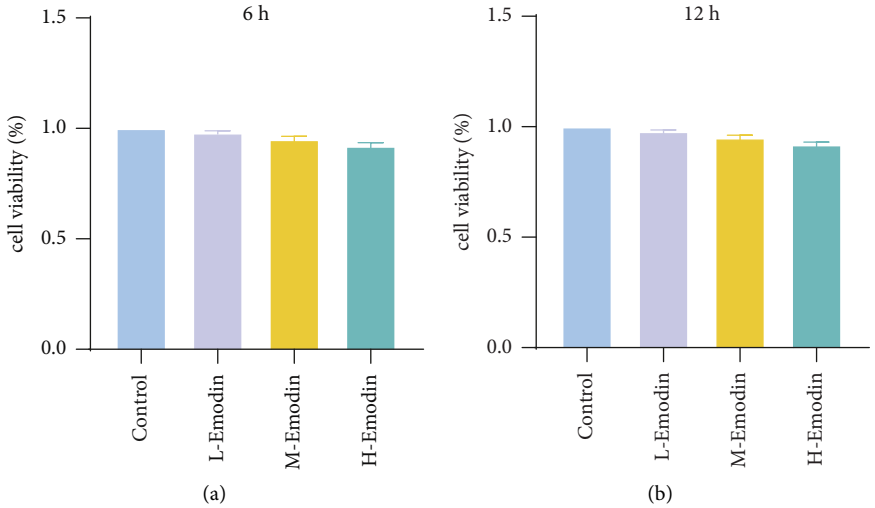

Figure 2: Emodin effects on RAW264.7 cell viability ($n = 3$). (a) Cell viability after 6 h of emodin treatment; (b) cell viability after 12 h treatment with emodin.

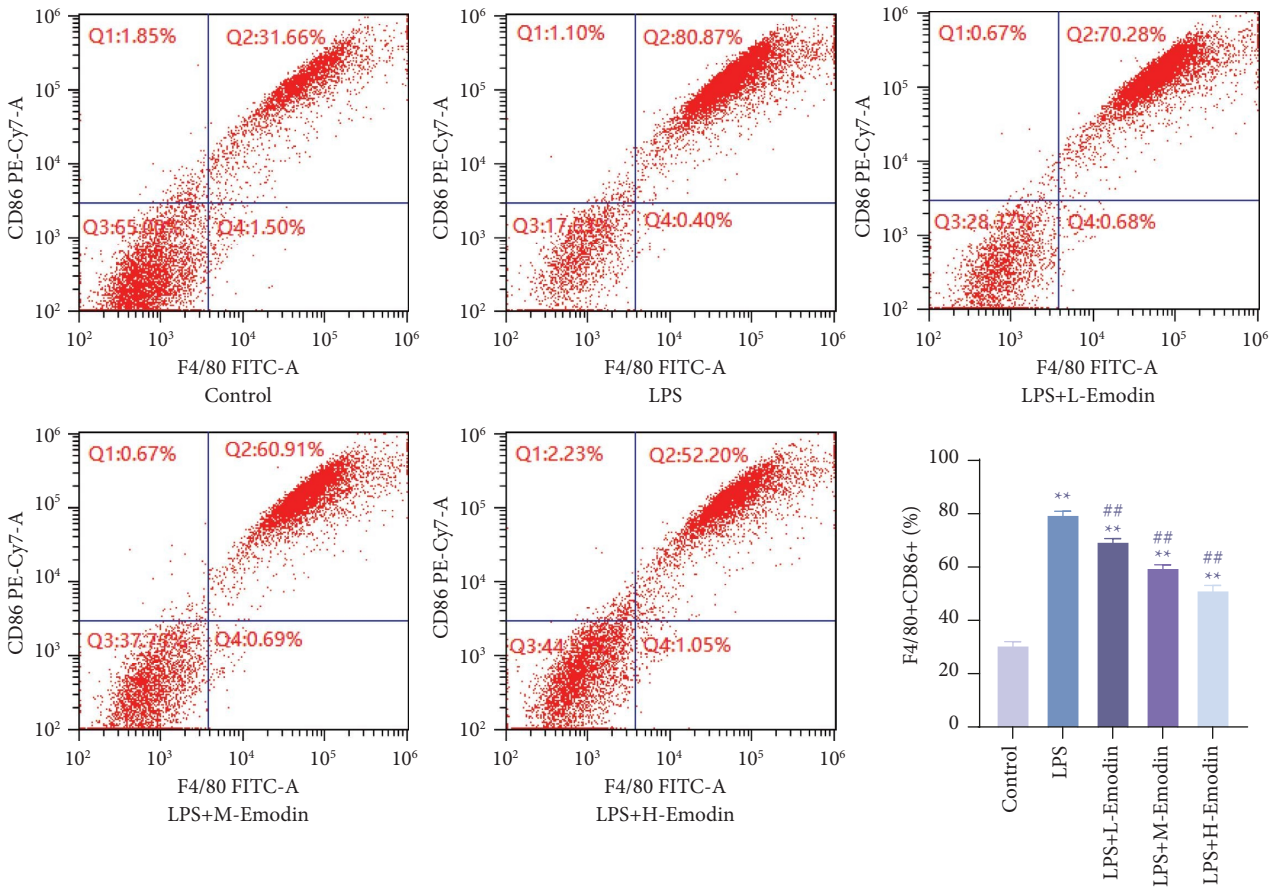

(a)

Figure 3: Continued.

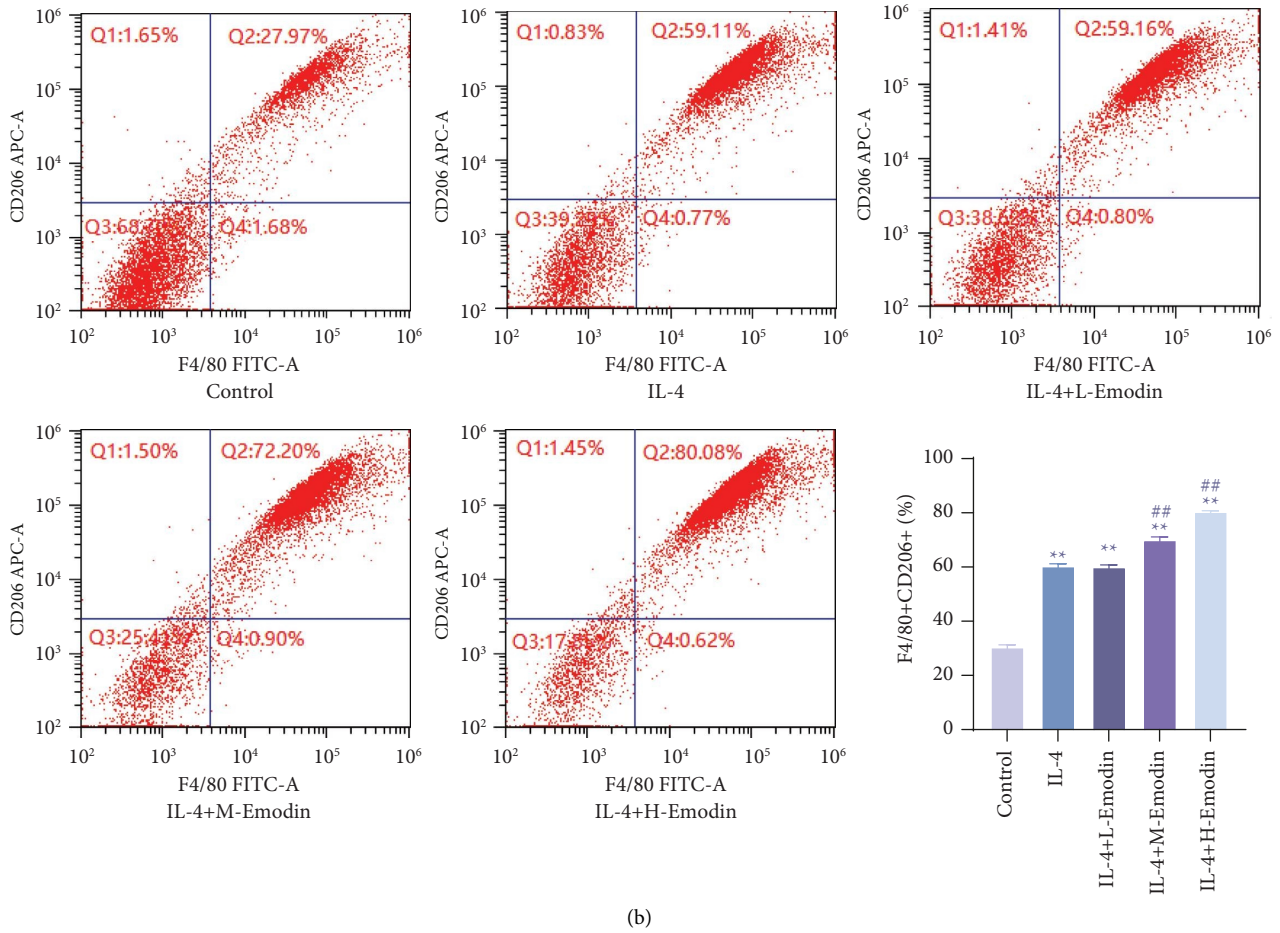

(b)

Figure 3: Emodin effects on the polarization of macrophages were detected by flow cytometry ($n = 3$). (a) Emodin inhibits LPS-induced polarization of M1 macrophages; (b) Emodin promotes IL-4-induced polarization of M2 macrophages. $^{**}P < 0.01$ vs. control; $^{\#\#}P < 0.01$ vs. IL-4 or LPS.

3.5. Emodin Ameliorates Kidney Injury in LN Rats. In order to better reveal the action of emodin, the present study constructed the rat LN model using 0.1% mercury chloride, collected the kidney, and observed pathological alternations in the renal structure through HE and PAS staining. HE staining indicated normal glomeruli in the control group in both size and shape, with clear boundaries, no inflammatory cell infiltration in the renal interstitium, and complete brush border margin structure inside the renal tubules without obvious abnormalities (Figure 5(a)). In the model group, the glomerular cavity was shrunk, part of the cyst wall adhered to the glomerulus, and a large number of red blood cells were infiltrated between the glomeruli. Inflammatory cell infiltration and obvious bleeding were seen in the renal interstitium. The tubule epithelial cells were swollen and protruded into the lumen, which occluded the lumen. The tubule epithelial cells were lytic necrotic and some cells vacuolated. In the interference group, some renal tubules were swollen, the epithelial cell structure was destroyed, and cell fragments and inflammatory cells were found in the lumen. Inflammatory cells are occasionally seen in the renal interstitium. In the emodin group, some renal tubular epithelial cells were atrophied and decreased, the renal tubular structure was destroyed, and intertubular space increased but decreased inflammatory cells. PAS findings revealed that the glomerular vascular loops in the control group were thin and clear with normal structure (Figure 5(b)). In the model group, glomerular pagination atrophy, a large number of PAS-positive substances in the mesangium, and positive deposits in the lumen of renal tubular epithelial cells were observed. The volume of the basal glomerulus was reduced, and PAS-positive substances were accumulated in the mesangium in the interference group vs. the control group. Glomerular atrophy was slight in the emodin group. These results suggest that emodin can effectively reduce the renal inflammatory response in LN rats, but the inflammatory response is aggravated after interfering with PPARG.

3.6. Emodin Decreases Urinary Protein and dsDNA Antibody Levels in LN Rats. Proteinuria is the main clinical urine index used to detect nephritis, and the dsDNA antibody is a serum marker of the autoimmune disease SLE. The detection of these two indicators can predict kidney inflammation and immune tolerance. Proteinuria and dsDNA antibody levels of experimental group rats were found markedly higher than in the control (Figures 6(a) and 6(b))

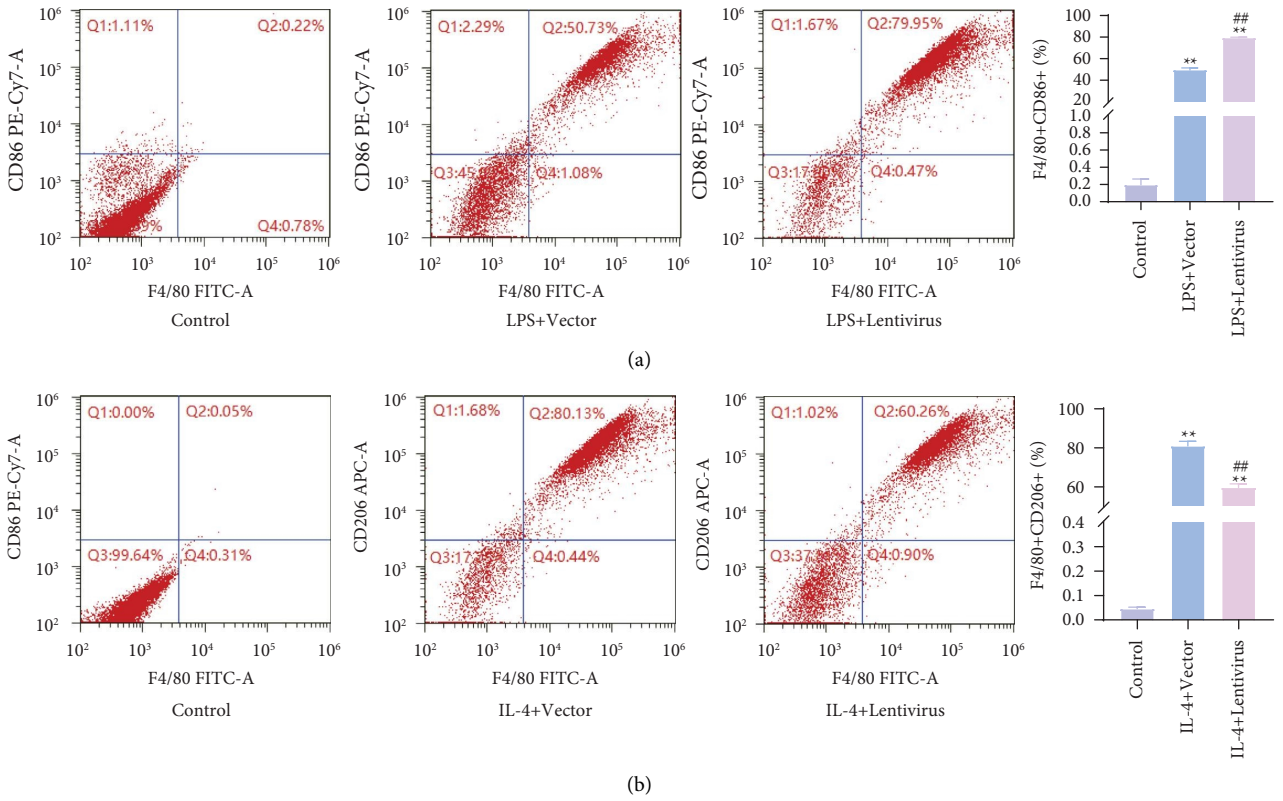

FIGURE 4: Effect of the PPARG interference on polarization of macrophages ($n = 3$). (a) Interference with PPARG promoted LPS-induced polarization of M1 macrophages; (b) interference with PPARG inhibits IL-4 induced polarization of M2 macrophages. $^{**}P < 0.01$ vs. Control; $^{\#\#}P < 0.01$ vs. Model.

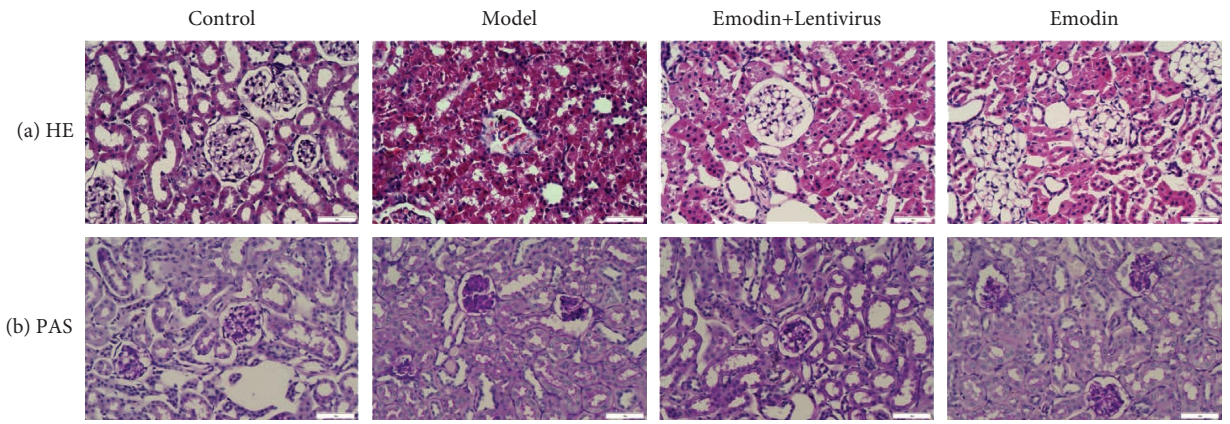

FIGURE 5: Effect of emodin on renal tissue injury in LN rats. (a) HE staining; (b) PAS staining. In PAS staining, the nucleus is blue, and the mesangial matrix, collagen fiber, basement membrane, fibrin, vascular hyaline, amyloidosis, and other positive reactions can be bright pink. Scale bar, 50 μm.

($P < 0.01$), indicating the presence of impairment in glomerular filtration function in experimental rats. After 14 d of administration of 70 mg/kg emodin by intraperitoneal injection, levels of urinary protein and dsDNA in rats were greatly lower than in the model ($P < 0.01$), indicating that emodin had a role in alleviating the damage to glomerular function caused by LN.

4. Discussion

In this study, 70 targets related to emodin therapy for LN were first screened through network pharmacology, and PPARG was predicted to play a vital role in the process. Then, through GO analysis, most of the targets were identified as being enriched in heat shock protein binding,

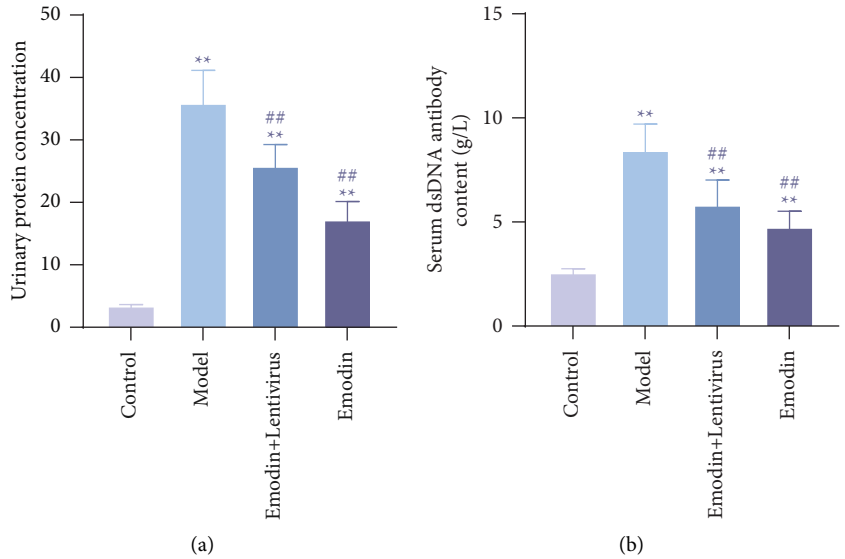

Figure 6: Effect of emodin on urinary proteins and serum dsDNA antibodies in LN rats ($n = 3$). (a) Urinary protein levels; (b) dsDNA antibody levels. $^{**}P < 0.01$ vs. Control; $^{\#\#}P < 0.01$ vs. Model.

immune response regulation, macrophage differentiation, etc. KEGG analysis found that the most related targets were involved in the PI3K-Akt signaling pathway. Therefore, based on network pharmacology analysis, we carried out subsequent related tests using cells and animals, respectively. First, the MTT assay was used to verify that emodin at 20, 40, and 80 μM had no significant toxicity to rat macrophages. Emodin inhibited polarization of the M1 phenotype while promoting polarization of the M2 phenotype. Then, after the targeted interference of the PPARG gene with lentivirus, the polarization direction of macrophages was significantly affected, namely, M1-type polarization increased while M2-type polarization decreased.

Macrophages are derived from monocytes in the blood circulation system (M0 macrophages) and differentiate into peripheral tissues, which are highly heterogeneous. Its role includes participating in immune response, regulating metabolism, maintaining homeostasis of the internal environment, and participating in angiogenesis, especially playing an important role in the inflammatory response [18, 19]. Mononuclear macrophages can develop into different subpopulations according to different activation stimuli, such as the proinflammatory macrophage population (M1) formed by the classical activation pathway or the anti-inflammatory macrophage population (M2) formed by substituted activation [20]. M0 macrophages are activated to M1 macrophages after being stimulated by lipopolysaccharide (LPS), tumor necrosis factor, interferon γ, and granulocyte-macrophage colony-stimulating factor, which highly express IL-12 and IL-23. Reactive oxygen species, TNF-α, nitric oxide, inducible nitric oxide synthase, monocyte chemoattractant protein 1 (MCP- 1), and other proinflammatory factors, participate in the immune process of antigen presentation and promote the inflammatory immune response [21]. M0 macrophages are activated into M2-type macrophages after induced stimulation by IL-1, IL-4, TGF-β, and glucocorticoid, which highly express anti-inflammatory factors TGF-β, IL-L0, IL-6, IL-10, and arginase-1 to inhibit immune response and inflammatory immune response promote angiogenesis, tissue repair, and remodeling [22]. M1- and M2-type macrophages can undergo phenotypic transformation under certain in vivo conditions or under the action of certain endogenous substances. For example, M1-type macrophages can transform into M2-type macrophages during renal repair to provide nutrients and promote renal tubule repair [23]. In LN, M1-type macrophages mainly promote inflammation and fibrosis, while M2-type macrophages mainly inhibit inflammation but facilitate the repair and reconstruction of injured tissues. It has been reported that the mouse model of nephritis has been greatly improved following M1-type macrophage depletion, recruitment inhibition, and polarization interruption of inflammatory macrophages [24]. Studies have suggested that LN renal damage is associated with M1-type macrophage infiltration and lymphocyte infiltration. Meanwhile, being an inflammatory factor IFN-γ, secreted by M1-type macrophages, promotes macrophage recruitment and up-regulates inflammatory immune response [25]. In addition, M1-type macrophages in LN have high expression of the proinflammatory factor MCP-1. Studies have used gene knockout mice or inhibitors to block MCP-1 or its receptors to minimize M1-type macrophage infiltration, thereby reducing inflammatory response [25, 26]. There are few studies on M2-type macrophages in LN, but it has been proven that M2 macrophages can secrete nutritional factors to promote angiogenesis through endocytosis, promote the remodeling of extracellular matrix, mediate tissue healing, and inhibit a variety of proinflammatory factors for anti-inflammation [27]. Thus, polarization and proliferation of macrophages are of great importance in LN pathogenesis.

Peroxisome proliferator-activated receptors (PPARs), recognized as a class of ligand-activated transcription factors, can realize macrophage polarization, regulate macrophage metabolism, inhibit proinflammatory genes, and promote the transformation of the M2 phenotype [27, 28]. Studies have shown that peroxisome proliferators-activated receptor gamma (PPARG) overbinds with other transcription factors to Arg1, Fizz1, and Ym1 gene promoter regions, thereby promoting Arg1 and Fizz1 gene expression and regulating the M2 polarization level of macrophages, and Arg1 expression is significantly down-regulated when PPARG macrophages are knocked out [29, 30]. PPARG can enhance LPL expression by interacting with PPARG response elements in the LPL gene promoter region and mediating TNF-α expression [31]. The regulation of NF-κB, signal transducers, and transcriptional activators inhibit the expression and secretion of cytokines and inflammatory factors IL-6 and IL-1β, thus playing an important anti-inflammatory role [32]. This suggests that PPARG drives macrophages into an anti-inflammatory state.

The results of cell and animal level tests showed that emodin promoted the transformation from M1 to M2 macrophages, and after interfering with PPARG, M2 macrophage markers were reduced, kidney inflammation was aggravated in rats, and urinary protein levels and serum dsDNA antibody levels were increased. Emodin indicated a role in promoting the transformation of M2 macrophages by activating PPARG, thus improving LN. The limitation of this study is that emodin action on improving LN was only preliminarily detected. Although it serves as an application reference against LN, the effect of emodin on the marker genes of both M1 and M2 macrophages was not further proven at the molecular level. The related pathway of PPARG (PI3K-Akt signaling pathway) has not been studied, so the mechanism of emodin is still unclear. In the future research plan, we will continue to improve the research at the molecular level based on the results of this experiment so as to more clearly explain the mechanism of emodin's action on LN and provide more favorable proof for the development and utilization of emodin in LN.

5. Conclusion

In the current work, emodin was demonstrated to inhibit polarization of the RAW 264.7 cell line towards the M1 phenotype and facilitate its polarization towards the M2 phenotype. Emodin improved the inflammatory injury of the kidneys in LN rats and reduced the levels of urinary protein and dsDNA antibodies. The therapeutic effect of emodin on the treatment of LN may be realized through the activation of PPARG. These findings offer a novel drug candidate for LN management.

Data Availability

The data used to support the finding of this study are available from the corresponding author upon request.

Ethical Approval

All animal experiments were performed as per the Guidelines for the Use of Experimental Animals issued by the Chongqing Hospital of Traditional Chinese Medicine and approved by the Ethical Management Committee of Experimental Animal Welfare of the Chongqing Hospital of Traditional Chinese Medicine.

Conflicts of Interest

The authors declare that they have no conflicts of interest.

Acknowledgments

The research was supported by the National Natural Science Foundation of China (No. 81904012) and Chongqing Science and Technology Bureau Project (cstc2018jxjl130048, cstc2018jcyjAX0818, cstc2021jxjl130003).

References

[1] M. Ostensen and M. Clowse, "Pathogenesis of pregnancy complications in systemic lupus erythematosus," *Current Opinion in Rheumatology*, vol. 25, no. 5, pp. 591–596, 2013.

[2] N. Schwartz, B. Goilav, and C. Putterman, "The pathogenesis, diagnosis and treatment of lupus nephritis," *Current Opinion in Rheumatology*, vol. 26, no. 5, pp. 502–509, 2014.

[3] S. Yung, D. Y. Yap, and T. M. Chan, "Recent advances in the understanding of renal inflammation and fibrosis in lupus nephritis," *F1000Research*, vol. 6, p. 874, 2017.

[4] H.-J. Anders, R. Saxena, M.-h Zhao, I. Parodis, J. E. Salmon, and C Mohan, "Lupus nephritis," *Nature Reviews Disease Primers*, vol. 6, no. 1, p. 7, 2020.

[5] J. J. Manson and D. A. Isenberg, "The pathogenesis of systemic lupus erythematosus," *The Netherlands Journal of Medicine*, vol. 61, no. 11, pp. 343–346, 2003.

[6] A. Davidson, R. Bethunaickan, C. Berthier, R. Sahu, W. Zhang, and M. Kretzler, "Molecular studies of lupus nephritis kidneys," *Immunologic Research*, vol. 63, no. 1-3, pp. 187–196, 2015.

[7] S. Lee, S. Huen, H. Nishio et al., "Distinct macrophage phenotypes contribute to kidney injury and repair," *Journal of the American Society of Nephrology*, vol. 22, no. 2, pp. 317–326, 2011.

[8] Y. Chen, J. Sun, K. Zou, Y. Yang, and G. Liu, "Treatment for lupus nephritis: an overview of systematic reviews and meta-analyses," *Rheumatology International*, vol. 37, no. 7, pp. 1089–1099, 2017.

[9] X. Dong, J. Fu, X. Yin et al., "Emodin: a review of its pharmacology, toxicity and pharmacokinetics," *Phytotherapy Research*, vol. 30, no. 8, pp. 1207–1218, 2016.

[10] C. Ma, B. Wen, Q. Zhang et al., ">>," *Drug Design, Development and Therapy*, vol. 13, pp. 601–609, 2019.

[11] W. T. Wei, S. Z. Lin, D. L. Liu, and Z. H. Wang, "The distinct mechanisms of the antitumor activity of emodin in different types of cancer (Review)," *Oncology Reports*, vol. 30, no. 6, pp. 2555–2562, 2013.

[12] G. Meng, Y. Liu, C. Lou, and H. Yang, "Emodin suppresses lipopolysaccharide-induced pro-inflammatory responses and NF-κB activation by disrupting lipid rafts in CD14-negative endothelial cells," *British Journal of Pharmacology*, vol. 161, no. 7, pp. 1628–1644, 2010.

[13] M. K. Ha, Y. H. Song, S. J. Jeong et al., "Emodin inhibits proinflammatory responses and inactivates histone deacetylase 1 in hypoxic rheumatoid synoviocytes," *Biological and Pharmaceutical Bulletin*, vol. 34, no. 9, pp. 1432–1437, 2011.

[14] A. Alisi, A. Pastore, S. Ceccarelli et al., "Emodin prevents intrahepatic fat accumulation, inflammation and redox status imbalance during diet-induced hepatosteatosis in rats," *International Journal of Molecular Sciences*, vol. 13, no. 2, pp. 2276–2289, 2012.

[15] Z. C. Song, Z. S. Wang, J. H. Bai, Z. Li, and J. Hu, "Emodin, a naturally occurring anthraquinone, ameliorates experimental autoimmune myocarditis in rats," *Tohoku Journal of Experimental Medicine*, vol. 228, no. 1, pp. 83–230, 2012.

[16] G. x Liu, R. g Ye, Z. m Tan et al., "Effect of emodin on biological behavior of fibroblasts in lupus nephritis," *Chinese Journal of Integrative Medicine*, vol. 7, no. 3, p. 205, 2001.

[17] X. L. Zhu, Y. J. Wang, Y. Z. Yang et al., "Suppression of lipopolysaccharide-induced upregulation of toll-like receptor 4 by emodin in mouse proximal tubular epithelial cells," *Molecular Medicine Reports*, vol. 6, no. 3, pp. 493–500, 2012.

[18] W. Zhang, H. Li, H. Q. Bu et al., "Emodin inhibits the differentiation and maturation of dendritic cells and increases the production of regulatory T cells," *International Journal of Molecular Medicine*, vol. 29, no. 2, pp. 159–164, 2012.

[19] F. Geissmann, M. G. Manz, S. Jung, M. H. Sieweke, M. Merad, and K. Ley, "Development of monocytes, macrophages, and dendritic cells," *Science*, vol. 327, no. 5966, pp. 656–661, 2010.

[20] Y. S. Schwartz and A. V. Svistelnik, "Functional phenotypes of macrophages and the M1-M2 polarization concept. Part I. Proinflammatory phenotype," *Biochemistry*, vol. 77, no. 3, pp. 246–260, 2012.

[21] D. A. Hume, "The many alternative faces of macrophage activation," *Frontiers in Immunology*, vol. 6, p. 370, 2015.

[22] C. Nathan, "Secretory products of macrophages: twenty-five years on," *Journal of Clinical Investigation*, vol. 122, no. 4, pp. 1189-1190, 2012.

[23] X. Hu, Y. Xu, Z. Zhang et al., "TSC1 affects the process of renal ischemia-reperfusion injury by controlling macrophage polarization," *Frontiers in Immunology*, vol. 12, Article ID 637335, 2021.

[24] S. A. Chalmers, V. Chitu, M. Ramanujam, and C. Putterman, "Therapeutic targeting of macrophages in lupus nephritis," *Discovery Medicine*, vol. 20, no. 108, pp. 43–49, 2015.

[25] C. E. Carvalho-Pinto, M. I. García, M. Mellado et al., "Autocrine production of IFN-gamma by macrophages controls their recruitment to kidney and the development of glomerulonephritis in MRL/lpr mice," *The Journal of Immunology*, vol. 169, no. 2, pp. 1058–1067, 2002.

[26] O. Kulkarni, R. D. Pawar, W. Purschke et al., "Spiegelmer inhibition of CCL2/MCP-1 ameliorates lupus nephritis in MRL-(Fas)lpr mice," *Journal of the American Society of Nephrology*, vol. 18, no. 8, pp. 2350–2358, 2007.

[27] Y. Wang, Y. P. Wang, G. Zheng et al., "Ex vivo programmed macrophages ameliorate experimental chronic inflammatory renal disease," *Kidney International*, vol. 72, no. 3, pp. 290–299, 2007.

[28] P. M. Ridker, B. M. Everett, T. Thuren et al., "Antiinflammatory therapy with canakinumab for atherosclerotic disease," *New England Journal of Medicine*, vol. 377, no. 12, pp. 1119–1131, 2017.

[29] M. Chandra, S. Miriyala, and M. Panchatcharam, "PPARγ and its role in cardiovascular diseases," *PPAR Research*, vol. 2017, Article ID 6404638, 10 pages, 2017.

[30] Q. Li, H. Peng, H. Fan et al., "The LIM protein Ajuba promotes adipogenesis by enhancing PPARγ and p300/CBP interaction," *Cell Death and Differentiation*, vol. 23, no. 1, pp. 158–168, 2016.

[31] L. Bai, Z. Li, Q. Li et al., "Mediator 1 is atherosclerosis protective by regulating macrophage polarization," *Arteriosclerosis, Thrombosis, and Vascular Biology*, vol. 37, no. 8, pp. 1470–1481, 2017.

[32] X. Zhang, M. H. Liu, L. Qiao et al., "Ginsenoside Rb1 enhances atherosclerotic plaque stability by skewing macrophages to the M2 phenotype," *Journal of Cellular and Molecular Medicine*, vol. 22, no. 1, pp. 409–416, 2018.

Hindawi
Journal of Chemistry
Volume 2023, Article ID 6298366, 8 pages
https://doi.org/10.1155/2023/6298366

Research Article

Exploring the Anticonvulsant Activity of Aqueous Extracts of *Ficus benjamina* L. Figs in Experimentally Induced Convulsions

Rajinder Singh,[1] Mohammad Khalid,[2] Nikhil Batra,[3] Partha Biswas,[4,5] Lovedeep Singh,[6] and Rajbir Bhatti[1]

[1]*Department of Pharmaceutical Sciences, Guru Nanak Dev University, Amritsar 143005, Punjab, India*
[2]*Department of Pharmacognosy, College of Pharmacy, Prince Sattam Bin Abdulaziz University, Al-Kharj, Saudi Arabia*
[3]*Department of General Medicine, Maharishi Markandeshwar Institute of Medical Sciences and Research, Maharishi Markandeshwar Deemed to be University, Ambala, India*
[4]*Laboratory of Pharmaceutical Biotechnology and Bioinformatics, Department of Genetic Engineering and Biotechnology, Jashore University of Science and Technology, Jashore 7408, Bangladesh*
[5]*ABEx Bio-Research Center, East Azampur, Dhaka 1230, Bangladesh*
[6]*University Institute of Pharma Sciences, Chandigarh University, Mohali 140413, Punjab, India*

Correspondence should be addressed to Partha Biswas; partha_160626@just.edu.bd and Lovedeep Singh; lovedeep.e13279@cumail.in

Received 24 September 2022; Revised 16 October 2022; Accepted 24 November 2022; Published 30 January 2023

Academic Editor: Romina Alina Marc Vlaic

Background. *Ficus benjamina* L. is an evergreen tree, native to Southeast Asia, and often known as a weeping fig. Its latex and fruit extracts are used by indigenous cultures to cure skin conditions, inflammation, vomiting, leprosy, malaria, and nasal ailments. The aqueous extract of the figs of *Ficus benjamina* L. has various therapeutic values, including biological activities on the central nervous system. *Materials and Methods*. The extract of the dried figs of *Ficus benjamina* L. (FBE) was prepared by defatting with petroleum ether for 16 h followed by soxhelation with 70% methanol (1 : 10 w/v) for 24 h, and standardization of the extract was carried out using HPLC with 5-HT as a standard. Electroconvulsions were induced by the maximal electroshock model, and chemoconvulsions were induced by picrotoxin. *Results*. The HPLC chromatogram of the *Ficus benjamina* L. extract showed an absorption peak with a retention time of 1.797 min, similar to that observed with standard serotonin (5-HT) solution. In the maximal electroshock model, FBE significantly reduced the duration of the tonic hind limb extensor and extensor-to-flexor ratio (E/F ratio) in a dose-dependent manner. Moreover, in the picrotoxin-induced seizure model, FBE increased the seizure latency and decreased the duration of tonic-clonic convulsions dose-dependently. We confirmed the anticonvulsant activity of the FBE extract as it attenuated both maximal electroshock and picrotoxin-induced convulsions. *Conclusion*. The *in vivo* studies revealed that the Ficus extract was found to protect the animals in electroshock-induced and picrotoxin-induced convulsions.

1. Introduction

Epilepsy is a neurological disorder, primarily caused by an imbalance between excitatory and inhibitory neurotransmission, which leads to abnormally synchronized firing of groups of neurons [1]. Approximately 50 million individuals worldwide suffer from epilepsy, which is a serious global health issue. It is one of the most widespread chronic neurological conditions in the world and, in some regions, has detrimental physical, financial, and discriminatory effects [2]. After a stroke and Alzheimer's disease, epilepsy is the third most frequent neurological condition [3]. Based on suspected underlying causes, epilepsy is divided into genetic and acquired epilepsy. Genetic epilepsy results from a genetic predisposition of the brain to produce seizures, while acquired epilepsy is due to acute insult or a lesion that alters the cellular, molecular, and physiological properties that give origin to seizures [4]. It has been suggested that altered

neuronal membrane permeability, decreased inhibitory neuronal regulation, or neurotransmitter imbalance may be the probable initiators of seizures, though the precise cellular effect is not fully clear [2].

Current anticonvulsant medicines can effectively manage epileptic seizures in approximately 50% of patients; 25% of cases may improve, while the remaining patients do not benefit appreciably [2]. Furthermore, unwanted side effects of clinically used medications frequently make therapy difficult [5, 6]. Benzodiazepines have dependence liability, along with an increased risk of glaucoma and respiratory depressive effects [5]. Moreover, drugs like carbamazepine cause upset stomach, serious skin reactions, and may reduce sodium levels. Phenobarbital and its derivative treatment can lead to memory loss, sedation, depression, and also possess chances of birth defects [6]. Pregabalin, $\alpha 2\delta$ calcium channel subunit ligand, is often associated with trouble in concentration, sedation, weight gain, and swelling of hands and feet [7].

Medicinal plants are used for the treatment of different infections. These plants contributed as a source of inspiration for novel therapeutic compounds. The medicinal value of plants is due to the presence of a wide variety of secondary metabolites including alkaloids, glycosides, tannins, volatile oil, and terpenoids [8, 9]. Several medicinal plants have been explored for their anticonvulsant activity in various animal models. These include *Carum copticum* [10], *Erythrina mulungu* [11], *Anisomeles malabarica* [12], *Anacyclus pyrethrum* [13], *Zizyphus jujuba*, *Passiflora incarnata* [14], *Acorus calamus, Crocus sativus, Emblica officinalis, Ginkgo biloba, Hypericum perforatum, Matricaria recutita,* and *Panax ginseng* [15]. *Ficus* is a large genus with as many as 800 species [16]. The methanol extract from leaves of *Ficus hispida* has been reported to inhibit chemically induced convulsions in mice [17]. The aqueous extract of roots of *F. religiosa* has been studied for its protective action in strychnine and pentylenetetrazole-induced seizures [18]. Figs of *F. religiosa* have also been documented to have anticonvulsant activity [19]. The anticonvulsant action of most of the *Ficus* species has been attributed to the rich content of serotonin (5-HT) in these plants [18, 19]. The most common cause of mortality in people with refractory epilepsy is sudden unexpected death. The pathophysiology of sudden unexpected death in epilepsy patients is heavily influenced by defects in central respiratory regulation and serotonin (5-HT) system malfunction [20]. Furthermore, it has been reported that the increased serotonin level is associated with a reduced incidence of seizure-related breathing problems in epilepsy patients [21].

Literature evidence delineates that its latex and fruit extracts are used by indigenous cultures to cure skin conditions, inflammation, vomiting, leprosy, malaria, and nasal ailments [22]. Moreover, many parts of the plant have long been widely utilized in traditional medicine to treat skin problems and dysentery [23]. A preliminary investigation of the *Ficus benjamina L.* fig extract revealed the presence of 5-HT. However, to date, no studies have been reported for its anticonvulsant potential. Therefore, the present study is designed to investigate the anticonvulsant effect of ripe figs of *Ficus benjamina* L.

2. Material and Methods

2.1. Drugs and Chemicals. Picrotoxin (Cat No. P1675) and serotonin (Cat No. 14927) were purchased from Sigma Aldrich, USA. All other solvents and chemicals were of analytical grade and purchased from local suppliers.

2.2. Collection of Plant Materials and the Extraction Procedure. Ripe figs of *Ficus benjamina* L. (Moraceae) were collected from the campus of Guru Nanak Dev University, Amritsar, between March and April, washed with water, and shade dried. Dried figs were then ground into a coarse powder. The powdered material was defatted with petroleum ether for 16 h and then extracted by soxhelation with 70% methanol (1 : 10 w/v) for 24 h. The hydroalcoholic extract FBE obtained was filtered, and the solvent was evaporated under reduced pressure using a rotary evaporator (Heidolph Laborota 4001) to obtain a semisolid mass that was stored in an airtight container in a refrigerator till further use. The yield was found to be 15%, w/w. The extract was reconstituted by dissolving it in 10% (v/v) dimethyl sulfoxide. Thereafter, it was suspended in 0.5% carboxymethylcellulose (DMSO 1: CMC 9) for a treatment purpose [19].

2.3. Preliminary Phytochemical Screening of FBE. Preliminary phytochemical screening of FBE was carried out to detect the presence of alkaloids, glycosides, tannins, saponins, etc.

2.4. HPLC Characterization of FBE. FBE was standardized w.r.t. the content of 5-HT as discussed in other species of *Ficus* [24]. 2 mg of pure 5-HT was dissolved in 100 mL of methanol and used as a standard; 50 mg of the *F. benjamina* extract was dissolved in 50 ml of methanol to prepare a sample solution (1 mg mL^{-1}). The solution was then centrifuged at $4500 \times g$ for 10 min, and the supernatant was used for further detections. The standard and sample solutions were filtered through a 0.45 μm membrane filter separately. The UV spectrum of pure 5-HT was determined by using a spectrophotometer with a scanning wavelength of 200–400 nm. Separation was performed on a 250 mm × 4.6 mm (5 μm particles) Hypersil GOLD C-18 RP column from Thermo Incorporated using 25 mM phosphate buffer (pH 2.5) and acetonitrile at 95 : 5 (v/v) at a flow rate of 1 mL min^{-1}. The injection volume was 10 μL, and the peaks were identified by comparison with the retention times of the standard solution.

2.5. Animals. Swiss albino mice of either sex were used in the present study. The animals were procured from Guru Angad Dev Veterinary and Animal Sciences University, Ludhiana, Punjab, and housed in the central animal house of Guru Nanak Dev University, Amritsar. Animals had free access to food (standard laboratory chow diet) and water and were maintained at a temperature of 24 ± 4°C in a 12-hour dark-light cycle. The protocol (Approval no. 1009/BT/Dated Aug 2011, Protocol No. 20) was approved by the institutional

animal ethics committee and was in accordance with the guidelines of the Committee for the Purpose of Control and Supervision of Experiments on Animals (CPCSEA).

2.6. Assessment of Anticonvulsant Activity. The animals were divided into 11 groups ($n = 6$) for the anticonvulsant study using maximal electroshock and picrotoxin-induced convulsion models as described below. FBE, picrotoxin, diazepam, and phenytoin were suspended in freshly prepared 1% carboxymethylcellulose (CMC). All the drugs were administered intraperitoneally. The schematic protocols are shown in Figure 1.

2.7. Maximal Electroshock-Induced Convulsions. A total of five groups (Figure 1) were studied according to the method in [25]. In each group, animals received the respective treatment for 30 min before an electric shock of 50 mA for 0.2 s through corneal electrodes using an electroconvulsiometer (INCO, Ambala, India); the duration of tonic hind limb extension was determined followed by recovery or death.

2.8. Picrotoxin-Induced Convulsions. A total of five groups (Figure 1) were included in picrotoxin-induced seizures according to the method described by [25]. Picrotoxin (5 mg kg^{-1}) was injected 30 min after the respective treatment in each group. The onset of mild jerks, tonic-clonic convulsion, and duration of convulsions were noted in all groups and compared with those in the vehicle-treated control.

2.9. Statistical Analysis. All results are expressed as the mean ± standard error of the mean (SEM). Statistical analysis was performed by the one-way analysis of variance (ANOVA), followed by post hoc analysis and Tukey's test using InStat software version 3.05 (Graphpad Inc., San Diego, USA). The Design-Expert 10.0 software (Stat-Ease, Inc.) was used to analyze the results of the response surface design.

3. Results

3.1. Preliminary Phytochemical Analysis of FBE. The hydroalcoholic extract of *F. benjamina* was found to contain saponins, flavonoids, tannins, alkaloids, and carbohydrates.

3.2. HPLC Standardization of FBE. The HPLC chromatogram of the standard 5-HT solution showed an absorption peak with a retention time of 1.797 min (Figure 2(a)). A similar peak was observed in the HPLC chromatogram of FBE at the same retention time, indicating the presence of 5-HT in the extract (Figure 2(b)) (Table 1).

3.3. Effect of Various Pharmacological Interventions on Maximal Electroshock-Induced Seizures. The treatment of mice with an electric shock of 50 mA for 0.2 s was found to produce the flexor and tonic hind limb extensor, followed by stupor or death. Maximal electroshock produced a tonic hind limb extensor of an average duration of 11.2 ± 0.8 s in the vehicle-treated control with a percentage mortality of 83.3%. Treatment with phenytoin was found to completely abolish the extensor phase with no mortality. The treatment with FBE was found to produce a decrease in the duration of the tonic hind limb extensor and the extensor-to-flexor ratio (E/F ratio) significantly and in a dose-dependent manner (Figures 3(a) and 3(b)). The percentage protection with FBE 400 mg kg^{-1} treatment was found to be 92.8 ± 11.6% (Figure 3(c)).

Treatment of animals with picrotoxin was found to precipitate tonic-clonic (T/C) convulsions after 11.9 ± 2.6 min in the vehicle-treated control group, and the duration of T/C convulsions was found to be 16.6 ± 1.5 s. Treatment with diazepam was found to completely abolish picrotoxin-induced convulsions (zero convulsions). Therefore, no latency was observed in the diazepam group, whereas FBE was found to produce a dose-dependent increase in seizure latency and a decrease in the duration of T/C convulsions at doses of 100, 200, and 400 mg kg^{-1} (Figures 4(a) and 4(b)). The respective percentage of protection was found to be 22.8, 44.5, and 66.2% (Figure 4(c)). The effect was statistically significant as compared to the vehicle control.

4. Discussion

Conventional anticonvulsant therapy is marred by several adverse drug reactions including cognitive deficits, teratogenicity, and behavioral and cosmetic side effects [26, 27]. These problems have led to a renewed interest in plant-based medicines due to their better tolerability and lower number of side effects. Plants have been used as medicine to maintain human health for ages and are also major natural sources of medicinal compounds in current pharmacopoeias [28, 29]. The current study demonstrated the protective effect of the hydroalcoholic fig extract of *Ficus benjamina* L. (FBE) on picrotoxin and maximal electroshock-induced convulsions in mice. FBE was found to produce a dose-dependent reduction in convulsions.

The HPLC investigation revealed the presence of 5-hydroxytryptamine (5-HT) in the extract. Earlier studies have revealed the presence of 5-HT in the figs of *Ficus religiosa* [30]. Although there are conflicting reports on the role of 5-HT in epilepsy [24], there is sufficient evidence in the literature that supports the inhibition of 5-HT reuptake to have beneficial effects in epilepsy. Selective serotonin reuptake inhibitors (SSRIs) have been documented to help treat epilepsy [31, 32]. Some agents like 5-hydroxytryptophan that increases the extracellular level of 5-HT have been found to inhibit focal and generalized seizures, and depletion of 5-HT evokes seizures [33]. Serotonergic neurotransmission has been documented to modulate a variety of experimentally induced seizures and drugs that increase the concentration of 5-HT to have an anticonvulsant effect [34]. It is reported that serotonergic agonists can directly affect the firing of cerebellar neurons and can

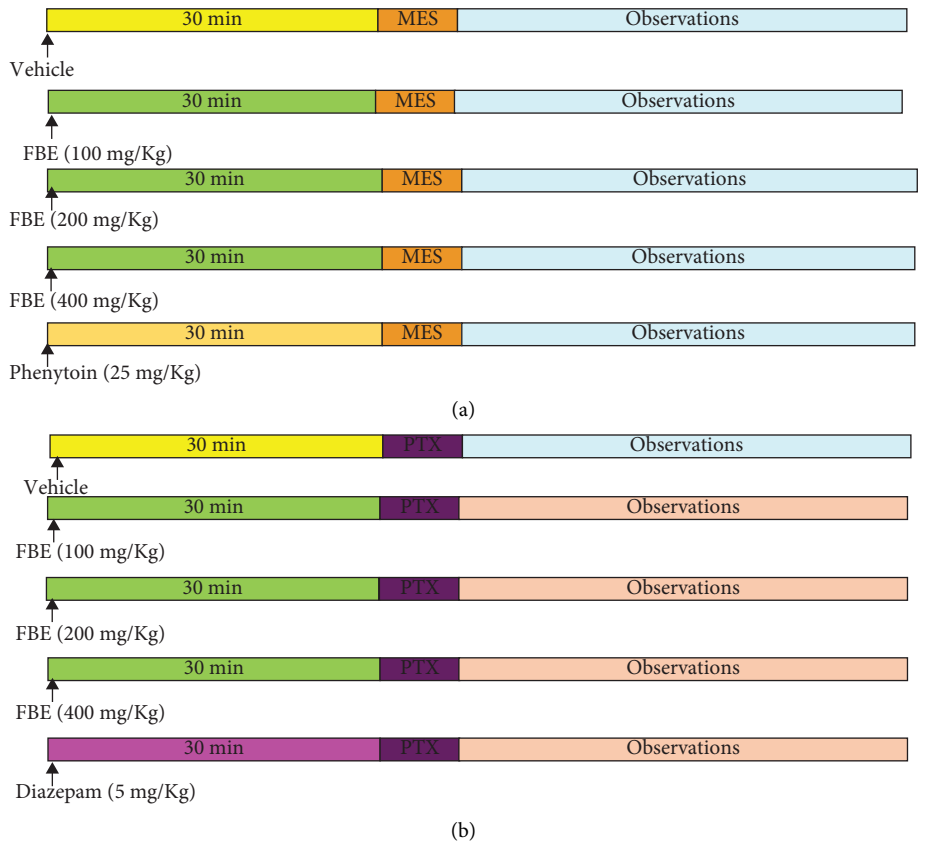

Figure 1: Schematic protocols for anticonvulsant activity of *Ficus benjamina* L. in (a) maximal electroshock-induced convulsions and (b) picrotoxin-induced convulsions in mice.

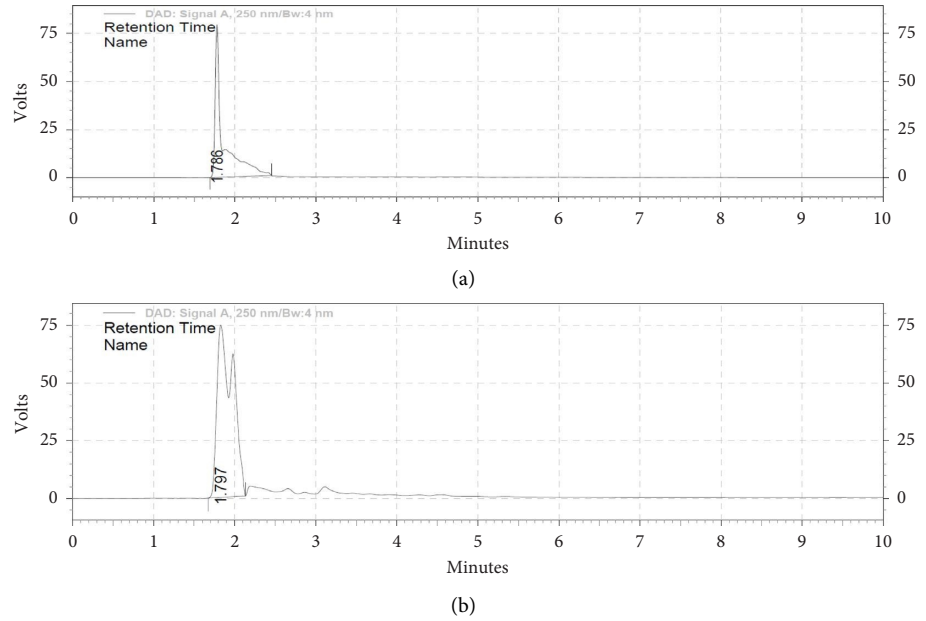

Figure 2: (a) HPLC of the 5-HT standard; (b) HPLC of the *Ficus benjamina* L. extract.

modulate the effect of excitatory amino acids [35]. In the genetic model of absence epilepsy, it is found that there is an interaction of glutamatergic and serotonergic mechanisms in the regulation of epileptic activity [33]. All the brain areas that are involved in epilepsy have an expression of 5-HT receptors, and currently, the role of 5-HT_{1A}, 5-HT_{2C}, 5-HT_3,

Table 1: HPLC data depicting the comparison of the standard and the extract.

	Retention time	Area	Area%	Height	Height%
Standard	1.786	1096963	100	166056	100
Extract	1.797	2129641	100	156272	100

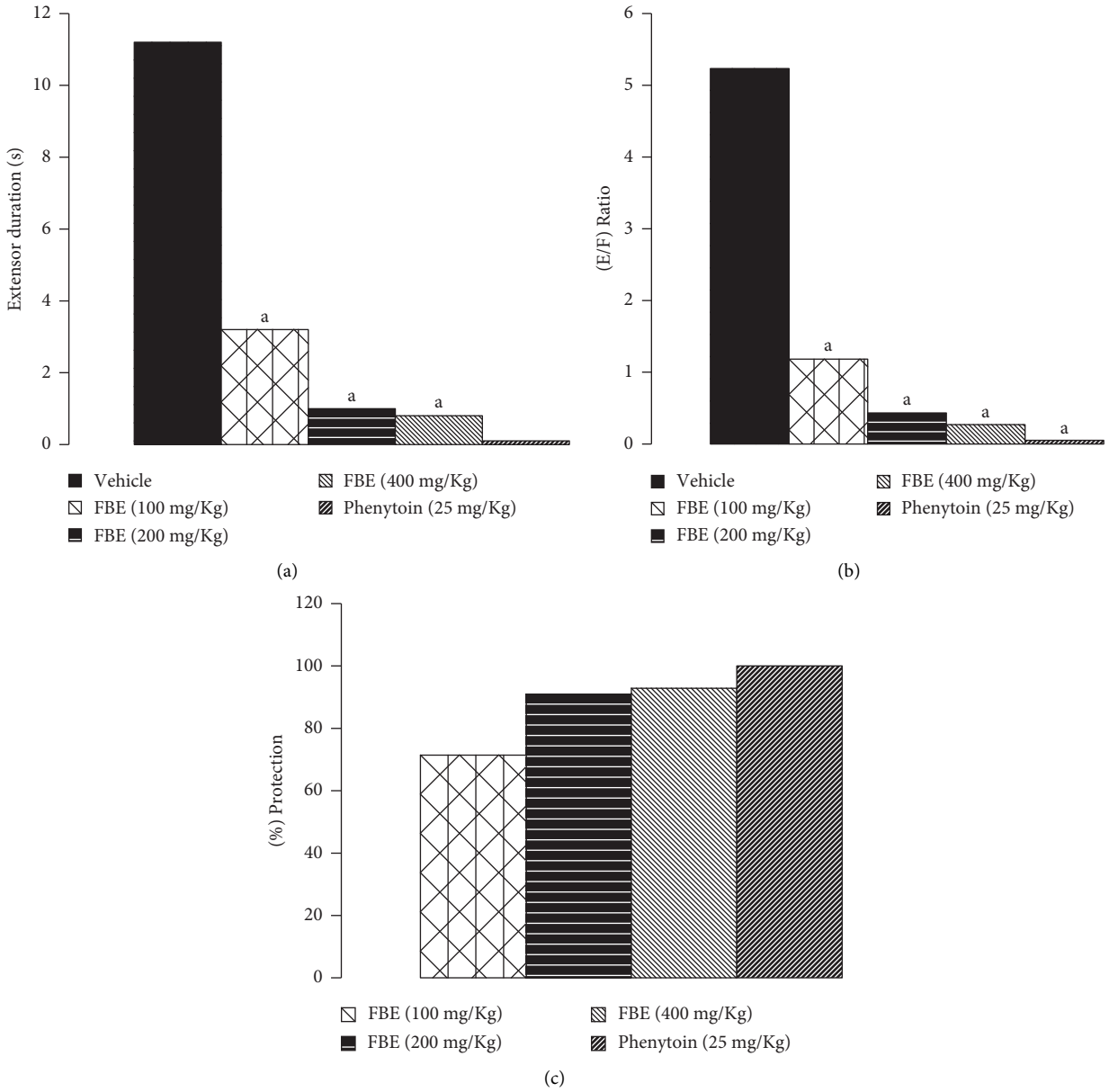

Figure 3: Effect of various pharmacological interventions on maximal electroshock-induced seizures. (a) Duration of the extensor, (b) extensor/flexor ratio, and (c) % protection. All values are expressed as the mean ± SEM. $^a p < 0.001$ compared to the vehicle control. The effect of various pharmacological interventions on picrotoxin-induced seizures.

and 5-HT_7 receptors has been described in epilepsy [33]. In general, hyperpolarization of glutamatergic neurons by 5-HT_{1A} receptors and depolarization of GABAergic neurons by 5-HT_{2C} receptors, as well as antagonists of 5-HT_3 and 5-HT_7 receptors, decrease neuronal excitability [32]. Various studies on experimental animals have reported that the activation of 5-HT_{2C} and 5-HT_7 receptors have an anticonvulsant effect [34]. The postictal phase is marked by a decrease in the 5-HT transporters in the brain and a decrease in the brain levels of tryptophan, the precursor of 5-HT, which is suggested to be related to some types of epilepsy [31]. The conventional antiepileptic therapy with drugs such as phenytoin and valproic acid is effective in treating the episodes of convulsions but is insufficient to manage

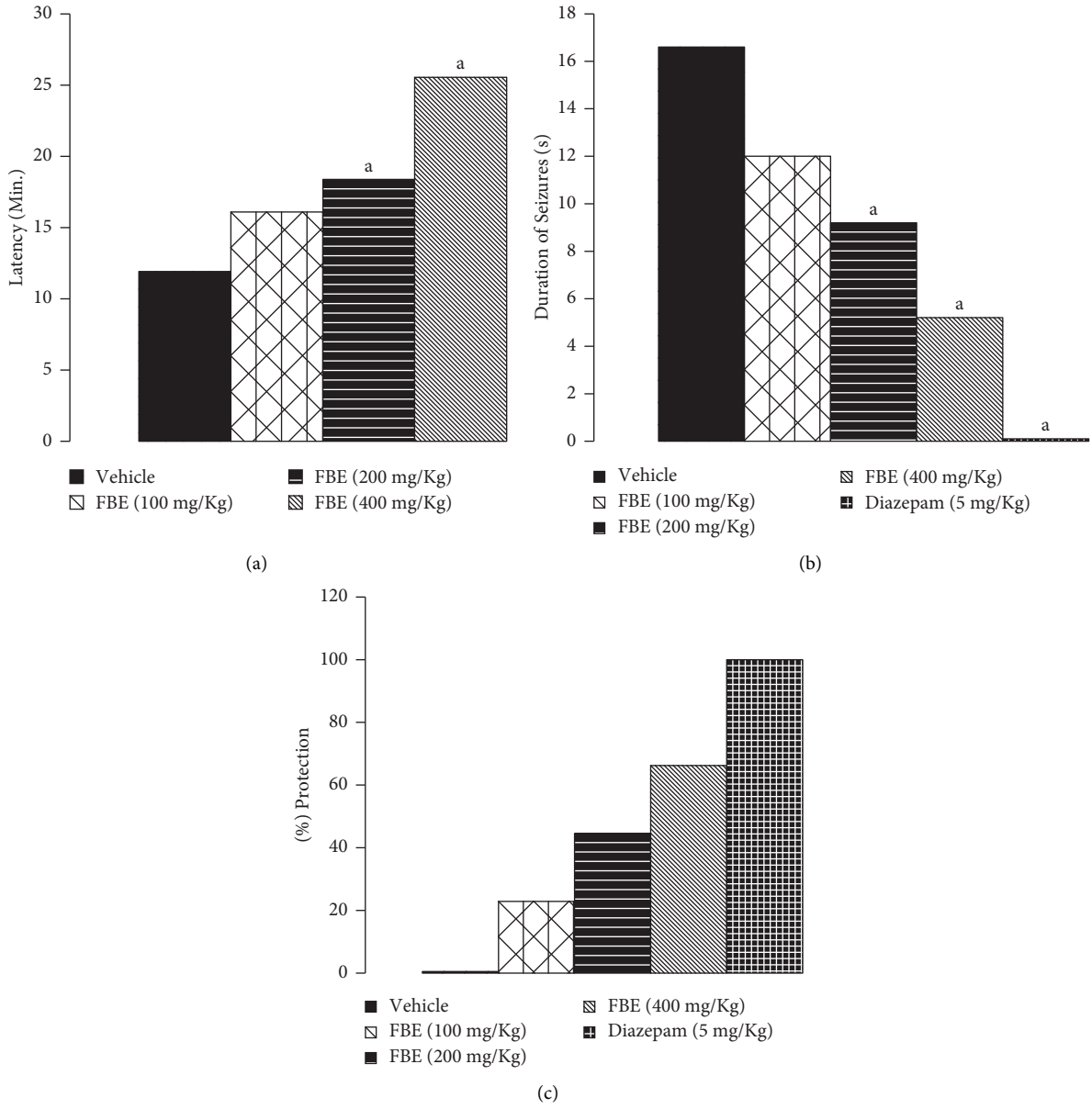

Figure 4: Effect of various pharmacological interventions on picrotoxin-induced seizures. (a) Latency to convulsions, (b) duration of convulsions, and (c) % protection. All values are expressed as the mean ± SEM. $^a p < 0.001$ compared to the vehicle control.

postictal depression. 5-HT present in FBE may act to replenish the depleted 5-HT levels in the brains of epileptic patients. The current study only screened the anticonvulsant activity of the *Ficus benjamina* L. extract along with determination of serotonin in the extract. One of the limitations of the current study is that only the activity of the hydroalcoholic extract was performed, and second, apart from serotonin, the estimation of other components of interest was not carried out. However, this study will give a base for researchers to perform the isolation of molecules of interest from this plant and further explore their potential in epilepsy.

5. Conclusion

Overall, the outcomes of the current investigation delineate that the hydroalcoholic fig extract of *Ficus benjamina* L. (FBE) exerted a protective effect against picrotoxin and maximal electroshock-induced convulsions in mice dose-dependently. The anticonvulsant effect of the *Ficus benjamina* L. extract might be attributed to the presence of 5-HT in the extract. However, this needs more direct and detailed studies to prove this contention. In terms of future prospects, it is necessary to continue the development of efficacious anticonvulsant agents that are cost-effective with

minimal side effects. Based on the outcome of the current study, it seems logical to presume that *Ficus benjamina* L. may contain some molecules which might have anticonvulsant activity. Characterization of secondary metabolites will reveal further health benefits.

Data Availability

Data used in this study are available on request to the corresponding author.

Conflicts of Interest

The authors declare that they have no conflicts of interest.

References

[1] D. C. Patel, B. P. Tewari, L. Chaunsali, and H. Sontheimer, "Neuron–glia interactions in the pathophysiology of epilepsy," *Nature Reviews Neuroscience*, vol. 20, no. 5, pp. 282–297, 2019.

[2] M. Lawal, H. Omobayo, and K. Lawal, "Epilepsy: pathophysiology, clinical manifestations and treatment options," *British Journal of Neuroscience Nursing*, vol. 14, no. 2, pp. 58–72, 2018.

[3] K. M. Fiest, K. M. Sauro, S. Wiebe et al., "Prevalence and incidence of epilepsy: a systematic review and meta-analysis of international studies," *Neurology*, vol. 88, no. 3, pp. 296–303, 2017.

[4] W. Loscher, L. J. Hirsch, and D. Schmidt, "The enigma of the latent period in the development of symptomatic acquired epilepsy-traditional view versus new concepts," *Epilepsy and Behavior*, vol. 52, pp. 78–92, 2015.

[5] S. C. Licata and J. K. Rowlett, "Abuse and dependence liability of benzodiazepine-type drugs: GABAA receptor modulation and beyond," *Pharmacology Biochemistry and Behavior*, vol. 90, no. 1, pp. 74–89, 2008.

[6] K. G. Bath and H. E. Scharfman, "Impact of early life exposure to antiepileptic drugs on neurobehavioral outcomes based on laboratory animal and clinical research," *Epilepsy and Behavior*, vol. 26, no. 3, pp. 427–439, 2013.

[7] C. Toth, "Pregabalin: latest safety evidence and clinical implications for the management of neuropathic pain," *Therapeutic Advances in Drug Safety*, vol. 5, no. 1, pp. 38–56, 2014.

[8] A. S. Alqahtani, R. Ullah, and A. A. Shahat, "Bioactive constituents and toxicological evaluation of selected antidiabetic medicinal plants of Saudi Arabia," *Evidence-based Complementary and Alternative Medicine*, vol. 2022, Article ID 7123521, 23 pages, 2022.

[9] R. Ullah and A. S. Alqahtani, "GC-MS analysis, heavy metals, biological, and toxicological evaluation of reseda muricata and marrubium vulgare methanol extracts," *Evidence-based Complementary and Alternative Medicine*, vol. 2022, Article ID 2284328, 9 pages, 2022.

[10] M. E. Rezvani, A. Roohbakhsh, M. H. Mosaddegh, M. Esmailidehaj, F. Khaloobagheri, and H. Esmaeili, "Anticonvulsant and depressant effects of aqueous extracts of Carum copticum seeds in male rats," *Epilepsy and Behavior*, vol. 22, no. 2, pp. 220–225, 2011.

[11] D. Santos Rosa, S. A. Faggion, A. S. Gavin et al., "Erysothrine, an alkaloid extracted from flowers of Erythrina mulungu Mart. ex Benth: evaluating its anticonvulsant and anxiolytic potential," *Epilepsy and Behavior*, vol. 23, no. 3, pp. 205–212, 2012.

[12] N. Choudhary, K. R. V. Bijjem, and A. N. Kalia, "Antiepileptic potential of flavonoids fraction from the leaves of anisomeles malabarica," *Journal of Ethnopharmacology*, vol. 135, no. 2, pp. 238–242, 2011.

[13] M. Pahuja, J. Mehla, K. Reeta, S. Joshi, and Y. K. Gupta, "Root extract of Anacyclus pyrethrum ameliorates seizures, seizure-induced oxidative stress and cognitive impairment in experimental animals," *Epilepsy Research*, vol. 98, no. 2-3, pp. 157–165, 2012.

[14] M. Nassiri-Asl, S. Shariati-Rad, and F. Zamansoltani, "Anticonvulsant effects of aerial parts of Passiflora incarnata extract in mice: involvement of benzodiazepine and opioid receptors," *BMC Complementary and Alternative Medicine*, vol. 7, no. 1, pp. 26–6, 2007.

[15] S. Kumar, R. Madaan, G. Bansal, A. Jamwal, and A. Sharma, "Plants and plant products with potential anticonvulsant activity–a review," *Pharmacognosy Communications*, vol. 2, no. 1, pp. 3–99, 2012.

[16] A. Chawla A, R. Kaur, and A. K. Sharma, "Ficus carica Linn.: a review on its pharmacognostic, phytochemical and pharmacological aspects," *International Journal of Pharmaceutical & Phytopharmacological Research*, vol. 1, no. 4, pp. 215–232, 2012.

[17] D. Sivaraman and P. Muralidaran, "Sedative and anticonvulsant activities of the methanol leaf extract of ficus hispida linn," *Drug Invention Today*, vol. 1, pp. 27–30, 2009.

[18] M. S. Patil, C. Patil, S. Patil, and R. Jadhav, "Anticonvulsant activity of aqueous root extract of Ficus religiosa," *Journal of Ethnopharmacology*, vol. 133, no. 1, pp. 92–96, 2011.

[19] D. Singh and R. K. Goel, "Anticonvulsant effect of Ficus religiosa: role of serotonergic pathways," *Journal of Ethnopharmacology*, vol. 123, no. 2, pp. 330–334, 2009.

[20] G. F. Buchanan, N. M. Murray, M. A. Hajek, and G. B. Richerson, "Serotonin neurones have anti-convulsant effects and reduce seizure-induced mortality," *The Journal of Physiology*, vol. 592, no. 19, pp. 4395–4410, 2014.

[21] A. Murugesan, M. R. S. Rani, L. Vilella et al., "Postictal serotonin levels are associated with peri-ictal apnea," *Neurology*, vol. 93, no. 15, pp. e1485–e1494, 2019.

[22] M. Imran, N. Rasool, K. Rizwan et al., "Chemical composition and biological studies of Ficus benjamina," *Chemistry Central Journal*, vol. 8, no. 1, p. 12, 2014.

[23] M. L. Dhar, M. M. Dhar, B. N. Dhawan, B. N. Mehrotra, and C. Ray, "Screening of Indian plants for biological activity: I," *Indian Journal of Experimental Biology*, vol. 6, no. 4, pp. 232–247, 1968.

[24] M. Leopoldo, E. Lacivita, F. Berardi, R. Perrone, and P. B. Hedlund, "Serotonin 5-HT7 receptor agents: structure-activity relationships and potential therapeutic applications in central nervous system disorders," *Pharmacology & Therapeutics*, vol. 129, no. 2, pp. 120–148, 2011.

[25] H. S. White, M. Johnson, H. H. Wolf, and H. J. Kupferberg, "The early identification of anticonvulsant activity: role of the maximal electroshock and subcutaneous pentylenetetrazol seizure models," *The Italian Journal of Neurological Sciences*, vol. 16, no. 1-2, pp. 73–77, 1995.

[26] M. S. Yerby, P. Kaplan, and T. Tran, "Risks and management of pregnancy in women with epilepsy," *Cleveland Clinic Journal of Medicine*, vol. 71, pp. 25–37, 2004.

[27] E. Perucca and K. J. Meador, "Adverse effects of antiepileptic drugs," *Acta Neurologica Scandinavica*, vol. 112, no. s181, pp. 30–35, 2005.

[28] A. Kabra, R. Sharma, S. Singla, R. Kabra, and U. S. Baghel, "Pharmacognostic characterization of Myrica esculenta leaves," *Journal of Ayurveda and Integrative Medicine*, vol. 10, no. 1, pp. 18–24, 2019.

[29] M. Ayaz, A. Nawaz, S. Ahmad et al., "Underlying anticancer mechanisms and synergistic combinations of phytochemicals with cancer chemotherapeutics: potential benefits and risks," *Journal of Food Quality*, vol. 2022, Article ID 1189034, 15 pages, 2022.

[30] N. Vyawahare, A. Khandelwal, V. Batra et al., "Herbal anti-convulsants," *Herbal Medicine and Toxicology*, vol. 1, pp. 9–14, 2007.

[31] C. Albano, A. Cupello, P. Mainardi, S. Scarrone, and E. Favale, "Successful treatment of epilepsy with serotonin reuptake inhibitors: proposed mechanism," *Neurochemical Research*, vol. 31, no. 4, pp. 509–514, 2006.

[32] K. M. Igelström, "Preclinical antiepileptic actions of selective serotonin reuptake inhibitors—implications for clinical trial design," *Epilepsia*, vol. 53, no. 4, pp. 596–605, 2012.

[33] G. Bagdy, V. Kecskemeti, P. Riba, and R. Jakus, "Serotonin and epilepsy," *Journal of Neurochemistry*, vol. 100, no. 4, pp. 857–873, 2007.

[34] F. M. Werner and R. Coveñas, "Classical neurotransmitters and neuropeptides involved in generalized epilepsy: a focus on antiepileptic drugs," *Current Medicinal Chemistry*, vol. 18, no. 32, pp. 4933–4948, 2011.

[35] A. Krishnakumar, P. M. Abraham, J. Paul, and C. Paulose, "Down-regulation of cerebellar 5-HT2C receptors in pilocarpine-induced epilepsy in rats: therapeutic role of Bacopa monnieri extract," *Journal of the Neurological Sciences*, vol. 284, no. 1-2, pp. 124–128, 2009.

Hindawi
Journal of Chemistry
Volume 2023, Article ID 2349713, 7 pages
https://doi.org/10.1155/2023/2349713

Research Article

Comparative Analysis of the Content of Sum of Hydroxycinnamic Acids from Leaves of *Actinidia arguta* Lindl. Collected in Ukraine and China

Nadiia Kovalska,[1] **Uliana Karpiuk**,[1] **Valentyna Minarchenko**,[1] **Iryna Cholak**,[1] **Natalia Zaimenko**,[2] **Nadiia Skrypchenko**,[2] **and Dejiang Liu**[3]

[1]*Department of Pharmacognosy and Botany, Bogomolets National Medical University, T Shevchenka Blvd 13, Kyiv 01601, Ukraine*
[2]*Department of Fruit Plants Acclimatization, M. M. Gryshko National Botanical Garden of National Academy of Sciences of Ukraine, Timiryazevska Str 1, Kyiv 01014, Ukraine*
[3]*College of Life Sciences, Jiamusi University, XueFu Str. 148, Jiamusi, Heilongjiang 154007, China*

Correspondence should be addressed to Uliana Karpiuk; uliana.karpiuk@gmail.com

Received 20 August 2022; Revised 26 September 2022; Accepted 24 November 2022; Published 23 January 2023

Academic Editor: Romina Alina Marc (Vlaic)

Leaves of *Actinidia arguta* Lindl. (*A. arguta*) are a promising raw material for pharmaceutical production. *Actinidia* is cultivated in Ukraine, and its homeland is China, so raw materials may have different origins. Hydroxycinnamic acids (HCAs) are one of the important biologically active substances of *A. arguta* leaves, which provide the pharmacological action of this raw material. The aim of the study was to identify and compare the quantitative content of HCAs in the leaves of *A. arguta* harvested in Ukraine and China in different phases of the growing season. Microscopic and phytochemical studies of the leaves of *A. arguta* are conducted. After histochemical reaction with the nitrite-molybdenum reagent, idioblast cells with HCAs in *A. arguta* leaves are stained on brick-red color. The amount of the sum of HCAs was determined by absorption UV-spectrophotometry in terms of rosmarinic acid at wavelength 505 nm after reaction with a nitrite-molybdenum reagent. It was found that the *A. arguta* leaves contain high levels of HCAs (to 2.69%). The highest HCAs level was recorded in July, which was decreased somewhat in August. Histochemical reactions for the detection of HCAs in fresh *A. arguta* leaves can be used to identify plants of the genus *Actinidia* Lindl., which are potential sources of HCAs. The content of HCAs is independent of the region of plant growth, but its quantity varies during the growing season. So, during July, the leaves can be collected from male plants, and during the end of August and start of September, leaves can be collected from both male and female plants. This indicates the prospect of using the leaves of *A. arguta* as a source of raw materials for pharmacy and medicine.

1. Introduction

The search for plant sources of biologically active substances includes the study of the influence of environmental factors from different places of plant growth on the content of compounds with medicinal potential. Plant growth conditions in different longitudes and latitudes are markedly different [1]. Various environmental limiting factors, such as ambient temperature, carbon dioxide levels, lighting, ozone, groundwater status, salinity, and soil fertility, have a significant impact on biochemical reactions in medicinal plants [2]. Plants can synthesize a variety of secondary metabolites to cope with the negative effects of stress. Secondary plant metabolites are a group of natural classes of compounds that are synthesized by various biochemical pathways. The content of these substances in plants is highly dependent on environmental influences [3]. The same plant species that grow in different environmental conditions have significant differences in the formation and accumulation of primary and secondary metabolites [3–8].

Secondary metabolites are used as important natural remedies with a wide range of pharmacological activities. One of the important groups of secondary metabolites are phenolic compounds, which perform many physiological functions for plant survival and are fundamental in the adaptation of plants to changes in the environment [9]. Hydroxycinnamic acids, which belong to the group of phenolic compounds, are an important group of secondary metabolites of plants that are involved in many important plant functions. For hydroxycinnamic acids, the directions of pharmacological action as anti-inflammatory, antiallergic, antiplatelet, antitumor, detoxifying, hepatoprotective, bactericidal, and antiviral is established [10–15].

Variations in the synthesis of plant metabolites often depend on growing conditions. Therefore, the study of differences in the quantitative content of secondary metabolites, in particular, hydroxycinnamic acids, in plants from different places of growth is essential for understanding the characteristics of plants of the same species, whose raw materials are harvested in different regions.

In the manufacture of medicines, the quality of the final product depends on the quality of the raw materials. The content of biologically active substances in plants is influenced by environmental conditions. Therefore, to effectively develop methods for standardizing plant raw materials for the content of secondary metabolites, it is important to take into account the different geographical origins of plant.

A promising source of hydroxycinnamic acids for pharmacy and medicine are the leaves of plants from the genus *Actinidia* Lindl. [16–18], which require more detailed phytochemical studies to develop methods of standardization.

Actinidia arguta Lindl. (*A. arguta*), named as kiwiberry, is distributed in the eastern and northern parts of China, Korea, Japan, Sakhalin, and the Kuril Islands cultivated in various regions of Asia, Europe, North America, New Zealand, and Australia. The northern limit of growth of *A. arguta* runs along 46°40′ north latitude. Due to its frost resistance, *A. arguta* is introduced into horticulture in Canada, Chile, France, and the United States. The largest *Actinidia* plantations are concentrated in the United States (Oregon). Frost-resistant varieties of *A. arguta* are also successfully cultivated in Poland [19].

The Global Biodiversity Database (https://www.discoverlife.org) contains an interactive map that includes registered wildlife habitats of *A. arguta* in the world, as well as marked botanical gardens where it is successfully cultivated (Figure 1). To obtain complete information about the indicated places of growth of *A. arguta*, you need to select the marked points on the map.

The homeland of kiwiberry is China, but it is well cultivated in Ukraine and has a high yield. Therefore, in Ukraine, kiwiberry is becoming increasingly popular in home gardens and industrial plantations. Researchers of the M. M. Grishko National Botanical Garden have for many years created the largest collection of plants of the genus *Actinidia* Lindl. in Ukraine, which includes not only well-researched and popular species but also new varieties and forms [20].

The vegetative mass of leaves in *Actinidia* vines is quite large and contains valuable biologically active substances. Therefore, it is important to study the presence and quantitative content of such phenolic compounds, such as hydroxycinnamic acids in *A. arguta* leaves cultivated in Ukraine, in comparison with raw materials harvested from wild plants of *A. arguta* in China to expand the raw material base for the development and creation of new herbal medicines.

2. Materials and Methods

2.1. Samples. The research study was conducted based on the Department of Pharmacognosy and Botany of the Bogomolets National Medical University (2020–2021).

The object of the study was generatively mature plants of kiwiberry (*A. arguta*), grown under different soil and climatic conditions, namely, from cultivated plants in Ukraine (Kyiv city, M. M. Grishko National Botanical Garden) on gray forest soil and from wild-growing plants in China (Jiamusi University, Heilongjiang province) on black earth. As a material for investigation, we used leaves of fifteen-year-old plants of *A. arguta*, which grew in the collection of M. M. Grishko National Botanical Garden (Ukraine) and in Jiamusi (China) during summer. Leaves samples of female and male plants were collected during June-September (Figure 2(a)). Leaf samples were dried by air-shadow drying (Figure 2(b)).

The male and female *A. arguta* leaves get into the plant raw material during the leaves collection from wild-growing plants in China. More leaves from female plants will be harvested as plant raw material in Ukraine because 5–7 female plants are planted next to one male plant during *A. arguta* cultivation. It means that leaves, as raw material will come more from female plants. Therefore, it is important to compare the HCAs content in female leaves collected in Ukraine and China. The harvesting time affected to the quantitative content of different BAS and to the HCAs also. We collected male and female *A. arguta* leaves in different months for a comparative determination of HCAs content.

Cultivated male plants of *A. arguta* can also become raw materials to expand the raw material base of medicinal plants. The content of HCAs in *A. arguta* leaves from male plants cultivated in Ukraine was also studied.

Jiamusi city is located in the eastern part of the northernmost province of China, Heilongjiang. The city is in a moderately cold zone with a humid continental climate. The average rainfall is 627 millimeters. The soils are mostly black soil with high humus content.

The climate of the area in which Kyiv is located is moderately continental, with an average annual temperature 9.4°C. M. M. Grishko National Botanical Garden, which located in Kyiv (N, 50°27′; E, 30°31′), is one of the biggest scientific and practical Ukrainian centers of introduction and acclimatization of nontraditional plants, selection and spreading of new cultivars, which may be successfully cultivated on commercial plantations and in private gardens.

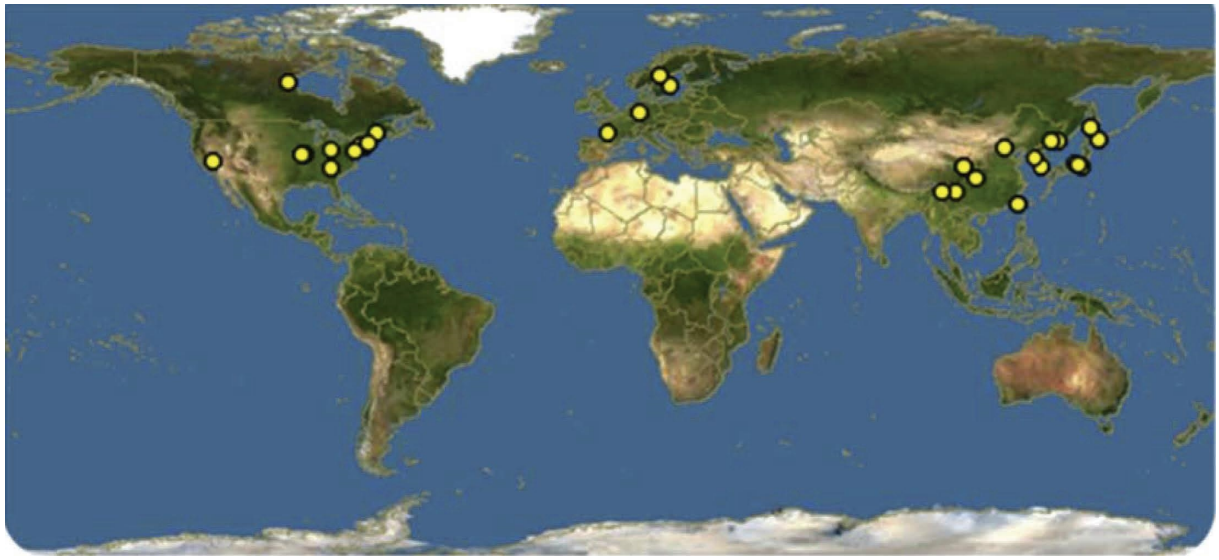

Figure 1: Distribution map of *Actinidia arguta* Lindl. in the world by Global Biodiversity Information Facility Database (https://www.discoverlife.org).

(a) (b)

Figure 2: Leaves of female plant *A. arguta* (a) freshly harvested and (b) dried collected in Ukraine.

The garden is located on the border of two climatic zones—wooded district and forest steppe in the southeastern part of city on the slopes of the Pechersk hills near the Dnipro River. The main type of soil is dark gray podzolic. Due to the crossing of locality, the garden soil is rather washed out and characterized by low humus content. The climate of the area is continental with an average annual temperature of 7.6°C; the average temperature in January is −5.5°C, in June −20.4°C. The winter in Kyiv is softened by the periodic invasion of Atlantic air masses. The frost-free period in Kyiv is 165–180 days on average. The average annual amount of precipitation in Kyiv is 550–650 mm, and the relative humidity is 73–76%. The duration of the period without frost, temperature conditions, and rainfall during the active growing season create a suitable possibility for the successful cultivation of different fruit and berry plants from regions with similar and sometimes more mild climatic conditions.

2.2. Determination of HCA*s in the A. arguta Leaves by Chemical and Histochemical Reactions.* Chemical reaction by using nitrite-molybdenum reagent as the Arnov test was performed as described by Gawlik-Dziki et al. [21].

2.2.1. Preparation of Extracts for the Detection of Hydroxycinnamic Acids. 3.00 g of crushed *A. arguta* leaves (separately from males and females) were filled with 50% alcohol. Extracted in a water bath in a flask under reflux for 20 minutes, the extract was cooled, and after cooling, it was filtered.

2.2.2. Preparation of Nitrite-Molybdenum Reagent. Reagent was prepared by dissolving 10% (m/v) sodium molybdate and 10% (m/v) sodium nitrite in distilled water. To prepare a dilute sodium hydroxide solution, 8.3 g of sodium hydroxide was made up to 100 ml with purified water in a volumetric flask. All reagents were prepared daily.

2.2.3. Reaction with Nitrite-Molybdenum Reagent. To 1 ml of each extract, 2 ml of 0.5 M hydrochloric acid solution, 2 ml of a mixture of 10% sodium molybdate solution and 10% sodium nitrite solution, and 2 ml of dilute sodium hydroxide solution were added in the specified order. The formed reaction products were brick-cherry in color.

The investigation of the character of the localization of HCAs in the *A. arguta* leaves was carried out by light microscopy after reaction on cross sections of petiole and central vein of the leaf with nitrite-molybdenum reagent [22]. Temporary micropreparations were examined in the light trinocular microscope XSP-146T of ULAB at a magnification of 40, 100, 400, and 1000 times. Snapshots were taken using the camera Canon EOS 550 DSLR.

2.3. Comparative Analysis of HCAs Content in the A. arguta Leaves by Spectrophotometry. The quantity of HCAs sum was defined by absorption UV-spectrophotometry in amounts equivalent to rosmarinic acid at wavelength 505 nm after reaction with the nitrite-molybdenum reagent. As a standard for comparison, rosmarinic acid was used, since after the reaction with a nitrite-molybdenum reagent, extracts from the studied types of raw materials form a maximum absorption at 505 nm, as well as rosmarinic acid (Figure 3). HCAs give maxima of absorption of the reaction product with the nitrite-molybdenum reagent in the wavelength range from 490 to 527 nm. In the aqueous alcoholic extract of *A. arguta* leaves, the sum of HCAs forms the maximum absorption with nitrite-molybdenum reagent at a wavelength of 493 nm. Therefore, we have chosen a unified method for calculating the content of the sum of HCAs in terms of rosmarinic acid at a wavelength of 505 nm, which is given in the monograph State Pharmacopeia of Ukraine 2.0 Java tea.

The quantitative determination of the HCAs sum in the investigated types of raw materials was carried out according to the method of quantitative determination of HCAs amount in Java tea described by the State Pharmacopeia of Ukraine 2.0 [23].

The statistical analysis of the results was carried out in accordance with the monograph of the State Pharmacopoeia of Ukraine 2.0 "Statistical analysis of the results of a chemical experiment" using Microsoft Excel 2010 for Windows.

3. Results

3.1. The Results of Determination of HCAs in the A. arguta Leaves by Chemical and Histochemical Reactions. As a result of the reaction of alcoholic extracts from the leaves of male and female plants of A. arguta with nitrite-molybdenum reagent, the formation of brick-cherry color of the formed reaction products was observed (Figure 4).

Histochemical reactions on cross sections of the petiole and central vein of the leaf with the nitrite-molybdenum reagent showed the presence and character of the localization of HCAs in *A. arguta* leaves.

In the study of the localization of HCAs in the studied leaves of female and male plants of *A. arguta*, we observed the formation of brick-red color in idioblast cells in the xylem area, phloem, as well as in the parenchyma under the integument. Figure 5 shows the result of histochemical reaction on the leaves of females and males of *A. arguta* with the nitrite-molybdenum reagent.

The result of our reaction was stable. The color did not disappear quickly over time. Conducted histochemical reactions provide additional information in establishing the identity of medicinal plant raw materials. They revealed the localization of the studied group of substances directly in tissues and cells.

3.2. Analysis of the Content of HCAs Collected in Different Regions and Different Months. The content of HCAs sum is in the range from $1.51 \pm 0.04\%$ to $2.69 \pm 0.13\%$ (Figure 6). There are different medicinal plant materials in Ukraine, which have standardized content of HCAs detected with spectrophotometry. For example, *Echinacea purpurea* radix must content not less than 2.0% HCAs in amounts equivalent to chicoric acid and dry raw material. *A. arguta* leaves contain almost the same amount of HCAs.

The HCA content in *A. arguta* leaves is independent of plant growth conditions. The leaves collected in different regions of China and Ukraine contained almost the same HCAs sum, although it was slightly higher in leaves mass collected in Jiamusi (Figure 6). Samples of leaves from China, which have a slightly higher content of HCAs, were collected from wild plants that grow in their natural range. It was found that the content of HCAs in cultivated plants on the territory of Ukraine is slightly lower than in wild plants of *A. arguta* from China. The maximum content of HCAs is observed in July, and in August it reduces slightly. It was determined that the content of HCAs decreases during the vegetation until the end of the summer in the same way in *A. arguta* leaves harvested in Jiamusi and in Kyiv. Therefore, it is advisable to harvest the leaves of *A. arguta* in July to obtain the raw materials with the highest content of HCAs for the next research study of pharmacological action. At this time, you can use leaves from the shoots of female *A. arguta* plants, the main function of which is to provide the plants with pollen during their flowering period.

3.3. Analysis of HCAs Content in the Leaves of Female and Male Plants. It should be noted that the leaves of female and male plants differ in their HCA content (Figure 7). Thus, in June, the leaves of female plants accumulated more HCAs ($2.26 \pm 0.10\%$) compared to male ones ($1.67 \pm 0.08\%$). In July, their contents were leveled, and in the following months of observation, there is a steady tendency of decrease in the level of acids in female plants that may be associated with the onset of the period of ripening of the fruit. Therefore, the collection of *Actinidia* leaves of male plants is recommended in July and August. At this time, the leaves of the shoots of female *A. arguta* plants, which are removed during the summer pruning, may be used. Raw materials can also be harvested from female plants in August because the content of HCAs remains relatively high ($1.51 \pm 0.04\%$). In September, after the harvest, you can collect leaves from all plants, regardless of sex, because the content of HCAs does not fall critically ($1.13 \pm 0.05\%$ in female and $1.85 \pm 0.09\%$ in male plants).

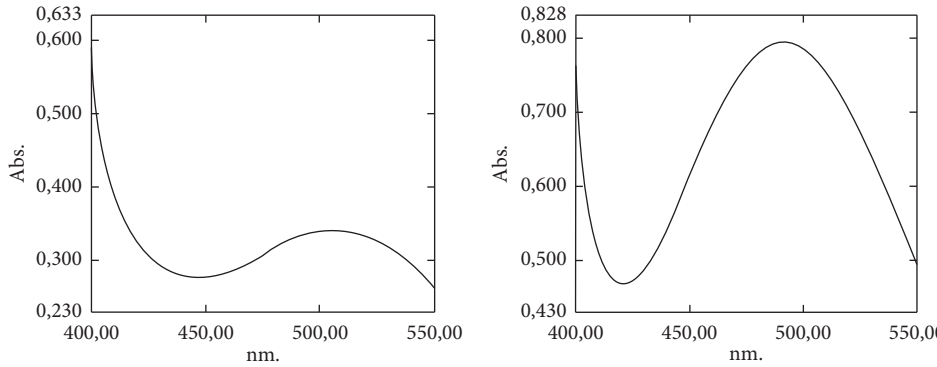

Figure 3: Electronic spectrum absorption of alcoholic solution of rosmarinic acid with the nitrite-molybdenum reagent (a). Electronic spectrum absorption of alcohol-aqueous extract of *A. arguta* leaves with nitrite-molybdenum reagent (b).

Figure 4: The result of the reaction with the detection of HCAs with an extract from the leaves of females of *A. arguta*.

4. Discussion

Chemical and histochemical reactions for the determination of HCAs in the leaves of *A. arguta* showed positive results and could be used for HCAs identification in this plant raw material. The reagents we have chosen are quite economical and easy to use. According to the saturation of the color of the reaction products and the number of idioblast cells in the section, it can be assumed that hydroxycinnamic acids contain approximately the same amount in the leaves of male and female individuals of *A. arguta*. The obtained results can be used as an auxiliary indicator to establish the identity of raw materials in the development of quality control method "*Actinidia* leaves."

The spectrophotometric pharmacopoeia method allows for the maximum absorption of the reaction products with the nitrite-molybdenum reagent to determine the sum of all HCAs in the raw material. We determined the content of HCAs in *A. arguta* leaves harvested from female and male plants during the whole vegetation period by the method of spectrophotometric research. In June, there is a fairly high content of HCAs, but for the plant harvest in this period is not useful, because the vegetative mass of leaves has yet to perform its assimilative function. In addition, young leaves harvested in June turn black quickly during drying. This indicates active enzymatic biochemical processes in the leaves during this period. In June, the leaves of male plants synthesize the least HCAs for the entire growing season ($1.67 \pm 0.08\%$). In the first two summer months, more HCAs accumulated in the leaves of female plants ($2.26 \pm 0.10\%$ in June and $2.37 \pm 0.12\%$ in July). In August and September, their content decreased compared to the content in July by 37% and 52%, respectively. This decrease in the content of HCAs in the leaves of female plants can be associated with the beginning of the process of fruit ripening. All biochemical processes involved in the formation of biologically active substances are concentrated during this period in fruits. In leaves harvested from male plants, the content of HCAs is highest in July ($2.20 \pm 0.11\%$), and in August their content decreases by only 8.6%. The results showed that the best period for collecting leaves to create potential drugs is the end of July–August because it was then that the spectrophotometric method revealed the highest amount of HCAs for rosemary acid (2.0% on average).

There is a positive correlation between the amount of HCAs in plants growing in Ukraine and China. Our research has shown that *A. arguta* leaves collected from cultivated plants in Ukraine have a slightly lower HCA content compared to wild plants collected in the natural growth zone in China. Thus, leaves harvested in July in the province of Jiamusi accumulate only 12% more HCAs than *A. arguta* leaves harvested in July at research sites in the M. M. Grishko National Botanical Garden in the city of Kyiv, Ukraine. This gives reason to believe that the leaves of the cultivated plant *A. arguta* are a promising raw material base for research to develop new potential remedies.

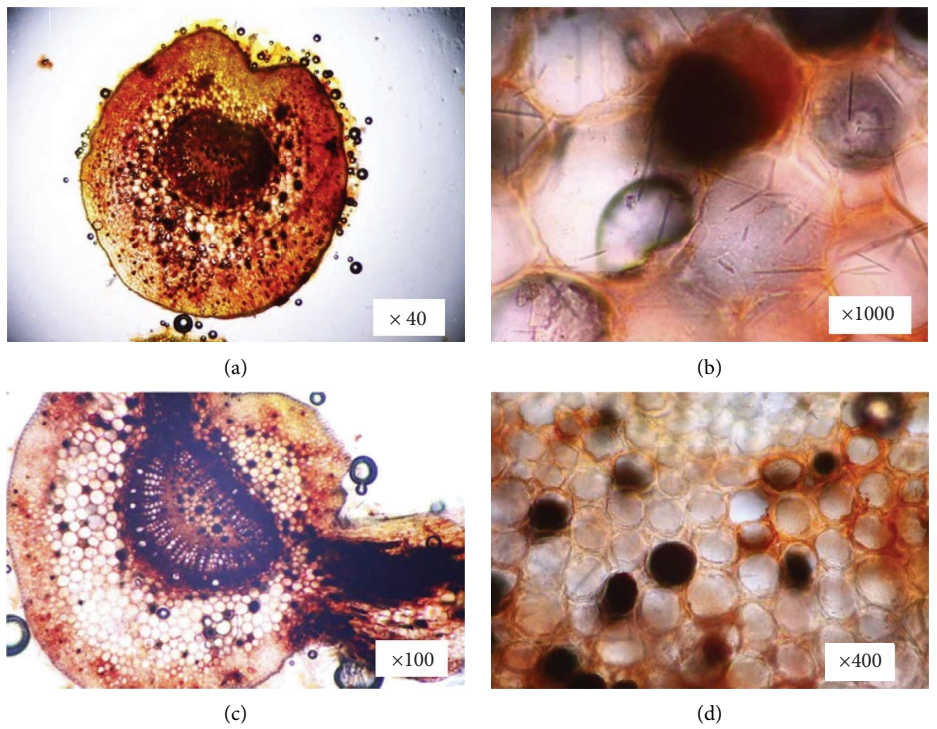

Figure 5: Locations of HCAs in the leaves of females (a, b) and males (c, d) of *A. arguta* by histochemical reaction with the nitrite-molybdenum reagent.

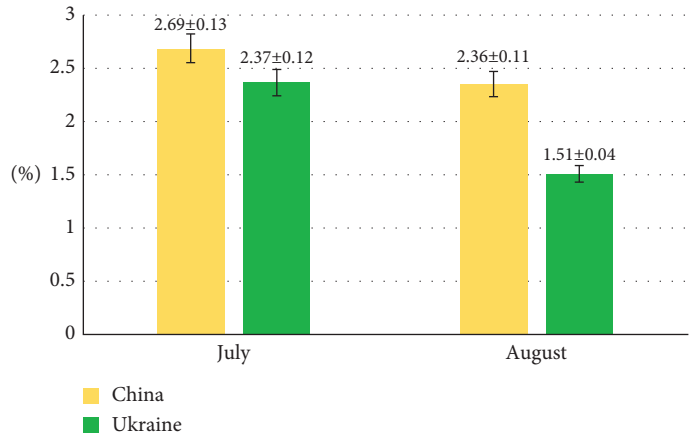

Figure 6: Content of the sum of HCAs in *A. arguta* leaves collected in Jiamusi (China) and Kyiv (Ukraine) (p-value < 0.05).

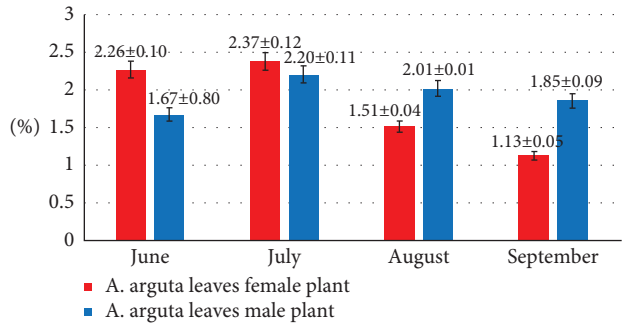

Figure 7: The content of the HCAs sum in *A. arguta* leaves collected in Kyiv (Ukraine) (p-value < 0.05).

5. Conclusions

A. arguta leaves contain a high level of HCAs (up to 2.0%), which is independent of the region of plant growth. Its quantity varies during the growing season, with the highest HCA content in July. During this period, the leaves of male plants, whose main function is to provide the process of pollination of female flowers during the flowering period in May, may be used to harvest raw materials. In August and in September, after harvesting fruits, the HCA content in *A. arguta* leaves decreases somewhat but remains rather high, so the leaf mass during this period may be harvested with both male and female plants. Therefore, the leaves of *A. arguta*, cultivated in Ukraine are a promising source for obtaining extracts with a high content of HCAs, which require future research on pharmacological activity. Certain features of the localization of hydroxycinnamic acids can be used to identify plant raw materials in the development of methods for quality control of raw materials.

We can note that *A. arguta* leaves collected in China have the higher content of HCAs. China is a homeland of *A. arguta*, and natural growth conditions contribute to the accumulation of secondary metabolites in plants.

Data Availability

The data used to support the findings of this study are included within the article.

Conflicts of Interest

The authors declare that they have no conflicts of interest.

Acknowledgments

This work was supported by the Ministry of Health of Ukraine (grant no. 012U001306).

References

[1] L. Jaakola and A. Hohtola, "Effect of latitude on flavonoid biosynthesis in plants," *Plant, Cell and Environment*, vol. 33, no. 8, pp. 1239–1247, 2010.

[2] P. Pant, S. Pandey, and S. Dall'Acqua, "The influence of environmental conditions on secondary metabolites in medicinal plants: a literature review," *Chemistry and Biodiversity*, vol. 18, no. 11, Article ID e2100345, 2021.

[3] D. P. Pavarini, S. P. Pavarini, M. Niehues, and N. P. Lopes, "Exogenous influences on plant secondary metabolite levels," *Animal Feed Science and Technology*, vol. 176, no. 1-4, pp. 5–16, 2012.

[4] B. L. Sampaio, R. Edrada-Ebel, and F. B. Da Costa, "Effect of the environment on the secondary metabolic profile of Tithonia diversifolia: a model for environmental metabolomics of plants," *Scientific Reports*, vol. 6, no. 1, Article ID 29265, 2016.

[5] R. Akula and G. A. Ravishankar, "Influence of abiotic stress signals on secondary metabolites in plants," *Plant Signaling & Behavior*, vol. 6, no. 11, pp. 1720–1731, 2011.

[6] B. Gutbrodt, S. Dorn, S. B. Unsicker, and K. Mody, "Species-specific responses of herbivores to within-plant and environmentally mediated between-plant variability in plant chemistry," *Chemoecology*, vol. 22, no. 2, pp. 101–111, 2012.

[7] V. V. Edreva, T. Tsonev, S. Dagnon, A. L. Gürel, and L. Aktas, "Stress-protective role of secondary metabolites: diversity of functions and mechanisms," *General and Applied Plant Physiology*, vol. 34, pp. 67–78, 2008.

[8] N. Theis and M. Lerdau, "The evolution of function in plant secondary metabolites," *International Journal of Plant Sciences*, vol. 164, no. S3, pp. S93–S102, 2003.

[9] N. Verma and S. Shukla, "Impact of various factors responsible for fluctuation in plant secondary metabolites," *Journal of Applied Research on Medicinal and Aromatic Plants*, vol. 2, no. 4, pp. 105–113, 2015.

[10] D. Vauzour, A. Rodriguez-Mateos, G. Corona, M. J. Oruna-Concha, and J. P. E. Spencer, "Polyphenols and human health: prevention of disease and mechanisms of action," *Nutrients*, vol. 2, no. 11, pp. 1106–1131, 2010.

[11] H. Abramovič, *Coffee in Health and Disease Prevention*, V. R. Preedy, Ed., p. 843, Academic Press, Cambridge, MA, USA, 2015.

[12] K. B. Martinez, J. D. Mackert, and M. K. McIntosh, *Nutrition and Functional Foods for Healthy Aging*, R. R. Watson, Ed., vol. 18, p. 191, Academic Press, Cambridge, MA, USA, 2017.

[13] G. B. Maru, G. Kumar, S. Ghantasala, and P. Tajpara, *Polyphenols in Human Health and Disease*, R. R. Watson, V. R. Preedy, and S. H. Zibadi, Eds., vol. Vol. 2, p. 1401, Academic Press, Cambridge, MA, USA, 2014.

[14] S. A. Heleno, A. Martins, M. J. R. P. Queiroz, and I. C. F. R. Ferreira, "Bioactivity of phenolic acids: metabolites versus parent compounds: a review," *Food Chemistry*, vol. 173, pp. 501–513, 2015.

[15] J. Teixeira, A. Gaspar, E. M. Garrido, J. Garrido, and F. Borges, "Hydroxycinnamic acid antioxidants: an electrochemical overview," *BioMed Research International*, vol. 2013, Article ID 251754, 2013.

[16] D. Almeida, D. Pinto, J. Santos et al., "Hardy kiwifruit leaves (Actinidia arguta): an extraordinary source of value added compounds for food industry," *Food Chemistry*, vol. 259, pp. 113–121, 2018.

[17] K. H. Heo, X. Sun, D. W. Shim et al., "Actinidia arguta extract attenuates inflammasome activation: potential involvement in NLRP3 ubiquitination," *Journal of Ethnopharmacology*, vol. 213, no. 1, pp. 159–165, 2018.

[18] N. V. Skrypchenko and V. F. Levon, "Antioxidant activity of biologically active substances of woody fruit vines," *Introduction of Plants*, vol. 1, pp. 60–63, 2016.

[19] A. R. Ferguson, "Kiwifruit cultivars: breeding and selections," *Acta Horticulturae*, vol. 498, pp. 43–52, 1999.

[20] N. Skrypchenko and P. Latocha, "'The genesis and current state of actinidia collection in M.M. Gryshko national botanical garden in Ukraine', polish," *Journal of Natural Sciences*, vol. 32, no. 3, pp. 513–525, 2017.

[21] U. Gawlik-Dziki, D. Dziki, B. Baraniak, and R. Lin, "The effect of simulated digestion in vitro on bioactivity of wheat bread with tartary buckwheat flavones addition," *LWT--Food Science and Technology*, vol. 42, no. 1, pp. 137–143, 2009.

[22] T. V. Dzhan, N. P. Kovalska, N. M. Guzio, O. Y. Konovalova, and S. V. Klimenko, *Method for Determining Localization of Hydroxycinnamic Acids in Plant Raw Materials by Histochemical Reaction Utility Model Patent of Ukraine*, 2018.

[23] J. Tea, "State pharmacopoeia of Ukraine," *Ukrainian Scientific Pharmacopoeial Center for Quality of Medicines*, p. 407, Kharkiv, 3 edition, 2014.

Hindawi
Journal of Chemistry
Volume 2022, Article ID 2755084, 21 pages
https://doi.org/10.1155/2022/2755084

Review Article

Photochemistry, Functional Properties, Food Applications, and Health Prospective of Black Rice

Muhammad Abdul Rahim,[1] Maryam Umar,[1] Ayesha Habib,[2] Muhammad Imran,[1] Waseem Khalid,[1] Clara Mariana Gonçalves Lima,[3] Aurbab Shoukat,[4] Nizwa Itrat,[2] Anum Nazir,[5] Afaf Ejaz,[1] Amna Zafar,[6] Chinaza Godswill Awuchi,[7] Rohit Sharma,[8] Renata Ferreira Santana,[9] and Talha Bin Emran[10,11]

[1]*Department of Food Science, Faculty of Life Sciences, Government College University, Faisalabad, Punjab, Pakistan*
[2]*Department of Nutritional Sciences, Faculty of Medical Sciences, Government College University Faisalabad, Faisalabad, Punjab, Pakistan*
[3]*Department of Food Science, Federal University of Lavras, Lavras, Minas Gerais, Brazil*
[4]*National Institute of Food Science & Technology, University of Agriculture, Faisalabad, Pakistan*
[5]*Department of Nutrition and Dietetics, University of Faisalabad, Faisalabad, Punjab, Pakistan*
[6]*Department of Home Economics, Faculty of Life Sciences, Government College University, Faisalabad, Punjab, Pakistan*
[7]*School of Natural and Applied Sciences, Kampala International University, Box 20000 Kansanga, Kampala, Uganda*
[8]*Department of Rasa Shastra and Bhaishajya Kalpana, Faculty of Ayurveda, Institute of Medical Sciences, Banaras Hindu University, Varanasi 221005, Uttar Pradesh, India*
[9]*Department of Food Science, Southwestern Bahia State University, Itapetinga, Bahia, Brazil*
[10]*Department of Pharmacy, BGC Trust University Bangladesh, Chittagong 4381, Bangladesh*
[11]*Department of Pharmacy, Faculty of Allied Health Sciences, Daffodil International University, Dhaka 1207, Bangladesh*

Correspondence should be addressed to Talha Bin Emran; talhabmb4@gmail.com

Received 12 August 2022; Revised 11 September 2022; Accepted 16 September 2022; Published 14 October 2022

Academic Editor: Muhammad Zia-Ul-Haq

This review investigates black rice's photochemistry, functional properties, food applications, and health prospects. There are different varieties of black rice available in the world. The origins of this product can be traced back to Asian countries. This rice is also known as prohibited rice, emperor's rice, and royal's rice. Black rice is composed of different nutrients including fiber, protein, carbohydrates, potassium, and vitamin B complex. It contains an antioxidant called anthocyanin and tocopherols. Antioxidants are found mostly in foods that are black or dark purple. Due to its nutritious density, high fiber level, and high antioxidant content, black rice is a good alternative to white and brown rice. Utilizing black rice in various foods can enhance the nutritional value of food and be transformed into functional food items. Many noncommunicable diseases (NCDs) can be prevented by eating black rice daily, including cancer cells, atherosclerosis, hypertension, diabetes, osteoporosis, asthma, digestive health, and stroke risk. This review aim was to discuss the role of nutritional and functional properties of black rice in the formation of functional food against different noncommunicable diseases.

1. Introduction

Black rice that belongs to the *Oryza sativa* L. species, scientifically known as *Zizania aquatica,* is cultivated in Asia. They are a viscous and nutrient-dense food. Its seed appears black due to the presence of an antioxidant pigment anthocyanin. Other popular names of black rice are forbidden rice, purple rice, heaven rice, king's rice, and prized rice. People often take it as an elixir as they are nutrient-dense and therapeutic. The food also called "long-life rice" is

known to raise the soundness and longevity of life. It has been grown in Southeast Asian countries including China, Thailand, and India for years [1]. There are 200 varieties of black rice around the world. 62% of the global production of black rice is by China alone. Around 45 modern black rice varieties are developed by China, which have high yield and multiple resistance genes [2]. Engrossment in black rice is shown by several successions that occurred in germ plasma collection, e.g., Bangladesh—24, the Philippines—25, Indonesia—42, and China—359 [3].

Black rice has minerals (Ca, P, Fe, and Zn) and dietary fiber, which are higher than brown and white rice. Being nutrient-dense, the demand for black rice is accelerating in the United States of America and European countries. Black rice is certainly a special breed that was grown in ancient times, but in modern agriculture, they are not grown on a larger scale. Black rice has both short and long grains. Black rice is openly pollinated, i.e., heirloom rice. One of its strains was called "Imperial Rice," which was reserved for the emperor's consumption only. The black color of rice turns royal purple when cooked. This characteristic color is due to anthocyanin; a strong antioxidant presents in the seed coat of anthocyanin. This characteristic color is typically observed in blueberries and blackberries [4].

Black rice contains about 26.3% anthocyanin, and the main functional constituents are chrysanthemum (cyanidin-3-O-glucoside) and methyl-cyanidin (peonidin-3-O-glucoside), which constitute 90% [5]. Anthocyanin present in black rice is mainly responsible for preventing DNA damage and artery endothelial degeneration and hardening [6]. Extracts of black rice have a better ability to scavenge superoxide anions than OH radicals [7]. Black rice is highly protected in Asian countries, and its intake in meals has become more common now. Black rice is particularly common among dieticians who recommend it to their clients due to its high nutritional value and therapeutic nature [8]. Black rice is usually sold with its fiber-rich black husk instead of polished rice. It is more commonly used either as savory or in dressings, and it is also a part of desserts in different parts of the world. This "Superfood" is praised and liked by people because of its rich color and nutritional value. It is often a part of fresh juices and other refreshments around the world. Once cooked, its black color converts into dark purple, which looks attractive to the consumer, and its taste is sweeter than white rice with a sticky texture. In Korea, they are consumed in combination with white rice, while in China it is part of many desserts, porridges, and bakery item. It was believed that looking at black rice in the morning is a good omen as it brings peace and happiness all day long. In ancient times, it was consumed by emperors due to its dual nature of being fluffy and good in taste first and being nutritious and curative food second. The consumption of black rice is more common among Europeans as compared to South Asians. Its antioxidant-rich nature and therapeutic effects make it a lifesaving food [9].

Black rice due to its strong antioxidant potential protects from thickening or hardening of arteries due to plaque formation by preventing the changes in low-density lipoproteins resulting from oxidative stress. Studies have shown that the Chinese took black rice as alternative medicine due to its antioxidant potential and they also believed that it was beneficial for vital organs of the body [10]. The fractional of minerals in black rice greatly depends on the nature of the soil where it is cultivated and its strain [11].

Rice is the staple food in many countries around the globe; thus, the consumption of black rice is a great option to enhance the supply of anthocyanins to the body [12]. Another way to consume anthocyanin is in the supplemental form, which can be costly All these aspects are contributing to giving black rice the status of novel organic food worldwide [13]. The consumption of black rice also has an antiaging, antiviral, anticancerous, and anti-inflammatory effect on its consumer [14].

Evidence-based studies have proven the physiological and pharmacological potential of black rice [15]. Harvesting and cultivation of black rice have also created many employment and career opportunities for people [16]. Excessive production of free radicals is the main cause of cancer. Breast cancer, colon cancer, and prostate cancer are greatly found to be associated with dietary choices and lifestyle. The risk of cancer can be reduced by consuming plant foods such as black rice. Many studies have suggested the role of black rice in health improvement and disease prevention. Alone anthocyanin in black rice is an undoubtedly potentially bioactive component that has come up with a great ability to improve metabolic mechanisms and conditions such as obesity, heart disease, stroke, and type 2 diabetes [17–20]. Whole seed black rice must have much more health benefits as they not only can prevent and improve conditions such as heart diseases, diabetes, and hypertension but also upgrade the quality of life.

2. Methodology

For the data collection about black rice, we used Science Direct, Google Scholar, Web of Science, and PubMed. We made the content first to make the proper design of the review and then made the conceptualization. By following the framework, we developed the partitions of the review and discussed the nutritional composition of black rice, food application of black rice foods, and the potential to combat noncommunicable diseases of black rice.

3. Classification of Black Rice

Black rice is classified into different categories according to the different shapes, sizes, nutrient contents, and colors. There are different varieties including black forbidden rice, black glutinous rice, black emperor's rice, and black jasmine or Chak Hao rice. Black rice is classified into various varieties as described as follows and in Figure 1.

3.1. Black Forbidden Rice. Black forbidden rice is a combination of mahogany medium-sized grain rice and black short grain rice. It has a characteristic earthy flavor along with a mild sweet spicy smack [21].

Figure 1: Classification of black rice.

3.2. Black Glutinous Rice. Black glutinous rice is commonly known as black sticky rice, which is a short grain variety of rice with a sticky texture and sweet taste. This rice has uneven pigmentation anis *d* mainly used as a part of desserts in Asia.

3.3. Black Emperor's Rice. Black emperor's rice is a combination of Chinese black rice and Italian rice. It is long grain rice with rich and buttery savor.

3.4. Black Jasmine or Chak Hao Rice. Thai black jasmine rice is basically of Thai origin, and they are a combination of medium grain rice with a mixture of jasmine rice and Chinese black rice. When cooked, a delicate floral aroma or fragrance can be felt [22].

4. History and Background

Black rice is a worthy grain consumed globally as a source of energy by both humans and animals. It is grown in over 100 countries in the world ranging from 45° S to 53° N latitudes [23]. Residents of at least fifteen countries in Asia, about ten countries in Latin America and the Caribbean, seven countries in Saharan Africa, and one country in North Africa consume black rice as a staple food [24]. Rice is quite a popular food among consumers as about half of the rice produced is consumed within 10 miles of where it was grown. Rice is found everywhere except Antarctica. About 95% of global rice production is from Asian countries [25]. Acknowledging the worth of another rice crop, 2004 was declared the "International Year of Rice" by the General Assembly of the United Nations. In Asia, food and rice are used synonymously. A single grain of rice can produce 3000 grains of rainout to production, and rice is second to corn. 1/5^{th} of human caloric intake is from rice, and when we talk about Asia, almost 60% to 70% of their caloric requirement is obtained from rice [26].

Oryza sativa L. that is commonly known as Asian rice is a monocotyledonous plant and a major cereal grain making up a food source for 3 billion people around the globe. Rice was a crop from East, Southeast, and South Asia. Later, it reached the European countries and America during the colonization of the subcontinent. Rice has more than 40,000 varieties, yet we know of only a few. These varieties grow in tropical and subtropical regions and are linked to the grass family Gramineae. It is often said that it was grown in India, China, and other Asian countries for 4,000 B.C. years ago. It is also believed that Japonica rice was first grown at a domestic level from which other types were merged including Indica [27]. Oryza has more than 25 varieties, and more of them are Indica, which is followed by Japonica and then Javanica. A perennial specie, which is known as *Oryza glaberrima,* is grown in Africa. Zizania aquatica, which is also known as "wild rice," is grown in the Great Lakes region of the United States. Wild rice is closer to oats than rice. Rice is partially aquatic grasses. Rice that is grown in winter is known as Rabi rice and those that are grown in summer/spring are called Boro rice. In tropical regions, once the ice is sown, it will take about six months to harvest this crop. Using conventional methods of rice cultivation, about 2500 liters of water is needed to produce a single kg of rice, but using modern techniques of rice cultivation, the water requirement for rice cultivation has greatly reduced. During the whole plantation period, flooding according to weather conditions keeps rice plants safe from weeds and pests. Rice plants can grow from 3′ to 6′ vertically depending on the variety, soil nutrition, and weather conditions. The consumption of polished white rice is more common worldwide. People usually think of white or brown rice, but they are found in a broad spectrum of colors from white to brown to red and with a deep purple hue. The taste of rice consumed with their hull or seed coat is nuttier than polished rice and those with removed seed coat. An expert can distinguish between different rice varieties. Before the Chinese dynastic period, black rice was grown in China, and they were a sign of luck because of its black color. Later, it was found that color depends on the concentration of pigment. In black rice, this black pigmentation is due to anthocyanin, and in red rice, it is due to tannins. If white rice is discussed, there is no pigmentation as no mutations occur at the genetic level, while in black rice, there is a mutation in the gene controlling the biosynthesis of pro-anthocyanin. During the Hung Dynasty, black rice was cultivated and eaten in Vietnam [28]. The origin of black rice is not clearly understood; however, it is believed that it originated from Asian countries including Japan, India, China, and Vietnam [29–32]. Chaudary and Tran [33] mentioned that this superfood might be originated from the Philippines, Sri Lanka, Bangladesh, Myanmar, Thailand, and Indonesia (Table 1).

Table 1: Different classification of black rice consumption in the different regions of the world.

Varieties	Species and subspecies	Description	Consumption regions	References
Black rice	*Oryza sativa L. indica*	Long and nonsticky rice	People of Southern Asia and Eastern Asia	[34]
Black Japonica rice	*Oryza sativa L. japonica*	Short and sticky or mahogany rice	People of Northern China, Japan, Southern Asia, and Latin America	
Black Chak Hao Amubi rice	*Oryza sativa Chak Hao Amubi*	Medium and long nonsticky rice	People of the Indian subcontinent	[35,36]
Black *Chak Hao Poireiton* rice	*Oryza sativa Chak Hao Poireiton*	Medium and long nonsticky rice	People of Thailand and Iran	[37]
Black forbidden rice	*Oryza sativa forbidden*	Medium-sized grain rice and black short grain	Mostly people of China and Asian countries	[21]
Black emperor's rice	*Oryza sativa emperor's*	Long grain rice	Mostly consumed in China, South Africa and Nigeria, and Italy	[38]

5. Botanical Description of Black Rice

Black rice is formed by the ripened ovary of the flower and is between 5 and 12 mm in length and pear-shaped (Figure 2). Oryza is the genus belongs to the Oryzeae of Poaceae family. Oryzeae has twelve genera, and the genus Oryza has almost 22 species. Among the cities, 20 are wild species and the rest of the two are cultivated: O. sativa and O. *glaberrima* [39]. Former is more common on a larger scale than *O. glaberrima* in different parts of the world including African, Asian, European, Middle Eastern, South, and North American countries. *O. glaberrima* is grown in West African countries. However, high-yielding hybrids of cultivating species are replacing *O. glaberrima* in African parts [40].

It is suggested by the researchers that Asian species are the ancestor of *O. sativa*. These ancestors are *O. nivara* and *O. rufipogon,* which are annual and perennial. They also added that among the developed varieties there is a similarity with wild ancestors. *O. glaberrima,* which are African cultivated rice, are the predecessors' wild ancestor species, *O. longistaminata* and *O. barthii.* The rest of the wild species belong to regions of Africa, Central and South America, Asia, and Oceania with conjoining spread. *Oryza sativa* has the smallest gene sequence and diploid genome among all food crops consisting of 430 million base pairs, and half of this genome is made up of repeated sequences. Some of the Oryza species are tetraploid with 48 chromosomes. Species in genes Oryza are classified into nine groups depending upon the similarity of the F_1 hybrids that are the first generation in meiosis [41, 42].

6. Chemical Properties

Rice comprises the hull (outside) and the caryopsis (inside). Hull makes the outer layer and consists of about 20% of the total paddy rice by weight, and it also has silica and cellulose. During the hulling process, the hull is removed and crypsis is exposed, which is brown rice that consists of bran, endosperm, and germ [43]. Then, in another process of millet, the bran layer and germ are removed, and white rice is obtained [44]. Bran and germ are rich in minerals, proteins, fiber, oil, and phytochemicals. When it comes to black rice, the hull is removed along with a small fraction of the bran [45]. The bran makes up 6%–7% of paddy rice by weight and

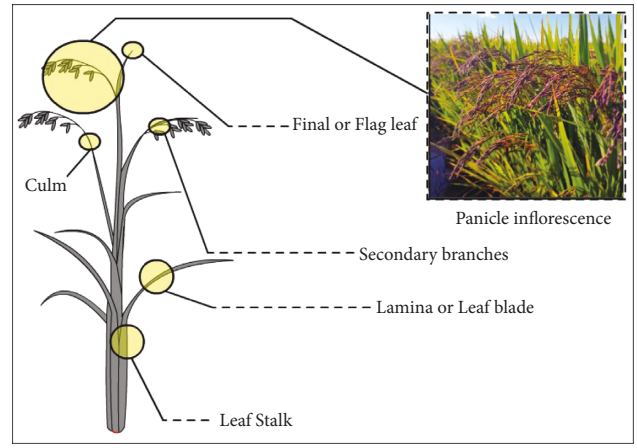

Figure 2: Formation of black rice.

comprises different layers [46]. Black rice is like other whole grains. The pericarp plays a protective color seed coat and has pigment, which makes rice appear brown, red, or black. Starch stores are majorly found in endosperm, which is about 75%, and proteins are found in an outer layer, which is sub-aleurone [47–49]. Mau et al. [50] believed that black rice contains lesser amounts of polysaccharides including dietary fibers (cellulose and hemicellulose, pectin, and resistant starch) and simple sugars. All these carbohydrates are mainly found in the outer layers. However, the germ of the seed has proteins and fat constituents of two to three percent (2%–3%) of the total weight of paddy rice.

Rice is a major crop that feeds more than half of the world's population. Aside from essential nutrients, black rice is a good source of phytochemicals, fiber, and minerals. In Asia, particularly in China, a variety of black rice cultivars are grown [51]. When compared to white rice, black rice has better nutritional and functional properties. This is owing to the presence of several bioactive and nutritious components in the embryo and the bran layers, such as functional lipids, essential amino acids, vitamins (A, B complex, and E), dietary fiber, minerals (Fe, K, Zn, Mg, Cu, P, and Mn), phenolic compounds, anthocyanins, y-oryzanol, tocopherols, phytic acid, tocotrienols, and phytosterols [47–49]. Black rice's endosperm contains around 75% carbohydrates, mostly starch and a protein-rich outer layer (sub-aleurone).

The maximum quantities of anthocyanin are found in black rice, which has a high nutritional value. The pericarp (outside part) of this rice's kernel is black due to an antioxidant pigment called anthocyanin [46]. The germ, which makes up around 2–3% of the overall mass of paddy rice, contains lipids and proteins. The inclusion of nutrients such as fiber, protein, B vitamins, minerals, vital amino acids, and others that are unique to sticky black rice is extremely helpful to human health. There is no other rice that comes close to black rice in terms of nutritional diversity. This rice is gluten-free, cholesterol-free, sugar-free, salt-free, and fat-free. Black rice is a high-fiber, antioxidant, anthocyanin, iron, vitamins B and E, thiamine, niacin, magnesium, and phosphorus whole grain rice [13].

6.1. Proteins. The germ, which makes up around 2 to 3 percent of the total weight of paddy rice, contains proteins and lipids. Although rice is primarily composed of starch, which provides energy, black rice also contains protein, which is found in the rice kernels. Rice protein can be classed based on how soluble it is. Glutelins, which are soluble in alkaline conditions and account for 60% of total protein, are accompanied by globulin (salt-water-soluble; 10%), a prolamin (alcohol-soluble; 25%), and albumin (albumin-like protein) (water-soluble; 5%) [38].

6.2. Minerals. Many vitamins and minerals, such as vitamin A, vitamin B, and iron, are found in black rice and are good for the overall prevention and health of heart diseases [52]. As compared to white rice, black rice contains more minerals, such as Zn, Fe, P, and Mn, and its mineral content is more variable, depending on the variety and soil type of the flowering location. The iron in black rice is required for healthy red blood cell synthesis, digestion, and energy expenditure, while potassium is required for muscle development [51].

6.3. Vitamins. This rice is high in fiber, vitamin E, iron, and a variety of other important minerals. A rice variety is used as both medicine and food [13]. Because of its high amounts of vitamins B and E, it is considered a "superfood" that may reduce the risk of cancer. Vitamins and minerals are beneficial for overall health and heart disease prevention [53].

6.4. Fiber. Black rice is thought to be a high-fiber food. Black rice is usually sold unmilled, which implies that the rice's fiber-rich black husks have not been removed. This rice is cholesterol-free, gluten-free, and low in salt, sugar, and fat [13]. Black rice is high-fiber whole grain rice that is extremely healthy. The most common type of fiber is insoluble fiber, which accounts for about 75% of the total. Black rice has higher fiber content than white rice, which is preferable [38]. The consumption of black rice in the diet was hypocholesterolemic. The hypocholesterolemic impact of black rice is thought to be due to a combination of dietary fiber and other bioactive components such as polyphenols [54].

6.5. Anthocyanin. Black rice is rich in anthocyanin and has a high nutritional value. Its dark purple color comes from a higher anthocyanin content than other colored grains. Anthocyanins are a collection of water-soluble reddish-purple flavonoids found on the pericarp, aleurone layer, and seed coat. Anthocyanin is one of the black rice ingredients that help protect arteries and prevent DNA damage by mopping up toxic chemicals. Anthocyanins are the flavonoid pigments found in black rice, and they are a source of antioxidants that can prevent or limit the generation of reactive cell-damaging free radicals [55].

7. Bioactive Composition of Black Rice

Preservation of pigmented rice is of prime importance for a sustainable environment and in providing a surety for food security in the future. Pigmented rice is gaining popularity due to its therapeutic potential [17]. They are also high in proteins, minerals, and vitamins [56]. They are anti-atherosclerosis, anti-allergic, and cancer-preventive. They also improve the condition of iron deficiency anemia [57]. The nutritional profile and bioactive components of this rice have gained popularity in research as well due to their ability to lower the chances of heart disease, diabetes, and inflammation. The formation of flavonoids requires phenolic compounds as their precursor [10]. The bran layer of rice has been shown to contain anthocyanin, which has antioxidant potential by scavenging free radicals. Rice is one of the most researched foods about fortified food and clinical research. Due to its antioxidant potential, pigmentary rice is gaining popularity in research studies in South America, Africa, and Europe [13]. Because of its nutritional profile, researchers and scientists have considered black rice as a superfood [58]. Black rice is a wholesome variety of rice that contains a generous amount of protein along with a high amount of fiber, vitamin B, antioxidants, iron, thiamine, vitamin E, magnesium, phosphorous, and niacin. It comprises the highest percentages of antioxidants, protein, and dietary fiber among all rice varieties [59]. Black rice has also been recognized as an excellent source of phytosterols, carotenoids, phenol carboxylic acids, bioflavonoids, and phytochemicals (Figure 3).

7.1. Phytosterols. Secondary metabolites are present in black rice grains in a wide range. An antioxidant g-oryzanol, which contains a combination of phytosterol, is present in high amounts in black rice than in white rice [60]. Campesterol ferulate, 24-methylenecycloartanyl ferulate, cycloartenol ferulate, and beta-sitosterol contribute to the nutrition. Zubair et al. [61]; Pereira-Caro et al. [62]; and Jesch and Carr [63] reported that phytosterols play important role in controlling several unwanted lipoproteins in blood inhibiting the cholesterol absorption in adipocytes.

7.2. Carotenoids. One of the important classes of nutritionally beneficial components is carotenoids [64]. About more than 90% of the carotenoids produced by rice comprise lutein and zeaxanthin. Trace amounts of lycopene and beta-

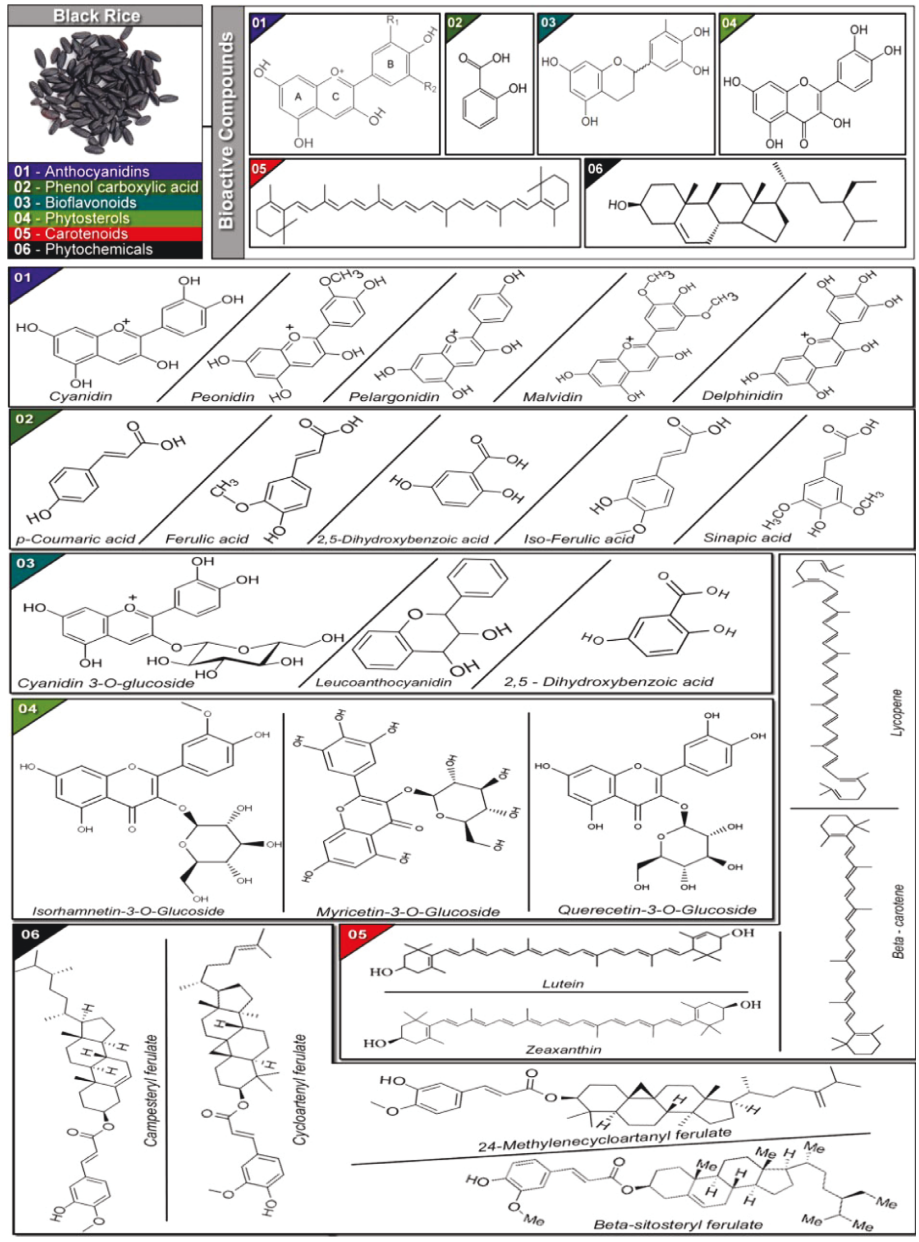

Figure 3: Bioactive components obtained from black rice.

carotene are found in carotenes [65]. The bran layer of black rice has a generous amount of these compounds. However, negligible amounts of carotenoids are found in milled rice [66]. Carotenoids are associated with pigmentation and genetic makeup, so they are mostly present in black rice [67]. A comparatively higher concentration of carotenoid is present in black and red rice as compared to white rice [66].

7.3. Phenol Carboxylic Acids. Zhang et al. [68] and Gunaratne et al. [69] reported that higher levels of phenolic carboxylic acids are found in black rice as compared to white rice. Cinnamic acid is a precursor for the making of several phenolic acids, including major p-coumaric acid, ferulic acid, 2, 5-dihydroxybenzoic acid, isoferulic acid, and sinapic acid [70]. Syringic acid is found in the extract of black, brown, and red rice [71], while pinellic acid is found in red and white rice and hydroxybenzoic acid is present in black rice [72, 73].

7.4. Bioflavonoids. The main flavonoids found in black rice are anthocyanins, and Galland et al. [74] reported that the synthesis of delphinidin, pelargonidin, and cyanidin is done by oxidization reaction and is catalyzed by anthocyanin synthase of leucoanthocyanidin. Flavonoids and particularly anthocyanins cause purple and blue color pigmentation in purple and black rice. The most prominent compounds are cyanidin-3-O-glucoside, peonidin-3-O-glucoside, cyanidin-3, 5-glucoside, pelargonidin-3-O-glucoside, peonidin-3-O-(600-O-p-coumaroyl) glucoside, cyanidin-3-O-(600-O-p-coumaroyl) glucoside, and cyanidin-3-O-arabidoside [62, 68].

7.5. Phytochemicals. Black rice is a vital and abundant source of phytochemicals, and the dehulled seeds of Japanese black-purple rice have twenty-three secondary metabolites, comprising anthocyanins, flavones, isorhamnetin-3-O-glucoside, and myricetin-7-O-glucoside, and flavonoid glycosides, quercetin-3-O-glucoside, vitamin E (tocopherols and tocotrienols), carotenoids, and y-oryzanol have been characterized both qualitatively and quantitatively, and they provide health benefits. They also make black rice a functional food [75, 76]. Anthocyanins are responsible for the dark color of the rice. 90% of anthocyanin components in black rice are about 26.3%, and cyanidin-3-O-glucoside and peonidin-3-O-glucoside are the main effective components. Anthocyanins are flavonoid pigments with antioxidant potential that protect the body against free radicals, thus slowing down aging and preventing cancer and other chronic diseases including cardiovascular diseases and diabetes. Improvement in memory and brain function and coordination is also reported by black rice [6]. Its antioxidant potential improves visual and neurological functions. It also shows antimicrobial properties. Anthocyanins are also used to treat a wide variety of other health problems such as blood pressure and urinary tract infections. Black rice has been reported to be the rival of blueberries in terms of its antioxidant power. Kushwaha [13] carried out a study at the American Chemical Society, and he reported that one spoonful of black rice bran contains more anthocyanin when compared with fresh blueberries.

8. Utilization of Black Rice and Its Components in the Food Industry

It is now clear that how black rice has a superior level of quality over the other varieties of rice regarding appearance and nutrition. It is rich in protein, fat, riboflavin, thiamine, zinc, tocopherols, and iron. Because of its health and nutritional advantages, black rice is becoming more common in the food choices of people and replacing white rice slowly. Utilizing black rice in various foods can enhance the nutritional value of food and be transformed into functional food items [4]. Functional foods may help with diverse health problems such as diabetes, obesity, high blood pressure, and heart diseases [20]. The black rice variety is not very well-known among the general population and can be thought of as a novel and healthier alternative to various food items for generations to come. The use of black rice in various food processing industries can enhance the nutritional value of traditional food items [13].

9. Applications and Quality Attributes of Black Rice

Due to numerous health-promoting and disease-preventing effects, black rice cultivars have been the subject of exploratory research regarding their potential applications and processing technologies to improve quality attributes and provide beneficial health properties. Black rice is utilized as a primary or small ingredient in paella, rice cakes, cooked rice, pancakes, and cereals [77]. Because of its unique functions, it has become a major ingredient in a variety of new foods such as drinks, puddings, children's meal porridge, desserts, classic Chinese white rice cake bread, pasta, and bread. The studies in Table 2 have inspired research into the physicochemical and functional characteristics of starches and flours derived from black rice along with other kinds. This is because various factors can impact the quality of these flours and starches, such as size and structure of the grain's composition, gelatinization type, crystal polymorph, ratios of amylose and amylopectin, and the amylose-lipid complex, and that of a noncarbohydrate portion of the starch [95]. For instance, the external amylopectin, as well as amylose chains, could create double helices and join to form crystal domains, but in most starches, these are restricted to the amylopectin portion. Amylopectin-rich starches are the cause of crystallinity because of the creation of double helices between the chains that are external to amylopectin's molecules. Amylose does not affect the amount of crystallinity that occurs in glutinous and normal black rice starches, but it can contribute to crystallinity in starches with high amylose [96]. Amylose is among the most important factors in the rice's quality, particularly when it comes to the properties of cooking and pasting. The rice that has a low amylose content will be dry and sticky when cooked, while black rice that has a moderate amount of amylose can be dry and airy after being cooked, and it retains its soft texture even after cooling as well. Black rice that has a high amount of amylose will also become dry and fluffy after being cooked, but it becomes harder as it cools because of the retrogradation of amylose molecules [97]. Starches from black rice that have more amylose typically have a higher temperature for pasting, a lower peak viscosity, and greater setback viscosity. In contrast, those with lower levels of amylose tend to have less retrogradation and a higher swelling capacity [98]. The black rice starch has distinct characteristics. It is a mild taste and smells odorless in addition to being white in color, nonallergenic, and digestible in the tiny granular form [47]. Starch granules made of black rice are comparable to other varieties of rice and are the smallest among cereal grains, having an average size of between 3 and 8 mm. They are polyhedral and with irregular shapes, sharp edges, and sharp angles [48], which makes them perfect for use as a cosmetic dusting powder, a fabric stiffener, and fat mimetics in food [99].

10. Processing Technologies of Black Rice

While rice starch is extensively used in its original form, its use is limited by factors such as high viscosity, insufficient solubility, high-temperature degradation, and the high likelihood of retrogradation. Therefore, both conventional and nonconventional sources of starch are altered by treatment (enzymatically and chemically) to meet the particular requirements of industries, by adjusting their functional and physicochemical properties. The methods for enzyme modification are complicated and time-consuming, which is why they are not widely used in the industry of food. Chemical modification is often employed because it is quicker, but there are risks with the presence of chemicals in the product [100]. There is a rising trend to modify the physical properties of black rice with green technology [101]. As per Zhu [102], the bioactive substances that are found in black rice may react with the starch in

Table 2: Food applications of black rice and their components.

Procurement	Black rice product	Mixing	Quantity and ratios	Phytochemicals	Conclusion	References
Rural Development Administration, Korea	Noodles	Bran powder: wheat flour	98 : 2; 95 : 5; 90 : 10, and 85 : 15 (w/w)	Polyphenolics, flavonoids, phytic acid, and anthocyanins	Improved the antioxidant activities when compared to the control noodles	[78]
Local Market of Manipur, India	Pasta	Black rice + Joha rice	30%, 55.32%, and 14.68%	Anthocyanin, total phenolic content, and DPPH scavenging activity	Conventional pretreatment method showed less degradation of anthocyanin and phenolic compound than sous vide and microwave processes	[79]
Chiang Mai, Thailand	Vinegar	Steamed rice	100 g	Total phenolic compounds, total acid, and acetic acid	Work as an antioxidant, anticancer, and antibacterial agent against various disorders	[80]
Zibo, Shandong Province, China	Beer	Black rice flour + malt	6.80 kg + 15.20 kg	Total polyphenol contents, Cyperus japonicus -3-O-glucoside (C3G), and paeoniflorin-3-0-glucoside (P3G)	The polyphenol content that influences the antioxidant ability and foam stability of extruded rice adjunct beer	[81]
Research Institute of Korea	Wine	Rice: black rice	1 kg: 0 + 800 g: 200 g + 600 g: 400 g + 400 : 600 g	Citric acid, malic acid, succinic acid, lactic acid, and acetic acid	The concentration of antioxidant was significantly increased with increasing amount of black rice. As a result of sensory evaluation, overall preference was high in rice wine made with less than 20% of black rice	[82]
Maha Sarakham Province, Thailand	Punch	Flavored yogurt	0.2, 0.4, and 0.6% by weight	γ-Oryzanol, total phenolics, and anthocyanins	A good stability of color and increasing phytochemicals contributed by black waxy rice bran	[83]
Nong Don District, Saraburi, Thailand	Milk chocolate	Anthocyanin powder + cocoa powder	3, 5, and 7 g	Antioxidant	Milk chocolate with 42% anthocyanin powder was selected as the most desirable health product with overall acceptance	[84]
Yogyakarta, Indonesia	Kefir	Black rice extract	Goat milk + inulin; goat milk and black rice extract (1 : 1); and goat milk + black rice extract (1 : 1) + inulin. Inulin was added in GM + IN and GM + BRE + IN as much as 0.5 g/100 ml	Total phenolic contents	Kefir can be used to treat diabetics as it acts as an antidiabetic agent	[85]

Table 2: Continued.

Procurement	Black rice product	Mixing	Quantity and ratios	Phytochemicals	Conclusion	References
Imphal, Manipur, India	Chicken nuggets	Rice flour + other ingredients	1, 3, and 5%	Antioxidants	The higher the nutritional value, the greater the textural properties of the final product and the better antioxidant activity	[86]
Chiang Mai Province, Thailand	Mayonnaise	Fish oil: black glutinous rice flour: soybean oil: vinegar: egg yolk: salt: potassium sorbate: mustard	Oil mixture (3 : 1 weight ratio of soybean oil to fish oil), 9.5 g, 8.9 g, 1.3 g, 1.0 g, and 0.7 g	Tocopherols, carotenoids, and antioxidants	The synergistic impact of all antioxidants can improve the oxidative stability of mayonnaise	[87]
Shaanxi Taiji Huaqing Technology, China	Bread	Black rice extract powder: bread flour	0%, 1%, 2%, and 4%	Anthocyanin	The experimental product may be an alternative to making active bread with the lower digestive rate and additional health benefits	[88]
Taichung, Central Taiwan	Chiffon cake	Black rice and wheat flour	0%, 20%, 30%, 40%, 50%, 60%, 70%, 80%, 90%, and 100% (w/w)	Total phenols, total anthocyanins, and antioxidant property	Black rice significantly enhanced the bioactive components in the experimental product than the control. Therefore, it can be incorporated into bakery products with more bioactive components and more effective antioxidant activity	[50]
Gimpo, Korea	Cookies	Powder	Control and 7%	Antioxidant	Significantly improve the total phenol content and DPPH radical scavenging ability in the product	[89]
Thailand	Crackers	Brown Brown oyster Brown mussels Black rice Black oyster Black mussels	100% 80% + 20% 80% + 20% 100% 80% + 20% 80% + 20%	Antioxidant properties and total phenolic content	Significantly improved the antioxidant activity and total phenolic content in both cracker types due to the addition of functional ingredients	[90]
Zlín, Czech Republic	Muesli mixture	Kamut, einkorn, red and black quinoa, or rice flakes together with hibiscus, mallow, rose	60–70% of nontraditional flakes and 30–40% of lyophilized fruits and edible flowers	Anthocyanins, cyanidin-3-glucoside, delphinidin-3-glucoside, quercetin, epigallocatechin, flavonoids, sinapic and protocatechuic acids	Nontraditional muesli blends can be a valuable source of nutrients and biological components	[91]

Table 2: Continued.

Procurement	Black rice product	Mixing	Quantity and ratios	Phytochemicals	Conclusion	References
Guilin, Guangxi Province, China	Porridge	Waxy and non-waxy black rice	40 g	Total phenolic content, total flavonoid content, condensed tannin content, monomeric anthocyanin content, cyanidin-3-glucoside, and peonidin-3-glucoside	Heat treatment in black rice porridge has significantly reduced these biological compounds. It can retain a lot of antioxidants (such as phenolics) and maintain the stability of the functional substances. Therefore, rice porridge in the form of cooking black rice can have more health-promoting effects	[58]
Kanpur, India	Soup	Black rice, okra, and barley	(50 : 10 : 40), (50 : 15 : 35), and (50 : 20 : 30)	Anthocyanin and antioxidants	The soup can be easily swallowed by patients, who cannot chew and keep human health away from any inflammatory conditions such as allergies, cancer, asthma, atherosclerosis, and arthritis	[92]
Assam, India	Kheer	Black rice and xylooligosaccharides	5%, 8%, and 10%	Antioxidants	It can be used against various noncommunicable diseases	[93]
Kuta Selatan, Indonesia	Skin cream	Bran and powder	35%	Antioxidant	It increased the expression of matrix metalloproteinase-1 and density of dermal collagen in the skin to UV rays	[94]

gelatinization, affecting its pasting, thermal, and digestibility characteristics. The principal methods employed to examine the various analysis of quality in the black rice include scanning electron microscopy (SEM) and differential scanning calorimetry (DSC) within the flour and X-ray diffractometry, rapid visco analysis (RVA) high-performance liquid chromatography (HPLC)-photodiode array (HPLC-PDA), mass spectrometry (LC-MS), liquid chromatography (LC-MS), ultraviolet/visible (HPLC-UV/Vis), a fluorescent detector (HPLC-FLD) and texture profile analysis within the grain [47], and polarized light microscopy (PLTM) and Fourier transform infrared (FTIR) spectrum within the starch [48, 101, 103, 104].

The applications for the development of new goods are generally treated by steaming, boiling pan-frying, or roasting. These techniques can affect the bioactive components such as anthocyanins and phenolic acids, which can cause an increase in antioxidant activity [77]. Ryu and Koh [105] examined their thermal stability for phenolic acids. They discovered that all cooking techniques resulted in significant increases in the total amount of phenolic acids. However, no significant change was observed in the quantity of inbound phenolic acids. The protocatechuic acid content free increased eleven-fold for cooked white rice as compared to raw rice. The acid showed a negative correlation with the total content of anthocyanins, which suggest that it is produced by the thermal breakdown of anthocyanins. Additionally, Melini et al. [106] reported that the main pigmented rice varieties have been recognized as a good source of carotenoids, total phenolic compounds, and anthocyanins. In this study, various cooking methods was used to investigate the impact of cooking methods on these ingredients. The results reveal that the main carotenoid (lutein), free anthocyanin, and phenolic compounds were reduced in all samples, while anthocyanins were observed only in black genotypes. On the other hand, it was observed that insoluble phenolics increased in some samples. Anthocyanins are potent natural colorants because of their high content of pigment and low toxicity. This means they could be utilized

within the industry of food as replacements for synthetic dyes. For instance, He et al. [107] created an easy method of removal and separation of the anthocyanins extracted from black rice, using water for extraction and membrane separation and resin adsorption to purify. However, using anthocyanins in food formulations, particularly in aqueous systems, is difficult because they can be reactive and are prone to degradation to brown or colorless compounds. Anthocyanins are believed to be affected by a variety of aspects, such as temperatures of heat treatment, storage temperature addition to exposure to UV and light pH value's chemical structure [108]. Therefore, the food industry is always looking for efficient and cost-effective methods to produce colorants that are powdered and condition-sensitive. A few studies have been conducted on the degradation of pH and thermal bioactive compounds' kinetics, particularly anthocyanins derived made from black rice [109].

A previous study assessed the effects of gamma radiation (0, 1, 2, and 3 kGy) on the thermal degradation and stability of anthocyanins and the stability of the total phenolic compound and antioxidant activity at various temperatures in the black rice flour [38]. The results revealed that combining radiation at different temperatures could enhance the shelf-life of black rice flour. According to Norkaew et al. [104], there is evidence to suggest that the stability of bioactive substances in rice may be affected by certain postharvest treatment methods, such as temperature and time of drying, storage, and packaging. Numerous studies have attempted to limit the depletion of bioactive substances in addition to improving the qualities of black rice, such as through the creation and selection of high-potential phytochemical genotypes [2, 110] and the high-temperature fluidization method [111]. Papillo et al. [112] have discovered polyphenolic anthocyanin-rich extracts made from Italian black rice. The rice was processed using spray drying and freezing to get ingredients that could remain more stable in baking and storage. The extracts in powdered form were tested as ingredients that could be used in a model food baked (biscuit). The biscuits with enriched ingredients had a greater number of polyphenols, anthocyanins, and antioxidants when compared to the unenriched biscuit. The researchers found that bioactive substances can be dried by spray to produce powders that are more stable components for nutraceuticals and functional foods.

11. Future Uses

More attention is being paid to the essential antioxidants and nutrients in black rice and bran. Research conducted by researchers from Louisiana State University in 2010 indicated that food manufacturers were adding black rice bran into certain food items such as cakes, cereals, cookies, and beverages to improve nutrition and make health improvements. Apart from its role as a diet or staple of grains, Chinese black rice is utilized to create vinegar that is black, specifically from the Zhejiang variety that comes from this area of China. Vinegar, when not transcribed into pinyin, is written with the correct spelling as Chekiang. This kind of vinegar is as balsamic vinegar. Chinese black rice can also be used to produce different types of wine. Most of them are fragrant and delicately scented. They are excellent for drinking and for cooking purposes. Black waxy rice is among the sources of plants with anthocyanins with a dark purple hue. The colorant powder has more phytochemicals than the untreated bran. The efficacy of using colorant powder has been realized by giving a pinkish-purplish color to yogurt, which results in the best durability of color, as well as the increase in phytochemicals produced by the rice bran that is black and waxy. This makes the powder a possibility to use in food products to act as an effective food colorant, but to make further use of this colorant for food use to other food products additional quality assessments are needed including safety and sensory evaluation. Jun et al. [113] discovered that black rice bran is a source of phenolic compounds with a high antioxidant capacity. Jun and others identified ferulic acid as the principal phenolic compound found in the bran of black rice and suggested the utilization of the bran of black rice as an organic source of antioxidants. Particularly, the ethyl-acetate subfraction 2 and its subfraction 1 are able to be utilized as food additives that can be used in cereals, breakfasts, snack foods, bread, cakes, beverages, cookies, and many other food items because they possess greater antioxidant power than butylated toluene (BHT). The black rice bran is a source of gallic, hydroxybenzoic, and protocatechuic acids with higher amounts than regular and red rice bran. In addition, adding 5% bran from black rice to wheat flour for bread making resulted in a significant increase in antioxidant and free radical scavenging activity, compared with regular bread [114]. The diverse physical properties of varieties of black rice have been studied, and the results can be used as baseline information for food processors to check the quality of black rice for special processing of food [115]. Kim et al. [5] claimed that adding the right amount of black and blueberry powders improved the general quality of Korean traditionally brewed rice wine Takju. It was found that the DPPH radical scavenging capability of the mead derived from black rice grains was greater than beverages made of polished rice. The inhibitory effect of lipid peroxidation from mead made of black rice grains was greater [116]. The anthocyanin content of beverages made with raw black rice was higher than the content of beverages prepared from the cooking of the black rice. The antioxidative capacity of alcohol drinks made from raw black rice was superior to drinks made from prepared black rice [117]. Therefore, the black rice (*Oryza sativa*) along with its derivatives is becoming increasingly sought-after and is consumed extensively throughout China, Japan, Korea, and other East Asian countries such as Thailand [62, 118].

12. Health Benefits of Black Rice

The health benefits of colorful black rice are numerous. The deep color of the grain is one of the most noticeable. Amino acids, fatty acids, antioxidants, flavonoids, anthocyanins, and other phenolic compounds are abundant in black rice. Black rice contains 18 amino acids, with an essential and nonessential type. Amino acids are essential for a variety of

Table 3: Role of black rice against various disorders.

Diseases	Animals	Duration	Analysis	*In vitro/ in vivo*	Results	References
Hypercholesterolemia disorder	48 Wistar male rats	30 days	Biological analysis	*In vivo*	Black rice significantly reduced the level of plasma cholesterol, triglycerides, and low-density lipoprotein levels in rats compared with rats fed with whole rice diet	[54]
Diabetic nephropathy	Sprague Dawley rats	8 weeks	Blood metabolites	*In vivo*	Supplementation of black rice significantly decreased blood glucose and serum insulin, improved the renal function, and relieved renal glomerular sclerosis and interstitial fibrosis of diabetic nephropathy rats	[119]
Breast cancer	Female immunodeficient BALB/*c* nude mice	28 days	Cell viability	*In vitro and in vivo*	The anticancer impact of anthocyanin-rich extract from black rice significantly works against human breast cancer cells in vitro and in vivo by affecting apoptosis and suppressing angiogenesis	[120]
Obesity	Sixty male-specific pathogen-free mice	12 weeks	Biochemical analysis	*In vivo*	Whole grain black rice significantly reduced lipid accumulation and normalized levels of protein or gene expression related to liver and intestinal lipid metabolism in treated mice	[121]
Osteoclastogenesis and osteoporosis	Female Sprague Dawley	16 weeks	Histomorphometric and biochemical analysis	*In vitro and in vivo*	Fermented black rice with Lactobacillus casei extract can inhibit the production of reactive oxygen species and the activation of mitogen-activated protein kinase and nuclear factor-kappa, thereby reducing the c-Fos and nuclear factor of activated T cells. Lastly, oral administration of Lactobacillus casei extract modified bone microarchitectural parameters and characteristics associated with ovariectomy-induced osteoporosis in rats	[122]
Liver damage	Male mice	12 weeks	Biochemical and gene expression analysis	*In vivo*	The complementary diet had significantly decreased serum triglycerides and LDL cholesterol levels in the liver and nonsignificant effect on serum and liver total cholesterol in mice	[123]

Table 3: Continued.

Diseases	Animals	Duration	Analysis	*In vitro/ in vivo*	Results	References
Atherosclerosis	Male Sprague Dawley rats	12 weeks	Hematological parameters	*In vivo*	The thrombogenic ratio of thromboxane A_2, prostacyclin, serum calmodulin and triglyceride, platelet hyperactivity, hypertriglyceridemia, optimal platelet function, and soluble P-selectin was significantly decreased, while raised in body weight, hepatic CPT-1 mRNA expression in rats fed a high-fat diet supplemented with anthocyanin extract from black rice	[124]
Diabetes mellitus	Adult male Wistar rats	12 weeks	Biochemical analysis	*In vivo*	The plasma glucose, cholesterol, triglyceride levels, insulin resistance, and glucose tolerance were reduced, while the degree of insulin secretion in rat plasma was significantly increased upon germinated black rice extract treatment	[125]
Hippocampal neuronal damage	Male mice	21 day	Histological analysis	*In vivo*	Black rice extract profoundly attenuated neuronal cell death, inhibited reactive astrogliosis, and prevented loss of glutathione peroxidase expression in the hippocampus when compared to vehicle treatment	[126]
Digestive disease	—	—	Glycemic index and hydrolysis	*In vitro*	Black rice extract significantly improved the gastrointestinal health and glycemic index of the prepared gels. Additionally, starch hydrolysis has been suppressed by inhibiting digestive enzymes	[127]
Hyperlipidemia	Male Sprague Dawley rats	8 weeks	Biochemical analysis and oxidative stress	*In vivo*	Black rice is significantly preventing and ameliorating the hyperlipidemia in rats fed with a high-fructose diet	[18]
Photoaging of the skin	—	—	Cell viability and proteomic analysis	*In vitro*	The black rice extract could be modulating mitogen-activated protein kinase, the inhibition of reactive oxygen species generation, and activator protein-1 signaling in prepared solution	[128]

bodily activities, including skin and tissue regeneration, energy production, and digestion (Table 3).

Anthocyanins are pigments that can be found in a variety of blue and purple foods and serve to protect your cells from harm. These pigments have also been linked to a reduction in inflammation and a lower risk of cardiovascular disease. Consuming black rice can help you improve your heart health and general fitness [129]. Tocopherol in combination with anthocyanins present in black rice shares a role towards health and reduces noncommunicable diseases (NCDs) [130]. They also show anticancerous potential by scavenging free radicals. Meals added with black rice can prevent and ameliorate conditions of diabetes, atherosclerosis, obesity, asthma, digestive health, stroke, and cancer. Anthocyanins of black rice also provide neurological protection, visual improvement, and antimicrobial potential. They are also

used to treat minute health issues including UTI, cold, and blood pressure. Black rice when added to meals is known to improve life span and quality of life [14]. Antioxidants were claimed to be abundant in black fragrant rice (Hom Nil variety). It contains 186.20 mg GAE/100 g of total phenolics and 24.55 mg/100 g of anthocyanins, respectively. When milling for 10 seconds (p 0.05), phenolic content dropped abruptly to 127.82 mg GAE/100 g and then progressively dropped to 61.01 mg GAE/100 g after 100 seconds. Changes in anthocyanin content during milling followed a similar pattern. Anthocyanin levels in raw black rice dropped to 7.46 mg/100 g after 10 seconds of milling (p 0.05), followed by minor changes for the next 30–60 seconds. Finally, grinding the black rice kernel for 100 seconds fully removed the anthocyanin pigments. During milling, antioxidants were lost. As a result, the DPPH scavenging activity of raw black rice (227 mg AAE/100 g) was demonstrably lowered to 175 mg AAE/100 g after only 10 seconds of milling (p 0.05). Additional milling (30–100 s) resulted in a small decrease in DPPH activity, which dropped to 118 mg AAE/100 g. Polyphenolics, flavonoids, vitamin E, phytic acid, and oryzanol are all antioxidants found in black rice. Other researchers such as Zhou et al. [131] and Walter et al. [132] found that the light brown pericarp (70–90%) and black pericarp (92–97%) had higher levels of phenolic chemicals. After milling, antioxidant activity decreased due to a decrease in antioxidants. Milling black grains had an effect on antioxidant activity that was similar to that of polyphenols. When black rice was polished, it decreased by about 88 percent. When all was confidently eliminated, only 35% of antioxidant activity was seen in this study. Black rice milled for 10 seconds showed 77% of the antioxidant activity of black rice [133].

Today, one of the most prevalent diseases is systematic inflammation. This inflammation can be regarded as the key factor contributing towards chronic diseases including asthma, Alzheimer's disease, cardiac disorders, and cancer. Inflammations at the cellular level are reduced due to the consumption of black rice. Reduction in cellular inflammation results in a reduction in systematic inflammations. It also improves the cell health and overall health [134]. Anti-inflammatory mediators including superoxide dismutase increase when black rice is consumed. Hence, it provides a shield from allergic reaction, joint pains due to inflammations, and aging [135]. Black rice bran when added to meals has shown to improve conditions such as dermatitis by reducing inflammation of dermal and epidermal cells [136]. An extract of black rice was discovered to help minimize edema and greatly suppress allergic contact dermatitis on the skin of mice in the study. This is a strong indication of black rice's ability to heal disorders related to chronic inflammation [137].

Gut health and digestion improve when food contains a high amount of fiber. Black rice contains a generous amount of fiber. Studies have shown that black rice contains double the fiber as compared to brown rice. Fiber promotes satiety as it passes through the gastrointestinal tract, results in reduced energy intake, and promotes weight loss [138]. Black rice also adds bulk to the stool and aids the easy release of stool from rectum, preventing the constipation. It also takes away toxic compounds by binding them with fiber, thus helps detoxifying the body. Black rice is low in calories, low in carbohydrates, and high in dietary fiber, all of which are important for weight control and weight loss. As a result, it makes you feel full and prevents hunger pangs. In fact, a study conducted in Korea compared the weight loss caused by white rice to a combination of brown and black rice in 40 overweight women over the course of six weeks. They discovered that the brown/black rice group lost considerably more weight and had a lower body mass index (BMI) and body fat percentage than the white rice group at the end of the trial. This merely goes to prove that both brown rice and black rice can be effective in obese women's diet therapy [139].

Black rice is reported to prevent cardiovascular health by preventing the formation of plaque in arteries. Plaque formation in arteries can cause blockage, which reduces or stops the flow of blood, thus leading to a condition called hypertension [140]. The addition of black rice to meals can reduce the levels of triglycerides (TGs) and low-density lipoproteins (LDLs). By lowering these parameters, heart health can be improved. Anthocyanins of black rice have the potential to reduce the risk of heart attack by preventing atherosclerosis. Recent research has shown that black rice can improve the high-density lipoprotein (HDL) levels. Black rice has also shown a ameliorative effect on hardening of arteries walls [141]. Research has shown that black rice has improved HDL and reduced the TGs and LDL level in rats when given in diet. A black rice-containing diet can improve the condition of hyperlipidemia. Black rice is proven to reduce the risk of heart disease and stroke by 57% [142]. White rice is replaced with black rice in your regular diet to protect your heart's health. High cholesterol, as we all know, is a leading cause of a variety of cardiovascular problems. However, several research investigations have indicated that the anthocyanin content of black rice has a substantial effect on lowering cholesterol in rats [143]. Atherosclerosis is a cardiovascular condition in which plaque builds up in the arteries, causing them to become clogged. This could lead to coronary artery disease, stroke, peripheral artery disease, or kidney problems, among other major issues. However, there is some good news! In rabbits, black rice consumption was reported to lower atherosclerotic plaque build-up by 50 percent [140].

Mutation in genes can cause uncontrolled cell division leading to a condition called cancer. Cancer formation that is also known as carcinogenesis consists of the following steps: initiation, promotion, and progression by uncontrolled cell division. Any damage to DNA of the cell leads to malignancy in the cells [144]. This damage to DNA can be due to any physiological or physical factor. These factors may be an error during cell division, toxins, environmental factors, stress, inflammation, or reactive oxygen species (ROS). These ROS can be formed by both exogenous and endogenous factors [145]. The body tries to maintain a balance by neutralizing these ROS with the help of defense mechanisms including glutathione, catalase, and superoxide dismutase. Excessive production of these free radicals or ROS can damage DNA and initiate cancer [142]. Excessive production of ROS is caused by the contribution and combination of factors such as

dietary choices, genetic factors, and environmental factors. Breast cancer, colon cancer, and prostate cancer are greatly found to be associated with dietary choices and lifestyle. Many studies have proven the association of colon cancer risk with increased consumption of red meat and saturated fats, and this risk can be reduced by consuming fibrous foods. In recent years, dietary choices have gained great attention in reducing the risk of cancer [132]. In vitro studies, active food components have been used to treat cancer, along with chemotherapy and radiotherapy, with chemo being unpropitious to healthy cells. Dietary components have shown great potential as an antioxidant, thus suppressing cancer development [146]. Protecting DNA from damage prevents the carcinogenesis by modulating initiation through phytochemicals. It also stops the proliferation of cancer cell and promotes cell death in cancer cells. Antioxidants prevent the onset of cancer development by the prevention of the formation of free radicals. Moreover, black rice has shown the potential to slow down metastasis. Black rice extract has also shown a cancer-preventive effect [147]. Terpenes, isothiocyanates, carotenoids, and flavonoids, which are widely present in fruits and vegetables, have cancer-preventive effect. Mode of actions of biological value such as anticancerous and antioxidative is shown by the secondary metabolites, i.e., flavonoids and its class anthocyanins. Peonidin, peonidin-3-glucoside, cyanidin-3-glucoside, and other major anthocyanins of black rice have been reported to show a shield from cancer cell invasion [4]. In the past few years, studies have proven that anthocyanins have an exceptional ability to suppress oxidative stress and initiation of apoptosis in cancerous cells, which shows the anticarcinogenic potential of anthocyanins. Cyanidin and peonidin-3-glucoside, which are present in the extract of black rice, have proven to show cancer inhibition potential and protective effect on endothelial cells from free radicals [12]. The anticancer properties of black rice are due to the anthocyanin concentration. An anthocyanin-rich extract of black rice successfully inhibited tumor growth and spread of breast cancer cells in mice, according to an experimental study done by China's Third Military University [120].

Phytosterols, carotenoids, polyphenols, and fatty acids have been studied in in vitro and in vivo studies as worthy alternative in the management of hepatotoxicity and associated complications. They have shown anti-inflammatory and liver protective potential [12]. Black rice has a direct influence on liver health, and it also shows the reduction in risk factors that lead to fatty liver. A healthy liver can protect the body from many other illnesses. Black rice mounts up liver functionality and detoxifies liver. Condition of increased blood glucose level and blood cholesterol level also improves as black rice enhances the metabolism of fatty acids [148]. Fatty liver disease is characterized by an accumulation of fat deposits in the liver, as the name implies. Mice were used to investigate the efficiency of black rice in treating this illness. The antioxidant activity of the black rice extract was found to control fatty acid metabolism and lower triglyceride and total cholesterol levels, lowering the risk of fatty liver disease [149].

Type II diabetes is one of the most widely found diseases around the globe that leads to insulin resistance and other complications associated with metabolism. Anthocyanins are found in fruits and vegetables. Black rice is also a good source of anthocyanins. Research based upon animal models, using cell lines and clinical trials including human subjects, has suggested that anthocyanins of black rice possess antidiabetic properties. Literature shows that anthocyanin has a role in improving the insulin resistance, protecting β cells, enhancing insulin output from cells, and decreasing absorption of sugar in intestine cells [150].

The bran, which is a repository of nutritional fiber, is intact in whole grain black rice. Because the fiber takes longer to digest, it ensures that the sugar in the grain is absorbed over a longer period, allowing blood sugar levels to remain stable. As a result, it can help prevent type 2 diabetes by preventing insulin levels from rising too high. In fact, in mouse research, the extract of germinated Thai black rice behaved similarly to the diabetic medicine metformin, preventing and managing diabetes mellitus complications. Anthocyanins, a type of flavonoid, affect blood sugar levels and diabetes control. Phytochemicals have a good impact on your body, boosting insulin sensitivity and allowing you to use glucose more effectively. They also aid in lowering blood sugar levels by slowing sugar digestion in the small intestine [125].

Clinical studies also showed that anthocyanins helped to improve learning capacity and reduce symptoms of depression. By adding black rice in the diet help to boost memory and prevent premature cognitive aging. Anthocyanins have antioxidant potential that imposes a positive impact on brain cells and their function. Age-related conditions such as dementia, Alzheimer's disease, and depression are prevented or reduced due to these anthocyanins of black rice. They also found to improve memory-related issues and improve cognition and learning abilities [149]. Many scientists feel that oxidative stress has a negative impact on cognitive performance. As a result, antioxidants such as anthocyanins (found in black rice) may help to minimize oxidative stress and protect brain health. Anthocyanins were discovered to increase learning and memory function in rats suffering from estrogen deficiency in a study conducted by the Medical University of Bulgaria. [151] Another six-year study of 16,000 adults found that eating anthocyanin-rich foods for a long time delayed the rate of cognitive deterioration by up to 2.5 years [152].

Atherosclerosis is a condition characterized by the formation of plaque in the walls of arteries, thus causing blockage to blood flow. This condition can lead to cardiovascular complications. The consumption of black rice can improve such condition and reduce the risk of death due to these conditions. Active components of black rice extract including anthocyanins and tocopherols are proven to lower down total cholesterol, LDL, and TGs. They also prevent the accumulation of fat and hypertension. The dietary fiber included in black rice (or any whole grain in general) has been shown to promote cardiovascular health by lowering cholesterol levels, regulating body weight, enhancing glucose metabolism, and reducing chronic inflammation, among other things [153, 154].

Black rice is loaded with fiber, behaves friendly to digestive system ecosystem, and improves bowel movements. It also prevents those conditions associated with gastrointestinal tract such as diverticulitis, irritable bowel syndrome, duodenal cancers, hemorrhoids, and constipation. Being high in fiber, it induces satiety and helps in weight loss. Black rice, as we saw in the nutrition profile, is a high-fiber food. This dietary fiber promotes regular bowel motions and helps to avoid bloating and constipation. It can also help with gastric reflux disease, duodenal ulcers, diverticulitis, constipation, and hemorrhoids, among other gastrointestinal issues [147, 155].

The anthocyanins in black rice have been shown to be useful in the treatment of asthma. In a study conducted in Korea, anthocyanins were found to be effective in treating (and even preventing) asthma in mice by lowering airway inflammation and mucus hypersecretion [156].

Black rice is high in lutein and zeaxanthin, two carotenoids renowned for their role in eye health, in addition to protective anthocyanins. These antioxidants aid in the protection of eye cells and the reduction in the harmful effects of ultraviolet (UV) radiation. Anthocyanins, which can be found in black rice, have long been known to help with vision. Anthocyanidins isolated from black rice were found to be significantly effective in preventing and decreasing retinal damage caused by fluorescent light in rats in a study [157, 158].

Flavonoid groups (anthocyanins, proanthocyanidins, flavonoids, flavones, flavanones, flavan-3-ols) control anthocyanins, which are most notably linked to hypertension prevention. The role of anthocyanin and tocopherol extracts from black rice bran has been studied, and it was discovered that the anthocyanin extract plays a significant role in cholesterol maintenance but not in fatty acid oxidation inhibition [159].

It is linked to age-related skeletal illness, which shows an increase in adipogenesis as osteogenesis expands from common osteoporotic bone marrow cells. Incorporating BRE (black rice extract) into our diet can help prevent the onset of osteoporosis [160].

Collagen is an extracellular matrix protein produced by fibroblasts in the dermis layer of the skin, and the regulation of collagen synthesis and degradation is critical for wound healing and skin rejuvenation. In comparison with the controls, the wound healing benefits of the KRB extract were expressed as percent migration and percent collagen production in the NHDF. The wound healing effects of the KRB extract were evident on day 1 and day 2, as evidenced by increased NHDF proliferation [161–164].

13. Conclusion

It is concluded that black rice is composed of different nutritional and bioactive compounds. Because of its high nutritional value, black rice is one of the most potent rice in our diet. It is essential for the promotion of health benefits. It is high in fiber, protein, iron, vitamins, and minerals, which help to balance out the effects of other foods in our bodies. Antioxidants known as anthocyanin and tocopherol are found in black rice. Black rice is also used as a functional ingredient in different foods. Individuals who consume black rice have shown that it has numerous health benefits, including the prevention of diabetes, atherosclerosis, obesity, and cancer.

Data Availability

The data used to support the findings of this study are included within the article.

Conflicts of Interest

The authors declare that they have no conflicts of interest regarding the publication of this study.

References

[1] L. Kong, Y. Wang, and Y. Cao, "Determination of Myo-inositol and D-chiro-inositol in black rice bran by capillary electrophoresiswith electrochemical detection," *Journal of Food Composition and Analysis*, vol. 21, 2008.

[2] R. Sompong, E. S. Siebenhandl-Ehn, M. G. Linsberger-Martin, and E. Berghofer, "Physicochemical and antioxidative properties of red and black rice varieties from Thailand, China and Sri Lanka," *Food Chemistry*, vol. 124, no. 1, pp. 132–140, 2011.

[3] R. C. Chaudhary, "Speciality rices of the world: effect of WTO and IPR on its production trend and marketing," *Journal of Food Agriculture and Environment*, vol. 1, no. 2, pp. 34–41, 2003.

[4] H. Ichikawa, T. Ichiyanagi, B. Xu, Y. Yoshii, M. Nakajima, and T. Konishi, "Antioxidant activity of anthocyanin extract from purple black rice," *Journal of Medicinal Food*, vol. 4, no. 4, pp. 211–218, 2001.

[5] K. K. Chang, S. Kikuchi, Y. K. Kim et al., "Computational identification of seed specific transcription factors involved in anthocyanin production in black rice," *Biochip journal*, vol. 4, no. 3, pp. 247–255, 2010.

[6] K. K. Adom and R. H. Liu, "Antioxidant activity of grains," *Journal of Agricultural and Food Chemistry*, vol. 50, pp. 6182–6187, 2002.

[7] S. H. Nam, S. P. Choi, M. Y. Kang, H. J. Koh, N. Kozukue, and M. Friedman, "Antioxidative activities of bran extracts from twenty one pigmented rice cultivars," *Food Chemistry*, vol. 94, no. 4, pp. 613–620, 2006.

[8] "Segen's medical Dictionary," 2012, https://medicaldictionary.thefreedictionary.com/healthcare+provider.

[9] Kristamtini, "Mengenal beras hitam Dari bantul," 2009, https://www.litbang.pertanian.go.id/artikel/238/pdf/Mengenal%20Beras%20Hitam%20dari%20Bantul.pdf.

[10] S. Chutipaijit and T. Sutjaritvorakul, "Comparative study of total phenolic compounds, flavonoids and antioxidant capacities in pigmented and non-pigmented rice of indica rice varieties," *Journal of Food Measurement and Characterization*, vol. 12, no. 2, pp. 781–788, 2018.

[11] M. W. Zhang, *Specialty Rice and its Processing Techniques*, China Light Industry Press, Beijing, Chiina, 2000.

[12] T. Oikawa, H. Maeda, T. Oguchi et al., "The birth of a black rice gene and its local spread by introgression," *The Plant Cell Online*, vol. 27, no. 9, pp. 2401–2414, 2015.

[13] U. K. S. Kushwaha, *Black Rice Research, Hiastor and Development*, Springer International Publishing, Berlin, Germany, 2016.
[14] N. Kanha, J. M. Regenstein, S. Surawang, P. Pitchakarn, and T. Laokuldilok, "Properties and kinetics of the in vitro release of anthocyanin-rich microcapsules produced through spray and freeze-drying complex coacervated double emulsions," *Food Chemistry*, vol. 340, Article ID 127950, 2021.
[15] B. J. Prasad, P. S. Sharavanan, and R. Sivaraj, "RETRACTED: health benefits of black rice—a review," *Grain & Oil Science and Technology*, vol. 2, no. 4, pp. 109–113, 2019.
[16] A. Agrawal, "Black rice the new black gold of India," *Food and Agriculture Spectrum Journal*, vol. 2, pp. 96–99, 2020.
[17] D. R. T. Sari, A. Safitri, J. R. K. Cairns, and F. Fatchiyah, "Anti-apoptotic activity of anthocyanins has potential to inhibit caspase-3 signaling," *Journal of Tropical life sciences*, vol. 10, pp. 15–25, 2020.
[18] J. B. Harborne and C. A. Williams, "Advances in flavonoid research since 1992," *Phytochemistry*, vol. 55, no. 6, pp. 481–504, 2000.
[19] J. A. Carney, *Black Rice: The African Origins of Rice Cultivation in the Americas*, Los Angeles Public Library, Los Angeles, CA, USA, 2003.
[20] J. A. Carney, "Black rice," in *Black Rice*Harvard University Press, Cambridge, MA, USA, 2001.
[21] S. Saha, "Black rice: the new age super food (an extensive review)," *American International Journal Research in Formal, Applied Natural Science*, vol. 16, no. 1, pp. 51–55, 2016.
[22] U. K. S. Kushwaha, I. Deo, N. K. Singh, and S. N. Tripathi, "Black rice (oryza sativa L.) breeding," in *The Future of Rice Demand: Quality beyond Productivity*Springer, Berlin, Germany, 2020.
[23] J. F. Monks, N. L. Vanier, J. Casaril et al., "Effects of milling on proximate composition, folic acid, fatty acids and technological properties of rice," *Journal of Food Composition and Analysis*, vol. 30, 2013.
[24] FAOSTAT, *Food and Agriculture Organization of the United Nations*, FAQ, Rome, Italy, 2005.
[25] P. Bhattacharjee, R. S. Singhal, and P. R. Kulkarni, "Basmati rice: a review," *International Journal of Food Science and Technology*, vol. 37, 2002.
[26] G. S. Khush, "What it will take to feed 5.0 billion rice consumers in 2030," *Plant Molecular Biology*, vol. 59, no. 1, pp. 1–6, 2005.
[27] J. Molina, M. Sikora, N. Garud et al., "Molecular evidence for a single evolutionary origin of domesticated rice," *Proceedings of the National Academy of Sciences*, vol. 108, no. 20, pp. 8351–8356, 2011.
[28] K. S. K. Ujjawal, *Black Rice—Research, History and Development*, Springer, Berlin, Germany, 2016.
[29] T. Natsumi and O. Noriko, "Physicochemical properties of kurogome, a Japanese native black rice. Part 1 Bull," *Gifu Women's Coll*, vol. 23, pp. 105–113, 1994.
[30] S. V. S. Sastry, "Inheritance of genes controlling glume size, pericarp colour, and their interrelationships in indica rice," *Oryza*, vol. 15, pp. 177–179, 1978.
[31] H. E. Hoahua, X. Pan, Z. Zao, and Y. Liu, "Properties of the pigment in black rice," *Chinese Rice Research Newsletter*, vol. 4, no. 2, pp. 11-12, 1996.
[32] L. H. Quan, "Selection of yeast for beverage production from black rice," *Nong Nghiep Cong Nghiep Thue Pham*, vol. 8, pp. 375-376, 1999.
[33] R. C. Chaudary and D. V. Tran, "Specialty rice of the world: a prologue," in *Specialty Rice of the World: Breeding, Production and Marketing*FAO and Science Publishers Inc, Rome, Italy, 2001.
[34] F. Fatchiyah, D. Ratih, D. Sari, A. Safitri, and J. Ketudat Cairns, "Phytochemical compound and nutritional value in black rice from java island, Indonesia," *Systematic Reviews in Pharmacy*, vol. 11, pp. 414–421, 2020.
[35] N. Borah, F. D. Athokpam, R. L. Semwal, and S. C. Garkoti, "Chakhao (black rice; oryza sativa L.): a culturally important and stress tolerant traditional rice variety of manipur," *Indian Journal of Traditional Knowledge*, vol. 17, 2018.
[36] S. Bhuvaneswari, S. Gopala Krishnan, H. Bollinedi et al., "Genetic architecture and anthocyanin profiling of aromatic rice from Manipur reveals divergence of Chakhao landraces," *Frontiers in Genetics*, vol. 11, 2020.
[37] K. Moirangthem, D. Jenkins, P. Ramakrishna, R. Rajkumari, and D. Cook, "Indian black rice: a brewing raw material with novel functionality," *Journal of the Institute of Brewing*, vol. 126, no. 1, pp. 35–45, 2020.
[38] V. C. Ito and L. G. Lacerda, "Black rice (Oryza sativa L.): a review of its historical aspects, chemical composition, nutritional and functional properties, and applications and processing technologies," *Food Chemistry*, vol. 301, Article ID 125304, 2019.
[39] D. A. Vaughan, "The wild relatives of rice," in *A Genetic Handbook*International Rice Research Institute, Manila, Philippines, 1994.
[40] O. F. Linares, "African rice (Oryza glaberrima): history and future potential," *Proceedings of the National Academy of Sciences*, vol. 99, no. 25, pp. 16360–16365, 2002.
[41] T. T. Chang, "Origin, domestication and diversification," in *Rice Origin, History, Technology and Production*John Wiley and Sons. Inc, Hoboken, NJ, USA, 2003.
[42] D. A. Vaughan and H. Morishima, "Biosystematics of the genus oryza," in *Rice Origin, History, Technology and Production*John Wiley and Sons inc, Hoboken, NJ, USA, 2003.
[43] B. O. Juliano, *Rice in Human Nutrition (No. 26)*, Int. Rice Res. Inst, Los Baños, Philippines, 1993.
[44] B. Burlando and L. Cornara, "Therapeutic properties of rice constituents and derivatives (Oryza sativa L.): a review update," *Trends in Food Science & Technology*, vol. 40, no. 1, pp. 82–98, 2014.
[45] S. Kraithong, S. Lee, and S. Rawdkuen, "Physicochemical and functional properties of Thai organic rice flour," *Journal of Cereal Science*, vol. 79, pp. 259–266, 2018.
[46] T. E. Callcott, B. A. Santhakumar, J. Luo, and L. C. Blanchard, "Therapeutic potential of rice-derived polyphenols on obesity-related oxidative stress and inflammation," *Journal of Applied Biomedicine*, vol. 16, no. 4, pp. 255–262, 2018.
[47] V. Ziegler, C. D. Ferreira, J. T. S. Goebel et al., "Changes in properties of starch isolated from whole rice grains with brown, black, and red pericarp after storage at different temperatures," *Food Chemistry*, vol. 216, pp. 194–200, 2017.
[48] V. C. Ito, E. Schnitzler, I. M. Demiate, M. E. S. Eusébio, L. G. Lacerda, and R. A. E. Castro, "Physicochemical, thermal, crystallographic, and morphological properties of biodynamic black rice starch, and of residual fractions from aqueous extraction," *Starch Stärke*, vol. 70, no. 12, Article ID 1700348, 2018a.
[49] M. Hiemori, E. Koh, and A. E. Mitchell, "Influence of cooking on anthocyanins in black rice (Oryza sativa *L. japonica* var. SBR)," *Journal of Agricultural and Food Chemistry*, vol. 57, no. 5, pp. 1908–1914, 2009.

[50] J.-L. Mau, C.-C. Lee, Y.-P. Chen, and S.-D. Lin, "Physico-chemical, antioxidant and sensory characteristics of chiffon cake prepared with black rice as replacement for wheat flour," *Lebensmittel-Wissenschaft & Technologie*, vol. 75, pp. 434–439, 2017.

[51] M. W. Zhang, B. J. Guo, and Z. M. Peng, "Genetic effects on grain characteristics of Indica black rice and their useson indirect selections for some mineral element contents in grains," *Genetic Resources and Crop Evolution*, vol. 52, no. 8, pp. 1121–1128, 2005.

[52] B. Thanuja and R. Parimalavalli, "Role of black rice in health and diseases," *International Journal of Health Sciences & Research*, vol. 8, pp. 241–248, 2018.

[53] V. A. Moyer and US Preventive Services Task Force, "Vitamin, mineral, and multivitamin supplements for the primary prevention of cardiovascular disease and cancer: U.S. Preventive services task force recommendation statement," *Annals of Internal Medicine*, vol. 160, no. 8, pp. 558–564, 2014.

[54] J. M. Salgado, A. G. C. de Oliveira, D. N. Mansi, C. M. Donado-Pestana, C. R. Bastos, and F. K. Marcondes, "The role of black rice (oryza sativaL.) in the control of hypercholesterolemia in rats," *Journal of Medicinal Food*, vol. 13, no. 6, pp. 1355–1362, 2010.

[55] T. Wu, X. Guo, M. Zhang, L. Yang, R. Liu, and J. Yin, "Anthocyanins in black rice, soybean and purple corn increase fecal butyric acid and prevent liver inflammation in high fat diet-induced obese mice," *Food & Function*, vol. 8, no. 9, pp. 3178–3186, 2017.

[56] R. Dash, T. B. Emran, M. M. N. Uddin, A. Islam, and M. Junaid, "Molecular docking of fisetin with AD associated AChE, ABAD and BACE1 proteins," *Bioinformation*, vol. 10, no. 9, p. 562, 2014.

[57] G. F. Deng, X. R. Xu, Y. Zhang, D. Li, R. Y. Gan, and H. B. Li, "Phenolic compounds and bioactivities of pigmented rice," *Critical Reviews in Food Science and Nutrition*, vol. 53, no. 3, pp. 296–306, 2013.

[58] Y. Tang, W. Cai, and B. Xu, "From rice bag to table: fate of phenolic chemical compositions and antioxidant activities in waxy and non-waxy black rice during home cooking," *Food Chemistry*, vol. 191, pp. 81–90, 2016.

[59] A. Gani, S. M. Wani, F. A. Masoodi, and H. Gousia, "Whole—grain cereal bioactive compounds and their health benefits," *Journal of Food Processing & Technology*, vol. 3, no. 3, pp. 1–10, 2012.

[60] K. Chakuton, D. Puangpronp, and M. Nakornriab, "Phytochemical content and antioxidant activity of colored and non-colored Thai rice cultivars," *Asian Journal of Plant Sciences*, vol. 11, no. 6, pp. 285–293, 2012.

[61] M. Zubair, F. Anwar, M. Ashraf, and K. Uddin, "Characterization of high-value bioactives in some selected varieties of Pakistani rice (Oryza sativa L.)," *International Journal of Molecular Sciences*, vol. 13, no. 4, pp. 4608–4622, 2012.

[62] G. Pereira-Caro, S. Watanabe, A. Crozier, T. Fujimura, T. Yokota, and H. Ashihara, "Phytochemical profile of a Japanese black-purple rice," *Food Chemistry*, vol. 141, no. 3, pp. 2821–2827, 2013.

[63] E. Jesch and T. P. Carr, "Food ingredients that inhibit cholesterol absorption," *Preventive Nutrition and Food Science*, vol. 22, no. 2, pp. 67–80, 2017.

[64] J. E. Roberts and J. Dennison, "The photobiology of lutein and zeaxanthin in the eye," *Journal of Ophthalmology*, vol. 2015, Article ID 687173, 8 pages, 2015.

[65] V. Melini and R. Acquistucci, "Health-promoting compounds in pigmented Thai and wild rice," *Foods*, vol. 6, no. 1, p. 9, 2017.

[66] K. Petroni, M. Landoni, F. Tomay, V. Calvenzani, C. Simonelli, and M. Cormegna, "Proximate composition, polyphenol content and anti-inflammatory properties of white and pigmented Italian rice varieties," *Universal Journal of Agricultural Research*, vol. 5, no. 5, pp. 312–321, 2017.

[67] H. Ashraf, I. Murtaza, N. Nazir, A. B. Wani, S. Naqash, and A. M. Husaini, "Nutritional profiling of pigmented and scented rice genotypes of Kashmir Himalayas," *Journal of Pharmacognosy and Phytochemistry*, vol. 6, pp. 910–916, 2017.

[68] H. Zhang, Y. Shao, J. Bao, and T. Beta, "Phenolic compounds and antioxidant properties of breeding lines between the white and black rice," *Food Chemistry*, vol. 172, pp. 630–639, 2015.

[69] A. Gunaratne, K. Wu, D. Li, A. Bentota, H. Corke, and Y. Cai, "Antioxidant activity and nutritional quality of traditional red-grained rice varieties containing proanthocyanidins," *Food Chemistry*, vol. 138, no. 3, pp. 1153–1161, 2013.

[70] Y. Shao, Z. Hu, Y. Yu, R. Mou, Z. Zhu, and T. Beta, "Phenolic acids, anthocyanins, proanthocyanidins, antioxidant activity, minerals and their correlations in non-pigmented, red, and black rice," *Food Chemistry*, vol. 239, pp. 733–741, 2018.

[71] A. Ghasemzadeh, M. T. Karbalaii, H. Z. E. Jaafar, and A. Rahmat, "Phytochemical constituents, antioxidant activity, and antiproliferative properties of black, red, and brown rice bran," *Chemistry Central Journal*, vol. 12, p. 17, 2018.

[72] G. ., R. Kim, E. S. Jung, S. Lee, S. Lim, S. Ha, and C. H. Lee, "Combined mass spectrometry-based metabolite profiling of different pigmented rice (Oryza sativa L.) seeds and correlation with antioxidant activities," *Molecules*, vol. 19, no. 10, pp. 15673–15686, 2014.

[73] P. Tantipaiboonwong, K. Pintha, W. Chaiwangyen et al., "Anti-hyperglycaemic and anti-hyperlipidaemic effects of black and red rice in streptozotocin-induced diabetic rats," *ScienceAsia*, vol. 43, no. 5, pp. 281–288, 2017.

[74] M. Galland, S. Boutet-Mercey, I. Lounifi et al., "Compartmentation and dynamics of flavone metabolism in dry and germinated rice seeds," *Plant and Cell Physiology*, vol. 55, no. 9, pp. 1646–1659, 2014.

[75] M. ., N. Irakli, V. F. Samanidou, C. G. Biliaderis, and N. Papadoyannis, "Simultaneous determination of phenolic acids and flavonoids in rice using solid-phase extraction and RP-HPLC with photodiode array detection," *Journal of Separation Science*, vol. 35, no. 13, pp. 1603–1611, 2012.

[76] T. Sriseadka, S. Wongpornchai, and M. Rayanakorn, "Quantification of flavonoids in black rice by liquid chromatography-negative electrospray ionization tandem mass spectrometry," *Journal of Agricultural and Food Chemistry*, vol. 60, no. 47, pp. 11723–11732, 2012.

[77] J. Surh and E. Koh, "Effects of four different cooking methods on anthocyanins, total phenolics and antioxidant activity of black rice," *Journal of the Science of Food and Agriculture*, vol. 94, no. 15, pp. 3296–3304, 2014.

[78] S. Kong, D. J. Kim, S. K. Oh, I. S. Choi, H. S. Jeong, and J. Lee, "Black rice bran as an ingredient in noodles: chemical and functional evaluation," *Journal of Food Science*, vol. 77, no. 3, pp. C303–C307, 2012.

[79] B. Laishram and A. B. Das, "Effect of thermal pretreatments on physical, phytochemical, and antioxidant properties of

black rice pasta," *Journal of Food Process Engineering*, vol. 40, no. 5, Article ID e12553, 2017.

[80] S. Taweekasemsombut, J. Tinoi, P. Mungkornasawakul, and N. Chandet, "Thai rice vinegars: production and biological properties," *Applied Sciences*, vol. 11, no. 13, p. 5929, 2021.

[81] T. Zhang, H. Zhang, Z. Yang, Y. Wang, and H. Li, "Black rice addition prompted the beer quality by the extrusion as pretreatment," *Food Sciences and Nutrition*, vol. 7, no. 11, pp. 3664–3674, 2019.

[82] O. S. Kim, S. S. Park, and J. M. Sung, "Antioxidant activity and fermentation characteristics of traditional black rice wine," *Journal of the Korean Society of Food Science and Nutrition*, vol. 41, no. 12, pp. 1693–1700, 2012.

[83] S. Nontasan, A. Moongngarm, and S. Deeseenthum, "Application of functional colorant prepared from black rice bran in yogurt," *Apcbee Procedia*, vol. 2, pp. 62–67, 2012.

[84] P. Ngamdee, A. Bunnasart, and A. Sonda, "Development of a functional food: milk chocolate fortified with anthocyanin from broken Riceberry," *Life Sciences and Environment Journal*, vol. 20, no. 1, pp. 81–89, 2019.

[85] S. I. Han, W. D. Seo, J. E. Na et al., "Characteristics of poprice and rice tea using black sticky rice with giant embryo," *Journal of Life Sciences*, vol. 25, no. 1, pp. 68–74, 2015.

[86] K. Richa, S. K. Laskar, A. Das et al., "Effect of black rice (Oryza sativa L.) flour on proximate composition, texture profile and microbiological qualities of chicken nuggets," *Journal of Entomology and Zoology Studies*, vol. 8, no. 6, pp. 412–416, 2020.

[87] K. Tananuwong and W. Tewaruth, "Extraction and application of antioxidants from black glutinous rice," *LWT—Food Science and Technology*, vol. 43, no. 3, pp. 476–481, 2010.

[88] X. Sui, Y. Zhang, and W. Zhou, "Bread fortified with anthocyanin-rich extract from black rice as nutraceutical sources: its quality attributes and in vitro digestibility," *Food Chemistry*, vol. 196, pp. 910–916, 2016.

[89] S. Y. Joo and H. Y. Choi, "Antioxidant activity and quality characteristics of black rice bran cookies," *Journal of the Korean Society of Food Science and Nutrition*, vol. 41, no. 2, pp. 182–191, 2012.

[90] C. Pandit, A. Roy, S. Ghotekar et al., "Biological agents for synthesis of nanoparticles and their applications," *Journal of King Saud University-Science*, vol. 34, no. 3, p. 101869, 2022.

[91] M. Mrázková, D. Sumczynski, and J. Orsavová, "Non-traditional muesli mixtures supplemented by edible flowers: analysis of nutritional composition, phenolic acids, flavonoids and anthocyanins," *Plant Foods for Human Nutrition*, vol. 76, no. 3, pp. 371–376, 2021.

[92] S. Sonkar, T. S. Saha, and A. Singh, "Development and standardization of soup mix based on black rice and okra powder value added with barley," *Plant Archives*, vol. 15, no. 2, pp. 909–911, 2015.

[93] A. Thakuria and M. Sheth, "An invitro study of the prebiotic properties of Xylooligosaccharide (XOS) and organoleptic evaluation of XOS added Prawn patia and Black rice kheer," *Bioactive Compounds in Health and Disease*, vol. 3, no. 1, pp. 1–14, 2020.

[94] A. Haryanto, W. Pangkahila, and A. A. G. P. Wiraguna, "Black rice bran (oryza sativa l. indica) extract cream prevented the increase of dermal matrix metalloproteinase-1 and dermal collagen reduction of male Wistar rats (rattus norvegicus) exposed to ultraviolet-B rays," *IJAAM (Indonesian Journal of Anti-Aging Medicine)*, vol. 4, no. 1, pp. 16–19, 2020.

[95] L.-J. Zhu, Q.-Q. Liu, J. D. Wilson, M.-H. Gu, and Y.-C. Shi, "Digestibility and physicochemical properties of rice (Oryza sativa L.) flours and starches differing in amylose content," *Carbohydrate Polymers*, vol. 86, no. 4, pp. 1751–1759, 2011.

[96] R. F. Tester, J. Karkalas, and X. Qi, "Starch-composition, fine structure and architecture," *Journal of Cereal Science*, vol. 39, no. 2, pp. 151–165, 2004.

[97] E. Adu-Kwarteng, W. O. Ellis, I. Oduro, and J. T. Manful, "Rice grain quality: a comparison of local varieties with new varieties under study in Ghana," *Food Control*, vol. 14, no. 7, pp. 507–514, 2003.

[98] N. Singh Sodhi and N. Singh, "Morphological, thermal and rheological properties of starches separated from rice cultivars grown in India," *Food Chemistry*, vol. 80, no. 1, pp. 99–108, 2003.

[99] C. R. Mitchell, "Rice starches," in *Starch*Academic Press, Cambridge, MA, USA, 2009.

[100] P. Kumar, K. S. Prakash, K. Jan et al., "Effects of gamma irradiation on starch granule structure and physicochemical properties of brown rice starch," *Journal of Cereal Science*, vol. 77, pp. 194–200, 2017.

[101] V. C. Ito, C. D. Bet, J. P. Wojeicchowski et al., "Effects of gamma radiation on the thermoanalytical, structural and pasting properties of black rice (Oryza sativa L.) flour," *Journal of Thermal Analysis and Calorimetry*, vol. 133, no. 1, pp. 529–537, 2018.

[102] F. Zhu, "Interactions between starch and phenolic compound," *Trends in Food Science & Technology*, vol. 43, no. 2, pp. 129–143, 2015.

[103] Y. Shao, F. Tang, F. Xu, Y. Wang, and J. Bao, "Effects of γ-irradiation on phenolics content, antioxidant activity and physicochemical properties of whole grainrice," *Radiation Physics and Chemistry*, vol. 85, pp. 227–233, 2013.

[104] O. Norkaew, P. Boontakham, K. Dumri et al., "Effect of postharvest treatment on bioactive phytochemicals of Thai black rice," *Food Chemistry*, vol. 217, pp. 98–105, 2017.

[105] D. Ryu and E. Koh, "Influence of cooking methods on free and bound phenolic acids in Korean black rice," *Journal of Food Processing and Preservation*, vol. 41, no. 2, Article ID e12873, 2017.

[106] V. Melini, G. Panfili, A. Fratianni, and R. Acquistucci, "Bioactive compounds in rice on Italian market: pigmented varieties as a source of carotenoids, total phenolic compounds and anthocyanins, before and after cooking," *Food Chemistry*, vol. 277, pp. 119–127, 2019.

[107] S. He, Q. Lou, J. Shi, H. Sun, M. . i. Zhang, and Q. Li, "Water extraction of anthocyanins from black rice and purification using membrane separation and resin adsorption," *Journal of Food Processing and Preservation*, vol. 41, no. 4, Article ID e13091, 2017.

[108] P. Loypimai, A. Moongngarm, and P. Chottanom, "Thermal and pH degradation kinetics of anthocyanins in natural food colorant prepared from black rice bran," *Journal of Food Science & Technology*, vol. 53, no. 1, pp. 461–470, 2016.

[109] Z. Hou, P. Qin, Y. Zhang, S. Cui, and G. Ren, "Identification of anthocyanins isolated from black rice (Oryza sativa L.) and their degradation kinetics," *Food Research International*, vol. 50, no. 2, pp. 691–697, 2013.

[110] M. W. Zhang, R. F. Zhang, F. X. Zhang, and R. H. Liu, "Phenolic profiles and antioxidant activity of black rice bran of different commercially available varieties," *Journal of Agricultural and Food Chemistry*, vol. 58, no. 13, pp. 7580–7587, 2010.

[111] D. Jaisut, S. Prachayawarakorn, W. Varanyanond, P. Tungtrakul, and S. Soponronnarit, "Accelerated aging of jasmine brown rice by high-temperature fluidization V.C. Ito and L.G. Lacerda Food Chemistry 301 (2019) 125304 11 technique," *Food Research International*, vol. 42, no. 5, pp. 674–681, 2009.

[112] V. A. Papillo, M. Locatelli, F. Travaglia et al., "Spray-dried polyphenolic extract from Italian black rice (Oryza sativa L., var. Artemide) as new ingredient for bakery products," *Food Chemistry*, vol. 269, pp. 603–609, 2018.

[113] H. Jun, J. W. Shin, G. S. Song, and Y. S. Kim, "Isolation and identification of phenolic antioxidants in black rice bran," *Journal of Food Science*, vol. 80, no. 2, 2015.

[114] T. Laokuldilok, C. F. Shoemaker, S. Jongkaewwattana, and V. Tulyathan, "Antioxidants and antioxidant activity of several pigmented rice brans," *Journal of Agricultural and Food Chemistry*, vol. 59, no. 1, pp. 193–199, 2011.

[115] M. Y. Kang, J. H. Kim, C. W. Rico, and S. H. Nam, "A comparative study on the physicochemical characteristics of black rice varieties," *International Journal of Food Properties*, vol. 14, no. 6, pp. 1241–1254, 2011.

[116] T. Katoh, K. Koguchi, S. Saigusa, and T. Teramoto, "Production and antioxidative activity of mead made from various types of honey and black rice (Oryza sativa var. Indica cv. Shiun)," *Food Science and Technology Research*, vol. 17, no. 2, pp. 149–154, 2011.

[117] Y. Teramoto, M. Koguchi, A. Wongwicharn, and N. Saigusa, "Production and antioxidative activity of alcoholic beverages made from Thai ou yeast and black rice (Oryza sativa var. Indica cv. Shiun)," *African Journal of Biotechnology*, vol. 10, no. 52, pp. 10706–10711, 2011.

[118] F. Hou, R. Zhang, M. Zhang et al., "Hepatoprotective and antioxidant activity of anthocyanins in black rice bran on carbon tetrachloride-induced liver injury in mice," *Journal of Functional Foods*, vol. 5, no. 4, pp. 1705–1713, 2013.

[119] H. X. Zheng, S. S. Qi, J. He et al., "Cyanidin-3-glucoside from black rice ameliorates diabetic nephropathy via reducing blood glucose, suppressing oxidative stress and inflammation, and regulating transforming growth factor β1/smad expression," *Journal of Agricultural and Food Chemistry*, vol. 68, no. 15, pp. 4399–4410, 2020.

[120] C. Hui, Y. Bin, Y. Xiaoping et al., "Anticancer activities of an anthocyanin-rich extract from black rice against breast cancer cells in vitro and in vivo," *Nutrition and Cancer*, vol. 62, no. 8, pp. 1128–1136, 2010.

[121] D. Liu, Y. Ji, J. Zhao, H. Wang, Y. Guo, and H. Wang, "Black rice (Oryza sativa L.) reduces obesity and improves lipid metabolism in C57BL/6J mice fed a high-fat diet," *Journal of Functional Foods*, vol. 64, Article ID 103605, 2020.

[122] Y. M. Lee, I. S. Kim, and B. O. Lim, "Black rice (Oryza sativa L.) fermented with lactobacillus casei attenuates osteoclastogenesis and ovariectomy-induced osteoporosis," *BioMed Research International*, vol. 2019, Article ID 5073085, 16 pages, 2019.

[123] H. Liu, L. Huang, and X. Pei, "Effects of sorghum rice and black rice on genes associated with cholesterol metabolism in hypercholesterolemic mice liver and intestine," *Food Sciences and Nutrition*, vol. 9, no. 1, pp. 217–229, 2021.

[124] Y. Yang, M. C. Andrews, Y. Hu et al., "Anthocyanin extract from black rice significantly ameliorates platelet hyperactivity and hypertriglyceridemia in dyslipidemic rats induced by high fat diets," *Journal of Agricultural and Food Chemistry*, vol. 59, no. 12, pp. 6759–6764, 2011.

[125] C. Chaiyasut, B. S. Sivamaruthi, N. Pengkumsri et al., "Germinated Thai black rice extract protects experimental diabetic rats from oxidative stress and other diabetes-related consequences," *Pharmaceuticals*, vol. 10, no. 1, p. 3, 2016.

[126] S. N. Hwang, J. C. Kim, M. I. H. Bhuiyan et al., "Black rice (Oryza sativa L., poaceae) extract reduces hippocampal neuronal cell death induced by transient global cerebral ischemia in mice," *Experimental Neurobiology*, vol. 27, no. 2, pp. 129–138, 2018.

[127] I. Y. Bae, J. S. An, I. K. Oh, and H. G. Lee, "Optimized preparation of anthocyanin-rich extract from black rice and its effects on in vitro digestibility," *Food Science and Biotechnology*, vol. 26, no. 5, pp. 1415–1422, 2017.

[128] M. Han, J. S. Bae, J. J. Ban, H. S. Shin, D. H. Lee, and J. H. Chung, "Black rice (Oryza sativa L.) extract modulates ultraviolet-induced expression of matrix metalloproteinases and procollagen in a skin cell model," *International Journal of Molecular Medicine*, vol. 41, no. 5, pp. 3073–3080, 2018.

[129] H. E. Khoo, A. Azlan, S. T. Tang, and S. M. Lim, "Anthocyanidins and anthocyanins: colored pigments as food, pharmaceutical ingredients, and the potential health benefits," *Food & Nutrition Research*, vol. 61, no. 1, Article ID 1361779, 2017.

[130] F. Shahidi and A. C. de Camargo, "Tocopherols and tocotrienols in common and emerging dietary sources: occurrence, applications, and health benefits," *International Journal of Molecular Sciences*, vol. 17, no. 10, p. 1745, 2016.

[131] Z. Zhou, K. Robards, S. Helliwell, and C. Blanchard, "The distribution of phenolic acids in rice," *Food Chemistry*, vol. 87, no. 3, pp. 401–406, 2004.

[132] M. Walter, E. Marchesan, P. F. S. Massoni, L. P. da Silva, G. M. S. Sartori, and R. B. Ferreira, "Antioxidant properties of rice grains with light brown, red and black pericarp colors and the effect of processing," *Food Research International*, vol. 50, no. 2, pp. 698–703, 2013.

[133] P. Sirisoontaralak, S. Keatikasemchai, C. Mancharoen, and N. Na Nakornpanom, "Development of lightly milled black rice with easy cooking and retaining health benefits," *Journal of Food Science & Technology*, vol. 57, no. 10, pp. 3762–3771, 2020.

[134] G. Nitenberg and B. Raynard, "Nutritional support of the cancer patient: issues and dilemmas," *Critical Reviews In Oncology-Hematology*, vol. 34, no. 3, pp. 137–168, 2000.

[135] T. Oki, M. Masuda, S. Nagai et al., "Radical-scavenging activity of red and black rice," in *World Rice Research Conference*International Rice Research Institute, Tsukuba, Japan, 2005.

[136] R. Chatthongpisut, S. J. Schwartz, and J. Yongsawatdigul, "Antioxidant activities and antiproliferative activity of Thai purple rice cooked by various methods on human colon cancer cells," *Food Chemistry*, vol. 188, pp. 99–105, 2015.

[137] S. P. Choi, S. P. Kim, M. Y. Kang, S. H. Nam, and M. Friedman, "Protective effects of black rice bran against chemically-induced inflammation of mouse skin," *Journal of Agricultural and Food Chemistry*, vol. 58, no. 18, pp. 10007–10015, 2010.

[138] S. W. Min, S. N. Ryu, and D. H. Kim, "Anti-inflammatory effects of black rice, cyanidin-3-O-β-d-glycoside, and its metabolites, cyanidin and protocatechuic acid," *International Immunopharmacology*, vol. 10, no. 8, pp. 959–966, 2010.

[139] J. Y. Kim, J. H. Kim, S. H. Lee, S. S. Kim, and S. S. Lee, "Meal replacement with mixed rice is more effective than white rice in weight control, while improving antioxidant enzyme

activity in obese women," *Nutrition Research*, vol. 28, no. 2, pp. 66–71, 2008.

[140] W. H. Ling, Q. X. Cheng, J. Ma, and T. Wang, "Red and black rice decrease atherosclerotic plaque formation and increase antioxidant status in rabbits," *Journal of Nutrition*, vol. 131, no. 5, pp. 1421–1426, 2001.

[141] V. Lobo, A. Patil, A. Phatak, and N. Chandra, "Free radicals, antioxidants and functional foods: impact on human health," *Pharmacognosy Reviews*, vol. 4, no. 8, p. 118, 2010.

[142] J. Zawistowski, A. Kopec, and D. D. Kitts, "Effects of a black rice extract (Oryza sativa L. indica) on cholesterol levels and plasma lipid parameters in Wistar Kyoto rats," *Journal of Functional Foods*, vol. 1, no. 1, pp. 50–56, 2009.

[143] M. Y. Um, J. Ahn, and T. Y. Ha, "Hypolipidaemic effects of cyanidin 3-glucoside rich extract from black rice through regulating hepatic lipogenic enzyme activities," *Journal of the Science of Food and Agriculture*, vol. 93, no. 12, pp. 3126–3128, 2013.

[144] M. J. Navas, A. M. Jiménez-Moreno, J. M. Bueno, P. Sáez-Plaza, and A. G. Asuero, "Analysis and antioxidant capacity of anthocyanin pigments. Part IV: extraction of anthocyanins," *Critical Reviews in Analytical Chemistry*, vol. 42, no. 4, pp. 313–342, 2012.

[145] M. Valko, D. Leibfritz, J. Moncol, M. T. Cronin, M. Mazur, and J. Telser, "Free radicals and antioxidants in normal physiological functions and human disease," *The International Journal of Biochemistry & Cell Biology*, vol. 39, no. 1, pp. 44–84, 2007.

[146] N. Khan, F. Afaq, and H. Mukhtar, "Cancer chemoprevention through dietary antioxidants: progress and promise," *Antioxidants and Redox Signaling*, vol. 10, no. 3, pp. 475–510, 2008.

[147] A. Satija and F. B. Hu, "Cardiovascular benefits of dietary fiber," *Current Atherosclerosis Reports*, vol. 14, no. 6, pp. 505–514, 2012.

[148] Z. Hou, P. Qin, and G. Ren, "Effect of anthocyanin-rich extract from black rice (Oryza sativa L. Japonica) on chronically alcohol-induced liver damage in rats," *Journal of Agricultural and Food Chemistry*, vol. 58, no. 5, pp. 3191–3196, 2010.

[149] H. H. Jang, M. Y. Park, H. W. Kim et al., "Black rice (Oryza sativa L.) extract attenuates hepatic steatosis in C57BL/6 J mice fed a high-fat diet via fatty acid oxidation," *Nutrition & Metabolism*, vol. 9, no. 1, pp. 27–11, 2012.

[150] R. A. S. Sancho and G. M. Pastore, "Evaluation of the effects of anthocyanins in type 2 diabetes," *Food Research International*, vol. 46, no. 1, pp. 378–386, 2012.

[151] M. G. Varadinova, D. I. Docheva-Drenska, and N. I. Boyadjieva, "Effects of anthocyanins on learning and memory of ovariectomized rats," *Menopause*, vol. 16, no. 2, pp. 345–349, 2009.

[152] E. E. Devore, J. H. Kang, M. M. Breteler, and F. Grodstein, "Dietary intakes of berries and flavonoids in relation to cognitive decline," *Annals of Neurology*, vol. 72, no. 1, pp. 135–143, 2012.

[153] A. Fardet, E. Rock, and C. Rémésy, "Is the in vitro antioxidant potential of whole-grain cereals and cereal products well reflected in vivo?" *Journal of Cereal Science*, vol. 48, no. 2, pp. 258–276, 2008.

[154] H. Jia, W. Chen, X. Yu et al., "Black rice anthocyanidins prevent retinal photochemical damageviainvolvement of the AP-1/NF-κB/Caspase-1 pathway in Sprague-Dawley Rats," *Journal of Veterinary Science*, vol. 14, no. 3, pp. 345–353, 2013.

[155] P. Goufo and H. Trindade, "Rice antioxidants: phenolic acids, flavonoids, anthocyanins, proanthocyanidins, tocopherols, tocotrienols, γ-oryzanol, and phytic acid," *Food science & nutrition*, vol. 2, no. 2, pp. 75–104, 2014.

[156] S. J. Park, W. H. Shin, J. W. Seo, and E. J. Kim, "Anthocyanins inhibit airway inflammation and hyperresponsiveness in a murine asthma model," *Food and Chemical Toxicology*, vol. 45, no. 8, pp. 1459–1467, 2007.

[157] M. A. Lila, "Anthocyanins and human health: an in vitro investigative approach," *Journal of Biomedicine and Biotechnology*, vol. 2004, Article ID 673916, 8 pages, 2004.

[158] M. A. Rahim, F. Saeed, W. Khalid, M. Hussain, and F. M. Anjum, "Functional and nutraceutical properties of fructo-oligosaccharides derivatives: a review," *International Journal of Food Properties*, vol. 24, no. 1, pp. 1588–1602, 2021.

[159] X. Zhang, Y. Shen, W. Prinyawiwatkul, J. M. King, and Z. Xu, "Comparison of the activities of hydrophilic anthocyanins and lipophilic tocols in black rice bran against lipid oxidation," *Food Chemistry*, vol. 141, no. 1, pp. 111–116, 2013.

[160] H. C. R. Sangma and S. Parameshwari, "Health benefits of black rice (Zizania aqatica)-a review," *Materials Today Proceedings*, vol. 68, 2021.

[161] I. T. Nizamutdinova, Y. M. Kim, J. I. Chung et al., "Anthocyanins from black soybean seed coats stimulate wound healing in fibroblasts and keratinocytes and prevent inflammation in endothelial cells," *Food and Chemical Toxicology*, vol. 47, no. 11, pp. 2806–2812, 2009.

[162] M. S. H. Kabir, M. M. Hossain, M. I. Kabir et al., "Phytochemical screening, antioxidant, thrombolytic, alpha-amylase inhibition and cytotoxic activities of ethanol extract of steudnera colocasiifolia K. Koch leaves," *Journal of Young Pharmacists*, vol. 8, no. 4, p. 391, 2016.

[163] S. Ahmed, A. Rakib, M. Islam et al., "In vivo and in vitro pharmacological activities of tacca integrifolia rhizome and investigation of possible lead compounds against breast cancer through in silico approaches," *Clinical Phytoscience*, vol. 5, no. 1, pp. 1–13, 2019.

[164] A. M. Tareq, S. Farhad, A. N. Uddin et al., "Chemical profiles, pharmacological properties, and in silico studies provide new insights on cycas pectinata," *Heliyon*, vol. 6, no. 6, p. e04061, 2020.

Hindawi
Journal of Chemistry
Volume 2022, Article ID 9632979, 10 pages
https://doi.org/10.1155/2022/9632979

Research Article

Phenolic Acid Patterns in Different Plant Species of Families Asteraceae and Lamiaceae: Possible Phylogenetic Relationships and Potential Molecular Markers

Oksana Sytar,[1] **Marek Zivcak**,[2] **Kiessoun Konate**,[3,4] **and Marian Brestic**[2,5]

[1]*Taras Shevchenko National University of Kyiv, Volodymyrska 64, Kyiv, Ukraine*
[2]*Institute of Plant and Environmental Sciences, Slovak University of Agriculture, A. Hlinku 2, Nitra 94976, Slovak*
[3]*Laboratory of Biochemistry, Food Biotechnology and Nutrition, Department of Biochemistry and Microbiology, University Joseph KI-ZERBO, 03 BP 7021, Ouagadougou, Burkina Faso*
[4]*Applied Sciences and Technologies Training and Research Unit, University of Dedougou, B. P. 176, Dedougou, Burkina Faso*
[5]*Department of Botany and Plant Physiology, Faculty of Agrobiology, Food and Natural Resources, Czech University of Life Sciences Prague, Kamycka 129, Prague 16500, Czech Republic*

Correspondence should be addressed to Oksana Sytar; oksana.sytar@gmail.com

Received 18 July 2022; Revised 9 September 2022; Accepted 27 September 2022; Published 13 October 2022

Academic Editor: Marwa Fayed

Nowadays, investigations of some specific secondary metabolites estimated near 10,000 various compounds of phenolic nature in different plant species. The interest in natural compounds is not only due to their antioxidant potential, but also to their economic impact, as most of them may be extracted from underexploited plant species. The presented research work presents an extended analysis of the most important phenolic acids of the selected known and underexploited plant species from the families *Asteraceae* and *Rosaceae* with the development of phylogenic tree analysis according to the nonparametric rate smoothing (NPRS) methods. HPLC-UV analysis revealed the original spectrum of phenolic acids in selected known and underexploited plant species of the families *Rosaceae* and *Asteraceae*. The analysis of phenolic acid's contribution from their total amount in the methanolic extract in *Asteraceae* found the high percentage of syringic acid in leaves varied between 64.13% and 95.13%. The detected high contribution of syringic acid among estimated phenolic acids in *Asteraceae* leaves suggests its possible prevalence in the representatives of the family *Asteraceae*. The content of draconic acid in the leaves of most representatives of the family *Rosaceae* which represented more than 30% of total phenolic acid content. The high presence of such phenolic acids may relate to the antioxidant activity of the studied herbal extracts.

1. Introduction

Nowadays, studies analyzing the role of some specific secondary metabolites of the phenolic group identified near 10,000 various compounds of phenolic nature in different plant species. It is known that common transitional secondary metabolites for phenolic compounds is phenylalanine or a precursor of phenylalanine-shikimic acid. Both compounds are presented mostly in conjugated forms and have one or more sugar residues connected to the hydroxyl groups. It is also known their possible connection with other compounds, like amines, lipids, carboxylic and organic acids, and other phenolic plant hormones, which develop huge phenolics biodiversity in the various plant varieties [1–3].

Several phenolic classes can be esteemed regarding to the quantity of phenol rings and specification of structural elements which also unite these rings [4]. The structural characteristics of the compounds of the most important groups of phenolic nature such as coumarins, tannins, flavonoids, and lignans are established on the existence in a core monocyclic carbon skeleton of phenolic and benzoic functional groups. The phenolic compounds have been characterized by high diversity and various ways of their

biosynthesis. Many secondary metbaolites of phenolic nature have a different structure but may have similar biological activities [5, 6].

Phenolic acids are a subgroup of phenolic compounds broadly presented in hydroxybenzoic and hydroxycinnamic acids with antioxidant capacity [7]. It is known about positive correlation between the content of phenolic compounds in plant extracts of various plants and their antioxidant potential [8–10]. Singh et al. has been discovered that gentisic acid among phenolic acids got the most higher antioxidant activity. The gentisic acid showed highest antioxidant activity. Gallic and caffeic acids got second and third places, respectively, regarding the level of antioxidant activity [11]. The salicylic acid is an important phenolic acid which participate in the responses to different abiotic stresses [12].

Plant phenolic compounds biodiversity is visible at variation of genetic lines within and between species [13, 14]. Different phenolics are intensively studied in various chemo-systematic learning with botanical, plant physiology orientation [15]. For example, phenolic compounds can be biochemical markers for identifying base species of plants in Ethiopia [16]. A taxonomic marker of *Ericaceous* species/genera (family: *Ericaceae*) is flavonol gossypetin [17]. The absence of some phenolic acids and specific phenolic compounds also can be a marker of some genus of the plants. It was typical absence of ellagic acid for the genus *Pittosporum* (*Pittosporaceae*) [18]. The connection between diversity of phenolics of bearberry (*Arctostaphylos uva-ursi, Ericaceae*) species and the lines with cytogenetic and genetic background was shown [19]. It was studied that phenolic acid derivatives may act as chemotaxonomic markers in the *Cardiocrinum* species leaves (*Liliaceae* family) [20]. Exploring the antioxidant activity of phenolic acids in a wide range of herbs can be used for further elucidation of their prospective healthful capacities in the biomembranes against oxidative stress and in chemotaxonomy studies of the genus and families [21–23].

Most of the phenolics compounds analysis, which were previously reported, are HPLC-UV qualitative analysis and less mass-spectrometry analysis. It also used the Folin–Ciocalteu method to estimate the total phenolics content of the plant extract together with the estimation of antioxidant activity [24]. It is known using common herbs and crops in human pharmaceutical and food, especially *Calendula officinalis*, *Rudbeckia* sp., *Echinacea purpurea* (*Asteraceae*), *Rosa canina*, *Rosa rubiginosa*, *Alchemilla mollis*, and *Eriobotrya japonica* (*Lamiaceae*) which have shown antioxidant properties [24–31]. The interest in antioxidant natural components is not only due to their biological capacity, but also to their economic impact, as most of them may be extracted from underexploited plant species. At the same time, analysis of the relationships among species in the plant genus or family based on the phenolic acid composition may bring new knowledge. Previously such analysis was done on complete chloroplast genomes, rbcL, and matK chloroplast genes, electrochemical fingerprints showed a series of oxidation peaks of flavonols, phenolic acids, procyanidins, alkaloids, and pigments in the plant tissue [32–34]. The proposed study presents an original phylogenetic tree analysis according to the NPRS methods based on the identified phenolic acids by high-performance liquid chromatography (HPLC) analysis of the selected known and underexploited plant genotypes from the families *Asteraceae* and *Rosaceae*.

2. Materials and Methods

2.1. Plant Object. The herbs and plants (representatives *Asteraceae* and *Rosaceae* families) at the flowering stage were taken in the area of the Botanical Park, Nitra, Slovak republic. Plant species of the family *Asteraceae*: *Calendula officinalis* L., *Achillea filipendulina* Lam., *Helianthus annuus* L., *Helianthus tuberosus* L., *Echinops ritro* L., *Echinacea purpurea* L., and *Rudbeckia fulgida* L. Plant species of the family *Rosaceae*: *Potentilla recta* L., *Rosa canina* L., *Rosa rubiginosa* L., *Cotoneaster horizontali* Decne., *Agrimonia eupatoria* L., *Alchemilla mollis (Buser)* Rothm., and *Eriobotrya japonica* L. A 15 cm of a petiole section of each leaf was taken for quality estimation. It was determined from the node toward the bottom. After collection, leaves were stored in liquid nitrogen to avoid the volatilization of biological compounds and lyophilized.

2.2. Estimation of the Antioxidant Activity. Estimation of the antioxidant activity (DPPH analysis) was done regarding Singleton and Rossi, 1965 [35]. 1 mL of distilled water was added to 0.02 g of the plant sample material in the Eppendorf tube. Then, the mixed samples (leaf lyophilized powder) during 15 min were heated at 95°C and centrifuged for 5 min at 12,000 rpm. The extract was transferred to a new tube and the same procedure was repeated. The supernatant from the two step procedure was collected to a new tube. 3.9 mL of the DPPH working solution was mixed with 0.1 mL of the experimental supernatant, shaking for 30 s and placed for further reaction time during 30 min. The absorbance was estimated with a Jenway UV/Vis 6405 spectrophotometer (Jenway, Chelmsford, UK) at 515 nm. The next formula was used for the antioxidant activity calculation: %Inhibition = $[(A_0—A_1)/(A_0)]^*100$. A_0 was control reaction absorbance and A_1 was the sample's presence absorbance.

2.2.1. Phenolic Acid Assay. Phenolic acid assays has been advanced by Cai et al. with some adaptations [36]. 0.75 mL of 70% methanol was mixed with 0.02 g of plant material samples. The mixture was placed for 15 min with additional centrifugation during 5 min at 6000 g. The extraction was done one more time with 70% methanol (0.5 mL) with further collection of supernatants. The final supernatant was diminished to nearby dryness (at 25°C) in a Speed Vac evaporator. As an internal standard were used 40 μL of 3 mM solution of coumaric acid or cinnamic acid (Sigma–Aldrich Chemie GmbH). The samples for HPLC analysis with added 1 mL of 40% acetonitrile were filtrated using Millex-GP filter (0.22 μm). The Dionex UltiMate 3000 HPLC system with a diode array detector (DAD-3000) was used for HPLC analysis (Dionex Corp., Sunnyvale, CA, USA).

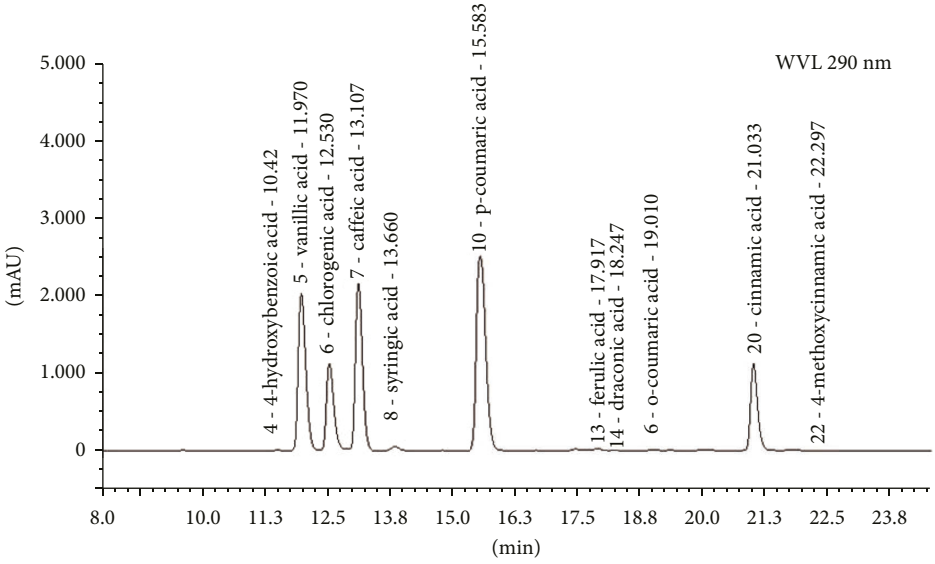

Figure 1: HPLC-UV standards chromatogram at 290 nm.

An initial injection volume was 40 μl at a flow rate of 0.4 mL/min. A temperature of the column (Narrow-Bore Acclaim PA C16-column (3 mm, 120A, 2.1 × 150 mm, Dionex) was 35°C. The eluent A (0.1% v/v phosphoric acid in ultrapure water) and eluent B (40% v/v acetonitrile in ultrapure water) were parts of 49-min gradient program with next steps: 0–5 min: 0.5% B, 5–9 min: 0–40% B, 9–12 min: 40% B, 12–17 min: 40–80% B, 17–20 min: 80% B, 20–24 min: 80–99% B, 24–32 min: 99–100% B, 32–36 min: 100–40% B, and 36–49 min: 40-1% B. Screening of peaks was done at 290 nm. HPLC-UV standards chromatogram and UV spectrum of phenolic acids at 290 nm was used for calculation of phenolic acids quantity (mg·g^{-1} DW) (Figures 1 and 2).

2.3. Statistical Analysis. Microsoft Office Excel 2003 program was applied for the estimation of average and standard deviations. The hierarchical cluster analysis of the phenolic acid contents was done using Euclidean coefficient and WARD methods. Statistical replication of the experimental samples was 6 times.

3. Results

The HPLC-UV analysis of experimental extracts of species of the family *Asteraceae* identified the phenolic acids such as syringic acid, draconic (*p*-anisic) acid, *p*-hydroxybenzoic acid, chlorogenic acid, vanillic acid, o-coumaric acid, *p*-coumaric acid, ferulic acid, salicylic acid, cinnamic acid, and *p*-methoxycinnamic acid (Figure 3). The content of phenolic acids depends on the variety and/or the place and time of cultivation [37]. The phenolic acids as cinnamic acid, o-coumaric acid, *p*-coumaric acid, caffeic acid, sinapic acid, and ferulic acid have a phenylalanine as metabolic precursor. The phenolic acids derivatives of benzoic acid are syringic acid, *p*-hydroxybenzoic, and vanillic acids. In general, benzoic acid derivatives are reached from analogous cinnamic acid derivatives by the way of the β-oxidation enzymatic reactions. That metabolic pathway can vary between representatives of plant families and inside the group. The syringic acid among identified phenolic acids in plant species of the family *Asteraceae* had a greatest level. The syringic acid antioxidant potential is well known [38]. A significant increase of superoxide dismutase (SOD), catalase (CAT) enzymes, and glutathione (GSH) levels was observed under additional treatment with syringic acid [39].

The percentage calculation of phenolic acid amounts in the extracts of representatives of the family *Asteraceae* found high presence of syringic acid in the experimental extracts of *Asteraceae* species varied between 64.13% and 95.13% (Figure 3). Such a significant presence in the extracts of the species of the *Asteraceae* family compared to the total content of identified phenolic acids can be a possible biochemical marker of the representatives of this plant family.

The analysis of results of phenolic acid composition in the representatives of the family *Rosaceae* found a high presence of draconic (*p*-anisic) acid in the assessed leaf extracts (Figure 4).

Moreover, the HPLC-UV analysis identified in this botanical family the following phenolic acids: draconic, chlorogenic, o-coumaric, *p*-coumaric, *p*-hydroxybenzoic, vanillic, syringic, ferulic, salicylic, *p*-methoxycinnamic, and cinnamic acids. From this group, o-coumaric acid was not estimated in the leaf methanolic extracts of *Potentilla recta* L., *Rosa canina*, *Alchemilla mollis*, and *Eriobotrya japonica*. It was found that high presence of draconic acid can be a possible biochemical marker of plant species of the family *Rosaceae* (Figure 4).

The great content of the syringic acid in the representatives of the family *Asteraceae* and draconic acid in the representatives of the family *Rosaceae* can be partly connected with the studied antioxidant activity of plant extracts (Figures 5(a) and 5(b)). The highest antioxidant capacity of

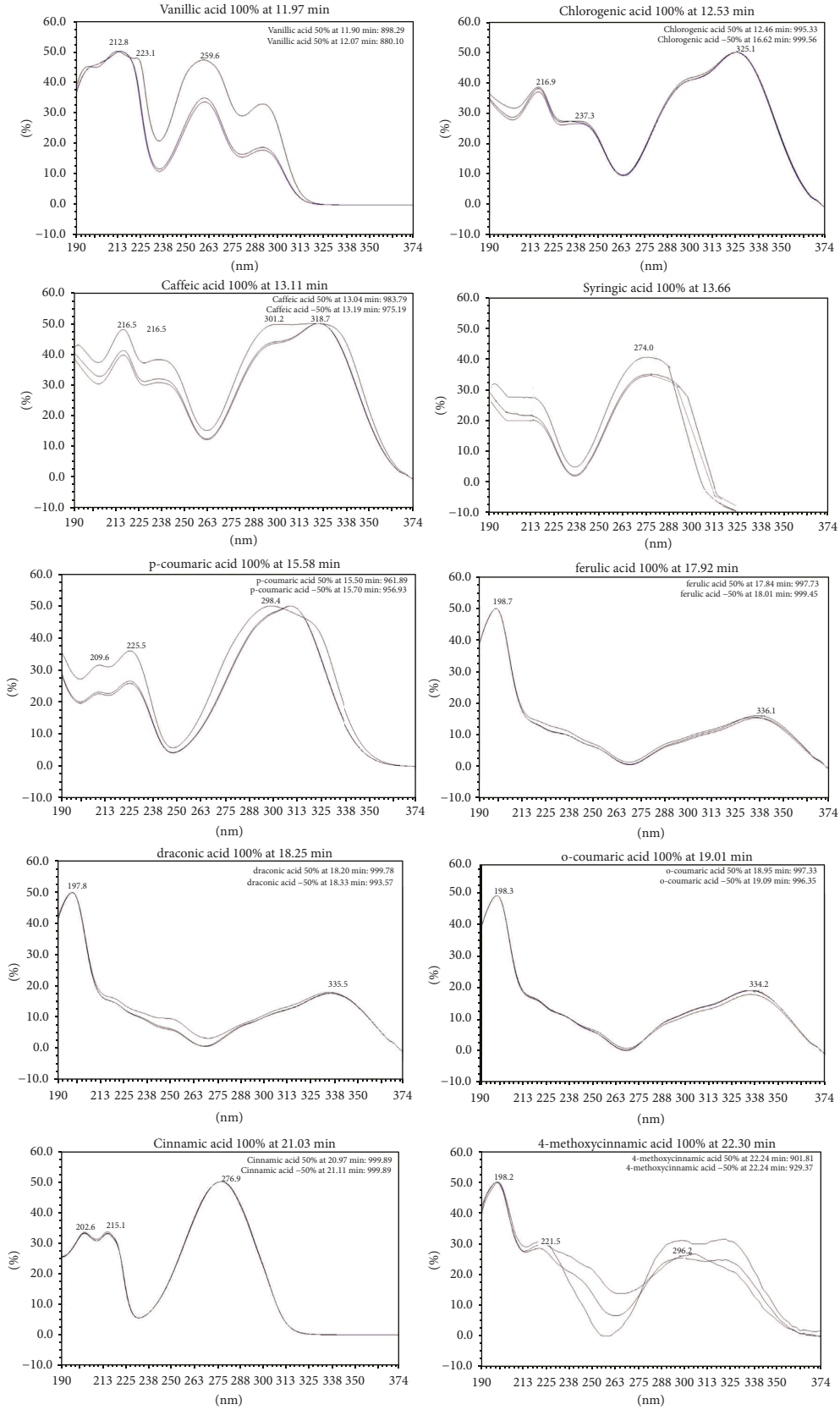

Figure 2: Phenolic acids UV spectrum at 290 nm.

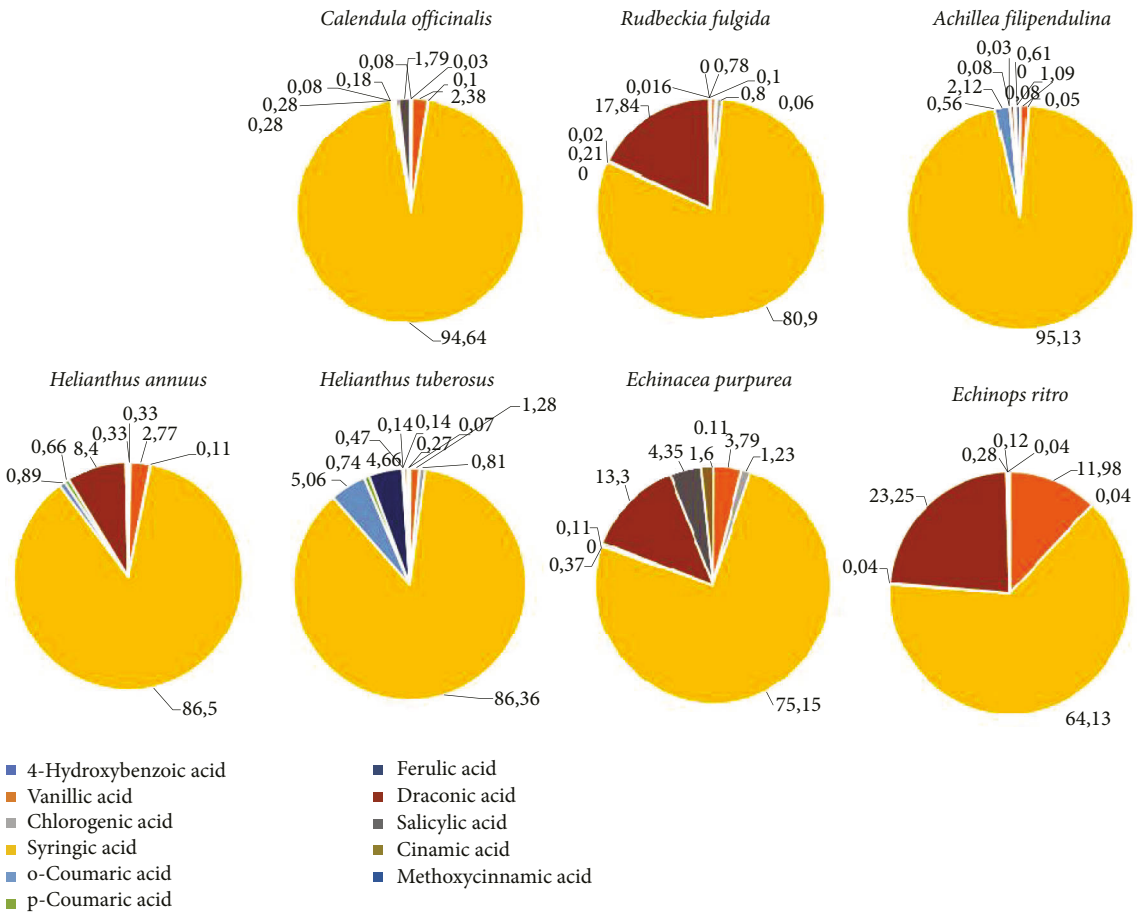

Figure 3: Percentage of phenolic acids amounts in the methanolic extract of representatives of the family *Asteraceae* (%).

experimental extracts was noticed in the extracts of *Potentilla recta* L., *Rosa canina*, and *Rosa rubiginosa*, where the percentage of draconic acid was 33.99%, 53.39%, and 57.76%, respectively. The low antioxidant activity among representatives of the family *Rosaceae* was identified in *Eribotrya japonica* L. Among representatives of the family *Asteraceae*, the significant high antioxidant potential was noticed in the extract of *Calendula officinalis* L, *Rudbeckia fulgida Aiton*, and *Achillea filipendulina* L.

At the same time, to detail the presence of phenolic acids in connection with analyzed plant species, the cluster analysis dendrogram (Figure 6) was created based on the analysis of clusters using the Euclidean coefficient and WARD method. The analogical analysis formed by the obtained data of phenolics composition and content in plant cultivars with a comparable phenolics concentration in another plant cultivars was previously used by Krochmal–Marczak et al. [37]. The cluster analysis group objects based on the data describing the objects and their relationships. The objects within a group are similar (or related) to one another but different or unrelated from the objects in other groups.

Cluster 1 in Figure 6(a) (family *Asteraceae*) contains data describing the similar phenolic acids composition in *Calendula officinalis* and *Achillea filipendulina* leaves; cluster 2 contains the similar phenolic acids composition in *Helianthus annuus* and *Helianthus tuberosus* species. Cluster 3 includes the similar phenolic acid composition in *Echinops ritro* and *Echinacea purpurea* leaves, whereas cluster 4 describes the phenolic acids composition in *Rudbeckia fulgida* L., which is significantly different from other representatives of the family *Asteraceae*.

Based on the cluster analysis, it is evident that the concentration of phenolic acids inside one family was differentiated by the plant species' genetic properties. The significant presence of syringic acid was a prevailing trait for all experimental representatives of the family *Asteraceae*.

The apparent data structure matches with the cluster analysis of the concentration of phenolic acids in the representatives of the family *Rosaceae*. As shown in Figure 6(b), intergroup relations reveal four main clusters characterized by the similar composition of phenolic acids inside each cluster. Cluster one in Figure 6(b) (family *Rosaceae*) contains data describing the similar phenolic acid composition in *Potentilla recta* L., *Alchemilla mollis*, and *Eriobotrya japonica*. Cluster 2 contains a similar phenolic acid composition in *Rosa rubiginosa* and *Cotoneaster horisontalis*, which are closer to representatives of cluster 1.

Interestingly, the *Rosa canina* is in cluster 4, and it is characterized by the different phenolic acid composition compared to the other studied representatives of the family

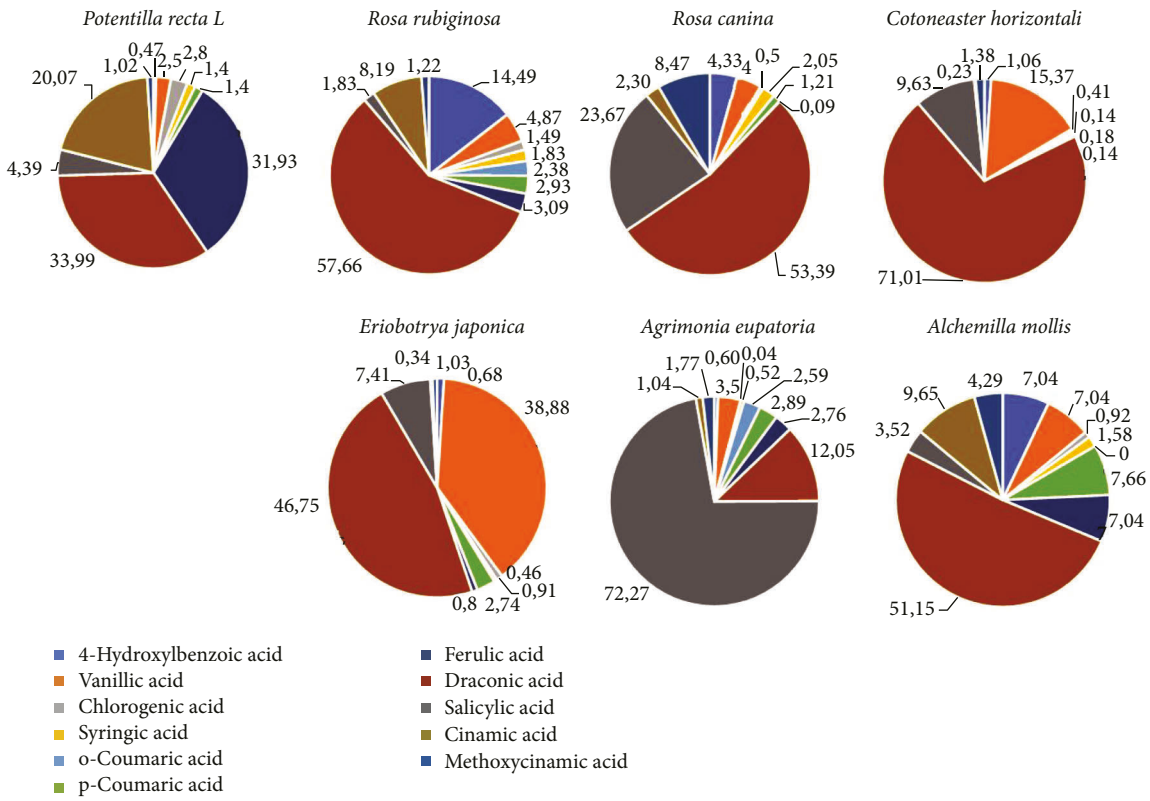

Figure 4: Percentage of phenolic acids amounts in the methanolic extract of representatives of the family *Rosaceae* (%).

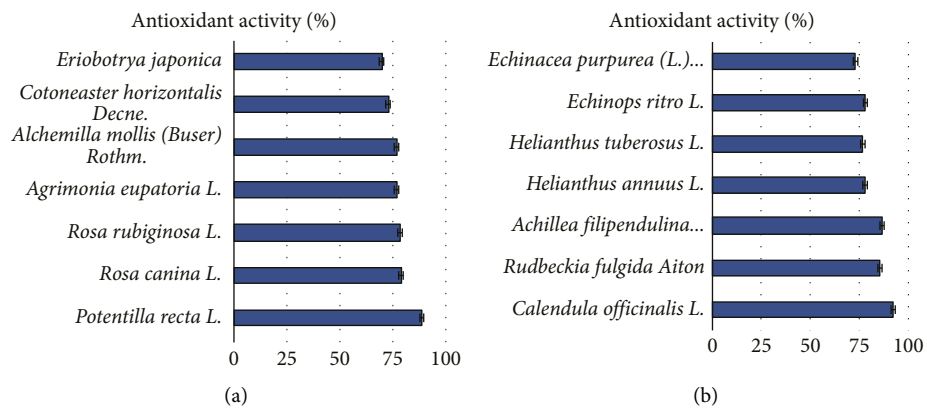

Figure 5: antioxidant activity of the experimental extracts of plant species *Rosaceae* (a) and *Asteraceae* (b) families.

Rosaceae. Cluster 3 includes the phenolic acid composition presented by *Agrimonia eupatoria*. The analysis of phenolic acids composition showed the substantial accumulation of specific phenolic acids in the plant leaf may indicate about their participation in plant defense.

4. Discussion

The percentage of phenolic acids can be calculated regarding phenolic acid amounts in the methanolic extract of the representatives *Asteraceae* family. It was found high syringic acid level in the experimental extracts of *Asteraceae* species.

Between 64.13% and 95.13%, such significant presence in the leaves of representatives of *Asteraceae* family can be a possible biochemical marker of plant species of this family. The formation of specific secondary metabolites in phylogenetic close families and genera of plants is possible due to the similarity of metabolic processes [39, 40]. The presence of syringic acid may be scientifically applied both as a specific marker for experimental plant species and as a source of this substance in the studied plant species in biofortification processes.

Quantitative analysis of phenolic compounds of other *Asteraceae* plants such as *Achillea millefolium L.* (common

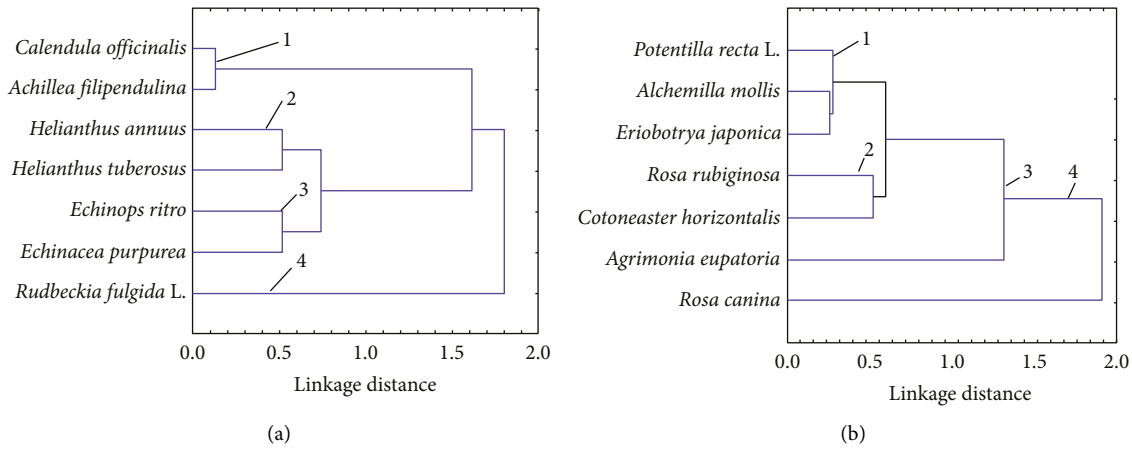

FIGURE 6: Dendrogram of the species family Asteraceae (a) and Rosaceae (b) obtained after applying hierarchical cluster analysis to the phenolic acids contents using Euclidean coefficient and WARD methods. 1, 2, 3, and 4 clusters. The similar composition of phenolic acids inside of each cluster.

yarrow), *Helichrysum arenarium L.* (immortelle) also shown high presence of syringic acid. At the same time, phenolic acids compostion was different between these studied plant species. For example, common yarrow got high level of rosmarinic acid but immortelle has no romarinic acid but high level of caffeic acid [41]. Syringic acid was discovered in some plants, such as Schumannianthus dichotomus (*Marantaceae*) and *Ardisia* elliptica (*Primulaceae*) [42, 43]. Syringic acid is one of the transitional compounds of the plant pigment malvidin. Syringic acid and plant anthocyanidin malvidin were described in vinegar and red wine [44]. The presence of methoxy groups attributes the therapeutic activity of syringic acid with the places 3 and 5 of the aromatic ring. Syringic acid is able to regulate the modifications of some biological functions such as factors of growth, transcriptional factors, and the level of signaling molecules implicated in the development of various human diseases such as cancer, liver damage, and diabetes. In the eantime, syringic acid has also huge spectrum of applications in industry counting on bioremediation and photocatalytic ozonation [38, 45].

It was confirmed anesthetic and sedative activities of syringic acid in the *Quercus infectoria* plant extract (Dar M.S., Ikram, 1979). The correlation between the percentage level of syringic acid and antioxidant activity has been observed for the studied representatives' family *Asteraceae—Calendula officinalis*, *Achillea filipendulina*, and *Rudbeckia fulgida* has shown a high percentage of syringic acid and also a high level of antioxidant potential (Figures 3 and 5). The intense antioxidant activity of syringic acid was discussed by Srinivasulu et al.[38]. The antioxidant activity potential can relate to the anti-inflammatory activity of the studied plant extracts [46]. Anti-inflammatory and antioxidant potential of plants from the *Asteraceae* family was noted [47]. The unique mechanisms of action of biological markers for the anti-inflammatory activity was described with assistance of the metabolic approach. The huge network and connections between the diversified range of tribes and genera of the family *Asteraceae* with the help of HPLC-ESI-HRMS metabolomic approach was described [48].

In our study, intergroup relations using cluster analysis reveal four main clusters characterized by shared variance in the representatives of the family *Asteraceae* (Figure 7(a)). The cluster analysis indicated that the identified phenolic acid concentrations were differentiated by the genetic properties of the plant species inside one family. The high presence of syringic acid in the experimental extracts of the family *Asteraceae* was a significant trait for all experimental plant species.

The further study with percentage calculation of phenolic acid amounts in methanolic extract of representatives of the family *Rosaceae* found that percentage of draconic acid in the studied leaf extracts of *Rosaceae* vary between 12.05% and 71.01%. Such significant presence in the leaves of mostly all representatives of the family *Rosaceae* which was higher than 30% of the total amount of identified phenolic acids can be used as a species-specific biochemical marker.

Draconic acid is another name, p-anisic acid or 4-methoxybenzoic acid. It is one of the isomers of draconic acid characterized by antioxidant and antiseptic properties [49]. It is also recommended to use as a transitional compound in the formation of more composite natural compounds. Draconic acid is found naturally in anise, fruits of figs *Ficus mucuso* (*Moraceae*) [50], leaves extract of *Rhododendron ferrugineum (Ericaceae)* [51], and in the mycelium of *Cordyceps sinensis* (*Ophiocordycipitaceae*) [52]. In our study all experimental plant extracts were characterized by the presence of draconic acid. The draconic acid content in the leaf extracts of the studied representatives was a great level in *Rosa canina* L., *Rosa rubiginosa* L.

Literature analysis has been revealed the presence of studies on the topic phenolic content and antioxidant activity mostly in the fruit of the representatives' family *Rosaceae*, but not many in the leaf extracts [53, 54]. Just one comparable study of phenolics extraction of black cherry leaves and flowers with simulating different traditional extraction procedures was done. Black cherry leaves were extracted with methanol, which is a standard extraction of phenolics. It was identified in the leaf extracts next phenolic

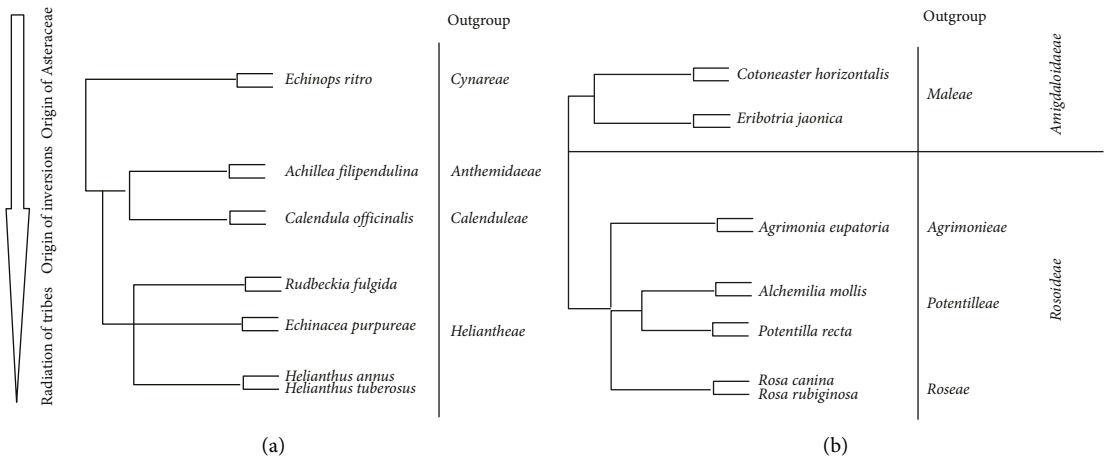

Figure 7: Presentations of phylogeny trees studied representatives' families *Asteraceae* (a) and *Rosaceae* (b).

acids: caffeic acid hexoside1,2, caffeic acid, p-coumaric hexoside 1,2,3, 5-Caffeoylquinic acid, 5-p-coumaroylquinic acid, 5-feruloylquinic acid, and dicaffeoylquinic acid [55].

The high level of syringic acid in members of the family *Asteraceae* and draconic acid in *Rosaceae* can be partly connected with the studied antioxidant capacity of plant extracts. The use of extracts in the study of antioxidant properties, antimicrobial effects may get different results compared to the study of the same effects from isolated biologically active compounds of the same plant extract. It is known that the impacts of activities of the compounds solute in extracts can have synergistic or antagonistic response [56, 57]. So, it is not correct to state that just major phenolic acid present in the leaf sample can influence the antioxidant potential of the plant extract.

The obtained data structure correlates with the cluster analysis of the concentration of phenolic acids in the family *Rosaceae* representatives. It is evident from the intergroup relations (Figure 7(b)) that the four main clusters appeared, characterized by similar phenolic acids inside each cluster. The *Rosa canina* is in cluster 4 and characterized by other phenolic acid composition than *Rosa rubiginosa,* representing the same genus. Medicinal herbs associated with the same genus are continually simply distracted because to their quite identical metabolites and structure. To comprehend them, naturally specific biological markers with assistance developed method which use HPLC analysis were analyzed profiles of metabolites [58]. Cluster analysis based on the composition and level of the identified flavonoids, ascorbic and citric acids suggested the effectiveness of the division of sect. Caninae into three subsections. Regarding this analysis, *Rosa rubiginosa* and *Rosa canina* were chosen in the different subsections [59]. The described data confirm the data of cluster analysis based on phenolic acid composition for *Rosa canina* and *Rosa rubiginosa*.

5. Conclusions

The plant extracts of the studied seven species family *Asteraceae* and seven species family *Rosaceaes* contained 11 phenolic acids. It was noticed species-dependent variations of phenolic acids composition. Based on the cluster analysis, it is evident that the level of the determined phenolic acids was differentiated by the genetic properties of the plant species inside one family. The experimental plant species can be the sources of specific phenolic acids with compatible antioxidant activity. The presented data regarding phenolic acids composition reveal that their profiles are significant biochemical markers of authenticity indication of the studied plant species. It was found significant appearance of syringic acid in the extracts of representatives of the family *Asteraceae*. At the same time, draconic acid have shown major presence in the extracts of *Rosaceae* family species. The explanation of the results is creative with applied scientific background for further studies of plants and herbs botanical, physiological features related to the phenolic acids composition and presence of other specific secondary metabolites.

Data Availability

The data analyzed in this study were a reanalysis of the existing data, which are openly available at locations cited in the reference section.

Ethical Approval

This paper does not contain any studies with human or animals.

Consent

The author approves processing of this manuscript for publication.

Conflicts of Interest

The authors declare that there are no conflicts of interest.

Authors' Contributions

Conceptualization was done by OS and MB. Investigation was done by OS, MB, and KK:. Data analysis contribution by

OS and MZ:. HPLC analysis by OS, cluster analysis by MZ, writing by OS, KK, and MB, funding acquisition by MB.

Acknowledgments

The authors would special like to thank for the arrangement of scientific support from Hindawi for Ukrainian scientist. This study was supported by the Research Agency of Slovak Republic within the project OPVaI-VA/DP/2018/no: 313011T81300 "Optimization of phenotyping methods: building a national phenotyping platform".

References

[1] T. P. Kondratyuk and J. M. Pezzuto, "Natural product polyphenols of relevance to human health," *Pharmacien Biologiste*, vol. 42, pp. 46–63, 2004.

[2] I. Faraone, D. Russo, M. Ponticelli et al., "Preserving biodiversity as source of health promoting compounds: phenolic profile and biological activity of four varieties of *Solanum lycopersicum*," *Plants*, vol. 10, no. 3, p. 447, 2021.

[3] W. Zhang, Y. Hu, J. Liu et al., "Progress of ethylene action mechanism and its application on plant type formation in crops," *Saudi Journal of Biological Sciences*, vol. 27, no. 6, pp. 1667–1673, 2020.

[4] O. Sytar, M. Brestic, M. Rai, and H. Shao, "Plant phenolic compounds for food, pharmaceutical and cosmetics production," *Journal of Medicinal Plants Research*, vol. 6, pp. 2526–2539, 2012.

[5] O. Sytar, M. Brestic, S. Hajihashemi et al., "COVID-19 prophylaxis efforts based on natural antiviral plant extracts and their compounds," *Molecules*, vol. 26, no. 3, p. 727, 2021.

[6] R. Marchiosi, W. D. dos Santos, R. P. Constantin et al., "Biosynthesis and metabolic actions of simple phenolic acids in plants," *Phytochemistry Reviews*, vol. 19, no. 4, pp. 865–906, 2020.

[7] N. Kumar and N. Goel, "Phenolic acids: Natural versatile molecules with promising therapeutic applications," *Biotechnology Reports*, vol. 24, Article ID e00370, 2019.

[8] Y. Z. Cai, Q. Luo, M. Sun, and H. Corke, "Antioxidant activity and phenolic compounds of 112 traditional Chinese medicinal plants associated with anticancer," *Life Sciences*, vol. 74, no. 17, pp. 2157–2184, 2004.

[9] R. Y. Gan, L. Kuang, X. R. Xu et al., "Screening of natural antioxidants from traditional Chinese medicinal plants associated with treatment of rheumatic disease," *Molecules*, vol. 15, no. 9, pp. 5988–5997, 2010.

[10] Li Fu, B. T. Xu, X. R. Xu et al., "Antioxidant capacities and total phenolic contents of 62 fruits," *Food Chemistry*, vol. 129, no. 2, pp. 345–350, 2011.

[11] D. P. Singh, S. Verma, and R. Prabha, "Investigations on antioxidant potential of phenolic acids and flavonoids: the common phytochemical ingredients in plants," *Journal of Plant Biochemistry & Physiology*, vol. 6, pp. 1–5, 2018.

[12] H. Lu, J. T. Greenberg, and L. Holuigue, "Editorial: salicylic acid signaling networks," *Frontiers of Plant Science*, vol. 7, p. 238, 2016.

[13] J. Hakulinen, R. Julkunen-Tiitto, and J. Tahvanainen, "Does nitrogen fertilization have an impact on the trade-off between willow growth and defensive secondary metabolism?" *Trees*, vol. 9, no. 4, pp. 235–240, 1995.

[14] J. Witzell, R. Gref, and T. Näsholm, "Plant-part specific and temporal variation in phenolic compounds of boreal bilberry (*Vaccinium myrtillus*) plants," *Biochemical Systematics and Ecology*, vol. 31, no. 2, pp. 115–127, 2003.

[15] V. Míka, V. Kubáň, B. Klejdus, V. Odstrčilová, and P. Nerušil, "Phenolic compounds as chemical markers of low taxonomic levels in the family Poaceae," *Plant Soil and Environment*, vol. 51, pp. 506–512, 2011.

[16] B. Lemma, C. Grehl, M. Zech et al., "Phenolic compounds as unambiguous chemical markers for the identification of keystone plant species in the Bale Mountains, Ethiopia," *Plants*, vol. 8, no. 7, p. 228, 2019.

[17] J. B. Harborne and C. A. Williams, "A chemotaxonomic survey of flavonoids and simple phenols in leaves of the Ericaceae," *Botanical Journal of the Linnean Society*, vol. 66, no. 1, pp. 37–54, 1973.

[18] M. Jay, "Chemotaxonomic researches on vascular plants XIX Flavonoid distribution in the Pittosporaceae," *Botanical Journal of the Linnean Society*, vol. 62, no. 4, pp. 423–429, 1969.

[19] E. Asensio, D. Vitales, I. Pérez et al., "Phenolic compounds content and genetic diversity at population level across the natural distribution range of bearberry (*Arctostaphylos uva-ursi*, *Ericaceae*) in the Iberian Peninsula," *Plants*, vol. 9, no. 9, p. 1250, 2020.

[20] K. Hori, T. Watanabe, and H. P. Devkota, "Phenolic acid derivatives, flavonoids and other bioactive compounds from the leaves of *Cardiocrinum cordatum* (Thunb.) Makino (*Liliaceae*)," *Plants*, vol. 10, no. 2, p. 320, 2021.

[21] L. Yao, Y. Jiang, R. Singanusong, N. Datta, and K. Raymont, "Phenolic acids and abscisic acid in Australian Eucalyptus honeys and their potential for floral authentication," *Food Chemistry*, vol. 86, no. 2, pp. 169–177, 2004.

[22] J. A. Ávila-Reyes, N. Almaraz-Abarca, A. I. Chaidez-Ayala et al., "Foliar phenolic compounds of ten wild species of *Verbenacea* as antioxidants and specific chemomarkers," *Brazilian Journal of Biology*, vol. 78, no. 1, pp. 98–107, 2017.

[23] S. Kiokias, C. Proestos, and V. Oreopoulou, "Phenolic acids of plant origin-a review on their antioxidant activity in vitro (O/W Emulsion Systems) along with their in vivo health biochemical properties," *Foods*, vol. 9, no. 4, p. 534, 2020.

[24] O. Sytar, "Phenolic acids in the inflorescences of different varieties of buckwheat and their antioxidant activity," *Journal of King Saud University Science*, vol. 27, no. 2, pp. 136–142, 2015.

[25] O. Sytar, I. Hemmerich, M. Zivcak, C. Rauh, and M. Brestic, "Comparative analysis of bioactive phenolic compounds composition from 26 medicinal plants," *Saudi Journal of Biological Sciences*, vol. 25, no. 4, pp. 631–641, 2018.

[26] S. Mishima, K. Saito, H. Maruyama et al., "Antioxidant and immuno-enhancing effects of *Echinacea purpurea*," *Biological and Pharmaceutical Bulletin*, vol. 27, no. 7, pp. 1004–1009, 2004.

[27] K. C. Preethi, G. Kuttan, and R. Kuttan, "Antioxidant potential of an extract of *Calendula officinalis* flowers in vitro. and in vivo," *Pharmaceutical Biology*, vol. 44, no. 9, pp. 691–697, 2006.

[28] I. Roman, A. Stănilă, and S. Stănilă, "Bioactive compounds and antioxidant activity of *Rosa canina* L. biotypes from spontaneous flora of Transylvania," *Chemistry Central Journal*, vol. 7, no. 1, p. 73, 2013.

[29] K. Maher, B. A. Yassine, and B. Sofiane, "Anti-inflammatory and antioxidant properties of *Eriobotrya japonica* leaves extracts," *African Health Sciences*, vol. 15, no. 2, pp. 613–620, 2015.

[30] R. Lukashou and N. Gurina, "Chemical composition and pharmacological potential of *Rudbeckia hirta* L. review," *Acta Scientific Medical Sciences*, vol. 3, no. 10, pp. 65–70, 2019.

[31] M. Polumackanycz, M. Kaszuba, A. Konopacka et al., "Phenolic composition and biological properties of wild and commercial dog rose fruits and leaves," *Molecules*, vol. 25, no. 22, p. 5272, 2020.

[32] L. Wu, L. Nie, Z. Xu et al., "Comparative and phylogenetic analysis of the complete chloroplast genomes of three paeonia section moutan species (*Paeoniaceae*)," *Frontiers in Genetics*, vol. 11, p. 980, 2020.

[33] S. Lav, D. Pooja, S. Ravi Prakash et al., "Phylogenetic and evolutionary relationships in selected Pinus species using rbcL and matK chloroplast genes," *Open Journal of Political Science*, vol. 6, no. 1, pp. 064–068, 2021.

[34] Q. Zhou, K. Liu, X. Li et al., "Voltammetric electrochemical sensor for phylogenetic study in acer linn," *Biosensors*, vol. 11, no. 9, 2021.

[35] V. L. Singleton, "Colorimentry of total phenolics with phosphomolybdic-phosphotungstic acid reagents," *American Journal of Enology and Viticulture*, vol. 16, pp. 144–158, 1965.

[36] Z. Cai, A. Kastell, C. Speiser, and I. Smetanska, "Enhanced resveratrol production in *Vitis vinifera* cell suspension cultures by heavy metals without loss of cell viability," *Applied Biochemistry and Biotechnology*, vol. 171, no. 2, pp. 330–340, 2013.

[37] B. Krochmal-Marczak, T. Cebulak, I. Kapusta, J. Oszmiański, J. Kaszuba, and N. Żurek, "The content of phenolic acids and flavonols in the leaves of nine varieties of sweet potatoes (*Ipomoea batatas* L.) depending on their development, grown in Central Europe," *Molecules*, vol. 25, no. 15, p. 3473, 2020.

[38] C. Srinivasulu, M. Ramgopal, G. Ramanjaneyulu, C. M. Anuradha, and C. Suresh Kumar, "Syringic acid (sa)—A review of its occurrence, biosynthesis, pharmacological and industrial importance," *Biomedicine & Pharmacotherapy*, vol. 108, pp. 547–557, 2018.

[39] Y. Li, L. Zhang, X. Wang, W. Wu, and R. Qin, "Effect of syringic acid on antioxidant biomarkers and associated inflammatory markers in mice model of asthma," *Drug Development Research*, vol. 80, no. 2, pp. 253–261, 2019.

[40] M. Wink, "Evolution of secondary metabolites from an ecological and molecular phylogenetic perspective," *Phytochemistry*, vol. 64, no. 1, pp. 3–19, 2003.

[41] I. G. Mekinić, D. Skroza, I. Ljubenkov, L. Krstulović, S. S. Možina, and V. Katalinić, "Phenolic acids profile, antioxidant and antibacterial activity of chamomile, common yarrow and immortelle (Asteraceae)," *Natural Product Communications*, vol. 9, no. 12, 2014.

[42] N. Malaj, B. C. De Simone, A. D. Quartarolo, and N. Russo, "Spectrophotometric study of the copigmentation of malvidin 3-O-glucoside with p-coumaric, vanillic and syringic acids," *Food Chemistry*, vol. 141, no. 4, pp. 3614–3620, 2013.

[43] M. M. Rob, K. Hossen, A. Iwasaki, K. Suenaga, and H. Kato-Noguchi, "Phytotoxic activity and identification of phytotoxic substances from *Schumannianthus dichotomus*," *Plants*, vol. 9, no. 1, 2020.

[44] M. C. Gálvez, C. G. Barroso, and J. A. Pérez-Bustamante, "Analysis of polyphenolic compounds of different vinegar samples," *Journal of Food Investigation and Research*, vol. 199, pp. 29–31, 1999.

[45] E. Adams, T. Miyazaki, J. Y. Moon et al., "Syringic acid alleviates cesium-induced growth defect in *Arabidopsis*," *International Journal of Molecular Sciences*, vol. 21, no. 23, p. 9116, 2020.

[46] M. Allegra, "Antioxidant and anti-inflammatory properties of plants extract," *Antioxidants*, vol. 8, no. 11, p. 549, 2019.

[47] A. Rolnik and B. Olas, "The plants of the *Asteraceae* family as agents in the protection of human health," *International Journal of Molecular Sciences*, vol. 22, no. 6, p. 3009, 2021.

[48] D. A. Chagas-Paula, T. Zhang, F. B. Da Costa, and R. A. Edrada-Ebel, "A metabolomic approach to target compounds from the Asteraceae family for dual COX and LOX inhibition," *Metabolites*, vol. 5, no. 3, pp. 404–430, 2015.

[49] M. Martinka Maksymiak, M. Zięba, A. Orchel, M. Musiał-Kulik, M. Kowalczuk, and G. Adamus, "Bioactive (Co)oligoesters as potential delivery systems of p-anisic acid for cosmetic purposes," *Materials*, vol. 13, no. 18, p. 4153, 2020.

[50] J. J. K. Bankeu, R. Khayala, B. N. Lenta et al., "Isoflavone dimers and other bioactive constituents from the figs of *Ficus mucuso*," *Journal of Natural Products*, vol. 74, no. 6, pp. 1370–1378, 2011.

[51] P. Seephonkai, R. Popescu, M. Zehl, G. Krupitza, E. Urban, and B. Kopp, "Ferruginenes A-C from *Rhododendron ferrugineum* and their cytotoxic evaluation," *Journal of Natural Products*, vol. 74, no. 4, pp. 712–717, 2011.

[52] M. L. Yang, P. C. Kuo, T. L. Hwang, and T. S. Wu, "Anti-inflammatory principles from *Cordyceps sinensis*," *Journal of Natural Products*, vol. 74, no. 9, pp. 1996–2000, 2011.

[53] Z. Kiran, M. Ahmed, and F. Khan, "Comparative evaluation of total phenolics, total flavonoids content and antiradical activity in six selected species of family *Rosaceae* using spectroscopic method," *American Journal of Biomedical Science & Research*, vol. 3, no. 4, 2019.

[54] A. Butkevičiūtė, R. Urbštaitė, M. Liaudanskas, K. Obelevičius, and V. Janulis, "Phenolic content and antioxidant activity in fruit of the genus *Rosa* L," *Antioxidants*, vol. 11, no. 5, p. 912, 2022.

[55] J. Brozdowski, B. Waliszewska, S. Gacnik, M. Hudina, R. Veberic, and M. Mikulic-Petkovsek, "Phenolic composition of leaf and flower extracts of black cherry (*Prunus serotina* Ehrh.)," *Annals of Forest Science*, vol. 78, no. 3, p. 66, 2021.

[56] K. C. Bulusu, R. Guha, D. J. Mason et al., "Modelling of compound combination effects and applications to efficacy and toxicity: state-of-the-art, challenges and perspectives," *Drug Discovery Today*, vol. 21, no. 2, pp. 225–238, 2016.

[57] L. K. Caesar and N. B. Cech, "Synergy and antagonism in natural product extracts: when $1+1$ does not equal 2," *Natural Product Reports*, vol. 36, no. 6, pp. 869–888, 2019.

[58] Hp. Wang, Y. Liu, C. Chen, and H. B. Xiao, "Screening specific biomarkers of herbs using a metabolomics approach: a case study of *Panax ginseng*," *Scientific Reports*, vol. 7, no. 1, p. 4609, 2017.

[59] A. Adamczak, W. Buchwald, J. Zieliński, and S. Mielcarek, "Flavonoid and organic acid content in rose hips (Rosa L., sect. Caninae dc. Em. Christ.)," *Acta Biologica Cracoviensia Series Botanica*, vol. 54, no. 1, pp. 105–112, 2012.

Hindawi
Journal of Chemistry
Volume 2022, Article ID 5426050, 9 pages
https://doi.org/10.1155/2022/5426050

Research Article

Chemical Compositions of Essential Oil from Aerial Parts of *Cyclospermum leptophyllum* and Its Application as Antibacterial Activity against Some Food Spoilage Bacteria

Yilma Hunde Gonfa,[1,2] **Fekade Beshah Tessema**,[1,3] **Abiy A. Gelagle**,[4] **Sileshi D. Getnet**,[4] **Mesfin Getachew Tadesse**,[1] **Archana Bachheti**,[5] **and Rakesh Kumar Bachheti**[1]

[1]*Department of Industrial Chemistry, College of Applied Sciences, Addis Ababa Science and Technology University, P. O. Box 16417, Addis Ababa, Ethiopia*
[2]*Department of Chemistry, College of Natural and Computational Sciences, Ambo University, P. O. Box 19, Ambo, Ethiopia*
[3]*Department of Chemistry, College of Natural and Computational Sciences, Woldia University, P. O. Box 400, Woldia, Ethiopia*
[4]*Ethiopian Public Health Institute, P. O. Box 1242, Addis Ababa, Ethiopia*
[5]*Department of Environment Science, Graphic Era University, Dehradun, India*

Correspondence should be addressed to Rakesh Kumar Bachheti; rkbachheti@gmail.com

Received 4 August 2022; Revised 10 September 2022; Accepted 20 September 2022; Published 3 October 2022

Academic Editor: Marwa Fayed

Cyclospermum leptophyllum is plant species known for its medicinal value and pleasant aroma. The aerial part and plant seeds are traditionally used as food additives as a spice. This study aims to isolate the chemical constituents of essential oil of the aerial part of the plant and study their potential antibacterial activities against some food contaminating bacteria. The essential oil of *C. leptophyllum* (CSEO) was isolated from aerial parts of the plant species and studied using GC-MS and FTIR techniques. The first four major chemical constituents determined from GC-MS analysis of CSEO (for peak area % ≥ 1.15%) were 2,5-dimethoxy-*p*-cymene (87.09%), 2-methoxy-1-methyl-4-(1-methylethyl) benzene (3.09%), 2-methoxy-4-methyl-1-(1-methylethyl) benzene (1.71%), and humulene (1.15%). 60%, 30%, 15%, 7.5%, and 3.75% of CSEO solutions were prepared and evaluated for their potential antibacterial activities against six food spoilage pathogenic bacterial strains. Three Gram-positive strains: *Staphylococcus aureus* (ATCC 25923), *Staphylococcus epidermidis* (ATCC 12228), *Streptococcus agalactiae* (ATCC 12386) and three Gram-negative strains: *Escherichia coli* (ATCC 25922), *Proteus mirabilis* (ATCC 35659), and *Pseudomonas aeruginosa* (ATCC 27853) were used as test microorganisms. Compared to ciprofloxacin, a positive control, the promising antibacterial activity was observed for CSEO against *S. aureus* at minimum and maximum test solutions as the values of the zone of inhibition diameter (ZID, mm) were recorded as 14.33 ± 0.58 for 3.75% CSEO solution and 30.67 ± 0.58 for 60% CSEO solution. Tests of CSEO solutions generally showed stronger antibacterial activities against Gram-positive than Gram-negative strains. Therefore, CSEO contains potent chemical constituents that might be applicable in treating pathogenic bacterial species.

1. Introduction

Medicinal plants have been widely used for various applications supported by *in vivo* and *in vitro* studies due to their easy affordability and fewer side effects [1–5]. The World Health Organization (WHO) has reported that about 80% population of the world uses plants and natural products to treat different pathogenic diseases [6, 7]. Medicinal plants have also been reported as the source for the invention of novel drugs, and 25% of modern drugs contain one or more active components of plant origin [8, 9]. Similarly, the world's top 25 best-selling medicines were obtained from the natural products of plants [10]. Some reports showed that about 17,500 aromatic plants are known for producing essential oils (EOs) [11, 12]. EOs are the mixtures of secondary metabolites with characteristic flavour and odour.

These phytochemicals protect plants from various bacterial, fungal, and viral diseases [13–17].

Plant ecology and growth conditions can affect the quantity and quality of isolated EOs [18]. These natural products are volatile oils and naturally occurring organic compounds in plants with various physical and chemical properties with multiple functions and health benefits [19]. Some studies showed that the EOs of different parts of medicinal plants have been widely applied for diverse biological and pharmacological applications because of their wide-spectrum bioactive compounds [20–22]. Various literature reviews also reported that EOs or their significant components are used as plausible alternatives for treating pathogenic bacteria due to their complex composition of secondary metabolites [23–26]. Currently, EOs of plants are known to be employed in food as preservatives/additives, medicine, and agricultural commodities for their potential antibacterial activities [27–33].

Cyclospermum leptophyllum (Pers.) belongs to the family *Apiaceae*. This family contains approximately 450 genera and 3,700 species [34]. *C. leptophyllum* is a small, spreading, erect, and much-branched annual herb (Figure 1) [35]. Its fruit is traditionally used to treat flatulence, dyspepsia, diarrheal, laryngitis, rheumatoid arthritis, bronchitis, asthma, and folk medicine [36]. The leaves and seeds of *C. leptophyllum* were reported to be applied to treat loss of appetite and disease, which are caused by sweet inflammation locally known as "mitch" in Ethiopia and food additives, respectively [37]. The EO of *C. leptophyllum* displayed significant activities against Gram-positive and Gram-negative pathogenic bacterial strains [38]. To the best of our knowledge, there have been a limited number of reports regarding the investigation of antibacterial activities of EO of the aerial part of *C. leptophyllum* against food-related pathogenic bacterial species. Hence, the main aim of this study was to isolate *C. leptophyllum* essential oil (CSEO), identify its chemical compositions, and finally evaluate its potential antibacterial activity against some pathogenic bacteria responsible for food contamination using ciprofloxacin, an antibiotic drug as a positive control. Antibacterial activities of CSEO were evaluated by using six food-contaminating pathogenic bacteria from three Gram-positive and three Gram-negative strains. The newly reported chemical compositions and antibacterial activity effects of CSEO might provide important information about the bioactivities of phytochemicals of this plant species and its diversified chemical compounds and potential applications.

2. Materials and Methods

2.1. Chemicals and Solvents. In this study, all chemicals and solvents of analytical grade from Sigma-Aldrich were used. The solutions were prepared using sterilized distilled water throughout the antibacterial activity tests.

2.2. Plant Samples' Collection, Authentication, and Preparation. C. leptophyllum, Figure 1, was collected from Tullu Dimtu, Addis Ababa, Central Ethiopia, located at the latitude of 8° 88′ 52″ North and longitude of 38° 80′ 98″ East, in November 2020. Voucher specimens YH21 were authenticated by Mr. Melaku Wondafrash and deposited at the National Herbarium (ETH), Department of Plant Biology and Biodiversity Management, Addis Ababa University, Addis Ababa, Ethiopia. The aerial parts of the plant sample were separated, cleaned carefully, and dried under shade for two weeks. Then, the dried sample was milled using the electric grinder, and the powdered sample was stored in nontransparent plastic bags until the hydrodistillation process.

Figure 1: Images of *C. leptophyllum* plant species.

2.3. Isolation of Essential Oils. Essential oil of *C. leptophyllum* (CSEO) was isolated from a 2 kg powdered sample (dry weight) by using the hydrodistillation technique in Clevenger-type apparatus for 3 hours based on the procedure from European Pharmacopoeia (Phar. Eur. Supplement 7.0). CSEO was separated and dried over anhydrous Na_2SO_4 from the aqueous phase and then stored in brown glass bottles in the refrigerator until further analysis.

2.4. Characterization of Essential Oil

2.4.1. Gas Chromatography-Mass Spectrometry (GC-MS) Analysis. Gas chromatography-mass spectrometry measurements were performed according to the procedure proposed by Freire et al. [39] with some minor modifications. GC-MS analysis of CSEO was carried out using an HP5890 Series II gas chromatograph, HP5972 mass selective detector, and Agilent 6890 Series autosampler (Agilent Technologies, Santa Clara, CA, USA). A Supelco MDN-5S, 30 m × 0.25 mm capillary column with a 0.5 μm film thickness was used with helium as the carrier gas at a 1.0 mL/min flow rate. CSEO was diluted in n-hexane (1 : 10), and GC-MS results were obtained using the following conditions: split 1 : 20; injection volume 0.1 μl; injection temperature 250°C; oven temperature progress from 60 to 130°C at 1°C/min, from 130–200°C at 2°C/min, from 200–250°C at 4°C/min and held at 250°C for 40 min; the ionization model used was an electronic impact at 70 eV. The chemical composition of CSEO was identified from their Kovats retention indices (KIs) on the capillary column. The chemical constituents of

CSEO were identified based on a homologous series of C_7-C_{25} n-alkanes, and we compared their mass spectral fragmentation patterns with those stored in the NIST spectral database and literature reports [39, 40].

2.4.2. Fourier Transform Infrared (FTIR) Analysis. Fourier transform infrared (FTIR) was performed based on the procedure reported by Getahun et al. [41] with some modifications. FTIR spectra of CSEO were recorded using an FTIR spectrophotometer (IS50 ABX, Thermo Scientific, USA) to identify the major functional groups in the CSEO sample. A few drops of CSEO were used with a resolution of 4 cm^{-1}, a spectral range of 400–4000 cm^{-1}, and several scans of 32.

2.5. Antibacterial Activities of Essential Oil

2.5.1. Bacterial Strains. Six food-related pathogenic bacterial strains, three from Gram-positive and three from Gram-negative, were used to study the antibacterial activities of CSEO. Gram-positive bacterial strains were *Staphylococcus aureus* (ATCC 25923), *Staphylococcus epidermidis* (ATCC 12228), and *Streptococcus agalactiae* (ATCC 12386), and Gram-negative bacterial strains were *Escherichia coli* (ATCC 25922), *Proteus mirabilis* (ATCC 35659), and *Pseudomonas aeruginosa* (ATCC 27853). The standard bacterial strains were obtained from the Traditional and Modern Medicine Research Directorate Laboratory, Ethiopian Public Health Institute, Addis Ababa, Ethiopia.

2.5.2. Preparation of Test Solutions. The concentrations of solution of CSEO, positive control, and negative control were prepared as follows: mixing 1.20 ml CSEO with 0.80 ml of 5% (v/v) Tween-80 to obtain 60% of CSEO solution. 60% CSEO was used as stock solution from which 30% CSEO solution was prepared. The solvent is 5% Tween-80 solution. All the remaining lower concentrations of test solutions such as 15%, 7.5% and 3.75% of CSEO solution were prepared from their preceding concentration of CSEO solution based on the same procedure. 5% (v/v) Tween-80 solution was prepared by mixing 5 ml of Tween-80 (purity 99.99%) with 95 ml of sterilized distilled water. 5 μg/ml (5 gm in 1000 ml) of ciprofloxacin and 5% (v/v) Tween-80 were prepared and used as a positive and negative control, respectively.

2.5.3. Agar Diffusion Method. The antibacterial activity test was performed according to the protocol described by Mungole and Chaturvedi [42] with some minor modifications. Cultures of bacterial strains were prepared in the Luria–Bertani (LB) media for assays. Muller–Hinton Agar (MHA) (Oxoid Ltd., Hampshire, UK) culture media were used in Petri dish plates to grow microorganisms. The culture media were boiled in the sterilized distilled water to dissolve the media and autoclaved at 121°C for 50 min. After cooling, 20 ml of MHA media were poured into the Petri dish plates (90 mm in diameter) using the pipette. The solidified culture media in plates were seeded with bacterial suspension using cotton swabs. For the standardization of test organisms, bacterial suspensions were diluted and adjusted to reach 0.5 McFarland (1.5×10^7 CFU/ml) turbidity at 625 nm using a UV spectrophotometer (Evolution 60S Thermo Scientific, USA), with an optical density of 0.08–0.1.

Wells with 8 mm diameter were punctured into the agar plates with a Cork borer. The wells were filled with 120 μl of EO and control solutions using a micropipette. Sterility and growth control plates were used in parallel to ensure the sterility of nutrient media and microorganism growth ability on media, respectively. All equipment and materials used in all activities were sterilized before use. The Petri dish plates were incubated for 24 hours at 37°C. The inhibition of bacteria growth was evaluated by measuring the diameter (in mm) of the clear zone around the wells [43]. Ciprofloxacin (5 μg/ml) and 5% (v/v) Tween-80 and 5 ml of 99.99% Tween-80 to 95 ml of sterilized distilled water were used as a positive and negative control. The zone of inhibition diameter (ZID, mm) was the mean of three replicates, and all values were expressed as mean ± standard deviation (SD).

2.6. Statistical Analysis. All antibacterial activity tests were performed in triplicate. All data were analyzed using IBM SPSS Package (Version 26.0) for statistical analysis. The experimental results were expressed as mean ± standard deviation (SD). The statistically significant differences between concentrations of CSEO solution were compared using a one-way ANOVA. Differences were considered significant when $p \leq 0.05$. Post hoc analysis was also carried out with Tukey's test.

3. Results

3.1. Essential Oil Yield. EO obtained from *C. leptophyllum* (CSEO) was light yellow in colour. The total percentage yield (% v/w) of CSEO obtained from the dry weight of the plant sample by using the hydrodistillation process was 0.84%.

3.2. Characterization of Essential Oil

3.2.1. GC-MS Analysis. GC-MS analysis of CSEO resulted in the identification of 16 chemical constituents (for relative peak area % ≥ 0.11), which represent 96.86% of the relative area percentage of the total EO compositions. CSEO has oxygenated monoterpenes (92.34%), oxygenated sesquiterpenes (0.57%), and nonoxygenated sesquiterpenes (3.95%). The identified chemical constituents of CSEO were 2,5-dimethoxy-*p*-cymene (87.09%), 2-methoxy-1-methyl-4-(1-methylethyl) benzene (3.09%), 2-methoxy-4-methyl-1-(1-methyl ethyl)-benzene (1.71%), humulene (1.15%), α-curcumene (0.91%), E-caryophyllene (0.90%), α-zingiberene (0.42%), humulene-1,2-epoxide (0.31%), δ-cadinene (0.23%), β-bisabolene (0.21%), 4-(1-methylethyl)-benzaldehyde (0.18%), carvacrol (0.16%), (+)-spathulenol (0.14%), α-amorphene (0.13%), eudesma-4(15),7-dien-1β-ol (0.12%), and *p*-cymene (0.11%). Chemical structures and all the related GC-MS results of chemical constituents of CSEO have been displayed in Figure 2 and Table 1. The result of

GC-MS analysis of CSEO regarding its chemical constituents' retention time (min), experimental Kovats retention indices ($KI_{exp.}$), literature Kovats retention indices ($KI_{lit.}$) chemical name, and relative peak area percentage is summarized and presented in Table 1.

3.2.2. Fourier Transform Infrared (FTIR) Analysis. FTIR spectra of CSEO are shown in Figure 3. CSEO displayed FTIR peaks at 2962 cm^{-1}, 1506 cm^{-1}, 1465 cm^{-1}, 1402 cm^{-1}, 1207 cm^{-1}, 1047 cm^{-1}, and 811 cm^{-1}.

3.2.3. Assessment of Antibacterial Activities. Antibacterial activity effects of various concentrations of CSEO solution were evaluated against six food-related pathogenic bacterial strains such as *S. aureus*, *S. epidermidis*, *S. agalactiae*, *E. coli*, *P. mirabilis*, and *P. aeruginosa*. The results of all zone of inhibition diameter (ZID, mm) are the mean ± SD of three replicates and are provided in Table 2. Values of $p \leq 0.05$ were considered significant.

In comparison with the control groups, antibacterial activities of different concentrations of CSEO solution against some bacterial strains were determined based on their relative zone of inhibition diameter percentage (% RZID) calculation as given in (Eq.(1)) [44, 45] and presented in Table 3.

$$\%\ \%\text{RZID} = \frac{\text{ZID sample} - \text{ZID negative control}}{\text{ZID positive control} - \text{ZID negative control}} \times 100, \quad (1)$$

where % RZID is the percentage relative zone of inhibition diameter, the ZID sample is the zone of inhibition diameter of CSEO (mm), the ZID positive control is the zone of inhibition diameter of ciprofloxacin (mm), and the ZID negative control is the zone of inhibition diameter of 5% Tween-80 (mm).

4. Discussion

In this study, the percentage yield and relative area percentage of the total composition of the isolated CSEO were 0.84% and 96.86%, respectively. In the earlier reports, 0.3–1.1% yields of EOs were reported from different parts of *C. leptophyllum*. Helal et al. [36] reported that 1.1% EO yield was obtained from the fruit part of the plant. Helal et al. [38] also determined the percentage yield of EOs of *C. leptophyllum* from its roots, green aerial part, unripe fruit, and ripe fruit as 0.1%, 0.4%, 0.8%, and 1.1%, respectively. Verma et al. [35] also demonstrated that the percentage yield of EO from the fresh aerial part of *C. leptophyllum* at the seed setting stage was 1.0%. In our study, as shown in Table 1, about 16 identified compounds such as 2,5-dimethoxy-*p*-cymene (87.09%), 2-methoxy-1-methyl-4-(1-methylethyl) benzene (3.09%), 2-methoxy-4-methyl-1-(1-methylethyl)-benzene (1.71%), humulene (1.15%), α-curcumene (0.91%), E-caryophyllene (0.90%), α-zingiberene (0.42%), humulene-1,2-epoxide (0.31%), δ-cadinene (0.23%), β-bisabolene (0.21%), 4-(1-methylethyl)-benzaldehyde (0.18%), carvacrol (0.16%), (+)-spathulenol (0.14%), α-amorphene (0.13%), eudesma-4(15), 7-dien-1β-ol (0.12%), and *p*-cymene (0.11%) which account for 96.86% were determined from GC-MS analysis (peak area % ≥ 0.11%). CSEO is a rich source of oxygenated terpenes (92.91%). 2,5-dimethoxy-*p*-cymene (87.09%) was reported as the major component of CSEO of the aerial part of *C. leptophyllum*. The highest relative area percentage of major chemical constituents (87.09%) is reported for this specific plant species. Some previous reports showed that 2,5-dimethoxy-*p*-cymene (46.8%), methyl ether thymol (14.6%), *p*-cymene (13.9%), γ-terpinene (8.9%), carvacrol methyl ether (7.5%), and γ-gurjunene (1.1%) were the first six major components reported from EO of aerial part of *C. leptophyllum,* and the relative area percentage of the total chemical composition of EO of the plant species was 97.7% (for peak area % > 0.05) [35]. Singh et al. [46] also revealed that the EO of *C. leptophyllum* contained 2,5-dimethoxy-*p*-cymene (50.7%) as a major chemical constituent. In this research work, some unidentified compounds with greater peak area percentages were obtained from the GC-MS analysis of CSEO, and even though their experimental Kovats retention indices (KI_{Expt}) were determined, the corresponding chemical compounds could not be identified from the NIST spectral database or literature survey.

For FTIR peak bands of CSEO, in Figure 3, the peak that appeared at 2962 cm^{-1} represents sp^3C-H symmetric stretching bond vibration. The absence of band absorption in the 1850–1600 cm^{-1} region indicates that a carbonyl group is not likely present. FTIR peaks at 1506 cm^{-1}, 1465 cm^{-1}, and 1402 cm^{-1} show the aromatic $C=C$ bond stretching. The strong peak at 1207 cm^{-1} and the medium peak at 1047 cm^{-1} describe an aromatic C-H bond in-plane bending and C-O bond stretching. The weak peak absorbed at 811 cm^{-1} is due to the aromatic C-H bond out-of-plane bending [47–49]. The FTIR results further supported the functional groups present in the major chemical constituents of CSEO.

The major components of CSEO with diversified functional groups are the most responsible organic compounds for potential antibacterial activities against most food-related pathogenic bacterial species. In the present study, as summarized in Tables 2 and 3, the variation of the zone of inhibition diameter (ZID, mm) and the relative zone of inhibition diameter percentage (% RZID) values depend on the type and concentrations of CSEO solution and bacterial strains used for evaluation. The treatments were compared by analysis of ANOVA on the various concentrations of CSEO solution and on the antibacterial activities measured. This analysis was followed by the post hoc Tukey HSD test (95% confidence level) to compare the effects of different conditions on the measured parameters. The concentrations of CSEO solution at lower concentrations revealed weak antibacterial activities against *S. agalactiae, P. mirabilis,* and *P. aeruginosa.*

The most potent antibacterial activity effects were observed for different concentrations of CSEO solution against *S. aureus* for both minimum and maximum concentrations of solution used (ZID at 3.75% CSEO

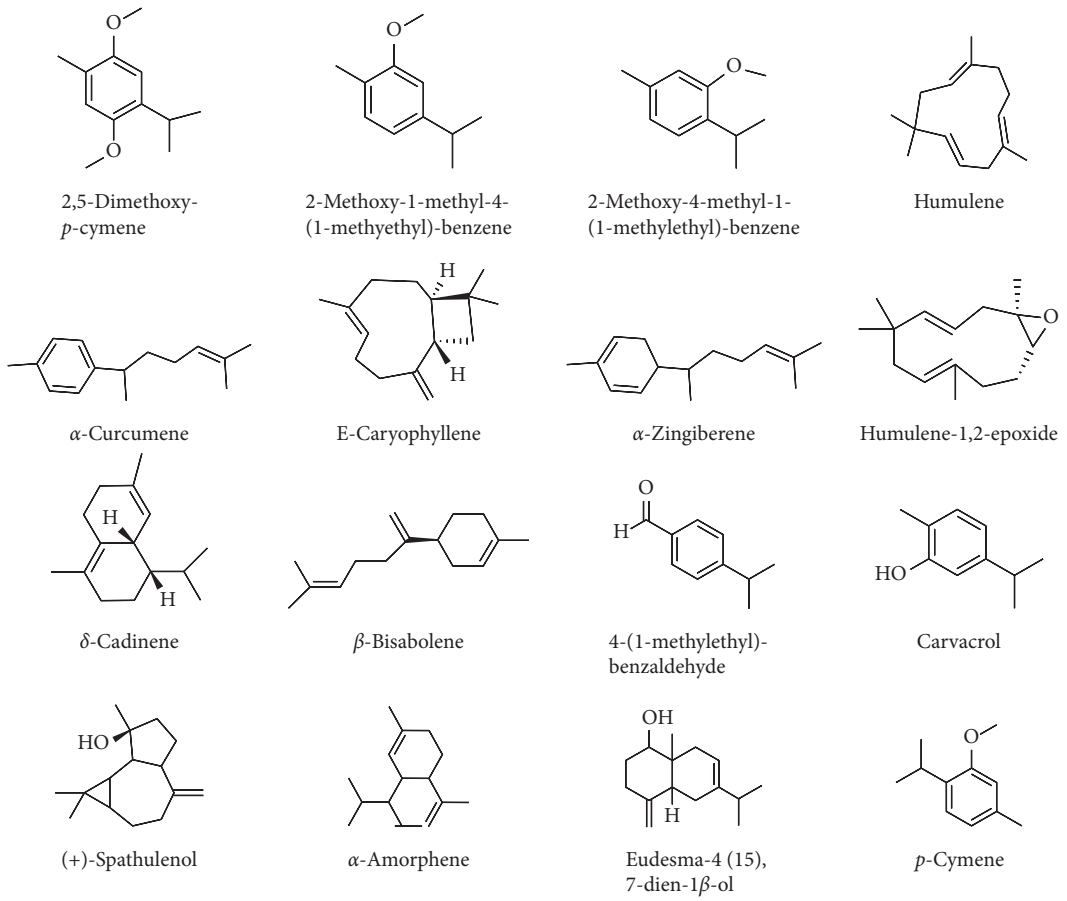

Figure 2: Chemical structures of the first 16 major components of CSEO. The chemical compounds with peak area percentage ≥0.11%.

Table 1: Chemical constituents of CSEO isolated from aerial parts of *C. leptophyllum*.

RT (min)	$KI_{exp.}$	$KI_{lit.}$	Chemical name	Peak area %
15.101	1025	1025	*p*-cymene	0.11
22.749	1224	1224	2-Methoxy-1-methyl-4-(1-methylethyl) benzene	3.09
22.935	1229	1229	2-Methoxy-4-methyl-1-(1-methylethyl) benzene	1.71
23.387	1242	1242	4-(1-methylethyl)-benzaldehyde	0.18
24.744	1280	1280	Carvacrol	0.16
29.297	1416	1415	2,5-Dimethoxy-*p*-cymene	87.09
29.411	1419	1419	E-caryophyllene	0.90
30.554	1456	1456	Humulene	1.15
31.135	1474	1474	α-Amorphene	0.13
31.325	1480	1479	α-Curcumene	0.91
31.749	1493	1493	α-Zingiberene	0.42
32.149	1506	1506	β-Bisabolene	0.21
32.454	1517	1517	δ-Cadinene	0.23
34.201	1576	1576	(+)-spathulenol	0.14
35.178	1608	1608	Humulene-1,2-epoxide	0.31
37.449	1689	1690	Eudesma-4(15), 7-dien-1β-ol	0.12
Class of compounds				% composition
Oxygenated monoterpenes				92.34%
Sesquiterpene compounds				4.52%
Oxygenated sesquiterpenes				0.57%
Sesquiterpene hydrocarbons				3.95%
Total				96.86%

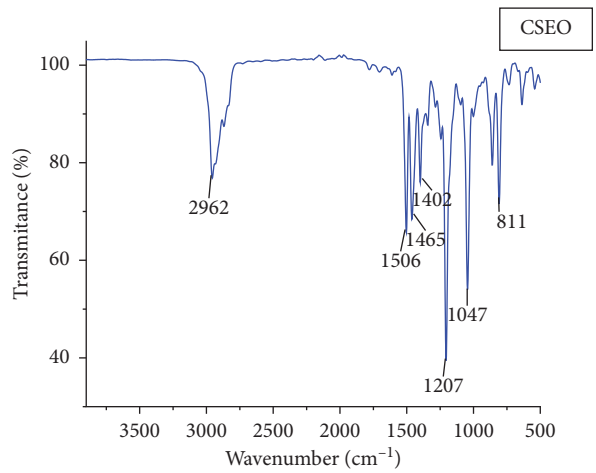

Figure 3: Fourier transform infrared (FTIR) spectra of CSEO.

Table 2: Antibacterial activity of various concentrations of CSEO solution against test microorganisms by agar well diffusion.

S.No.	Test microorganisms	Zone of inhibition diameter (ZID)* mm					Cipro.
		60% CSEO	30% CSEO	15% CSEO	7.5% CSEO	3.75% CSEO	5 μg/ml
1	*S. aureus*	30.67 ± 0.58	24.00 ± 0.00	20.00 ± 0.00	17.67 ± 0.58	14.33 ± 0.58	32.00 ± 0.00
2	*S. epidermidis*	26.67 ± 0.58	23.00 ± 0.00	16.67 ± 0.58	12.00 ± 0.00	9.00 ± 0.00	38.67 ± 1.15
3	*S. agalactiae*	17.00 ± 1.00	8.00 ± 0.00	8.00 ± 0.00	8.00 ± 0.00	8.00 ± 0.00	32.00 ± 1.73
4	*E. coli*	20.00 ± 1.00	14.67 ± 0.58	9.00 ± 0.00	9.00 ± 0.00	9.00 ± 0.00	34.00 ± 1.00
5	*P. mirabilis*	20.33 ± 0.58	11.67 ± 0.58	8.67 ± 0.58	8.00 ± 0.00	8.00 ± 0.00	39.00 ± 1.00
6	*P. aeruginosa*	16.33 ± 0.58	15.00 ± 0.00	12.67 ± 0.58	9.00 ± 0.00	8.00 ± 0.00	32.00 ± 1.00

*ZID values are expressed as the mean ± SD of three replicates. Cipro: ciprofloxacin (positive control), Tween-80 (negative control), and ZID values including well diameter, 8 mm; $p \leq 0.05$ significant as compared to the control.

Table 3: Relative zone of inhibition diameter percentage (% RZID) of different concentrations of CSEO solution against test microorganisms.

Test microorganism	% RZID					
	60% CSEO	30% CSEO	15% CSEO	7.5% CSEO	3.75% CSEO	Cipro.
S. aureus	94.44 ± 2.40	66.67 ± 0	50.00 ± 0	40.28 ± 2.41	26.39 ± 2.41	100.00 ± 0.00
S. epidermidis	60.97 ± 4.09	48.96 ± 1.80	28.27 ± 1.67	13.05 ± 0.48	3.26 ± 0.12	100.00 ± 0.00
S. agalactiae	47.64 ± 4.90	0.00 + 0.00	0.00 ± 0.00	0.00 ± 0.00	0.00 ± 0.00	100.00 ± 0.00
E. coli	46.23 ± 5.63	25.62 ± 1.49	3.85 ± 0.15	3.85 ± 0.15	3.85 ± 0.15	100.00 ± 0.00
P. mirabilis	39.81 ± 2.23	11.80 ± 1.57	2.18 + 1.89	0.00 ± 0.00	0.00 ± 0.00	100.00 ± 0.00
P. aeruginosa	34.82 ± 3.79	29.20 ± 1.22	19.52 ± 3.09	4.17 ± 0.18	0.00 ± 0.00	100.00 ± 0.00

solution = 14.33 ± 0.58 mm and at 60% CSEO solution = 30.67 ± 0.58 mm as compared to ciprofloxacin = 32.00 ± 0 mm), respectively. Generally, Gram-negative bacterial strains showed more resistance to various concentrations of CSEO solution than Gram-positive strains. Some previous reports displayed that some Gram-negative bacteria strains, including *E. coli*, were more resistant, and Gram-positive bacteria including *S. aureus* were more susceptible microorganisms to various concentrations of EO solution of *C. leptophyllum* [35, 38]. Studies of EO solution of *C. leptophyllum* also revealed stronger inhibitory activity against Gram-positive and Gram-negative bacterial strains such as *S. aureus* and *P. aeruginosa,* respectively, as compared to kanamycin and gentamicin antibiotic drug standards [46].

The antibacterial activity effects of CSEO solution on bacterial test strains were further expressed by the calculated values of the relative zone of inhibition diameter percentage (% RZID). The calculated results of % RZID exhibited higher values at higher concentrations of CSEO solution due to the presence of bioactive compounds in the solution. For instance, as shown in Table 3, 60%, 30%, and 15% test solutions of CSEO inhibited the growth of *S. aureus* bacterial species by 94.44%, 66.67%, and 50.00%, respectively, as compared to ciprofloxacin. Similarly, the growth of *S. epidermidis* was inhibited by 60.97% and 48.96% using 60% and 30% CSEO solutions. 60% CSEO solution also showed the relative zone of inhibition diameters of 47.67% and 46.23% against *S. agalactiae* and *E. coli* compared to the positive control. The significant difference ($p \leq 0.05$) of antibacterial activity of different concentrations of CSEO solution against the test

bacterial strains has been more supported by post hoc multiple comparisons between zones of inhibition diameter percentage values.

Besides antibacterial activity tests, the mechanism of action of bioactive compounds of EOs was also the subject of numerous studies [35, 50]. Even though the mechanisms of action of chemical components are not fully answered, actions of chemical compounds of CSEO against bacterial species most probably follow the same mechanisms reported in the previous related research findings [51, 52]. Hydrophobic properties of major chemical components are mainly responsible for the antibacterial action of EO. Even though the action of EO is due to its constituent's synergic effect, the antibacterial activity of CSEO more probably relies on the highly dominant component CSEO, 2,5-dimethoxy-*p*-cymene, which accounts for 87.09% of the total composition. After 2, 5-dimethoxy-*p*-cymene penetrates through the cell membrane; it destroys the cytoplasm membrane and changes membrane permeability and integrity of bacterial cells. Thus, these phenomena make bacteria leak components necessary for their existence and finally cause the death of bacteria. This proposed action mechanism of CSEO is supported by some literature reviews [34]. Some previous reports displayed that Gram-negative bacterial strains are more resistant to EO than Gram-positive bacteria because the former species have an outer membrane surrounding the cell wall, preventing diffusion of hydrophobic chemical components through their lipopolysaccharide layer [35, 50, 53]. The components in the EOs were reported for alteration of structure, functionality, blockage of energy metabolism system, disruption of whole-cell protein, and DNA of the bacterial strains. This was reported as the frequently proposed mechanism of action of EOs for antibacterial activities [54, 55].

5. Conclusions

GC-MS analysis of CSEO identified the dominant chemical constituents in oxygenated terpenes and diversified functional groups. Their chemical compositions are also known to contain different aromatic compounds. The maximum ever reported total composition percentages of CSEO were obtained as 96.86%. This study reported the major compound, 2,5-dimethoxy-*p*-cymene, with a greater relative area percentage, 87.09%, for the first time from the EO of the aerial part of *C. leptophyllum*. Compared to ciprofloxacin, the relative zone of inhibition diameter percentage (% RZID) of 15–60% of CSEO solution displayed average or above average growth inhibition activities against *S. aureus*. Similarly, 30% and 60% of CSEO solution inhibited the above average percentage of growth of S. epidermidis. *S. agalactiae* exhibited the strongest resistant effect towards all test solutions except 60% CSEO solution. Generally, stronger inhibition activities were observed for Gram-positive bacterial strains than Gram-negative bacterial strains. Bioactive compounds in CSEO potentially inhibit the growth of some food spoilage bacterial strains. Therefore, this study contributes to the scientific evidence required for supporting the traditional medicinal practices exercised by some communities using natural products of *C. leptophyllum*. This research work is also used to strengthen the current efforts of scientific investigation regarding the application of EOs of various medicinal plants from the ecology of Ethiopia as natural antibacterial agents. To evaluate the effectiveness of the antibacterial activities of CSEO, it needs more evaluation of CSEO against a vast number of pathogenic bacterial strains responsible for food contamination.

Abbreviations

EOs: Essential oils
CSEO: *Cyclospermum leptophyllum* essential oil
FTIR: Fourier transform infrared
GC-MS: Gas chromatography-mass spectrometry
ATCC: American Type Culture Collection
RZID: Relative zone of inhibition diameter
KI_{Lit}: Literature-based Kovats retention index
KI_{Exp}: Experimental-based Kovats retention index
MHA: Muller–Hinton agar
LB: Luria–Bertani
NIST: National Institute Standard and Technology.

Data Availability

The datasets used and/or analyzed during the current study are available from the corresponding author upon reasonable request.

Conflicts of Interest

The authors declare that they have no conflicts of interests.

Authors' Contributions

YHG conceived, designed, performed, and analyzed the experiments and prepared the original manuscript. AAG performed all the in vitro antibacterial activities. SDG carried out the reading of the results of incubated plates. FBT and AB helped revise the prepared manuscript and adjust the tables and figures. MGT and RKB supervised the research work. All authors read and agreed to the published version of the manuscript.

Acknowledgments

The authors are grateful to Cadila Pharmaceuticals PLC (Ethiopia) for providing ciprofloxacin. The authors also want to extend their appreciation to the Ethiopian Public Health Institute for allowing them to use their laboratory and resource facilities to conduct antibacterial activity tests.

References

[1] R. A. Mothana, M. S. Alsaid, and N. M. Al-musayeib, "Phytochemical analysis and in vitro antimicrobial and free-radical-scavenging activities of the essential oils from *Euryops arabicus* and *Laggera decurrens*," *Molecules*, vol. 16, no. 6, pp. 5149–5158, 2011.

[2] S. F. Bashir and G. Kumar, "Preliminary phytochemical screening and in vitro antibacterial activity of *Plumbago indica* (Laal chitrak) root extracts against drug-resistant *Escherichia coli* and *Klebsiella pneumoniae*," *Open Agriculture*, vol. 6, no. 1, pp. 435–444, 2021.

[3] Y. H. Gonfa, F. Beshah, M. G. Tadesse, A. Bachheti, and R. K. Bachheti, "Phytochemical investigation and potential pharmacologically active compounds of *Rumex nepalensis*-An appraisal," *Beni-Suef University Journal of Basic and Applied Sciences*, vol. 10, no. 1, pp. 18–11, 2021.

[4] J. Mehta, R. Rolta, D. Salaria et al., "Phytocompounds from Himalayan medicinal plants as potential drugs to treat multidrug-resistant *Salmonella typhimurium*-An in silico approach," *Biomedicines*, vol. 9, no. 10, pp. 1402–1419, 2021.

[5] S. Shabab, Z. Gholamnezhad, and M. Mahmoudabady, "Protective effects of medicinal plant against diabetes-induced cardiac disorder-A review," *Journal of Ethnopharmacology*, vol. 265, pp. 113328–113425, 2021.

[6] W. Kooti, Z. Hasanzadeh-Noohi, N. Sharafi-Ahvazi, M. Asadi-Samani, and D. Ashtary-Larky, ""Phytochemistry, pharmacology, and therapeutic uses of black seed (*Nigella sativa*)," *Chinese Journal of Natural Medicines*, vol. 14, no. 10, pp. 732–745, 2016.

[7] V. Gupta, R. Guleri, M. Gupta et al., "Anti-neuro-inflammatory potential of *Tylophora indica* (Burm.F) Merrill and development of an efficient in vitro propagation system for its clinical use," *PLoS One*, vol. 15, no. 3, pp. 02301422–e230220, 2020.

[8] Y. S. Ghebremariam, M. S. Demoz, and N. A. Fissehaye, "Phytochemical screening and antimicrobial potential of *Lepidium sativium* and *Rumex nervosus* in Eritrea," *Journal of Advances in Medical and Pharmaceutical Sciences*, vol. 19, no. 1, pp. 1–8, 2018.

[9] A. Manilal, K. R. Sabu, M. Shewangizaw et al., "In vitro antibacterial activity of medicinal plants against biofilm-forming methicillin-resistant *Staphylococcus aureus*: efficacy of *Moringa stenopetala* and *Rosmarinus of ficinalis* extracts," *Heliyon*, vol. 6, pp. e03303–e03308, 2020.

[10] A. Enyew, Z. Asfaw, E. Kelbessa, and R. Nagappan, "Ethnobotanical study of traditional medicinal plants in and around Fiche district, Central Ethiopia," *Current Research Journal of Biological Sciences*, vol. 6, no. 4, pp. 154–167, 2014.

[11] H. T. Huang, C. C. Lin, T. C. Kuo, S. J. Chen, and R. N. Huang, "Phytochemical composition and larvicidal activity of essential oils from herbal plants," *Planta*, vol. 250, no. 1, pp. 59–68, 2019.

[12] A. Limenew, B. Archana, K. B. Rakesh, A. Husen, M. Getachew, and D. P. Pandey, "Potential role of forest-based plants in essential oil production: an approach to cosmetic and personal health care applications," in *Non-Timber Forest Products*Springer, Berlin, Germany, 2021.

[13] E. Kavetsou, S. Koutsoukos, D. Daferera et al., "Encapsulation of *Mentha pulegium* essential oil in Yeast Cell Microcarriers: an approach to environmentally friendly pesticides," *Journal of Agricultural and Food Chemistry*, vol. 67, no. 17, pp. 4746–4753, 2019.

[14] J. S. Neves, Z. Lopes-da-silva, M. de Sousa Brito Neta et al., "Preparation of terpolymer capsules containing *Rosmarinus officinalis* essential oil and evaluation of its antifungal activity," *RSC Advances*, vol. 9, no. 39, pp. 22586–22596, 2019.

[15] M. Osanloo, A. Abdollahi, A. Valizadeh, and N. Abedinpour, "Antibacterial potential of essential oils of *Zataria multiflora* and *Mentha piperita*, micro- and nano-formulated forms," *Iranian Journal of Microbiology*, vol. 12, no. 1, pp. 43–51, 2020.

[16] N. A. S. Rozman, W. Y. Tong, C. R. Leong et al., "*Homalomena pineodora* essential oil nanoparticle inhibits diabetic wound pathogens," *Scientific Reports*, vol. 10, pp. 3307–3311, 2020.

[17] B. J. Okoli, Z. Ladan, F. Mtunzi, and Y. C. Hosea, "Vitex negundo L. Essential oil: odorant binding protein efficiency using molecular docking approach and studies of the mosquito repellent," *Insects*, vol. 12, pp. 1061–1126, 2021.

[18] D. Kotagiri and K. B. Shaik, *Antimicrobial and Antioxidant Properties of Essential Oil Isolated from Coleus zeylanicus under Normal and Salinity Stress Conditions, Free Radicals, Antioxidants and Diseases*, IntechOpen, London, UK, pp. 107–119, 2018.

[19] G. O. Silva, A. T. Abeysundara, and M. M. W. Aponso, "Extraction methods, qualitative and quantitative techniques for screening of phytochemicals from plants," *American Journal of Essential Oils and Natural Products*, vol. 5, no. 2, pp. 29–32, 2017.

[20] S. K. Bardaweel, B. Bakchiche, H. A. Alsalamat, M. Rezzoug, A. Gherib, and G. Flamini, "Chemical composition, antioxidant, antimicrobial and antiproliferative activities of essential oil of *Menthaspicata* L. (*Lamiaceae*) from Algerian Saharan atlas," *BMC Complementary and Alternative Medicine*, vol. 18, pp. 201–207, 2018.

[21] M. S. Ali-Shtayeh, R. M. Jamous, S. Y. Abu-Zaitoun, A. I. Khasati, and S. R. Kalbouneh, "Biological properties and bioactive components of *Mentha spicata* L. essential oil: focus on potential benefits in the treatment of obesity, Alzheimer's disease, dermatophytosis, and drug-resistant infections," *Evidence-based Complementary and Alternative Medicine*, vol. 2019, Article ID 383426, 11 pages, 2019.

[22] H. A. S. El-Nashar, W. M. Eldehna, S. T. Al-Rashood, A. Alharbi, R. O. Eskandrani, and S. H. Aly, "GC/MS analysis of essential oil and enzyme inhibitory activities of *Syzygium cumini* (*Pamposia*) grown in docking studies," *Molecules*, vol. 26, no. 22, pp. 6984–7011, 2021.

[23] J. C. Lopez-Romero, H. González-Ríos, A. Borges, and M. Simões, "Antibacterial effects and mode of action of selected essential oils components against *Escherichiacoli* and *Staphylococcus aureus*," *Evidence-based Complementary and Alternative Medicine*, vol. 2015, Article ID 795435, 9 pages, 2015.

[24] C. Saviuc, B. Ciubuca, G. Dinca et al., "Development and sequential analysis of a new multi-agent, anti-acne formulation based on plant-derived antimicrobial and anti-inflammatory compounds," *International Journal of Molecular Sciences*, vol. 18, pp. 175–211, 2017.

[25] A. Thesing, J. do Nascimento, R. G. Jacob, and J. F. Santos, "Eucalyptus oil-mediated synthesis of gold nanoparticles," *Journal of Chemistry and Chemical Engineering*, vol. 12, no. 2, pp. 52–59, 2018.

[26] D. Nartey, J. Gyesi, and L. S. Borquaye, "Chemical composition and biological activities of the essential oils of Chrysophyllum albidum G. Don (african star apple)," *Biochemistry Research International*, vol. 2021, Article ID 9911713, 11 pages, 2021.

[27] E. Majewska, M. Kozłowska, D. Kowalska, and E. Gruczyńska, "Characterization of the essential oil from cone-berries of *Juniperus communis* L. (*Cupressaceae*)," *Herba Polonica*, vol. 63, no. 3, pp. 48–55, 2017.

[28] M. Chandra, O. Prakash, R. Kumar et al., "β-Selinene-rich essential oils from the parts of *Callicarpa macrophylla* and

their antioxidant and pharmacological activities," *Medicines*, vol. 4, no. 3, 2017.

[29] R. K. Bachheti, B. Archana, and S. S. Ramachandran, "Chemical Composition of the essential oil from Schinus molle L.(Peruvian pepper)," *Der Pharma Chemica*, vol. 10, no. 10, pp. 139–147, 2018.

[30] M. C. Queiroga, M. Pinto Coelho, S. M. Arantes, M. E. Potes, and M. R. Martins, "Antimicrobial activity of essential oils of *Lamiaceae* aromatic spices towards sheep mastitis-causing *Staphylococcus aureus* and *Staphylococcus epidermidis*," *Journal of Essential Oil Bearing Plants*, vol. 21, no. 5, pp. 1155–1165, 2018.

[31] L. Jin, J. Teng, L. Hu et al., "Pepper fragrant essential oil (PFEO) and functionalized MCM-41 nanoparticles: formation, characterization, and bactericidal activity," *Journal of the Science of Food and Agriculture*, vol. 99, no. 11, pp. 5168–5175, 2019.

[32] E. Majewska, M. Kozłowska, E. Gruczyńska-Sekowska, D. Kowalska, and K. Tarnowska, "Lemongrass (*Cymbopogon citratus*) Essential oil: extraction, composition, bioactivity and uses for food preservation-a review," *Polish Journal of Food and Nutrition Sciences*, vol. 69, no. 4, pp. 327–341, 2019.

[33] S. Siddique, Z. Parveen, F. Bareen, and S. Mazhar, "Chemical composition, antibacterial and antioxidant activities of essential oils from leaves of three *Melaleuca* species of Pakistani flora," *Arabian Journal of Chemistry*, vol. 13, no. 1, pp. 67–74, 2020.

[34] M. Kürkçüoglu, "Essential oil composition from fruits and aerial parts of *Bilacunaria anatolica* A. Duran (*Apiaceae*) endemic in Turkey," *Journal of Essential Oil Bearing Plants*, vol. 19, no. 2, pp. 379–383, 2016.

[35] Y. Zhang, X. Liu, Y. wang, P. Jiang, and S. Y. Quek, "Antibacterial activity and mechanism of cinnamon essential oil against escherichia coli and staphylococcus aureus," *Food Control*, vol. 59, pp. 1–21, 2015.

[36] R. S. Verma, R. C. Padalia, S. K. Verma, A. Chauhan, and M. P. Darokar, "Chemical composition and antibacterial activity of the essential oils of *Laggera crispata* (vahl) hepper and wood, *Cyclospermum leptophyllum* (pers.) eichler and *Perilla frutesc*ens (L.) Britton," *Analytical Chemistry Letters*, vol. 5, no. 3, pp. 162–171, 2015.

[37] I. Helal, A. Galala, H. E. Saad, and A. F. Halim, "Bioactive constituents from *Apium leptophyllum* fruits," *British Journal of Pharmaceutical Research*, vol. 14, no. 3, pp. 1–8, 2016.

[38] C. Pande, G. Tewari, C. Singh, and S. Singh, "Essential oil composition of aerial parts of *Cyclospermum leptophyllum* (Pers.) Sprague ex Britton and P. Wilson," *Natural Product Research*, vol. 25, no. 6, pp. 592–595, 2011.

[39] I. Helal, A. Galala, H. A. Saad, and A. F. Halim, "Chemical composition and α-amylase inhibitory activity of *Apium leptophyllum* essential oils," *Journal of American Science*, vol. 11, no. 4, pp. 1–7, 2015.

[40] I. D. A. Freires, R. M. Murata, V. F. Furletti et al., "(*Coriander*) essential oil: antifungal activity and mode of action on *Candida* spp., and molecular targets affected in human whole-genome expression," *PLoS One*, vol. 9, no. 6, Article ID e, 2014.

[41] M. A. Elfotoh, K. A. Shams, K. P. Anthony et al., "Lipophilic constituents of Rumex vesicarius L. and Rumex dentatus L." *Antioxidants*, vol. 2, no. 3, pp. 167–180, 2013.

[42] T. Getahun, V. Sharma, and N. Gupta, "The genus *Laggera* (*Asteraceae*) ethnobotanical and ethnopharmacological information, chemical composition as well as biological activities of its essential oils and extracts-A review," *Chemistry and Biodiversity*, vol. 16, no. 8, 2019.

[43] A. Mungole and A. Chaturvedi, "Determination of antibacterial activity of two medicinally important Indian taxa," *Der Pharma Chemica*, vol. 3, no. 1, pp. 83–89, 2011.

[44] S. B. Bataineh, Y. H. Tarazi, and W. A. Ahmad, "Antibacterial efficacy of some medicinal plants on multidrug resistance bacteria and their toxicity on eukaryotic cells," *Applied Sciences*, vol. 11, pp. 1–13, 2021.

[45] B. Singh, N. Dutt, D. Kumar, S. Singh, and R. Mahajan, "Taxonomy, ethnobotany and antimicrobial activity of *Croton bonplandianum, Euphorbia hirta* and *Phyllanthus fraternus*," *Journal of Advances in Developmental Research*, vol. 2, no. 1, pp. 21–29, 2011.

[46] A. Salayová, Z. Bedlovicova, N. Daneu et al., "Green synthesis of silver nanoparticles with antibacterial activity using various medicinal plant extracts: morphology and antibacterial efficacy," *Nanomaterials*, vol. 11, no. 4, pp. 1005–1020, 2021.

[47] C. Singh, S. Singh, C. Pande, G. Tewari, V. Pande, and P. Sharma, "Exploration of antimicrobial potential of essential oils of *Cinnamomum glanduliferum, Feronia elephant, Bupleurum hamiltonii* and *Cyclospermum leptophyllum* against foodborne pathogens," *Pharmaceutical Biology*, vol. 51, no. 12, pp. 1607–1610, 2013.

[48] S. Aswathy Aromal and D. Philip, "Green synthesis of gold nanoparticles using *Trigonella foenum-graecum* and its size-dependent catalytic activity," *Spectrochimica Acta Part A: Molecular and Biomolecular Spectroscopy*, vol. 97, pp. 1–5, 2012.

[49] S. Groiss, R. Selvaraj, T. Varadavenkatesan, and R. Vinayagam, "Structural characterization, antibacterial and catalytic effect of Iron oxide nanoparticles synthesised using the leaf extract of *Cynometra ramiflora*," *Journal of Molecular Structure*, vol. 1128, pp. 572–578, 2017.

[50] S. I. Shofia, K. Jayakumar, A. Mukherjee, and N. Chandrasekaran, "Efficiency of brown seaweed (*Sargassum longifolium*) polysaccharides encapsulated in nanoemulsion and nanostructured lipid carrier," *RSC Advances*, vol. 8, no. 29, pp. 15973–15984, 2018.

[51] K. Chebbac, A. Moussaoui, M. Bourhia, A. M. Salamatullah, A. Alzahrani, and R. Guemmouh, "Chemical analysis and antioxidant and antimicrobial activity of essential oils from *Artemisia negrei* L. against drug-resistant microbes," *Evidence-Based Complementary and Alternative Medicine*, vol. 2021, Article ID 5902851, 9 pages, 2021.

[52] E. Dănilă, Z. Moldovan, M. Popa, M. C. Chifiriuc, A. D. Kaya, and M. A. Kaya, "Chemical composition, antimicrobial and antibiofilm efficacy of *C. limon* and *L.* Angustifolia EOs and of their mixtures against *Staphylococcus epidermidis* clinical strains," *Industrial Crops and Products*, vol. 122, pp. 483–492, 2018.

[53] R. Iseppi, R. Tardugno, V. Brighenti et al., "Phytochemical composition and in vitro antimicrobial activity of essential oils from the *Lamiaceae* Family against *Streptococcus agalactiae* and *Candida albicans* biofilm," *Antibiotics*, vol. 9, pp. 592–616, 2020.

[54] P. Tongnuanchan and S. Benjakul, "'Essential oils: extraction, bioactivities, and their uses for food preservation," *Journal of Food Science*, vol. 79, no. 7, pp. 1231–1249, 2014.

[55] C. Zhou, C. Li, S. Siva, H. Cui, and L. Lin, "Chemical composition and antibacterial activity and study of the interaction mechanisms of the main compounds present in the *Alpinia galanga* rhizomes essential oil," *Industrial Crops and Products*, vol. 165, 2021.

Hindawi
Journal of Chemistry
Volume 2022, Article ID 2000237, 10 pages
https://doi.org/10.1155/2022/2000237

Research Article

Essential Oil from Hibiscus Flowers through Advanced Microwave-Assisted Hydrodistillation and Conventional Hydrodistillation

Hesham H. A. Rassem,[1] **Abdurahman H. Nour**,[2] **Gomaa A.M. Ali**,[3] **Najat Masood**,[4,5] **Amal H. Al-Bagawi**,[4] **Tahani Y. A. Alanazi**,[4] **Sami Magam**,[5,6] **and Mohammed A. Assiri**[7]

[1]*Chemistry Department, Faculty of Science, Hodeidah University, Hodeidah City, Yemen*
[2]*Faculty of Chemical and Natural Resources Engineering, Universiti Malaysia Pahang (UMP), Pahang, Malaysia*
[3]*Chemistry Department, Faculty of Science, Al–Azhar University, Assiut 71524, Egypt*
[4]*Department of Chemistry, College of Science, University of Ha'il, Ha'il City, Saudi Arabia*
[5]*Department of Marine Chemistry and Pollution, Faculty of Marine Science and Environment, Hodeidah University, Hodeidah City, Yemen*
[6]*Basic Science Department, Preparatory Year, University of Ha'il, Ha'il City 1560, Saudi Arabia*
[7]*Department of Chemistry, Faculty of Science, King Khalid University, Abha 61413, P.O. Box 9004, Saudi Arabia*

Correspondence should be addressed to Hesham H. A. Rassem; hesham_rassem@yahoo.com

Received 7 July 2022; Revised 21 August 2022; Accepted 10 September 2022; Published 30 September 2022

Academic Editor: Romina Alina Marc (Vlaic)

Due to the increased demand and importance of essential oils in medicinal applications, advanced essential oil extraction techniques have been employed. Both conventional hydrodistillation (HD) and microwave-assisted hydrodistillation (MAHD) were employed to extract the essential oils from the hibiscus flower. Extraction time and solvent polarity were the most critical factors. Scanning electron microscopy (SEM) was used to investigate the surface morphologies of raw powdered hibiscus flowers (not exposed to any pretreatment) and pretreated powdered hibiscus flowers (exposed to methanol absorption for 60 minutes prior to extraction). Extractive chemistry analysis utilizing Fourier transform infrared (FTIR) spectroscopy was performed on the volatile oil obtained by MAHD. Different peaks in the gas chromatography/mass spectrometry (GC/MS) analysis indicated the presence of thirty-seven different compositions. MAHD was more energy efficient, had higher yield production, and was environmentally friendly, reducing HD's overall carbon footprint by 40%. Oxygenated monoterpene, sesquiterpene, and sesquiterpene hydrocarbons were found in the hibiscus flower's crude extract. Moreover, the methanolic extract of Hibiscus rosa-sinensis has potent antioxidant properties. A hibiscus flower extract had scavenging activities of 51.2% at 0.2 mg/mL, 0.3% at 0.6 mg/mL, 0.8% at 1.0 mg/mL, and 68.5% at 1.2 mg/mL against DPPH free radicals. Therefore, the MAHD method is well-suited to extracting essential oils from hibiscus flowers, and the resulting oil has the potential to provide significant therapeutic advantages.

1. Introduction

Aromatic chemical compounds are found in essential oils, which are volatile industrial oils. Important chemical compounds in essential oils include phenols, hydrocarbons, aldehydes, ketones, alcohols, and esters [1]. Essential oils extracted from several plants can be purchased commercially [2]. A ton of research shows that even tiny amounts of essential oils can significantly impact biological activity [3, 4].

Numerous bioassays are frequently performed to detect the antioxidant from plant extracts such as flowers. Neoteric reports indicate an inverse connection between the consumption of antioxidant-rich foods and the incidence of human disease [5]. Therefore, the food industry heavily uses synthetic antioxidants such as butylated hydroxyanisole (BHA) and butylated hydroxytoluene (BHT), which may contribute to cancer development and liver toxicity [6]. Plants have been the basis of conventional medicine

worldwide [7–9]. Using currently known methodologies and techniques for finding natural antioxidants in plants has much potential. Many experts have discussed many ways in which these plants can be put to good use [10–12].

Hibiscus rosa-sinensis is a small, evergreen tree growing up to 1.5–3.0 m (5.0–10 ft) wide and 2.5–5.0 m (8.0–16 ft) tall, with shiny leaves and red flowers in summer. Different parts of this plant, such as leaves, roots, and flowers, have been known to possess medicinal features such as laxatives, aphrodisiacs, and contraceptives. Hibiscus rosa-sinensis is well-known in the *Malvaceae* implant family as an evergreen grassy plant.

Fatty acids, flavonoids, carbohydrates, proteins, and minerals are all found in hibiscus flowers [13]. The flowers have been studied for their anti-inflammatory, antihypertensive, hepatoprotective, anticancer, antidiabetic, antinociceptive, cytotoxicity, antibacterial, and antioxidant properties [14].

Techniques such as solvent extraction, steam distillation, hydrodistillation (HD), maceration, and expression are commonly used to extract essential oils from plants [15, 16]. Even though these methods are labeled as "traditional extraction procedures," HD is utilized multiple times throughout [15, 17]. However, several disadvantages are associated with traditional techniques, such as damage to volatile compounds, high energy consumption, and long extraction time [17–19]. Extraction methods have evolved due to increase in extraction yield, decrease in extraction time, improvement in soil quality, and decrease in operating costs. Modern styles include pressurized solvent extraction, ultrasound-assisted extraction, supercritical fluid extraction, microwave-assisted extraction, and microwave-assisted hydrodistillation (MAHD) [15, 20]. There are many advantages of using microwave-assisted hydrodistillation, such as its low cost, and it is one of the modern and fast methods, and it is possible to get better yield from the extracted oils [21, 22].

Recent studies [23, 24] have shown that microwave ovens can be used to remove active plant components effectively. There is a close relationship between the dielectric constant of the solvent and the sample and the effectiveness of MAHD [25, 26]. The extraction process limits the examination of various components in plant material because traditional procedures are thermally hazardous, solvent-intensive, and time-consuming [27, 28]. This novel, promising MAHD method can potentially reduce solvent usage, protect thermolabile elements, and facilitate rapid, high-yield extraction.

Since MAHD allows for solvent selectivity, it can reduce extraction time and allows for precise temperature control, and it is widely employed as a method for chemical extraction. As it produces less carbon dioxide (CO_2), MAHD is better for the environment [29]. Conventional methods for bioactive component extraction are laborious and lack precise temperature regulation [27]. Many bioactive components of plants have also been extracted using this method. Although it is more effective than traditional steam distillation [23, 30], its use depends on the solvent's dielectric constants and the sample [25].

Healing with MAHD relies on its direct effect on polar materials or solvents because this is where the action is most concentrated. Ionic conduction and the rotation of two dipoles drive this phenomenon [31]. Some of the many advantages of MAHD include targeted heating, higher output, sufficient temperature maintenance, fewer required process steps, quicker start-up, smaller equipment footprint, and lower temperature disparities. Moreover, unlike conventional oil, the oils produced through MAHD do not harm the planet [32]. Furthermore, there are scant studies on functional group analysis of the chemicals recovered from hibiscus flowers using MAHD or on the impact of pretreatment input materials. Furthermore, no reports compare the effectiveness of MAHD and the traditional HD method in extracting the oil from the hibiscus flower's functional groups. This study compares MAHD to HD to extract the volatile oils found in hibiscus blooms. The hibiscus flower was studied morphologically before and after pretreatment to determine the impact of the process. GC-MS was used to determine the chemical makeup of the sample. Parts of the compounds recovered by each method were compared, and FTIR analysis was used to look at structural changes in the functional groups of the components. The financial, energy, and ecological effects of MAHD and HD extraction were also studied.

2. Materials and Methods

2.1. Materials. The mature and fresh flowers of hibiscus were collected in February 2016 from a location in Gambang Campus, Universiti Malaysia Pahang, Malaysia. In addition, the ecosystem for planting the flower was the system accustomed to climate change; whether it is summer or winter, it grows throughout the year. It does not tolerate low temperatures below 10°C. As defined by the climate of Malaysia, temperatures do not reach this degree in winter. This study used chemicals exclusively for analysis to verify that the extracted essential oil is safe for the environment. A small number of chemicals utilized in this work, including dimethyl sulfoxide (DMSO), anhydrous sodium sulfate (Na_2SO_4), and potassium dichromate ($K_2Cr_2O_7$), were supplied from Sigma-Aldrich (USA).

2.2. Pretreatment. Some dirt and sticky material, such as tiny sand grains, were found in the hibiscus flowers. The material was cleaned to eliminate harmful chemicals as much as possible. This method required fresh hibiscus flower samples, which were washed in distilled water for 60 minutes and then air-dried for 24 hours at temperature between 60 and 70°C. After that, the particle size of the sample was reduced by crushing and grinding about 70 g of dried hibiscus flower petals. Using a mechanical sieve shaker, 80 μm of hibiscus flower powder was obtained after grinding and sieving the samples. It was determined that drying the flower powder at 105 ± 5°C would provide a constant weight. The following formula determined the flower powder's moisture content:

$$\text{Moisture content } (\%) = \frac{W_1 - W_2}{W_1} x100, \quad (1)$$

W_1 and W_2 are the weight of the flower powder before and after drying (g), respectively. The moisture content of the flower powder was about 22.2%.

The thoroughly dried hibiscus flower powder sample was kept as an indicator. Before extraction, 35 g of the powdered hibiscus flowers were weighed and presoaked for 1 h in distilled methanol at a ratio of 8 : 1 w/w of methanol to whole dried hibiscus flower powder, respectively [33]. All results were based on the weight of the dried samples.

2.3. Scanning Electron Microscopy Analysis. SEM images were taken at 60 and 120 minutes in MAHD and HD of untreated dried hibiscus flower powder, presoaked hibiscus flower powder, and hibiscus flower powder that has had its essential oils extracted. The TM3030 Plus tabletop microscope was used to examine the specimens. All samples were analyzed at an analytical working distance of 11.3 mm and an accelerating voltage of 5.0–15 kV (15–600,000 magnification). Electrical discharge was prevented by sputter coating prior to SEM observation. The powdered hibiscus flowers underwent SEM analysis to detect morphological alterations throughout the extraction process.

2.4. Extraction of Hibiscus Oil via Microwave-Assisted Hydrodistillation. The Clevenger-type equipment described in the literature [23] could be microwaved in a Milestone MWS Ethos E Solvent Extraction system (2.5 kW; 230 V-60 Hz; 2450 MHz). The microwave oven cavity was filled with a 1 L reactor (round bottom flask) holding 35 g of the powdered hibiscus flower matrix (which had been presoaked in methanol at a weight-to-weight ratio of 8 : 1 of methanol to dried hibiscus flower powder). The extracted oil was collected using the clenching equipment placed on the microwave outside. For a total of 120 minutes, the microwave was set to 400 W of power. When the oil in the flask evaporates, it leaves vapor behind. A condenser reduces the pressure of steam and the vapors of essential oils. Methanol and essential oil are combined in the condensate before being collected and separated using dichloromethane in a separating funnel.

2.5. Extraction of Hibiscus Flower Oil through Hydrodistillation. The essential oil of hibiscus flowers was extracted using a Clevenger machine and the HD method. The extraction was heated with an electromantle (Nahita model 655). HD extraction works similar to MAHD extraction. Nevertheless, what sets apart the various methods is the heat source used. To make a fair comparison between HD and MAHD, we used the same sample size (1.0 L) and concentration (35 g of powdered hibiscus flowers in the same volumes of methanol) for both extraction procedures. The conventional methods reqiure a longer extraction time to attain maximal oil recovery [23, 29], while this extraction was conducted at an operating power of 300 W for only 180 minutes. The collected condensate containing a mixture of methanol and essential oil is poured into the separating funnel with solvent dichloromethane.

2.6. Gas Chromatography-Mass Spectrometry Analysis. The analysis was carried out with a DB-WAX-fused silica column (30 m × 0.25 mm i.d. and film thickness 0.25 μm) and Agilent 5975C Series GC/MS, Agilent, USA. The oven was set to 60°C for 10 minutes, then increased by 20°C every minute to 230°C, and finally maintained at 250°C for 10 minutes. In order to achieve a 30 cm/s linear velocity, helium was used as the carrier gas.

Both MAHD extract samples were diluted to a concentration of 3.0% in dichloromethane by mixing 1.0 μL of pure essential oil of flowers with 10 μL of dichloromethane. The split ratio was maintained when injecting the diluted samples into GC. Mass spectral data collected from the sample were compared to data obtained from pure, commercially available standards injected under identical conditions to identify the components.

Mass spectral data of essential oils from the National Institute of Standard and Technology (NIST MS collection) were compared to the components found in the extracted oil. The retention times of the chemicals found in the hibiscus flower oil were similar enough for a quantitative analysis to be performed using both techniques. The relative abundance of individual components in the purified hibiscus flower oil was determined by measuring the area under respective peaks. When estimating the size of each peak, the normalization approach was used, with 100% being the full extent of the peaks.

2.7. Fourier Transform Infrared Spectroscopy. Oil extracted using HD and MAHD was analyzed for functional groups. The purpose was to learn more about the bonding structures and alterations in the oil's chemical compositions that had taken place during the extraction process. For the analysis, we used a Thermo Scientific Nicolet iS5 FTIR spectrometer, made in USA by Thermo Scientific®. The FTIR spectrum was recorded between 4000 and 400 cm^{-1}.

2.8. Calculation of Energy Consumption. The total amount of energy expended during MAHD and HD extraction of hibiscus flower oil was determined to assess its environmental effect. The formula for determining energy consumption for both approaches is shown in the following equation:

$$\text{Energy consumed (kWh)} = \frac{(\text{Power consumed for the extraction process} / \text{Extraction time})}{1000}. \quad (2)$$

2.9. Antioxidant (DPPH Radical Scavenging) Assay. Methanol extract of hibiscus flower (Cass.) was tested for its ability to quench free radicals with 2,2-diphenyl-1-picrylhydrazyl (DPPH). 95% of methanol was used to make a DPPH solution (0.004% w/v). The investigated medication was prepared in test tubes with five distinct concentrations. We added 1.0 mL of newly produced DPPH reagent to the test tubes and left them to incubate overnight in the dark. The absorbance was checked at 517 nm after incubating the sample for 10 minutes (Systronics UV: Visible spectrophotometer, USA). The positive control used in this process was ascorbic acid.

Scavenging activity (%) of the DPPH free radical was measured using the following equation [34]:

$$\text{Inhibition}\,(\%) = \left(\frac{A_0 - \mathrm{A}_1}{A_0}\right) * 100, \tag{3}$$

where A_0 is the absorbance of the control and A_1 is the absorbance of the test.

3. Results and Discussion

The yield of flower oil can be affected by variables in the extraction process [35]. These variables include the solvent ratio, extraction power, and extraction time. Previous studies have looked into how different extraction settings affect the effectiveness of HD and MAHD procedures. Results from those analyses provided insights into the selection of extraction settings for MAHD and HD that yielded the best overall performance.

3.1. Scanning Electron Microscopy Analysis of Hibiscus Flower Powder

3.1.1. Surface Morphology of Untreated and Pretreated Hibiscus Flower Powder. Figures 1(a) and 1(b) illustrate the surface morphologies of raw powdered hibiscus flower (without soaking in methanol before extraction) and pretreated hibiscus flower (soaked in methanol for 60 min). The raw powdered flower shown in Figure 1(a) is slender and dry. Conversely, the powdered hibiscus flower undergoes discernible physical changes after being pretreated. As shown in Figure 1(b), when the hibiscus flower is dried and ground into a powder, it has an enlarged and puffy appearance. The hibiscus flower swelled up after soaking it in methanol, which suggests that the plant had taken in the solvent. This would increase tissue swelling and subsequent rupture, allowing the volatile oils to flow more easily into the methanol during extraction [32].

3.1.2. Morphological Variations in Hibiscus Flowers following MAHD and HD Extraction. As shown in Figure 2(a), the oil glands in the powder have a strong propensity to swell and expand upon soaking. This could aid in refining oil extraction by facilitating the clean and rapid release of oil from the substance. However, if the material is extracted without soaking, contractile oil glands will be subjected to greater stress, resulting in less oil being released. The internal pressure of the oil glands would need to be raised to a higher level before rupturing for oil emancipation to be possible. Soaking plant materials before extracting essential oils is recommended so that the induction time and overall energy usage can be shortened.

Figure 2(b) shows the oil gland following MAHD extraction. In contrast, Figure 2(c) shows an SEM image of the oil gland after HD extraction. The oil gland appears to have experienced different types of disruption (highlighted in red) in both the images. The oil gland is damaged in MAHD, which may be related to how the oil is heated. Methanol's high dielectric qualities allow it to absorb and transform microwave radiation into heat which is then delivered to the plant material in microwave-assisted hydrodistillation (MAHD) [36]. Because of this, heat energy can be focused precisely where the oil glands are located, allowing for the most efficient and least invasive method of oil release possible (Figure 2(b)). In the case of HD, however, the gland shows signs of a particularly severe fracture (Figure 2(c)). The high mechanical strain on the oil glands may be a side effect of the HD technique, suggesting that an aggressive attitude accompanies it. This is because the heat energy from HD first reaches the solvent surface through conduction and convection before heating the intended plant material [36]. This would cause the glands to explode, allowing the oil to be extracted. Based on what is shown in the SEM image [37], the gland ruptures violently when HD is extracted could be explained.

3.2. Analysis of the Chemical Structure of an Essential Oil. Figure 3 shows the FTIR spectra of hibiscus flower oils acquired using MAHD and HD. These spectra show that the absorption spectra of various oil components overlap. This is because volatile oils are such a complicated mixture. Since the peaks for the distinctive fingerprint of hibiscus flower oil are located in the region from 4000 to 400 cm^{-1}, their spectrum is highly instructive.

Essential oil functional groups were identified by comparing the FT-IR spectrophotometer's sample vibration frequencies in wave numbers to those listed on an IR correlation chart. The FT-IR spectrum of the essential oil from hibiscus flowers showed the presence of O-H stretch for alcohol and phenol in the absorption band of frequency at 3052 cm^{-1}. Aldehyde was detected thanks to an absorbance band at 1629 cm^{-1} (m). The aromatic components' C = C skeletal vibration gives rise to the peak at 1420 cm^{-1}. Specifically, ring stretching is responsible for the 1264 cm^{-1} peak. The peak at 1057 cm^{-1} represents the C-H stretching vibration. Vibrational bending absorption of C-N groups is responsible for the 895 cm^{-1} peak. The absorption peak at 736 cm^{-1} reflects the nitro group's vibrations. Table 1 provides a visual summary of the significant peaks.

The spectra of oils extracted using these two processes are typically very close to one another. These oils' complexity and the similarity in their chemical fingerprints make it challenging to identify their distinguishing features. This demonstrates that MAHD may be used to safely extract essential oils from hibiscus flowers without altering the oil's chemical composition.

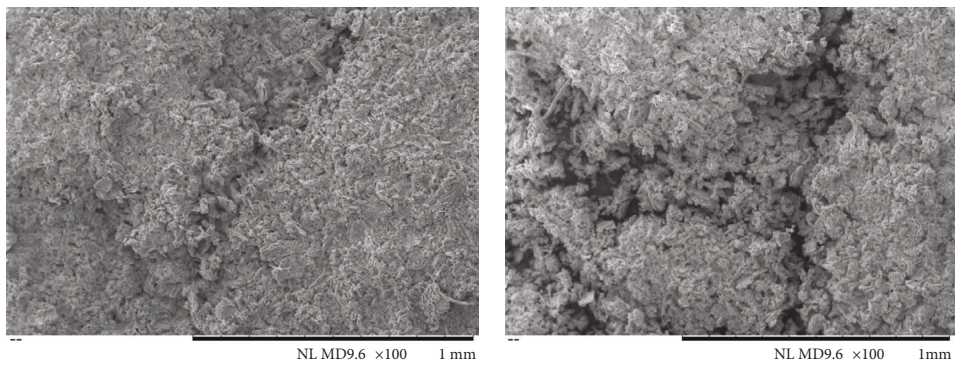

Figure 1: SEM images of (a) untreated raw hibiscus flower powder and (b) pretreated hibiscus flower powder after being soaked for 60 min.

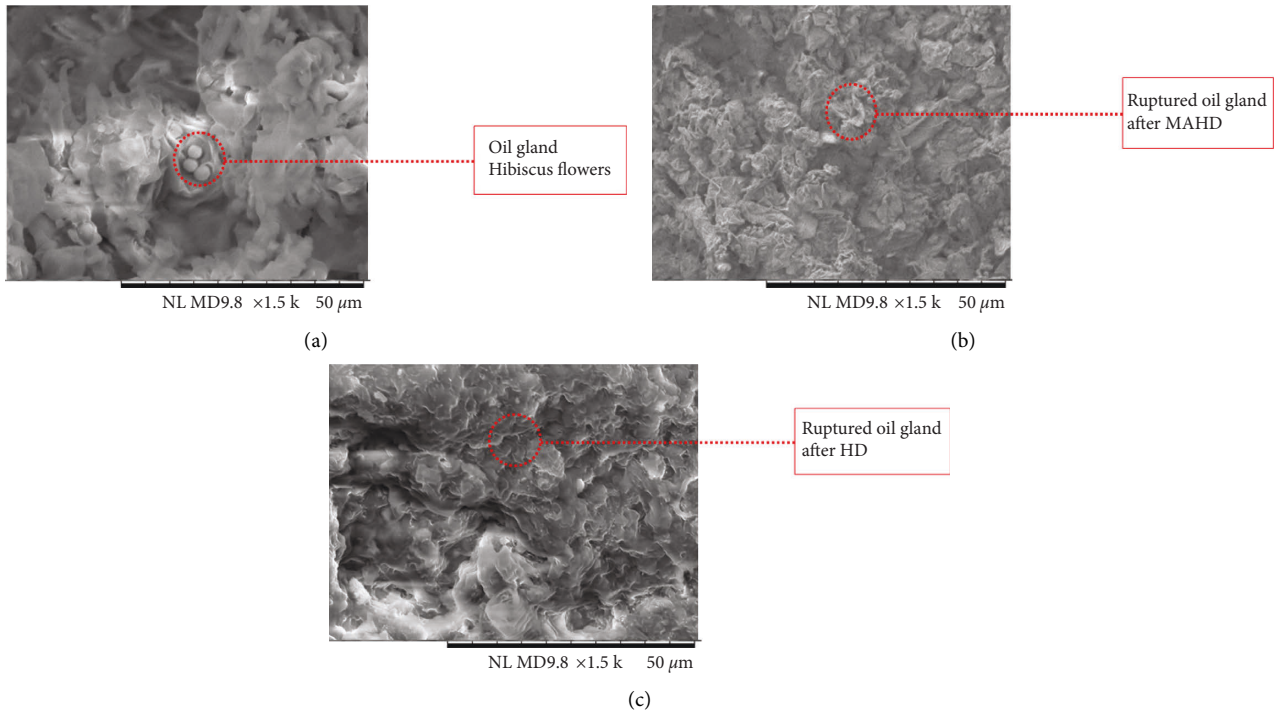

Figure 2: SEM images of oil cell glands of hibiscus flower (a) after pretreatment (soaking for 60 min), (b) after MAHD extraction (120 min), and (c) after HD extraction (160 min).

Table 1: Details of hibiscus flower oil functional groups derived from HD and MAHD.

Functional group representation	Vibration assignment (cm^{-1}) HD	MAHD
O-H	3052.76	3053.10
C = O stretching	1629.29	1629.29
C = C stretching	1420.77	1420.94
Ring stretching	1264.18	1264.42
C-H wagging	1057.00	1019.85
C-N bending	895.36	895.56
NO_2 wagging	736.08	735.70

3.3. Compositional Examination of Chemical Compounds in Hibiscus Flower Oil Obtained by MAHD and HD. Essential oils are complex substances that may even contain oxygenated molecules. For hibiscus flowers, the essential oils include only three elements: carbon, hydrogen, and oxygen. Terpenes (primarily monoterpenes and sesquiterpenes), phenolics, and alcohols are just a few of the volatile compounds found in these mixtures [29]. Aldehydes, ketones, acids, ethers, and esters are oxygenated derivatives of hydrocarbon terpenes [38]. In the treatment of cardiovascular illness [39], such as malaria [40] and cancer [41], several terpenes have proven to be highly effective medications.

The MAHD and HD extraction procedures obtained the crude extract of hibiscus flowers, and both were compared and evaluated for their chemical components and quality. The chemical components of MAHD and HD-obtained crude extract (%) of hibiscus flower oil are compared in Table 2. The table shows the results of a direct comparison between the percentage of chemical compounds in crude

Table 2: The average chemical composition of compounds in hibiscus flower oil.

Types	Compounds	Molecular formula	MW	Mass percentage of chemical compounds in crude extract (%)	
				MAHD	HD
Aldehyde	2,3-Dihydroxy propanal	$C_3H_6O_3$	90.10	12.58 ± 0.1	10.34 ± 0.1
	Acetaldehyde	C_2H_4O	44.04	0.62 ± 0.1	0.53 ± 0.1
	1,4-Butanediol	$C_4H_6O_2$	86.10	1.65 ± 0.2	1.43 ± 0.1
	Bicyclo[4.1.0]heptane-7-carbaldehyde	$C_8H_{12}O$	124.2	2.80 ± 0.1	3.50 ± 0.1
Amine	1-Isopropyldiaziridine	$C_4H_{10}N_2$	86.13	0.75 ± 0.1	0.92 ± 0.1
	Ethylenediamine	$C_2H_8N_2$	60.10	6.71 ± 0.1	5.42 ± 0.2
	1,3,5-Triazine-2,4,6-triamine	$C_3H_6N_6$	126.12	2.48 ± 0.1	2.32 ± 0.1
	Methylguanidine	$C_2H_7N_3$	73.10	0.73 ± 0.1	0.83 ± 0.3
	2-Butanamine, (S)-	$C_4H_{11}N$	73.13	2.72 ± 0.1	2.53 ± 0.2
	N-Formyl-β-alanine	$C_4H_7NO_3$	117.10	2.36 ± 0.1	2.22 ± 0.1
	2-Methyl-piperazine	$C_5H_{12}N_2$	100.20	0.80 ± 0.1	0.69 ± 0.1
Amide	N-ethyl-propanamide	$C_5H_{11}NO$	101.20	10.69 ± 0.1	9.89 ± 0.1
	2-Methyl- propanamide	C_4H_9NO	87.12	0.58 ± 0.1	0.74 ± 0.2
	1-(2-Adamantylidene)semicarbazide	$C_{11}H_{17}N_3O$	207.30	0.68 ± 0.2	0.47 ± 0.2
Alcohol	2-Propen-1-ol	C_3H_6O	58.10	0.98 ± 0.1	1.00 ± 0.2
	Tetrahydro-, trans-3,4-furandiol	$C_4H_8O_3$	104.10	0.91 ± 0.2	0.76 ± 0.1
	3-Piperidinol	$C_5H_{11}NO$	101.14	0.28 ± 0.1	0.45 ± 0.1
	1,5-Pentanediol	$C_5H_{12}O_2$	104.15	0.48 ± 0.1	0.54 ± 0.2
	2-Methyl-1-propanol	$C_4H_{10}O$	74.12	1.57 ± 0.1	1.32 ± 0.1
	(Z)6,(Z)9-pentadecadien-1-ol	$C_{15}H_{28}O$	224.40	1.70 ± 0.1	1.90 ± 0.1
Alkyne	1-Octyne	C_8H_{14}	110.20	0.45 ± 0.1	0.62 ± 0.2
Acid	Succinamic acid	$C_4H_7NO_3$	117.10	0.66 ± 01	0.58 ± 0.1
	Thioacetic acid	C_2H_4OS	76.12	1.08 ± 0.1	1.10 ± 0.2
	Citramalic acid	$C_5H_8O_5$	148.10	0.36 ± 0.1	0.50 ± 0.2
Ester	Dodecahydropyrido[1,2-b]isoquinolin-6-one	$C_{13}H_{21}NO$	207.30	0.35 ± 0.1	0.23 ± 0.2
	Ethanimidic acid, ethyl ester	C_4H_9NO	87.12	31.43 ± 0.2	29.23 ± 0.2
	Carbamic acid, ethylnitroso-, ethyl ester	$C_5H_{10}N_2O_3$	146.14	0.82 ± 0.1	0.90 ± 0.1
	Propanedioic acid, oxo-, bis(2-methylpropyl) ester	$C_{11}H_{18}O_5$	230.25	0.08 ± 0.1	—
	o-Methylisourea hydrogen sulfate	$C_2H_8N_2O_5S$	172.20	4.06 ± 0.1	3.90 ± 0.2
	6-Acetyl-β-d-mannose	$C_8H_{14}O_7$	222.20	0.08 ± 0.1	—
	Hexadecanoic acid, methyl ester	$C_{17}H_{34}O_2$	270.45	2.99 ± 0.1	3.01 ± 0.1
	Decanoic acid, ethyl ester	$C_{12}H_{24}O$	200.32	0.77 ± 0.1	0.98 ± 0.1
Ether	Trimethyl-oxirane	$C_5H_{10}O$	86.13	0.78 ± 0.1	0.90 ± 0.1
	1-(3-Methyloxiranyl)-ethanone	$C_5H_8O_2$	100.11	0.18 ± 0.1	0.20 ± 0.1
	Ethoxy-ethene	C_4H_8O	72.10	3.63 ± 0.2	3.49 ± 0.1
Other	Isothiazole	C_3H_3NS	85.12	0.17 ± 0.1	0.21 ± 0.2
	2,3-Dioxabicyclo[2.2.1] heptane	$C_5H_8O_2$	100.10	0.07 ± 0.1	—

(-) not detected, [a]mean, and ± standard deviation.

extractants under ideal conditions and the marker components, ethanimidic acid and ethyl ester. Under ideal conditions, the median concentrations of ethanimidic acid and ethyl ester in MAHD and HD were 31.43 and 29.23%, respectively. Certain chemical families were found in the crude extract of hibiscus flowers. These include oxygenated monoterpenes, sesquiterpene hydrocarbons, and other oxygenated chemicals. Hemiterpenes (C5) and sesquiterpenes (C15) are the most common chemicals in essential oils. Monoterpenes and sesquiterpenes are said to be "oxygenated" or "oxygenated" when an oxygen molecule is incorporated into their molecular structure. Our findings corroborate previous findings [42–46]. The crude extract percentages, however, were not the same between the two extraction strategies. MAHD could be suggested as a useful approach for extracting more oxygenated chemicals from hibiscus flowers. However, the total percentage of essential oil acquired from MAHD and HD might be very close. MAHD resulted in a more significant proportion of oxygenated compounds and a smaller proportion of sesquiterpene hydrocarbon than HD.

As a result, MAHD-obtained compounds are pretty helpful. These chemicals' high aromatherapy characteristics and high toxicity to insects and pests make them indispensable to pharmaceutical and other sectors [47]. As a result, the constituents are less likely to undergo partial degradation typical of HD extractions, which can be associated with a shorter extraction time [48]. This suggests that the essential oil extracted from hibiscus flowers using MAHD has excellent therapeutic potential.

3.4. Energy, Economy, and Environmental Impact. In light of the data presented here, it can be said that the MAHD method of hibiscus flower oil extraction is superior to the

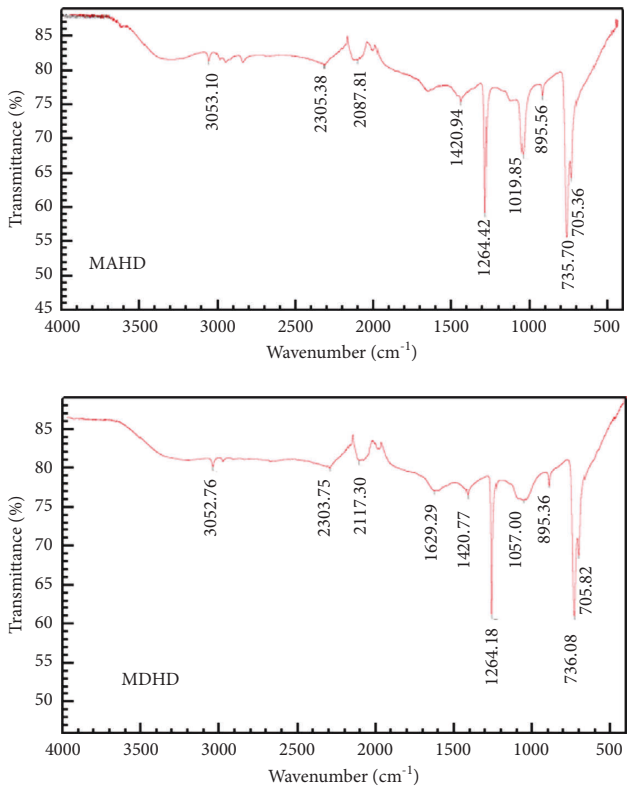

Figure 3: FTIR spectrum of essential oil for hibiscus flower through MAHD and HD.

HD method (conventional). This work aims to compare and contrast the two methods by considering their effects on the natural world, the economy, and the energy supply. This is essential for foreseeing the commercial viability of the MAHD extraction process.

In order to reach the boiling point of the plant matrix during HD extraction, 280 mL of methanol containing 35 g of hibiscus powder had to be heated for roughly 15 minutes [35]. The hibiscus oil was recovered entirely after 160 minutes of the HD procedure. Amazingly, the MAHD technique only needed 8.0 minutes to reach its induction time at 300 W and start making hibiscus oil. The oil from the hibiscus flowers was retrieved entirely in less than an hour. Table 3 shows how two extraction strategies stack up regarding energy use and CO_2 emissions. The energy consumption calculations show that 0.639 kWh of energy was used for MAHD extraction, and 1.087 kWh was needed for HD extraction. The wattmeter in the microwave and the power cord for the electric heater was used to calculate power consumption. As shown in Table 3, HD requires more energy to produce essential oil, and its energy requirements are more than MAHD. Noticeably, the yield produced by MAHD (1.25%) was higher than that obtained from HD (1.15%). In addition, MAHD consumed less energy than HD. These results were better than those obtained for essential oil yield from Sideritis raeseri, where the product was found to be 0.61–0.67% using microwave-assisted distillation [49]. In addition, the current work yield was higher than that obtained by Hibiscus sabdariffa L. using different methods,

Table 3: Summary of energy consumption and CO_2 emission of MAHD and HD methods.

Parameters	MAHD	HD
Total operating time (min)	128	181
Electricity consumption (kWh)	0.639	1.087
CO2 released (g)	511.2	869.6
Yield (%)	1.25	1.15

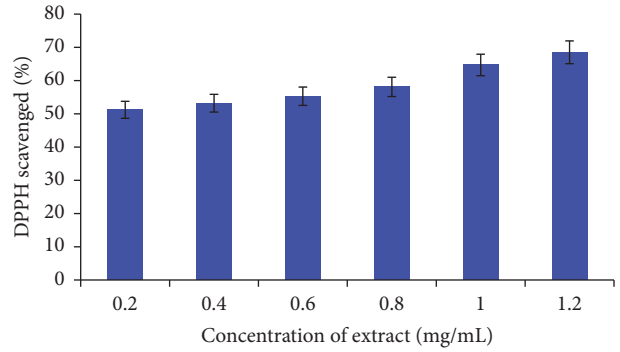

Figure 4: DPPH radical scavenging activity of essential oil and the methanol extract of hibiscus flower and the IC_{50} of essential oil 0.7 mg/mL.

where it was 0.86, 0.54, and 1.10% using HD, steam distillation, and solvent-free microwave-assisted extraction [50]. Concerning the environmental impact, the amount of carbon dioxide released to the environment is higher in HD (869.6 g CO_2/g of hibiscus flower oil) than that in MAHD (511.2 g CO_2/g of hibiscus flower oil). According to [37], 1 kWh energy consumption from coal or fuel releases almost 800 g of carbon dioxide into the environment during combustion. The calculation of energy consumption was carried out using equation (2).

From these findings, we deduce that the MAHD method is a green extraction process that benefits the natural world. MAHD is a solvent- and energy-efficient method that does not require chemicals to extract high-quality essential oil.

3.5. In Vitro Antioxidant Assay

3.5.1. DPPH Radical Scavenging Assay. Antioxidants are expected to neutralize DPPH radicals because of their hydrogen-donating capacity. Radical scavenging actions are essential to prevent many illnesses, including cancer [51]. Extracts of hibiscus flowers are commonly tested for their antioxidant capacity using the DPPH assay. Figure 4, shows the DPPH antioxidant capability of a hibiscus flower extract. The DPPH free radical scavenging activity of a hibiscus flower extract was 51.2%, 53.2%, 55.3%, 58.1%, 64.7%, and 68.5% at concentrations of 0.2, 0.4, 0.6, 0.8, 1.0, and 1.2 mg/mL, respectively. Scavenging activity for DPPH is shown in Figure 4 and Table 4. These results demonstrate that higher quantities of the extract have higher radical scavenging activity (see Figure 4). The IC50 for essential oil in the DPPH assay method was 0.7 mg/ml (Table 4). Methanol extract of hibiscus flower has a scavenging action comparable to ascorbic acid [52].

Table 4: DPPH assay of methanol extract of hibiscus flower.

No.	Concentration of extract (mg/mL)	DPPH scavenged (%)	IC_{50} (mg/mL)
1	0.2	51.2	
2	0.4	53.2	
3	0.6	55.3	
4	0.8	58.1	0.7
5	1.0	64.7	
6	1.2	68.5	
7	Ascorbic acid (5 mg/mL)	81.85	

4. Conclusion

Hibiscus flowers were used to create an eco-friendly essential oil using the modern green extraction methodology MAHD and the traditional HD method. The characteristics of hibiscus flower essential oils extracted using MAHD and HD techniques were compared. A scanning electron microscopy (SEM) study of powdered hibiscus flowers that had previously undergone oil extraction found that MAHD yielded the purest oil with minimally damaged sebaceous glands. FTIR testing confirmed that MAHD contained the same chemical constituents as that of the oil recovered from hibiscus flowers using HD. Based on the data, it is clear that the MAHD method is superior in terms of cost-effectiveness, environmental friendliness, and the number of oxygenated compounds it generates. The MAHD-obtained hibiscus flower raw material was put through the DPPH radical scavenging assay to determine its antioxidant quality. The MAHD crude extract has an intriguing IC50 value of 0.7 ppm. These findings demonstrate that MAHD crude extracts have more significant therapeutic potential. The MAHD procedure yielded higher quality hibiscus flower oil than the conventional HD method. This study reveals that MAHD may be used to successfully extract volatile oils from hibiscus flowers without disrupting their original chemical structures. Due to its high yield and low energy consumption, MAHD proved to be an eco-friendly option for separating essential oils compared to HD.

Data Availability

The data used to support the findings of this study are included within the article.

Conflicts of Interest

The authors declare that they have no conflicts of interest.

Acknowledgments

The authors would like to thank Universiti Malaysia Pahang for assisting with this study under the research (UIC 190806). In addition, M.A. Assiri extends his appreciation to the Deanship of Scientific Research at King Khalid University for funding this work through the research group project under grant number (KKU/RCAMS/G015-21).

References

[1] A. Younis, A. Riaz, M. Khan, A. Khan, and M. Pervez, "Extraction and identification of chemical constituents of the essential oil of Rosa species," *Proceedings of the XXVII International Horticultural Congress-IHC2006: International Symposium on Ornamentals*, pp. 485–492, Seoul, Korea, November 2006.

[2] K. H. Kubeczka and V. Formaceck, *Essential Oil by Capillary Gas Chromatography and Carbon 13 NMR Spectroscopy*, John Wiley & Sons, Hoboken, NJ, USA, 1982.

[3] M. Oussalah, S. Caillet, L. Saucier, and M. Lacroix, "Antimicrobial effects of selected plant essential oils on the growth of a Pseudomonas putida strain isolated from meat," *Meat Science*, vol. 73, no. 2, pp. 236–244, 2006.

[4] M. Oussalah, S. Caillet, L. Saucier, and M. Lacroix, "Inhibitory effects of selected plant essential oils on the growth of four pathogenic bacteria: *E. coli* O157: H7, Salmonella typhimurium, Staphylococcus aureus and Listeria monocytogenes," *Food Control*, vol. 18, no. 5, pp. 414–420, 2007.

[5] H. Sies, "Strategies of antioxidant defense," *European Journal of Biochemistry*, vol. 215, no. 2, pp. 213–219, 1993.

[6] H. Grice, "Safety evaluation of butylated hydroxyanisole from the perspective of effects on forestomach and oesophageal squamous epithelium," *Food and Chemical Toxicology*, vol. 26, no. 8, pp. 717–723, 1988.

[7] J. Sharifi-Rad, C. Quispe, M. Kumar et al., "Hyssopus essential oil: an update of its phytochemistry, biological activities, and safety profile," *Oxidative Medicine and Cellular Longevity*, vol. 202210 pages, 2022.

[8] D. N. Reddy, "Essential oils extracted from medicinal plants and their applications," in *Natural Bio-Active Compounds: Volume 1: Production and Applications*, M. S. Akhtar, M. K. Swamy, and U. R. Sinniah, Eds., pp. 237–283, Springer Singapore, Singapore, 2019.

[9] H. S. Kusuma, A. Altway, and M. Mahfud, "Solvent-free microwave extraction of essential oil from dried patchouli (Pogostemon cablin Benth) leaves," *Journal of Industrial and Engineering Chemistry*, vol. 58, pp. 343–348, 2018.

[10] S. Karakaya, Z. Bingol, M. Koca et al., "Identification of non-alkaloid natural compounds of Angelica purpurascens (Avé-Lall.) Gilli. (Apiaceae) with cholinesterase and carbonic anhydrase inhibition potential," *Saudi Pharmaceutical Journal*, vol. 28, pp. 1–14, 2020.

[11] A. Matkowski, "Plant in vitro culture for the production of antioxidants—a review," *Biotechnology Advances*, vol. 26, no. 6, pp. 548–560, 2008.

[12] H. Kusuma, D. Putri, I. Dewi, and M. Mahfud, "Solvent-free microwave extraction as the useful tool for extraction of edible essential oils," *Chemistry & Chemical Technology*, vol. 10, no. 2, pp. 213–218, 2016.

[13] S. a. P. K. N Mahadevan, "Hibiscus sabdariffa Linn.–An overview," *Natural Product Radiance*, vol. 8, pp. 77–83, 2009.

[14] K. L. Higginbotham, K. P. Burris, S. Zivanovic, P. M. Davidson, and C. N. Stewart Jr, "Antimicrobial activity of Hibiscus sabdariffa aqueous extracts against Escherichia coli O157: H7 and Staphylococcus aureus in a microbiological medium and milk of various fat concentrations," *Journal of Food Protection*, vol. 77, no. 2, pp. 262–268, 2014.

[15] A. Djouahri, L. Boudarene, and B. Y. Meklati, "Effect of extraction method on chemical composition, antioxidant and anti-inflammatory activities of essential oil from the leaves of Algerian Tetraclinis articulata (Vahl) Masters," *Industrial Crops and Products*, vol. 44, pp. 32–36, 2013.

[16] M. Mahfud, D. Putri, I. Dewi, and H. Kusuma, "Extraction of essential oil from cananga (Cananga odorata) using solvent-free microwave extraction: a preliminary study," *Rasayan Journal of Chemistry*, vol. 10, pp. 86–91, 2017.

[17] M. Gavahian, A. Farahnaky, K. Javidnia, and M. Majzoobi, "Comparison of ohmic-assisted hydrodistillation with traditional hydrodistillation for the extraction of essential oils from Thymus vulgaris L," *Innovative Food Science & Emerging Technologies*, vol. 14, pp. 85–91, 2012.

[18] E. de Rijke, P. Out, W. M. Niessen, F. Ariese, C. Gooijer, and U. A. Brinkman, "Analytical separation and detection methods for flavonoids," *Journal of Chromatography A*, vol. 1112, no. 1-2, pp. 31–63, 2006.

[19] M. Lo Presti, S. Ragusa, A. Trozzi et al., "A comparison between different techniques for the isolation of rosemary essential oil," *Journal of Separation Science*, vol. 28, no. 3, pp. 273–280, 2005.

[20] N. Jeyaratnam, A. H. Nour, R. Kanthasamy, A. H. Nour, A. R. Yuvaraj, and J. O. Akindoyo, "Essential oil from Cinnamomum cassia bark through hydrodistillation and advanced microwave assisted hydrodistillation," *Industrial Crops and Products*, vol. 92, pp. 57–66, 2016.

[21] H. S. Kusuma and M. Mahfud, "Kinetic studies on extraction of essential oil from sandalwood (Santalum album) by microwave air-hydrodistillation method," *Alexandria Engineering Journal*, vol. 57, no. 2, pp. 1163–1172, 2018.

[22] H. S. Kusuma and M. Mahfud, "Microwave-assisted hydrodistillation for extraction of essential oil from patchouli (Pogostemon cablin) leaves," *Periodica Polytechnica Chemical Engineering*, vol. 61, pp. 82–92, 2017.

[23] M.-T. Golmakani and K. Rezaei, "Comparison of microwave-assisted hydrodistillation withthe traditional hydrodistillation method in the extractionof essential oils from Thymus vulgaris L," *Food Chemistry*, vol. 109, no. 4, pp. 925–930, 2008.

[24] H. S. Kusuma and M. Mahfud, "The extraction of essential oils from patchouli leaves (Pogostemon cablin Benth) using a microwave air-hydrodistillation method as a new green technique," *RSC Advances*, vol. 7, no. 3, pp. 1336–1347, 2017.

[25] A. Brachet, P. Christen, and J. L. Veuthey, "Focused microwave-assisted extraction of cocaine and benzoylecgonine from coca leaves," *Phytochemical Analysis*, vol. 13, no. 3, pp. 162–169, 2002.

[26] H. Kusuma and M. Mahfud, "Comparison of kinetic models of oil extraction from sandalwood by microwave-assisted hydrodistillation," *International Food Research Journal*, vol. 24, 2017.

[27] V. Mandal, Y. Mohan, and S. Hemalatha, "Microwave assisted extraction–an innovative and promising extraction tool for medicinal plant research," *Pharmacognosy Reviews*, vol. 1, pp. 7–18, 2007.

[28] H. S. Kusuma, T. I. Rohadi, E. F. Daniswara, A. Altway, and M. Mahfud, "Preliminary study: comparison of kinetic models of oil extraction from vetiver (vetiveria zizanioides) by microwave hydrodistillation," *Korean Chemical Engineering Research*, vol. 55, pp. 574–577, 2017.

[29] M. E. Lucchesi, F. Chemat, and J. Smadja, "An original solvent free microwave extraction of essential oils from spices," *Flavour and Fragrance Journal*, vol. 19, no. 2, pp. 134–138, 2004.

[30] A. Farhat, C. Ginies, M. Romdhane, and F. Chemat, "Eco-friendly and cleaner process for isolation of essential oil using microwave energy: experimental and theoretical study," *Journal of Chromatography A*, vol. 1216, no. 26, pp. 5077–5085, 2009.

[31] M. Letellier, H. Budzinski, L. Charrier, S. Capes, and A. M. Dorthe, "Optimization by factorial design of focused microwave assisted extraction of polycyclic aromatic hydrocarbons from marine sediment," *Fresenius Journal of Analytical Chemistry*, vol. 364, no. 3, pp. 228–237, 1999.

[32] A. Filly, X. Fernandez, M. Minuti, F. Visinoni, G. Cravotto, and F. Chemat, "Solvent-free microwave extraction of essential oil from aromatic herbs: from laboratory to pilot and industrial scale," *Food Chemistry*, vol. 150, pp. 193–198, 2014.

[33] M. Nor Azah, Y. Chang, J. Mailina, S. Saidatul Husni, H. Nor Hasnida, and Y. Nik Yasmin, "Comparison of chemical profiles of selected gaharu oils from Peninsular Malaysia," *Malaysian Journal of Analytical Sciences*, vol. 12, pp. 338–340, 2008.

[34] Y. Li, B. Jiang, T. Zhang, W. Mu, and J. Liu, "Antioxidant and free radical-scavenging activities of chickpea protein hydrolysate (CPH)," *Food Chemistry*, vol. 106, no. 2, pp. 444–450, 2008.

[35] H. H. Rassem, A. H. Nour, and R. M. Yunus, "GC-MS analysis of bioactive constituents of Hibiscus flower," *Australian Journal of Basic and Applied Sciences*, vol. 11, pp. 91–97, 2017.

[36] M. Desai, J. Parikh, and P. A. Parikh, "Extraction of natural products using microwaves as a heat source," *Separation and Purification Reviews*, vol. 39, no. 1-2, pp. 1–32, 2010.

[37] M. A. Ferhat, B. Y. Meklati, J. Smadja, and F. Chemat, "An improved microwave Clevenger apparatus for distillation of essential oils from orange peel," *Journal of Chromatography A*, vol. 1112, no. 1-2, pp. 121–126, 2006.

[38] F. Bakkali, S. Averbeck, D. Averbeck, and M. Idaomar, "Biological effects of essential oils–a review," *Food and Chemical Toxicology*, vol. 46, no. 2, pp. 446–475, 2008.

[39] T. Liebgott, M. Miollan, Y. Berchadsky, K. Drieu, M. Culcasi, and S. Pietri, "Complementary cardioprotective effects of flavonoid metabolites and terpenoid constituents of Ginkgo biloba extract (EGb 761) during ischemia and reperfusion," *Basic Research in Cardiology*, vol. 95, no. 5, pp. 368–377, 2000.

[40] I. A. Parshikov, A. I. Netrusov, and J. B. Sutherland, "Microbial transformation of antimalarial terpenoids," *Biotechnology Advances*, vol. 30, no. 6, pp. 1516–1523, 2012.

[41] S. S. Ebada, W. Lin, and P. Proksch, "Bioactive sesterterpenes and triterpenes from marine sponges: occurrence and pharmacological significance," *Marine Drugs*, vol. 8, no. 2, pp. 313–346, 2010.

[42] S. Agarwal and R. Prakash, "Essential oil composition of solvent extract of Hibiscus rosasinensis flower," *Oriental Journal of Chemistry*, vol. 29, no. 2, pp. 813-814, 2013.

[43] Y. Pieracci, L. Pistelli, M. Lari et al., "Hibiscus rosa-sinensis as flavoring agent for alcoholic beverages," *Applied Sciences*, vol. 11, no. 21, p. 9864, 2021.

[44] A. L. Ogundajo, I. A. Ogunwande, T. M. Bolarinwa, O. R. Joseph, and G. Flamini, "Essential oil of the leaves of Hibiscus surattensis L. from Nigeria," *Journal of Essential Oil Research*, vol. 26, no. 2, pp. 114–117, 2014.

[45] S. Chakraborty, S. Majumder, A. Ghosh, and M. Bhattacharya, "Comprehensive profiling of aroma imparting biomolecules in foliar extract of Hibiscus fragrans Roxburgh: a metabologenesis perspective," *Journal of biomolecular structure & dynamics*, pp. 1–14, 2021.

[46] O. R. Alara and N. H. Abdurahman, "GC–MS and FTIR analyses of oils from Hibiscus sabdariffa, Stigma maydis and Chromolaena odorata leaf obtained from Malaysia: potential sources of fatty acids," *Chemical Data Collections*, vol. 20, Article ID 100200, 2019.

[47] E. A. Petrakis, A. C. Kimbaris, D. C. Perdikis, D. P. Lykouressis, P. A. Tarantilis, and M. G. Polissiou, "Responses of Myzus persicae (Sulzer) to three Lamiaceae essential oils obtained by microwave-assisted and conventional hydrodistillation," *Industrial Crops and Products*, vol. 62, pp. 272–279, 2014.

[48] M. Gavahian, A. Farahnaky, R. Farhoosh, K. Javidnia, and F. Shahidi, "Extraction of essential oils from Mentha piperita using advanced techniques: microwave versus ohmic assisted hydrodistillation," *Food and Bioproducts Processing*, vol. 94, pp. 50–58, 2015.

[49] Z. Drinić, D. Pljevljakušić, T. Janković, G. Zdunić, D. Bigović, and K. Šavikin, "Hydro-distillation and microwave-assisted distillation of Sideritis raeseri: comparison of the composition of the essential oil, hydrolat and residual water extract," *Sustainable Chemistry and Pharmacy*, vol. 24, Article ID 100538, 2021.

[50] M. F. Ibrahim, F. S. Robustelli della Cuna, C. Villa et al., "A chemometric assessment and profiling of the essential oils from Hibiscus sabdariffa L. from Kurdistan, Iraq," *Natural Product Research*, vol. 36, no. 9, pp. 2409–2412, 2022.

[51] H. Wang, Y. Liu, S. Wei, and Z. Yan, "Application of response surface methodology to optimise supercritical carbon dioxide extraction of essential oil from Cyperus rotundus Linn," *Food Chemistry*, vol. 132, no. 1, pp. 582–587, 2012.

[52] M. Jainu and C. S. Devi, "*In vitro*. and*In vivo*. Evaluation of free-radical scavenging potential of*Cissus quadrangularis*," *Pharmaceutical Biology*, vol. 43, no. 9, pp. 773–779, 2005.

Hindawi
Journal of Chemistry
Volume 2022, Article ID 3059725, 11 pages
https://doi.org/10.1155/2022/3059725

Research Article

Optimizing Extractability, Phytochemistry, Acute Toxicity, and Hemostatic Action of Corn Silk Liquid Extract

Zead Helmi Abudayeh,[1] **Uliana Karpiuk**,[2] **Viktoriia Kyslychenko**,[3] **Qais Abualassal**,[1] **Loay Khaled Hassouneh**,[4] **Sami Qadus**,[1] **and Ahmad Talhouni**[1]

[1]*Department of Applied Pharmaceutical Sciences, Faculty of Pharmacy, Isra University, Amman, Jordan*
[2]*Department of Pharmacognosy and Botany, Faculty of Pharmacy, Bogomolets National Medical University, Kyiv, Ukraine*
[3]*Department of Chemistry of Natural Compounds and Nutriciology, National University of Pharmacy, Kharkiv, Ukraine*
[4]*Department of Respiratory Therapy, Faculty of Allied Medical Sciences, Isra University, Amman, Jordan*

Correspondence should be addressed to Zead Helmi Abudayeh; zead.abudayeh@iu.edu.jo

Received 19 July 2022; Accepted 29 August 2022; Published 29 September 2022

Academic Editor: Marwa Fayed

The technological parameters and quality indicators of corn silk were evaluated in this study: specific density, volumetric density, bulk density, porosity, spatial layer, free volume of the layer, the absorption coefficient, weight loss on drying, and extractives. The technology for obtaining a liquid extract of corn silk was developed. The most effective extractant was discovered to be 40% ethanol, with an extraction time of 120 minutes. The qualitative composition and quantitative content of the major groups of biologically active substances (BAS) in the obtained liquid extract were determined. The qualitative composition of the main groups of BAS was determined by conventional chemical reactions. This extract contained free reduced sugars, glycosides (bound reduced sugars), phenols, tannins, flavonoids, saponins, and hydroxycinnamic acids. The quantitative content of phenolic compounds was performed by UV-vis-spectrophotometry. Total phenols, tannins, flavonoids, and hydroxycinnamic acids had quantitative contents of $8.25 \pm 0.33\%$, $1.4 \pm 0.03\%$, $2.20 \pm 0.06\%$, $3.30 \pm 0.13\%$, respectively. The acute toxicity study was carried out with a single intragastric administration to outbred unanesthetized white rats of both sexes. Duration of observation of animals was 14 days. It was revealed that corn silk extract at doses of up to 5.0 ml/kg is safe. A single injection of a liquid extract has no effect on internal organs when compared to a control group. Corn silk liquid extract's hemostatic efficacy was assessed using blood clotting time, prothrombin time, and blood clot retraction index. The corn silk liquid extract reduces blood coagulation time, decreases prothrombin time, and increases the blood clot retraction index. According to these findings, corn silk liquid extract is rich in phytochemicals and possesses a potential therapeutic effect on bleeding disorders. Furthermore, it could be used in the pharmaceutical sciences industry to develop medicines for testing in the treatment of various diseases.

1. Introduction

Bleeding (hemorrhagia) is the outflow of blood from damaged vessels into tissues, body cavities, and external environments [1–3].

The hemostasis system is responsible for halting the bleeding and ensuring that the aggregate state of blood in the body is ideal. The blood artery wall, blood cells (mainly platelets), and both enzymatic and non-enzymatic plasma systems are all part of the hemostasis system. Hemostasis has two mechanisms: vascular platelet and coagulation [1–4].

There is no single approach for the treatment of bleeding. This is due to the different etiology of their occurrence. A fairly common cause of bleeding is a violation of the integrity of the vascular wall that occurs as a result of trauma, vessel erosion in various purulent and pathological processes, increased blood pressure in the vessel, a sharp drop in atmospheric pressure, and increased vessel permeability [1].

Angiospasm is an essential component of the hemostatic system. The main result of its manifestations is the achievement of a persistent spasm of the damaged vessel, which limits blood loss. In addition to vascular spasm, the thrombogenic potential of the vascular wall includes its ability to produce and exhibit, when damaged, molecular activators of platelet adhesion and aggregation, as well as stimulators of fibrin formation. The vascular link of hemostasis depends on the state of the blood vessel [1].

In addition to vascular wall defects, the presence of bleeding, hemorrhage, and a tendency to recur, indicates a decrease in the ability of blood to coagulate—hypocoagulation. The main causes of hypocoagulation are genetic or acquired deficits and/or defects of hemostasis factors [1–3].

Bleeding associated with disorders of the plasma-coagulation link of hemostasis is characterized by hemorrhages in the cavity and soft tissues. Hemorrhages of the mucous membranes are common with defects in the vascular-platelet connection, including nasal, gastrointestinal, uterine hemorrhages, intradermal ecchymosis, and petechiae [1].

Bleeding can be a manifestation of self-bleeding diseases such as hemophilia A and B, Willebrand's disease; complication of local vascular tissue damage during infection, inflammation; a complication of another pathology such as cholemic bleeding in patients with jaundice, spontaneous nasal, skin, muscle bleeding during surgery and in the postoperative period. Uterine hemorrhage can also develop as a result of hypotension and atony of the muscles of the uterus. Microcirculation problems cause increased bleeding in people with diabetes. Scurvy causes gum bleeding owing to a lack of vitamin C. Patients suffering from osteoporosis due to an acute calcium deficiency, which is one of the components in blood coagulation, have more bleeding [1, 3, 5].

Based on the above, bleeding refers to both emergencies and systemic diseases. Accordingly, the treatment of bleeding of different etiology requires a different approach.

Hemostatic agents of plant origin, as a rule, accelerate blood clotting and have a moderate hemostatic effect. They are prescribed internally to reduce bleeding in hemorrhagic diathesis, hemorrhoids, nasal, pulmonary, renal, uterine and intestinal bleeding, externally for bleeding gums, after surgical treatment of wounds, etc [4–6].

Bleeding herbal medicine is a set of treatments aimed at eliminating the clinical manifestations and causes of bleeding, as well as preventing and eliminating complications [5, 6].

There is corn among such medicinal plants. Corn is also called maize, with its botanical name–*Zea mays* L. Corn belongs to the cereal family *Poaceae* [7, 8].

Corn plant raw material is a corn silk (*Zeae maydis styli cum stigmatis*). Corn silk is made up of soft silky threads that are gathered in bunches or partially tangled, with bilobed stigmas at the top. Silk is curved and flat, measuring 0.1–0.15 mm in width and 0.5–20.0 cm in length, with stigmas measuring 0.4–3.0 mm in length. Corn silk comes in a variety of colors, including brown, brown-red, and light yellow [8–10].

The most studied BAS in corn silk are phenolic compounds. The presence of tannin and tannin-like polyphenols (approximately 13%) has been established: anthocyanidins and flavan-4-ols luteoforol, apiforol [8, 11]. Furthermore, studies on flavonoids such as luteolin and apigenin glycosides such as orientin, vitexin, isovitexin, homoorientin, and maisin have been conducted [8, 11, 12]. Rutin and formononetin are also present [8, 11, 13]. Corn silk was reported to contain chlorogenic, ferulic, and caffeic acids [9].

According to previous researches, corn silk contains up to 80% carbohydrates, 8% fiber, 3.8% potassium-rich mucus, 10% protein, 3.5% lipophilic substances, 2.5% fatty oil, 3.18% saponins, and sterols (β-sitosterol and stigmasterol) [7–11, 14].

Corn silk is used in traditional medicine as a choleretic, diuretic, and hemostatic agent, as well as to suppress appetite and normalize lipid metabolism [8, 9, 14, 15]. Corn silk is also used in official medicine for medicinal purposes. Corn silk preparations have choleretic, diuretic, anti-inflammatory, hemostatic, and hypoglycemic properties and are used for hypertension prevention and treatment, as well as weight loss [7–9, 14, 16]. Corn silk has been shown to have antioxidant and antibacterial properties [7, 8, 17, 18].

Corn is an agricultural plant. According to the Food and Agriculture Organization of the United Nations (FAO), corn seeds rank seventh among the most widely produced raw materials in the world. According to FAO, the total global corn seeds production in 2018 was 1,147 million 155 tons, with the American continent accounting for slightly more than half of the total (50.4%), followed by Asia (31.5%), Europe (11.2%), Africa (6.9%), and Oceania (0.1%). The United States of America, China, Brazil, *Argentina*, Ukraine, Indonesia, India, Mexico, Romania, and Canada were the top ten maize producers in the world [3] Jordan's corn production is annual production is under 10,000 metric tons. Domestic corn production is largely for human consumption [19].

The development of highly effective and safe medicines based on medicinal herbs with hemostatic action is still extremely important and relevant to humanity. Modern conditions for the development of new pharmaceuticals in the context of the pharmaceutical industry's evolution necessitate not only their efficacy and safety, but also the verification of their quality, economic, social, and medical forecasting of the need for their development.

As a result of the preceding, the current study aimed to determine the technological parameters and quality indicators of corn silk, optimize extractability for obtaining of a liquid extract from corn silk, its' qualitative composition and quantitative content of the major groups of BAS, investigation of its acute toxicity and hemostatic action.

2. Materials and Methods

2.1. Plant Material. Corn silk was purchased at a local market in Amman, Jordan during June and August. The plant material was authenticated by Dr. Khaled Abulaila (Director of Biodiversity Research Department, National Agricultural Research Center, Amman, Jordan). The raw

components were rinsed twice using tap water. They were dried in an air-shadowed environment. The plant sample was ground into a fine powder (3,0 mm) and stored in airtight vials until usage.

2.2. Standards and Chemicals. All chemicals were analytical-reagent grade and the water was distilled. The chemicals included: cholesterol solution (Sigma-Aldrich), vanillin (Sigma-Aldrich), sulfuric acid, chloroform, ferric chloride (Sigma-Aldrich), lead acetate (Sigma-Aldrich), sodium hydroxide (Sigma-Aldrich), iron ammonium alum (Sigma-Aldrich), gelatin, magnesium shavings, hydrochloric acid, aluminum chloride (Sigma-Aldrich), Fehling's reagent, nitrite-molybdenum reagent (Sigma-Aldrich), Folin-Ciocalteu reagent (Sigma-Aldrich), anhydrous sodium carbonate (Synth®), pyrogallol (Fluka), luteolin 7-glucoside (Sigma-Aldrich), and chlorogenic acid (Fluka).

2.3. Technological Parameters and Quality Indicators of Raw Materials. The technological parameters and quality indicators of corn silk of plant raw materials were determined using commonly established methods [20, 21], including: specific density, volumetric density, bulk density, porosity, spatial layer, free volume of the layer, the absorption coefficient, weight loss on drying, and extractives.

2.3.1. Specific Density. A 100 ml pycnometer was filled at 2/3 volume with distilled water and weighed. Then about 5.0 g of the powdered raw material was placed into a dry empty 100 ml pycnometer, distilled water was added at 2/3 volume, and weighted. A pycnometer with the sample was heated in a water bath for 1.5–2 h, occasionally stirring to completely remove from the plant raw material air. Then cooled to a temperature of 20°C, the volume was distilled to the mark with water, and weighted. A specific density (d_n, (g/cm^3)) was calculated according to the formula:

$$d_n = \frac{P \times d_p}{P + G - F}, \tag{1}$$

where P–the mass of the plant raw material, (g); G–the mass of the pycnometer with distilled water, (g); F–the mass of the pycnometer with distilled water and the plant raw materials, (g); d_p–the specific density of water, (g/cm^3), ($d = 0{,}9982$ Г/см^3).

2.3.2. Volumetric Density. About 5.0 g of the powdered raw material was quickly placed into a measuring cylinder (50 ml) with 25 ml of distilled water. The volume of the plant raw material was measured. The volume occupied by the raw material was measured as the difference between measuring a cylinder with distilled water and the raw material and a cylinder with distilled water. A volumetric density (d_0, (g/cm^3)) was calculated according to the formula:

$$d_0 = \frac{P_o}{V_o}, \tag{2}$$

where P_o–the mass of the plant raw material, g; V_o–the volume occupied by the plant raw materials, (cm^3).

2.3.3. Bulk Density. About 5.0 g of the powdered raw material was placed in the measuring cylinder, shaking slightly for alignment. The volume of the plant raw material was measured. A bulk density (d, (g/cm^3)) was calculated according to the formula:

The bulk mass was calculated according to the formula:

$$d = \frac{P_n}{V_n}, \tag{3}$$

where P_n–the mass of the plant raw material, (g); V_n–the volume, which takes the plant raw material, (cm^3).

2.3.4. Porosity. The porosity (P_s) of the plant raw material is the size of the cavities within the cellular tissue. It's calculated as the ratio of the difference between the specific density and the volumetric density to the specific density. The formula is:

$$P_s = \frac{d_n - d_o}{d_n}, \tag{4}$$

where d_n–the specific density of the plant raw material, (g/cm^3); d_o–the volumetric density of the plant raw material, (g/cm^3).

2.3.5. Spatial Layer. The spatial layer (P) characterizes the size of the cavity between parts of powdered plant raw material. It's calculated as the ratio of the difference between volumetric and bulk density to the bulk density. The formula is given as follows:

$$P = \frac{d_o - d}{d}, \tag{5}$$

where d_o–the volumetric density of the plant raw materials, (g/cm^3); d–the bulk density of the plant raw materials, (g/cm^3).

2.3.6. Free Volume of the Layer. The free volume of the layer is calculated as the ratio of the difference between the specific density and bulk density to the specific density. The formula is given as follows:

$$V = \frac{d_n - d}{d_n}, \tag{6}$$

where d_n–the specific density of the plant raw materials, (g/cm^3), d–the bulk density of the plant raw materials, (g/cm^3).

2.3.7. Absorption Coefficient. The absorption coefficient is the amount of solvent that irreversibly permeates air cavities, intracellular pores, and vacuoles in the plant herbal drug. It's calculated as the ratio of the plant raw material mass after percolation with an extractant and squeezing to the plant raw material mass before percolation. Water was used as a

Table 1: Results of corn silk technological parameters and quality indicators determination.

Technological parameters and quality indicators	Results
Specific density, (g/см^3)	1.53 ± 0.07
Volumetric density, (g/см^3)	0.46 ± 0.02
Bulk density, (g/см^3)	0.30 ± 0.01
Porosity	0.69 ± 0.02
Spatial layer	0.34 ± 0.01
Free volume of the layer	0.80 ± 0.03
Absorption coefficient	
Water	5.00 ± 0.25
Ethanol 40%	4.30 ± 0.17
Weight loss on drying, (%)	12.0 ± 0.54
Extractives:	
Water	23.88 ± 0.47
Ethanol 40%	24.70 ± 0.64
Ethanol 50%	23.45 ± 0.40
Ethanol 70%	18.95 ± 0.70
Ethanol 96%	19.38 ± 0.40

common extractant. 40% ethanol solution was used as the most suitable for obtaining of corn silk extract according to the extractives results (Table 1). An absorption coefficient (K) was calculated according to the formula:

$$K = \frac{P_2}{P_1}, \tag{7}$$

where P_1– the mass of the plant raw material before percolation, (g); P_2– the mass of the plant raw material after percolation, (g).

The determination of weight loss on drying and extractives was performed according to the method described in the SPhU (2.2.32) [20, 21].

2.3.8. Loss on Drying. Loss on drying is a widely used test method to determine the residual moisture and any volatile matter content of a plant raw material sample. Loss on drying is the difference in the mass of the sample before and after drying, expressed as a percentage. Flat-bottomed empty weighted dish with a lid was put in the drying cabinet, at 100–105°C for 30 min. Cooled to a temperature of 20°C in a desiccator, weighted and then brought to a constant mass. In a flat-bottomed dish, 1.0 g of the powdered herbal drug was added, dried in drying cabinet at 100–105°C for 30 min. Cooled to a temperature of 20°C in a desiccator, weighted, and then brought to a constant mass. Sample mass is the difference between a mass flat-bottomed dish with a sample and an empty flat-bottomed dish. The total number of measurements was $n = 5$.

2.3.9. Extractives. The distilled water and ethanol solutions (40%–96%) were used as extractants for the determination of extractives (the solvents indicated in Table 1). To 1.0 g of the powdered plant raw material were placed in a flask with 200–250 ml, 50.0 ml of the solvent were added, then heated for 30 min from the moment the solvent boils. Cooled to a temperature of 20°C, diluted to 50.0 ml with a suitable solvent, and filtered. 20.0 ml of the filtrate were dried on a water bath, then the residue was dried in the drying cabinet, at 100–105°C, then weight. The total number of measurements was $n = 5$.

The content of extractives in percentages (X, (%)), calculated on the basis of absolutely dry raw materials, was calculated by the formula:

$$X = \frac{m \times 200 \times 100}{m_1 \times (100 - W)}, \tag{8}$$

where m–the mass of the dry residue, (g). m_1– the mass of the plant raw materials, (g). W–the weight loss on drying, (%).

2.4. Optimizing Extractability of a Corn Silk Liquid Extract (CSLE). The extractant and time for extraction were selected by an experiment based on the yield of extractive compounds (Table 1), cost, and environmental safety.

The raw material-extractant ratio was 1 : 1. A liquid extract is a liquid medicinal form in which one part by weight or volume is equivalent to one part by weight of the dried medicinal plant raw material.

Then the extraction time was selected according to the extractives amount also. 100 g of dried corn silk was grounded, loaded into the extractor, and filled with 40% ethanol (according to the result of extractives determination Table 1) at the ratio of raw material-extractant 1 : 1, taking into account the absorption coefficient of the extractant. Then heated during 15 min, 30 min, 45 min, 60 min, 90 min, 120 min, 180 min, and 240 min from the moment the solvent boils (80–90°C). The extract was cooled to a temperature of 20°C, filtered, and squizzed. 20.0 ml of the filtrate were dried on a water bath, then the residue was dried in the drying cabinet, at 100–105°C, then weight. The content of extractives (%), calculated on the basis of absolutely dry raw materials, was calculated by formula (8). The total number of measurements taken was $n = 5$ [21].

2.5. Phytochemical Investigation of CSLE. The qualitative compositions of the main groups of BAS were determined for the obtained extract by chemical reactions:

(1) *Saponins* [22–26]:

Foam test: 5.0 ml of distilled water was combined with around 0.2 ml of the CSLE. It was violently shacked for five minutes. Foam persistence is used as a saponins indicator.

Salkowski test: 2.0 ml of CSLE were combined with 1.0 ml of chloroform and 5-6- drops of concentrated sulfuric acid. The red ring that appeared between two layers indicates the presence of saponins.

Reaction with 1% alcohol cholesterol solution: 2.0 ml of CSLE were combined with 1.0 ml of 1% cholesterol alcoholic solution. The precipitate indicates the presence of saponins.

Vanillin-sulphate reaction: 2.0 ml of CSLE were combined with 1.0 ml of 0.5% alcohol vanillin

solution, 3-4 drops of concentrated sulfuric acid and heat in water bath at a temperature of 60°C. The red color indicates the presence of saponins.

(2) Phenolic compounds [25, 26]:

Ferric chloride test: 1.0 ml of 3% ferric chloride solution was mixed with 1.0 ml of CSLE. The presence of phenolic compounds is indicated by a greenish-black or a bluish-black color solution.
Reaction with lead acetate solution: the formation of a precipitate following adding 0.5 ml of 1% lead acetate solution to 10.0 ml of CSLE shows the presence of phenolic chemicals.
Reaction with sodium hydroxide solution: 1.0 ml of the CSLE add 1-2 drops of 10% alcohol-aqueous solution of sodium hydroxide. Intense yellow color indicating the presence of phenols.

(3) *Tannins* [25–27]:

Reaction with iron ammonium alum solution: 2.0 ml of analyzed extract were mixed with 4-5 drops of 1% iron ammonium alum solution. The presence of tannins is indicated by a greenish-black (condensed tannins) or a bluish-black (hydrolyzed tannins) color solution.
Gelatin test: a few drops of gelatine solution was added to 2.0 ml of the CSLE. Cloudiness is formed, and disappears after the addition of gelatine surplus. It indicates the presence of tannins.

(4) *Flavonoids* [25, 26]:

Cyanidin test (Shinoda's test): 10.0 ml of CSLE was handled with magnesium ribbons, and a few drops of concentrated hydrochloric acid were added. Magenta coloration is a sign of the presence of flavonoids.
Reaction with aluminum chloride solution: 2.0 ml of CSLE were combined with 2.0 ml of 3% aluminum chloride solution. The lemon yellow color indicates the presence of flavonoids.
Reaction with vanillin in concentrated hydrochloric acid: few drops of 1% solution of vanillin in concentrated hydrochloric acid were added to 1.0 ml of CLSE. Bright red color indicates the presence of flavonoids.

(5) Free and bound reducing sugars [26, 27]:

Fehling's test before and after hydrolysis: Fehling A and Fehling B reagents were combined in equal proportions and 2.0 ml of this mixture was added to the CSLE. Then gently boiled. The same reaction was done after hydrolysis of CLSE. A brick red precipitate indicated the presence of reducing sugars.

(6) Hydroxycinnamic acids [28]:

Reaction with nitrite-molybdenum reagent: 1,0 ml of CSLE was mixed with 2.0 ml of 0.5 M hydrochloric acid, 2,0 ml of a mixture of 10% sodium molybdate solution and 10% sodium nitrite solution, 2.0 ml of diluted sodium hydroxide solution in the specified order. A brick red color indicated the presence of hydroxycinnamic acids.

2.6. Determination of Total Flavonoid Content in CSLE. Spectrophotometry was used to determine the quantitative amount of flavonoids in liquid extract, according to the SPhU 2.0 Vol.3 monograph "Matricariae flos^{N}" in terms of luteolin-7-glucoside, wavelength 410 nm [29]. Spectrophotometer Shimadzu UV-1900 (Japan) was used for the experiment.

2.7. Determination of Total Tannin Content in CSLE. The quantitative content of tannins was determined using the spectrophotometry method indicated in section 2.8.14 of the SPhU 2.0 Vol. 1 in terms of pyrogallol and dry raw materials, wavelength 760 nm [30]. Spectrophotometer Shimadzu UV-1900 (Japan) was used for the experiment.

2.8. Determination of Total Phenolic Compounds Content in CLSE. The content of polyphenolic compounds was determined using the Folin–Ciocalteu method and spectrophotometry method (Shimadzu UV-1900 (Japan)), in terms of pyrogallol and dry raw materials, wavelength of 765 nm [24, 31].

2.9. Determination of Total Hydroxycinnamic Acids Content in CSLE. The studies of the quantitative content of hydroxycinnamic acids were carried out in accordance with the methodology given in the SPhU 2.0 Vol.3 in the monograph "Urticae folium," in terms of chlorogenic acid, wavelength 330 nm [30]. The spectrophotometry method was used. The spectrophotometer was Shimadzu UV-1900 (Japan).

2.10. Pharmacological Studies of CSLE

2.10.1. Experimental Animals. Pharmacological studies of CSLE were conducted on mature white (nonlinear) Wister albino rats. The rats were obtained from the vivarium at Isra University's Faculty of Pharmacy in Amman, Jordan. The protocol (SREC/22/09/053) of the study was approved by the Ethical Committee of the Faculty of Pharmacy, Isra University. Rats of both sexes were kept on a standard diet in a vivarium at a temperature of 22-23°C, with free access to food and water, according to the "day-night" retention regimen. All animals were kept in plastic cages with bedding as required [32]; animals of each sex were kept separately. Before the start of each experiment, the animals were transferred to the laboratory, where they were quarantined for 14 days under similar conditions [32].

The experiments were conducted in accordance with the principles outlined in the Convention for the Protection of Vertebrate Animals, which was used in the experiment [32].

2.10.2. Acute Toxicity Study. The acute toxicity study of the liquid extract was carried out with a single intragastric administration in dosage of 2.0–10.0 ml/kg to outbred unanesthetized 32 white rats of both sexes with an initial average weight of 162.2 ± 4.2 g. Duration of observation of animals - 14 days.

The registration of external signs of damage, disorders of autonomic functions, reactions to external stimuli, and the ability to consume food and water were carried out by visual inspection. To exclude possible sexual sensitivity to drugs, the analysis of the results was performed separately for females and males.

The criterion points for determining the toxic effect of liquid extract were dead animals, that registered for 14 days [33]. Animals of different groups were administered the appropriate doses of liquid extract recommended by this method. The toxic effect of the extract was assessed by the mean lethal dose of LD_{50}. The animals had free access to food and water 30 minutes after drug administration. Mass and body temperature were measured at 3, 7 and 14 days; the reaction of animals to external stimuli was evaluated at the same time. At the end of this period, the euthanasia of surviving animals was performed, and a macroscopic examination of the internal organs was performed, and their mass coefficients were determined [34].

2.10.3. Investigation of the Liquid Extract's Specific Hemostatic Activity in terms of Blood Coagulation. The trials were conducted on sexually mature white rats of both sexes (21 individuals). Random sampling was used to divide the animals into three groups: the first group (8 rats) received intact animals (control); the second group (8 rats) received a corn silk liquid extract orally at a dose of 1 ml/kg once a day for 5 days; and the third group (5 rats) received the reference preparation—water pepper liquid extract (WPLE), orally at a dose of 1 ml/kg once a day for 5 days.

It's important to compare the pharmacological action of the new extract and existing plant medicine with proven effectiveness. Water pepper extract is registered as a medicine in the State Register of Medicinal Products of Ukraine with a hemostatic activity which is produced by PJSC Pharmaceutical Factory "Viola" (Ukraine). Therefore, WPLE was chosen as a comparison medicine for CSLE-specific hemostatic activity investigation.

The blood clotting time and prothrombin time (PT) terms were used to evaluate the hemostatic activity. The blood clotting time of the studied extract on the process of blood coagulation was studied by the appearance of fibrin threads in the second drop of blood from the tail vein of rats. The drops of blood in free fall fell on the spherical (temporary) glass. The temperature in the laboratory was 22–25°C.

A stopwatch was used to record the time required to draw a drop of blood. Every 20–30 seconds, a thin glass rod touched a drop of blood from its center to its perimeter until the first fibrin strands emerged. The start of blood clotting was recorded at this time.

The stopwatch stopped once a blood clot had formed. The start of blood coagulation (the development of fibrin strands, sec) and the completion of blood coagulation (the formation of a clot, sec) was thus determined [35].

The prothrombin time was calculated using the Owren method. Noncontact blood was drawn from rats and collected in vials containing EDTA before being centrifuged at 13,000 rpm for 10 minutes at 4°C. For 2 minutes, the clear platelet-free plasma was placed in a 37°C water bath. Each sample received 100l (100 g/ml) suspended in 3% v/v Tween 85, which was mixed with 1 ml of plasma. Coagulation time was measured three times. The vehicle served as the control.

The retraction of the blood clot in the same rats which were injected with the examined preparations (CSLE and WPLE) into the stomach for 5 days, including the rats in the control group, was also evaluated. In the process of euthanasia of sedated (urethane, 1.5 mg/kg, intraperitoneally) rats, mixed blood in a volume of 3 ml was taken from each rat and placed into measured graduated tubes. All tubes were left at room temperature for 24 hours. The degree of peeling of the blood clot and the volume of serum was assessed a day later. The retraction index was determined by dividing the volume of serum separated by the total volume of blood drawn for the trial (3 ml) [36].

2.11. Statistical Analysis. The results were mean ± SD of three parallel measurements. All statistical comparisons and reliability were made by Student's criterion to determine the standard deviation with a level of significance of 95%.

Statistical analysis of the results obtained was carried out by the method of the smallest squares according to the SPhU monograph "5. 3. N. 1. Statistical analysis of the results of the chemical experiment" (2015). GraphPad Prism software, version 8, was used to evaluate significant differences between experimental groups using one-way ANOVA, followed by Tukey's post hoc test for multiple comparisons. A $p < 0.05$ difference was considered statistically significant.

3. Results and Discussion

3.1. Technological Parameters and Quality Indicators of Raw Materials. Table 1 shows the technological parameters and quality indicators of corn silk (3,00 mm): specific density, volumetric density, bulk density, porosity, spatial layer, free volume of the layer, the absorption coefficient, weight loss on drying, and extractives. These indicators were assessed based on the development of high-quality raw materials, the effectiveness, safety, reproducibility of the imposed collection, and the maximum yield of extractive and active substances [37].

Furthermore, as shown in Table 1, 40% ethanol is the most effective extractant, with a yield of 24,70 ± 0,64% when compared to ethanol in various degrees and water. On the other hand, it is inexpensive and environmentally safe.

3.2. Optimizing Extractability of the CSLE. The best extraction time for obtaining of CSLE was determined experimentally based on the amount of extractives obtained.

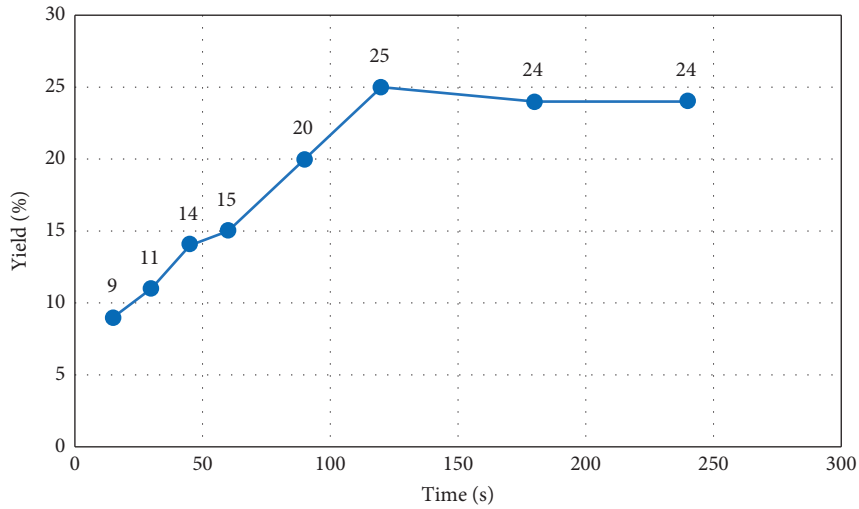

Figure 1: Optimization of the extractability of the CSLE, (%).

Table 2: Preliminary phytochemical screening of corn silk liquid extract.

Test	Free of reduced sugars	Glycosides (bound reduced sugars)	The sum of phenols	Tannins	Flavonoids	Saponins	Hydroxycinnamic acids
Qualitative determination	+	+	+	+	+	+	+
Quantitative content, (%)	–	–	8.25 ± 0.33 (In terms of *p* pyrogallol)	1.4 ± 0.03 (In terms of *p* pyrogallol)	2.20 ± 0.06 (In terms of luteolin 7-glucoside)	–	3.30 ± 0.13 (In terms of chlorogenic acid)

+ = present. – = the indicator is not defined. the quantitative content of saponins and sugars was not determined. data are presented as mean ± standard deviation ($n = 3$).

Figure 1 shows the percentage of extractive substances yield that was achieved depending on time extraction (min).

According to Figure 1, the maximum amount of extractive substances could be extracted in 120 minutes using the selected extractant. Furthermore, after 120 minutes of extraction, the yield was 25,30 ± 0,64%. Meanwhile, there were no significant changes in yield as the extraction time was increased. As a result, the determined extraction time is optimal for this type of raw material.

3.3. Phytochemical Investigation of CSLE. Table 2 depicts the qualitative and quantitative content of BAS of CSLE. Several chemical tests were carried out to detect the presence of BAS. The findings of this research confirmed the presence of free reduced sugars, glycosides (bound reduced sugars), phenols, tannins, flavonoids, saponins, and hydroxycinnamic acids in the CSLE. Based on the availability of the BAS, total phenols, tannins, flavonoids and hydroxycinnamic acids were 8.25 ± 0.33%, 1.4 ± 0.03%, 2.20 ± 0.06%, 3.30 ± 0.13% respectively.

The presence of numerous active substances in the CSLE demonstrated potential health benefits such as antioxidant properties against a variety of chronic and age-related diseases such as diabetes, hypertension, cancer, inflammation, hyperlipidemia, depression, hepatic and cardiovascular diseases [8, 38–40].

3.4. Pharmacological Studies of CSLE

3.4.1. Acute Toxicity Study. The acute toxicity of corn silk extract was investigated. Table 3 shows that a single intragastric administration of the liquid extract in a dose up to 5.0 ml/kg did not result in the death of rats, both females, and males. Physiological excess weight was observed in all groups of animals. White rats actively consumed food and water. They responded adequately to external stimuli an hour after administration. Their body temperature, social relationships, and behavioral responses were all normal [34]. Our findings showed that corn silk extract at a dose up to 5.0 ml/kg is safe.

An increase in the drug's experimental doses exacerbated the symptoms of poisoning, characterized by excitation of animals within 10 minutes of administration of corn silk extract, and a subsequent change in inhibition of motor activity, gradual loss of appetite, and decreased response to external stimuli. The deaths of rats (more animals) were mostly observed in the first two days following a single injection of the liquid extract [34].

The extract's average Lethal dose per os was almost the same for males (5.15 ml/kg) and females (5.64 ml/kg). The findings confirm the absence of sexual sensitivity to corn silk extract.

The animals were euthanized by an overdose of diethyl ether 14 days after receiving corn silk extract, and their cross-section was taken. Binocular dandruff was used for

Table 3: Study of acute toxicity of CSLE.

Route of administration	Sex	Dose, (ml/kg)	Weight of rats, (g) ($M \pm m$)		Result*	LD_{50} ml/kg
			Initial	At the end of the experiment		
Per os	Male	2.0	164.3 ± 5.4	174.0 ± 5.0	0/2	5.15
		2.5			0/2	
		3.1			0/2	
		3.9			0/2	
		5.0			1/2	
		6.3			2/2	
		7.9			2/2	
		10.0			0/2	
	Female	2.0	160.0 ± 4.2	170.4 ± 2.8	0/2	5.64
		2.5			0/2	
		3.1			0/2	
		3.9			0/2	
		5.0			0/2	
		6.3			2/2	
		7.9			2/2	
		10.0			2/2	

Note. * - the number of animals that died about the total number of rats in the group.

Table 4: Rat internal organ mass (g) following a single injection.

Treatment	Sex	Liver	Kidneys	Heart	Adrenal glands	Lungs	Testicles
Control (intact animals)	Male	7.80 ± 0.15	0.80 ± 0.06	0.86 ± 0.07	0.019 ± 0.002	0.77 ± 0.07	1.20 ± 0.12
	Female	7.95 ± 0.60	0.75 ± 0.08	0.80 ± 0.04	0.020 ± 0.002	0.85 ± 0.08	—
CSLE	Male	8.10 ± 0.07	0.77 ± 0.05	0.88 ± 0.07	0.021 ± 0.001	0,82 ± 0,06	9,50 ± 0,67
		$p > 0.05$	$p > 0.05$	$p > 0.05$	$p > 0.05$	$p > 0.05$	$p > 0.05$
		$p1 > 0.05$	$p1 > 0.05$	$p1 > 0.05$	$p1 > 0.05$	$p1 > 0.05$	$p1 > 0.05$
	Female	7.90 ± 0.07	0.80 ± 0.06	0.79 ± 0.05	0.021 ± 0.002	0.92 ± 0.07	
		$p > 0.05$	$p > 0.05$	$p > 0.05$	$p > 0.05$	$p > 0.05$	—
		$p1 > 0.05$	$p1 > 0.05$	$p1 > 0.05$	$p1 > 0.055$	$p1 > 0.05$	

Note. data are expressed as mean ± SEM. CSLE - corn silk liquid extract; p - the level of significance of the difference when compared to intact animals; $p1$ - the level of consistency of the difference when compared to animals of the opposite sex.

Table 5: Effect of CSLE on blood clotting time in white rats.

Treatment	Start of blood coagulation, $M \pm m$, s	End of coagulation (blood clot formation), $M \pm m$, s
Control (intact animals), $n = 8$	62.1 ± 3.58	132.5 ± 5.58
CSLE, $n = 8$	33.1 ± 2.48*	81.3 ± 2.48*
WPLE, $n = 5$	33.0 ± 3.85*	92.0 ± 12.05*

Note. CSLE-corn silk liquid extract; WPLE-water paper liquid extract; Data are expressed as mean ± SEM; * = $p < 0.05$ significant difference in comparison to intact animals values.

macroscopic examination of the internal organs, and the mass of the internal organs was recorded. Table 4 displays the results.

According to the findings, a single injection of a liquid extract does not cause visible changes in the internal organs; they remain in their normal location and color, the lungs retain their specific structure, the intestines are not filled with air, and the size and mass of internal organs do not change significantly ($p > 0.05$). Thus, the obtained results confirm the absence of organotropism for corn silk extract [34].

3.4.2. Investigation of the Liquid Extract's Specific Hemostatic Activity in terms of Blood Coagulation. The presence of an effect on blood clotting time in white rats was demonstrated by a study of the specific hemostatic activity of corn silk liquid extract in terms of blood coagulation determining the beginning of blood clotting by the appearance of fibrin filaments and its ending by the formation of a blood clot (Table 5).

As a result, as shown in Table 5, the time of onset of blood clotting in white rats after the use of corn extract and the reference drug is reduced significantly ($p < 0.05$) by nearly 47% when compared to intact animals. Furthermore, the time of onset of blood clotting in white rats treated with CSLE is comparable to that of white rats treated with WPLE. Moreover, CSLE reduces the end of blood coagulation by 38.6%, while the reference preparation reduces it by 30.5%.

The coagulometric determination of blood clotting time and prothrombin time are shown in Table 6. Blood clotting

Table 6: The effect of CSLE on hemocoagulation parameters in rats.

Treatment	Blood clotting time, $M \pm m$, s	Prothrombin time, $M \pm m$, s	Retraction index
Control (intact animals), $n = 8$	138.9 ± 6.78	23.23 ± 1.58	0.40 ± 0.03
CSLE, $n = 8$	$89.1 \pm 2.48^*$	$13.9 \pm 1.48^*$	0.52 ± 0.04
WPLE, $n = 5$	$94.8 \pm 8.85^*$	$15.6 \pm 2.05^*$	0.49 ± 0.06

Note. CSLE-corn silk liquid extract; WPLE-water paper liquid extract; data are expressed as mean ± SEM; $^* = p < 0.05$ significant difference in comparison to intact animals values.

times for CSLE, WPLE and the control were 89.1 ± 2.48, 94.8 ± 8.85 and 138.9 ± 6.78 seconds, respectively. The prothrombin times for CSLE, WPLE and control were 13.9 ± 1.48, 15.6 ± 2.05 and 23.23 ± 1.58 seconds, respectively.

In addition Table 6 also shows that when white rats are given CSLE, their blood clotting rate is shorter by 35.9% and their prothrombin time is reduced by 40% when compared to the control group. Similarly, both CSLE and WPLE showed the same effect (Table 6).

The retraction index increased by 30% and 22.5% with the use of corn silk extract and liquid pepper water extract, respectively.

The results of this experiment demonstrated that CSLE contributes to hemostasis by shortening the time required for plasma-coagulation (PT) and blood clotting. BAS, particularly polyphenols (tannins, flavonoids) may play an important role in hemostasis by preventing bleeding from injured vessels through protein coagulation to form a vascular plug. Hemostasis is defined by spontaneous blood stoppage, which includes vascular spasms of ruptured vessels, platelet aggregation, and blood coagulation [35]. These findings imply that CSLE may cause vasoconstriction and reduce bleeding from injuries or wounds.

Blood clotting is a complex phenomenon that involves a cascade of reactions in addition to platelet aggregation and vasoconstriction. This process begins with prothrombin activation, followed by thrombin conversion, which converts fibrinogen to insoluble fibrin. CSLE reduces coagulation time and raises the possibility that the extract affects with the blood coagulation process [35]. These findings suggested that CSLE may compel the hemostasis effect via the coagulation pathway, resulting in a decrease in clotting time and vasoconstriction, both of which are required to reduce blood loss from injuries.

The current study's findings suggest that CSLE may have clinical implications as a coagulant in the treatment of various pathological states.

Thus, a five-fold preliminary administration of CSLE into the stomach of white rats results in a reduction in blood clotting time, a decrease in prothrombin time, and an increase in the blood clot retraction index. Changes in the studied parameters with the use of CSLE were comparable in the degree of manifestation to those observed with the introduction of the reference drug. The reduction in blood clotting time in white rats when using CSLE, as well as the comparison drug, could be due to an increase in prothrombinase formation.

4. Conclusions

Technological parameters and quality indicators of corn silk were studied: specific density, volumetric density, bulk density, porosity, spatial layer, free volume of the layer, the absorption coefficient, weight loss on drying, and extractives. These results could be used during the industrial production of corn silk medicines.

The technology of obtaining a corn silk liquid extract was developed. It was found that the most effective extractant, according to the extractives yield, is ethanol 40% and the time of extraction is 120 min.

Phytochemical investigation of liquid extract confirmed the presence of free reduced sugars, glycosides (bound reduced sugars), phenols, tannins, flavonoids, saponins, and hydroxycinnamic acids. The research of quantitative content allows us to draw a conclusion that phenolic compounds are a main BAS group of CSLE: total phenols −8.25 ± 0.33%, tannins −1.4 ± 0.03%, flavonoids −2.20 ± 0.06% and hydroxycinnamic acids −3.30 ± 0.13%.

An acute toxicity study showed that corn silk extract at a dose up to 5.0 ml/kg is safe. A single injection of a liquid extract does not cause visible changes in the internal organs. The obtained results confirm the absence of organotropism for CSLE.

The preliminary administration of CSLE to white rats results in a reduction in blood clotting time, a decrease in prothrombin time, and an increase in the blood clot retraction index.

According to the findings, corn silk liquid extract is high in phytochemicals and has therapeutic potential in bleeding disorders. Furthermore, it could be used in pharmaceutical sciences and industry to develop medicines for testing in the treatment of a variety of diseases.

Data Availability

The data used to support the findings of this study are available from the corresponding author upon request.

Conflicts of Interest

The authors declare that they have no conflicts of interest.

Acknowledgments

The authors are grateful for the institutional support provided by the faculties of pharmacy at Isra University and Bogomolets National Medical University.

References

[1] S. Petros, "Pathophysiology of bleeding," *Medizinische Klinik - Intensivmedizin und Notfallmedizin*, vol. 116, no. 6, pp. 475–481, 2021.

[2] P. P. Clive, C. Michael, C. S. Morley, and W. Michael, *Integrated Pharmacology*, Mosby, Maryland Heights, MO, USA, 2006.

[3] J. Loscalzo and A. I. Schafer, *Thrombosis and Hemorrhage*, Lippincott Williams & Wilkins, Philadelphia, PA, USA, 2003.

[4] J. Ferguson, M. Quinn, and J. Moake, "The physiology of normal platelet function," *Antiplatelet Therapy in Clinical Practice*, Taylor & Francis, London, UK, 2000.

[5] R. Nayal, M. Y. Abajy, and S. Takla, "Investigating in vitro the hemostatic effect of some medicinal plants," *Research Journal of Aleppo University*, 2015.

[6] F. Ebrahimi, M. Torbati, J. Mahmoudi, and H. Valizadeh, "Medicinal plants as potential hemostatic agents," *Journal of Pharmacy & Pharmaceutical Sciences*, vol. 23, no. 1, pp. 10–23, 2020.

[7] A. O. Oyabambi, A. B. Nafiu, A. Okesina, S. S. Babatunde, E. K. Dominic, and D. O. Oreoluwa, "Corn silk methanolic extract improves oxidative stress and inflammatory responses in rats' excision wound model," *Ceylon Journal of Science*, vol. 50, no. 1, pp. 39–46, 2021.

[8] S. B. Mada, L. Sani, and G. D. Chechet, "Corn silk from waste material to potential therapeutic agent: a mini review," *Fuw Trends in Science & Technology Journal*, vol. 5, no. 3, pp. 816–820, 2020.

[9] M. Parle and I. Dhamija, "Zea maize: a modern craze," *International Research Journal of Pharmacy*, vol. 4, no. 6, pp. 39–43, 2013.

[10] C. W. Fennell, *Food Plants of the World, Identification, Culinary Uses and Nutritional Value*, Briza Publications, Toronto, Canada, 2006.

[11] J. Barnes, L. A. Anderson, and J. D. Phillipson, *Herbal Medicines*, Pharmaceutical Press, London, UK, 2007.

[12] R. Suzuki, M. Iijima, Y. Okada, and T. Okuyama, "Chemical constituents of the style of *Zea mays* L. with glycation inhibitory activity," *Chemical & Pharmaceutical Bulletin*, vol. 55, no. 1, pp. 153–155, 2007.

[13] N. W. Widstrom and M. E. Snook, "Recurrent selection for maysin, a compound in maize silks, antibiotic to earworm," *Plant Breeding*, vol. 120, no. 4, pp. 357–359, 2001.

[14] K. Chandler-Ezell and S. F. Austin, "Understanding medicinal plants their chemistry and therapeutic action," *Economic Botany*, vol. 60, no. 3, p. 298, 2006.

[15] D. Kumar and A. N. Jhariya, "Nutritional, medicinal and economical importance of corn: a mini review," *Research Journal of Pharmaceutical Sciences*, vol. 2319, p. 555, 2013.

[16] B. V. Owoyele, M. N. Negedu, S. O. Olaniran et al., "Analgesic and anti-inflammatory effects of aqueous extract of *Zea mays* husk in male Wistar rats," *Journal of Medicinal Food*, vol. 13, no. 2, pp. 343–347, 2010.

[17] E. Alam, "Evaluation of antioxidant and antibacterial activities of Egyptian Maydis stigma (*Zea mays* hairs) rich in some bioactive constituents," *Journal of American Science*, vol. 7, no. 4, pp. 726–729, 2011.

[18] Z. Maksimović and N. Kovačević, "Preliminary assay on the antioxidative activity of maydis stigma extracts," *Fitoterapia*, vol. 74, no. 1-2, pp. 144–147, 2003.

[19] FAO, *Production/Yield Quantities of Maize in World*, FAO, Rome, Italy, 2020.

[20] K. Volodymyr, C. Serhii, K. Anastasiia, and M. Olga, "Establishment of the main technological parameters of Iris raw material," *Research Journal of Pharmacy and Technology*, vol. 12, no. 7, pp. 3359–3364, 2019.

[21] Derzhavna Farmakopeya Ukrayiny, *Derzhavne Pidpryyemstvo "Ukrainskyi Naukovyi Farmakopeynyy Tsentr Yakosti Liarskih Zasobiv"*, Kharkiv: Derzhavne pidpryiemstvo, Ukrainskyi naukovyi farmakopeinyi tsentr yakosti likarskykh zasobiv, Ukrine, 2015.

[22] A. S. Ashour, M. M. A. El Aziz, and A. S. Gomha Melad, "A review on saponins from medicinal plants: chemistry, isolation, and determination," *Journal of Nanomedicine Research*, vol. 7, no. 4, pp. 282–288, 2019.

[23] S. Hiai, H. Oura, and T. Nakajima, "Color reaction of some sapogenins and saponins with vanillin and sulfur1c acid," *Planta Medica*, vol. 29, no. 2, pp. 116–122, 1976.

[24] T. Pasaribu, A. P. Sinurat, E. Wina, and T. Cahyaningsih, "Evaluation of the phytochemical content, antimicrobial and antioxidant activity of cocos nucifera liquid smoke, garcinia mangostana pericarp, syzygium aromaticum leaf, and *Phyllanthus niruri* L. extracts," *Veterinary World*, vol. 14, no. 11, pp. 3048–3055, 2021.

[25] N. O. Olha, "Pharmacognostic study of the galls of wild representatives of *Quercus robur* L., created by insects," *Research Journal of Pharmacy and Technology*, vol. 14, no. 1, pp. 122–128, 2021.

[26] R. Junaid and M. Patil, "Qualitative test for preliminary phytochemical screening," *International Journal of Chemical Studies*, vol. 8, no. 2, pp. 603–608, 2020.

[27] B. K. Das, M. M. Al-Amin, S. M. Russel, S. Kabir, R. Bhattacherjee, and J. M. A. Hannan, "Phytochemical screening and evaluation of analgesic activity of oroxylum indicum," *Indian Journal of Pharmaceutical Sciences*, vol. 76, no. 6, pp. 571–575, 2014.

[28] U. Gawlik-Dziki, D. Dziki, B. Baraniak, and R. Lin, "The effect of simulated digestion in vitro on bioactivity of wheat bread with tartary buckwheat flavones addition," *LWT--Food Science and Technology*, vol. 42, no. 1, pp. 137–143, 2009.

[29] Derzhavna Farmakopeya Ukrayiny, *Derzhavne Pidpryyemstvo "Ukrainskyi Naukovyi Farmakopeynyy Tsentr Yakosti Liarskih Zasobiv"*, Kharkiv: Derzhavne pidpryiemstvo, Ukrainskyi naukovyi farmakopeinyi tsentr yakosti likarskykh zasobiv, Ukrine, 2014.

[30] Derzhavna Farmakopeya Ukrayiny, *Derzhavne Pidpryyemstvo "Ukrainskyi Naukovyi Farmakopeynyy Tsentr Yakosti Liarskih Zasobiv"*, Kharkiv: Derzhavne pidpryiemstvo, Ukrainskyi naukovyi farmakopeinyi tsentr yakosti likarskykh zasobiv, Ukrine, 2021.

[31] J. Singh, B. S. Inbaraj, S. Kaur, P. Rasane, and V. Nanda, "Phytochemical analysis and characterization of corn silk (*Zea mays*, G5417)," *Agronomy*, vol. 12, no. 4, p. 777, 2022.

[32] National Research Council, *Guide for the Care and Use of Laboratory Animals*, National Academy Press, Washington, D.C., USA, 2010.

[33] OECD, *OECD Guideline for Testing of Chemicals: Acute Oral Toxicity-Fixed Dose Procedure*, OECD, Paris, France, 2001.

[34] A. W. Ha, H. J. Kang, S. L. Kim, M. H. Kim, and W. K. Kim, "Acute and subacute toxicity evaluation of corn silk extract," *Preventive Nutrition and Food Science*, vol. 23, no. 1, pp. 70–76, 2018.

[35] M. Sajid, M. R. Rashid Khan, N. A. Shah et al., "Evaluation of artemisia scoparia for hemostasis promotion activity," *Pakistan Journal of Pharmaceutical Sciences*, vol. 30, no. 5, pp. 1709–1713, 2017.

[36] E. E. Jansen and M. Hartmann, "Clot retraction: cellular mechanisms and inhibitors, measuring methods, and clinical implications," *Biomedicines*, vol. 9, no. 8, p. 1064, 2021.

[37] A. Kriukova and I. Vladymyrova, "Determination of technological parameters and indicators of the quality of new herbal collection," *Eureka: Health Science*, vol. 6, pp. 61–68, 2018.

[38] S. Tian, Y. Sun, and Z. Chen, "Extraction of flavonoids from corn silk and biological activities in vitro," *Journal of Food Quality*, vol. 2021, Article ID 7390425, 9 pages, 2021.

[39] A. Nurhanan and W. R. Wi, "Evaluation of polyphenol content and antioxidant activities of some selected organic and aqueous extracts of corn silk (*Zea mays* hairs)," *Journal of Medical and Bioengineering*, vol. 1, no. 1, pp. 48–51, 2012.

[40] K. Hasanudin, P. Hashim, and S. Mustafa, "Corn silk (*Stigma maydis*) in healthcare: a phytochemical and pharmacological review," *Molecules*, vol. 17, no. 8, pp. 9697–9715, 2012.

Hindawi
Journal of Chemistry
Volume 2022, Article ID 9212872, 8 pages
https://doi.org/10.1155/2022/9212872

Research Article

Total Active Compounds and Mineral Contents in *Wolffia globosa*

Orawan Monthakantirat,[1] **Yaowared Chulikhit**,[1] **Juthamart Maneenet**,[2] **Charinya Khamphukdee**,[3] **Yutthana Chotritthirong**,[2] **Suphatson Limsakul**,[2] **Tanakorn Punya**,[2] **Buntarawan Turapra**,[2] **Chantana Boonyarat**,[1] **and Supawadee Daodee**[1]

[1]*Division of Pharmaceutical Chemistry, Faculty of Pharmaceutical Sciences, Khon Kaen University, Khon Kaen 40002, Thailand*
[2]*SOJY Lab, Faculty of Pharmaceutical Sciences, Khon Kaen University, Khon Kaen 40002, Thailand*
[3]*Division of Pharmacognosy and Toxicology, Faculty of Pharmaceutical Sciences, Khon Kaen University, Khon Kaen 40002, Thailand*

Correspondence should be addressed to Supawadee Daodee; csupawad@kku.ac.th

Received 6 July 2022; Revised 7 September 2022; Accepted 16 September 2022; Published 28 September 2022

Academic Editor: Marwa Fayed

Wolffia globosa, or watermeal, is an aquatic plant belonging to the Lemnaceae family that is consumed as food and sold in local markets of Thailand. The aim of this study was to quantify selected active compounds and minerals in *W. globosa* ethanolic extract and evaluate its antioxidant activity. Total phenolic, flavonoid, and anthocyanin contents were analyzed. High-performance liquid chromatography was used for the determination of beta-carotene, ferulic acid, luteolin-7-O-β-D-glucoside, and kaempferol. Mineral contents (iron, potassium, calcium, magnesium, zinc, and sodium) were determined by atomic absorption spectroscopy. Antioxidative activity was evaluated by DPPH (2,2-diphenyl-1-picrylhydrazyl) and ABTS (2,2′-azobis (3-ethylbenzothiazoline-6-sulfonic acid)) radical scavenging assays. The beta-carotene, ferulic acid, luteolin-7-O-β-D-glucoside, and kaempferol contents of the extract were 2.52 ± 0.10, 1.40 ± 0.10, 2.42 ± 0.50, and 1.57 ± 0.14 mg/g extract, respectively. The highest mineral content in the *W. globosa* extract was magnesium. The wet extract of *W. globosa* showed higher amounts of all minerals than the dry extract. Freshly prepared and boiled *W. globosa* extracts showed radical scavenging activity at 1000 μg/milliliter with $75.77 \pm 0.93\%$ and $67.10 \pm 0.20\%$ inhibition of DPPH and $70.40 \pm 7.20\%$ and $59.78 \pm 3.16\%$ inhibition of ABTS, respectively. This plant is a promising novel source of natural phytochemical constituents and antioxidants and has potential for development as a plant-based nutraceutical product for the treatment of diseases caused by free radicals.

1. Introduction

Several classes of natural compounds generally found in plants have been reported to have antioxidant properties and reduce oxidative stress. Various kinds of plants such as *Moringa oleifera* and *Glycine max* (L.) Merr are sources of phytonutrients and minerals which have many biological activities [1–4]. These include flavonoids, phenolics, carotenoids, alkaloids, and some minerals [5, 6]. The accumulation of damage caused by free radicals arising from oxidative stress plays a crucial role in aging and diseases such as cancer, cardiovascular disease, and neurodegenerative diseases [7, 8]. The scavenging and deactivation of free radicals is one important mechanism of antioxidant activity. Free radicals are unstable atoms or molecules with unpaired electrons that react with proteins and DNA in human cells. Antioxidant defense mechanisms in plants and animals deactivate and remove these reactive molecules to prevent damage to tissues, but under conditions of oxidative stress, free radicals can overwhelm this defense system. Dietary intake of antioxidant compounds can prevent cell damage from oxidative stress and stabilize damaged cells by supplying electrons to free radicals and then eliminating them from the body. Many kinds of plants are used as sources of active compounds and elements in herbal products, nutraceuticals, cosmeceuticals, and food products.

Identifying active compounds and minerals in plants have received much attention, not only because of the perceived safety of natural products but also due to the synergistic mechanisms among the various kinds of compounds contained in plants.

Wolffia globosa, known as watermeal, khai nam, or khai phum, is a small, aquatic plant belonging to the Lemnaceae family of duckweeds as shown in Figure 1. The leaves and stem of this plant are fused together in a highly reduced rootless structure called a frond, which is less than 1 mm in diameter with a globular or oval shape, flattened upper surface [9, 10]. It has been reported that *W. globosa* fronds absorb nutrients through the underside, which is in contact with the water. This plant grows readily and is commonly found in nature. *W. globosa* is consumed as a vegetable in Myanmar, Laos, and the northern parts of Thailand. This plant has high protein content (approximately 40% dry weight) and high amounts of chlorophyll, carotenoids, flavonoids, and vitamins such as cyanocobalamin. All nine essential amino acids are also found in this plant [11]. Previous studies have revealed the presence of 20–35% protein, 4–7% fat, and 4–10% starch in plants from Lemnaceae, and *W. globosa* has been used as a protein source in animal feed and as a raw material for many industrial products including bioalcohol and biodegradable plastics [12, 13].

The nutritional value of this plant has long been recognized in the culinary traditions of Southeast Asia including Thailand. One study showed that consumption of *W. globosa* might have beneficial postprandial glycemic effects [14]. Another showed that the presence of cyanocobalamin, iron, and folic acid in this plant improved the health of prediabetic patients when included in a standard Mediterranean style diet [15]. *W. globosa* was also found to help maintain iron and folic acid status in humans and completely reverse iron deficiency anemia in an experimental rat model [16].

Thus, this plant is a rich, potential source of biologically active compounds. However, although the health-promoting effects of this plant have been reviewed, the plant components responsible for such biological effects have not yet been completely identified. Therefore, the aim of this research was to determine the biologically active components and minerals present in *W. globosa* and investigate its antioxidant activity in support of developing this plant as a nutraceutical product.

2. Materials and Methods

2.1. Materials and Equipment. *W. globosa* was collected from Nonmuang area, Muang District, Khon Kaen, Thailand. A specimen of the plant material (voucher number: SD10) was identified and authenticated by Assistant Professor Dr. Prathan Luecha, Division of Pharmacognosy and Toxicology, Faculty of Pharmaceutical Sciences, Khon Kaen University, Khon Kaen, Thailand.

Folin-Ciocalteu phenol reagent, β-carotene, sodium acetate, ferulic acid, luteolin-7-O-β-D-glucoside, Trolox, kaempferol, and quercetin were purchased from Sigma-Aldrich (SM Chemical supplies Co., LTD., Bangkok, Thailand), ethanol, methanol, and ethyl acetate were purchased from VWR Chemicals BDH (SM Chemical supplies Co., LTD., Bangkok, Thailand), and gallic acid, hexane, and hydrochloric acid were purchased from Merck (Merck, Bangkok, Thailand). Sodium carbonate (Loba chemie, India), aluminum chloride (Ajax Finechem, Australia), potassium chloride (QRëC, New Zealand), acetone (RCI Labscan, Thailand), and ultrapure water were also used in this study. A rotary vacuum evaporator (Buchi: R-114, Switzerland), a freeze dryer (Labconco: 710611130, USA), an atomic absorption spectrophotometer (Perkin Elmer Inc: PinAAcle 900F, USA), a high-performance liquid chromatograph (Agilent Technologies:1260, USA), and an incubator microplate reader (Perkin Elmer Inc: HH3400, USA) were used.

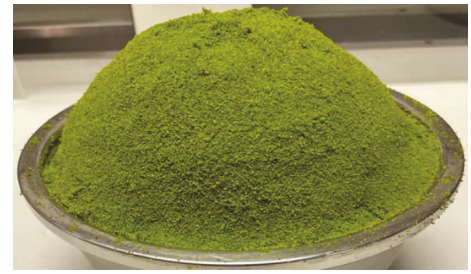

Figure 1: Fresh *Wolffia globosa* (watermeal, khai nam, or khai phum).

2.2. Preparation of Crude Extract. *W. globosa* was washed under running water until the water was clean and then boiled for 15 min. Then, the raw materials were dried at 50 degree Celsius and macerated with 95% ethanol (1000 ml) twice within 7 days. The extracts were filtered and evaporated using a vacuum rotary evaporator. The crude extracts were stored at −20 degree Celsius until needed for analysis.

2.3. Determination of Total Phenolic Content. The total phenolic content in *W. globosa* extract was determined using the Folin-Ciocalteu method [17, 18]. In brief, 20 microliters of the extract solution (1 mg of extract dissolved in 1,000 μl of ethanol) were added into 100 μl of the Folin-Ciocalteu reagent (10%) and 80 μl of sodium carbonate (7%). The reaction is shown as follows. After 30 minutes of incubation in the dark, the absorbance was measured at 760 nm using a microplate reader. The calibration curve of standard gallic acid solution was prepared in the range of 10–100 μg/ml and used to calculate the gallic acid equivalent content from the measured absorbance. The otal phenolic content is expressed as milligram gallic acid equivalents per gram of the extract (mg GAE/g extract).

$$\mathrm{Mo}(VI) + e^{-}\ (\text{antioxidant}) \mathrm{Mo}(V) \longrightarrow \mathrm{Mo}(V)\,(\lambda\mathrm{max} = 760\,\mathrm{nm}). \quad (1)$$

2.4. Determination of Total Flavonoid Content. The total flavonoid content in the extract was determined using the aluminum chloride colorimetric method [19]. The principle of this method involves the addition of $AlCl_3$ which could

form a stable acid complex with the ketone groups, hydroxyl groups, or orthodihydroxyl groups in flavonoid compounds which have a maximum absorption at a wavelength of 432 nm. In brief, twenty microliters of the extract solution were added to 15 μl of aluminum chloride, 20 μl of sodium acetate (10%), and 145 μl of distilled water. After 15 minutes of incubation in the dark, the absorbance was measured at 430 nm with a microplate reader. The calibration curve of standard quercetin solution (5–100 μg/ml) was prepared and used for the calculation of the quercetin equivalent from the measured absorbance. The otal flavonoid content is expressed as milligram quercetin equivalents per gram of the extract (mg QE/g extract).

2.5. Determination of Total Anthocyanin Content. The total anthocyanin content was determined using the pH differential method by measuring the absorbance at pH 1.0 and pH 4.5 with a UV-visible spectrophotometer [20]. Twenty microliters of the extract were mixed with 100 μl of 0.025 m potassium chloride solution (pH 1) or 100 μl of 0.4 m sodium acetate solution (pH 4.5). The absorbance was measured at 535 and 700 nm with a microplate reader. The total anthocyanin content is expressed as milligram cyanidin-3-glucoside equivalents per gram of the extract (mg c3g/g extract) and was calculated according to the following equation:

$$\text{monomeric anthocyanin} = (A \times M \times D \times 1000) \div (\text{molar absorptivity} \times 1), \quad (2)$$

where A is the absorbance, M is the molecular weight of a reference pigment (cyanidin-3-glucoside: 449.2 g/mol), D is the dilution factor = 10, and the molar absorptivity is the reference anthocyanin (extinction factor 26,900 $\text{L}\cdot\text{cm}^{-1}\cdot\text{mol}^{-1}$).

2.6. HPLC Analysis of Beta-Carotene. The analytical method for beta-carotene was adopted from the study by Khamphukdee et al. [21]. The analysis was carried out using HPLC with a diode array detector (Agilent Technologies: 1260, USA). The extract solution (10 mg in 1 ml of 80% acetone) was injected into a Hypersil ODS column (Thermo Scientific: 30105–254030, 250 × 4.0 mm i.d.; 5 μm particle size). The mobile phase consisted of acetonitrile, dichloromethane, and methanol in the ratio of 70 : 20 : 10. The flow rate for all the analyses was 1.0 ml/min. The absorbance was measured at a wavelength of 450 nm. The beta-carotene content was determined using the standard curve plotted between the peak area and concentration of standard solutions (0.25–30 μg/ml) and calculated.

2.7. HPLC Analysis of Ferulic Acid, Luteolin 7-O-β-D-Glucoside, and Kaempferol and Validation Method. The modified HPLC method with a diode array detector (Agilent Technologies:1260, USA) was carried out for the analysis of these three compounds [22]. A reversed phase HPLC column (ACE Generix 5, C18, 150 × 4.6 mm) was used. The mobile phase consisted of solvent A (ultrapure water) and solvent B (0.25% acetic acid in 80% methanol) which was run in gradient elution (0–3 min, solvent A was changed from 98 to 80%; 3–15 min, solvent A was changed from 80 to 0%; 15–20 min, solvent A was changed from 0 to 10%; and 20–25 min, solvent A was changed from 10 to 98%). The flow rate was 1.0 ml/min, and the total run time was 25 min. The detection wavelength was set at 340 nm. The analytical method was validated using some parameters to ensure the reliability. Accuracy, precision, linearity, limit of detection, and limit of quantitation were tested.

2.8. Elemental Analysis by Atomic Absorption Spectroscopy (AAS). An atomic absorption spectrophotometer was used for the analysis of potassium, sodium, magnesium, calcium, iron, and zinc. The type of hollow cathode lamp and the detection wavelengths were selected depending on each mineral (λ589.0 for sodium, λ248.33 for iron, λ213.86 for zinc, λ766.49 for potassium, λ422.67 for calcium, and λ285.21 for magnesium). An air-acetylene flame was used for the analysis. Samples were prepared by the dry ashing method. Two kinds of raw materials, wet and dry samples, were analyzed in this study. Dry samples were dried at 50 degree Celsius. For the wet sample, three grams of *W. globosa* were weighed in a porcelain dish and burned in a muffle furnace at 250 degree Celsius for 20 min and then 480 degree Celsius for 8 hr. The sample ash was cooled, 50 milliliters of 25% nitric acid were added, and the mixture was filtered. The filtrate was analyzed by AAS. For dry samples, one gram of the dried sample was burned using the same process as for the wet sample, and the filtrate was then analyzed by AAS. Stock standard solutions of all elements (40 ppm) were diluted to 0.8–4.8 ppm for the determination of iron, potassium, and calcium, 0.032–0.8 ppm for the determination of magnesium, 0.4–2 ppm for the determination of zinc, and 0.48–3.84 ppm for the determination of sodium. Standard curves of each set of standard solutions were prepared for the determination of each element by AAS.

2.9. Determination of Radical Scavenging Activity Using the DPPH Reagent. The free-radical scavenging method was adopted according to the method of some researchers [23]. In brief, the DPPH reagent was prepared by dissolving DPPH (7.9 mg) in ethanol (100 ml), which was then stored at −20 degree Celsius prior to use. The extract (10 mg/milliliter, 100 microliters) and DPPH reagent (100 microliters) were transferred into microplate wells and kept for 30 minutes at room temperature. Then, the absorbance was measured at 517 nm using a microplate reader (Perkin Elmer Inc: HH3400, USA). A calibration curve was plotted for

10–50 μM concentrations of Trolox, the reference standard. The inhibitory percentage of DPPH was calculated by the following formula:

$$\%\text{inhibition} = \left[\left(A_{\text{DPPH}} - A_{\text{sample}}\right) \div \left(A_{\text{DPPH}} - A_{\text{blank}}\right)\right] \times 100, \quad (3)$$

where A_{DPPH} is the absorbance of DPPH radical solution (without sample or standard) and A_{sample} is absorbance of a DPPH solution (with sample or control). The inhibitory concentration at 50% (IC50) was then calculated.

2.10. Determination of Radical Scavenging Activity Using ABTS Radical Cation Decolorization. This method was adapted from a method formerly published [21, 24]. The $ABTS^{\bullet+}$ was prepared by incubating ABTS with potassium persulfate and keeping in the dark at room temperature for 12 hr. One milliliter of $ABTS^{\bullet+}$ solution was diluted by adding ethanol (50 milliliter) to obtain an absorbance of 0.70 ± 0.02 at wavelength 734 nm. The extract (50 μl) in various concentrations and $ABTS^{\bullet+}$reagent (100 μl) were transferred into microplate wells and kept at room temperature for 2 hr. Absorbance was measured at 734 nm. The calibration curve fromTtrolox standard solution (10–50 μM) was plotted.

The percentage inhibition of ABTS was calculated using the following formula:

$$\%\text{inhibition} = \left[\left(A_{\text{ABTS}} - A_{\text{sample}}\right) \div \left(A_{\text{ABTS}} - A_{\text{blank}}\right)\right] \times 100, \quad (4)$$

where A is the absorbance. Inhibitory concentration at 50% (IC50) was then calculated.

2.11. Statistical Analysis. All results are expressed as the mean ± standard deviation (SD) of three replicates for the antioxidant activity assays and the determination of the active content of the samples.

3. Results and Discussion

3.1. The Content of Total Active Compounds and Beta-Carotene in W. globosa Extract. Total active contents were analyzed using standard curves of quercetin and gallic acid for the total flavonoid and total phenolic content. The total anthocyanin content was calculated as described above. The beta-carotene content in *W. globosa* extract was determined by HPLC and using a standard curve of beta-carotene. The total flavonoid, total phenolic, total anthocyanin, and beta-carotene contents of *W. globosa* extract are shown in Table 1. Phenolic, flavonoid, and beta-carotene contents found in the *W. globosa* extract in the present study were similar to those of other studies [25, 26]. Anthocyanin content has not been previously reported for *W. globosa*. These compounds have previously been shown to have biological activities, especially in protection against cell damage by oxidative stress, which plays an important role in aging, cancer, cardiovascular disease, and Alzheimer's disease.

An HPLC method was developed and used for the analysis of ferulic acid, luteolin 7-O-β-D-glucoside, and kaempferol in the *W. globosa* extract. All three peaks were separated in the HPLC chromatogram, and the resolution between peaks was more than 2, which shows complete separation. The validation of the HPLC method for determination of these compounds was satisfactory for some important parameters including accuracy (% recovery is in the range of 80–110), within-day precision, between-day precision (% RSD less than 7.3), linearity (r^2 more than 0.995), limit of detection, and limit of quantitation (Table 2). Thus, this developed HPLC method was appropriate to analyze these compounds in the *W. globosa* extract. Fingerprint HPLC chromatograms of the *W. globosa* extract are shown in Figure 2. The ferulic acid, luteolin 7-O-β-D-glucoside, and kaempferol contents in *W. globosa* extract were 1.40 ± 0.10, 2.42 ± 0.50, and 1.57 ± 0.14 mg/g extract, respectively, from three replicates. These three active compounds might be used as markers for the quality control of *W. globosa* raw materials, and their levels support the development of a nutraceutical product from this plant [21, 23]. However, this study had the limitation that the confirmation to improve the identification of each compound should be performed by some specific techniques such as liquid chromatography-mass spectrometry.

Table 1: Total active contents of the *W. globosa* extract.

Active compounds	Content (mg/g extract ± SD, three replications)
Total flavonoid	38.99 ± 0.44
Total phenolic	40.83 ± 4.99
Total anthocyanin	0.47 ± 0.08
Beta-carotene	2.52 ± 0.10

3.2. Mineral Content in the W. globosa Extract by AAS. Potassium, sodium, magnesium, calcium, iron, and zinc were analyzed by atomic absorption spectrophotometry. The analytical method was tested to confirm the reliability of the method, and the contents of all minerals are shown in Table 3. A comparison of the mineral content of wet and dry samples is shown in Figure 3.

The highest mineral content in both wet and dry *W. globosa* samples was magnesium.The mineral content in the wet sample was higher than in the dry sample except calcium. However, no definite conclusion could be drawn as which method is the best. This study was the only case study which showed the effect of different characteristics of samples on the mineral content. Probably, this might be due to the heating effect of the drying minerals which do escape or vaporize, and as such, lower values of minerals such as Mg was seen in this study. A previous study showed that the iron content in *W. globosa* extract was bioavailable and efficient at treating iron deficiency anemia in a rat model [16]. The important value-added elements of this plant are iron, potassium, calcium, magnesium, zinc, and sodium. Magnesium is an essential mineral for humans. One of magnesium's main roles is acting as an enzyme cofactor in biochemical reactions involved in energy creation, protein formation, gene maintenance, muscle movement, and nervous system regulation. Magnesium has also been shown to reduce symptoms of depression and have beneficial effects against type 2 diabetes [27]. Magnesium can also exhibit

Table 2: Validation results of the analysis of ferulic acid, luteolin 7-O-β-D-glucoside, and kaempferol in the *W. globosa* extract by the HPLC method.

Parameters	Ferulic acid	Luteolin 7-O-β-D-glucoside	Kaempferol
Range (μg/milliliter)	4–15	20–100	4–15
Linearity			
Regression equation	$y = 73.341x - 65.298$	$y = 59.273x - 68.148$	$y = 57.638x - 40.183$
Coefficient of determination	0.9988	0.9951	0,9989
Percentage recovery	102.59 ± 1.57	98.77 ± 4.67	101.39 ± 4.48
Precision (%RSD)			
Within-day	0.45–1.39	1.02–1.72	1.81–2.54
Between-day	1.81–5.38	2.99–3.64	3.82–6.20
Limit of detection (μg/milliliter)	2.0	2.5	2.0
Limit of quantitation (μg/milliliter)	4.0	10.0	4.0
Retention time (minute)	11.2	11.8	15.3
Wavelength detection (λ, nm)	340	340	340

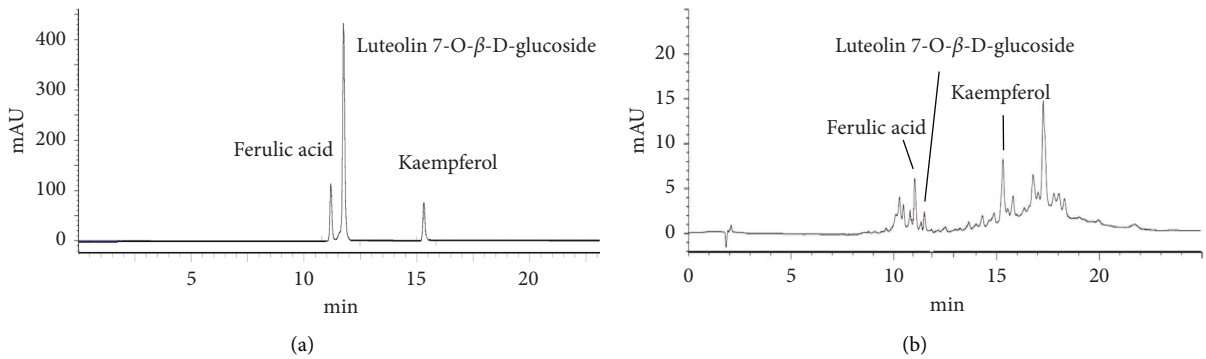

Figure 2: HPLC chromatograms of standard ferulic acid, luteolin 7-O-β-D-glucoside, and kaempferol solutions (a) and the fingerprint HPLC chromatograms of *W. globosa* extract (b) at wavelength 340 nm.

Table 3: The contents of all minerals in *W. globosa* and their validation results.

Parameters	Fe	K	Ca	Mg	Zn	Na
Range (μg/milliliter)	1.60–4.80	0.80–4.00	0.80–4.00	0.032–0.800	0.40–2.00	0.48–3.84
Linearity						
Regression equation	$y = 0.039x - 0.424$	$y = 0.231x + 0.281$	$y = 0.052x + 0.094$	$y = 0.981x + 0.073$	$y = 0.267x + 0.109$	$y = 0.210x + 0.090$
Coefficient of determination	0.9971	0.9923	0.9988	0.9938	0.9927	0.9943
Percentage recovery	99.33 ± 2.85	100.49 ± 10.71	100.99 ± 2.83	101.84 ± 4.87	101.50 ± 5.18	103.39 ± 6.54
Precision (% RSD)						
Within-day	0.00–1.89	1.18–1.70	2.32–3.76	0.49–4.57	0.00–0.91	1.01–2.98
Between-day	0.00–2.79	1.43–2.81	0.33–0.76	1.09–3.78	0.49–2.21	0.56–5.56
Limit of detection (μg/milliliter)	0.037	0.003	0.016	0.001	0.009	0.009
Limit of quantitation (μg/milliliter)	0.120	0.012	0.058	0.005	0.030	0.030
Amount						
Wet sample (mg/g)	0.419 ± 0.020	1.007 ± 0.044	0.059 ± 0.006	1.447 ± 0.321	0.425 ± 0.020	1.087 ± 0.543
Dry sample (mg/g)	0.137 ± 0.011	0.279 ± 0.036	0.282 ± 0.054	0.937 ± 0.076	0.001 ± 0.000	0.647 ± 0.259

anti-inflammatory benefits, and low magnesium intake has been linked to chronic inflammation, one of the drivers of aging, obesity, and chronic disease [28]. *W. globosa* might be counted among pumpkin seeds, boiled spinach, boiled swiss chard, dark chocolate, black bean, cooked quinoa, almonds, cashews, avocado, and salmon as excellent food sources of magnesium [28]. Sodium and potassium were the minerals with the succeeding highest values found in *W. globosa* in this study. These minerals can stimulate cell proliferation and mitochondrial activity, which decreased the expression of some aging markers and showed beneficial effect on keratinocytes damaged by UV exposure [29].

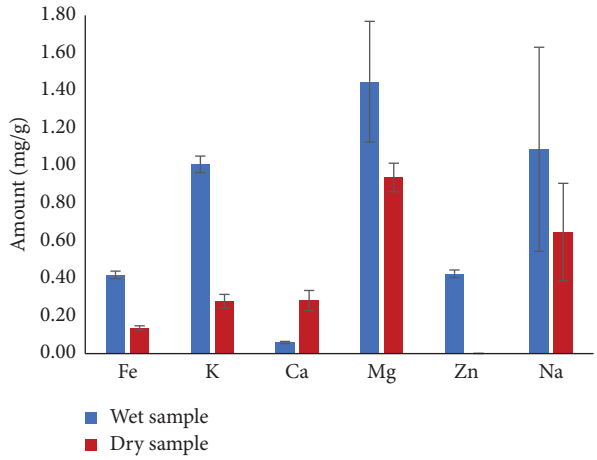

Figure 3: The content of all minerals in wet and dry extracts of *W. globosa*.

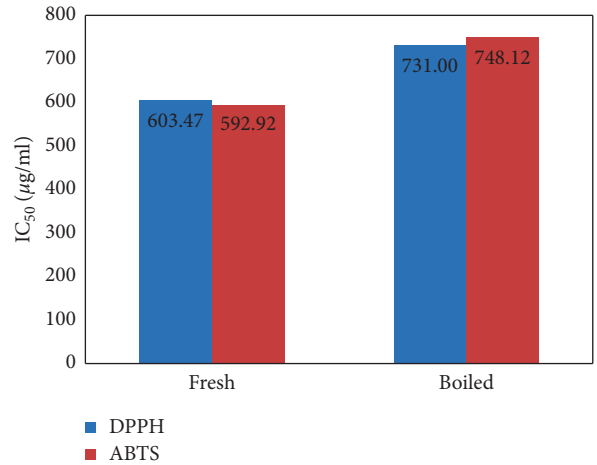

Figure 4: IC_{50} of the free-radical scavenging assay of extracts from fresh and boiled *W. globosa*.

However, the origin of a plant and the season of harvesting can affect the levels of minerals [30]. Generally, *W. globosa* is harvested in the rainy season. Thus, changes in the growth conditions, the harvest season, and the source or origin of the plants should all be studied to improve the plant materials and increase the potential of this plant to be a super food in the future.

3.3. Radical Scavenging Activity of the W. globosa Extract by DPPH and ABTS. The free-radical scavenging ability of freshly prepared and boiled samples of the *W. globosa* extract was tested using DPPH and ABTS assays. At a concentration of 1000 μg/milliliter, the fresh and boiled samples showed percentage inhibition of scavenging activity by DPPH at $75.77 \pm 0.93\%$ and $67.10 \pm 0.20\%$, respectively. By ABTS, the fresh and boiled samples showed percentage inhibition of scavenging activity of $70.40 \pm 7.20\%$ and $59.78 \pm 3.16\%$, respectively, at the same concentration. IC_{50} of the standard Trolox solution was $26.07 \pm 0.02\,\mu$M for DPPH and $21.05 \pm 0.07\,\mu$M for ABTS. Their IC_{50} is shown in Figure 4.

This result corresponded with a previous report that showed freshly prepared *W. globosa* extract had higher radical scavenging activity than boiled *W. globosa* extract [25]. The scavenging activity of *W. globosa* might be related to the amounts of the specific phytochemical constituents found in *W. globosa*. A previous study revealed that the total phenolic and beta-carotene contents of the boiled *W. globosa* extract were less than of the freshly prepared sample. This might be due to the effects of high temperature during boiling, which can cause degradation and loss of some phytochemical constituents. The antioxidant activity of *W. globosa* has previously been attributed to the phenolic compounds and flavonoids present in extracts [26]. Phenolic and flavonoid compounds have been reported to be associated with antioxidation activity in various plants [31–33]. The result of this study conformed to the study by Tipnee in 2017, which reported the anti-inflammatory and antioxidant activities were as a result from the phytosterols, carotenoids, and tocopherols. Moreover, the *W. globosa* extract was not toxic to the human fibroblast (HDFn) cells [26]. Antioxidant activities from these natural compounds might perform many mechanisms of action such as radical scavenging, chain breaking, and metal chelation. Several types of compounds found in the plant raw material might show synergistic effect. The phytochemical compounds found in this study were flavonoids, phenolics, anthocyanins, and carotenoids. Because different phytochemical constituents in this plant could show different mechanisms of action, further study about the other antioxidant tests should be carried out to get enough information about its activities. A few studies examined the phytochemical constituents of this plant. The phytochemical content could be used in the quality control aspect. This could be used to confirm the quality of raw material in different batches or different sources of the raw material. Moreover, a previous study revealed a moderate correlation between the potassium content of vegetables and their antioxidative activity, as determined by DPPH and ABTS radical scavenging assays [34]. Thus, the total active compounds and minerals found in *W. globosa* in the present study could be a key performance indicator for antioxidant activity of *W. globosa*. This study revealed some interesting aspects regarding to the value-added and sustainable food sources. The biodiversity of plants is related to the chemical constituent in the plant. Thus, knowledge about the quality control of the raw material will be the appropriate channel to improve the potential of this plant.

4. Conclusions

This study was an overall view of the phytochemical composition of *W. globosa* that included the determination of the total phenolic, flavonoid, and anthocyanin contents, the identification of potential biomarkers (beta-carotene, ferulic acid, luteolin 7-O-β-D-glucoside, and kaempferol), and the levels of selected minerals (iron, potassium, calcium, magnesium, zinc, and sodium), coupled with the evaluation of its radical scavenging activity. This plant exhibited free-radical scavenging activity that correlated with the beta-carotene, ferulic acid, luteolin- 7-O-β-D-glucoside, and kaempferol

phytochemical contents, all of which have been shown to have antioxidant activity. However, as this study covered only some antioxidant mechanisms, further investigation of other mechanisms is needed prove the efficiency and potential of this plant as a new promising source of nutraceutical compounds. The comparison among sample characteristics should be further investigated to confirm the content of minerals in the raw material.

Data Availability

The main part of the data is included within the content. Other datasets can be made available from the corresponding author upon request.

Conflicts of Interest

The authors declare that there are no conflicts of interest regarding the publication of this paper.

Acknowledgments

The authors thank Dr Glenn Borlace for English language assistance via the Khon Kaen University Publication Clinic and also thank Ms. Kingphai Buahom and Ms. Lalida Suttiart for their kind assistance. This work was financially supported by the Khon Kaen University, Thailand (Contract No. 591601).

References

[1] M. Busani, J. M. Patrick, H. Arnold, and M. Voster, "Nutritional characterization of Moringa (*Moringa oleifera* lam.) leaves," *African Journal of Biotechnology*, vol. 10, no. 60, pp. 12925–12933, 2011.

[2] V. Pakade, E. Cukrowska, and L. Chimuka, "Metal and flavonol contents of *Moringa oleifera* frown in South Africa," *South African Journal of Science*, vol. 109, no. 3/4, pp. 1–7, 2013.

[3] M. Udikala, Y. Verma, S. Sushma, and S. Lal, "Phytonutrient and pharmacological significance of *Moringa oleifera*," *International Journal of Life-Sciences Scientific Research*, vol. 3, no. 5, pp. 1387–1391, 2017.

[4] T. R. Mensah, M. Eklou-Lawson, E. H. Gbekley, S. D. Karou, Y. Ameyapoh, and C. A. deSouza, "Glycine max and *Moringa oleifera*: nutritional values, processing methods and mixed foods," *Journal de la Recherche Scientifique de l'Universite de Lome*, vol. 19, pp. 1–14, 2017.

[5] M. D. Awouafack, P. Tane, and H. Morita, *Isolation and Structure Characterization of Flavonoids, Flavonoids - from Biosynthesis to Human Health*, Intech Open, London, UK, 2017.

[6] M. A. Alam, A. S. Juraimi, M. Y. Rafii et al., "Evaluation of antioxidant compounds, antioxidant activities, and mineral composition of 13 collected purslane (*Portulaca oleracea* L.) accessions," *BioMed Research International*, vol. 2014, Article ID 296063, 10 pages, 2014.

[7] I. Peluso, A. Raguzzini, G. Catasta et al., "Effects of high consumption of vegetables on clinical, immunological, and antioxidant markers in subjects at risk of cardiovascular diseases," *Oxidative Medicine and Cellular Longevity*, vol. 2018, Article ID 5417165, 9 pages, 2018.

[8] A. I. O. Jideani, H. Silungwe, T. Takalani, A. O. Omolola, H. O. Udeh, and T. A. Anyasi, "Antioxidant-rich natural fruit and vegetable products and human health," *International Journal of Food Properties*, vol. 24, no. 1, pp. 41–67, 2021.

[9] D. J. Crawford, E. Landolt, D. H. Les, and R. T. Kimball, "Speciation in duckweeds (Lemnaceae): phylogenetic and ecological inferences," *Aliso*, vol. 22, no. 1, pp. 231–242, 2006.

[10] F. A. Bernard, J. M. Bernard, and P. Denny, "Flower structure, anatomy and Wolffia Australiana (Benth.) den Hartog&van der Plas," *Bulletin of the Torrey Botanical Club*, vol. 117, pp. 18–26, 1990.

[11] A. Kaplan, H. Zelicha, G. Tsaban et al., "Protein bioavailability of Wolffia globosa duckweed, a novel aquatic plant: a randomized controlled trial," *Clinical Nutrition*, vol. 38, no. 6, pp. 2576–2582, 2019.

[12] L. L. Rusoff, E. W. Blakeney, and D. D. Culley, "Duckweeds (Lemnaceae Family): a potential source of protein and amino acids," *Journal of Agricultural and Food Chemistry*, vol. 28, no. 4, pp. 848–850, 1980.

[13] G. H. Baek, M. Saeed, and H. K. Choi, "Duckweeds: their utilization, metabolites and cultivation," *Applied Biological Chemistry*, vol. 64, no. 1, p. 73, 2021.

[14] H. Zelicha, A. Kaplan, A. Yaskolka Meir et al., "The effect of Wolffia globosa mankai, a green aquatic plant, on postprandial glycemic response: a randomized crossover-controlled trial," *Diabetes Care*, vol. 42, no. 7, pp. 1162–1169, 2019.

[15] I. Sela, A. Yaskolka Meir, A. Brandis et al., "Wolffia globosa-mankai plant-based protein contains bioactive vitamin B12 and is well absorbed in humans," *Nutrients*, vol. 12, no. 10, p. 3067, 2020.

[16] A. Yaskolka Meir, G. Tsaban, H. Zelicha et al., "A green-mediterranean diet, supplemented with mankai duckweed, preserves iron-homeostasis in humans and is efficient in reversal of anemia in rats," *Journal of Nutrition*, vol. 149, no. 6, pp. 1004–1011, 2019.

[17] V. L. Singleton and J. A. Rossi, "Colorimetry of total phenolics with phosphomolybdic-phosphotungstic acid reagents," *American Journal of Enology and Viticulture*, vol. 16, pp. 144–158, 1965.

[18] N. Ngamkhae, O. Monthakantirat, Y. Chulikhit et al., "Optimized extraction method for Kleeb Bua Daeng formula with the aid of the experimental design," *Journal of Chemistry*, vol. 2021, Article ID 1457729, 10 pages, 2021.

[19] C. C. Chang, M. H. Yang, H. M. Wen, and J. C. Chern, "Estimation of total flavonoid content in propolis by two complementary colometric methods," *Journal of Food and Drug Analysis*, vol. 10, no. 3, pp. 178–182, 2020.

[20] J. Lee, R. W. Durst, R. E. Wrolstad et al., "Determination of total monomeric anthocyanin pigment content of fruit juices, beverages, natural colorants, and wines by the pH differential method: collaborative study," *Journal of AOAC International*, vol. 88, no. 5, pp. 1269–1278, 2005.

[21] C. Khamphukdee, Y. Chulikhit, O. Monthakantirat, J. Maneenet, C. Boonyarat, and S. Daodee, "Phytochemical constituents and antioxidative activity of schleichera oleosa fruit," *Tropical Journal of Natural Product Research*, vol. 5, no. 8, pp. 1445–1449, 2021.

[22] S. Daodee, O. Monthakantirat, K. Ruengwinitwong et al., "Effects of the ethanol extract of dipterocarpus alatus leaf on the unpredictable chronic mild stress-induced depression in ICR mice and its possible mechanism of action," *Molecules*, vol. 24, no. 18, p. 15, 2019.

[23] J. Maneenet, S. Daodee, O. Monthakantirat et al., "Kleeb bua daeng, a Thai traditional herbal formula, ameliorated unpredictable chronic mild stress-induced cognitive impairment in ICR mice," *Molecules*, vol. 24, no. 24, pp. 4587–4616, 2019.

[24] R. Apak, M. Özyürek, K. Güçlü, and E. Çapanoğlu, "Antioxidant activity/capacity measurement 1 classification, physicochemical principles, mechanisms, and electron transfer (ET)-based assays," *Journal of Agricultural and Food Chemistry*, vol. 64, no. 5, pp. 997–1027, 2016.

[25] W. Saengthongpinit, B. Sricharoen, and M Krangpreecha, "Effect of blanching in sodium chloride solution on phenolic content and antioxidant activity of water meal (Wolffia globosa)," in *Proceedingsof the 55th KU Annual Conference*, Bangkok, Thailand, 2017January.

[26] S. Tipnee, A. Jutiviboonsuk, and P. Wongtrakul, "The bioactivity study of active compounds in Wolffia globosa extract for an alternative source of bioactive substances," *Cosmetics*, vol. 4, no. 4, pp. 53–10, 2017.

[27] J. Y. Dong, P. Xun, K. He, and L. Q. Qin, "Magnesium intake and risk of type 2 diabetes: meta-analysis of perspective cohort studies," *Diabetes Care*, vol. 34, no. 9, pp. 2116–2122, 2011.

[28] F. H. Nielsen, "Effects of magnesium depletion on inflammation in chronic disease," *Current Opinion in Clinical Nutrition and Metabolic Care*, vol. 17, no. 6, pp. 525–530, 2014.

[29] S. H. Jung, Y. K. Seo, M. Y. Youn, C. S. Park, K. Y. Song, and J. K. Park, "Anti-aging and anti-inflammation effects of natural mineral extract on skin keratinocytes," *Biotechnology and Bioprocess Engineering*, vol. 14, no. 6, pp. 861–868, 2009.

[30] M. Grembecka and P. Szefer, "Evaluation of honeys and beeproducts quality based on their mineral composition using multivariate techniques," *Environmental Monitoring and Assessment*, vol. 185, no. 5, pp. 4033–4047, 2013.

[31] C. A. Manach, A. Scalbert, C. C. Morand, C. Rémésy, and L. Jiménez, "Polyphenols: food sources and bioavailability," *The American Journal of Clinical Nutrition*, vol. 79, no. 5, pp. 727–747, 2004.

[32] C. A. Rice-Evans, N. J. Miller, and G. Paganga, "Structure-antioxidant activity relationships of flavonoids and phenolic acids," *Free Radical Biology and Medicine*, vol. 20, no. 7, pp. 933–956, 1996.

[33] M. López-Vélez, F. Martínez-Martínez, and C. D. Valle-Ribes, "The study of phenolic compounds as natural antioxidants in wine," *Critical Reviews in Food Science and Nutrition*, vol. 43, no. 2, pp. 233–244, 2003.

[34] C. Tamuly, B. Saikia, M. Hazarika, J. Bora, M. J. Bordoloi, and O. P. Sahu, "Correlation between phenolic, flavonoid, and mineral contents with antioxidant activity of underutilized vegetables," *International Journal of Vegetable Science*, vol. 19, no. 1, pp. 34–44, 2013.

Hindawi
Journal of Chemistry
Volume 2022, Article ID 8581515, 9 pages
https://doi.org/10.1155/2022/8581515

Research Article

An Improved Method of Theabrownins Extraction and Detection in Six Major Types of Tea (*Camellia sinensis*)

Tzan-Chain Lee,[1,2] **Qian-Nan Zang**,[1] **Kuan-Hung Lin**,[3] **Hua-Lian Hu**,[1] **Ping-Yuan Lu**,[1] **Jing-Yao Zhang**,[1] **Chun-Qin Kang**,[1] **Yan-Jie Li**,[4] **and Tzu-Hsing Ko**[5]

[1]*Department of Tea Science, Anxi College of Tea Sciences, Fujian Agriculture and Forestry University, Fuzhou 350002, China*
[2]*Department of Foods and Pharmaceutical Engineering, Wuzhou University, Wuzhou 543002, Guangxi, China*
[3]*Faculty of Applied Sciences, Ton Duc Thang University, Ho Chi Minh 700000, Vietnam*
[4]*Department of Horticulture, Guangxi University, Nanning 530004, Guangxi, China*
[5]*Fujian Provincial University Key Laboratory of Green Energy and Environment Catalysts, College of Chemistry and Materials, Ningde Normal University, Ningde, Fujian 352100, China*

Correspondence should be addressed to Tzu-Hsing Ko; hsingko@gmail.com

Received 13 July 2022; Revised 17 August 2022; Accepted 20 August 2022; Published 27 September 2022

Academic Editor: Marwa Fayed

Tea pigments consisting of theabrownins (TBs), theaflavins (TFs), and thearubigins (TRs) affect the color and taste of tea. TBs include a variety of water-soluble compounds, but do not dissolve in n-butanol and ethyl acetate. Previously, the traditional method of TB extraction only mixed tea with n-butanol, and TBs were retained in the water phase. However, without ethyl acetate extraction, TFs and TRs remained in the water phase and affected the detection of TB content. Although an improved method had been devised by adding an ethyl acetate extraction step between tea production and n-butanol extraction, the proportional equation for calculating TB content (%) was not yet developed. In this study, we compared the absorbance at 380 nm (A_{380}) of TB solutions from six major types of tea (green, yellow, oolong, white, black, and dark teas) extracted by improved and traditional methods from the same tea samples. Significantly lower A_{380} values were obtained from TB solutions via the improved method compared to the traditional method for six major types of tea, and the highest and lowest slops in TB concentrations from A_{380} analyses were from dark tea and green tea, respectively. Moreover, newly developed equations for TB content in those six tea types extracted by the improved methods were also established.

1. Introduction

Tea is either prepared by infusion or decoction of *Camellia sinensis* dried leaves, which are classified into six major types (green, oolong (or cyan), black, white, yellow, and dark) based on the manufacturing process. Both black and oolong teas are two kinds of aerated tea leaves. After plucking, these fresh leaves are processed by withering, rolling, aeration, and then inactivation by drying (Figure 1(a)). During the aeration process, polyphenols are oxidized by endogenous enzymes such as polyphenol oxidase and peroxidase, thus producing many oxidative compounds. Polyphenol oxidation results in the pigment's dynamic transition into tea pigments that include TFs, TRs, and TBs [1, 2]. The relationship among TFs, TRs, and TBs is shown in Supplementary Figure 1. The transition induces color changes in tea leaves ranging from green to red brown [3]. All the pigments affect the color and flavor of liquid tea [3–7]. TBs give tea leaves a brown color and can be formed by TFs or TRs oxidation or polyphenol aggregation with other sugars and acidic compounds [8, 9]. The leaves of oolong tea are green with red edges (Figure 1(b)III) due to the formation and accumulation of oxidized polyphenols from leaf margins during the aeration process. As the aeration period proceeds, the surfaces of all tea leaves become reddish brown (Figure 1(b)I) and black tea leaves are produced. Therefore,

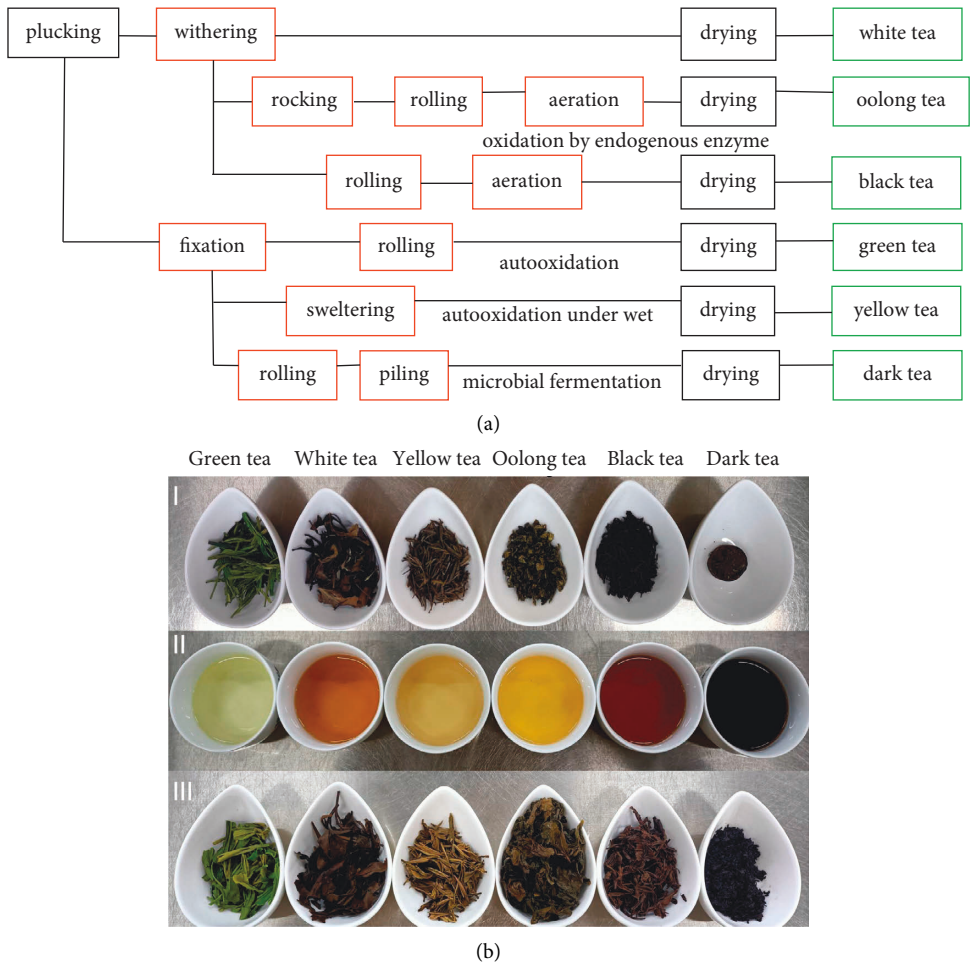

FIGURE 1: Manufacture processes of six major types of tea (a) and the dried leaves (b) (I), tea soups (b-II), and tea leaves after imbibed with hot water at 90°C (b-III) of six major types of tea.

oolong tea is "semioxidized" tea, and black tea is "fully oxidized" tea [10]. White tea is obtained by only withering and drying, as more prolonged withering leads to a severe water deficiency that induces membrane disintegration and polyphenol oxidization by endogenous enzymes. In addition, white tea can be stored for a long time, during which chemical reactions such as catechin and amino acid oxidation can occur that induce better flavor and taste (more sweetness and smoothness) and more health benefits [11–13].

The objective of our study was to "improve" (Figure 2) the abovementioned "traditional" method by adding an ethyl acetate extraction step between liquid tea production and n-butanol extraction. Moreover, our method's new equations for the TB content (%) of the six major types of tea extraction had different absorbance values at 380 nm (A_{380}) and slope compared to black tea analyses by the traditional method.

2. Materials and Methods

2.1. Samples. The six major types of tea samples obtained are listed in Table 1. All were purchased from local tea markets located in Anxi, Fujian Province, Dali, Yunnan Province, and Chongqing City, China. Each tea sample was ground into tea powder using a grinder (Joyoung Co., Shandong, China) and then stored in sealed cans until analysis.

2.2. Preparation of Liquid Tea Samples. Boiling distilled and deionized water (d.d. H_2O; 125 mL) was added to 3.0 grams of tea powder in a 250 mL conical flask and shaken in a water bath at 90°C for 10 min. The liquid tea was then centrifuged at 1,800 × *g* for 10 min at 4°C. The supernatant was diluted to 125 mL with d.d. H_2O and then divided into two aliquots, one for TB extraction by the traditional method and the other by our improved method (Figure 2).

2.3. TB Extraction. The traditional method was based on Yao et al. [33] and Roberts and Smith [35, 36], with a few modifications. Briefly, 25 mL of tea solution was extracted with the same volume of *n*-butanol (Xilong Scientific Co., Guangdong, China) and shaken for 3 min. The lower layer of the solution was then centrifuged at 1,800 × g for 10 min at 4°C. Two mL of the supernatant was then mixed with 2 mL of saturated (10.2%) oxalic acid (SINOPHARM Co., Shanghai,

China) and 6 mL of d.d. H_2O was then added, followed by dilution to 25 mL with 95% (v/v) ethanol (SINOPHARM Co., Shanghai, China). A_{380} values of the above solutions were measured using a UV-1750 spectrophotometer (Shimadzu, Japan), and 95% (v/v) ethanol was used as a blank. TB content (%) = $[7.06 \times 2 \times A_{380} \times 100\%]/ [w \times 1/3 \times (1\text{-M})] = [21.18 \times 2 \times A_{380} \times 100\%]/w \times (1\text{-M})$, where "$w$" is the weight (gram) of the tea sample, "M" is the moisture content (%) of the tea sample, and 21.18 is the inverse slope of A_{380}.

The improved method with TB concentrations from TB extracted samples was modified from the abovementioned traditional method. Mainly, 35 mL of ethyl acetate (SINOPHARM Co., Shanghai, China) was added to samples of the six tea types (35 mL) in a 125 mL separating funnel and shaken for 3 min. After discarding the upper layer, the lower layer (25 mL) was then extracted with 25 mL of *n*-butanol (Xilong Scientific Co., Guangdong, China) and shaken for 3 min; the lower layer solution was used for centrifugation at 1,800 × g for 10 min at 4°C. The A_{380} detections of the solutions were done the same way as in the abovementioned traditional method, and TB contents (%) were determined by the six equations for the improved method. TB in the six tea types was extracted by the improved method and then freeze-dried. Freeze-dried samples were dissolved in d.d. H_2O, various concentrations of TB solution (2 mL) were mixed with 2 mL of saturated oxalic acid, 6 mL of d.d. H_2O was added, and the samples were then diluted to 25 mL with 95% (v/v) ethanol. Samples were then measured at A_{380}.

2.4. Moisture. Moisture in the tea powder was measured using a vacuum oven according to an international standard method (ISO1573 (BS6049-2), 1980).

2.5. Data Analysis. Paired data with A_{380} values of both traditional and improved methods were subjected to paired *t*-tests using Microsoft Excel 2019. TB contents (%) are presented as mean values ± standard deviations (SD) of twelve independent sets of experiments with similar results. Paired *t*-tests were calculated with high significance at $p \leq 0.01$using SPSS version 23.0 (SPSS, Chicago, USA). Linear equations were established by regression analysis between A_{380} measurements and TB concentrations of the six tea types using SigmaPlot ver. 12.5 (SYSTAT Software, San Jose, CA).

3. Results and Discussion

3.1. Comparisons of TB Extractions between Traditional and Improved Methods. Figure 3 illustrates A_{380} values from TB solutions extracted by traditional and improved methods. Readings from the improved method were significantly lower (around 80–90%) compared to the traditional method in all six tea types, indicating that ethyl acetate extraction removes TFs and portions of TRs from liquid tea [33] and decreases TB A_{380} values. TB compositions were different between these extraction methods, and revised parameters for the improved method should therefore be established.

After plucking, yellow, green, and dark tea leaves are first fixed by steaming or pan-frying (Figure 1(a)) to inactivate all endogenous enzymes. Green tea is produced after rolling and drying. Yellow tea is obtained when tea leaves are kept wet and under high temperatures for 6 to 12 h (Figure 1(a)) between fixing and drying, during which chlorophylls are degraded and polyphenols are auto-oxidized. Dark tea is harvested after leaves have been kept wet and microorganisms grow on their surfaces for many days between fixing and drying (Figure 1(a)). During this piling process, microbes (mainly *Aspergillus fumigatus*, *Aspergillus Niger,* and *Saccharomyces cerevisiae*) secrete many enzymes to induce polyphenol oxidation, cell wall degradation, and fermentation [14–17]. TB content increases during dark tea processing [18], and the leaves become dark brown (Figure 1(b)).

Similar plant secondary metabolites can reduce the risk of age-related chronic diseases and promote health benefits [19, 20]. TBs have physiological functions such as reducing blood lipid and blood sugar levels [21–23]; controlling of diabetes mellitus [24]; attenuation of hypercholesterolemia [25, 26]; reducing serum levels of total cholesterol, low-density cholesterol, and triglycerides [27]; and osteoclastogenesis suppression and prevention of bone loss [28], together with inhibition of cell cycling and tumor cell growth [29]. In addition, TB content is a positive parameter in evaluating fragrance and flavor in dark tea and white tea [9, 18, 30, 31]. Zhu et al. [32] and Cheng et al. [18] reported that stringent taste levels were decreased and stale and fungal aromas increased with TB content. Furthermore, dark tea and white tea leaves can be stored for a long time, and longer storage times result in higher TB content [14]. In contrast, during storage, an increased TB content worsens tea quality in both black tea and oolong tea due to the loss of aroma and sweetness molecules [5, 7, 33]. Therefore, TB content may be an objective measure of tea quality [34]. Yao et al. [33] combined three methods [35–37] to analyze TF, TR, and TB contents and constructed a "traditional" method of TB extraction (Figure 2). However, TBs are defined as a variety of water-soluble compounds but are not dissolved in n-butanol and ethyl acetate [22, 27]. In the traditional method, without ethyl acetate extraction, TFs or TRs would be retained in the TB layer solution and thus affect the accuracy of TB content analysis, because A_{380} is detected from TF, TR, and TB solutions. In addition, the TB equation was based on black tea samples extracted from the traditional method [33, 35, 36]. Whether the slop parameter of the black tea equation is the same as other types of tea remains unknown.

3.2. Equations Established for the Improved Method. The traditional method's empirical equation for determining TB content (%) is $[21.18 \times 2 \times A_{380} \times 100\%]/w$ (1-M), where "w" stands for the weight (in grams) of tea sample powder and 21.18 is the inverse slope of A_{380} based on black tea [33, 35, 36]. In our study, six major types of tea were extracted by the improved method, their solutions were freeze-dried, and TB powder was collected. After TB

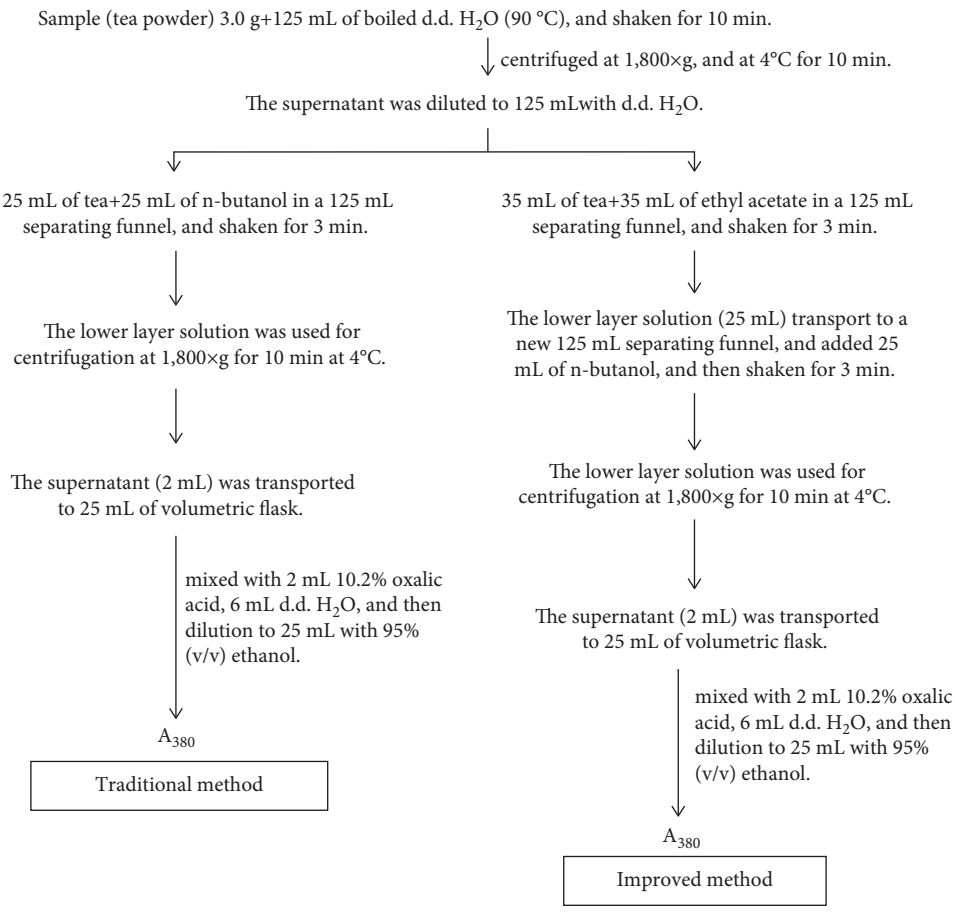

Figure 2: Flow chart of the traditional and improved methods of TB extractions.

Table 1: List of six major types of tea sample and producing location.

Type of tea	Tea sample and producing location
Black tea	Lapsang Souchong, produced in Fujian province, China Yunnan black tea, produced in Yunnan province, China
Oolong tea	Wuyi Dahongpao, produced in Fujian province, China Anxi Tieguanyin, produced in Fujian province, China
Dark tea	Ripened Pu-Erh teas, produced in Yunnan province, China, storage for 4 years Ripened Pu-Erh caked tea, produced in Yunnan province, China, storage for 4 years
White tea	Gong Mei, produced in Fujian province, China, storage for 4 years Baimudan, produced in Fujian province, China, storage for 4 years
Yellow tea	Huoshan Huangya, produced in Anhui province, China
Green tea	Longjing, produced in Zhejiang province, China Jinyun Maofeng, produced in Chongqing city, China

powders were dissolved in d.d. H_2O, different A_{380} values were observed from the samples. Figure 4 shows that A_{380} values were significantly ($p < 0.0001$) and positively correlated with the TB concentrations of green tea ($r = 0.9963$, $R^2 = 0.9926$), yellow tea ($r = 0.9961$, $R^2 = 0.9922$), oolong tea ($r = 0.9977$, $R^2 = 0.9954$), black tea ($r = 0.9987$, $R^2 = 0.9975$), white tea ($r = 0.9973$, $R^2 = 0.9947$), and dark tea ($r = 0.9975$, $R^2 = 0.9950$). Regression equation slopes for dark tea, white tea, black tea, oolong tea, yellow tea, and green tea were 0.0704, 0.0475, 0.0381, 0.0350, 0.0166, and 0.0160, respectively. Furthermore, the inverse slopes of dark tea, white tea, black tea, oolong tea, yellow tea, and green tea were 14.205, 21.053, 26.247, 28.571, 60.241, and 62.5, respectively. The equations for the six tea types using the improved method were as follows: dark tea:

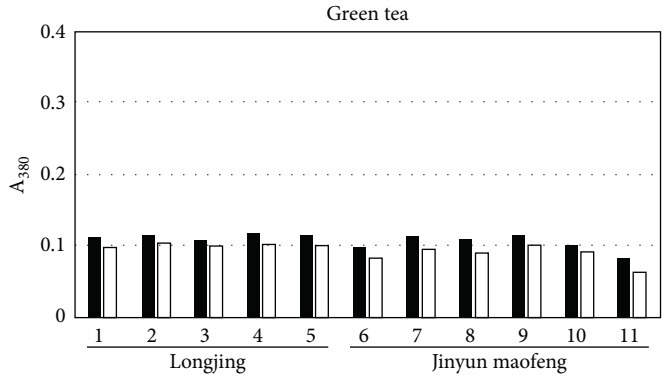

(a)

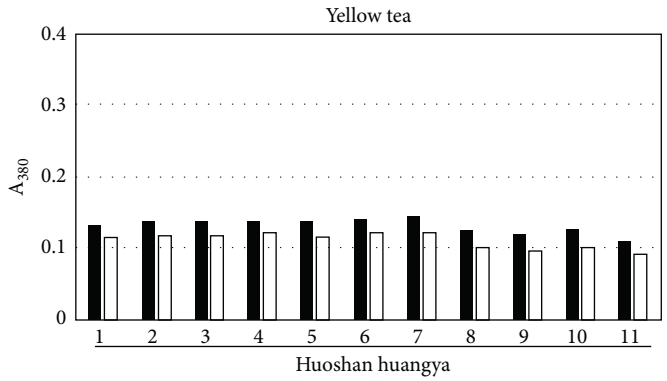

(b)

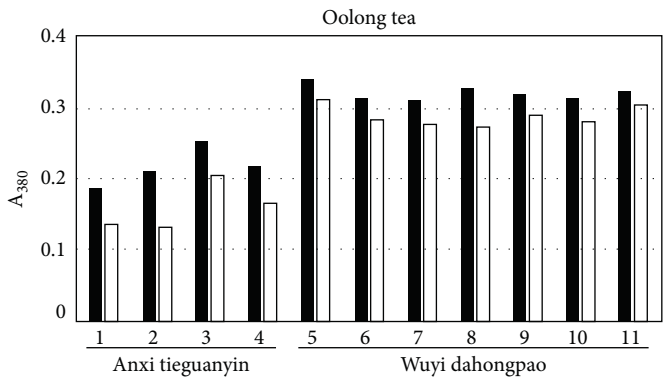

(c)

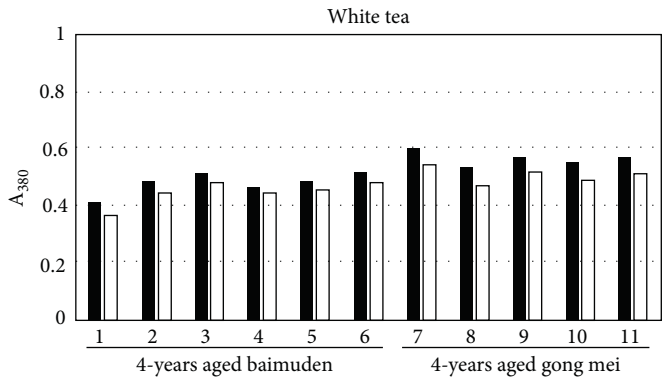

(d)

Figure 3: Continued.

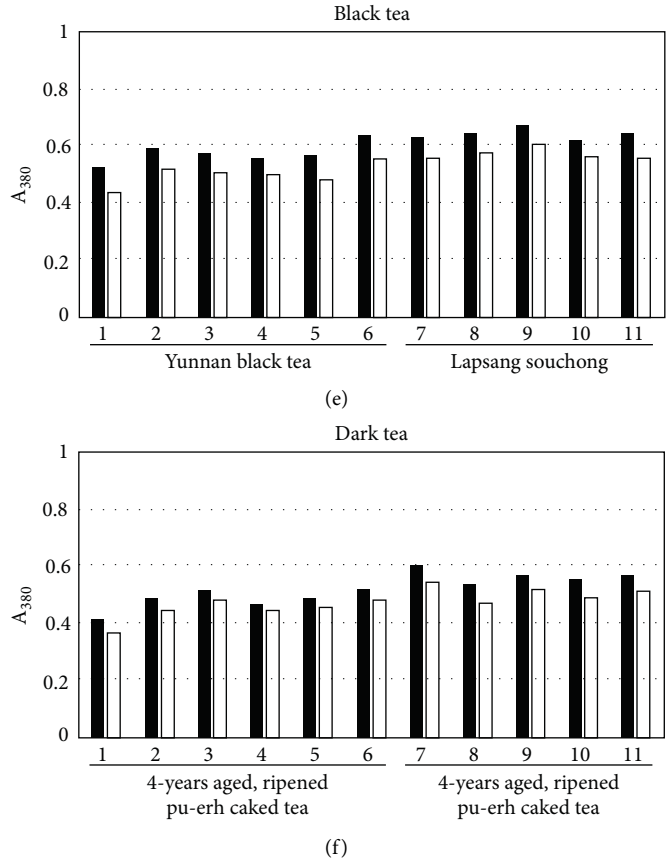

FIGURE 3: Comparisons of A_{380} values with TB extractions by the traditional method (black bar) and the improved method (white bar) of six major types of tea: green tea (a), yellow tea (b), oolong tea (c), white tea (d), black tea (e), and dark tea (f). Test numbers of tea samples (1~11) in each major type of tea: (a) 1–5, Longjing, and 6–11, Jinyun Maofeng in green tea. (b) 1–11, Huoshan Huangya in yellow tea. (c) 1–4, Anxi Tieguanyin, and 5–11, Wuyi Dahongpao in oolong tea. (d) 1–6, four-years-old Baimudan, and 7–11, four-years-old Gong-Mei white tea. (e) 1–6, Yunnan black tea, and 7–11, Lapsang Souchong black tea. (f) 1–6, four-years-old, ripened Pu-Erh teas, and 7–11, four-years-old, ripened Pu-Erh caked dark tea.

$[14.205 \times 2 \times A_{380} \times 100\%]/w \times (1\text{-M})$, white tea: $[21.053 \times A_{380} \times 100\%]/w \times (1\text{-M})$, black tea: $[26.247 \times 2 \times A_{380} \times 100\%]/w \times (1\text{-M})$, oolong tea: $[28.571 \times 2 \times A_{380} \times 100\%]/w \times (1\text{-M})$, yellow tea: $[60.241 \times 2 \times A_{380} \times 100\%]/w \times (1\text{-M})$, and green tea: $[62.5 \times 2 \times A_{380} \times 100\%]/w \times (1\text{-M})$.

In those empirical equations, "M" means the tea sample's moisture content (%) and "w" stands for the weight (in grams) of tea sample powder. Figure 4 shows that two types of aerated tea (black tea and oolong tea) had similar variations, but green tea and yellow tea almost completely overlapped, indicating that the TB compositions were similar in these two types of tea. Wang et al. [38] demonstrated that green tea and yellow tea had similar chemical components according to metabolome analysis. After high-temperature treatments in fixation and drying processes during storage, isomer flavanols and chlorophyll metabolites (e.g., pheophytins) were produced in the autooxidation process, and the color of tea leaves turned olive brown [39–43]. The slope of white tea was higher than that of black tea and lower than that of dark tea (Figure 4), implying that the TB composition in white tea is notably different from that in dark tea and black tea. Although liquid chromatography-mass spectrometry analysis was used to determine the chemical composition in white tea after long-term storage [11, 12, 44], the TB composition still remained unknown. In addition, the TB of dark tea contains some fungi-specific metabolites detected by gas chromatography-mass spectrometry or liquid chromatography-mass spectrometry-based metabolomics [18, 23, 32, 45–49].

3.3. Comparison of TB Content between Traditional and Improved Methods in Tea Extractions. TBs were extracted by both traditional and improved methods, and calculations were made with appropriate equations at A_{380}. Figure 5 shows that the TB contents of these two methods were significantly different ($p < 0.01$) in all types of liquid teas.

We repeated many studies by using the traditional extraction method and found that dark tea had the highest TB content (10%~14%) of the six tea types [14, 15, 50, 51], followed by black tea (7%~9%) [14, 50, 52], and ranges of 2%~3.5% in green tea and yellow tea [50, 52]. The improved method showed that black tea had the highest TB content (7.97%~11.19%, average 9.75%), and oolong tea ranged

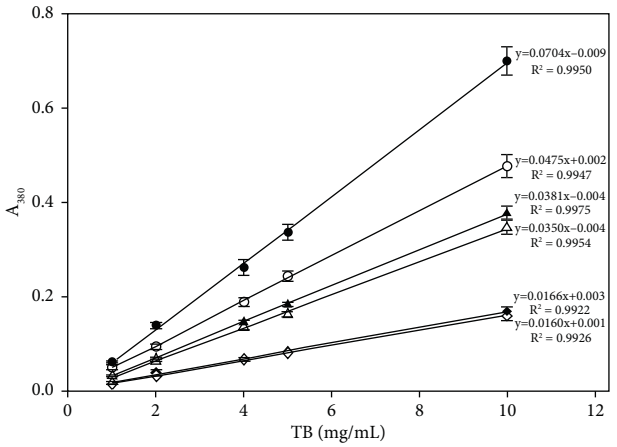

FIGURE 4: The A_{380} variations of TB concentrations extracted by the improved method from six major types of tea (◇: green tea, ◆: yellow tea, △: oolong tea, ▲: black tea, ○: white tea, and ●: dark tea). Linear equations were established by regression analysis of linear relationships between TB concentrations and A_{380} measurements. Each data point represents the mean ± SD of three independent measurements.

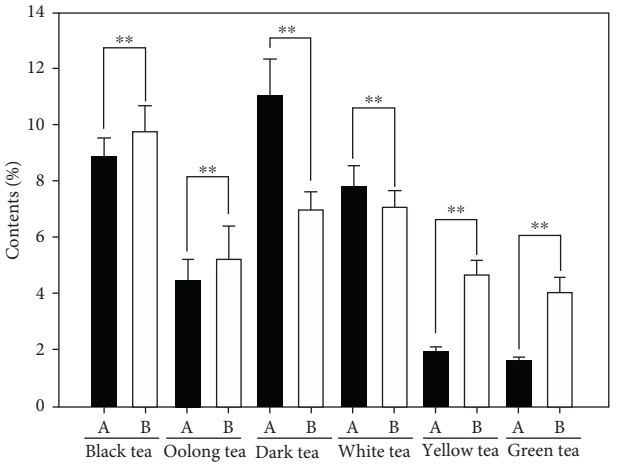

FIGURE 5: Paired comparisons of TB contents (%) of six major types of tea extracts between the traditional method (a) and improved method (b). Each bar represents the mean ± SD of twelve independent measurements. Asterisk (∗ ∗) indicates high significance at $p \leq 0.01$.

2.65%~6.23% with an average of 5.25%. Black tea and oolong tea were oxidized by endogenous enzymes in a longer aeration process and had higher TB contents. The TB contents of white tea ranged from 5.35% to 8.02%, averaging 7.03%, suggesting that four years of storage was sufficient to transfer high levels of TB content in the leaves. The TB contents of dark tea ranged from 5.66 to 7.66%, averaging 6.96%, while green tea and yellow tea ranged from 2.63 to 4.46% with an average of 4.03% and 3.87 to 5.2% with an average of 4.61%, respectively, indicating that their values differed significantly from levels derived from the traditional extraction method. Dark tea had the highest A_{380} of the six tea types (Figure 3); however, high slop in TB concentrations (Figure 4) resulted in TB content not being as high as with the traditional method (Figure 5). TB composition is formed during tea processing, and the aeration procedure is one of the most important steps in black tea and oolong tea processing, while it does not occur in other teas. Therefore, different equations are proposed to calculate TB content in different types of tea, especially dark tea, yellow tea, and green tea.

4. Conclusion

This study provided an improved method for the analysis of TB content (%) from six major types of tea. This method decreases the A_{380} values of TBs with differing TB absorbance capabilities in six major types of tea. Six equations have been developed to analyze TB content (%) in those six tea types extracted by an improved method, and the ranges of TB content (%) showed significant differences compared to the traditional method.

Abbreviations

SD: Standard deviation

Data Availability

The data used to support this study are available from the corresponding author upon request.

Conflicts of Interest

The authors declare that there are no conflicts of interest regarding the publication of this article.

Authors' Contributions

T-C L. designed the experiments; T-C L. and Q-N Z. collected the sample, conducted experiments, and analyzed the data. T-C L. and K-H L. wrote the article; T-C L., Q-N Z., H-L H., P-Y L., J-Y Z., C- K., and Y-J L. collected the sample and investigated the study; T-H Ko projected-ministration and reviewed and edited the manuscript.

Acknowledgments

This work was supported by the Starting Research Fund from the Fujian Agriculture and Forestry University (KXR19001), and the Starting Research Fund from the Wuzhou University (WZUQDJJ30173).

Supplementary Materials

Supplementary Figure 1: the simplified scheme of relationship among TF, TR, and TB. (*Supplementary Materials*)

References

[1] E. Haslam, "Thoughts on thearubigins," *Phytochemistry*, vol. 64, pp. 61–73, 2003.

[2] G. S. Gill, A. Kumar, and R. Agarwal, "Monitoring and grading of tea by computer vision–a review," *Journal of Food Engineering*, vol. 106, pp. 13–19, 2011.

[3] C. Dong, G. Liang, B. Hu et al., "Prediction of congou black tea fermentation quality indices from color features using non-linear regression methods," *Scientific Reports*, vol. 8, Article ID 10535, 2018.

[4] M. Obanda, P. Okinda O, and R. Mang'Oka, "Changes in the chemical and sensory quality parameters of black tea due to variations of fermentation time and temperature," *Food Chemistry*, vol. 75, no. 4, pp. 395–404, 2001.

[5] M. Obanda, P. O. Owuor, R. Mang'oka, and M. M. Kavoi, "Changes in thearubigin fractions and theaflavin levels due to variations in processing conditions and their influence on black tea liquor brightness and total colour," *Food Chemistry*, vol. 85, no. 2, pp. 163–173, 2004.

[6] M. Cavia-Saiz, M. D. Busto, M. C. Pilar-Izquierdo, N. Ortega, M. Perez-Mateos, and P. Muñiz, "Antioxidant properties, radical scavenging activity and biomolecule protection capacity of flavonoid naringenin and its glycoside naringin, a comparative study," *Journal of the Science of Food and Agriculture*, vol. 90, no. 7, pp. 1238–1244, 2010.

[7] K. Wang, Q. Chen, Y. Lin, and Z. Liu, "Comparison of phenolic compounds and taste of Chinese black tea," *Food Science and Technology Research*, vol. 20, no. 3, pp. 639–646, 2014.

[8] J. T. Dwyer and J. Peterson, "Tea and flavonoids: where we are, where to go next," *The American Journal of Clinical Nutrition*, vol. 98, no. 6, pp. 1611S–1618S, 2013.

[9] Q. P. Wang, J. S. Gong, Y. Chisti, and S. Sirisansaneeyakul, "Production of theabrownins using a crude fungal enzyme concentrate," *Journal of Biotechnology*, vol. 231, pp. 250–259, 2016.

[10] Q. Zhang, J. Ruan, B. Caballero, P. M. Finglas, and F. Toldrá, "Tea: analysis and tasting," in *Encyclopedia of Food and Health*Academic Press, Oxford, U K, 2016.

[11] J. M. Ning, D. Ding, Y. S. Song, Z. Z. Zhang, X. Luo, and X. C. Wang, "Chemical constituents analysis of white tea of different qualities and different storage times," *European Food Research and Technology*, vol. 242, pp. 2093–2104, 2016.

[12] D. Qi, A. Miao, J. Cao et al., "Study on the effects of rapid aging technology on the aroma quality of white tea using GC-MS combined with chemometrics: in comparison with natural aged and fresh white tea," *Food Chemistry*, vol. 265, pp. 189–199, 2018.

[13] F. Y. Fan, C. S. Huang, Y. L. Tong et al., "Widely targeted metabolomics analysis of white peony teas with different storage time and association with sensory attributes," *Food Chemistry*, vol. 362, Article ID 130257, 2021.

[14] Q. Wang, C. Peng, and J. Gong, "Effects of enzymatic action on the formation of theabrownin during solid state fermentation of Pu-erh tea," *Journal of the Science of Food and Agriculture*, vol. 91, no. 13, pp. 2412–2418, 2011.

[15] W. N. Wang, L. Zhang, S. Wang et al., "8-C N-ethyl-2-pyrrolidinone substituted flavan-3-ols as the marker compounds of Chinese dark teas formed in the post-fermentation process provide significant antioxidative activity," *Food Chemistry*, vol. 152, pp. 539–545, 2014.

[16] D. Haas, B. Pfeifer, C. Reiterich, R. Partenheimer, B. Reck, and W. Buzina, "Identification and quantification of fungi and mycotoxins from Pu-erh tea," *International Journal of Food Microbiology*, vol. 166, no. 2, pp. 316–322, 2013.

[17] Z. J. Zhao, H. R. Tong, L. Zhou, E. X. Wang, and Q. J. Liu, "Fungal colonization of Pu-erh tea in Yunnan," *Journal of Food Safety*, vol. 30, no. 4, pp. 769–784, 2010.

[18] L. Cheng, Q. Yang, Z. Chen et al., "Distinct changes of metabolic profile and sensory quality during qingzhuan tea processing revealed by LC-MS-based metabolomics," *Journal of Agricultural and Food Chemistry*, vol. 68, no. 17, pp. 4955–4965, 2020.

[19] I. Shah, M. A. Shah, M. A. Nawaz et al., "Analysis of other phenolics (capsaicin, gingerol and alkylresorcinols)," *Recent Advances in Natural Products Analysis*, Elsevier, Amsterdam, Netherland, 2020.

[20] M. Bule, I. A. Issa, F. Khan et al., "Development of new food products based on phytonutrients," *Phytonutrients in Food from Traditional to Rational Usage*, Woodhead Publishing, Cambridge, UK, 2020.

[21] R. A. Anderson and M. M. Polansky, "Tea enhances insulin activity," *Journal of Agricultural and Food Chemistry*, vol. 50, no. 24, pp. 7182–7186, 2002.

[22] J. S. Gong, C. X. Peng, T. Chen, B. Gao, and H. J. Zhou, "Effects of theabrownin from Pu-erh tea on the metabolism of serum lipids in rats: mechanism of action," *Journal of Food Science*, vol. 75, no. 6, pp. H182–H189, 2010.

[23] Y. Xiao, M. Li, Y. Wu, K. Zhong, and H. Gao, "Structural characteristics and hypolipidemic activity of theabrownins from dark tea fermented by single species *Eurotium cristatum* PW-1," *Biomolecules*, vol. 10, no. 2, Pub. ID. 204, 2020.

[24] S. Culas, R. A. U. J. Marapana, I. R. Palangasinghe, and A. C. Liyanage, "Development of liquid-based tea and its antidiabetic effect," *Journal of Chemistry*, vol. 20216 pages, Article ID 8863936, 2021.

[25] Y. Hou, W. F. Shao, R. Xiao et al., "Pu-erh tea aqueous extracts lower atherosclerotic risk factors in a rat hyperlipidemia model," *Experimental Gerontology*, vol. 44, no. 6-7, pp. 434–439, 2009.

[26] F. Huang, X. Zheng, X. Ma et al., "Theabrownin from Pu-erh tea attenuates hypercholesterolemia via modulation of gut microbiota and bile acid metabolism," *Nature Communications*, vol. 10, no. 1, Pub. ID. 4971, 2019.

[27] C. X. Peng, Q. P. Wang, H. R. Liu, B. Gao, J. Sheng, and J. S. Gong, "Effects of Zijuan pu-erh tea theabrownin on metabolites in hyperlipidemic rat feces by Py-GC/MS," *Journal of Analytical and Applied Pyrolysis*, vol. 104, pp. 226–233, 2013.

[28] T. Liu, Z. Xiang, F. Chen et al., "Theabrownin suppresses in vitro osteoclastogenesis and prevents bone loss in ovariectomized rats," *Biomedicine & Pharmacotherapy*, vol. 106, pp. 1339–1347, 2018.

[29] L. Zhou, F. Wu, W. Jin et al., "Theabrownin inhibits cell cycle progression and tumor growth of lung carcinoma through c-myc-related mechanism," *Frontiers in Pharmacology*, vol. 8 Pub. ID. 75, 2017.

[30] P. O. Owuor and M. Obanda, "The use of green tea (*Camellia sinensis*) leaf flavan-3-ol composition in predicting plain black tea quality potential," *Food Chemistry*, vol. 100, no. 3, pp. 873–884, 2007.

[31] P. Tang, D.-Y. Shen, Y.-Q. Xu, X.-C. Zhang, J. Shi, and J.-F. Yin, "Effect of fermentation conditions and plucking standards of tea leaves on the chemical components and sensory quality of fermented juice," *Journal of Chemistry*, vol. 2018, Article ID 4312875, 7 pages, 2018.

[32] M. Z. Zhu, N. Li, F. Zhou et al., "Microbial bioconversion of the chemical components in dark tea," *Food Chemistry*, vol. 312, Article ID 126043, 2020.

[33] L. H. Yao, Y. Jiang, N. Caffin et al., "Phenolic compounds in tea from Australian supermarkets," *Food Chemistry*, vol. 96, no. 4, pp. 614–620, 2006.

[34] Z. Feng, Y. Li, M. Li et al., "Tea aroma formation from six model manufacturing processes," *Food Chemistry*, vol. 285, pp. 347–354, 2019.

[35] E. A. H. Roberts and R. F. Smith, "Spectrophotometric measurements of theaflavins and thearubigins in black tea liquors in assessments of quality in teas," *Analyst*, vol. 86, no. 1019, pp. 94–98, 1961.

[36] E. A. H. Roberts and R. F. Smith, "The phenolic substances of manufactured tea. IX. –The spectrophotometric evaluation of tea liquors," *Journal of the Science of Food and Agriculture*, vol. 14, no. 10, pp. 689–700, 1963.

[37] L. H. Yao, Y. Chen, and C. Cheng, "The kinetics of black tea infusion," *Journal of Food and Fermentation and Industry*, vol. 19, pp. 38–44, 1993.

[38] Y. Wang, Z. Kan, H. J. Thompson et al., "Impact of six typical processing methods on the chemical composition of tea leaves using a single *Camellia sinensis* cultivar, Longjing 43," *Journal of Agricultural and Food Chemistry*, vol. 67, no. 19, pp. 5423–5436, 2019.

[39] J. L. Lu, S. S. Pan, X. Q. Zheng, J. J. Dong, D. Borthakur, and Y. R. Liang, "Effects of lipophillic pigments on colour of the green tea infusion," *International Journal of Food Science and Technology*, vol. 44, no. 12, pp. 2505–2511, 2009.

[40] V. Sai, P. Chaturvedula, and I. Prakash, "The aroma, taste, color and bioactive constituents of tea," *Journal of Medicinal Plants Research*, vol. 5, pp. 2110–2124, 2011.

[41] L. Kusmita, I. Puspitaningrum, and L. Limantara, "Identification, isolation and antioxidant activity of pheophytin from green tea (*Camellia sinensis*, (L.) Kuntze)," *Procedia Chemistry*, vol. 14, pp. 232–238, 2015.

[42] X. Li, R. Zhou, K. Xu et al., "Rapid determination of chlorophyll and pheophytin in green tea using fourier transform infrared spectroscopy," *Molecules*, vol. 23, no. 5, Pub. ID. 1010, 2018.

[43] X. Yu, S. Hu, C. He et al., "Chlorophyll metabolism in postharvest tea (*Camellia sinensis* L.) leaves: variations in color values, chlorophyll derivatives, and gene expression levels under different withering treatments," *Journal of Agricultural and Food Chemistry*, vol. 67, no. 38, pp. 10624–10636, 2019.

[44] D. Xie, W. Dai, M. Lu et al., "Nontargeted metabolomics predicts the storage duration of white teas with 8-C N-ethyl-2-pyrrolidinone-substituted flavan-3-ols as marker compounds," *Food Research International*, vol. 125, Article ID 108635, 2019.

[45] L. Zhang, W.-W. Deng, and X.-C. Wan, "Advantage of LC-MS metabolomics to identify marker compounds in two types of Chinese dark tea after different post-fermentation processes," *Food Science and Biotechnology*, vol. 23, no. 2, pp. 355–360, 2014.

[46] P. Long, M. Wen, D. Granato et al., "Untargeted and targeted metabolomics reveal the chemical characteristic of pu-erh tea (*Camellia assamica*) during pile-fermentation," *Food Chemistry*, vol. 311, Pub. ID. 125895, 2020.

[47] Y. Ma, T.-J. Ling, X.-Q. Su et al., "Integrated proteomics and metabolomics analysis of tea leaves fermented by *Aspergillus niger, Aspergillus tamarii* and *Aspergillus fumigatus*," *Food Chemistry*, vol. 334, Article ID 127560, 2021.

[48] J. Shi, W. Ma, C. Wang et al., "Impact of various microbial-fermented methods on the chemical profile of dark tea using a single raw tea material," *Journal of Agricultural and Food Chemistry*, vol. 69, no. 14, pp. 4210–4222, 2021.

[49] W. Zhang, J. Cao, Z. Li et al., "HS-SPME and GC/MS volatile component analysis of Yinghong No. 9 dark tea during the pile fermentation process," *Food Chemistry*, vol. 357, Article ID 129654, 2021.

[50] G. Xie, M. Ye, Y. Wang et al., "Characterization of pu-erh tea using chemical and metabolic profiling approaches," *Journal of Agricultural and Food Chemistry*, vol. 57, no. 8, pp. 3046–3054, 2009.

[51] C. Tan, J. S. Gong, and L. P. Bao, "Study on theabrownin physicochemical and microbial change in the fermentation process of Zijuan green tea," *Food and Fermentation Industries*, vol. 12, pp. 43–48, 2011.

[52] C. X. Peng, J. Liu, H. R. Liu, H. J. Zhou, and J. S. Gong, "Influence of different fermentation raw materials on pyrolyzates of Pu-erh tea theabrownin by Curie-point pyrolysis-gas chromatography–mass spectroscopy," *International Journal of Biological Macromolecules*, vol. 54, pp. 197–203, 2013.

[53] W. Tao, Z. Zhou, B. Zhao, and T. Wei, "Simultaneous determination of eight catechins and four theaflavins in green, black and oolong tea using new HPLC–MS–MS method-flavins ingreen, black and oolong tea using new HPLC–MS–MS method," *Journal of Pharmaceutical and Biomedical Analysis*, vol. 131, pp. 140–145, 2016.

Hindawi
Journal of Chemistry
Volume 2022, Article ID 9046780, 10 pages
https://doi.org/10.1155/2022/9046780

Research Article

Antioxidant, Antidiabetic, and Antihypertension Inhibitory Potentials of Phenolic Rich Medicinal Plants

Amir Hassan,[1,2] **Numan Zada Khan Mohmand**,[3] **Himayat Ullah**,[3] **and Abrar Hussain**[4]

[1]*Department of Natural Sciences, Novosibirsk State University, Novosibirsk 630090, Russia*
[2]*Boreskov Institute of Catalysis, Novosibirsk 630090, Russia*
[3]*Department of Chemistry, Government Post Graduate College, Mardan 23200, Pakistan*
[4]*Department of Biological Sciences, International Islamic University, Islamabad 44000, Pakistan*

Correspondence should be addressed to Amir Hassan; amirhassan741@gmail.com

Received 12 June 2022; Revised 18 July 2022; Accepted 20 July 2022; Published 11 August 2022

Academic Editor: Marwa Fayed

Veronica (Plantaginaceae) and *Schoenoplectus* have a unique chemotaxonomic and phytochemical importance and are widely utilized in Turkish and Traditional Chinese Herbal Medicine (TCM) for treating tonics, influenza, diuretics, expectorants, restoratives, and respiratory diseases, and both are very useful in treating infectious and metabolic disorders as well. This study evaluates two medicinal plant species, *Veronica biloba* and *Schoenoplectus triqueter* (L.) Palla; extraction was performed through Soxhlet and maceration methods as well as determination of free and bound phenolics. Evaluated biological screening of (extracts and phenolics) angiotensin-I converting enzyme (ACE), Type-II diabetes (α-glucosidase and α-amylase), and antioxidants potential was performed using modified assays. The angiotensin-I converting enzyme (ACE) 50% inhibition potential in *Veronica biloba* was found at $IC_{50} = 210.68\ \mu g/mL$ and in *Schoenoplectus triqueter* (L.) Palla at $IC_{50} = 229.40\ \mu g/mL$, respectively. Meanwhile Type-II diabetes with α-amylase 50% inhibition shown by bound phenolics of *Veronica biloba* at $IC_{50} = 219.66\ \mu g/mL$ and its water extract at $IC_{50} = 110.09\ \mu g/mL$ possesses higher potential, and α-glucosidase potential by free phenolics was found to be active at $IC_{50} = 469.56\ \mu g/mL$, while water and ethyl acetate extracts showed higher potential, $IC_{50} = 78.65\ \mu g/mL$ and $IC_{50} = 97.03\ \mu g/mL$, than the standard acarbose, recorded lower. In case of amylase, α-glucosidase showed $IC_{50} = 88.73\ \mu g/mL$. Our results showed that both plants possess a direct relationship with the increase in the concentration of extracts and inhibited very strongly angiotensin-I converting enzyme (ACE) and Type-II diabetes (α-glucosidase and α-amylase). The properties of enzyme hindrance may be associated with phenolic compounds and rich phenolic plant antioxidant potential provides a route to the elucidation of natural antihypertension and antidiabetes.

1. Introduction

Natural products are God-gifted, such as extracts from plants that possess a variety of biologically active compounds, and their purification, characterization, and isolation are very helpful for synthesizing a novel drug with chemical diversity to cure a number of health-related diseases utilized as pure compounds or standard extracts [1, 2]. Approximately 10–20% of plants in pharmaceutical studies were revealed positively for harmful diseases including cancer [3]. The extracts from medicinal plants contain several bioactive compounds, and each of them is responsible for any specific bioactivity [4]. According to ecological studies, synthetic drugs have several side effects, while drug or standard extract from medicinal plants shows high and effective results with no or few side effects and is more preferred [5–7]. The *Veronica* (Plantaginaceae) genus has 79 popular species in a total of 450, and 26 are endemic species present in both temperate and hemisphere regions [8, 9]. This genus has a unique chemotaxonomic and phytochemical importance and is widely utilized in Turkish and Traditional Chinese Herbal Medicine (TCM) for treating

tonics, influenza, diuretics, expectorants, restoratives, and respiratory diseases [10]. Previously, we have determined a strong antibacterial and antifungal potential of *Veronica biloba* extracts [11] as well as phytochemicals and antioxidants comparable with standard acarbose potential [12]. The family Cyperaceae mostly possesses fibrous halophytic plants; one genus of this family is *Schoenoplectus* present in the river territories of Pakistan, India, Africa, Morocco, and Spain at the extreme Mediterranean [13, 14]; about 49 compounds are extracted from the specie of *Schoenoplectus lacustris* and evaluated for eutrophic spots; a bioindicator was tested on algae green *Selenastrum capricornutum* and showed positive potential in comparison with copper sulphate, algaecide [15]. Cyperaceae contains 4231 chromosomes found in only 16% of its species which are helpful for biological activities [16]. Previously, we have reported that *Schoenoplectus triqueter* (L.) Palla extracts possess potential against both bacterial strains, Gram-positive and Gram-negative, as well as antioxidant potential [17, 18]. Type-II diabetes mellitus represents more than 90% of all elicit diabetes in both developing and developed countries. Around 382 million individuals are viewed as living with diabetes from one side of the planet to the other, and scientific predictions reveal that the number will increase to around 471 million individuals by 2035 [19]. Postprandial hyperglycemia has been embroiled in the advancement of insulin opposition [20], being quite possibly the earliest marker of glucose homeostasis liberation [21]. Furthermore, hypertension, cardiovascular illness, and diabetic neuropathy are linked to this issue [22, 23]. A hyperglycemia therapeutic prevention is carried out by the inhibition of key enzymes such as alpha-amylase and alpha-glucosidase, which are involved in the hydrolysis of carbohydrates and disaccharides to diminish the absorption of glucose. Some commonly available drugs such as miglitol and acarbose are efficient to decrease the glucose level in the blood, but they possess severe long-term side effects; therfore, its uses are very low [24, 25]. According to Bakriset al. [26], hypertension arises mainly due to long-term diabetes and may lead to severe chronic renal failure, a cardiovascular disease [26]. In phenomena of ACE, an important Zn-Metallopeptidase enzyme plays a role in breaking and conversion of bradykinin (vasoconstrictor, vasodilator) and angiotensin-I to angiotensin-II. In therapeutics, the efficient inhibition of ACE (angiotensin-I converting enzyme) is much preferred, which helps in lowering hypertension in normal and hyperglycemic diabetic persons [27]. In medicinal plants, mainly phytochemicals (such as phenolics) show antihypertension and antidiabetes potential [28, 29]. The ongoing hyperglycemia in diabetes stimulates oxidative pressure on organs and tissues [24], which might be constrained by cell reinforcement. Interest in natural antioxidants is presently growing [30–33]. Phenolic compounds address enormous gathering of biologically active phytochemicals which are present in practically all restorative and food plants, as a result of their extremely high environmental pertinence in plant life forms [34–39]. Due to fewer side effects and the high importance of natural antioxidants, phenolics, and phytochemicals, this study evaluates two medicinal plant species, *Veronica biloba* and *Schoenoplectus triqueter* (L.) Palla; extraction was performed through Soxhlet and maceration methods as well as determination of free and bound phenolics and investigation of inhibitory activity of phenolic-rich extracts on key enzymes involved in hypertension and diabetes, that is, α-amylase, α-glucosidase, and ACE.

2. Materials and Methods

2.1. Identification and Collection of Plants. The two different medicinal plant species, *Schoenoplectus triqueter* (L.) Palla and *Veronica biloba*, were confirmed from various botanical flora databases of plants, a comparison of literature survey, and a botanical export of Government Post Graduate College Mardan, Faculty of Botany. Professor Muhammad Israr confirmed voucher specimen of *Veronica biloba* (ID: 19-VB.PMI-PGCM) and *Schoenoplectus triqueter* (ID: 22-ST.PMI-PGCM). The specie Veronica biloba (A-VB) plant used in the project was the whole plant selected. Fresh whole plants in their floweringstage were collected from Sang-e-mar mar, near Par Hoti District Mardan andalso from Surkh Dheri, Rustam, Mardan. The plant collection was done during themonth of February–March. Healthy plants are collected from a fertile land. Whilespecies Schoenoplectus triqueter (L.)Palla (B-ST), only stem part collected in the month of January-February, locations;East 72° 4′ 49″ and North 34° 21′38″ coordinates from river areas of KatlangAsia Mardan 23200 Khyber Pakhtunkhwa Pakistan..

2.2. Drying and Grinding of the Plant. After collection of both plant species, A-VB and B-ST were introduced for surface cleaning first by tap water and then by distilled water slowly for the removal of any small particles of mud and other dust on surface. With the help of scissors and knives, plants were separately cut into smaller pieces and kept in a dust-free protective environment to avoid contamination for 3 weeks without exposure to any light at room temperature. After complete drying of both species, they were ground via a normal grinder to increase the surface area and obtain uniform size particles for a better extraction process in less time with a high yield.

2.3. Extractions

2.3.1. Soxhlet Extraction. The Soxhlet hot continuous method of extraction was followed according to reports [11, 12, 17, 18] for both plants. At first, two sterilized porous bags were manually prepared, in which each possesses 20 gm by weight of the fully powdered plant. 250 ml ethanol was placed in the Soxhlet round bottom (R.B) flask lower section. In the second, porous cellulose bags were kept in the Soxhlet thimble chamber upper section. Additionally, water outflow and inflow were provided to the upper condenser section for the successive extract process and liquid condensation; a fixed temperature in the range of 35–45°C was provided by the Monteux heater. After 14–18 hours, a clear liquid from the Soxhlet siphon arm was obtained without leaving residue

in cycling. Each plant extract obtained was fractionated into different solvents, n-hexane, dichloromethane, water, and ethyl acetate fractions under a controllable water bath; each dried fraction was saved and used for further biological analysis.

2.3.2. Maceration Extraction. The maceration method of extraction was followed according to reports [11, 12, 17, 18] for both plants. In this setup, two sterilized Pyrex-glass jars were used, in which each possesses 30 gm by weight of the fully powdered plant; a solvent of 300 mL ethanol for successive extractions was used. At room temperature in shade placed jars for 22 days with air-tight cap, at least twice for 10–15 minutes, daily shaking with stirring was performed to transfer slowly soluble metabolites to solvent. After filtration, each plant extract obtained was fractionated into different solvents, n-hexane, dichloromethane, water, and ethyl acetate fractions under a controllable water bath; each dried fraction was saved and used for further biological analysis.

2.4. Phenolic Extractions. The phenolic contents were extracted according to Chu et al. [40]. Free phenolics were extracted from ethanol fraction by filtration (Whatman filter paper) and evaporation in rotary (<45°C); for stability, dry extract was subjected to lyophilization and then stored (<−6°C). Meanwhile bound phenolics were extracted from the residue of free phenolics and ethyl acetate fractions, with condition of room temperature 22 ± 6°C, NaOH ($M = 2$) 15 mL for hydrolysis, $\text{pH} = 2.1 \pm 0.1$ (adjusted by HCl), and constant stirring of mixture for 45 minutes. Then ethyl acetate was subjected to dryness and evaporation (<45°C) and kept for further processing.

2.5. Determination of Total Phenolics. The content of phenolics was determined as illustrated by Singleton et al. [41]. At first, Folin-Ciocalteu's reagent (10%, 3 mL) and extracts were taken under Na_2CO_3 (8%, 2 mL) for oxidation and neutralization and subjected to an incubation period (40°C, 30 min). At last, the absorbance was recorded at a wavelength of 765 nm by UV-spectrophotometer. The standard gallic acid was used for specified values.

2.6. Determination of Reducing Power. The reducing power was determined as illustrated by Oyaizu [42], which is based on the reduction power of $FeCl_3$ solution. At first, $K_3[Fe(CN)_6]$ (Potassium Ferricyanide) 1%, 3 mL, Na_2HPO_4 (Sodium Phosphate) having $M = 200$ mM and $\text{pH} = 6.5 \pm 0.2$ amount 3 mL and same amount of samples were mixed and subjected to incubation (40°C, 20 min). Secondly, Trichloroacetic acid (TCA), $C_2HCl_3O_2$ 10%, 3 mL, was added and mixture was obtained at 2600 rpm/10 minute after centrifugation; clear supernatant (5 mL) mixed with $FeCl_3$ (Ferric Chloride) 0.1%, 1.5 mL, in distilled water. At last, the absorbance was recorded at a wavelength of 710 nm by UV-spectrophotometer. The standard ascorbic acid was used for specified values.

2.7. Total Antioxidant Potential. The total antioxidant potential was evaluated as illustrated by Sharifi Rad et al. [43], using ABTS (2,2′-azino-bis(3-ethylbenzothiazoline-6-sulfonic acid)). First, ABTS generation was performed by treating ABTS with Potassium Persulfate ($K_2S_2O_8$); both compositions are 6 mM, and2.3 mM, with duration of 12 hours at dark (to avoid decomposition). After dilution of the extracts with ABTS (amount fixed 0.5 mL+2 mL) solution, at last, the absorbance was recorded at a wavelength of 730 nm by UV-spectrophotometer. The standard trolox was used for specified values.

2.8. Alpha-Amylase. The α-amylase inhibitory potential was evaluated as illustrated by Yousaf et al. [44] using a series of phenolics (free and bound) and A-VB fraction extract dilution in the range of 5–150 μL. First, α-amylase (porcine pancreatic) solution, 0.5 mg/mL, 500 μL buffer ($\text{pH} = 6.9 \pm 0.02$) of Sodium Phosphate ($M = 0.02$) and Sodium Chloride ($M = 0.006$), was incubated for 15 min at 25°C. Then, individually 1% 500 μL solution of starch was added subsequently in the buffer ($\text{pH} = 6.9 \pm 0.02$) of Sodium Phosphate ($M = 0.02$) and Sodium Chloride ($M = 0.006$); again the whole mix was incubated for 15 min at 25°C, for countering over, 1 mL DNS (dinitrosalicyclic acid) added. Afterward, the reaction mixture for 15 minutes was transferred to a controllable water bath (containing distilled water) at room temperature range of 22 ± 4°C. At last, for dilution, 10 ml sterilized water was added and the absorbance was recorded at a wavelength of 540 nm by UV-spectrophotometer. The data are illustrated in percent inhibition placed standard acarbose [45, 46].

2.9. Alpha-Glucosidase. The α-glucosidase inhibitory potential was evaluated as illustrated by Sharifi Rad. et al. [47], using a series of phenolics (free and bound) and A-VB fraction extract dilution in the range of 5–150 μL. First, α-glucosidase (1.0 U/mL) solution 100 μL, 500 μL buffer ($\text{pH} = 6.9 \pm 0.02$) with Sodium Phosphate ($M = 0.1$), was incubated for 15 min at 25°C. Second, p-Nitrophenyl-α-D-Glucopyranoside ($M = 5$ mM) 50 μL solutions were added and the same incubation was repeated. At last, the absorbance was recorded at a wavelength of 405 nm by UV-spectrophotometer. The data are illustrated in percent inhibition placed standard acarbose [48].

2.10. Angiotensin-I Converting Enzyme Inhibition. The ACE (angiotensin-I converting enzyme) inhibition potential determination, using the Cushman and Cheung procedure, was followed as reported in [47]. In the first incubation period (15 minutes at 37°C), the standard ACE 50 μL and diluted phenolics in 5–50 μL were mixed; solution was fixed at 4 mU/mL. Second, Bz–Gly–His–Leu substrate ($M = 8.33$ mM) supported by buffer pH 8.3 of Tris-HCl

($M = 125$ mM) in a fixed amount of 150 μL was added for initiation of the enzymatic reaction. In the second incubation period (30 minutes at 35°C), HCl ($M = 1$) was added with amount 250 μL for countering the reaction. After bond breaking of Gly–His ethyl acetate, 1 mL was added to isolate Bz–Gly by centrifugation and evaporation from reaction. The sterilized water was added for residue analysis in UV-spectrophotometer, calibration, and absorbance recorded at a wavelength of 228 nm. The results were plotted as % inhibition.

2.11. Determination of IC_{50}. The Median Inhibitory Concentration (IC_{50}) was determined for 50% inhibition potential in each case of biological activity α-amylase, α-glucosidase, and angiotensin-I converting enzyme using Excel, Prism, and Origin software.

3. Results and Discussion

The extraction fractionation, phenolics (both free and bound phenolics), ACE (angiotensin-I converting enzyme), α-amylase, and α-glucosidase were determined in both plants, *Veronica biloba* (A-VB) and *Schoenoplectus triqueter* (L.) Palla (B-ST), according to the reports of [11, 12, 17, 18, 40–48]. The total phenolics determination results are shown in Table 1. The numbers of bound phenolics found in species *Veronica biloba*, 62.02 ± 5.2, are higher than those of bound phenolics found in *Schoenoplectus triqueter*, 41.6 ± 2.5. Meanwhile, for free phenolics, 81.34 ± 0.5, for *Veronica biloba* and those, 54.11 ± 1.5, for *Schoenoplectus triqueter*, the results are derived with standard *gallic acid* mg/100 gm as mean ± standard deviation (having P significantly $=< 0.05$). That closely resembles previous literature [40, 49–52]. The total antioxidant potential or capacity results are in Table 1 and are determined via standard mmol *trolox*/100 g; the species *Veronica biloba* possesses higher potential in both cases of free and bound phenolics, 12.21 ± 1.5 and 16.09 ± 1.2, than *Schoenoplectus triqueter* which showed 9.8 ± 0.05 and 11.03 ± 0.1, respectively, as mean having P significantly < 0.05, and the higher antioxidant potential is due to phenol content in the plants [24, 48]. The reducing power determination with standard ascorbic acid as mean ± standard deviation (P significantly $=< 0.05$) is presented in Table 1, with higher values recorded in the case of free phenolics only for *Veronica biloba*, 14.08 ± 1.5, and *Schoenoplectus triqueter*, 9.08 ± 2.05. Polyphenols are antioxidants of the plant, which have an important function in breaking up peroxides, neutralizing and absorbing free radicals, and extinguishing singlet and triplet oxygen [53]. Phenolics can be found as conjugated forms or free aglycones in different tissues with glucose as glycosides or other moieties in almost every plant organism [54].

The decrease in the antioxidant capacity normally occurs by conjugation present in the phenolic backbone through the hydroxyl groups; hence, the free radical resonance stabilization depends on the free hydroxyl groups present on the phenolic rings. Some lines of evidence suggest that *Veronica* species possess antioxidant activity marked as insufficient; however, limited studies claimed that few of *Veronica* species show antioxidant activity [55, 56]. It was observed that the aerial part of *Veronica persica* contains Persicoside, a phenylethanoid glycoside [57–59]; however, lots of phenylethanoid glycosides have been discovered which possess a wide range of biological activities, containing anticancer and antioxidant properties [60, 61].

The high phenolics containing compounds like phenylethanoids and flavonoids suppress the effect of *Veronica* species on NO production [62]. It has been investigated that most of the phenolic compounds discovered from *Veronica* species are beneficial for human health [37, 56, 63]. The antioxidant activity of phenolic compounds is also valuable for delaying or lowering the growth of inflammation [64]. In this way, we identified that *Veronica biloba* and *Schoenoplectus triqueter* phenolic extracts showed reducing power in the form of ascorbic acid equivalents (Table 1), exposing that the phenolic extract for bounding had lower reducing power than the free phenolic extract [65, 66].

The therapeutic approaches toward the control or reduction of hypertension and hyperglycemia involve the inhibition of carbohydrates metabolism enzymes that are ACE (angiotensin-I converting enzyme), α-glucosidase, and α-amylase [67–69]. The experimental results of ACE, α-glucosidase, and α-amylase activity of *Veronica biloba* and *Schoenoplectus triqueter* (L.) Palla of the extracts, free and bound phenolics, are as shown in Table 2 and Figures 1–8.

The α-amylase inhibition activity of *Veronica biloba* fraction extracts showed higher efficiency in the following order: water (110.25 μg/mL) > ethyl acetate > dichloromethane > acarbose > n-hexane (148.01 μg/mL); 50% median inhibition for water fraction appeared at a very lower concentration than standard acarbose and it is shown in Figure 1 that in the range of 50–75 μg/mL there is a direct relation found between inhibition and concentration; the exception was that n-hexane fraction pushed slowly. Meanwhile, in the case of α-glucosidase, the overall activity of water extract was found to be >75% and the results described the following order: water (78.65 μg/mL) > acarbose > ethyl acetate > dichloromethane > n-hexane (149.71 μg/mL); the 50% inhibition for first sequence order appeared at 75 μg/mL as shown in Figure 2.

The α-amylase inhibition activity for both plants, *Veronica biloba* and *Schoenoplectus triqueter*, and free and bound phenolics in comparison are shown in Figures 3 and 4, respectively; in both plant species, bound phenolics showed 50% activity, while *Veronica biloba* (219.66/mL) potential was noticed to be higher and more potent with change in concentration. In the case of α-glucosidase inhibition, free phenolics were active for *Veronica biloba*, 50% = 469.56 μg/mL, and *Schoenoplectus triqueter*, 50% = 673.05 μg/mL, significantly having $P = < 0.05$, as shown in Figures 5 and 6. Dose-depending antihypertensive activities of both species extracts (bound and free phenolics) are carried out via ACE inhibition in both plants. Bound phenolics showed greater efficiency than free phenolics.

Phenolics of *Veronica biloba* 50% = 210.68 μg/mL > *Schoenoplectus triqueter* 50% = 229.40 μg/mL as shown in Figures 7 and 8 and Table 2; in both cases, free

Table 1: The total antioxidants and phenolics potential in medicinal plants A-VB and B-ST.

Samples extracts	Total phenolics	Total antioxidants	Reducing power
Bound phenolic$^{(A\text{-}VB)}$	62.02 ± 5.2	12.21 ± 1.5	10.66 ± 2.0
Bound phenolic$^{(B\text{-}ST)}$	41.6 ± 2.5	9.8 ± 0.05	7.2 ± 1.5
Free phenolic$^{(A\text{-}VB)}$	81.34 ± 0.5	16.09 ± 1.2	14.08 ± 1.5
Free phenolic$^{(B\text{-}ST)}$	54.11 ± 1.5	11.03 ± 0.1	9.08 ± 2.05

The statistical data in triplicate ($n = 3$) are represented as mean ± standard deviation (having $P = < 0.05$); total antioxidant equivalent is determined via trolox standard, and reducing power equivalent is determined via ascorbic acid standard. (A-VB) = *Veronica biloba*; (B-ST) = *Schoenoplectus triqueter* (L.) Palla.

Table 2: Inhibitory potential of medicinal plants A-VB and B-ST.

Extracts	50% median inhibitory potential (IC_{50} μg/mL)		
	ACE	α-amy	α-glu
Bound phenolic$^{(A\text{-}VB)}$	210.68	219.66	608.31
Bound phenolic$^{(B\text{-}ST)}$	229.40	741.19	>749.35
Free phenolic$^{(A\text{-}VB)}$	249.05	573.39	469.56
Free phenolic$^{(B\text{-}ST)}$	319.59	>749.52	673.05
Water$^{(A\text{-}VB)}$	—	110.25	78.65
Ethyl acetate$^{(A\text{-}VB)}$	—	121.09	97.03
n-Hexane$^{(A\text{-}VB)}$	—	148.01	>149.71
Dichloromethane$^{(A\text{-}VB)}$	—	123.68	139.93
Acarbose	—	138.79	88.73

The statistical data in triplicate ($n = 3$) are represented as mean ± standard deviation (having $P = < 0.05$), calculated by software. (A-VB) = *Veronica biloba*; (B-ST) = *Schoenoplectus triqueter* (L.) Palla; ACE = angiotensin-I converting enzyme; α-amy = α-amylase; α-glu = α-glucosidase.

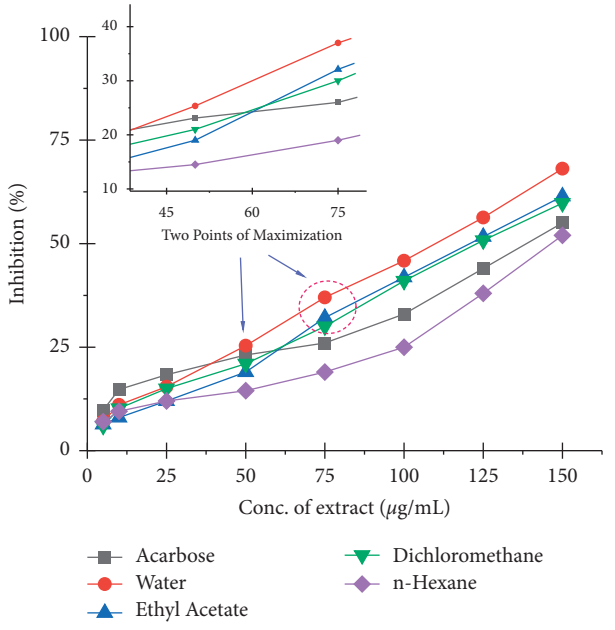

Figure 1: α-Amylase median inhibitory potential of *Veronica biloba* extracts.

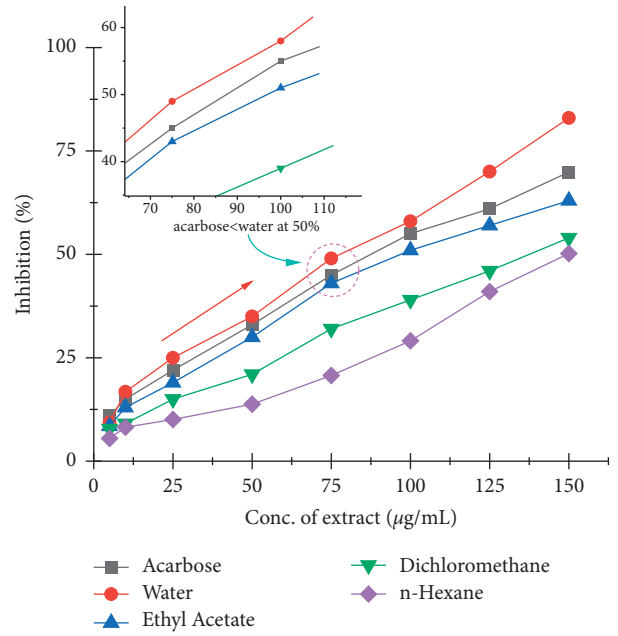

Figure 2: α-Glucosidase median inhibitory potential of *Veronica biloba* extracts.

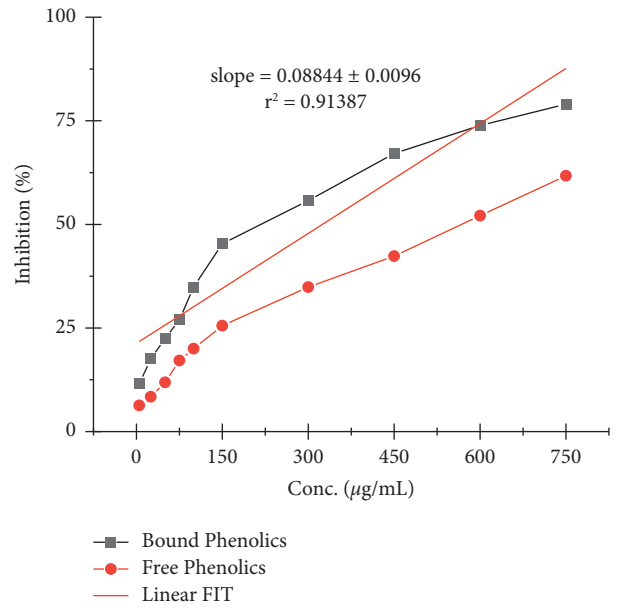

Figure 3: α-Amylase median inhibitory potential of *Veronica biloba* phenolics.

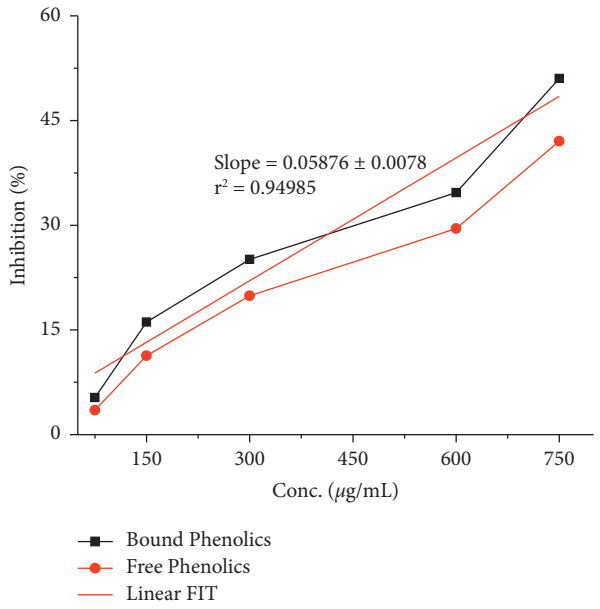

Figure 4: α-Amylase median inhibitory potential of *Schoenoplectus triqueter* phenolics.

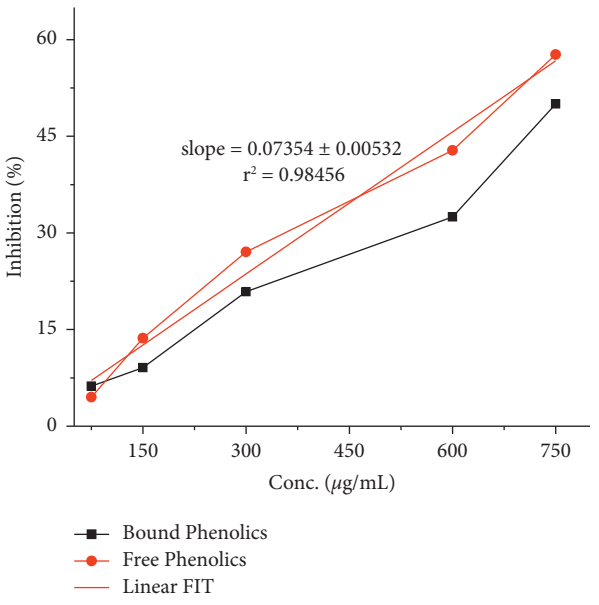

Figure 6: α-Glucosidase median inhibitory potential of *Schoenoplectus triqueter* phenolics.

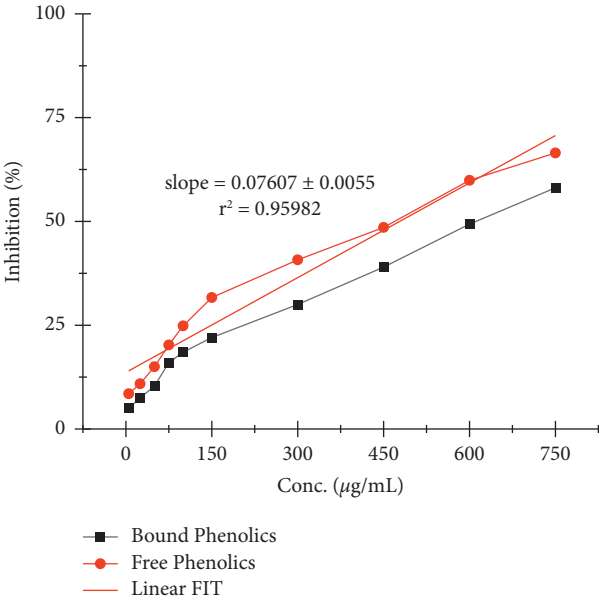

Figure 5: α-Glucosidase median inhibitory potential of *Veronica biloba* phenolics.

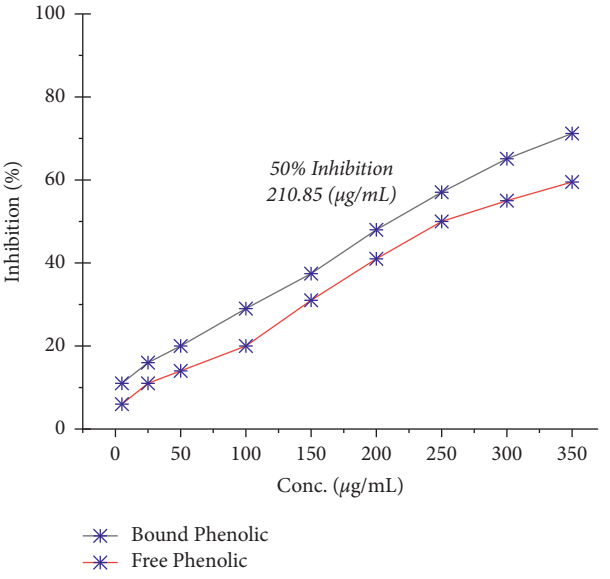

Figure 7: ACE (angiotensin-I converting enzyme) median inhibitory potential of *Veronica biloba* phenolics.

phenolics were lower. However, previous studies showed that phytochemicals have lower α-amylase inhibition than α-glucosidase inhibition [49, 50, 70, 71]. The antidiabetic and acarbose possess excess α-amylase inhibition which would avoid the side effects [72]. Thus, plant phenolics with high α-glucosidase and mild α-amylase inhibitory activities have been suggested as suitable substitutes for the clinician to the analogous synthetic inhibitors [67]. Moreover, the antihypertensive potential of phenolic extracts has also been examined through the inhibition of ACE. As shown in Figures 7 and 8, both extracts exhibited a high ACE inhibitory activity in adose-dependent manner. In specific, bounded phenolic extracts ($P < 0.05$) had very high inhibiting activity on enzymes compared to free phenolic extracts. Further studies on the physical structure of human ACE have given us evidence of the presence of a group of amino acids in the protein molecule cysteine (cysteine is responsible for the formation of disulfide bridges [69]. That is why ACE controlling activity of *Veronica persica* may be because of the interactions between (bound and free) phenolics and disulfide (cysteines which are oxidized) that

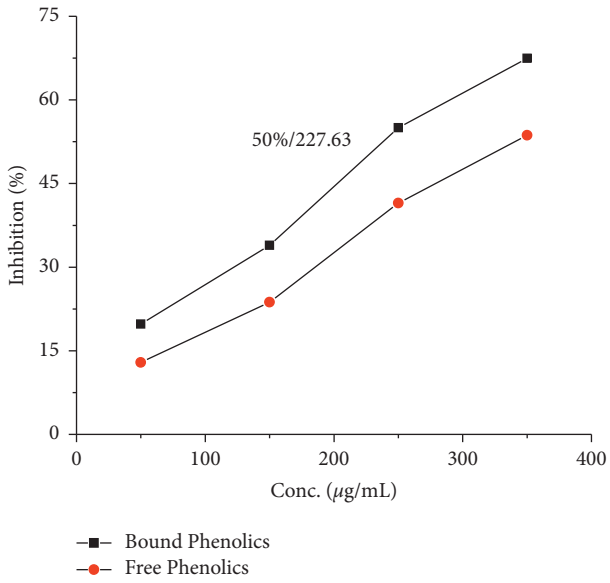

Figure 8: ACE (angiotensin-I converting enzyme) median inhibitory potential of *Schoenoplectus triqueter* phenolics.

are located over the surfaces of macromolecules responsible for functional and structural changes which are in turn associated with enzymes stopping [69]. Our results support the greater α-glucosidase, α-amylase, and ACE reducing activities as shown in Figures 1–8 with bounded extract of phenolics in comparison with the unbounded phenolic extract. The main reason may be associated with the higher water loving of bound phenolics, which are greatly in the form of glycosides. Compared to the free phenolics which are mainly in the form of a-glycones, enzymes (ACE and alpha-amylase) are active in medium containing water, which are inhibitors directing toward positive mean; it increases the interaction between inhibitors and enzymes; the interaction effects of bonded phenolics are greater compared to unbounded phenolics. These studies revealed the inhibition activity of phenolic compounds which might be involved in bridges, that is, disulfide bridges located on the outer layer of α-amylase, thus the enzyme responsible for the modification of the function and structure [68–73]. The reason for the inhibition of ACE, α-amylase, and α-glucosidase potential of both plant species maybe is due to the direct interaction of the phenolics with the disulfide bridges of the enzymes. Furthermore, the activity will be confirmed with the purification of extracts and isolation of phenolics; more consideration is required.

4. Conclusions

It is concluded that both plants, *Veronica biloba* and *Schoenoplectus triqueter* (L.) Palla, showed a quiescent hindrance in *in vitro* ACE (angiotensin-I converting enzyme), α-glucosidase, α-amylase, and antioxidant bioactivities and are helpful in the therapeutic investigation of hypertension and hyperglycemia, linked to Type-II diabetes. The properties of enzyme hindrance may be associated with phenolic compounds. Additional analysis and studies are firmly suggested to clarify the basic phenolics compounds which are moderated by free radicals; the identification and isolation of the components chemical outfit of plants may lead to utilization in clinical trials.

Data Availability

All data used to support the findings of this study are included within the article.

Conflicts of Interest

The authors declare that they have no conflicts of interest.

Acknowledgments

The authors thank Amir Hassan of the Department of Natural Sciences, Novosibirsk State University, 630090, Novosibirsk, Russia, for writing and handling the manuscript and also acknowledge Professor Himayat Ullah for project assessment and evaluation, in addition to experimental credit to Abrar Hussain, Department of Biological Sciences, International Islamic University, 44000, Islamabad, Pakistan.

References

[1] C. W. Huie, "A review of modern sample-preparation techniques for the extraction and analysis of medicinal plants," *Analytical and Bioanalytical Chemistry*, vol. 373, no. 1-2, pp. 23–30, 2002.

[2] P. Cos, A. J. Vlietinck, D. V. Berghe, and L. Maes, "Anti-infective potential of natural products: how to develop a stronger in vitro "proof-of-concept"," *Journal of Ethnopharmacology*, vol. 106, no. 3, pp. 290–302, 2006.

[3] M. Naczk and F. Shahidi, "Phenolics in cereals, fruits and vegetables: occurrence, extraction and analysis," *Journal of Pharmaceutical and Biomedical Analysis*, vol. 41, no. 5, pp. 1523–1542, 2006.

[4] I. O. Kibwage, J. W. Mwangi, and G. Thoithi, "Quality control of herbal medicines," *East and Central African Journal of Pharmaceutical Sciences*, vol. 8, no. 2, pp. 27–30, 2006.

[5] K. A. Hammer, C. F. Carson, and T. V. Riley, "Antimicrobial activity of essential oils and other plant extracts," *Journal of Applied Microbiology*, vol. 86, no. 6, pp. 985–990, 1999.

[6] I. B. Suffredini, H. S. Sader, A. G. Gonçalves et al., "Screening of antibacterial extracts from plants native to the Brazilian amazon rain forest and atlantic forest," *Brazilian Journal of Medical and Biological Research*, vol. 37, no. 3, pp. 379–384, 2004.

[7] F. Soldati, "The registration of medicinal plant products, what quality of documentation should be required? The industrial point of view," in *Proceedings of the World Congress on Medicinal and Aromatic Plants for Human Welfare*, Mendoza, Argentina, November 1997.

[8] R. M. Taskova, T. Kokubun, K. G. Ryan, P. J. Garnock-Jones, and S. R. Jensen, "Phenylethanoid and iridoid glycosides in the New Zealand snow hebes (veronica, Plantaginaceae)," *Chemical & Pharmaceutical Bulletin*, vol. 58, no. 5, pp. 703–711, 2010.

[9] P. Davis, *Flora of Turkey and the East Aegean Islands*, Edinburgh University Press, Edinburgh, UK, 1978.
[10] U. S. Harput, "Radical scavenging effects of different Veronica species," *Records of Natural Products*, vol. 5, no. 2, p. 100, 2011.
[11] A. Hassan and H. Ullah, "Antibacterial and antifungal activities of the medicinal plant veronica biloba," *Journal of Chemistry*, vol. 2019, Article ID 5264943, 7 pages, 2019.
[12] A. Hassan, H. Ullah, and M. Israr, "The antioxidant activity and phytochemical analysis of medicinal plant veronica biloba," *Letter In Applied NanoBioscience*, vol. 8, no. 4, pp. 732–738, 2019.
[13] M. Qasim, S. Gulzar, and M. A. Khan, "Halophytes as medicinal plants," in *Proceedings of the NAM Meeting*.
[14] P. Jimenez-Mejıas, M. Luceno, and S. Castroviejo, "Schoenoplectus corymbosus: a tropical old-world sedge (Cyperaceae) discovered in Spain and Morocco," *Nordic Journal of Botany*, vol. 25, no. 1-2, pp. 70–74, 2007.
[15] B. D'abrosca, M. Dellagreca, A. Fiorentino, M. Isidori, P. Monaco, and S. Pacifico, "Chemical constituents of the aquatic plant Schoenoplectus lacustris: evaluation of phytotoxic effects on the green alga Selenastrumcapricornutum," *Journal of Chemical Ecology*, vol. 32, no. 1, pp. 81–96, 2006.
[16] E. H. Roalson, "A synopsis of chromosome number variation in the Cyperaceae," *The Botanical Review*, vol. 74, no. 2, pp. 209–393, 2008.
[17] N. Khan, A. Hassan, H. Ullah, Z. Akmal, M. Y. Khan, and S. U. Khan, "Antibacterial potential test for *scheonoplectus triqueter* (L) Palla," *Letter in Applied NanoBioScience*, vol. 9, no. 1, pp. 941–944, 2020.
[18] A. Hassan, Z. Akmal, and N. Khan, "The phytochemical screening and antioxidants potential of *Schoenoplectus triqueter* L. Palla," *Journal of Chemistry*, vol. 2020, Article ID 3865139, 8 pages, 2020.
[19] F. Aguirre, A. Brown, N. H. Cho, G. Dahlquist, S. Dodd, and T. Dunning, *IDF Diabetes Atlas*, International Diabetes Federation, Brussels, Belgium, 6th edition, 2013.
[20] A. Ceriello, "Postprandial hyperglycemia and diabetes complications: is it time to treat?" *Diabetes*, vol. 54, no. 1, pp. 1–7, 2005.
[21] L. Monnier, C. Colette, G. J. Dunseath, and D. R. Owens, "The loss of postprandial glycemic control precedes stepwise deterioration of fasting with worsening diabetes," *Diabetes Care*, vol. 30, no. 2, pp. 263–269, 2007.
[22] T. Nishikawa, D. Edelstein, X. L. Du et al., "Normalizing mitochondrial superoxide production blocks three pathways of hyperglycaemic damage," *Nature*, vol. 404, no. 6779, pp. 787–790, 2000.
[23] T. H. W. Huang, G. Peng, B. P. Kota et al., "Anti-diabetic action of flower extract: activation of PPAR-γ and identification of an active componentflower extract: activation of PPAR-γ and identification of an active component," *Toxicology and Applied Pharmacology*, vol. 207, no. 2, pp. 160–169, 2005.
[24] M. Brownlee, "The pathobiology of diabetic complications: a unifying mechanism," *Diabetes*, vol. 54, no. 6, pp. 1615–1625, 2005.
[25] A. Abirami, G. Nagarani, and P. Siddhuraju, "In vitro antioxidant, antidiabetic, cholinesterase and tyrosinase inhibitory potential of fresh juice from Citrus hystrix and C. maxima fruits," *Food Science and Human Wellness*, vol. 3, no. 1, pp. 16–25, 2014.
[26] G. L. Bakris, M. Williams, L. Dworkin et al., "Preserving renal function in adults with hypertension and diabetes: a consensus approach," *American Journal of Kidney Diseases*, vol. 36, no. 3, pp. 646–661, 2000.
[27] M. F. McCarty, "ACE inhibition may decrease diabetes risk by boosting the impact of bradykinin on adipocytes," *Medical Hypotheses*, vol. 60, no. 6, pp. 779–783, 2003.
[28] Y. I. I. Kwon, D. A. Vattem, and K. Shetty, "Evaluation of clonal herbs of Lamiaceae species for management of diabetes and hypertension," *Asia Pacific Journal of Clinical Nutrition*, vol. 15, no. 1, pp. 107–118, 2006.
[29] G. Oboh and A. O. Ademosun, "Phenolic rich extracts from orange peels (Citrus sinensis) inhibits key enzyme linked to non-insulin dependent diabetes mellitus (NIDDM) and hypertension," *RivItalSostanze Gr*, vol. 88, no. 1, pp. 16–23, 2011.
[30] S. Raeisi, M. Sharif-Rad, S. Young Quek, B. Shabanpour, and J. SharifRad, "Evaluation of antioxidant and antimicrobial effects of shallot (Allium ascalonicum L.) fruit and ajwain (*Trachy spermumammi* (L.) Sprague) seed extracts in semi-fried coated rainbow trout (Oncorhynchusmykiss) fllets for shelf-life extension," *Food SciTechnol*, vol. 65, pp. 112–121, 2016.
[31] G. Bagheri, M. Mirzaei, R. Mehrabi, and J. Sharifi-Rad, "Cytotoxic and antioxidant activities of alstoniascholaris, alstoniavenenata and moringaoleifera plants from India," *Jundishapur Journal of Natural Pharmaceutical Products*, vol. 11, no. 3, 2016.
[32] M. Sharifi-Rad, G. S. Tayeboon, A. Miri et al., "Mutagenic, antimutagenic, antioxidant, anti-lipoxygenase and antimicrobial activities of *Scandixpectenveneris* L," *Cellular & Molecular Biology*, vol. 62, no. 6, pp. 8–16, 2016.
[33] J. Sharifi-Rad, M. Sharifi-Rad, S. M. Hoseini-Alfatemi, M. Iriti, M. Sharifi-Rad, and M. Sharifi-Rad, "Composition, cytotoxic and antimicrobial activities of SaturejaintermediaC.A.Mey essential oil," *International Journal of Molecular Sciences*, vol. 16, no. 8, pp. 17812–17825, 2015.
[34] A. Haasan, S. Shahzeb, M. Waqas, and N. Khan, "Extraction and antibacterial potential of traditional medicinal plant Cypreuscompressus," *TMR Modern Herbal Medicine*, vol. 4, no. 3, p. 22, 2021.
[35] J. Sharifi-Rad, S. M. Hoseini-Alfatemi, M. Sharifi-Rad et al., "Phytochemical compositions and biological activities of essential oil from *Xanthium strumarium* L," *Molecules*, vol. 20, no. 4, pp. 7034–7047, 2015.
[36] A. Hassan, I. Ullah, and W. Ahmad, "Isolation and evaluation of antibacterial potential test of plant carthamusoxycantha," *Journal of Tropical Pharmacy and Chemistry*, vol. 5, no. 4, pp. 299–308, 2021.
[37] D. S. Stojković, J. Živković, M. Soković et al., "Antibacterial activity of Veronica Montana L. extract and of protocatechuic acid incorporated in a food system," *Food and Chemical Toxicology*, vol. 55, pp. 209–213, 2013.
[38] A. Hassan, M. Ashfaq, A. Khan, and M. S. Khan, "Isolation of caffeine from carbonated beverages," *Journal of Tropical Pharmacy and Chemistry*, vol. 5, no. 1, pp. 33–38, 2020.
[39] N. Khan, A. Hassan, H. Ullah, Z. Akmal, Y. K. Muhammad, and S. Khan, "Antibacterial potential test for *scheonoplectus triqueter* (L) Palla," *Letter In Applied NanoBioscience*, vol. 9, pp. 941–944, 2020.
[40] Y. F. Chu, J. Sun, X. Wu, and R. H. Liu, "Antioxidant and antiproliferative activities of common vegetables," *Journal of Agricultural and Food Chemistry*, vol. 50, no. 23, pp. 6910–6916, 2002.
[41] V. L. Singleton, R. Orthofor, and R. M. Lamuela-Raventos, "Analysis of total phenols and other oxidation substrates and

antioxidants by means of Folin-Ciocaltau reagent," *Methods in Enzymology*, vol. 299, pp. 152–178, 1999.

[42] M. Oyaizu, "Studies on products of browning reaction: antioxidative activity of products of browning reaction prepared from glucosamine," *The Japanese Journal of Nutrition and Dietetics*, vol. 44, no. 6, pp. 307–315, 1986.

[43] J. Sharifi Rad, S. M. Hoseini-Alfatemi, M. Sharifi Rad, and M. Iriti, "Free radical scavenging and antioxidant activities of different parts of *Nitraria schoberi* L," *Journal of Biologically Active Products from Nature*, vol. 4, no. 1, pp. 44–51, 2014.

[44] M. Yousaf, A. Hassan, S. Ahmad et al., "2, 4-Dinitrophenyl hydrazone derivatives as potent alpha amylase inhibitors," *Indian Journal of Chemistry, Section B*, vol. 60, no. 2, pp. 277–282, 2021.

[45] V. Worthington, "Alpha amylase," in *Worthington Enzyme Manual. Worthington V*, pp. 36–41, Worthington Biochemical Corp, Freehold, NJ, USA, 1993.

[46] R. K. Shukla, P. Deepak, S. Abha, J. Singh, A. Porval, and S. Vats, "In vitro biological activity and total phenolic content of Morusnigra seeds," *Journal of Chemical and Pharmaceutical Research*, vol. 6, pp. 200–210, 2014.

[47] M. Sharifi Rad, G. S. Tayeboon, J. Sharifi Rad, M. Iriti, E. M. Varoni, and S. Razazi, "Inhibitory activity on type 2 diabetes and hypertension key-enzymes, and antioxidant capacity of Veronica persica phenolic-rich extracts," *Cellular and Molecular Biology*, vol. 62, pp. 80–85, 2016.

[48] E. Apostolidis, Y. I. Kwon, and K. Shetty, "Inhibitory potential of herb, fruit, and fungal enriched cheese against key enzymes linked to type 2 diabetes and hypertension," *Innovative Food Science & Emerging Technologies*, vol. 8, no. 1, pp. 46–54, 2007.

[49] G. Oboh, A. O. Ademiluyi, A. J. Akinyemi, T. Henle, J. A. Saliu, and U. Schwarzenbolz, "Inhibitory effect of polyphenol-rich extracts of jute leaf (Corchorusolitorius) on key enzyme linked to type 2 diabetes (α-amylase and α-glucosidase) and hypertension (angiotensin I converting) in vitro," *Journal of Functional Foods*, vol. 4, no. 2, pp. 450–458, 2012.

[50] J. A. Saliu, A. O. Ademiluyi, A. J. Akinyemi, and G. Oboh, "In vitro antidiabetes and antihypertension properties of phenolic extracts from Bitter Leaf (Vernoniaamygdalina Del)," *Journal of Food Biochemistry*, vol. 36, no. 5, pp. 569–576, 2011.

[51] G. Oboh, A. O. Ademiluyi, and A. A. Akindahunsi, "Changes in polyphenols distribution and antioxidant activity during fermentation of some underutilized legumes," *Food Science and Technology International*, vol. 15, no. 1, pp. 41–46, 2009.

[52] A. O. Ademiluyi and G. Oboh, "Soybean phenolic-rich extracts inhibit key enzymes linked to type 2 diabetes (α-amylase and α-glucosidase) and hypertension (angiotensin I converting enzyme) in vitro," *Experimental & Toxicologic Pathology*, vol. 65, no. 3, pp. 305–309, 2013.

[53] N. K. Upadhyay, M. S. Yogendra Kumar, and A. Gupta, "Antioxidant, cytoprotective and antibacterial effects of Sea buck thorn (*Hippophae rhamnoides* L.) leaves," *Food and Chemical Toxicology*, vol. 48, no. 12, pp. 3443–3448, 2010.

[54] D. A. Vattem and K. Shetty, "Solid-state production of phenolic antioxidants from cranberry pomace by Rhizopusoligosporus," *Food Biotchnology*, vol. 16, no. 3, pp. 189–210, 2002.

[55] B. Kiss, D. S. Popa, G. Crişan, M. Bojiţă, and F. Loghin, "The evaluation of antioxidant potential of Veronica offcinalis and rosmarinus offcinalis extracts by monitoring malonildialdehide and glutathione levels in rats," *Farmacia*, vol. 57, no. 4, pp. 432–441, 2009.

[56] J. H. Kwak, H. J. Kim, K. H. Lee, S. C. Kang, and O. P. Zee, "Antioxidativeiridoid glycosides and phenolic compounds from Veronica peregrina," *Archives of Pharmacal Research*, vol. 32, no. 2, pp. 207–213, 2009.

[57] U. S. Harput, I. Saracoglu, M. Inoue, and Y. Ogihara, "Phenylethanoid and iridoid glycosides from Veronica persica," *Chemical and Pharmaceutical Bulletin*, vol. 50, no. 6, pp. 869–871, 2002.

[58] C. Andary, *Poliphenolic Phenomena*, pp. 237–255, INRA, Paris, France, 1993.

[59] C. Jimenez and R. Riguera, "Phenylethanoid glycosides in plants: structure and biological activity," *Natural Product Reports*, vol. 11, no. 6, pp. 591–606, 1994.

[60] I. Saracoglu, M. Inoue, I. Calis, and Y. Ogihara, "Studies on constituents with cytotoxic and cytostatic activity of two Turkish medicinal plants Phlomisarmeniaca and Scutellariasalviifolia," *Biological and Pharmaceutical Bulletin*, vol. 18, no. 10, pp. 1396–1400, 1995.

[61] I. Saracoglu, I. Calis, M. Inoue, and Y. Ogihara, "Selective cytotoxic and cytostatic activity of some phenylpropanoid glycosides," *Fitoterapia*, vol. 68, no. 5, pp. 434–438, 1997.

[62] I. Beara, J. Ž ivkovic, M. Lesjak et al., "Phenolic profile and anti-inflammatory activity of three Veronica species-flammatory activity of three Veronica species," *Industrial Crops and Products*, vol. 63, pp. 276–280, 2015.

[63] D. C. Albach, R. J. Grayer, S. R. Jensen, F. Özgökce, and N. C. Veitch, "Acylated flavone glycosides from Veronica-flavone glycosides from Veronica," *Phytochemistry*, vol. 64, no. 7, pp. 1295–1301, 2003.

[64] C. Frontela-Saseta, R. Lopez-Nicolas, C. A. Gonzalez-Bermudez, C. Martinez-Gracia, and G. Ros-Berruezo, "Anti-inflammatory properties of fruit juices enriched with pine bark extract in an in vitro model of inflamed human intestinal epithelium: the effect of gastrointestinal digestion.flammatory properties of fruit juices enriched with pine bark extract in an in vitro model of inflamed human intestinal epithelium: the effect of gastrointestinal digestion," *Food ChemToxicol*, vol. 53, pp. 94–99, 2013.

[65] K. Dastmalchi, H. Damien Dorman, M. Kosar, and R. Hiltunen, "Chemical composition and in vitro antioxidant evaluation of a water soluble Moldavian balm (*Dracocephalummoldavica* L.) extract," *LWT—Food Science and Technology*, vol. 40, no. 2, pp. 239–248, 2007.

[66] S. Meir, J. Kanner, B. Akiri, and S. Philosoph-Hadas, "Determination and involvement of aqueous reducing compounds in oxidative defense systems of various senescing leaves," *Journal of Agricultural and Food Chemistry*, vol. 43, no. 7, pp. 1813–1819, 1995.

[67] Y. I. Kwon, E. Apostolidis, Y. C. Kim, and K. Shetty, "Health benefits of traditional corn, beans and pumpkin: in vitro studies for hyperglycemia and hypertension management," *Journal of Medicinal Food*, vol. 10, no. 2, pp. 266–275, 2007.

[68] R. R. Ortiz-Andrade, S. Garcia-Jimenez, P. Castillo-Espana, G. Ramírez-Avila, R. Villalobos-Molina, and S. Estrada-Soto, "alpha-Glucosidase inhibitory activity of the methanolic extract from Tournefortia hartwegiana: an anti-hyperglycemic agent," *Journal of Ethnopharmacology*, vol. 109, no. 1, pp. 48–53, 2007.

[69] P. McCue, Y. I. Kwon, and K. Shetty, "Anti-diabetic and anti-hypertensive potential of sprouted and solid state bioprocessed soybean," *Asia Pacific Journal of Clinical Nutrition*, vol. 14, no. 2, pp. 145–152, 2005.

[70] A. O. Ademiluyi and G. Oboh, "Phenolic-rich extracts from selected tropical underutilized legumes inhibit α-amylase, α-glucosidase, and angiotensin I converting enzyme in vitro," *Journal of Basic and Clinical Physiology and Pharmacology*, vol. 23, no. 1, pp. 17–25, 2012.

[71] G. Oboh, A. J. Akinyemi, A. O. Ademiluyi, and S. A. Adesegha, "Inhibitory effects of aqueous extract of two varieties of ginger on some key enzymes linked to type-2 diabetes in vitro," *Journal of Food and Nutrition Research*, vol. 49, no. 1, pp. 14–20, 2010.

[72] H. Bischoff, "Pharmacology of alpha-glucosidase inhibition," *European Journal of Clinical Investigation*, vol. 24, no. 3, p. 3, 1994.

[73] P. McCue, D. Vattem, and K. Shetty, "Inhibitory effect of clonal oregano extracts against porcine pancreatic amylase in vitro," *Asia Pacific Journal of Clinical Nutrition*, vol. 13, no. 4, pp. 401–408, 2004.